# JOURNAL OF ATMOSPHERIC AND TERRESTRIAL PHYSICS

EDITORIAL ADVISORY BOARD

H. O. G. ALFVÉN–STOCKHOLM · J. BARTELS–GÖTTINGEN · W. J. G. BEYNON–ABERYSTWYTH · P. M. S. BLACKETT–LONDON · H. G. BOOKER–ITHACA, N.Y. E. G. BOWEN–SYDNEY · SIR DAVID BRUNT–LONDON · R. BUREAU–BAGNEUX S. CHAPMAN–ALASKA · J. EGEDAL–COPENHAGEN · V. F. HESS–NEW YORK · E. O. HULBURT–WASHINGTON, D.C. · H. ISRAEL–AACHEN · D. K. MENZEL–CAMBRIDGE, MASS. · S. K. MITRA–CALCUTTA · M. NICOLET–UCCLE · E. H. NORINDER–UPSALA · B. van der POL–GENEVA · N. V. PUSHKOV–MOSCOW · J. A. RATCLIFFE–CAMBRIDGE · O. E. H. RYDBECK–GOTHENBURG · J. C. W. SCOTT–OTTAWA SIR GEORGE SIMPSON–LONDON · H. SOLBERG–OSLO · J. VELDKAMP–DE BILT M. WALDMEIER–ZÜRICH · J. ZENNECK–ALTHEGNENBERG

EDITOR-IN-CHIEF

SIR EDWARD APPLETON, F.R.S.

EDINBURGH

VOLUME 15

1959

Nos. 1/2. Proceedings of Fifth Meeting of the Mixed Commission on the Ionosphere of ICSU

Nos. 3/4. Proceedings of Fourth Meeting of the Joint Commission on Radio-Meteorology of ICSU

PERGAMON PRESS

LONDON · NEW YORK · PARIS · LOS ANGELES

J. Atmosph. Terr. Phys.

VOL.
15
1959

INTERNATIONAL COUNCIL OF SCIENTIFIC UNIONS

MIXED COMMISSION ON THE IONOSPHERE

# PROCEEDINGS OF FIFTH MEETING

NEW YORK UNIVERSITY
14–16 AUGUST 1957

DL.
15
959

*Editor:*

W. J. G. BEYNON
*Department of Physics, University College of Wales, Aberystwyth*

PERGAMON PRESS LTD.
LONDON NEW YORK PARIS LOS ANGELES

VOL
15
195

## Foreword

THIS Volume contains the Proceedings of the Fifth Meeting of the Mixed Commission on the Ionosphere held at New York on 14–16 August 1957 together with the papers submitted to the Commission. It is regretted that a number of factors combined to delay seriously the preparation and publication of this Volume and apologies are tendered to those concerned. The initial submission of manuscripts was considerably retarded by the intense preoccupation of many authors with the International Geophysical Year, and further delays were experienced due to an unavoidable change of publication plans. The delay in publication is in no way due to the present publishers and the Editor wishes to acknowledge the very efficient manner in which Pergamon Press has now expedited publication. The assistance of Sir Harold Spencer-Jones (I.C.S.U. General Editor) with some of the proof reading is also gratefully acknowledged.

VOL.
15
1959

## Membership of the Mixed Commission on the Ionosphere

*International Scientific Radio Union (U.R.S.I.)*

Sir EDWARD APPLETON, Old College, South Bridge, Edinburgh 8, Scotland. Chairman of the Commission.

Dr. D. F. MARTYN, Commonwealth Scientific and Industrial Research Organization, Radio Research Laboratories, Camden, N.S.W., Australia.

Dr. L. V. BERKNER, President, Associated Universities Inc., 10 Columbus Circle, New York 19, N.Y., U.S.A.

Father P. LEJAY, Bureau Ionosphérique Francais, 106 rue de Paris, Bagneux.

*International Union of Geodesy and Geophysics (U.G.G.I.)*

Prof. S. CHAPMAN, The Geophysical Institute, College, Alaska, U.S.A.

Prof. D. R. BATES, Department of Applied Mathematics, The Queen's University of Belfast, Belfast, N. Ireland.

Dr. M. NICOLET, c/o Service du Rayonnement, I.R.M.3, Avenue Circulaire, Uccle, Belgium.

Dr. J. BARTELS, Director Geophysikalisches Institut, University of Göttingen, Göttingen, Germany.

*International Astronomical Union (I.A.U.)*

Dr. V. G. FESSENCOV, Sternberg State Astronomical Institute, Poroulok Morosova 5, Moscow 155, U.R.S.S.

Dr. D. H. MENZEL, Harvard College Observatory, Cambridge, Mass., U.S.A.

Dr. J. L. PAWSEY, Radiophysics Laboratory, C.S.I.R.O., Sydney, Australia.

*International Union of Pure and Applied Physics (I.U.P.A.P.)*

Prof. H. S. W. MASSEY, University College, Gower Street, London.

Prof. M. ALFVEN, Royal Institute of Technology, Stockholm 70, Sweden.

---

Prof. W. J. G. BEYNON, Department of Physics, University College of Wales, Aberystwyth, Wales. Secretary of the Commission.

The following were present at the New York meeting:

| | |
|---|---|
| Sir EDWARD APPLETON (President) | Dr. D. H. MENZEL |
| Dr. L. V. BERKNER | Dr. M. NICOLET |
| Prof. S. CHAPMAN | Dr. J. L. PAWSEY |
| Father P. LEJAY | Col. E. HERBAYS |
| Dr. D. F. MARTYN | Prof. W. J. G. BEYNON (Secretary) |
| | |
| Mr. D. K. BAILEY | Dr. M. G. MORGAN |
| Prof. H. G. BOOKER | Mr. P. NEWMAN |
| Dr. J. W. CHAMBERLAIN | Dr. N. J. OLIVER |
| Mr. K. P. CHOPRA | Mlle. G. M. PILLET |
| Mr. M. GALLET | Mr. J. A. RATCLIFFE |
| Dr. A. HAUBERT | Dr. K. RAWER |
| Prof. MORRIS KLINE | Dr. R. RIVAULT |
| Dr. D. LÉPÉCHINSKY | Dr. J. W. C. SCOTT |
| Dr. K. MAEDA | Dr. S. F. SINGER |
| Prof. L. A. MANNING | Dr. R. J. SLUTZ |
| Dr. S. MATSUSHITA | Dr. E. K. SMITH |
| Mr. E. METZLER | Mr. J. M. WATTS |

Dr. T. YONEZAWA

VOL. 15 1959

J. W. Chamberlain: Excitation of the oxygen red lines in twilight . . . . . 95
J. W. Chamberlain: Recombination in the *F2*-layer and the oxygen red lines in the airglow . . . . . 96
G. J. Gassmann: Tides in the *F*-layer . . . . . 99
A. R. Robbins and J. O. Thomas: The disturbed *F*-layer over Slough . . . . . 102
T. Shimazaki: Dynamical structure of the ionospheric *F2*-layer as deduced from the world-wide daily variations . . . . . 108
T. Sato: Ionospheric *F2*-disturbances associated with geomagnetic storms . . . . 116
R. W. Wright and N. J. Skinner: Equatorial spread-*F* . . . . . 121
I. Kasuya: On the occurrence of the $F1\frac{1}{2}$-layer at Tokyo . . . . . 126
M. Ôse, K. Aida and H. Okamoto: Latitude dependence of $f_0F2$ over the range of 20°N to 69°S, obtained by ship-borne ionospheric sounder . . . . . 130
W. G. Elford: Winds in the upper atmosphere . . . . . 132
L. A. Manning: Air motions at meteoric heights . . . . . 137
K. Rawer: Drift in the *E*-region . . . . . 141
A. Haubert: A propos des grands mouvements verticaux de la région-*F* . . . . 145
M. Hirono, H. Maeda and S. Kato: Wind systems and drift motions in the ionosphere deduced from the dynamo theory . . . . . 146
K. Sinno: On the origin of the long-lived solar corpuscular streams which appeared during the last solar cycle, 1950–53 . . . . . 151
S. Akasofu: Magneto-hydrodynamic waves in the ionosphere . . . . . 156
W. Pfister and J. C. Ulwick: Analysis of pulse-delay data from rockets for the determination of electron density . . . . . 161
W. J. G. Beynon and G. M. Brown: Region *E* and solar activity . . . . . 168
L. Vegard: Report on spectrographic work at Tromsö and Oslo . . . . . 175
Author Index 176

VOL
15
195

# CONTENTS


Preface . . . . . 183

*Session* I. *Radio Scattering by Inhomogeneities*

A. D. WHEELON: Radio scattering by tropospheric irregularities . . . . . 185

Discussion . . . . . 204

K. A. NORTON: Recent experimental evidence favouring the $\rho K_1(\rho)$ correlation function for describing the turbulence of refractibility in the troposphere and stratosphere . 206

*Session* II. *Convection and Inhomogeneities*

V. G. PLANK: Convection and refractive index inhomogeneities . . . . . 228

Discussion . . . . . 245

*Session* III. *Lightning*

M. G. H. LIGDA: Radar observation of lighting . . . . . 248

L. G. SMITH: Electric field-change studies of lightning . . . . . 251

Discussion . . . . . 252

D. R. FITZGERALD and H. R. BYERS: Aircraft observations of convective cloud electrification . . . . . 254

Discussion . . . . . 260

*Session* IV. *Radar Studies of "Angels"*

D. ATLAS: Radar studies of meteorological "angel" echoes . . . . . 262

Discussion . . . . . 284

*Session* V. *Radar Weather*

W. F. HITSCHFELD: Convective processes in the atmosphere as revealed by weather radar 288

Discussion . . . . . 292

*Session* VI. *Administration*

Minutes . . . . . 294

Resolutions . . . . . 295


VOL. 15 1959

VOL.
15
1959

# CONTENTS

## PART 1. PROCEEDINGS OF THE MEETING


*Session* I

SIR EDWARD APPLETON: Global morphology of the *E*- and *F1*-layers of the ionosphere 9

W. J. G. BEYNON: Vertical drift effects in region-*E* . . . . . 13

*Session* II

J. A. RATCLIFFE, A. R. ROBBINS and J. O. THOMAS: Movements in the quiet *F*-layer over Slough . . . . . 21

*Session* III

P. LEJAY: Irrégularités ionosphériques . . . . . 27

S. CHAPMAN: Disturbances in the lower auroral ionosphere . . . . . 29

K. RAWER: Irregularities and movements in the *F*-region . . . . . 38

*Sessions* IV *and* V

S. CHAPMAN: The outermost ionosphere . . . . . 43

S. F. SINGER: Geophysical effects of solar corpuscular radiation . . . . . 48

J. L. PAWSEY: The question of radio emission by the ionosphere . . . . . 51

M. G. MORGAN: Whistlers . . . . . 54

K. MAEDA and I. KIMURA: Calculation of the propagation path of whistling atmospherics 58

*Session* VI

Resolutions . . . . . 66


---

## PART 2. PAPERS SUBMITTED TO THE COMMISSION


S. MATSUSHITA: The morphology of the lower ionospheric region in auroral latitudes 68

J. M. WATTS: Interpretation of some features of low-frequency ionograms . . . 73

T. SHIMAZAKI: Effect of the $S_q$ current system on the ionospheric *E*- and *F1*-layers . 77

A. HAUBERT: Les gradients de température dans les régions-*E* et -*F1*, d'après les sondages ionosphériques effectués à Casablanca . . . . . 83

A. HAUBERT: L'ionisation nocturne de la région-*E* et l'activité géomagnétique . . 84

Y. INOUE: On the importance of the resonance-lines of atomic oxygen to the ionospheric ionization . . . . . 85

T. YONEZAWA: A new theory of formation of the *F2*-layer . . . . . 89

J. W. Chamberlain: Excitation of the oxygen red lines in twilight . . . . . 95
J. W. Chamberlain: Recombination in the *F2*-layer and the oxygen red lines in the airglow . . . . . 96
G. J. Gassmann: Tides in the *F*-layer . . . . . 99
A. R. Robbins and J. O. Thomas: The disturbed *F*-layer over Slough . . . . . 102
T. Shimazaki: Dynamical structure of the ionospheric *F2*-layer as deduced from the world-wide daily variations . . . . . 108
T. Sato: Ionospheric *F2*-disturbances associated with geomagnetic storms . . . . 116
R. W. Wright and N. J. Skinner: Equatorial spread-*F* . . . . . 121
I. Kasuya: On the occurrence of the $F1\frac{1}{2}$-layer at Tokyo . . . . . 126
M. Ôse, K. Aida and H. Okamoto: Latitude dependence of $f_0F2$ over the range of 20°N to 69°S, obtained by ship-borne ionospheric sounder . . . . . 130
W. G. Elford: Winds in the upper atmosphere . . . . . 132
L. A. Manning: Air motions at meteoric heights . . . . . 137
K. Rawer: Drift in the *E*-region . . . . . 141
A. Haubert: A propos des grands mouvements verticaux de la région-*F* . . . . 145
M. Hirono, H. Maeda and S. Kato: Wind systems and drift motions in the ionosphere deduced from the dynamo theory . . . . . 146
K. Sinno: On the origin of the long-lived solar corpuscular streams which appeared during the last solar cycle, 1950–53 . . . . . 151
S. Akasofu: Magneto-hydrodynamic waves in the ionosphere . . . . . 156
W. Pfister and J. C. Ulwick: Analysis of pulse-delay data from rockets for the determination of electron density . . . . . 161
W. J. G. Beynon and G. M. Brown: Region *E* and solar activity . . . . . 168
L. Vegard: Report on spectrographic work at Tromsö and Oslo . . . . . 175
Author Index 176

VOL. 15 1959

INTERNATIONAL COUNCIL OF SCIENTIFIC UNIONS

MIXED COMMISSION ON THE IONOSPHERE

# PROCEEDINGS OF FIFTH MEETING

NEW YORK UNIVERSITY
14–16 AUGUST 1957

DL.
5
959

*Editor:*

W. J. G. BEYNON
*Department of Physics, University College of Wales, Aberystwyth*

PERGAMON PRESS LTD.
LONDON NEW YORK PARIS LOS ANGELES

VOL.
15
1959

## Foreword

THIS Volume contains the Proceedings of the Fifth Meeting of the Mixed Commission on the Ionosphere held at New York on 14–16 August 1957 together with the papers submitted to the Commission. It is regretted that a number of factors combined to delay seriously the preparation and publication of this Volume and apologies are tendered to those concerned. The initial submission of manuscripts was considerably retarded by the intense preoccupation of many authors with the International Geophysical Year, and further delays were experienced due to an unavoidable change of publication plans. The delay in publication is in no way due to the present publishers and the Editor wishes to acknowledge the very efficient manner in which Pergamon Press has now expedited publication. The assistance of Sir Harold Spencer-Jones (I.C.S.U. General Editor) with some of the proof reading is also gratefully acknowledged.

OL.
15
959

VOL.
15
1959

## Membership of the Mixed Commission on the Ionosphere

*International Scientific Radio Union (U.R.S.I.)*

Sir EDWARD APPLETON, Old College, South Bridge, Edinburgh 8, Scotland. Chairman of the Commission.

Dr. D. F. MARTYN, Commonwealth Scientific and Industrial Research Organization, Radio Research Laboratories, Camden, N.S.W., Australia.

Dr. L. V. BERKNER, President, Associated Universities Inc., 10 Columbus Circle, New York 19, N.Y., U.S.A.

Father P. LEJAY, Bureau Ionosphérique Francais, 106 rue de Paris, Bagneux.

*International Union of Geodesy and Geophysics (U.G.G.I.)*

Prof. S. CHAPMAN, The Geophysical Institute, College, Alaska, U.S.A.

Prof. D. R. BATES, Department of Applied Mathematics, The Queen's University of Belfast, Belfast, N. Ireland.

Dr. M. NICOLET, c/o Service du Rayonnement, I.R.M.3, Avenue Circulaire, Uccle, Belgium.

Dr. J. BARTELS, Director Geophysikalisches Institut, University of Göttingen, Göttingen, Germany.

*International Astronomical Union (I.A.U.)*

Dr. V. G. FESSENCOV, Sternberg State Astronomical Institute, Poroulok Morosova 5, Moscow 155, U.R.S.S.

Dr. D. H. MENZEL, Harvard College Observatory, Cambridge, Mass., U.S.A.

Dr. J. L. PAWSEY, Radiophysics Laboratory, C.S.I.R.O., Sydney, Australia.

*International Union of Pure and Applied Physics (I.U.P.A.P.)*

Prof. H. S. W. MASSEY, University College, Gower Street, London.

Prof. M. ALFVEN, Royal Institute of Technology, Stockholm 70, Sweden.

---

Prof. W. J. G. BEYNON, Department of Physics, University College of Wales, Aberystwyth, Wales. Secretary of the Commission.

The following were present at the New York meeting:

Sir EDWARD APPLETON (President)
Dr. L. V. BERKNER
Prof. S. CHAPMAN
Father P. LEJAY
Dr. D. F. MARTYN
Dr. D. H. MENZEL
Dr. M. NICOLET
Dr. J. L. PAWSEY
Col. E. HERBAYS
Prof. W. J. G. BEYNON (Secretary)

Mr. D. K. BAILEY
Prof. H. G. BOOKER
Dr. J. W. CHAMBERLAIN
Mr. K. P. CHOPRA
Mr. M. GALLET
Dr. A. HAUBERT
Prof. MORRIS KLINE
Dr. D. LÉPÉCHINSKY
Dr. K. MAEDA
Prof. L. A. MANNING
Dr. S. MATSUSHITA
Mr. E. METZLER
Dr. M. G. MORGAN
Mr. P. NEWMAN
Dr. N. J. OLIVER
Mlle. G. M. PILLET
Mr. J. A. RATCLIFFE
Dr. K. RAWER
Dr. R. RIVAULT
Dr. J. W. C. SCOTT
Dr. S. F. SINGER
Dr. R. J. SLUTZ
Dr. E. K. SMITH
Mr. J. M. WATTS
Dr. T. YONEZAWA

VOL.
15
1959

Journal of Atmospheric and Terrestrial Physics 1959, Vol. 15, pp. 9 to 12. Pergamon Press Ltd. Printed in Northern Ireland

# PART 1: PROCEEDINGS OF THE MEETING

## SESSION I

### Global morphology of the *E*- and *F1*-layers of the ionosphere

Sir EDWARD APPLETON

(1) IT has been accepted now for many years that the classical theory of ionized layer production, developed by CHAPMAN (1931, 1939), can be considered as providing a fairly satisfactory explanation of *E*-layer and *F1*-layer behaviour. As radio-sounding measurements of the characteristics of these two layers have become more experimentally accurate and globally extensive, however, small but significant departures from simple layer characteristics have been recognized in both cases. Some of these anomalies have been reported to the Commission, by the author, at previous meetings (APPLETON, 1955). These particular examples have been identified in work carried out, at Edinburgh, by TURNBULL, LYON and the writer.

The theory of CHAPMAN is based on two simple assumptions: the earth's atmosphere is considered to be of uniform temperature and composition, and the process by way of which electrons disappear is taken to be that of recombination with positive ions. The basic continuity equation for electrons according to this theory, may therefore be written:

$$\frac{\partial}{\partial t} N(h, t) = q(h, \chi) - \alpha[N(h, t)]^2 \tag{1}$$

where $N(h, t)$ is the electron density at height $h$ and at time $t$; $q(h, \chi)$ is the rate of electron production per unit volume and thus is a function of both height and solar zenith distance $\chi$; while $\alpha$ is the recombination coefficient assumed independent of $H$ and $t$. In an isothermal atmosphere it is found that the maximum value of $q$ is given by

$$q_m = \left(\frac{S_\alpha}{H \exp (1)}\right) \cos \chi = q_0 \cos \chi \tag{2}$$

where $S_\alpha$ is the photon flux of the ionizing radiation outside the earth's atmosphere and $H$ is the scale height of the atmospheric absorbing constituent.

However, in vertical radio-sounding, we measure $N_m$ directly, a quantity not given simply in CHAPMAN's original investigation. This has led APPLETON and LYON (1955) to consider the matter afresh with the object of obtaining explicit theoretical expressions for the value of $N_m$. These authors have shown that, under sufficiently quasi-stationary conditions, we can write, instead of (1),

$$\frac{dN_m}{dt} = q_0 \cos \chi - \alpha N_m^2 \tag{3}$$

a relation of fairly wide applicability in studies of the *E*- and *F1*-layers.

If, however, we make the further assumption that the conditions are completely stationary, we can write (3) as

$$N_m = \sqrt{\left(\frac{q_0 \cos \chi}{\alpha}\right)} \tag{4}$$

Expressing $N_m$ in terms of $fE$ (in Mc/s), we can derive the familiar relations

$$\frac{(fE)^4}{\cos \chi} = K \tag{5}$$

where

$$K = \frac{1}{(1{\cdot}24 \times 10^4)^2} \frac{S_\alpha}{\alpha H \exp (1)} \tag{6}$$

The literature also describes many instances where (5) is written, more generally,

$$\frac{(fE)^n}{\cos \chi} = K \tag{7}$$

and ionospheric measurements of the relation between $fE$ and $\chi$ are used to find the value of $n$.

(2) It should be explained that many of the results described below, indicating departures from Chapman theory behaviour in the *E*- and *F1*-layers, have been obtained using published data from the world's routine sounding stations. Some doubt therefore exists concerning the accuracy and uniformity of the data employed, notably in connexion with the values of $fE$. It is well known that values of $fE$ round the period of noon in summer are specially difficult to read from ionograms. For example the influence of sporadic-*E* may have the effect of reducing the recorded $fE$ below the true value, if the *E*-layer "cusp" is relied on. Also, when absorption is marked over the critical frequency range, a reliance on the first appearance of an *F1*-reflection will yield values of $fE$ which are too high. Such difficulties become specially significant, for example, in finding the value of $n$, in equation (7), for the summer diurnal relation between $fE$ and $\chi$, when values of $fE$ at high and low values of $\chi$ are read with differing degrees of reliability.

Nevertheless it is believed that all the *E*-layer departures from Chapman theory identified cannot be wholly ascribed to errors in $fE$ determinations.

(3) The Edinburgh group have examined especially *E*-layer diurnal asymmetry. For this purpose they have used two theoretical relations, derivable from equation (3) above. The first relation is:

$$\Delta N_m = \frac{|dN_m/dt|}{\alpha \bar{N}_m} \tag{8}$$

where $|dN_m/dt|$ is the numerical magnitude of the mean rate of change of $N_m$ at two corresponding times, a.m., and p.m., at which $\chi$ is the same; and $\Delta N_m$ is the difference of $N_m$ at these two corresponding times, and $\bar{N}_m$ is their mean value.

The other relation is the formula for noon delay:

$$\Delta t = \frac{1}{2 \alpha N_0} \tag{9}$$



VOL. 15 1959

where $\Delta t$ is the delay between noon and the time of maximum $N_m$, and $N_0$ is the noon value of $N_m$.

It will be seen that an *effective* value of $\alpha$ can be determined using both relations.

The most cursory examination of $E$-layer data shows that (8) and (9) are not generally applicable, if $\alpha$ is assumed constant. One result easily identifiable, obtained by APPLETON and LYON (unpublished), is the "low-cos $\chi$ anomaly." Here, for low values of cos $\chi$, the value of $\Delta N_m$ in (8) is found to be zero or even negative! This means, for example, that evening values of $fE$ can be actually less than the corresponding morning values, both determinations being made at times when critical frequency measurements are least suspect.

Edinburgh studies of noon delay (APPLETON *et al.*, 1955a,b) over a wide range of latitudes, in terms of (9), have led to the identification of a motor influence of the $S_q$-current system on the $E$-layer. This can be noted in diurnal curves of both $fE$ and $h'E$. In the higher latitudes an east–west $S_q$-current, reaching its maximum round about 11 a.m., local time, causes a diminution of both $fE$ and $h'E$. In lower latitudes a west–east $S_q$-current has opposite effects.

The general result that an east–west $S_q$-current decreases $fE$, while a west–east current increases the same quantity, can be used to explain certain global characteristics of $fE$. It has been reported to the Commission previously (APPLETON, 1955) that, at the solstices, $fE$ does not attain its maximum value at the sub-solar point, but at a latitude displaced therefrom by some 10° towards the equator. This is due to the fact that the $S_q$-current system tends to raise the value of $fE$ at low latitudes, independently of the season; thus $fE$ ceases to be uniquely dependent on cos $\chi$.

The above results have been recently confirmed by SHIMAZAKI (1957, 1958).

(4) Mention has been made above of the effect of $S_q$-currents on the equivalent height of the $E$-layer. This prompts the recollection of the pioneer work of MARTYN (1947) who identified anomalous effects in the diurnal variation of $h'E$ and $h'F1$. This author showed that forenoon values of these quantities were lower than afternoon values in high latitudes, whereas the reverse was the case in low latitudes. MARTYN further identified these effects as due to a *semi-diurnal* variation of vertical drift which, for example in low latitudes, attains its maximum upward value at 0900 hours and its maximum downward value at 1500 hours. As will have been seen above, later workers have adopted a somewhat different interpretation, correlating drift effects with the known *diurnal* variations of $S_q$-currents which attain their maximum values at 1100 hours local time.

(5) The ionospheric literature dealing with the relation between $fE$ and cos $\chi$ for diurnal, seasonal and latitude variations is already voluminous. This all relates to the determination of $n$ in equation (7), or of $p$, if the same equation is alternatively written:

$$\frac{fE}{(\cos \chi)^p} = K \tag{7a}$$

For example HARNISCHMACHER (1950) finds that, in terms of (7a),

$$\left.\begin{aligned} K &= 2{\cdot}25 + 1{\cdot}5 \cos \phi + (0{\cdot}01 - 0{\cdot}007 \cos \phi)^R \\ p &= 0{\cdot}21 + 0{\cdot}12 \cos \phi + 0{\cdot}0002\ R \end{aligned}\right\} \tag{10}$$

where $\phi$ is the geographic latitude and $R$ the sunspot number. According to simple Chapman theory $K$ and $p$ should, of course, be independent of $\phi$ and $R$, while $p$ should be universally equal to 0·25.

More recently Beynon and Brown have made the striking discovery that the value of $n$ in equation (7), as applied to the seasonal variation of noon $fE$, has a characteristic variation with latitude, reaching two sharp maxima at middle latitudes in both the northern and southern hemispheres. The positions of these maxima are identified as being associated in some way with the positions of the $S_q$-current foci. Beynon will no doubt give a fuller account of this very remarkable result.

(6) Some of the anomalous effects identified in the $E$-layer are found to be paralleled in the case of the $F1$-layer. For example, the different types of diurnal height asymmetry in high and low latitudes, noted in $h'E$, are also recognizable in $h'F1$. Some authors conclude that there is also slight, but definite, evidence of geomagnetic distortion in the $F1$-layer recognizable in diurnal and seasonal studies of $fF1$. But, in the most recent paper, Shimazaki (1957) concludes that the only departure from Chapman theory exhibited by the $F1$-layer is due to variable temperature influences.

(7) In conclusion I add a word on the subject of nomenclature. I suggest that we should use the symbol $\Delta$ for the distortion of any quantity brought about by influences (e.g. electron transport) not envisaged in Chapman theory. We can then write, for example in the case of the $F2$-layer where transport effects are known to be specially marked,

$$\Delta_q(fF2) = \frac{S_q(fF2)}{\text{theor.}(fF2)} \tag{11}$$

or, alternatively,

$$\Delta_q(fF2) = S_q(fF2) - \text{theor. } (fF2) \tag{12}$$

The same equations on magnetically disturbed days would be written with a $d$ instead of $q$ subscript.

I leave the choice between (11) and (12) as a matter for discussion by the Commission.

VOL. 15 1959

## References


| | | |
|---|---|---|
| Appleton E. V. | 1955 | *Proceedings Fourth Meeting Mixed Commission on the Ionosphere* p. 14. |
| Appleton E. V. and Lyon A. J. | 1955 | *Physics of the Ionosphere* p. 20. Physical Society, London. |
| Appleton E. V., Lyon A. J. and Pritchard A. G. | 1955a | *J. Atmosph. Terr. Phys.* **7,** Nos. 4–5, 292. |
| Appleton E. V., Lyon A. J. and Turnbull A. G. | 1955b | *Nature, Lond.* **176,** 897. |
| Chapman S. | 1931a | *Proc. Phys. Soc.* **43,** 26. |
| Chapman S. | 1931b | *Proc. Phys. Soc.* **43,** 483. |
| Chapman S. | 1939 | *Proc. Phys. Soc.* **51,** 93. |
| Harnischmacher E. | 1950 | *C.R. Acad. Sci., Paris* **230,** 1301. |
| Martyn D. F. | 1947 | *Proc. Roy. Soc.* A **189,** 241; **190,** 273. |
| Martyn D. F. | 1948 | *Proc. Roy. Soc.* A **194,** 429, 445. |
| Shimazaki T. | 1957 | *J. Radio Res. Lab.* **4,** 37. |
| Shimazaki T. | 1958 | *J. Radio Res. Lab.* **5,** 35. |

Journal of Atmospheric and Terrestrial Physics, 1959, Vol. 15, pp. 13 to 20. Pergamon Press Ltd. Printed in Northern Ireland

# Vertical drift effects in region-*E*

W. J. G. Beynon

In 1947–1948 Martyn called our attention to some of the important perturbations in electron density and height which can arise as a result of vertical drifts from the vertical component of the transport term div($Nv$) which occurs in the usual equilibrium equation. The effect of vertical drift in distorting the electron density profile of Chapman-like layers was later discussed by Kirkpatrick (1948) and more recently by Appleton and Lyon (1955). Martyn pointed out that in region-*E* the distortion due to vertical drift is unlikely to be large, since in this region the lifetime of the ions is comparatively small and the loss of ionization due to transport is offset by the normal replenishment by solar radiation. He has shown that, under typical conditions, vertical drift in the *E*-layer may change the peak density by a few per cent. The results which I present here show that under certain circumstances this distortion of the *E*-layer due to vertical drift, although small, can readily be detected.

Appleton and Lyon have shown that the fractional change in the peak electron density, $\Delta N_m/N_m$, of an ionized stratum of *E*-layer type due to vertical drift effects is given approximately by the expression

$$\frac{\Delta N_m}{N_m} = -\frac{1}{2\alpha N_m}\cdot\frac{\partial v}{\partial h} - \frac{1}{4H^2}\left(\frac{v}{2\alpha N_m}\right)^2 \tag{1}$$

and that the height of the peak electron density changes by the amount

$$(\Delta h)_{N_m} = \frac{v}{2\alpha N_m} \tag{2}$$

where $v$ is the *vertical* velocity of electron drift, reckoned positive upwards. It will be seen from the second term on the right-hand side of equation (1) that the change of the maximum ionization density is independent of the *direction* of drift (upwards or downwards). If there is negligible height-gradient of the drift velocity, or if there is positive gradient $\partial v/\partial h$, then distortion due to vertical drift may always be expected to *reduce* the peak density. The direction of drift will determine whether the height of the electron peak rises or falls (equation 2), but in either case the ionization will be spread out vertically resulting in a diminished peak density. However, if there is a *negative* velocity gradient then vertical drift will compress the ionization vertically, tending to give an enhanced peak density. The drift velocity itself will, of course, tend to remove this peak to another height, which will no longer be the height of maximum electron production. Whether the net result is then an increase or decrease in $N_m$ clearly depends on the relative magnitudes of the two terms in expression (1). In general, the term in $\partial v/\partial h$ may be expected to be of greater magnitude than that in $v^2$ and for a negative velocity gradient an increase in peak density may be anticipated.

All this, of course, presupposes a constant $H$ and $\alpha$.

## Analysis of $fE$-data

Two years ago my colleague Brown and I examined a large body of data on the normal $E$-layer critical frequency $fE$ with a view to detecting a possible influence of vertical drift. If initially we omit consideration of drift effects then under equilibrium conditions (e.g. at noon) the general equilibrium equation yields the simple relationship between $fE$ and cos $\chi$ namely:

$$fE^n = A \cos \chi$$

Hence, whenever this relationship applies we should expect logarithmic plots of $fE$ against cos $\chi$ to be straight lines of slope $n$ and intercept $A$. For a simple recombination process $n$ should of course have the value 4·0. If the effect of drift is important then we might expect the consequences of neglecting it to show in the value of the index $n$. In fact the index is extremely sensitive to small perturbations in $fE$.

Now when such plots are made, using monthly mean noon values for stations in various latitudes, we find that almost invariably for *each* station a good straight line is obtained but the slope varies with latitude in a systematic but remarkable manner. This is shown in Fig. 1 in which the top curve shows the values of $n$ for

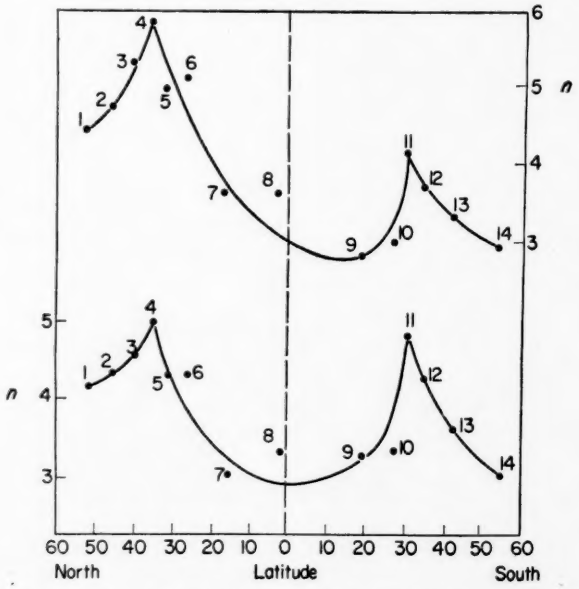


Fig. 1. (*upper curve*)—Index $n$ for stations centred approximately on the 150°E meridian, derived from noon values of $fE$ for 1952–1954. (*lower curve*)—The same, but reduced to a common solar distance.

Station key: 1, Adak; 2, Wakkanai; 3, Akita; 4, Tokyo; 5, Yamagawa; 6, Okinawa; 7, Baguio; 8, Singapore; 9, Townsville; 10, Brisbane; 11, Watheroo; 12, Canberra; 13, Hobart; 14, Macquarie Island.

fourteen stations near the 150°E meridian. It will be seen that there is a systematic variation with latitude and that marked peaks occur at Tokyo and Watheroo.

There is also considerable asymmetry between the hemispheres and much of this we can attribute to the 3 per cent change in the earth–sun distance between January and July. It is to be remembered that these logarithmic plots are based on the *seasonal* variation in *noon* values. A typical plot for a northern hemisphere station would be of the form shown in Fig. 2. If we correct the winter and summer points for the fact that the earth is nearer the sun in December than in June, then the December value of $fE$ must be decreased slightly and the June value increased slightly, giving a reduced slope. For southern hemisphere stations the correction produces *increased* values of the slope $n$. Hence when we correct for the varying

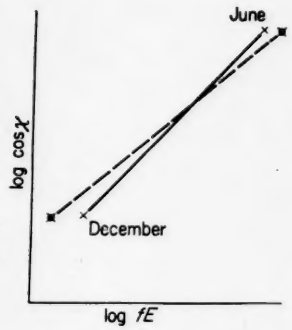


Fig. 2. Effect of changing solar distance on index $n$. Full line, uncorrected; broken line, corrected to a common distance.

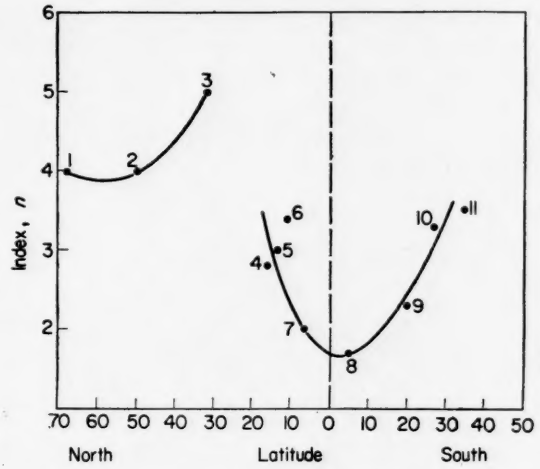


Fig. 3. Latitude variation in index $n$ for stations centred around 10°E meridian. Key to stations: 1, Kiruna; 2, Slough; 3, Casablanca; 4, Dakar; 5, Khartoum; 6, Djibouti; 7, Ibadan; 8, Leopoldville; 9, Tananarive; 10, Johannesburg; 11, Capetown.

earth–sun distance we largely remove the asymmetry between the hemispheres and get the lower curve in Fig. 1. Outside the peaks there is still a degree of asymmetry and this is probably associated with the magnetic asymmetry of the earth.

We have made a similar study of $n$ for stations in two other longitude zones and although the data are far less complete than for the 150°E zone, nevertheless the two peaks are clearly present (Figs. 3 and 4). An interesting additional feature of Fig. 4 is the bodily displacement of the curve towards the south. This is probably associated with the pronounced displacement of the magnetic equator towards the south at these longitudes.

Before discussing the possible cause of these remarkable latitude variations in the index $n$ I might briefly mention three other experimental facts:

(i) There is a marked *diurnal* variation in the index $n$, maximum values occurring near 1000 or 1100 hours. Fig. 5 shows this variation for Slough.

(ii) The remarkable maxima in noon values of $n$ near latitudes $\pm 35°$ are completely absent in the values for 1500 hours. Fig. 6 shows the latitude variation at 1500 hours for the same stations as are included in Fig. 1.

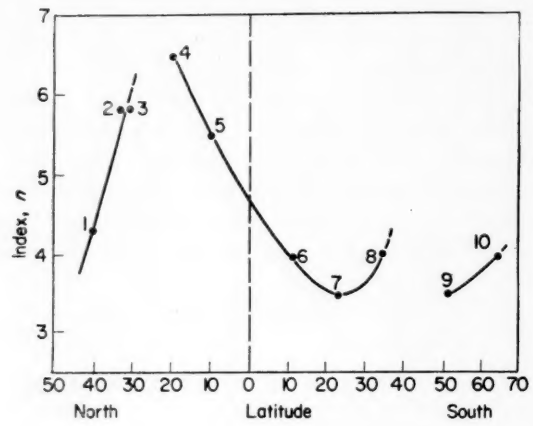


Fig. 4. Latitude variation in index $n$ for stations centred around 75°W meridian. Key to stations: 1, Washington; 2, White Sands; 3, Baton Rouge; 4, Puerto Rico; 5, Panama; 6, Huancayo; 7, Sao Paulo; 8, Buenos Aires; 9, Falkland Islands; 10, Port Lockroy.

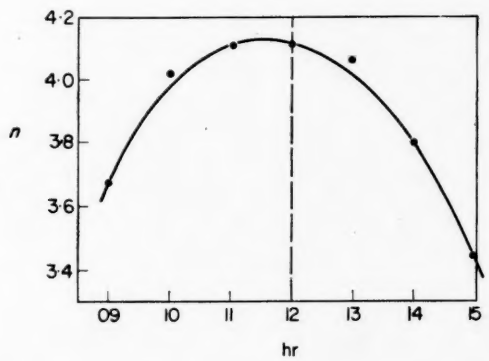


Fig. 5. Diurnal variation of index $n$ derived from values of $fE$ for Slough for 1952–1954, reduced to the common sunspot number $R = 16$.

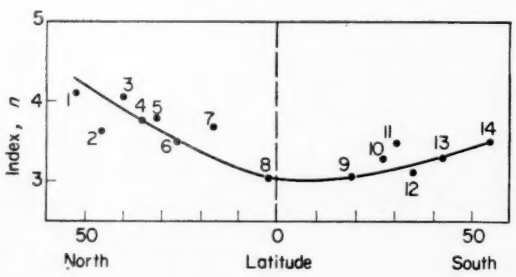


Fig. 6. Index $n$ for stations centred approximately on the 150°E meridian, derived from values of $fE$ at 1500 hours for 1952–1954. Station key as for Fig. 1.

(iii) At temperate latitude stations there is much evidence for a "bite-out" in the forenoon period in the curve showing the diurnal variation of $fE$. Attention to this point has already been called by APPLETON *et al.* (1955). We have confirmed its existence at temperate latitude stations but have been unable to find conclusive evidence for any corresponding anomaly in $fE$ at this time of day at equatorial stations.

## Influence of the $S_q$-current System

The high values of $n$ obtained for stations between latitudes 30° and 40°, and the other experimental facts just mentioned, suggest some influence on $fE$ of the current systems responsible for the quiet day solar magnetic variation ($S_q$). Three relevant features of these current systems may be noted here:

(i) The maximum E–W component of the current usually occurs not at noon but 1–2 hr before noon. Furthermore at 1500–1600 hours there is little or no E–W component of current.

(ii) The current intensities are much larger in local summer than local winter.

(iii) Although the foci are, on the average, located near latitudes $\pm 35°$ there is much evidence for both day to day and seasonal variations in this latitude.

If now the $S_q$-current system is located in or near region-$E$, then under the combined influence of the current and the earth's magnetic field, we may expect vertical drift effects in this region. At any latitude the magnitude of the vertical drift will be determined by the magnitude of the E–W component of the current and by the strength of the horizontal component of the earth's field. Hence from the magnetic studies we should expect maximum drift to occur near 1000–1100 hours, and to be directed downwards at latitudes on the poleward sides of the foci, and upwards on the equatorial sides of the foci. Also minimum drift effects should occur near 1500 hours. If downward is associated with a depression of $fE$, and vice versa, possible explanations for the latitude variation in the index $n$ may be sought along the following lines:

(i) A seasonal shift in the latitudes of the foci of the $S_q$ current systems.

(ii) The seasonal change in the intensity of the $S_q$-current systems.

(iii) A seasonal change in the vertical gradient of vertical drift velocity.

In our preliminary report on this work (1956) Brown and I inclined to an explanation in terms of a seasonal shift in the latitudes of the $S_q$-current foci, but recently we have been able to obtain some detailed magnetic data from Japanese observatories near the foci, and this does not support the suggestion for a seasonal shift in the sense required. Additional ionospheric studies will be necessary before we can decide between the other two possibilities.

If the "bite-out" in $fE$ which is often observed at temperate stations an hour or so before noon is due to an $S_q$-effect then one might expect a corresponding *elevation* of $fE$ to show itself in the diurnal variation at equatorial stations. So far we have been unable to detect such an elevation. At equatorial latitudes the magnitude of the vertical drift velocity is expected to be very large and in these circumstances the second term in equation (1) may possibly be of sufficient magnitude to offset the first and so result in negligible distortion.

## Sporadic-$E$ Ionization

I should also like to refer briefly to a subsidiary analysis involving considerations of the world distribution of sporadic-$E$ ionization which are relevant to these $E$-layer studies.

Those who are familiar with ionograms will know that, quite often, the estimation of the true value of $fE$ is made difficult or impossible by the presence of sporadic-$E$ ionization. It is thus important to examine carefully the possibility

that these anomalous results for $fE$ may perhaps be due to the influence of sporadic-$E$ ionization.

Recently a very comprehensive survey of the world distribution of $E_s$-ionization was made by SMITH (1957) and a study of these results reveal some interesting features of this distribution. Three such features are relevant to the present discussion:

(i) At temperate latitude stations in local summer there would appear to be a marked tendency for the "intensity" of $E_s$ (as measured by the percentage of time for which it exceeds an arbitrary level) to be a maximum 1–2 hr *before* local noon. On the other hand, in local winter the diurnal variation at temperate latitude stations appears to be more symmetrical, with maxima near noon or even slightly after noon.

(ii) At the June solstice the latitude variation in the incidence of $E_s$ appears to show a maximum near 30°N (rather than near 23½°N). At the December solstice the southern hemisphere latitude of maximum occurrence is less well defined, but there is again evidence that it may be greater than 23½°S.

(iii) There would appear to be quite marked asymmetry between the two hemispheres in the incidence of $E_s$-ionization. This is particularly evident when the June and December solstice conditions are compared. Thus, in June the latitude variation shows a maximum near 30°N and $fE_s$ then exceeded 5 Mc/s for about 65 per cent of the time. In December the corresponding maximum in the southern hemisphere only amounts to about 35 per cent.

It will be seen that these three general features of the distribution of $E_s$-ionization are analogous to those found for the anomalies in $fE$ and strongly suggest that either (i) the perturbations in $fE$ are really due to the presence of $E_s$-ionization or (ii) that both normal and sporadic $E$-ionization show a geomagnetic distortion due to the influence of the $S_q$ current system.

From a careful study of a large body of data BROWN and I conclude that (i) is most unlikely and that the features of $E_s$-ionization outlined above probably represent some influence of the $S_q$-current system.

VOL. 15 1959

## REFERENCES


| | | |
|---|---|---|
| APPLETON E. V. and LYON A. J. | 1955 | *Physics of the Ionosphere* p. 20. Physical Society, London. |
| APPLETON E. V., LYON A. J. and TURNBULL A. G. | 1955 | *Nature, Lond.* **176,** 897. |
| BEYNON W. J. G. and BROWN G. M. | 1956 | *Nature, Lond.* **177,** 583. |
| KIRKPATRICK C. B. | 1948 | *Aust. J. Sci. Res.* A **1,** 423. |
| MARTYN D. F. | 1947 | *Proc. Roy. Soc.* **189,** 241, **190,** 273. |
| SMITH E. K. | 1957 | *Nat. Bur. Stand. Circ.* 582. |


## DISCUSSION

PROFESSOR CHAPMAN—Since the distortion is small I suggest the definitions be

$$\Delta(fE) = \frac{S_q(fE)}{\text{theor. } fE} - 1, \text{ etc.}$$

One might also insert $S$ or $L$ in front to indicate solar or lunar effects.

DR. MARTYN—I doubt whether the magnitude of the $v^2$ term is likely to be large enough to nullify the effect due to $\partial v/\partial h$ as suggested by Dr. BEYNON. I think that the precise interpretation of the remarkable latitude variation in the index $n$, described by Dr. BEYNON, may prove complex. What we all agree about are the departures in the height of the $E$-layer—that at high latitudes the height is depressed and at the equator it is probably elevated. The expression for the vertical velocity $v$ is

$$v = \frac{E}{H} \cdot \frac{\omega^2}{\omega^2 + \nu^2}$$

This is not a particularly convenient form for discussion since $E$, $\omega$ and $\nu$ all change with height. An alternative approach is to think in terms of a conductor in a viscous medium moving with a velocity which depends on the viscosity. In the case of region-$E$ we have height gradients in the conductivity, in the velocity and in the current and the problem is, at the moment, too complex in that there are several possible ways of explaining the observed phenomena. We do not know precisely what the height gradient of velocity is in region-$E$ and we need further rocket experiments to tell us exactly the levels at which currents flow.

SIR EDWARD APPLETON—The perturbations in height are of considerable interest and it is hoped that, during the IGY, accurate data for further studies of asymmetry in $h'E$ and $h'F1$ will become available. The Edinburgh work suggests that $S_q$-influences are recognizable in $h'F1$ as well as in $h'E$.

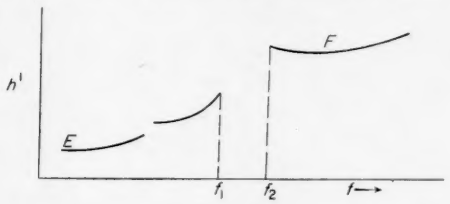


Fig. D1.

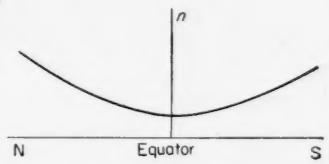


Fig. D2.

DR. MARTYN—One would not expect effects in region-$F1$. I think it desirable to ensure that we sort out quiet and disturbed ionospheric effects.

DR. BERKNER—In the ionospheric field we might follow the magneticians and separate data for the quiet and disturbed days. (See Resolution (2)—Ed.)

MR. J. A. RATCLIFFE—Recently at Cambridge we have been examining closely the form of the $h'(f)$ curve during the transition from region-$E$ to $F$. In the winter, day-time curves of the form shown in Fig. D1 are often obtained.

We often observe a slight frequency gap between frequencies indicated by $f_1$ and $f_2$. We find that published data often give $f_2$ as the normal $E$-layer critical frequency whereas we find that the critical frequency marked $f_1$ behaves like a normal Chapman region in winter with the expected slight noon-delay in its maximum value. We find that for the same days the $N(h)$ profiles are also Chapman-like and move up and down in the course of a day in the manner expected for a Chapman layer.

On the other hand, in summer, owing to the influence of $E_s$ we do not find this Chapman-like variation of $N_{\max}$ with time.

At Cambridge we have also examined the diurnal variation in *fF1* for some twenty stations and determined the value of the index $n$ in the expression $fF1 \propto (\cos \chi)^n$. We find that the value of $n$ is always less than 0·25 and shows a latitude variation of the form shown in Fig. D2.

Dr. K. Rawer—The URSI Sub-committee on Worldwide Soundings has discussed at some length the difficulties attached to scaling *fE* and *fF1*. It is often especially difficult to measure the latter and considerable caution should be exercised in the interpretation placed upon *fF1*.

In the case of *h'E* we find that if measurements are made to an accuracy of $\pm 2$ km then the value of *h'E* varies with the frequency of the measurement and at a fixed frequency shows the expected dependence on the value of the critical frequency *fE*.

Sir Edward Appleton—It would be extremely valuable to determine lunar tides in all the principal parameters for both sporadic-*E* and normal-*E* layers. We badly need a check on the latitude situation of the foci in the $L_q$ current system.

Dr. Matsushita—We have used published sporadic-*E* layer data and found them accurate enough to permit the determination of lunar tides.

Dr. Beynon—It is clear that accurate measurements of *E*-layer parameters are becoming essential and I think that some degree of accuracy is being lost due to the compressed height scale of the *E*-layer trace on the usual type of ionogram. Some advantage might come from the use of an expanded height scale at the lower frequency end.

Dr. Lépéchinsky—I should strongly support such a proposal.

Dr. Pawsey—It would also be worthwhile proposing that certain stations should make especially careful measurement of some ionospheric parameters so that small, but important, perturbations might be reliably determined.

Father P. Lejay—I do not think that a simple expansion of the height scale will give the accuracy required to determine lunar tidal phenomena. When consideration is given to the analysis by Lépéchinsky of the quasi-longitudinal and quasi-transverse approximations it will be found that for certain ionospheric parameters it is not possible to make a direct comparison between values from stations in different latitudes.

Dr. Menzel—The lunar tidal effects are difficult to disentangle from those due to the solar rotation period and to the solar activity variation. I think it would be profitable to invite IGY stations to extend the period of observations well beyond the 18 months of the IGY.

Mr. Bailey—A resolution on the need for extending the period of observation of certain IGY stations has been formulated by CCIR.

Dr. Martyn—I should like to comment on the cusp effects in *fE* referred to by Mr. Ratcliffe. In Australia Munro has extended his earlier region-*F2* analysis to region-*E* and concludes that many of the observed perturbations in the *E*-layer trace are due to non-vertical reflections. Such non-vertical reflections can be especially important in the study of eclipse and sunrise effects.

Mr. Ratcliffe—I do not think the effects observed at Cambridge can be explained in this way. We have also observed the transient phenomena referred to by Dr. Martyn but the cusp effects, to which I referred, are quite regular from day to day.



VOL. 15 1959

Journal of Atmospheric and Terrestrial Physics, 1959, Vol. 15, pp. 21 to 26. Pergamon Press Ltd. Printed in Northern Ireland

## SESSION II

# Movements in the quiet *F*-layer over Slough

J. A. Ratcliffe, Audrey R. Robbins and J. O. Thomas

**Abstract**—Electron density profiles have been deduced from $h'(f)$ curves recorded at Slough once per hour on every day of each of six representative months. Allowance was made for the effects of the earth's magnetic field and the ionization below the *F*-layer. The average behaviour on magnetically quiet days is described and discussed, with particular reference to the possible magnitude and phase of vertical movements in the *F*-region.

Recent theories of the *F*-layer have supposed that the peak of electron density corresponds, not to a peak in the rate of production of electrons, but to the balancing of two or more processes (such as rate of production, rate of loss, or rate of accretion by diffusion) whose magnitudes vary with height. Until there is a well-established theory to explain the existence of the peak it is difficult to base theories of the ionosphere on measured magnitudes of this peak density. Recently, however, several computations have been made of complete electron-density profiles which show the electron density $N$ as a function of height $h$, and it is the purpose of this note to draw attention to the significance of these profiles (or $N(h)$ curves) in relation to movements in the *F*-region.

The $N(h)$ curves to be discussed here have been deduced from $h'(f)$ records made at Slough once per hour on every day of 6 months representing summer, equinox and winter at high and low sunspot number, and have been published in a booklet by Thomas *et al.* (1957). In the computations, allowance was made for the effects of the earth's magnetic field and the ionization below the *F*-layer.

When a detailed knowledge of the electron distribution is available, it is possible to concentrate attention on the electron density ($N$) at a fixed height, not necessarily near the peak of the layer, and to consider it in the light of the equation of continuity

$$dN/dt = q - L - \text{div } (Nv) \tag{1}$$

in which $q$ represents the rate of production of electrons, $L$ the rate of loss by processes of attachment or recombination, and div $(Nv)$ the rate of loss resulting from movement of the electrons with a drift velocity $v$.

In a first attempt to understand the behaviour of the *F2*-region it seems reasonable to suppose that the rate of production $q$ varies with the sun's zenith angle as given by the well-known theory of Chapman, and that the loss-term ($L$) is probably "attachment-like" and may be written $K(h) \,.\, N$ where the loss coefficient $K(h)$ is a function of height. Detailed suggestions about $q$ and $K(h)$ have been made by Ratcliffe *et al.* (1956) who suggested that

$$K(h) = 10^{-4} \exp \{(300 - h)/50\} \text{ sec}^{-1} \tag{2}$$

with $h$ measured in kilometres.

It is interesting to enquire what magnitude must be given to the movement term in equation (1) if it is to represent the observed results. For the enquiry the

computed values of $N(h)$ have been used to construct curves to show how the monthly average value $\bar{N}(t)$ of the electron density at a given height, varied with time of day ($t$). Results are available from all the months, at night, for heights of 340, 300 and 260 km and, during the day, for heights of 220 km and for 260 km near sunspot maximum.

Examination of the daytime results shows that $\bar{N}(t)$ is approximately symmetrical about midday but with values of $\bar{N}$ somewhat greater in the afternoon

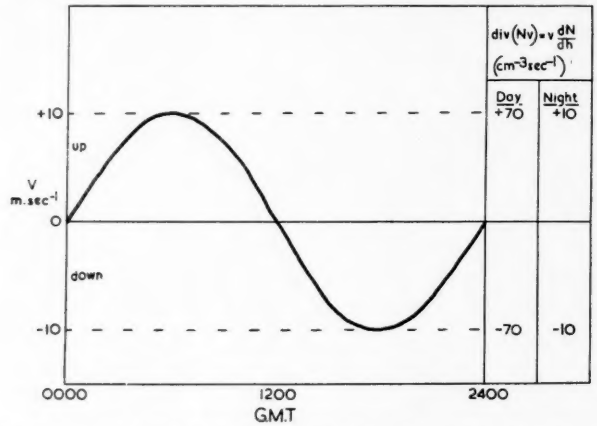


Fig. 1. The variation of vertical velocity ($v$) with local time at medium latitudes (Martyn, 1954). The right-hand scale gives the orders of magnitude for div ($Nv$) by day and by night.

than in the morning. They can be described, to a first approximation, by the equation

$$dN/dt = q(t) - K(h) \,.\, N \tag{3}$$

where $K(h)$ is given by equation (2), $q(t)$ is symmetrical about midday, and the movement term of equation (1) is omitted. The night-time results, with the exception of those for winter in years of few sunspots, can likewise be described, to a first approximation, by the corresponding equation

$$dN/dt = -K(h)N \tag{4}$$

It thus appears, at first sight, that the movement term is small compared with the other terms in equation (1), or that it varies with time in such a way that it becomes confused with one of the other terms. For example, it might become confused with $q(t)$ by day if it were symmetrical about midday, or with $KN$ by night if it simulated an attachment process.*

It has sometimes been supposed (Martyn, 1954) that the movement term represents the effect of a vertical velocity which varies throughout the day as shown in Fig. 1. With the observed gradients of electron density, a velocity of this kind would give rise to movement terms in equation (1) whose maximum magnitude would be of the order of 70 $cm^{-3}$ $sec^{-1}$ by day and 10 $cm^{-3}$ $sec^{-1}$ by night as indicated on the right-hand scales of Fig. 1.

* Martyn (1956) and others have pointed out that, under certain circumstances, movements resulting from diffusion might simulate an attachment process.

Now, with the exception of those for winter at times of few sunspots, the night-time $\bar{N}(t)$ curves can be described to a first order by equation (4), and the observed magnitude of $dN/dt$ is of the order $-10$ cm$^{-3}$ sec$^{-1}$. There does not seem to be any room for an additional movement term, at night, of the kind shown in Fig. 1.

By day the results are approximately represented by equation (3) and the midday magnitudes of the two terms on the right-hand side are of the order 100–400 cm$^{-3}$ sec$^{-1}$ according to the height or the season. If a movement term were to be included with the magnitude and phase shown in Fig. 1 the representations would be much worse.

It is concluded that movements associated with a vertical velocity of the kind described by Fig. 1 do not occur in the $F2$-region. If an oscillating velocity with this phase is present at all it cannot have an amplitude greater than about 300 cm-sec$^{-1}$ otherwise it would be detectable from the observations.

It may well be that a movement of this kind can explain some of the smaller anomalies in the behaviour of the region, but it does not seem that it can play an important part in a first order theory.

## References


| | | |
|---|---|---|
| Martyn D. F. | 1954 | *The Physics of the Ionosphere* p. 254. Physical Society, London. |
| Martyn D. F. | 1956 | *Aust. J. Phys.* **9,** 161. |
| Ratcliffe J. A., Schmerling E. R., Setty C. S. G. K. and Thomas J. O. | 1956 | *Phil. Trans.* A **248,** 621. |
| Thomas J. O., Haselgrove J. and Robbins A. R. | 1957 | *Tables of Ionospheric Electron Density, Slough.* Series B, No. 1. Cavendish Laboratory, Cambridge. |


## Discussion

Sir Edward Appleton—Undoubtedly the most valuable information of all comes from $N(h)$ studies. But these take time and some problems cannot wait.

I think that present-day knowledge of the $F2$-layer would suggest that the appropriate continuity equation describing the behaviour of this layer would be written

$$\frac{dN}{dt} = q(t) - \beta N - \text{div}\,(Nv)$$

and, as we go from sunspot minimum to sunspot maximum, we can picture $q(t)$ altering to $\lambda q(t)$ where $\lambda$ is a small positive number. Now, if $v$ remains constant, we have, generally,

$$N(\text{S.S. max}) = \lambda N(\text{S.S. min})$$

That is to say, the values of $N$ at all heights and at all times are merely multiplied by $\lambda$ as we go from sunspot minimum to sunspot maximum conditions. Edinburgh global studies of the ratio $fF2$ (max)/$fF2$ (min) show that this is definitely not the case. We therefore conclude that a different basic continuity equation is required.

Dr. Martyn—I think the solar radiation might be expected to have different spectral composition at sunspot maximum from that at sunspot minimum. In this case $q$ and $\beta$ would be different at the two epochs.

Sir Edward Appleton—Is there not good reason for expecting drift velocities to be the same at sunspot maximum and minimum?

Dr. Berkner—I understand that Professor Waynick's group have been studying the problem of calculating time height and that a convenient analogue method which has certain advantages over the digital method has been developed by Mr. Schmerling. This can be used for the rapid reduction of $N(h)$ profiles from the ionograms.

Mr. Ratcliffe—During the IGY the Radio Research Station, Slough, will compute $N(h)$ profiles for selected periods for four of their stations.

Dr. Martyn—In Australia $N(h)$ curves will also be calculated for a number of stations.

Dr. Morgan—Professor Waynick's group will make calculations for three stations.

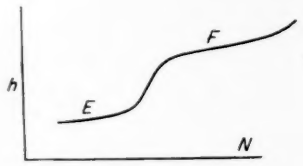


Fig. D3.

Sir Edward Appleton—In an attempt to get some idea of the nature of geomagnetic distortion in the *F2*-layer I have made the simple assumption that the layer is more Chapman-like at sunspot maximum than at sunspot minimum. By plotting diurnal curves of the ratio $fF2$ (S.S. max)/$fF2$ (S.S. min) at different latitudes it is then possible to get some idea of the diurnal variation of distortion, $\Delta(fF2)$, all over the world. The phase of this diurnal wave of distortion varies with latitude in a manner which can be described by Fourier coefficients.

Studies of this kind emphasize the importance of the anomalous *F2*-layer belt which I have found to be centred on the magnetic equator. For example the phase of diurnal $\Delta(fF2)$ within this belt and over the summer hemisphere is fairly uniform. There is, however, an abrupt change of phase at the winter boundary of the anomalous belt.

Dr. Rawer—I should like to ask Mr. Ratcliffe what is the relative importance of the corrections for magnetic field and *E*-layer effects?

Mr. Ratcliffe—When $fF2$ is small the group retardation effects in region *E* can be quite important. We assumed a semi-parabola for the *E*-region with the level between *E* and *F* "more than" filled up (see Fig. D3).

Dr. Rawer—But could this be assumed for all stations?

Mr. Ratcliffe—If the calculations are made for both the *o* and *x* components then one can get a check on the assumption. At night we assume a full parabolic *E*-layer with the peak estimated from recombination data.

Dr. Chamberlain—Barbier's work makes it pretty definite that the red lines in the airglow are in the *F2*-layer. These airglow results suggest that high up in *F2* we have an $\alpha$ and lower down in the layer a $\beta$ term. There is an increase in intensity after midnight.



VOL.
15
1959

Dr. Martyn—Green and red line observations are now being made at Camden, N.S.W.

I should like to comment on the equatorial anomaly mentioned by Sir Edward and also on Mr. Ratcliffe's discussion of what happens to the *F2*-region at different levels—I think the two are related.

Mr. Ratcliffe has presented certain experimental facts but only a part of the theory. What he has said affects the theory of drift concerning *F2*. Consider the full equation

$$\frac{\partial N}{\partial t} = q - \phi(N) + \left[ d_0 e^z \sin^2 I \left( \frac{\partial^2 N}{\partial z^2} + \frac{3}{2} \frac{\partial N}{\partial z} + \frac{N}{2} \right) \right] - \operatorname{div} (Nv)$$

The $\phi(N)$ may be either a $\beta$ or $\alpha$ term. The term in square brackets, the diffusion term, cannot be neglected.

Mr. Ratcliffe—But it depends on the height concerned.

Dr. Martyn—Let us go to some extreme cases and isolate some of these effects. I suggest we concentrate attention on the moving maximum and move with it. If we remain at one height as Mr. Ratcliffe does then one gets important $\partial N/\partial z$ and $\partial^2 N/\partial z^2$ terms. If however, we concentrate on the maximum then one gets a much simpler equation. Thus we can set $\partial v/\partial z = 0$ for *F2* (the control lying in region-*E*). At the maximum $\partial N/\partial z = 0$ and furthermore for a Chapman or parabolic layer $\partial^2 N/\partial z^2 \sim -N/2$. At night $q = 0$ and we are left simply with $\partial N/\partial t = -\phi(N)$. The layer settles into a Chapman shape soon after sunset—about 2 hr afterwards.

Mr. Ratcliffe—The part of the motion term concerned with diffusion increases rapidly upwards and is one not justified in supposing diffusion is not important at any height? Also if one takes the accepted values of $d_0$ in conjunction with the new low heights then the magnitude of the diffusion term is small.

Dr. Martyn—In the day the diffusion term is probably unimportant but at dawn, when the height may be about 320 km, it is important. I should also like to point out that on all days Mr. Ratcliffe will have a disturbance term coming in and this will tend to give symmetry about noon. I think that what happens in the equatorial zone lends point to what happens elsewhere. The general expression for $W$, the vertical velocity at the layer peak, is

$$W = \frac{2\beta^2}{N} \frac{\partial q}{\partial z} - 2\beta^2 N \frac{\partial \alpha}{\partial z} + v + \frac{d_0 e^z \sin^2 I}{2} (2\beta^2 - 5) - 2\beta^2 \frac{\partial^2 v}{\partial z^2} + v$$

At the equator $\sin I = 0$ and the velocity $v$ comes in. For a Chapman layer $\beta = 1$. In general the diffusion term operates on the height but at the equator this diffusion term cannot operate—the layer is here not free to diffuse down whereas at moderate latitudes one can get drift downwards although the other terms tend to lift it up.

Sir Edward Appleton—Perhaps I should add that, while the Slough $N(h)$ profile data, used by Mr. Ratcliffe and his colleagues, enable them to discuss the need for a transport term in the basic continuity equation, we must not assume that the same can be done in discussing effects at lower latitudes. The simplicity of the conclusions for Slough follows from the stated result that the $(N, t)_h$ relation is

"symmetrical about midday, but with values of $N$ somewhat greater in the afternoon than in the morning".

However, as we move south from Slough, we encounter $F$-layer behaviour which is entirely different. At Huancayo, for example, we frequently find the $(N,t)_h$ relation showing that $N$ is much greater in the forenoon than in the afternoon, for heights exceeding 200 km. So we cannot discuss transport effect here.

VOL.
15
1959

Journal of Atmospheric and Terrestrial Physics, 1959, Vol. 15, pp. 27 to 28. Pergamon Press Ltd. Printed in Northern Ireland

# SESSION III

## Irrégularités ionosphériques

Père P. LEJAY

SI nous remontons dans le passe, nous constatons que la mise en evidence des correlations étroites qui existent entre certains phénomènes solaires et certaines irrégularités de l'ionosphère, et le rapprochement non moins évident qui s'impose immédiatement entre les perturbations de l'ionosphère et celles du magnétisme terrestre, ont conduit tout naturellement à appliquer à l'étude des perturbations ionosphériques les méthodes qui ont été précédemment utilisées par les magnéticiens.

Des résultats ont été immédiatement obtenus, qui ont permis, dans une certaine mesure, de séparer l'influence de l'heure locale sur l'évolution des orages ionosphériques en une station donnée, et également d'étudier l'influence de la latitude des stations. On est parvenu ainsi à établir des prévisions utilisables, avec une certaine chance de succès, dans l'organisation des télécommunications.

Cependant, on a rencontré dans ces études de grandes difficultés qui semblent avoir quelque peu arrêté les progrès auxquels, dès le début de ces recherches, on était en droit de s'attendre. Le but de cette réunion est sans doute de faire le point, de rechercher s'il ne pourrait se rencontrer des vues nouvelles qui permettraient de reprendre le problème.

Il est clair qu'il existe, entre les perturbations magnétiques et ionosphériques, des ressemblances, mais que les phénomènes, dans les deux cas, présentent aussi des différences notables, et que, par suite, il apparaît trop simple de chercher à appliquer de trop près les mêmes méthodes d'analyse. En particulier, si les perturbations magnétiques présentent, en beaucoup de cas, un début bien marqué qui permet une définition précise de l'heure d'orage, il n'en est pas de même des perturbations ionosphériques. L'analyse des fréquences critiques de $F2$ en particulier est rendue difficile du fait des fluctuations pratiquement continues qui les affectent même par jours calmes, à tel point qu'après MARTYN, la plupart des auteurs ont adopté, pour caractériser l'heure du début des perturbations ionosphériques, précisément l'heure du début de la perturbation magnétique concommittante, comme s'il y avait en toute certitude une correspondance étroite entre les deux phénomènes. Or ceci n'est pas tellement évident puisque, si une certaine corrélation ne peut être niée, il n'en existe pas moins de très notables exceptions.

(1) L'évolution d'un orage ionosphérique, en une station donnée, reste encore très mystérieuse. Pourquoi certains orages sont-ils marqués d'une phase positive, tandis que d'autres ne le sont pas; pourquoi ces phases positives sont-elles si

variables en durée suivant les saisons? Quels sont les rapports entre la phase positive des tempêtes ionosphériques et celle des tempêtes magnétiques? Autant de questions auxquelles il ne semble pas qu'il ait été encore donné de réponse précise, bien que cependant quelques travaux aient été déjà présentés dans ce sens par plusieurs spécialistes.

(2) Un autre aspect du problème doit être envisagé, sur lequel nous manquons plus encore d'études complètes. Il s'agit des comparaisons entre les caractères des diverses tempêtes en des lieux différents. Il est bien connu que chaque tempête se présente à diverses latitudes et à diverses longitudes de façon variée. Une tempête qui présente une phase positive marquante en Europe par exemple, peut n'en présenter aucune en Amérique ou inversement. Il y a évidemment à tenir compte de l'heure locale qui sera, dans les deux cas, différente; mais il semble que d'autres facteurs interviennent aussi, qui nous échappent entièrement.

Il semble que sur ce sujet les données ionosphériques que nous possèdons maintenant en grand nombre n'ont pas été utilisées jusqu'ici complètement. Nous devrions savoir comment une tempête ionosphérique se développe dans le monde entier, et nous devrions pouvoir prévoir dès son commencement comment elle doit normalement évoluer; ceci serait d'un intérêt spéculatif et pratique considérable.

Il est vrai que les travaux d'analyse sont laborieux, mais il vaudrait certainement la peine qu'ils soient entrepris de façon systématique. Ne serait-il pas opportun que le Dst soit déterminé en toute station qui possède des séries d'observations depuis de longues années?

A l'occasion de l'Année Géophysique, lorsque nous possèderons toutes les données des stations de sondage, et particulièrement les données rapprochées dans le temps pour les jours spéciaux, il est absolument nécessaire que ces donnés soient systématiquement analysées; une organisation devra être fondée dans ce but, car le travail à fournir dépasse les possibilités d'organisations individuelles; ce sera une oeuvre à entreprendre en commun, qui pourrait être un des objectifs principaux d'une commission internationale.

VOL. 15 1959

Journal of Atmospheric and Terrestrial Physics, 1959, Vol. 15, pp. 29 to 37. Pergamon Press Ltd. Printed in Northern Ireland

# Disturbances in the lower auroral ionosphere

S. CHAPMAN*

**Abstract**—The solar particles that enter the atmosphere and produce the luminous aurora are known to include protons, which also *ionize* the atmosphere. As suggested by BATES, their ionizing action may extend below the level of their own penetration, by the Lyman α-photons they emit. These can penetrate to about 75 km, and ionize nitric oxide. Recent rocket researches by VAN ALLEN and his colleagues prove that the primary auroral particles also include electrons, with energies up to 100 keV. These penetrate to about 80 km, thus directly extending the auroral ionization well below the level of auroral luminosity. Indirectly these electrons ionize the atmosphere down to far lower levels, by the X-rays emitted by a small fraction of the electrons. WINCKLER's balloon results show that such ionization extends at least down to 32 km. This ionization below the level of the visible aurora accounts for most of the absorption, in auroral regions, of high frequency radio waves. Though the primary electron flux at night probably exceeds that by day, the secondary electrons are often more numerous (and absorbent) by day than by night. This is because, by day, photodetachment prolongs the free life of these electrons, despite their ready attachment to oxygen.

## 1. INTRODUCTION

RADIO researches (APPLETON *et al.*, 1937) during the second International Polar Year indicated that during notable auroras and magnetic disturbances the auroral ionosphere is strongly disturbed. Since then this region has been much studied by various radio methods—measuring vertical incidence reflection, absorption and auroral echoes—and also by rockets. Magnetic records indicate that at such times strong electric currents flow in the polar ionosphere, and especially along the auroral zone. It is clear that strong ionization accompanies the auroral luminosity.

It has in the past often been tacitly assumed that the regions of ionization and luminosity are the same (though the "polar blackouts" observed in auroral latitudes suggested ionization at lower levels). This would imply that the extra ionization during auroras usually lies above about 95 km, the normal lower limit of auroral luminosity (STÖRMER, 1955, Figs. 55, 56, pp. 70, 71). The assumption is not unnatural, as the luminosity (at least during the first auroral phase,† of homogeneous arcs) is generally ascribed to solar corpuscular bombardment. This will ionize and excite the atmospheric particles, until the solar corpuscles have reached the limit of their penetration.

The observations of atomic hydrogen radiations in the auroral light (VEGARD and TÖNSBERG, 1937) and especially of the Doppler displacement of the hydrogen lines (GARTLEIN, 1950; MEINEL, 1951), proved that protons are among the incoming solar particles. MEINEL estimated their extreme speeds of descent as of order 3000 km/sec, corresponding to an energy of 47 keV. The primary protons produce hydrogen radiation only after they have gained an electron; they may lose this and gain another, perhaps more than once before their descent ceases. Thus the hydrogen radiation will be emitted over a range of height. The initial energy of the protons will exceed 47 keV. Their degree of penetration into the atmosphere suggests that the energy may range up to 100 keV or even more.

* Geophysical Institute, College, Alaska, and High Altitude Observatory, Boulder, Colorado, there engaged in a program of research supported by the National Bureau of Standards and the Sacramento Peak Observatory of the Air Force Cambridge Research Center.

† SUCKSDORFF (1954) and others have suggested that the mode of production of the auroral luminosity changes radically after the first phase. Instead of being a direct effect of incoming particles, it is attributed to some kind of electric discharge (cf. CHAMBERLAIN, 1956).

It could be expected, and was expected, that electrons as well as protons would reach the earth from the sun. But where, when, and with what numbers, speeds and energies they would enter the atmosphere were matters only of speculation.

## 2. Primary Auroral Electrons and their Production of X-rays

New light on these questions has recently come from the rocket researches on the arctic ionosphere, by the physicists of the State University of Iowa (Meredith *et al.*, 1955; Van Allen, 1957). These researches have so far been confined to day observations, but during the coming months night observations will also be made. The past researches indicate that electrons with energies up to 100 keV must enter the atmosphere in auroral latitudes. This is inferred from Van Allen's interpretation of the rocket observations as due to X-rays (Bremsstrahlung) whose energies range, according to his estimates, from 10 to 100 keV. They are detected down to levels as low as 40 km. Their detection only in auroral latitudes implies that they are produced by charged particles, which enter the atmosphere after being deflected by the geomagnetic field. The production of the X-rays cannot be ascribed to particles of atomic mass such as protons, as this would require them to have a far greater energy than their observed penetration indicates. Hence the X-rays must be produced by electrons. About one electron in 1000 will make a sufficiently close impact with an atmospheric atom to generate an X-ray photon. This may have any fraction, up to the whole, of the energy of the primary electron (Massey and Burhop, 1952, p. 342). Thus the primary electrons must have energies ranging up to 100 keV.

Electrons of energy 100 keV can penetrate the atmosphere to slightly below 80 km—well below the usual limit of auroral luminosity, which is the inferred limit of penetration of the protons. Thus the primary electrons will directly ionize the atmosphere down to about 80 km. The X-rays produced by a small minority of the primary electrons will ionize a still lower layer, of considerable thickness, extending below 40 km.

## 3. Auroral Luminosity below 95 km

The question arises: why is the ionization below 95 km not accompanied by luminosity? The answer must, of course, involve questions of intensity; doubtless with more delicate detectors it is possible to observe luminosity of auroral arcs at levels below what would normally be regarded as their lower limit. But the existence of a moderately sharp auroral lower limit may be ascribed to two main factors. One is the degree of sharpness shown by the final penetration of a beam of fairly homogeneous particles of atomic mass projected into a mass of *uniform* gas. The other factor is the downward increase of density in the atmosphere.

The absorption of a similarly homogeneous beam of electrons is less concentrated. If the beam is in the form of a limited sheet, like an auroral arc, the luminosity it produces will be more spread out vertically than if produced by protons. This will reduce the surface brightness of the luminous sheet produced by the electron beam as compared with a proton beam.

The auroral spectrum consists of atomic lines (chiefly of atomic oxygen) and



VOL. 15 1959

molecular bands (chiefly of nitrogen). BATES (1949) has shown that the latter must be ascribed mainly to excitation by particles of atomic mass (the excitation will be more effective after the protons have gained an electron). Such particles can raise nitrogen molecules to the high levels of vibrational energy indicated by the spectrum. Electrons cannot easily change the vibrational levels; they could produce the observed nitrogen light only in a gas where the vibrationally excited molecules are already present; this would require a temperature of many thousand degrees, far exceeding that of the ionosphere. Hence the primary electrons below 95 km can produce much less nitrogen light than is produced above 95 km by a similar number of equally energetic protons or hydrogen atoms.

Both kinds of primary particle, protons and electrons will produce secondary electrons (and associated ions) from the particles of the air they traverse. These secondary electrons are largely responsible for the excitation of the oxygen atoms to the metastable states $^1D$ and $^1S$, from which the main oxygen atomic light is produced. These states have long lives—about 0·75 sec for $^1S$, which gives the yellow-green line 5577 Å, and much longer for $^1D$, which gives the red doublet 6300, 6364 Å. The lower the level in the atmosphere, the greater the chance that a collision will de-activate an atom in these metastable states. This must reduce the production of the main oxygen light at levels below 95 km as compared with higher levels.

If the primary electrons that penetrate below 95 km do not produce much auroral luminosity, it is not to be expected that the X-rays will do so, because their aggregate energy is less than one-thousandth of that of the primary electrons, and they operate at still lower levels. Moreover their main effect on the atmosphere is to produce electrons of energy that may range nearly up to that of the X-ray photons. The electrons, like the secondary electrons produced by the primary particles, produce secondary ionization and most of the excitation. Thus the X-rays are intrinsically no more effective than the primary electrons in producing luminosity.

However, at times the auroral luminosity extends to more than usually low levels. HARANG and BAUER (1932) have even reported an auroral arc with deep crimson lower border that descended, for a few minutes only, down to about 65 km. If produced directly by solar corpuscles, as its form would suggest, this arc would imply abnormally high energy and speed—the energy requirement being much greater for primaries of atomic mass than for electrons. It is perhaps surprising that particles of such abnormal energy can appear in the same geomagnetic latitude as the particles that produced the arc at much higher levels just before and after. Such events seem to be very rare. It will be of interest to learn whether any very low-level auroras are revealed by the all-sky cameras that are providing an extensive and intensive auroral watch during the International Geophysical Year. Unless such auroras recur, and are more completely observed than in the case mentioned above, it does not seem profitable to speculate as to their mechanism.

Less outstanding cases of low auroral luminosity may be ascribed to more energetic protons, or perhaps to a larger proportion than usual of primary particles of greater mass (e.g. $\alpha$-particles or still heavier ions) that may accompany the protons.

## 4. IONIZATION BY HYDROGEN RADIATION

BATES (1956) has pointed out that the observed auroral light emitted by hydrogen atoms, in the visible spectrum, implies also the emission of Lyman $\alpha$-photons (1216 Å); and that these also may contribute to the ionization below 95 km. Such photons can penetrate to about 70 km. They are absorbed by oxygen, but cannot ionize oxygen or nitrogen, whether atomic or molecular. They can, however, ionize nitric oxide (NO), which seems likely to be present.

The recombination of electrons with the incoming auroral protons can produce photons with energies up to the ionization potential (13·6 eV) of atomic hydrogen; these can ionize oxygen molecules, but are likely to be relatively few.

Only a small part of the energy of the primary protons seems to be emitted as atomic hydrogen radiation. Only part of this radiation (which is emitted in all directions) will go downwards, and ionize the minor constituent NO in the air below 95 km. This process seems unlikely to make an important contribution to the ionization at those levels; but quantitative estimates of the amount and height-distribution of the ionization so created are desirable.

## 5. COMPARISON OF THE PROTON AND ELECTRON BEAMS

As it appears that both electrons and protons enter the atmosphere with energies of the same order of magnitude (50 to 100 keV), it is clear that the electrons must have much the greater speeds. For the energy 100 keV, the electron speed (allowing for the relativistic increase of mass) is 30 times that of an equally energetic proton; for 50 keV, the ratio is 55.

The rocket evidence indicates that the electrons enter only in auroral latitudes, but as yet does not show whether they come in limited "sheets" like the auroral arcs. These arcs imply considerable magnetic focusing of the proton beam.

The rate of influx of the X-ray photons is variable; VAN ALLEN gives its order of magnitude as ranging from $10^3$ to $10^5$/cm$^2$-sec, and infers a corresponding electron flux ranging from $10^6$ to $10^8$/cm-sec. The electron energies being taken to range from 10 to 100 keV, the corresponding energy flux ranges from 0·01 to 1 erg/cm$^2$-sec.

The X-ray photons are emitted in all directions, but mostly have a considerable component *normal* to the direction of motion of the generating electron. Their component speed along this direction is predominantly forward. The polar diagram has a minimum on the axis of the electron beam (MASSEY and BURHOP, 1952 p. 360). Thus the X-rays from a limited "sheet" of inflowing electrons will spread out downwards and extend further in the horizontal direction, the lower the level they attain. On this account it seems likely that the intensity of the primary electron flux and the energy flux exceed by 10 or more the above estimates by VAN ALLEN. If so, the energy flux seems likely to be at least comparable with that associated with the protons.

It is most desirable to explore the distribution of entry of the electrons and protons by means of rockets travelling nearly horizontally at levels of about 100 km. This should be done by night as well as by day. If their instruments can detect and distinguish between electrons and protons (and heavier particles) and determine their flux or number densities and speeds, they can indicate whether there is any *net* flux of charge into the atmosphere. If there is no such flux, the number density

of the electrons in the entering stream, multiplied by the cross-section of the stream, must be less than the corresponding product for the positive charges, in the inverse ratio of their speeds.

## 6. The Non-deviative Absorption of High-frequency Radio Waves in Auroral Latitudes

The rocket aeronomer can contribute greatly to our knowledge of auroral physics, but cost and difficulty limit the number and duration of his measurements. The radio aeronomers and geomagnetists can obtain *continuous* records of their data, in whose interpretation the rocket results can give crucial help.

One type of radio data that is important for auroral physics is the absorption of high-frequency radio waves. At College*, Alaska such absorption for 30 Mc/s cosmic radio waves has been continuously recorded. The receiving antenna is directed vertically; its cone of reception is of wide angle, about 60° to half-power. The absorption (denoted by $D$, when reckoned in decibels) varies irregularly, and may be strong at any hour of the day or night. The highest values, up to 10 dB around noon, or 2·5 dB around midnight, generally occur in the equinoctial months. The frequency of high values is strongly correlated with (a) polar black-outs recorded on a C-3 vertical incidence equipment, (b) the 3 hr magnetic $K$-indices, and (c) at night, with auroras. But by day there may be considerable absorption unaccompanied by much magnetic disturbance. Independent radio observations suggest that the absorption is patchily distributed.

Chapman and Little (1957) have discussed this absorption, which they attribute to levels between 55 and 90 km at noon, and from 60 to 100 km at midnight—mainly well below the luminous aurora. The low-level ionization they ascribe to primary electrons, acting directly or, in the lowest regions, by the X-rays produced by a small minority of the primary electrons.

They constructed tentative "model" distributions of $Q$, $N$, $N_+$, $N_-$ and of the absorption, for noon and for midnight, which would make $D$ approximately equal to 10 (noon) and 2·5 (midnight). Here $Q$ denotes the rate of production of electron-ion pairs, and $N$, $N_+$, $N_-$ denote the number densities of electrons, positive ions and negative ions, respectively. Their height distributions of $Q$, $N$, $N_+$ and the absorption are shown in Figs. 1 and 2; the scales for $N$ and $N_+$ differ by a factor of 10.

In constructing these curves, it was rather arbitrarily assumed that at all heights $Q_{\text{midnight}}$ was $20Q_{\text{noon}}$. This assumption was made because magnetic disturbance at midnight is much more frequent and intense than at noon. The height-distribution $Q(h)$ was chosen so as to limit $N$ (up to 105 km) to $5 \times 10^5/\text{cm}^3$ at most (this restriction was based on the C-3 records).

The model distributions $Q(h)$ were made to fit not only the supposed high values of the absorption $D$ at noon and midnight, but also to be consistent with a set of values of various rate-coefficients. These were the recombinances ($\alpha_e$, $\alpha_-$) for electron–ion and ion–ion recombination, and the coefficients of attachment ($\eta n$) and photodetachment ($\rho S$) of electrons to and from negative ions. Here $n$ denotes

* At 64°.9′ N, 167°.8′ W; geomagnetic latitude 64°.5′ ; magnetic dip 77°.

the number density of the particles (probably mainly $O_2$) to which the electrons attach themselves; and $S$ denotes the intensity of the photodetaching radiation. As this radiation is probably red or infra-red, and only slightly absorbed, $S$ is taken to be independent of height. Collisional detachment was *not* taken into account. Thus the equations for $N$, $N_+$, $N_-$ were taken to be:

$$dN_+/dt = Q - \alpha_e N N_+ - \alpha_- N_- N_+$$
$$dN/dt = Q - \alpha_e N N_+ - \eta n N + \rho S N_-$$
$$dN_-/dt = \eta n N - \rho S N_- - \alpha_- N_- N_+$$

These are consistent because

$$N_+ = N + N_-$$

The adopted values were:

$$\alpha_e = 10^{-8}, \qquad \alpha_- = 10^{-9}, \qquad \eta n \text{ (see Table 1)}, \qquad \rho S = 0{\cdot}1 \text{ (noon)}$$

At midnight the photodetachment term is of course zero ($S = 0$). Values of $n$ and of the electron collision frequency $\nu$ were adopted in approximate accord with the Rocket Panel (1952) atmosphere. Table 1 gives $Q_{\text{noon}}$, $\eta n$ and $\nu$ at various heights.

Table 1
(Numbers here expressed as $a^b$ signify $a \times 10^b$)

| Height (km) | 45 | 55 | 65 | 75 | 85 | 95 | 105 |
|---|---|---|---|---|---|---|---|
| $\eta n$ | $89{\cdot}4$ | $26{\cdot}9$ | $7{\cdot}4$ | $1{\cdot}7$ | $0{\cdot}33$ | $0{\cdot}064$ | $0{\cdot}0159$ |
| $\nu$ | $4{\cdot}0^8$ | $1{\cdot}2^8$ | $3{\cdot}3^7$ | $7{\cdot}6^6$ | $1{\cdot}5^6$ | $3{\cdot}1^5$ | $7{\cdot}1^4$ |
| $Q_{\text{noon}}$ | 8 | 62 | 300 | 900 | 1200 | 1100 | 1060 |

For 30 Mc/s waves at College, Alaska, taking the gyromagnetic frequency to be 1·68 Mc/s,

$$D = A/31{\cdot}68^2$$

where
$$A = 1{\cdot}17 \times 10^{-14} \int g N \nu \, dS,$$

and

$$1/g = 1 + (\nu/2 \times 10^6 \pi 31{\cdot}68)^2$$

The factor $g$ differs appreciably from unity only from 65 km downwards; its values at 45, 55 and 65 km are 0·20, 0·74 and 0·97, respectively. Hence

$$D = 1{\cdot}17 \times 10^{-17} \int g N \nu \, dS,$$

$$\int g N \nu \, dS = 8{\cdot}54 \times 10^{16} D$$

From the adopted functions $Q(h)$, and the above equations, the values of $N$, $N_-$, $N_+$ were calculated, assuming a steady state ($dN/dt$, $dN_+/dt$, $dN_-/dt$ all zero).

The decibels of absorption contributed by each of seven 10 km layers from 40 to 100 km were then determined. Finally an allowance was made for a supposed incompleteness or patchiness of the ionization at certain heights. The layers up to

70 km were supposed completely and uniformly ionized within the cone of reception; above 70 km the area within the cone was taken to contain an unabsorbing (non-ionized) fraction; this fraction was taken to be 0·15, 0·3, 0·5, 0·8 for the successive 10 km layers from 70 to 110 km. The method used to allow for these clear areas

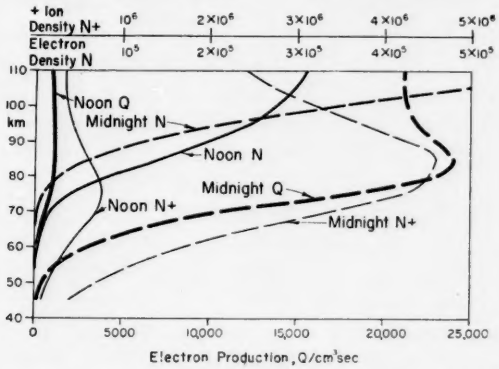


Fig. 1. Extreme conditions of radio absorption on 30 Mc/s at College, Alaska.

was too crude, and overestimated the resulting absorption. Thus the actual values of $D$ at noon and midnight would be less than the calculated values 9·22 and 2·39. Consequently to account for observed absorptions of 10 (noon) and 2·5 (midnight) dB, the electron densities and electron production rates would have to exceed the values indicated in Figs. 1 and 2.

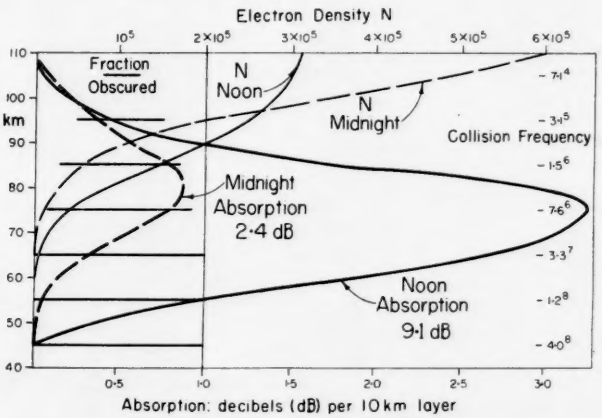


Fig. 2. Extreme conditions of radio absorption on 30 Mc/s at College, Alaska, noon and midnight.

I am in the process of revising these models of electron production and absorption distribution; at the same time I am taking account of collisional detachment, and examining generally how $D$ depends on the rate-coefficients, on the function $Q(h)$, and on the patchiness of the upper layers. The adopted values of $Q$ in the lower X-ray ionized layers should probably be reduced.

I find that a reasonable amount of collisional detachment has little effect on the daytime absorption, but materially increases $D$ at midnight, for any given $Q(h)$. Hence the midnight/noon ratio of $Q(h)$ may be rather less than the value (20) adopted by CHAPMAN and LITTLE, for the same noon/midnight ratio (4) for $D$.

The revision of the calculations does not alter the main conclusion drawn by CHAPMAN and LITTLE—that the absorption takes place mainly well below the level of the luminous aurora, and that the excess absorption by day results from photodetachment of electrons from negative ions. These conclusions are reinforced by consideration of the rapidity of the irregular changes of absorption.

A comparison between the magnetic disturbances associated with strong noon and strong midnight absorption may lead to conclusions regarding the degree of parallelism between the flux changes of primary electrons and those of the auroral protons. The absorbing layer contributes only slightly to the electrical conductivity of the auroral ionosphere, which seems likely to depend mainly on ionization produced above 95 km by the incoming protons. At these upper levels the electron density decays less rapidly than it does at 70 or 80 km. The auroral arcs will be regions of active electron production by protons. As the arcs move across the sky, they will leave ionization behind them, that will persist in some degree for an hour or more.

Thus in auroral regions there will be a long strip of ionized atmosphere over the band of latitude traversed by the auroral arcs; and this strip appears to extend considerably below the level of luminosity, owing to the primary electrons. In particular, it extends much lower down towards the weather and thunderstorm levels of the atmosphere than was formerly supposed.

VOL.
15
1959

## REFERENCES


| | | |
|---|---|---|
| APPLETON E. V., NAISMITH R. and INGRAM L. J. | 1937 | *Phil. Trans.* **A236,** 191. |
| BATES D. R. | 1949 | *Proc. Roy. Soc.* **A196,** 217. |
| BATES D. R. | 1956 | Private communication. |
| CHAMBERLAIN J. W. | 1956 | *The Airglow and the Aurora* pp. 206–224. Pergamon Press, London. |
| CHAPMAN S. and LITTLE C. G. | 1957 | *J. Atmosph. Terr. Phys.* **10,** 20. |
| GARTLEIN C. W. | 1950 | *Trans. Amer. Geophys. Un.* **31,** 18. |
| HARANG L. and BAUER W. | 1932 | *Gerlands Beitr. Geophys.* **37,** 109. |
| MASSEY H. S. W. and BURHOP E. H. S. | 1952 | *Electronic and Ionic Impact Phenomena,* Oxford. |
| MEINEL A. B. | 1951 | *Astrophys. J.* **113,** 50, **114,** 431. |
| MEREDITH L. H., GOTTLIEB M. B. and VAN ALLEN J. A. | 1955 | *Phys. Rev.* **97,** 201. |
| *Rocket Panel* | 1952 | *Phys. Rev.* **88,** 1027. |
| SEATON M. J. | 1953 | *Phil. Trans.* **A265,** 469. |
| STÖRMER C. | 1955 | *The Polar Aurora.* Oxford. |
| SUCKSDORFF G. E. | 1954 | *Naturw. Rundsch.* **1,** 7. |
| VAN ALLEN J. A. | 1957 | *Proc. Nat. Acad. Sci., Wash.* **43,** 57; see also earlier papers there cited. |
| VEGARD L. and TÖNSBERG E. | 1937 | *Geophys. Publ.* **11,** No. 16. |

## Discussion

Sir Edward Appleton—Measurements of ionospheric absorption show that as soon as the sun rises the absorption also increases very markedly. This idea of photodetachment during the day-time fits in nicely with this observation.

Professor Chapman—There is a store of positive and negative ions at low level which are ionized by long wavelength radiation as soon as the sun rises. In these photodetachment processes there is an analogy between the ozone layers and the ionosphere layers. I should like to suggest that the Commission recommends that the letter *A* be used to designate auroral ionization resulting directly or indirectly from solar particles (see Resolution 12(iii)—Ed.)

---

Mr. J. A. Ratcliffe—I should like to draw attention to the dangers involved in using the minimum equivalent height of the *F*-layer. This parameter can be very misleading especially in the study of magnetic storm phenomena. Our studies of ($N$, $h$) profiles under storm conditions show that the total electron content of the *F*-layer follows the variation in the peak value—both being reduced during the storm. The increase in layer thickness only offsets by a factor of about one-half the decrease in peak density. We have also studied some cases in which a sudden commencement type magnetic disturbance occurred but without a subsequent storm—we found that the level of the peak of the layer then increased by some 100 km.

(At this stage there was considerable discussion on the use of $h'_{\min}$ and it was finally agreed to continue with this parameter but that it should be used with proper caution.—Ed.)

Journal of Atmospheric and Terrestrial Physics, 1959, Vol. 15, pp. 38 to 42. Pergamon Press Ltd. Printed in Northern Ireland

# Irregularities and movements in the *F*-region

K. Rawer

Bibl (1952) published some provisional results which he had obtained with a new technique of observation, namely, moving pictures of ionograms at a sequence of about 5 per minute. Some years before, Wells had used this same technique and some of the phenomena were then seen by him for the first time. The most striking feature Bibl reported was a rapidly downwards-moving perturbation, which he identified on the ionograms as a small deformation of the trace or only as a break in the echo amplitude. Such forms of perturbation are seen fairly often on daytime ionograms but their motion is most strikingly observed on moving pictures. The deformations always move along the *F*-trace, beginning at the high-frequency end and going towards lower frequencies. (Fig. 1).

There could be no doubt from the records that something really moved downwards but it was not certain that this downward motion was really only a component of an oblique movement. We expressed this opinion in 1954, indicating that some pressure wave could be the background of the observations (Bibl *et al.*, 1954). Meanwhile Nakata *et al.* (1953), with their new technique of automatic recording of critical frequency and minimum height, observed a horizontal component of the motion of such perturbations. Akasofu (1956), discussing the different magneto-hydrodynamic waves in the ionosphere, suggested that the phenomenon could be explained by a "retarded sound-wave". This is a shock wave of rather small but finite amplitude, the movement of particles being strongly controlled by the magnetic field to the extent that it is no longer in the direction of propagation but approaches the direction of the (terrestrial) magnetic field. Using Akasofu's equation the velocity $C$ of such a retarded sound-wave, written as a Mach number, can be expressed as

$$\frac{C}{U} = \sqrt{\left(\frac{2}{\gamma}\right)} \cdot R^{\frac{1}{2}} \cdot \sin \phi$$

(where $\gamma$ is the ratio of specific heats, $\phi$ the angle between the shock wave front and the magnetic field vector, $R$ the ratio of kinetic to potential energy at the front of the wave, $U$ normal sound velocity). With a density variation of about 10 per cent in the shock front, $\phi = 6°$, and conditions are such that the magnetic energy is much more important than the acoustical. Akasofu finds the velocity of the shock front (as a Mach number) to be about 0·1. This is about the magnitude of observed velocities. Independently from this theoretical work, these perturbations have meanwhile been studied by Bibl in different ways and at different places. These phenomena have been observed nearly in the same form in the tropics at Djibouti, in northern Europe at Bergen, and in central Europe at Freiburg where most of Bibl's observations have been made. They are quite



VOL. 15 1959

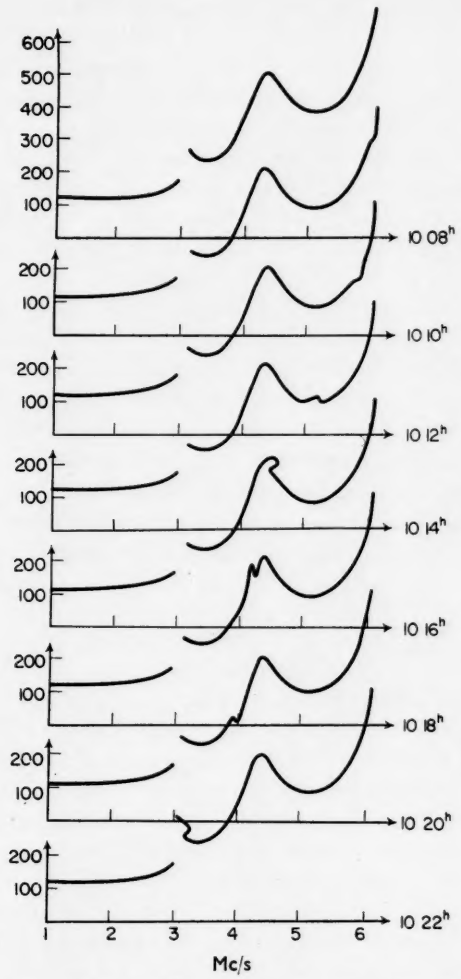


Fig. 1. Development of a transitory phenomenon in the *F*-region. Freiburg 5 June 1952.

usual as daytime phenomena, occurring several times per hour, up to ten per hour. The velocity of *apparent* movement as found from virtual height goes up to 300 m/sec.

It seems thus likely that AKASOFU's identification is justified, and that the downwards-moving perturbations are retarded sound-waves coming from outside into the earth's atmosphere. He has suggested that there may be a correlation with the so-called *M*-type solar perturbations which are revealed by geomagnetic observations.

Some relation was found with the stratification at the lower limit of the *F*-region, which has been called *F0* and which often transforms into an intermediate layer, *E2*. This intermediate layer appears with the same downwards

motion but at a slower rate. It becomes more and more flattened such that we often have finally a layer of $E_s$-type (Fig. 2). In the majority of cases the perturbation seems to disappear between the $F$- and $E$-regions. On the trace corresponding to the normal $E$-layer the motion of the deformation has not been observed—perhaps because it is too small to be resolved.

During these investigations the phenomenon which in the past has been called "$G$-layer" has also been studied. This stratification seems not to be a stable one. In all cases observed with motion pictures, it precedes a rapid shock-wave perturbation and is the very beginning of it. On the other hand it seems to be related to the slower variations in the $F$-region.

Slower dynamical changes in the $F$-region are revealed by routine soundings. Especially with $\frac{1}{4}$-hr observations, BIBL found by statistical methods that changes occur having quasi-periods between $\frac{1}{2}$ and 8 hr. After elimination of the normal daily variation, BIBL finds that this sort of perturbation has the same sign for more than 1 hr generally, but that it lasts only very rarely for more than 4 hr. (A pretty period of about 4 hr appeared at the tropical station Lwiro.) The corresponding variation of the critical frequency is nearly as large as is its day-to-day variation. The phenomena are even more clearly shown with the characteristic MUF 3000-*F2*. This shows that a decrease of height and an increase of ionization density occur together. BIBL supposes that oscillations of the atmosphere are thus observed, the scale of which may be some hundred kilometres. A "superposed epoch" examination of $f_0F2$ (or better of MUF 3000-*F2*) has been made using observation of the "$G$-layer" as the "event"; it then appears that a depression of MUF 3000-*F2* occurs immediately *before* the event. BIBL's hypothesis is that the extra layer is formed as a consequence of this rapid depression and thus in some way, the large-scale oscillations, e.g. by phase focusing. The depression has been found for two stations, one in central Africa and the other in Europe (see Figs. 3 and 4). It seems that the variation is somewhat slower in the tropics but quite marked in intensity, some 20 per cent for the MUF.

The variations of the ionization in the $F$-region have certainly two quite different sources, namely, variations of the solar ionizing radiation on one hand and variations in the earth's atmosphere on the other. Apart from tidal movements and oscillations, we have amongst the latter rapidly-moving shock waves of the retarded-sound type and also slow changes of finite amplitude; the latter may be part of a system of "cellular oscillations" according to MARTYN's theory (1950). Unfortunately, our system of characteristics must be based on electron density and thus it is rather sensitive to both influences. If a characteristic like the "total electron content" could be reliably evaluated it would be much less sensitive to atmospheric movements or pressure oscillations.

Some further details seen from cine films concerning the formation of the *F2*-layer may be noted. When the *F2*-layer has practically disappeared during the night, e.g. in the equatorial region when the scatter-type $F$-trace appears, the re-formation with sunrise seems to start at greater heights, the new layer is then "coming down". Now during the African eclipse of 14 December 1955 the *F2*-layer was also strongly affected and disappeared at greater heights. But on this occasion the re-formation of the layer at the end of the eclipse started from



VOL.
15
1959

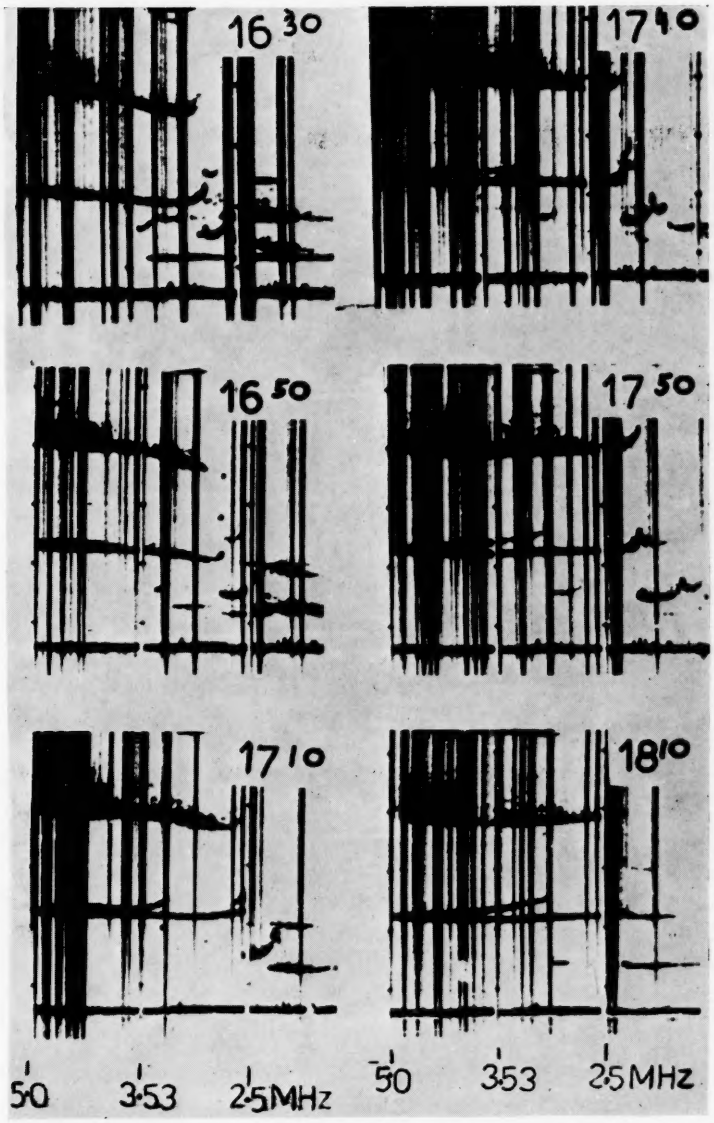


Fig. 2.

VOL.
15
1959

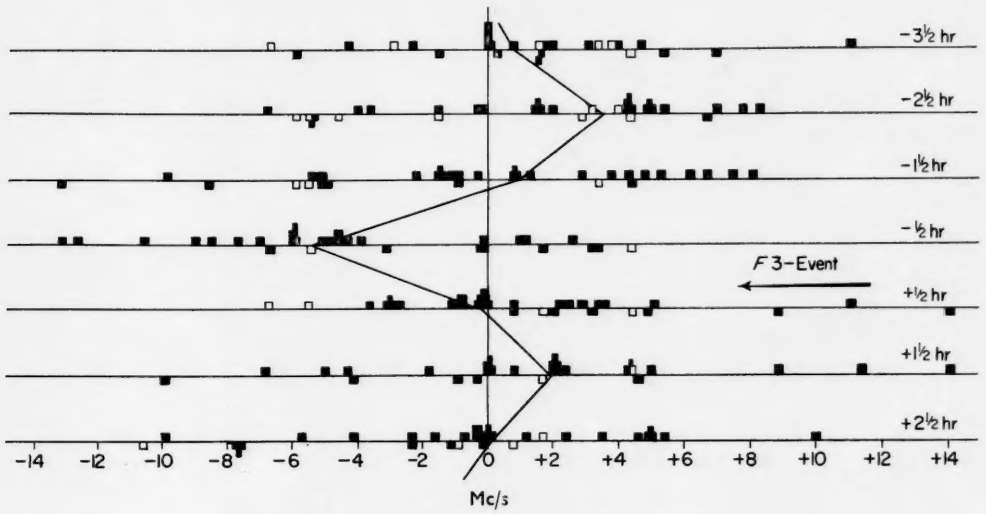


Fig. 3. Depression of MUF 3000-*F2* at Lwiro, August 1954.
■ Isolated perturbation
□ Serial perturbation

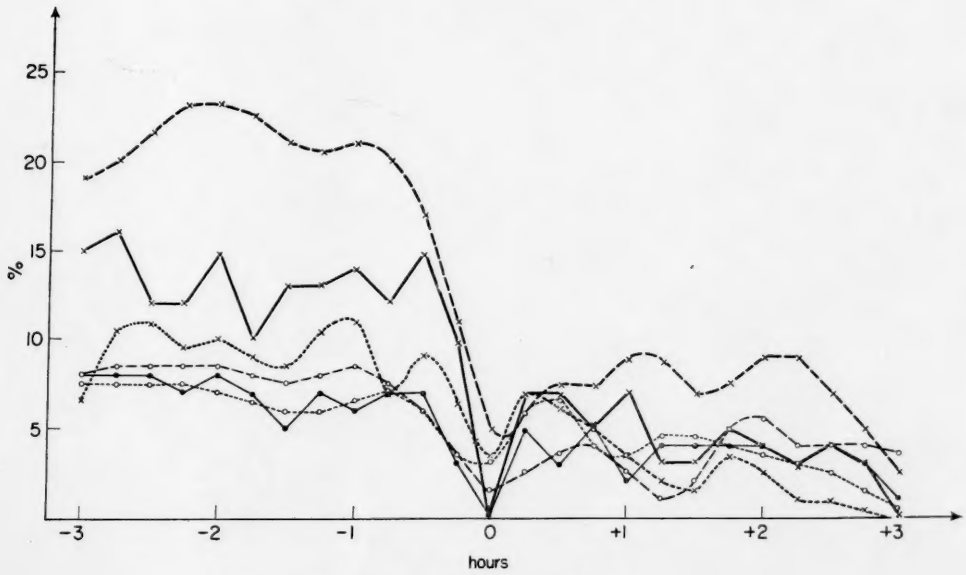


Fig. 4. Depression of MUF 3000-*F2*. (Freiburg)

| MUF-*F2* | $f_0F2$ | |
|---|---|---|
| ×———× | ○———○ | Averaged night values |
| ×———× | ●———● | ¼-hourly values (wholeday) |
| ×– – – – – × | ○– – – – – ○ | Averaged day values |

below. This important observation was first noted by Durand and Lejay (1956).

I do not intend to give an explanation here but it may be stated that all sorts of variations which are important for conclusions concerning the physical or meteorological state of the upper atmosphere can be seen very readily on cine films. More stations should be encouraged to use this technique and trials for their dynamical evaluation should be made in order to arrive later at some conventions.

## References


| | | |
|---|---|---|
| Akasofu S. | 1956 | *Sci. Rep. Tôhoku Univ.* Ser. 5 **8,** 24. |
| Bibl K. | 1952 | *C. R. Acad. Sci., Paris* **235,** 734. |
| Bibl K., Harnischmacher E. and Rawer K. | 1955 | *Physics of the Ionosphere* pp. 113–118. Physical Society, London. |
| Durand J. and Lejay P. | 1956 | *J. Atmosph. Terr. Phys.* Suppl. 6, 86. |
| George D. E., Watts J. M. and Wells H. W. | 1946 | *Phys. Rev.* **69,** 540. |
| Martyn D. F. | 1950 | *Proc. Roy. Soc.* A **201,** 216. |
| Nakata Y., Kan M. and Uyeda N. | 1953 | *Rep. Ionos. Res. Japan* **7,** 129. |


## Discussion

Dr. Martyn—Munro in Australia has done a great deal of work (both $P't$ and $P'f$) on the movement of irregularities in region-$F2$. He has been unsuccessful in his efforts to detect downward motion and we feel that these are really inclined wave-fronts with considerable horizontal width of 2000 km or more. We are not convinced about this propagation downwards as suggested by Akasofu.

Dr. Berkner—I think that about one in ten of these goes back up again.

Dr. Martyn—Dr. Tuve presented evidence for this at Oslo in 1948 but we have concluded that they do not represent disturbances coming down and that they are in fact travelling horizontally. I doubt this suggestion about disturbances going down through the $F$-layer to the sporadic-$E$ layer.

Dr. Berkner—I think the records showing these phenomena are probably still available at DTM.

Journal of Atmospheric and Terrestrial Physics, 1959, Vol. 15, pp. 43 to 47. Pergamon Press Ltd. Printed in Northern Ireland

# SESSIONS IV and V

## The outermost ionosphere

S. CHAPMAN*

**Abstract**—Speculations made by the writer regarding the extension of the solar corona up to and beyond the earth's orbit are considered in connexion with the constitution of the outer ionosphere, above the *F2*-peak. If the sun's magnetic field is radially limited so as not to affect the outward flow of heat from the corona, the earth must be immersed in a very hot (200,000°) interplanetary atmosphere mainly consisting of ionized atomic hydrogen—the protons and electrons numbering about a thousand per cubic centimetre. Heat must flow from this gas into the earth's atmosphere. Above the *F2*-peak the atmosphere will first consist increasingly of ionized atomic oxygen, under-lying an extensive layer of nearly neutral atomic hydrogen. The temperature continually increases upwards and at high levels the atomic hydrogen gradually merges with the interplanetary gas. Above the neutral hydrogen layer, the heat inflow is greatest in polar latitudes.

### THE IONOSPHERE ABOVE THE *F2*-PEAK

THE ionosphere has been much explored up to the peak of the *F2*-layer—at about 300 km height—by vertical-incidence reflection methods. Our observational knowledge for the regions above that level is still very imperfect. Some information can be gained from the change of polarization of signals returned by reflection from the moon. The study of whistlers and other low-frequency signals is another source of information as to the electron density many thousands of kilometres above the earth.

Theoretical speculations as to the ionosphere above the *F2*-peak vary considerably. As regards the temperature $T$, one view is that there is an isothermal layer, the exosphere, above the level where collisions become rare; the estimated values of $T$ in the exosphere are of the order 1500°K or perhaps 2000°K.

SPITZER has pointed out that below the *F2*-peak there is a significant downward flow of heat by thermal conduction. BATES has indicated another process by which the *F2*-layer may lose energy, namely by radiation from atomic oxygen, corresponding to transitions between the two low levels of the ground term; he has also examined whether the supply of energy of sunlight absorbed in the *F2*-layer suffices to meet the estimated losses. According to his calculations the supply is inadequate. He made tentative suggestions as to supplementary supplies of solar energy absorbed in the layer.

### THE EXTENDED SOLAR ATMOSPHERE

I have speculatively proposed another picture of the outer ionosphere, which leads to an alternative explanation of part of the downward energy flux below

* Geophysical Institute, College, Alaska, and High Altitude Observatory, Boulder, Colorado—there engaged in a program of research supported by the National Bureau of Standards and the Sacramento Peak Observatory of the Air Force Cambridge Research Center.

the *F2*-peak. According to these ideas the terrestrial ionosphere decreases upwards in density until it merges with the far extension of the solar atmosphere. The particle density of this interplanetary atmosphere, at the distance of the earth's orbit, is estimated (from purely solar data) to be of order $10^3/cm^3$ (mainly protons and electrons); its temperature there is estimated to be about 200,000°. The estimated density agrees in order of magnitude with estimates independently made on the basis of quite different observational data—the zodiacal light and whistlers. The ionospheric temperature must increase continually upwards to the temperature of the solar interplanetary atmosphere.

If this picture be correct, heat must flow inwards from the hot solar interplanetary atmosphere towards the cool earth that moves through it; this flow of energy is tentatively identified with part of the downward heat flux in the *F2*-layer, namely with the part that cannot be explained by absorption of sunlight in the layer. Thus the excess energy flux inferred from BATES's calculations is not attributed to an unapparent source within the layer—it is ascribed to heat flow coming through the layers from far above.

These ideas are speculative and open to much-needed criticism. It is hoped also that it will be possible to apply to them some observational checks.

The approach to the above new conceptions of the outer ionosphere began with an idealized study of the solar atmosphere. The starting point was the existence of the solar corona, the high outer layer of the sun's atmosphere, consisting mainly of ionized atomic hydrogen (protons and electrons) at a temperature of the order of a million degrees. A first step was a simple limited treatment of some properties that would characterize a *model* solar corona, which (unlike the actual corona) is static and spherically symmetrical. At the level of maximum $T$ for the actual corona (namely 1·06 solar radii from the sun's centre) the model corona was taken to have the same density as the actual mean coronal density, estimated by VAN DE HULST to be $2{\cdot}3 \times 10^8$ particles (of each sign) per cubic centimetre, and the temperature $T_0$ for the model corona at that level was taken to be of order $10^6$ degrees.

The simple nature of the solar gas enables its thermal conductivity to be estimated; this varies very nearly as $T^{5/2}$. Assuming a constant outward flow of heat to infinity, it results that $T$ varies as $1/r^{2/7}$ at the radial distance $r$. This indicates that at the distance of the earth's orbit $T$ is 220,000°, if $T_0$ is $10^6$ degrees. Knowing $T$ as a function of $r$, it is possible to infer from the equation of statical equilibrium of the extended solar atmosphere how the number density $n$ of the gas varies with $r$; at the earth's orbit $n$ is calculated to be about 340, 1300 or 4200, according as $T_0$ is $10^6$, $1{\cdot}1 \times 10^6$ or $1{\cdot}2 \times 10^6$.

## UNCERTAINTIES AS TO THE INTERPLANETARY GAS

The solar corona is obviously not spherically symmetrical; eclipse photographs show greater extension in some directions than in others, and the coronal form changes characteristically in the course of a sunspot cycle. If the changes are slow compared with the time required to achieve a quasi-static equilibrium of the extended atmosphere, the inequalities in different directions should be increasingly reduced with increasing distance from the sun.



VOL. 15 1959

If there are magnetic fields in the hottest coronal regions, and at greater radial distances, the thermal conductivity for the outward flow of heat will be reduced. This will result in steeper radial temperature gradients, and lower temperatures at the earth's orbital distance. The density of the solar gas at this distance would also be reduced. The values of this density estimated from the zodiacal light and from whistlers seem to agree fairly well with those of the model corona. This suggests that the influence of solar magnetic fields is unimportant, and tends to support the above estimate of the temperature where the ionosphere merges with the extended corona.

The sun appears to emit clouds and streams of solar gas, with speeds of the order 500 to 1500 km/sec; this gas is ionized (but neutral). BIERMANN has shown that such gas may accelerate comets' tails, through interaction with their ionized constituents. It seems likely that the extended coronal atmosphere is also affected, and the action of such clouds and streams moving through that atmosphere may explain the marked irregularities in the form of the corona as shown by eclipse photographs. In conjunction with Dr. W. E. BRITTIN, I am now examining this possibility. It may be that the moving gas partly sweeps away the nearly stationary interplanetary atmosphere; but as the solar stream moves onward (owing to the rotation of the sun), there will be a tendency for the atmosphere to return to its normal state, by flow from the regions above and below the sun's equatorial plane, and also radially outward.

Owing to these uncertainties it is improper to dogmatize as to the state of the solar gas through which the earth moves in its orbit. But for the present it seems worth while to consider the possibility that it is very hot, and that it has a density of order $10^3/cm^3$ near the earth.

## THE COMPOSITION OF THE OUTER IONOSPHERE

The height variation of the composition of the atmosphere has been much discussed. It is now generally agreed to be likely that above about 100 km oxygen is increasingly dissociated to the atomic form by the photochemical action of sunlight. However, as has been shown by the important work of NICOLET (1954a, b, c) and MANGE (1955) on diffusion at high levels, some molecular oxygen will still be present at great heights, where chemical reactions are very slow, by the action of diffusion. Nitrogen, on the other hand, may be mainly molecular even at the *F2*-peak, but some dissociation will occur, and diffusion will carry a small amount of atomic nitrogen downward to lower levels.

In the *E*- and *F*-layers of the ionosphere, these two gases, nitrogen and oxygen, neutral and ionized, molecular and atomic, seem to be the predominant constituents. Their upward extension depends on their different scale heights, and on their relative proportions at the level where diffusion becomes rapid enough to overcome turbulent mixing. The greatest scale heights correspond to the effective molecular weights (8 and 7) of ionized atomic oxygen and nitrogen. If no other constituents were present, the outermost ionosphere would be composed of atomic nitrogen, singly ionized, with perhaps an outer fringe multiply ionized.

But there is certainly another constituent which has a much larger scale height, namely neutral atomic hydrogen. Its occurrence in the *D*- and *E*-layers has been reliably inferred by BATES and NICOLET, in the course of their important study of the photochemistry of atmospheric water-vapour; the presence of the associated compound OH is manifested by strong airglow emissions. BATES and NICOLET very tentatively estimated the number density $n(\mathrm{H})$ of atomic hydrogen to be about $10^{8.5}$ at 100 km; thus only one in about $10^5$ particles at that level is atomic hydrogen. The ratio may be somewhat smaller at the higher level where diffusive equilibrium begins. But above that level, the ratio $n(\mathrm{N}^+)/n(\mathrm{H})$ decreases by a factor $10^{-6}$ in one decimal scale height of atomic hydrogen; and the ratio for the other constituents decreases still faster. Thus after rising through two such decimal scale heights the atmosphere must consist almost entirely of neutral atomic hydrogen, with a small percentage of ionized atomic hydrogen (protons and electrons). This percentage, however, is likely to be small until the supposedly upward rising temperature reaches a value of the order 30,000°. The number density of the atmosphere, with mounting temperature and diminishing gravity, will fall off ever more slowly, till the ionosphere merges with the extended solar atmosphere.

Model calculations of the atmospheric density at heights well above the *F2*-peak are being made, based on a variety of empirical assumptions. These refer not only to the value of $n(\mathrm{H})$ at the level where mixing ceases, and to the height of this level; they refer also to the variation of thermal conductivity with height. As long as the proportion of neutral atomic hydrogen is appreciable, the thermal conductivity is unlikely to be much influenced by the geomagnetic field; but at higher levels, except in polar regions, the vertical mount rate of temperature will be reduced by the magnetic field.

The deceleration of the IGY earth satellites may provide a valuable indication of the density of the outer atmosphere, and provide a check on the above speculations.

These ideas suggest that the thermo-incline (or region of mounting temperature) continues indefinitely upwards, but that the *F2*-layer is limited above by a nearly neutral layer of atomic hydrogen, above which lies another ionized layer of protons and electrons.

VOL. 15 1959

## REFERENCES


| | | |
|---|---|---|
| BATES D. R. | 1951 | *Proc. Phys. Soc. Lond.* B**54,** 805. |
| BATES D. R. and NICOLET M. | 1950 | *J. Geophys. Res.* **55,** 301. |
| BIERMANN L. | 1951 | *Z. Astrophys.* **29,** 274. |
| CHAPMAN S. | 1957 | *Smithsonian Inst. Publ. Contrib. Astrophys.* **2,** 1. |
| CHAPMAN S. | 1957 | *The Threshold of Space* (Edited by ZELIHOFF) pp. 65–72. Pergamon, London. |
| VAN DE HULST H. C. | 1953 | *The Sun* (Edited by KUIPER) pp. 207–321. University of Chicago Press. |
| MANGE P. | 1955 | *Ann. Géophys.* **11,** 153. |
| NICOLET M. | 1954a | *J. Atmosph. Terr. Phys,* **5,** 132. |
| NICOLET M. | 1954b | *Rocket Exploration of the Upper Atmosphere* (Edited by BOYD R. L. F. and SEATON M. J.) pp. 357–360. Pergamon Press, London. |

NICOLET M. 1954c *Rocket Exploration of the Upper Atmosphere* (Edited by BOYD R. L. F. and SEATON M. J.) pp. 361–365. Pergamon Press, London.

SPITZER L. 1952 *The Atmospheres of the Earth and Planets* p. 221 (1949 Ed., p. 213). University of Chicago Press.

## DISCUSSION

DR. SINGER—Has Professor CHAPMAN considered the dynamics of this interplanetary gas?

PROFESSOR CHAPMAN—I have not thought much about that. It would involve a reconsideration of the Chapman–Ferraro theory of magnetic storms.

DR. PAWSEY—What is the order of the mean free path of particles in the solar corona near the earth?

PROFESSOR CHAPMAN—It will be very large. In my analysis I had to consider whether the usual expressions for thermal conductivity are applicable. I concluded that they could be reasonably applied to the problem.

DR. PAWSEY—The mean free paths will thus be less than the layer thicknesses.

PROFESSOR CHAPMAN—No, not necessarily.

DR. BERKNER—As the satellite passes it can be observed both visually and on 108 Mc/s radio signals. In general these two paths will not coincide but at the zenith they will be identical and we can compute the total ionization along the path.

DR. PAWSEY—One can make a similar measurement on radio star signals, and from moon echoes.

DR. BERKNER—Provided the measurements are accurate. One requires a Markowitz camera to fix the moon position accurately.

Journal of Atmospheric and Terrestrial Physics, 1959, Vol. 15, pp. 48 to 50. Pergamon Press Ltd. Printed in Northern Ireland

# Geophysical effects of solar corpuscular radiation*

S. F. SINGER†

DURING the past 2 years we have investigated some of the prominent geophysical effects produced by the emission of solar gas of high velocity. The chief phenomena are *magnetic storms*, *aurora* and their various ramifications, as well as variations in the *cosmic ray* intensity which are correlated with magnetic storms. It is important that the theory tries to explain all of these in terms of a model of interplanetary space and of the "outer ionosphere" of the earth (defined as the region from the exosphere, about 400 km, outwards to about ten earth radii).

## MAGNETIC STORMS

Our theory tries to take account of the fact that the outer ionosphere is a very good conductor of electricity because of the high electron density there (as shown by whistler experiments (STOREY, 1953)). With the electron density of the order of 600 per cubic centimetre, the conductivity is already so high that phenomena occurring at the limit of the outer ionosphere will not be propagated instantaneously to the earth itself. Instead one needs to study the propagation of phenomena through the ionized gas in the presence of magnetic fields, i.e. we have to treat a magneto-hydrodynamic problem. Such problems are difficult to solve, particularly in the case of a three-dimensional model (it must be three-dimensional in order to be realistic), and in the presence of a dipole (non-uniform) field. Our approach instead has been to use hydrodynamic analogies and geophysical evidence where available. Thus we adduce evidence for two types of magnetic storm effects. One, identified with the *sudden commencement*, *SC*, is caused by currents flowing in the inner ionosphere and shows typical features associated with normal ionospheric currents. These *SC*-currents are set up in the following way (SINGER, 1957e). The solar eruption ejects high-velocity gas which arrives at the earth about a day later. In interacting with the ambient interplanetary gas where weak magnetic fields are present, the phenomenon develops a sharp front ("shock wave").‡ In the vicinity of the earth where the magnetic field strength increases, the gas is retarded by body forces at the equator but can penetrate into the ionosphere through the auroral zones. As the shock wave is compressed in the converging channel formed by the earth's magnetic lines of force, the gas pressure pushes the lines of force apart and thus creates a phenomenon known as the reverse *SC* (*SC*$^\star$). The *SC*$^\star$ has been observed repeatedly but the present theories of magnetic storms have not tried to explain it; our magneto-hydrodynamic model gives what we consider a natural explanation. On penetrating into the ionophere itself, in the auroral zone, e.m.f.s are set up which drive the *SC*-currents through the ionosphere.

* This work has been supported in part by the Air Force Office of Scientific Research under Contract AF # 18(600)-1038.

† University of Maryland, College Park, Maryland.

‡ The theoretical basis for formation of a hydromagnetic shock is not quite clear; the Larmor radius may take the place of the mean free path as the organizing length.

The form of these current systems has been shown beautifully by NAGATA and ABE (1955) for the *SC** and by JACOBS and OBAYASHI (1956) for the *SC*.

While the analyses by SUGIURA (1953) and FORBUSH and VESTINE (1955) show fairly conclusively that the *SC*-currents do flow in the inner ionosphere, it is very likely that only a portion of the main phase currents flow in the inner ionosphere. We must hold to the idea of an extra atmospheric ring current first worked out by CHAPMAN and FERRARO. We have developed a model for the main phase ring current which differs from that of CHAPMAN and FERRARO (1955) and also from ALFVÉN's (1955); in our model the current is produced by high-speed solar particles which enter into the normally forbidden regions of the earth dipole field, are trapped there, and execute motions and drifts which produce the main phase current. Particles with small pitch angles to the magnetic field can reach the earth's atmosphere and will disappear from the current but contribute to aurora and ionospheric ionization. These particles are replenished by perturbations; thus the time constant of the ring current can be calculated to be from 1 to 2 days A calculation has been made of the distribution of this ring current and shows a maximum in the vicinity of seven earth radii in gratifying accord with auroral data.

## AURORA

One of the outstanding problems for the aurora is the acceleration of solar corpuscles to auroral energies, i.e. from velocities of the order of $10^8$ cm/sec to velocities of the order of $10^9$ cm/sec. BENNETT and HULBURT (1954) solved this problem in an *ad hoc* way by granting these velocities initially. MARTYN (1951) has extended the Chapman–Ferraro theory in an important way by using the polarization voltage appearing across the ring current to accelerate protons to auroral energies; but this model has not been worked out in detail nor are we sure that it can work in the presence of ambient ionized gas of high density such as exists in the outer ionosphere. ALFVÉN (1955) on the other hand considers that the aurora is due to an electric discharge which in turn is caused by an electric field supposed to exist within the solar corpuscular beam. In our view the acceleration takes place quite close to the earth by a type of betatron effect in which the great mass of the protons contribute energy through a non-linear process which in turn accelerates a few of the protons to the required high energies. The details of the process will be given separately.

## COSMIC RAYS

Finally we must seek to explain the so-called Forbush decreases of cosmic rays which often occur during magnetic storms, although the correlation is by no means perfect. For this reason, and also because of the observation of decreases near the pole, we must rule out a ring current as their cause (SINGER, 1957c). Arguments can also be given which rule out any geocentric mechanism such as the admirable model proposed recently by PARKER (1956). In fact no magnetic screening effect has yet been found which will give the observed decreases with reasonable values of magnetic fields and interplanetary gas densities. In common with ALFVÉN we favour a deceleration by electric fields as the cause of Forbush decreases. However, our deceleration mechanism is a diffusive one and works in a manner similar to but inverse to the well-known Fermi acceleration mechanism for cosmic rays. We

assume that cosmic rays are trapped in collisions between receding centres in an expanding turbulent cloud which issues from the solar eruption. In this adiabatic expansion cosmic rays lose the required amount of energy; then by virtue of Liouville's theorem the intensity decrease occurs (SINGER, 1957a). We also explain the low energy cutoff ("knee") of cosmic rays in terms of diffusive deceleration on which ionization loss (for non-relativistic particles) is superimposed (SINGER, 1957b). Here again magnetic screening does not seem to lead to a satisfactory explanation for the absence of low-energy cosmic-ray primary particles.

## PROPOSED OBSERVATIONS

A large number of experiments can be proposed to test crucial features of theories of magnetic storms and aurora. Chief among them are experiments with rockets and satellites. In particular we would like to measure the amount of current flowing in the inner ionosphere during the sudden commencement and during the main phase of magnetic storms. According to our views the sudden commencement current would flow chiefly in the inner ionosphere and the main phase current chiefly in the outer ionosphere (SINGER, 1956). Sensitive microphones carried in balloons may be able to detect the incoming auroral shock wave during the sudden commencement. Scintillators carried in high-altitude aircraft may be able to detect nuclear $\gamma$-rays produced by incoming auroral protons which are captured by nitrogen-14 in the ionosphere. Cosmic ray measurements in satellites as a function of latitude, and cosmic ray measurements with extremely high-altitude vehicles up to several earth radii may decide between geocentric magnetic screening theories and the diffusive deceleration model proposed by us (SINGER, 1956, 1957c).

## REFERENCES


| | | |
|---|---|---|
| ALFVÉN H. | 1955 | *Tellus* **7,** 50. |
| BENNETT W. H. and HULBURT E. O. | 1954 | *Phys. Rev.* **95,** 315. |
| FERRARO V. C. A. | 1955 | *Ann. Géophys.* **11,** 284. |
| FORBUSH S. E. and VESTINE E. H. | 1955 | *J. Geophys. Res.* **60,** 299. |
| JACOBS J. A. and OBAYASHI T. | 1956 | *The Sudden Commencement of Magnetic Storms.* University of Toronto Physics Dept., Sci. Rpt. 3. |
| MARTYN D. F. | 1951 | *Nature, Lond.* **167,** 984. |
| NAGATA T. and ABE S. | 1955 | *Rep. Ionos. Res. Japan* **9,** 39. |
| PARKER E. N. | 1956 | *J. Geophys. Res.* **61,** 625. |
| SINGER S. F. | 1956 | Geophysical research with artificial earth satellites. *Advances in Geophysics* Vol. III. Academic Press, New York. |
| SINGER S. F. | 1957a | *Nuovo Cim.* Suppl. II. 334 |
| SINGER S. F. | 1957b | *Nuovo Cim.* Suppl. II. 342 |
| SINGER S. F. | 1957c | *Nuovo Cim.* Suppl. II. 326 |
| SINGER S. F. | 1957d | The primary cosmic radiation and its time variations. *Progress in Cosmic Ray and Elementary Particle Physics* Vol. IV. Interscience. New York and North Holland Publishing Company |
| SINGER S. F. | 1957e | *Trans. Amer. Geophys. Un.* **38,** 175. |
| STOREY L. R. O. | 1953 | *Phil. Trans.* A **246,** 113. |
| SUGIURA M. | 1953 | *J. Geophys. Res.* **58,** 558. |




VOL.
15
1959

Journal of Atmospheric and Terrestrial Physics, 1959, Vol. 15, pp. 51 to 53. Pergamon Press Ltd. Printed in Northern Ireland

# The question of radio emission by the ionosphere

J. L. Pawsey

It is natural for a radio astronomer to ask if the ionosphere emits radio waves. Much of the radiation with which he is familiar originates in ionized gases, some in thermal processes and some in non-thermal processes on the nature of which he can only speculate. Thermal emission from the ionosphere is known. Non-thermal emission might well originate in some forms of disturbance, e.g. the aurora, and if it exists it might offer a reasonable chance of observing conditions at the source and possibly of elucidating mechanisms. The probability of recognition of such radiation is suggested by the traditional reports of "radio noise from the aurora".

But a search of the literature does not substantiate this tradition; evidence is extremely meagre. It is the purpose of this note to point this out and to emphasize the importance which non-thermal emission, if it occurs, would have in ionospheric and astronomical studies.

It has been conclusively demonstrated (Pawsey *et al.*, 1951; Gardner, 1954) that thermal emission from the *D*-region can, under favourable conditions, be observed on about 2 Mc/s throughout a large part of the daylight hours in temperate latitudes. This implies the absence of regular or frequent intense non-thermal components. It does not preclude occasional bursts which might have been mistaken for interference, nor intense emission from the *F*-layer which would be cut off by the *E*-layer.

On metre wavelengths (25–110 Mc/s), intense noise from all over the sky has been reported (Cottony, 1950, Washington; and unpublished Canadian reports, Ottawa). On 10 cm Covington (1947, 1950) has reported bursts of radiation from the sky which coincided in time with magnetic disturbances or aurorae, and on 480 Mc/s Reber reported, on the occasion of a severe solar noise storm, "swishes" which continued, though with much reduced intensity, through the night. Forsythe *et al.* (1949), also on 10 cm, reported series of short-duration (micro-seconds) pulses at the time of aurorae, and Hartz *et al.* (1956) observing on v.h.f. frequencies reported noise at such times. Of these observations, those of Covington and Reber appear highly reliable but, until they can be reliably reproduced, must be regarded as clues rather than evidence.

Brief increases of noise level on a frequency of 33 Mc/s coinciding with meteors have been reported by McKinley and Millman (1949) but they were unable to tell if the noise originated in the meteor or was simply due to an enhancement of propagation from a distant noise source by the meteor trail.

There are three more recent points worth mentioning. The first is a negative result found by R. L. Dowden (unpublished) at Macquarie Island. He repeated the thermal noise measurements at 2 Mc/s and found, at this point which is in the auroral zone, results very like those found in temperate latitudes. He still found

no evidence for non-thermal emission. The second is speculation; it has been suggested by ALCOCK (in press) that the "dawn chorus" is due to excitation of the outer atmosphere by some sort of matter ejected from the sun. The third is argument by analogy. It has been found by SHAIN and GARDNER (unpublished) that the emission from Jupiter is in bursts or groups of bursts, the bursts never being of shorter duration than about $\frac{1}{4}$ sec. In this the bursts contrast with the very short duration impulses occurring in terrestrial atmospherics but appear analogous to solar bursts. The emission also appears to show a maximum around 20 Mc/s. On this evidence the authors suggest the most plausible origin is in the Jovian ionosphere.

These results are sufficient to provoke curiosity but none appeared sufficiently definite to justify launching a systematic investigation. But the results reported by Gallet at this meeting, in which he gives reasons for supposing the "dawn chorus" is indeed generated in the outer reaches of the ionosphere, are of a different order of plausibility. Here are clues well worthy of investigation.

## REFERENCES


| | | |
|---|---|---|
| ALCOCK G. McC. | 1959 | *Aust. J. Phys.* In press. |
| COTTONY H. V. | 1950 | *Science* **3,** 41. |
| COVINGTON A. E. | 1947 | *Terr. Magn. Atmos. Elect.* **52,** 1947. |
| COVINGTON A. E. | 1950 | *J. Geophys. Res.* **55,** 33. |
| FORSYTHE P. A., PETRIE W. and CURRIE B. W. | 1949 | *Nature, Lond.* **164,** 453. |
| GARDNER F. F. | 1954 | *J. Atmosph. Terr. Phys.* **5,** 298. |
| HARTZ T. R., REID G. C. and VOGAN E. L. | 1956 | *Canad. J. Phys.* **34,** 728. |
| McKINLEY D. W. R. and MILLMAN P. M. | 1949 | *Proc. Inst. Radio Engrs., N.Y.* **37,** 364. |
| PAWSEY J. L., McCREADY L. L. and GARDNER F. F. | 1951 | *J. Atmosph. Terr. Phys.* **1,** 261. |
| REBER G. | 1946 | *Nature, Lond.* **158,** 945. |


## DISCUSSION

DR. J. W. CHAMBERLAIN—I have investigated the possibility of a dispersion in velocities of the protons that are incident on the atmosphere during auroral arcs. A velocity dispersion, in the incident flux of particles, varying approximately as $v^{-2}$ over a wide range of velocities could give a consistent explanation to the luminosity curves and hydrogen-line profiles. The angular dispersion is probably proportional to $\cos^2 \theta$. There seems to be no way to explain all the observations with mono-energetic particles. The data are inadequate to show whether protons alone are the cause of auroral arcs or whether additional processes (e.g. fast incident electrons, electric fields) need be invoked. Insofar as a theory of primary auroral particles is concerned, it appears that an acceleration mechanism close to the earth is required. (Complete details are given in *Astrophys. J.*, **127,** 1957).

PROFESSOR CHAPMAN—Do the particles spiral in? Presumably near the end of their path they will be deflected by collisions.

DR. CHAMBERLAIN—Yes they do spiral in—they will be almost stopped before they are deflected.



VOL. 15 1959

DR. MENZEL—Is the maximum near 500 km explained if the electrons travel with the protons? High-energy protons entering the earth's atmosphere would have difficulty in picking up electrons.

DR. CHAMBERLAIN—No this is just the assumption that would place the maximum at 1000 km and not 500 km. When the particles are going at a speed comparable with that of the Bohr electron it captures them.

OL.
15
959

Journal of Atmospheric and Terrestrial Physics, 1959, Vol. 15, pp. 54 to 57. Pergamon Press Ltd. Printed in Northern Ireland

# Whistlers

M. G. MORGAN*

THE theory of whistlers was completed in 1951 by STOREY in his graduate studies at Cambridge University. It was deduced from his phenomenological observations and an extension of the work of ECKERSLEY some 15–20 years earlier. STOREY's colleague, RATCLIFFE, reported the new theory to the Tenth General Assembly of URSI in Sydney, Australia in 1952. This, together with STOREY's subsequent publication of his work, set off much new interest in this remarkable phenomenon.

During World War I, stray earth currents associated with field telephones were intercepted by both sides. From terminals in the ground a few hundred metres apart, wires were brought to a common point and applied to a high-gain audio amplifier. On the German side, BARKHAUSEN noted phenomena which he reported as "whistling tones from the earth".

For some time there remained confusion between tweeks and whistlers. Tweeks are developed from lightning impulses by multiple-reflection between the earth and the ionosphere. At a distant point of observation, a succession of impulses is received as the signal arrives by a greater and greater number of reflections. BURTON (1930) first recognized the clear difference between these phenomena and properly explained the generation of tweeks. Tweeks are developed only when the *D*-layer absorption is low and therefore only at night. BURTON heard them commence during a solar eclipse.

By 1935, ECKERSLEY recognized that BURTON had correctly explained tweeks but that his own theory of dispersive propagation would undoubtedly lead to the correct explanation of whistlers. He had shown that at audio-frequencies, the extraordinary magneto-ionic wave component in the ionosphere, when travelling in the direction of the earth's magnetic field, has a suitable dispersion.

STOREY (1953) showed that such a signal must in fact be guided along the field flux and he concluded that the necessary paths of great length are provided by propagation along the flux of the geomagnetic field into the far outer atmosphere and down to earth at the conjugate point in the opposite hemisphere. This idea was strongly supported by certain observational details. Its greatest difficulty was that it required a minimum electron density of about 400/cm$^3$ at the crest of the path. The geomagnetic flux lines passing through middle latitudes, where whistlers are commonly observed, rise to an earth diameter or more as they cross the equator. A prediction of the particle density at so great a height, based upon the lapse rate known for the first few hundred kilometres, falls far short of this requirement.

In 1955, ALLCOCK and I (MORGAN and ALLCOCK, 1956) found from the simultaneous observation of whistlers at conjugate positions in the northern and southern hemispheres, that the essential details of STOREY's hypothesis were borne out.

* Dartmouth College.



VOL. 15 1959

HELLIWELL and GEHRELS (1957) have found that v.l.f. broadcast signals can be received near the conjugate point in the opposite hemisphere after propagation in the whistler mode. Because the guiding action falls off with increasing frequency, the signals are very weak at the lowest available frequency (15·5 kc/s).

There have been a number of discoveries corroborating these basic facts:

(1) It is not uncommon to have two or more separate whistlers produced from a single lightning flash. During a given period of activity, the time-spacing of the whistlers within such a group is the same from one group to another, and the

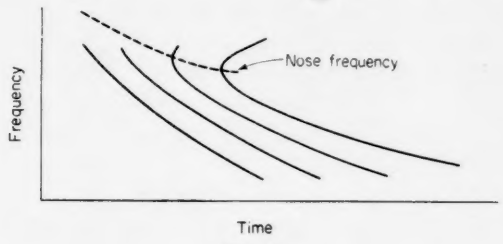


Fig. 1.

whistlers arriving later within a group have greater dispersion. These facts clearly indicate that the multiples are produced by distinct propagation paths of successively greater delay. CURTIS and I (MORGAN and CURTIS, 1957) have found an example in which there were two widely separated multiples followed by a complicated echo train. We have succeeded in explaining the train by showing that successive transits were made over the two paths in various sequential combinations. One of the original whistlers was stronger than the other, indicating that that path had the smaller attenuation. It was found accordingly that there was a preference for that path in the echoes.

(2) GALLET, HELLIWELL and ELLIS have independently pointed out that ECKERSLEY's approximation for the refractive index at very low frequencies was improperly made, and when properly carried out shows a reversal of the dispersion at a frequency lying between the gyrofrequency in the lower ionosphere and one-quarter the minimum gyrofrequency (proportional to the minimum magnetic field strength) encountered over the path. HELLIWELL has called the frequency at which the reversal occurs the nose-frequency. The energy in the whistler at the nose-frequency is rather low because of the reduced guiding. As the observer's latitude is increased, the nose-frequency decreases because the magnetic field strength at the crest of the propagation path decreases. Fig. 1 shows this effect in a group of multiple whistlers generated by one lightning flash and propagated over a group of paths. The whistler with the greatest delay rose to the greatest height and therefore exhibits the lowest nose-frequency (Fig. 1).

(3) DINGER and I (MORGAN and DINGER, 1956) have examined whistlers observed simultaneously at points separated 5° in geomagnetic latitude, and have found a given whistler to have the same dispersion at both locations though at the higher latitude the nose-effect may be greater at the highest frequency observed.

(4) It has been noted on some occasions that an echo may be stronger than the

original whistler. In a long train of echoes, the intensity may increase for several echoes and then fall off rapidly. MAEDA and KIMURA (1956) have examined the theoretical considerations of the guiding and have shown the extent to which it may be imperfect. Their investigation shows how successive echoes may come down at progressively higher latitudes. Thus the observation is explained if the first whistler comes down at a latitude lower than that of the observer, and the echoes come down at successively higher latitudes, passing by that of the observer. The effect has been dubbed "the polar creep"!

(5) Whistlers have been heard from 25°N to 65°N geomagnetic latitude and at a number of places in the southern hemisphere within this latitude range. There is evidently a low-latitude cut-off in the occurrence of long whistlers (those originating in the observer's hemisphere). IWAI and OUTSU (1956) have found them at 35°N, but have found only short whistlers (those originating in the opposite hemisphere) at 25°N. They have shown on the basis of simple geometrical considerations, that a whistler reflected from the earth cannot produce an upgoing longitudinal component if the reflection occurs below 26·5° latitude.

(6) Throughout the development of the theory of whistlers, observers have found that they do not hear whistlers produced from lightning which they can see. There have been two unelucidated exceptions reported, but on 27 May 1958 I experienced an occasion which removed all doubt. For 1 hr or more, lightning flashes were occurring 3–4 min apart and each produced a loud whistler with echoes. The association was very positive because it was dark, the flashes were infrequent, there were no other whistlers and no other significant atmospherics. Why such an observation is not ordinarily successful is not known. One would expect that it must be either a matter concerning the lightning or the propagation conditions, or some combination thereof. IWAI and OUTSU have pointed out that *D*-layer absorption is very important and must be taken into consideration at both ends of the path.

(7) ALLCOCK and I (ALLCOCK and MORGAN, 1958) have found some statistical evidence that the dispersion of whistlers has increased with the rising solar activity of the current cycle.

With this account before us, it is evident that whistlers are ideally suited to synoptic study. Twenty-seven stations have been set up in a co-ordinated western hemisphere IGY programme. There is also a co-ordinated Australia–Japan programme. In addition, there are stations at Kerguelen, Poitiers and Cambridge, and there will undoubtedly be others of which I have not yet had word. In the western hemisphere programme, 2-min recordings are being made hourly commencing precisely at 35 min past the hour. The recordings are made on magnetic tape up to 15 kc/s (in some cases higher). Time marks good to $\pm 1/20$ sec are mixed with the signals so that events recorded simultaneously at different stations can be identified and compared. The programme also provides a large amount of information on atmospherics fixes.

All magnetic tape recordings in the western hemisphere programme will be preserved. From the study of these, there can be no doubt that our knowledge of the ionosphere and the earth's field will be notably widened.

HERLOFSON and BLOCK (1956) have computed a table of geomagnetic conjugate



VOL.
15
195

pairs including the quadrupole field. The table bears out the great perturbation towards the south of the lines of constant surface dip in the vicinity of 75°W geographic. Already, there is limited evidence that this perturbation will be confirmed by the synoptic whistler studies.

## References


| | | |
|---|---|---|
| Allcock G. McK. and Morgan M. G. | 1958 | *J. Geophys. Res.* **63,** 573. |
| Barkhausen H. | 1919 | *Phys. Z.* **20,** 401. |
| Burton E. T. | 1930 | *Nature, Lond.* **126,** 55. |
| Burton E. T. | 1933 | *Nature, Lond.* **131,** 81. |
| Eckersley T. L. | 1925 | *Phil. Mag.* **49,** 1250. |
| Eckersley T. L. | 1928 | *Nature, Lond.* **122,** 768. |
| Eckersley T. L. | 1935 | *Nature, Lond.* **135,** 104. |
| Ellis G. R. | 1956 | *J. Atmosph. Terr. Phys.* **8,** 338. |
| Helliwell R. A. *et al.* | 1956 | *J. Geophys. Res.* **61,** 139. |
| Helliwell R. A. and Gehrels E. | 1957 | *USA-URSI Spring Meetings.* |
| Herlofson N. and Block L. | 1956 | *Tellus* **8,** 210 |
| Iwai A. and Outsu J. | 1956 | *Proc. Res. Inst. Atmos. (Nagoya Univ., Japan)* **4,** 29. |
| Maeda K. and Kimura I. | 1956 | *Rep. Ionos. Res. Japan* **10,** 105. |
| Morgan M. G. and Allock G. McK. | 1956 | *Nature, Lond.* **177,** 30. |
| Morgan M. G. and Curtis H. W. | 1959 | *VLF Symposium CRPL, Boulder, Colorado, 1957.* In press. |
| Morgan M. G. and Dinger H. E. | 1956 | *Nature, Lond.* **177,** 30. |
| Storey L. R. O. | 1953 | *Phil. Trans.* **246,** 113. |


OL.
15
959

## Discussion

Sir Edward Appleton—Have you observed whistlers during a magnetic storm? Such observations might provide evidence for ionization far out from the earth.

Dr. Morgan—We have not found any correlation but 10 years ago some observations suggested a correlation with whistlers and Dr. Gallet has observed a strong correlation with magnetic storms.

Dr. J. W. C. Scott—Dr. Storey working recently in Canada has looked for correlation between whistlers, dawn chorus and magnetic storms but has not found any.

Journal of Atmospheric and Terrestrial Physics, 1959, Vol. 15, pp. 58 to 65. Pergamon Press Ltd. Printed in Northern Ireland

# Calculation of the propagation path of whistling atmospherics

KEN-ICHI MAEDA and IWANE KIMURA*

**Abstract**—An approximate method is worked out of calculating the propagation path of a whistler by using Fermat's principle. The paths calculated under some appropriate assumptions of the electron density distribution above the ionosphere show appreciable deviations from the line of magnetic force and are generally asymmetric with respect to the magnetic equator. As to the frequency characteristics of the whistler path, the higher the wave frequency is, the more inside travels the wave.

## 1. INTRODUCTION

SINCE STOREY (1953) presented a theory on the propagation mechanism of a whistler, its paths have been simply treated, so far, as if they coincide with the lines of magnetic force. But it is necessary to know the exact propagation path in order to investigate the state of the outer ionosphere. A method to determine the path by numerical calculation was devised by the writers (MAEDA and KIMURA, 1956).

## 2. RAY PATH TRACING

The method is a ray theoretical one and is derived from Fermat's principle. In a plane-stratified ionized medium with constant magnetic field, the wave-normal of a wave is governed by Snell's law, which can be derived from Fermat's principle. In a spherically stratified ionized medium with a magnetic field the direction of which changes with latitude, we also obtain Snell's law by the following approximate treatment for the waves travelling in the magnetic meridian plane. We divide the meridian plane into many small sectors with regards to the latitude and in each sector the angle ($\psi$) between the magnetic field and the radial vector is assumed to be constant. At the boundary of two sectors the angle ($\psi$) changes discontinuously. Then Fermat's principle is converted to Euler's differential equation in its solvable form and yields Snell's law for the wave-normal both in each sector and at the boundary.

The refractive index ($\mu$) for the whistler waves is approximately represented as

$$\mu^2 \simeq \frac{x}{y_L - 1} = \frac{f_0^2}{ff_H} \frac{1}{\cos\Theta - f/f_H} \qquad \left(\text{for } \frac{x}{y_L} \gg 1\right) \tag{1}$$

$$\simeq \frac{x}{y_L} = \frac{f_0^2}{ff_H \cos\Theta} \qquad \left(\text{for } \frac{x}{y_L} \gg 1, \quad y_L \gg 1\right) \tag{2}$$

where $f_0$, $f_H$, $f$ and $\Theta$ are, respectively, critical frequency of the ionized medium, gyro-frequency, wave frequency, and the angle between the wave-normal and magnetic field, and $x = f_0^2/f^2$, $y = f_H/f$ and $y_L = y\cos\Theta$. Then by using this refractive index, Snell's laws for each case mentioned above, are as follows :

(I) Plane-stratified layer (the direction of magnetic field is constant)

$$\mu \sin\beta = \text{const.} \tag{3}$$

* Department of Electronic Engineering, Kyoto University.

(II) Concentrically stratified layer (the direction of magnetic field may change with latitude).

(a) in each sector (the angle $\psi$ is constant)

$$\mu r \sin \beta = \text{const.} \tag{4}$$

(b) at the boundary ($\psi$ changes discontinuously but the other medium parameters are uniform).

$$\mu \cos \beta = \text{const.} \tag{5}$$

$\beta$ is used to denote the angle between the wave normal and the vertical (I) or the radial (II) direction, and $r$ is the radial distance.

It is to be noticed that these Snell's laws are for the wave-normal and not for the ray direction which is needed for the determination of the path. According to BREMMER (1949), the angle ($\alpha$) between the wave-normal and the ray direction is obtained by

$$\tan \alpha = \frac{1}{\mu} \frac{\partial \mu}{\partial \Theta} \tag{6}$$

Hence if the refractive index is given by a simple formula such as (2) and (1), the ray direction can be obtained by the equalities (3) to (5). The equation (3) is applicable to the path determination inside the ionosphere ($E$-, $F$-layer). It is, however, unnecessary to know the complete path in the ionosphere, because the layers are very thin as compared with the total path length of a whistler. Therefore (3) is used only for obtaining the initial ray direction of the path at the top of the ionosphere (the level of the maximum electron density, about 300 km above the ground). We then calculate the path in the outer ionosphere by (4) and (5). In the ionosphere, (3) is approximately written as

$$\frac{f_0}{\sqrt{f f_H}} \frac{\sin \beta}{\sqrt{\cos \Theta}} = \text{const.} \tag{7}$$

provided that (2) is applied to (3). The ratio of $f_0$ at the top of the ionosphere to $f_0$ at the bottom of the ionosphere is very large, say, order of 100. Then $\beta$ must become very small at the top, since $|\cos \Theta| \leq 1$. Consequently by taking $\beta$ as zero, we find the initial value ($i_0$) of the angle ($i$) between the ray direction and the radial vector as

$$\tan i_0 = \tfrac{1}{2} \tan \psi \tag{8}$$

Next, the refractive index (1) and Snell's laws (4) and (5) provide the fundamental equations for ray tracing. That is,

(a)
$$\frac{r f_0}{\sqrt{f f_H}} \frac{\sin \beta}{\sqrt{(\cos \Theta - f/f_H)}} = \text{const.} \tag{9}$$

(b)
$$\frac{f_0}{\sqrt{f f_H}} \frac{\cos \beta}{\sqrt{(\cos \Theta - f/f_H)}} = \text{const.}$$

or
$$\frac{\cos \beta}{\sqrt{(\cos \Theta - f/f_H)}} = \text{const.} \tag{10}$$

In this case, $\beta = (\Theta + \psi)$ (see Fig. 1) and $i = \Theta + \alpha + \psi$, where $\alpha$ is calculated from (1) and (6) as

$$\tan \alpha = -\frac{1}{2}\frac{\sin \Theta}{\cos \Theta - f/f_H} \tag{11}$$

Therefore

$$\sin \beta / \sqrt{(\cos \Theta - f/f_H)} \tag{12}$$

and

$$\cos \beta / \sqrt{(\cos \Theta - f/f_H)} \tag{13}$$

are regarded as functions of $i$ with $\psi$ and $f/f_H$ as parameters. Accordingly we find the angle $i$ of the ray at every height provided that in advance we prepare the

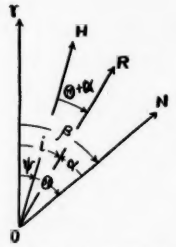


Fig. 1. Diagram showing radial direction ($r$), magnetic field ($H$), ray direction ($R$) and wave-normal ($N$).

charts of (12) and (13) vs. $i$ with $\psi$ and $f/f_H$ as parameters. Then the path in each sector is calculated by (9) and the variation of $i$ at the boundary is determined by (10) through the use of the above explained charts.

## 3. CALCULATION

In the calculation, we have to know $f_0$ or the electron density as a function of $r$. But no plausible electron density distribution in the outer ionosphere has been presented, although a few reports were published such as that by DUNGEY (1954). In our calculation, the following distribution is used on the basis that the observed dispersion ($D$) must agree with the computed value. For the altitudes from 1000 km to 16,500 km over all latitudes,

$$N = 1{\cdot}8 \times 10^{11} \exp\{-6{\cdot}57 \times 10^{-4}(h - 300)\} \quad \text{per m}^3 \tag{14}$$

And for the altitudes from 300 km to 1000 km, two types of distribution are adopted for low-latitude and high-latitude zones, respectively:

(i) for low latitudes (35°N ~ 35°S)

$$N = 1{\cdot}24 \times 10^{12} \exp\{-3{\cdot}45 \times 10^{-3}(h - 300)\} \quad \text{per m}^3 \tag{15}$$

(ii) for high latitudes (90°N ~ 35°N, 35°S ~ 90°S)

$$N = 1{\cdot}8 \times 10^{11} \exp\{-6{\cdot}57 \times 10^{-4}(h - 300)\} \quad \text{per m}^3 \tag{14}$$

where $h$ is the height in kilometres. For heights greater than 16,500 km, we assume the distribution to follow the relation

$$rf_0/\sqrt{f_H} = \text{const.} \tag{16}$$

As to the gyrofrequency, the earth's magnetic field is regarded as that produced by a centred magnetic dipole.

The calculation of the paths was carried out for those starting from the latitudes 15°, 30° and 50°N on the ground under the approximation $f/f_H \simeq 0$. These paths are independent of the frequency $f$. Another calculation was also made using the equations (9) and (10), that is, without the approximation $f/f_H \simeq 0$. These paths depend on the frequency, hence the different paths of $f = 10$, 20 and 30 kcs starting from the same latitude 40°N were obtained. The calculated paths are illustrated in Fig. 2. The arrows on it show the starting points (lightning flash).

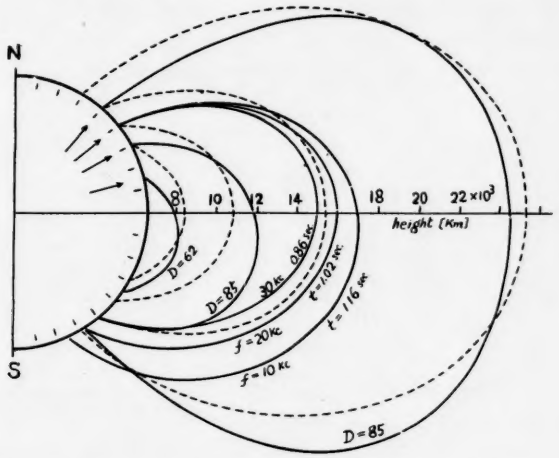


Fig. 2. Ray paths (solid curves) and the lines of magnetic force (dotted curves) produced by a centred magnetic dipole; $t$ on the curves indicates the calculated propagation time.

As seen in the figure, the paths are generally asymmetric with respect to the magnetic equator. This tendency is more predominant for the paths from lower latitudes. These configurations, however, may alter according to the distribution of the electron density. And after several trials, we find that the more slowly the electron density decreases above the ionosphere, the more asymmetrical the path becomes. The result obtained when $f/f_H$ was not ignored shows the frequency characteristics of the path, that is, higher frequency components of a whistler take more inner paths than the lower frequency components.

The propagation time of a whistler is computed by an integration

$$t = \frac{1}{\sqrt{f}} \frac{1}{2c} \int \frac{f_0}{\sqrt{f_H}} \frac{\cos \alpha}{\sqrt{(\cos \Theta - f/f_H)}} \frac{\cos \Theta}{(\cos \Theta - f/f_H)} ds \tag{17}$$

The numerical computation of (17) over the calculated paths gives the frequency vs. time characteristics. This characteristics will be able to explain the nose whistler observed in high latitudes, although our calculation for the paths of 10, 20 and 30 kcs from 40°N does not show exactly a nose figure. Needless to mention,

for the path calculated under the assumption $f/f_H \simeq 0$ the dispersion ($D$) (the proportional constant of $t \propto f^{-\frac{1}{2}}$) is obtained by the numerical integration

$$\frac{1}{2c}\int \frac{f_0}{\sqrt{f_H}} \frac{\cos\alpha}{\sqrt{\cos\Theta}}\, ds \tag{18}$$

## 4. CONCLUSION

According to our calculation the paths deviate much from the lines of the magnetic field and we cannot expect that the paths are always symmetrical with respect to the magnetic equator. This conclusion will cause much trouble in the explanation of the long whistler and the whistler train. But this trouble will be removed if we consider that under an appropriate distribution of the electron density the paths become nearly symmetrical especially for the waves starting from higher latitudes as seen from Fig. 2.

## REFERENCES


| | | |
|---|---|---|
| BREMMER H. | 1949 | *Terrestrial Radio Waves* p. 301. |
| DUNGEY J. W. | 1954 | *The Physics of the Ionosphere* pp. 229–236 |
| MAEDA K. and KIMURA I. | 1956 | *Rep. Ionos. Res. Japan* **10,** No. 3, 105. |
| STOREY L. R. O. | 1953 | *Phil. Trans.* A **246,** 113. |


VOL. 15 1959

## DISCUSSION

SIR EDWARD APPLETON—The original experiments of C. T. R. WILSON showed that there is a discontinuity in the electric field due to an electric moment having been destroyed. Then F. W. CHAPMAN and I increased the time scale and detected a slow destruction of the moment and this gives rise to the leader flash. Then we have a thermal tongue current going down and then comes the atmospheric. The frequency after the main discharge tended to decrease.

DR. MORGAN—At the Radio Meteorology Commission yesterday we discussed why most lightning flashes do not produce whistlers. Dr. HELLIWELL and myself have both found that those which do produce whistlers have maximum energy at frequencies as low as 5 kc/s. Recent lightning studies suggest that some flashes may be as long as 100 miles.

DR. BERKNER—The current intensity in a lightning flash varies enormously and this needs to be considered. Associated with large currents one must of course have many dipoles. The implication of the whistler work is that longer wavelengths travel over longer paths. Is this the whole explanation or is it a question of a lower group velocity?

DR. MANNING—I should like to report very briefly on the whistler studies which Dr. HELLIWELL is conducting at Stanford. In the first "conjugate point" test of STOREY's theory in December 1954 we found that lightning discharges causing "short" whistlers can produce outstanding atmospherics at the receiver. Thus very strong atmospherics recorded on the U.S.S. *Atka* in the southern hemisphere were correlated with short whistlers at Stanford. In a later co-operative experiment between Boulder and Stanford the discharges producing long whistlers

were located with direction finders and the broadband waveforms were obtained. We found that the effective atmospherics were quite dispersive and showed a peak intensity at frequencies lower than average (~5 kcs). We also found that whistler-producing atmospherics occurred more often over water than over land. A discrepancy of up to 0·4 sec was observed between the actual time of origin and that obtained from the Eckersley-law extrapolation of the whistler. This discrepancy can be explained in terms of "nose" whistler theory.

Wideband recordings at Stanford with low-noise equipment have demonstrated the existence of quite important high-frequency components above 10 kcs and extending sometimes to 35 kcs. The observations have led to the development of a new dispersion equation which is valid for these higher frequencies. We have observed at medium latitudes "nose" whistlers having the predicted nose frequencies and from nose-whistler data we estimate that the electron density varies from several thousand per cubic centimetre at one or two earth radii to a few hundred per cubic centimetre at four or five earth radii.

These observations of whistler components above 10 kcs were the basis of the first man-made test of the Eckersley–Storey theory of whistler propagation. In January 1957 whistler-made echoes from station NSS on 15·5 kcs were detected at Cape Horn. The measurements confirmed whistler theory and furthermore showed that the path, or magneto-ionic duct, is open far more often than the occurrence of whistlers would indicate. We found that there was severe and relatively rapid fading together with frequent echo splitting, an observation which demonstrated the existence of multiple and unstable propagation paths such as could account for multiple whistlers. The apparent attenuation in the magneto-ionic duct must be interpreted with care since the energy of the signal may be influenced as the result of interaction with incoming solar corpuscular streams.

Dr. Morgan—My evidence does not support the suggestion that atmospherics over sea are more effective in producing whistlers than those occurring over land.

Sir Edward Appleton—Atmospheric studies always indicate more lightning flashes over land than over sea.

Professor Chapman—Is there any difficulty in having a neutral layer above the ionosphere—it would not appear that a continuous distribution of electron density is required? Does my theory of the outermost ionosphere offer any difficulties to whistler theory?

Dr. Manning—As far as I can see, there are no serious difficulties.

Dr. Gallet—In recent months we have had considerable success in observing whistlers using a large antenna some 2800 ft long and 800 ft high supported between two hilltops. Some of our findings are as follows:

(i) The number of whistlers is really always very great. With this large aerial and using low-noise amplifiers there is no difficulty in always observing large numbers of whistlers.

(ii) The number of whistlers observed shows a rapid fall from winter to summer. This effect we believe is due to transmission changes and not to a seasonal change in the incidence of lightning.

(iii) The area of "receivability" of a given whistler is really quite large. The same whistlers have been observed at Stanford and Boulder.

(iv) Whistlers do not seem to be propagated during the first part of a magnetic storm but the number of whistlers is definitely greater about $1\frac{1}{2}$ days after the day of storm maximum.

(v) The so-called "dawn chorus" can be observed at all times and is not necessarily a dawn phenomenon.

We have also observed two types of v.l.f. emissions ("continuous" and "discrete") which are strongly related to magnetic disturbance but which have nothing to do with lightning discharges. These v.l.f. emissions are associated with the incidence of aurorae and the production of these emissions seems closely related to magnetic storms and corpuscular streams. The continuous hiss suggests a continually flowing stream and the discrete types of emission suggest sharp clouds. The two types of v.l.f. emission are not mutually exclusive and sometimes we observe them occurring together. The required clouds would appear to be small—of the order of 50 km or so—I do not know how these might be produced. This v.l.f. emission and whistlers are sometimes associated and sometimes whistlers appear to degenerate into the discrete v.l.f. hiss. There is plenty of evidence that the propagation of these v.l.f. emissions is similar to that for whistlers and shows the same order of dispersion. We suggest that the physical process is that of the travelling wave tube mechanism with an electromagnetic wave interacting with a stream of ionized gas. The interaction between the wave and the ionization stream (which is really a modulation of the density of ionization), is strongest when they are moving at approximately the same velocity. The interaction is a selective phenomenon in that the whistler electromagnetic wave will interact with those electrons which have the appropriate velocity. The delay in the e.m. wave can be quite appreciable and theoretically the velocity may be as low as c10 to c100—it can be as low as 3000 km/sec.

If we accept an explanation in terms of interaction between the e.m. wave and corpuscular streams then we find that the velocity required is at least 10,000 km/sec which fits with that required to explain aurorae but is, of course, much too large for the usual delay time between solar phenomenon and magnetic storms.

One can show that the electron density at great distances from the earth might be expected to be proportional to the magnetic field intensity $H$ and this to fall off as $1/r^3$. Our observations of whistlers and v.l.f. emissions show clearly that the electron density cannot be constant around the earth and the distribution required to explain our results fits in well with the $1/r^3$ law. If the electron density increases faster than $1/r^3$ as we approach the earth then we should expect whistlers with rising tones and vice versa. We have been able to study the electron density/distance distribution well above the *F2* maximum and, although there is a general fall off as $1/r^3$, we have found evidence for a secondary maximum at a height of 2000 km or so with a scale height of 300 to 400 km.

SIR EDWARD APPLETON—Has anyone measured the polarization of whistlers?



VOL. 15 1959

MR. J. WATTS—We have tried at Boulder but have not obtained any satisfactory answer.

MR. RATCLIFFE—But surely it will be very complex since a wide range of angles of incidence is involved.

DR. GALLET—The area of reception is certainly large.

DR. SINGER—The velocities of the particles will change as they progress along the field—except for those with very small pitch angles. Fast-moving particles may be expected to emit Cerenkov radiation and the mechanism proposed by Dr. GALLET raises problems of the bunching of particles and of the power of the radiation.

DR. GALLET—In the case of Cerenkov radiation we are concerned with radiation of single particles whereas here we have a stream of particles in a highly dispersive medium. We have a sort of e.m. shock wave.

I have considered another mechanism involving the deceleration of particles because of pitch but I have not worked this out in any detail. There is a theoretical objection relating to the magnetic fields associated with clouds of particles.

DR. MENZEL—Your mechanism will work with clouds of electrons but not protons?

DR. GALLET—No. I need a neutral stream.

DR. MENZEL—But the energies of the protons are such that they will drag the electrons along with them.

DR. CHAMBERLAIN—Even if electrons are dragged along with protons, there must be some slowing down of the mechanism.

DR. SINGER—One must consider the variation in pitch angle and somehow bring this into the theory.

DR. GALLET—Computation shows that it is difficult to separate positive and negative particles, but I do not suggest that there is no dispersion or diffusion of these clouds along the lines of force.

OL.
15
959

Journal of Atmospheric and Terrestrial Physics, 1959, Vol. 15, pp. 66 to 67. Pergamon Press Ltd. Printed in Northern Ireland

# SESSION VI

## Resolutions

At the final session the following Resolutions were drafted:

1. *Ionospheric current systems*

(i) The MCI expresses the hope that new determinations of the $S_q$ and $S_D$ electric current systems in the ionosphere will be made on the basis of the IGY magnetic records.

(ii) The MCI invites the International Association of Geomagnetism and Aeronomy to consider the possibility of determining the latitudes of the foci of the $S_q$ current systems at one or more longitude on as many days as possible during the IGY.

2. *Ionospheric data for quiet and disturbed days*

The MCI recommends that in ionospheric tabulations the data for the five selected international magnetically quiet and disturbed days should be extracted and mean values tabulated.

3. *Region-E parameters*

The MCI reaffirms its earlier resolutions on the need for accurate scaling and timing of region-$E$ parameters. It recommends that recordings of the $E$-region trace on ionograms should be made on expanded frequency scales. It further recommends that especial attention should be given to the measurement of $h'E$ at stations located near the magnetic equator.

4. *Ionospheric tidal phenomena*

The MCI calls attention to the need for studies during the IGY of lunar tidal oscillations in the $E$ and sporadic-$E$ layer parameters—$h'E$, $fE$, $h'E_s$.

5. *Region-E isoelectronic contours*

The MCI recommends that some central organization should compute, from all available IGY data maps showing normal region-$E$ isoelectronic contours. Such contour maps would greatly facilitate the study of perturbations from normality in this region.

6. *Height and frequency scales of ionograms*

The MCI recommends that during the IGY, the URSI World Soundings Subcommittee should be charged with the control of relative and absolute scales of height and frequency. The increased reading accuracy might then permit not only studies of relative changes but also inter-station comparison.



VOL.
15
1959

7. *Measurements of horizontal ionospheric movements*

The MCI recommends that there should be the fullest co-operation between stations studying horizontal movement so that the world pattern of such motion may be elucidated.

8. *Electron density/height profiles* ($N,h$)

The MCI recommends that organizations which undertake the calculation of $N,h$ profiles should interchange sample ionograms and the corresponding calculated profiles, so as to ensure agreement on the results obtained by different methods.

9. *Rocket investigations in auroral latitudes*

The MCI recommends that a more intensified small rocket programme should be carried out in auroral latitudes to study particle and other radiation at levels below 90 km.

10. *Region-F2*

The MCI recommends that each IGY vertical sounding station, or the responsible central organization should be invited to calculate the hourly departures of $fF2$ from the smooth curve drawn through the monthly mean or median values.

OL.
15
959

11. *Ionospheric irregularities*

The MCI recommends that groups observing rapidly moving ionospheric irregularities should be encouraged to continue this work and to interchange results. It is also strongly recommended that studies of all ionospheric movements should be arranged on a local or regional basis.

12. *Nomenclature*

The MCI recommends:

(i) That the total ionization content per unit column in that part of an ionized region below its peak be designated the "sub-peak electron content" of the region.

(ii) that the present terminology on "whistlers" ("nose-whistlers", etc.,) should be regarded as tentative and that a study of a more appropriate terminology should be immediately undertaken.

(iii) that the letter $A$ be used to designate auroral ionization resulting directly or indirectly from the entry into the earth's atmosphere of solar particles: also that the subdivisions of this ionization be indicated as follows:

$Aa$ auroral ionization due to primary atomic particles
$Ae$ auroral ionization due to electrons
$Ax$ auroral ionization due to X-radiation
$Au$ auroral ionization due to ultra-violet radiation
$Ar$ auroral ionization due to photo-detachment by red radiation.

*Secretary of Mixed Commission on the Ionosphere.* W. J. G. Beynon
*August*, 1957.

Journal of Atmospheric and Terrestrial Physics, 1959, Vol. 15, pp. 68 to 72. Pergamon Press Ltd. Printed in Northern Ireland

## PART 2: PAPERS SUBMITTED TO THE COMMISSION

# The morphology of the lower ionospheric region in auroral latitudes

S. MATSUSHITA*

IN auroral latitudes, lower ionospheric regions show special phenomena, compared with those in middle latitudes. Special types of sporadic-$E$ which are named "auroral", "slant" and "retardation" $E_s$ often occur during the night in this region. Distributions of these $fE_s$ values at night on geomagnetic latitudes increase at latitudes higher than about geomagnetic 60°N, and reach the maximum at about 69°N (MATSUSHITA, 1953), as shown in Fig. 1. However, $fE_s$ in the daytime does not show such a distribution. Another interesting phenomenon in auroral latitudes is no-echo in ionograms called "polar blackout". This phenomenon has been studied by many workers in the field. APPLETON *et al.* (1937) found that the phenomenon occurred at Tromsö during magnetic disturbances, and WELLS, (1947) using data from College, Alaska, for 1942, reported briefly that polar blackouts occurred during magnetic bays. However, the polar blackouts also occur even on magnetically quiet days. In connexion with the study of ionospheric storminess, MEEK (1952) examined the diurnal and seasonal variation of the occurrence of blackouts. PIGGOTT (1953) and AGY (1954 a, b) obtained geographic and temporal distributions of polar blackouts. These reported results are not always consistent in showing correlations between ionospheric blackouts (hence radio absorbing region) and geomagnetic phenomena. In this communication, the writer describes relations among blackouts, complete blanketing of *F2* by abnormal-$E$, slant-$E_s$ and geomagnetic bay. Interesting correlations between lower ionospheric and geomagnetic phenomena are obtained. The morphological results are two types of absorbing regions in auroral latitudes. An effect of X-rays generated from auroral particles to form these absorbing regions (MATSUSHITA, 1956) is then described in this report.

The data used were both ionograms obtained every 15 min with vertical-incidence ionosondes (NBS, Model C-3) and magnetograms made at College (64·9°N, 147·8°W; g.m. lat. 64·5°N) and Point Barrow (71·3°N, 156.8°W; g.m. lat. 68°N), Alaska, during the period of 1 year starting from March 1955. For purposes of analysis, the data were classified into quiet ($Ap < 16$) and disturbed days ($Ap \geq 16$) during three seasons—summer months (from May to Aug.), equinoctial months (March, April, Sept. and Oct.) and winter months (from Nov. to Feb.). Ionograms made during periods in which there were troubles of the ionosonde were carefully eliminated to distinguish real blackouts.

In auroral latitudes, large magnetic bays often occurred at night, most frequently at 0100–0300 hours local time, even on small $Ap$ days, particularly in equinoctial

* Geophysical Institute, Kyoto University, Japan.

months. Average occurrence frequencies of bays during an equinoctial month were about 30 per cent for negative bays, and about 15 per cent for positive bays. The positive bay occurred before 2200 or 2300 hours local time, and the negative bay occurred after that time. When the range of horizontal component of the bay at College was moderate (100–200$\gamma$ ($Ap < 16$) and 200–300$\gamma$ ($Ap \geq 16$) for positive bays, and about 200$\gamma$ ($Ap < 16$) and 300–400$\gamma$ ($Ap \geq 16$) for negative bays), complete blanketing of *F2* by increased $E_s$ always occurred, corresponding to the time at which the bay took place. The above-mentioned $fE_s$ distribution

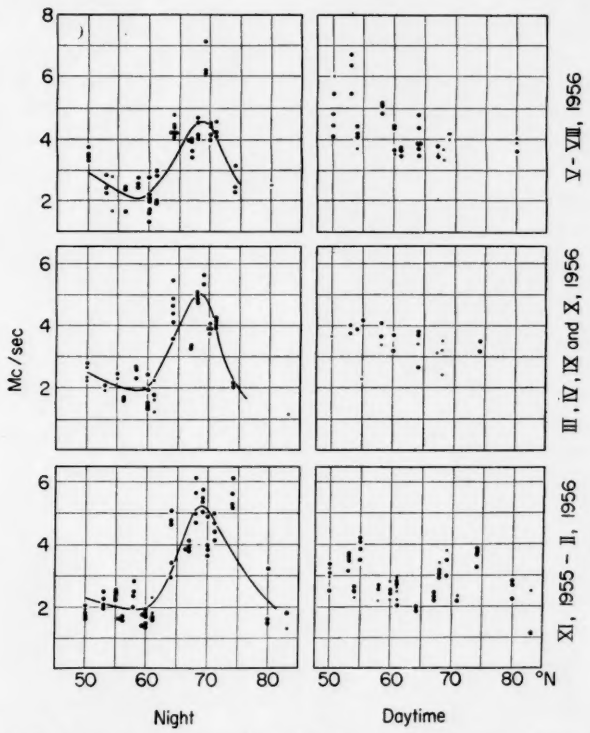


Fig. 1. $fE_s$ distributions on geomagnetic latitudes at night (mean of monthly median values from 2200 hours to 0200 hours local time) and in the daylight hours (mean values from 1000 hours to 1400 hours) during three seasons. Small dots express less reliability than large dots.

at night may be explained by this relation. The storm-*E* named by PIGGOTT (1953) seems to be this phenomenon. When the range of bays was larger than above values, the blackout usually occurred after the incidence of complete blanketing of *F2*. This is called "gradual blackout" in the present study. Fig. 2 shows examples of these relations. When the range of bays was smaller than about 100$\gamma$, no remarkable variation occurred in ionograms. In this study the multiple type of $E_s$ which blanketed the upper ionosphere was ignored; in fact, it did not frequently occur. This type of $E_s$ had no correlation with magnetic variations.

As will be seen in Fig. 1, a type of sporadic-$E$, called "slant-$E_s$", occasionally appeared during bays, particularly during positive bays (half of the positive bays were associated with the slant-$E_s$ at College), and it never occurred except during bays or bay-type variations during magnetic storms. The time of most frequent occurrence of slant-$E_s$ was 1800–2000 hours local time on disturbed days. From the modes of radio propagation for slant-$E_s$, which have been suggested by SMITH (1955), the occurrence of slant-$E_s$ indicates the formation of an ionized region which scatters radio waves under the $E$-level. In other words, an ionized region is occasionally formed under the $E$-level during magnetic bays.

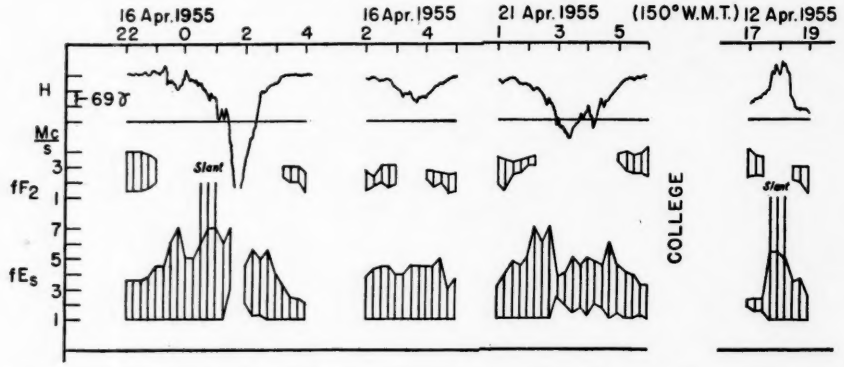


Fig. 2. Examples of the occurrence of complete blanketing of $F2$, gradual blackouts, and slant-$E_s$, associated with magnetic bays, at College, Alaska. Variations of $f_0F2$, $f$-min-$F$, $fE_s$ and $f$-min, every 15 min, and of geomagnetic horizontal component are compared in this figure.

These results on the occurrence of gradual blackouts, complete blanketing of $F2$ by increased $E_s$, and slant-$E_s$, associated with bays, imply an increase of ionization for middle magnitude of bays, and of night-time absorption of radio waves for large magnitude of bays, in the level of 80–100 km which are responsible for the electric current producing the magnetic variation.

During the daytime, 0800–2000 hours in auroral latitudes, blackouts often occurred suddenly both on quiet and disturbed days without any relating magnetic variations. This is named "sudden blackout" in the present study, and has maximum occurrence frequency at 1100–1400 hours on disturbed days. This sudden blackout means that the height of absorbing region during daylight hours is lower than that at night; in other words, lower than the level responsible for the geomagnetic variation. Accordingly, $fE_s$ distribution in the daytime on geomagnetic latitudes is vague as shown in Fig. 1. We may conclude, therefore, that there are two different blackouts—gradual blackout which occurs only at night and sudden blackout in the daytime—and that the radio absorbing regions for the two are situated at different heights. Many morphological works on polar blackouts were confused for these two different blackouts, since they treated the two together.

For non-deviative absorption of the ordinary component of radio waves, the



VOL. 15 1959

absorption along the path through a stratum of $S$ (APPLETON, 1937) is expressed in decibels as follows:

$$\int K\,ds \simeq \frac{A}{(f+f_L)^2}\int N\nu\,ds$$

where $N$ is electron number density, $\nu$ is the effective electron collision frequency, $A = 1{\cdot}17 \times 10^{-14}$, and $f$ and $f_L$ are the radio and gyromagnetic frequencies expressed in Mc/s:

$$f_L = 10^{-6}eH\cos\theta/2\pi mc = 2{\cdot}80\,H\cos\theta \qquad \text{(e.s.u.)}$$

in which $c$ is the velocity of electromagnetic waves in a vacuum, $e$ and $m$ are electron charge and mass, and $\theta$ is the angle between the direction of wave propagation and the geomagnetic field $H$ (gauss).

At College, $H\cos\theta$ for vertical incidence is 0·55 gauss, and $f_L$ is 1·54 Mc/s. For the phenomenon of polar blackouts, 15 Mc/s may be sufficient for the value of $f$. Accordingly,

$$\int K\,ds = 4{\cdot}27 \times 10^{-17}\int N\nu\,ds$$

To find the order of the value $N$, we assume that the thickness of the layer responsible for the polar blackout is 10 km. The order of the values $\nu$ in different heights is assumed as follows:

| Height (km) | 50 | 70 | 85 | 100 |
|---|---|---|---|---|
| $\nu$ | $10^8$ | $10^7$ | $10^6$ | $10^5$ |

Then the order of magnitude of $N$ for the absorption of 10 db is

| Height (km) | | 50 | 70 | 85 | 100 |
|---|---|---|---|---|---|
| $N$ | $2{\cdot}34\times$ | $10^3$ | $10^4$ | $10^5$ | $10^6$ |

From this calculation, we must have $10^3$–$10^4$ electrons per unit volume in the daytime and $10^5$–$10^6$ at night, to explain the statistical results. The solar charged particles of high energy may ionize to this extent at 90–100 km. Accordingly, the complete blanketing of *F2* and the gradual blackouts at night may occur due to auroral particles. However, these particles seem to be difficult to reach and ionize to the extent of the above obtained order of $N$ at levels lower than 80 km.

VAN ALLEN (1955) observed by a rockoon that X-rays penetrated to levels as low as 50 km in auroral latitudes. He estimated that the production of electron–ion pairs by these X-rays was $10^8$/cm²-column/sec. During intense absorption, it may be reasonable to estimate that the value is $2 \times 10^9$/cm² sec in a 10 km thickness at 70–80 km. Then the electron production rate $Q$ is $2 \times 10^3$/cm³/sec. If $Q/(1+\lambda) = \alpha N^2$, (where $\alpha$ is the effective recombination coefficient and $\lambda$ is the ratio of the density of negative ions to that of electrons, which is maintained for steady states) then $N = 10^4$ for $\alpha = 10^{-6}$ and $\lambda = 20$ in the daytime at about 70 km. Accordingly, these X-rays generated by the primary bombarding particles from the sun, as also suggested by CHAPMAN and LITTLE (1957), may be an important factor in explaining the absorption in auroral latitudes, particularly

the sudden blackout in the daytime. Lyman-$\alpha$ radiation generated by the auroral protons, which was pointed out by BATES (1956), may also contribute to the absorbing region.

The electrons become increasingly attached to form negative ions below about 100 km. However, $\lambda$ may be smaller, by photo-detachment, than that at night. Therefore, the same X-ray produces a weaker absorbing region by night than by day, at lower levels than the $E$. This effect may be sufficient to outweigh that of a greater flux of primary particles at night, as CHAPMAN (1957) has suggested. The difference between sudden blackouts in the daytime and gradual blackouts at night may be explained by this effect.

The magnetic bay seems to occur in a patchy structure due to patchy flux of primary particles. The increase of electron number density due to these particles (and X-rays) causes an increase of electric conductivity in the region responsible for the magnetic variation mainly at night; hence, bays are explained by the dynamo theory in the same way as the calculation of the $S_D$ variation (FUKUSHIMA, 1949; MATSUSHITA, 1953). For the tendency of recurrence of bays during 2–4 days even on quiet days and for its patchy structure, we may suggest an effect of deflection of the path of solar particles due to the magnetic field of magnetized gas clouds (PARKER, 1956) which may be situated in the interplanetary space.

We may finally conclude that these obtained morphological results on sporadic-$E$ and absorbing regions in auroral latitudes are explained by the effect of solar particles deflected by magnetic gas clouds, and of X-rays generated by these particles.

VOL. 15 1959

In conclusion, the author wishes to express his sincere gratitude to Dr. W. O. ROBERTS, Mr. A. H. SHAPLEY, Dr. S. CHAPMAN and Mr. V. AGY for their kind help and advice.

## REFERENCES


| | | |
|---|---|---|
| AGY V. | 1954a | *J. Geophys. Res.* **59,** 267, 499. |
| AGY V. | 1954b | *Nature, Lond.* **173,** 445. |
| APPLETON E. V. | 1932 | *J. Inst. Elect. Engrs.* **71,** 642. |
| APPLETON E. V. | 1937 | *Proc. Roy. Soc.* A **162,** 451. |
| APPLETON E. V., NAISMITH R. and INGRAM L. J. | 1937 | *Phil. Trans.* A **236,** 191. |
| BATES D. R. | 1956 | *Ann. Geophys.* |
| CHAPMAN S. and LITTLE C. G. | 1957 | *J. Atmosph. Terr. Phys.* **10,** 20. |
| FARMER F. T. and RATCLIFFE J. A. | 1935 | *Proc. Roy. Soc.* A **151,** 370. |
| FUKUSHIMA N. | 1949 | *Geophys. Notes, Tokyo Univ.* **2,** No. 21. |
| MATSUSHITA S. | 1953 | *J. Geomagn. Geoelect. Kyoto* **5,** 109. |
| MATSUSHITA S. | 1956 | *J. Geomagn. Geoelect. Kyoto* **8,** 156. |
| MEEK J. H. | 1952 | *J. Geophys. Res.* **57,** 177. |
| MEREDITH L. H., GOTTLIEB M. B. and VAN ALLEN J. A. | 1955 | *Phys. Rev.* **97,** 201. |
| PARKER E. N. | 1956 | *Phys. Rev.* **103,** 1518. |
| PIGGOTT W. R. | 1953 | *Nature, Lond.* **171,** 124. |
| SMITH E. K. | 1955 | National Bureau of Standards Report No. 3575. |
| VAN ALLEN J. A. | 1955 | *Phys. Rev.* **99,** 609. |
| WELLS H. W. | 1947 | *Terr. Magn. Atmos. Elect.* **52,** 315. |

Journal of Atmospheric and Terrestrial Physics, 1959, Vol. 15, pp. 73 to 76. Pergamon Press Ltd. Printed in Northern Ireland

# Interpretation of some features of low-frequency ionograms

J. M. WATTS*

BY the routine use of a low-frequency ionosonde in the frequency range 50 kcs to 2 Mcs reliable observations of detailed reflections at normal incidence from the $E$-region at night are possible (WATTS and BROWN, 1954). At the National Bureau of Standards Boulder Laboratory recordings of this type are being made using a large mountain-suspended antenna, which is particularly effective at the low frequencies.

This paper will discuss only one aspect of the low-frequency ionograms, a type of retardation which has proved interesting and which seems to be of definite value in the study of the night-time ionosphere. It is illustrated by Figs. 1 and 2. Fig.1 contains the ordinary, $O$, and extraordinary, $X$, traces from the $F$-layer. Both are eclipsed at their low-frequency ends by reflections from the region below. In the region near 0·9 Mcs they are separated owing to the retardation of the extraordinary ray near the gyrofrequency. Since the extraordinary ray suffers high absorption near the gyrofrequency, it is undetectable above 1 Mcs. There is no obvious indication of the distribution of ionization below the $F$-layer, except perhaps the small cusp at the low-frequency end of the ordinary ray trace. The reflections from near 100 km virtual height will not be discussed except to mention that the region is obviously transparent to extraordinary ray polarization above 0·1 Mcs since the extraordinary trace from the $F$-layer is perfectly recorded above it.

The reader's attention is next called to Fig. 2, an ionogram made later the same night. The separation of the $O$- and $X$-traces of the $F$-layer is much greater than in Fig. 1. There is a definite cusp at the low-frequency end of the $O$-trace, causing it to cross the $X$-trace at a frequency near which a distinct perturbation (at $A$) of the $X$-trace occurs. This perturbation takes the form of increased retardation and is almost always associated with the frequencies near the cusp on the $O$-trace. Examination of many night-time records has shown that this phenomenon always occurs when there is a distinct layer between the $F$-layer and $E$-region and suggests an interdependence of the $O$- and $X$-rays not observed in ordinary high-frequency ionograms, where the reflections are almost entirely from a region having plasma frequencies above the gyromagnetic frequency. However, the curves of refractive index in Fig. 3 suggest an important difference in the propagation of the extraordinary waves for frequencies above and below the gyromagnetic frequency (BOOKER, 1950). Here, as usual, $X$ is equal to the square of the ratio, plasma frequency to wave frequency; and $Y$ is the ratio of gyromagnetic frequency to wave frequency. A high-frequency wave proceeds to the reflection level $X = 1 - Y$ without incident, the ordinary wave penetrates further and is reflected at the $X = 1$

* National Bureau of Standards, Boulder Laboratories.

level. In the case of a frequency below the gyromagnetic value ($\omega = 1/2\omega_H$ in Fig. 3) the extraordinary wave not only penetrates farther than the ordinary, until reflected at the $X = 1 + Y$ level, but also passes through a region of inflexion in refractive index near the $X = 1$ level. The abruptness of the inflexion is determined by the angle with respect to the earth's magnetic field of the direction of phase propagation. For purely transverse propagation the effect disappears completely and for longitudinal propagation it becomes a definite discontinuity. Because of this difference in character between ordinary and extraordinary

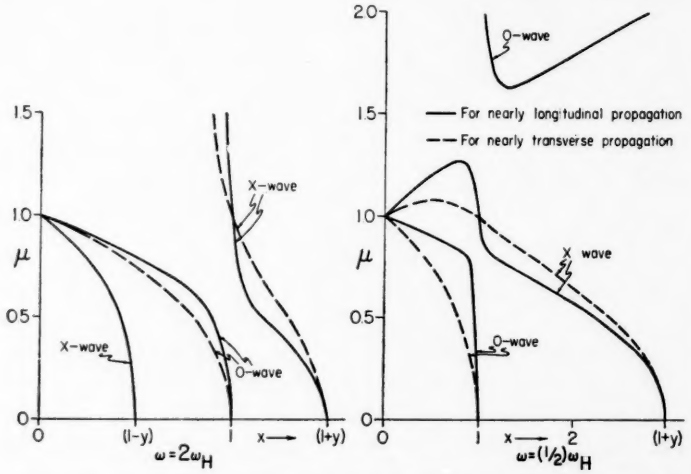


Fig. 3. Refractive index as a function of $X$, no. collisions, for different angles relative to the earth's magnetic field (after BOOKER).

refractive indices it was decided to calculate group velocity of the extraordinary ray, on a sweep-frequency basis, for regions having plasma frequencies below the gyrofrequency. One set of results is shown in Fig. 4 for a plasma frequency of 400 kcs, and the retardation required to explain the observed phenomenon appears as the group-velocity minimum at $A$ on the dashed (extraordinary ray) curve. The writer is indebted to GALLET and ROGERS of the Boulder Laboratories for programming the group velocity on the electronic computor and providing Fig. 4 as one set of results.

SHINN and WHALE (1952), in their investigation of group delays, were interested primarily in high-frequency propagation, but one of their curves (their Fig. 5) when unfolded and replotted on Fig. 4 results in the circled points. The fit is good because the angle of the earth's magnetic field used by SHINN and WHALE was very nearly the same as the one used by GALLET and ROGERS for Boulder, Colorado, conditions.

Some implications of the phenomenon are shown in Fig. 5. Three types of electron distribution below a slab-like $F$-layer are shown: linear, ledge and separate layer. Five frequencies were chosen and the retardations of the extraordinary ray near the $X = 1$ levels are shown—being proportional to the areas in black—on the lines $A$, $B$, $C$, $D$ and $E$. Retardation near the reflection levels is omitted for



VOL. 15 1959

OL.
15
959

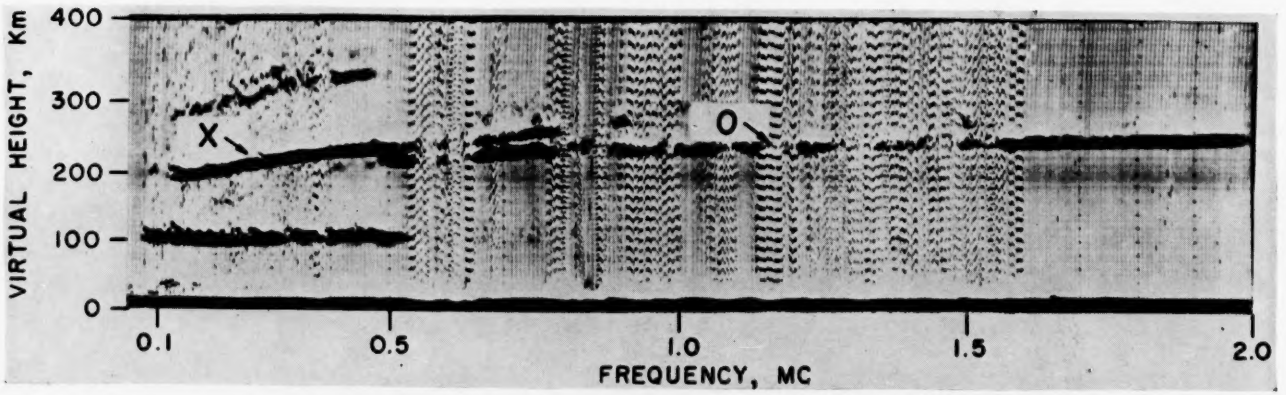


Fig. 1. Low-frequency ionogram 14 March, 1957, 2230 hours MST.

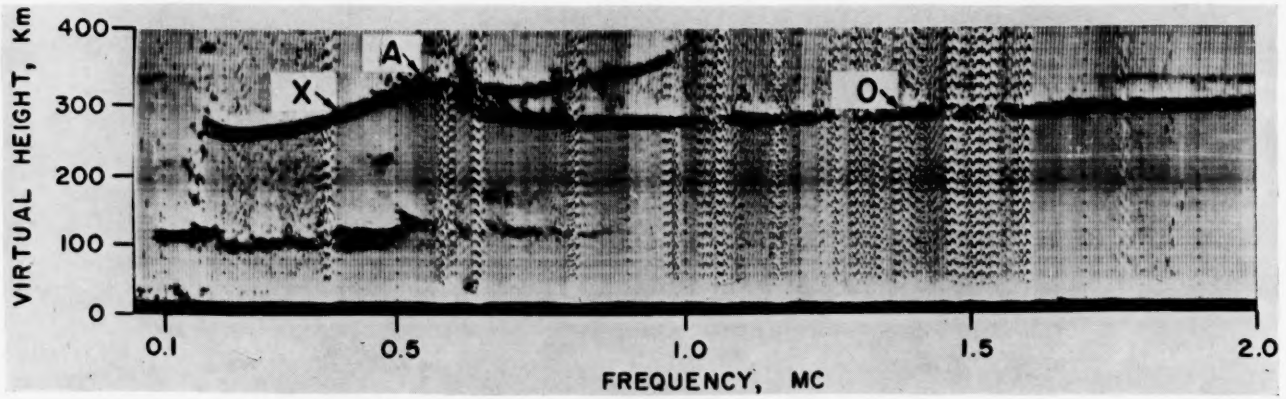


Fig. 2. Low-frequency ionogram 15 March, 1957, 0445 hours MST.

VOL.
15
1959

simplicity, as well as any due to the gyrofrequency proximity (see Fig. 4). It is seen that, in the case of linear distribution, the retardation shows no pronounced maximum at any frequency, although it is still evident after the layer has been penetrated. For a ledge of ionization some frequency can be found so that the wave travels a considerable distance through a density near $X = 1$ (line $B$) and a large maximum in group delay would be observed at that frequency, although complete penetration of the region has already occurred at a lower frequency. In the case of a separate layer, a similar situation can be found (line $C$) and the nose of the layer is indicated by a maximum of group delay after penetration.

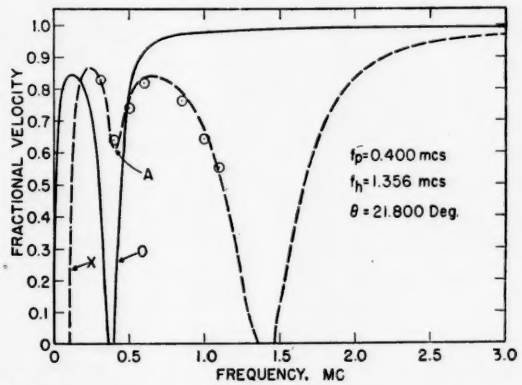


Fig. 4. Group velocity vs. frequency for a critical frequency of 0·400 Mcs at Boulder, Colorado.

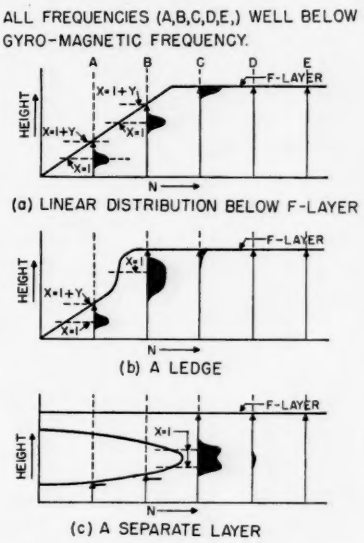


Fig. 5. Retardation of the extraordinary wave for different frequencies and ion distributions.

It is pointed out that the foregoing describes the application of simple ray theory, in the absence of collisions, to explain a phenomenon observed when the intermediate layer (WATTS and BROWN, 1954) affects the appearance of low-frequency ionograms. In the height range, 120 km to 200 km, and frequency range, 150 to 700 kcs, over which the layer may be observed the region seems to be "slowly varying" in its characteristics since the simple theory explains the observed retardation.

As a practical application, the phenomenon allows a layer or ledge to be detected even though no reflection from it is observed. Its critical frequency (or a frequency very near the critical frequency) can be measured by taking the center frequency of the perturbation marked $A$. In addition, by observing the retardation of the extraordinary ray relative to that of the ordinary ray as close to the gyrofrequency as possible, still assuming the $F$-layer to be a reflecting slab, a measure of the total ionization below the $F$-layer may be had. The best procedures for accomplishing these have still to be worked out, and seem to be quite complicated. However,

the opportunity of adding new information concerning night-time *E*-region ionization seems important enough to warrant further study.

## References


| | | |
|---|---|---|
| Booker H. G. | 1950 | *An Outline of the Magneto-Ionic Theory.* Technical Report No. 1, Cornell University School of Electrical Engineering. |
| Shinn D. H. and Whale H. A. | 1952 | *J. Atmosph. Terr. Phys.* **2,** 85. |
| Watts J. M. and Brown J. N. | 1954 | *J. Geophys. Res.* **59,** No. 1, **71.** |


VOL.
15
1959

Journal of Atmospheric and Terrestial Physics, 1959, Vol. 15, pp. 77 to 82. Pergamon Press Ltd. Printed in Northern Ireland

# Effect of the $S_q$ current system on the ionospheric *E*- and *F1*-layers

TATSUO SHIMAZAKI*

**Abstract**—The discrepancy between the observed $f_0E$ or $f_0F1$ and those predicted by the Chapman theory was examined in detail. The result shows that the *F1*-layer varies in a manner more regular than the *E*-layer, and that the discrepancy in the *E*-layer may be attributed partly to the effect of scale height gradient, but the principal cause certainly lies in the effect of $S_q$ overhead current system. Discussion is made on the non-uniform motion of vertical drift velocity produced by this effect, as well as on the recombination coefficient and the scale height gradient in these regions.

## 1. INTRODUCTION

IT has long been believed that the maximum electron density of the ionospheric *E*- and *F1*-layers varies in a fairly regular manner with the $\sqrt{(\cos \chi)}$ law of variation of the simple Chapman layer. Recently, however, more detailed studies of these regions were made by APPLETON *et al.* (1955) and by BEYNON and BROWN (1956), who found a definite departure from the Chapman norm in the *E*-layer. This was considered to be due to the vertical drift effects by the $S_q$ overhead current system that flows in or near the *E*-layer and is responsible for the daily solar magnetic variations. In the present paper the author intends to treat the problem from a more general viewpoint and to evaluate the value of div $v$ which may arise from the vertical drift effect of the $S_q$ current system, as well as the value of recombination coefficient or of the scale height gradient in the ionospheric *E*- and *F1*-regions.

## 2. MATERIAL AND METHOD

Generally speaking, the rate of increase in electron density in the ionosphere can be given by the following well-known equation of

$$\partial N/\partial t = q_0 . F(z,t) - \alpha . N^2 - \text{div}\,(Nv) \tag{1}$$

where the three terms on the right-hand side indicate, respectively, the rate of electron production, of true electron disappearance by recombination, and of apparent increase by electron transport phenomena; $q_0$ is the rate at the production peak when the sun is in the zenith, and is expected to vary with the epoch in the solar cycle.

If it is permissible to assume, as may be fairly justified in the *E*- and *F1*-layers, that the maximum electron density is produced at the level of maximum electron production, the ionization function takes the form

$$F(z_m, t) = (\cos \chi)^{1+\Gamma} \tag{2}$$

where $\Gamma$ is the scale height gradient. Then by following these levels hour after hour, we can get from equation (1)

$$dN_m/dt = q_0 (\cos \chi)^{1+\Gamma} - \alpha . N_m{}^2 - (\text{div } v) . N_m \tag{3}$$

* Radio Research Laboratories, Kokubunji, Tokyo, Japan.

As is easily understood by the order estimation of each term in equation (3), the first two terms on the right-hand side are much greater than the other two terms, i.e. while the first two terms are of the order of $10^2$ cm$^{-3}$-sec$^{-1}$, the last term of the order of 10 cm$^{-3}$-sec$^{-1}$ and the left-hand side term of the order of 1 cm$^{-3}$-sec$^{-1}$ at 0900 or 1500 hours, becoming zero particularly near noon. Thus it can be safely asserted that the first two terms on the right-hand side define the general tendency of variations and the remaining terms only give the effect of perturbation. Consequently we have as the first approximation,

$$(f_0E)^4 \quad \text{or} \quad (f_0F1)^4 = K \,.\, (\cos\chi)^{1+\Gamma} \tag{4}$$

with

$$K = 1/(1{\cdot}24 \times 10^4)^2 \,.\, q_0/\alpha \tag{5}$$

For evaluating the numerical value of parameters such as $K$ and $\Gamma$ from observational data, the writer used the monthly median values of $f_0E$ and $f_0F1$ in March during the years 1952–1954 (near the sunspot minimum) for all available observatories in the world. Then the solar zenith distance $\chi$ was calculated for every observatory for each hour of 0900–1500 hours, taking into account the difference between the geographical longitude of the observatory and that corresponding to the standard local time used at the same observatory.

We illustrate in Fig. 1 the observed distribution of $f_0E$ and $f_0F1$ with $\chi$ by black circles, which indicate the centre of mass of all observational points in every ten degrees of $\chi$ centering at every five degrees. Then against these observational data the most probable values of $K$ and $\Gamma$ in equation (4) are determined for each hour by the least square method. The curves in Fig. 1 indicate the relation of equation (4) thus determined, which shows a noticeable difference from the observed points, particularly in the $E$-layer. This difference is certainly due to the effect of additional perturbing factors which were neglected in equation (4). As is known from the above-mentioned estimates of order, the major effect of these perturbing factors seems to originate in the last term of the right-hand side in equation (3), from which the following formula for obtaining div $v$ can be derived:

$$\operatorname{div} v = q_0 \cdot \left\{ \frac{(\cos\chi)^{1+\Gamma}}{N_m} - \frac{\alpha}{q_0} \,.\, N_m \right\} - \frac{1}{N_m} \cdot \frac{dN_m}{dt} \tag{6}$$

This term produces the effect of non-uniform motion in the ionosphere and the most important effect may arise from the vertical gradient of vertical drift velocity $-\partial v/\partial h$.

## 3. Results and Discussion

We can see in Fig. 1 that the curve is more fitted to the observations in the $F1$-layer than in the $E$-layer. This apparently indicates that the $F1$-layer undergoes a Chapman-like variation according to $\sqrt{(\cos\chi)}$ law. On the other hand in the $E$-layer there can be seen a general tendency for the observed $f_0E$ to be greater (or smaller) at lower (or higher) latitudes as compared with theoretical values of the Chapman layer (broken lines in Fig. 1). This characteristic tendency of discrepancies between experimental and theoretical values in the $E$-layer is somewhat reduced (see solid lines in Fig. 1), if we take account of the effect of scale

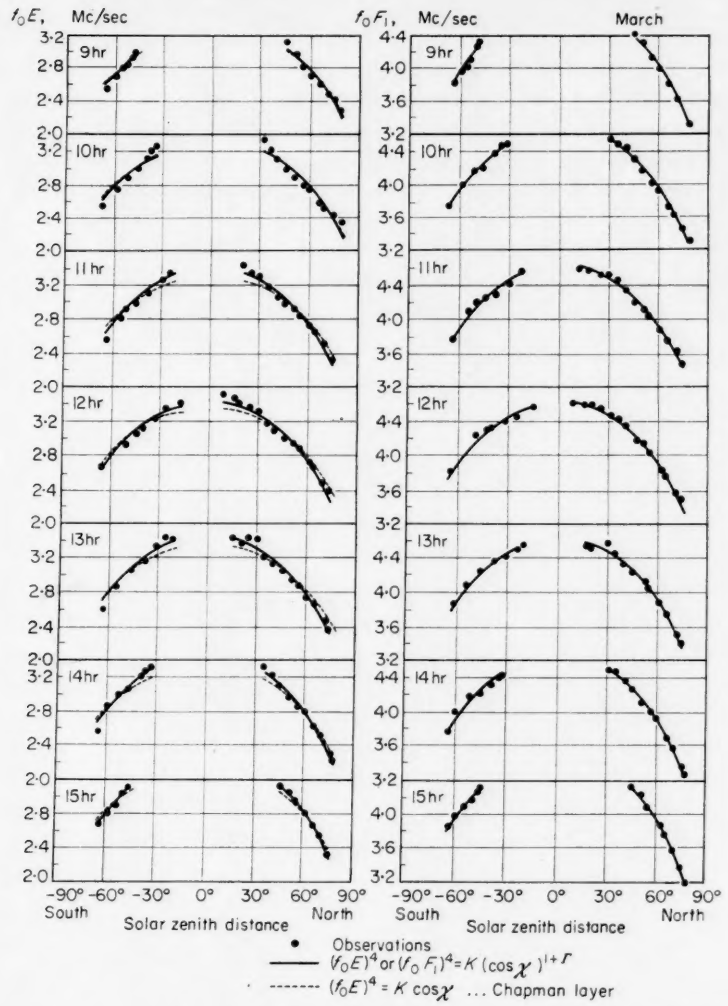


Fig. 1. Comparison of observed $f_0E$ and $f_0F1$ with theoretical curves. Numerical values of $K$ and $\Gamma$ available for each hour are given in Fig. 2.

height gradient and take different values of $\Gamma$ at different hours, which are shown in Fig. 2. It must, however, be noted that even in the latter case there remain observable discrepancies particularly at 1000 or 1100 hours.

### 3.1. *Recombination coefficient* $\alpha$

From the value of $K$ obtained by the least squares method we calculate the value of $\alpha$ at each hour by the use of equation (5). The value of $q_0$ is assumed to be 200 $cm^{-3}$ $sec^{-1}$ in the $E$-layer and 280 $cm^{-3}$ $sec^{-1}$ in the $F1$-layer, so that we may get, on the average, the well-known values of $\alpha \sim 10^{-8}$ and $4 \times 10^{-9}$ $cm^3$ $sec^{-1}$ for these two layers, respectively.

We can see in Fig. 2 a quite different time-dependency of $\alpha$ in these two layers, i.e. in the $E$-layer $\alpha$ is comparatively large in the forenoon and becomes rather small in the afternoon. On the other hand in the $F1$-layer it takes the largest value at noon and gradually decreases as time passes from noon. This difference of variation in $\alpha$ between $E$- and $F1$-layers could supposedly arise from the difference of factors, which are primarily responsible for the variations. Such factors may be the temperature in the $E$-layer and the height of the layer in the case of the $F1$-layer.

3.2. *Scale height gradient* $\Gamma$

As will be seen in Fig. 2 an essential difference does exist between the two layers with regard to the quantity of $\Gamma$ and its temporal variations. In the $E$-layer $\Gamma$ is

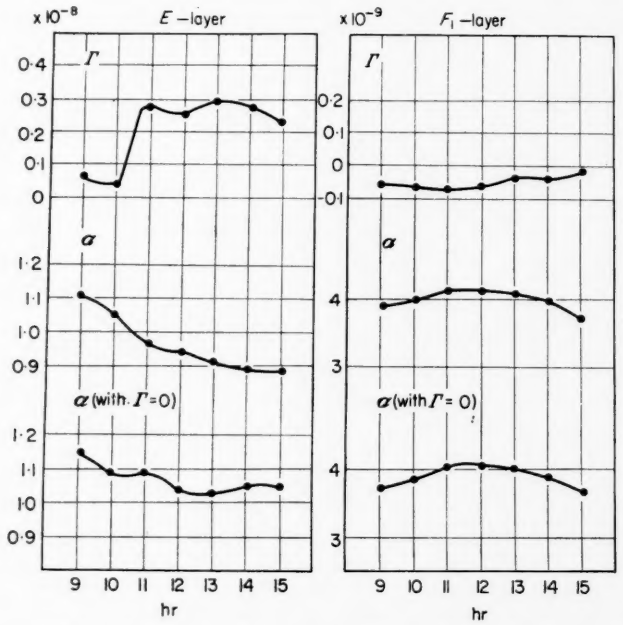


Fig. 2. Hourly variations in the scale height gradient $\Gamma$ and the recombination coefficient $\alpha$ in the $E$- and $F1$-layers in March 1952–1954.

positive throughout all hours and has larger values for 1100–1500 hours with the maximum at 1300 hours. This may lead us to the supposition that the temperature in the regions above the $E$-layer rises considerably during these hours around noon 1100–1400 hours.

On the contrary in the $F1$-layer, $\Gamma$ keeps always negative, although its quantity is very small. However, this small negative value of $\Gamma$ must be apparent, because it is hardly possible to suppose that the scale height gradient is negative in these regions. And these inappropriate values of $\Gamma$ may be due to the fact that the $F1$-layer will not be produced *exactly* at the level of maximum electron production, as was assumed in equations (2) and (3).



VOL. 15 1959

### 3.3. *Effect of $S_q$ current system*

We can present evidence to indicate that the discrepancies between experimental and theoretical values of $f_0E$ should be attributed to the effect of $S_q$ overhead current system. First, they have opposite signs at lower and higher latitudes, changing signs somewhere at middle latitudes. Secondly, they predominate particularly around 1100 hours, when the east–west component of $S_q$ current reaches the maximum. Thirdly, they are hardly observed in the $F1$-layer, which exists apart from the dynamo regions, in which $S_q$ current flows.

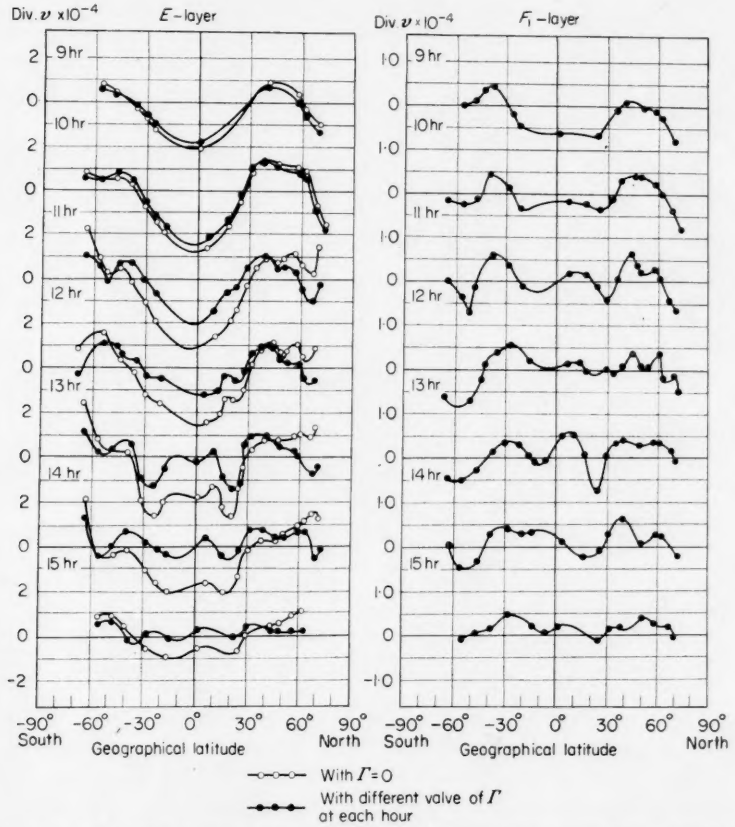


Fig. 3. Latitudinal distribution of div $v$ in the $E$- and $F1$-regions for each hour of 0900–1500 hours in March 1952–1954. Note the difference between the scales in these two layers.

Now, the effect of $S_q$ current system will be shown by the non-uniform vertical drift motions produced by the joint effect of this current and the earth's magnetic field. The result of calculations of div $v$ thus produced is illustrated in Fig. 3, in which we can see comparatively small values and non-systematic variations in the $F1$-layer. On the contrary in the $E$-layer div $v$ is comparatively large and has systematic variations being negative at lower latitudes and positive at higher latitudes except at very high latitudes.

According to the geomagnetic dynamo theory, the vertical drift velocity would be upward ($v > 0$) at lower latitudes and downward ($v < 0$) at higher latitudes. It may, therefore, be concluded that div $v$ and $v$ have opposite signs throughout all ranges of latitudes: div $v < 0$ and $v > 0$ at lower latitudes and div $v > 0$ and $v < 0$ at higher latitudes. In other words, the vertical drift velocity decreases with heights in the *E*-regions. According to the writer's study (SHIMAZAKI, 1956) on the non-uniform motion in the *F2*-regions, it has been concluded that the vertical drift velocity increases and its phase advances with heights in the *upper F2*-regions, while, on the contrary, the amplitude decreases and the phase lags with heights in the *lower F2*-regions. These *upper* and *lower F2*-regions are bounded by a certain level—about 350 km in sunspot maximum years and 280 km in sunspot minimum. This may correspond to the fact that the kinematic viscosity in the upper atmosphere has its maximum value at 240–350 km, as was suggested by YERG (1953). If the characteristics of these *lower F2*-regions are considered to be preserved in the *E*-regions, the above-mentioned characteristics of the non-uniform motions in the *E*-regions may be easily understood.

## REFERENCES


| | | |
|---|---|---|
| APPLETON E. V., LYON A. J. and TURNBULL A. G. | 1955 | *Nature, Lond.* **176,** 897. |
| BEYNON W. J. G. and BROWN G. M. | 1956 | *Nature, Lond.* **177,** 583. |
| SHIMAZAKI T. | 1956 | *Rep. Ionos. Res. Japan* **10,** 124 |
| YERG D. G. | 1953 | *Scientific Report* No. 45. Ionosphere Res. Labor., State University, Penn., U.S.A. |


VOL.
15
1959

Journal of Atmospheric and Terrestrial Physics, 1959, Vol. 15, p. 83. Pergamon Press Ltd. Printed in Northern Ireland

# Les gradients de température dans les régions-*E* et -*F1*, d'après les sondages ionosphériques effectués à Casablanca

A. Haubert

**Résumé**—L'interprétation des mesures effectuées à Casablanca sur les régions-*E* et -*F1* se conduit à admettre, d'après la théorie de Chapman, que le gradient de température est en moyenne positif dans la région-*E* et en moyenne légèrement négatif dans la région-*F1*, avec une variation saisonnière assez marquée pour y provoquer l'inversion.

On sait que les densités maxima d'ionisation des régions-*E* et -*F1* obéissent à la loi de Chapman. Si l'on porte sur un graphique les logarithmes des médianes

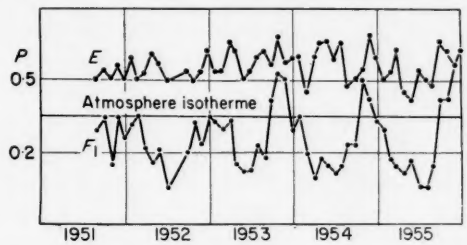


Fig. 1

horaires mensuelles des fréquences critiques ordinaires, en fonction du logarithme du cosinus de la hauteur zénithale solaire correspondante (valeur horaire du 15 de chaque mois), on obtient un ensemble de points se groupant le long d'une ligne droite. La pente de cette ligne droite détermine la valeur moyenne mensuelle de l'exposant $p$ de la formule:

$$f_0 = f_m (\cos Z)^p$$

La théorie montre que si le milieu est isotherme, $p$ doit être égal à 0,25; si le gradient de température est positif $p$ est plus grand que 0,25 et si le gradient est négatif $p$ est plus petit que 0,25.

Nous avons tracé, Fig. 1, les courbes des valeurs de $p$ obtenues à Casablanca au cours des années 1951, 1952, 1953, 1954 et 1955.

On ne trouve, pour la région-*E*, aucune variation saisonnière caractérisée; la moyenne des valeurs de $p$ se situe vers 0,32 avec une variation erratique relativement faible, indiquant un gradient de température fermement positif.

Par contre, pour la région-*F1*, on observe une variation saisonnière marquée; la moyenne de $p$ se situant vers 0,22, on peut en déduire que le gradient de température y est en général négatif, mais avec une tendance à l'inversion au début de l'hiver.

Journal of Atmospheric and Terrestrial Physics, 1959, Vol. 15, p. 84. Pergamon Press Ltd. Printed in Northern Ireland

# L'ionisation nocturne de la région-$E$ et l'activité géomagnétique

A. HAUBERT

**Résumé**—Une bonne corrélation a été trouvée à Casablanca entre l'apparition sur les ionogrammes d'une couche épaisse nocturne, en dessous de la région-$F$, et l'accroissement de l'activité magnétique. Une constatation semblable avait été faite à la station de Fribourg en 1957. Ce phénomène mériterait d'être étudié à l'échelle mondiale.

LA comparaison systématique des phénomènes solaires et magnétiques avec le comportement de l'ionosphère à Casablanca, nous a permis de mettre en évidence une bonne corrélation entre l'apparition nocturne sur les ionogrammes d'une couche $E2$ (couche épaisse), vers 150 km de hauteur virtuelle, et le renforcement de l'activité magnétique. Une confirmation de cette corrélation vient de nous être fournie par l'écoute de whistlers à Poitiers et à Rabat.

La fréquence limite inférieure du sondeur de Casablanca, qui est de 1,5 Mc/s, ne permet généralement pas de mesurer les fréquences critiques ordinaire et extraordinaire de cette couche nocturne; pour cette raison, l'étude de ce phénomène avait été négligée. Cependant la coincidence des cas où $f_xE2$ (même parfois $f_0E2$) pouvait être mesurée de nuit et l'existence simultanée d'une forte activité magnétique, nous a fait rechercher dans le passé (de 1951 à 1956) tous les cas où un retard des échos de la région-$F$ permettait de déceler une augmentation de l'ionisation dans une couche épaisse inférieure. Nous avons ainsi constaté que cela se produisait presqu'à coup sûr lorsque $K_p$ était égal ou supérieur à 5.

Une constatation semblable avait été faite par E. THEISSEN en 1947 à la station de Neuershausen (Fribourg).

Nous profitons de l'occasion qui nous est ici offerte, pour rappeler la suggestion présentée dans le Rapport de Comité Marocain à la XIe Assemblée Générale à La Haye, à savoir: que les stations de sondages devraient publier dans leurs bulletins mensuels, en plus des données de base, la liste, avec mention des dates et heures d'occurence, des anomalies ionosphériques observées. Celà permettrait de se rendre compte de l'étendue géographique de certains phénomènes anormaux.

C'est ainsi qu'une vue mondiale sur le phénomène de $E2$ nocturne permettrait sans doute de préciser ses rapports avec le géomagnétisme et de jeter peut-être quelque lumière sur l'altitude des courants invoqués dans la dynamo-théorie.

Journal of Atmospheric and Terrestrial Physics, 1959, Vol. 15, pp. 85 to 88. Pergamon Press Ltd. Printed in Northern Ireland

# On the importance of the resonance-lines of atomic oxygen to the ionospheric ionization

YUJI INOUE*

**Abstract**—A new interpretation of the effective recombination-coefficients of an electron in the ionosphere is advocated. A new theory for the ionization mechanism in the ionosphere is also brought forward. The resonance lines of atomic oxygen are of 1302–1306 Å, $3s\,^3S^0$–$2p^3P$, and 1025·7 Å, $3d\,^3D^0$–$2p^3P$. These lines were observed at 115 km as a strong emission. The new theories of the ionosphere are discussed, relating to the interpretation of the formation of these emission-lines in the ionosphere.

## 1. INTRODUCTION

### 1.1. Chapman's *original idea relating to the formation of the ionized layers and the directive principle of its development*

Chapman first proposed that an ionized layer can be produced by solar radiation. His idea may be expressed as follows. In a hydrostatic atmosphere of a uniform temperature, an incident monochromatic radiation from the sun is absorbed by a gas molecule of a particular kind, ionizing it, and the photon-flux decreases with increase of the optical depth, $\tau$, appropriate to the absorbing agency, in proportion to $e^{-\tau}$. As a consequence, the rate of ionization at any height becomes proportional to $\tau e^{-\tau}$, since $\tau$ may be considered to be proportional to the gas density there. This function $\tau e^{-\tau}$ has a maximum at the place where $\tau = 1$, so that one ionized layer can be formed.

Following Chapman's original idea, various workers have done theoretical work on the formation of the ionosphere. Their directing principle is to seek among possible ionospheric constituents the probable one whose absorption-coefficient for photo-ionization is satisfied, so that the predicted layer can be formed at the observed height of the layer under consideration in the atmosphere of the assumed density-distribution. As a natural consequence of this avenue of approach, the research has had a tendency to give a solution for different layers separately. However, in this paper, the writer attempts to clarify the problem synthetically by considering all the observed layers together.

### 1.2. *Difficulties in explaining the formation of the ionosphere*

The difficulties have been described in the writer's paper sent to the XII General Assembly of URSI, 1957. Its conclusion is that a new theory of the formation of the ionosphere is urgently needed.

### 1.3. *Solar spectrum in* 1000–1800 Å *by rocket-spectroscopic experiments*

U.S. Naval Research Laboratory recorded the solar spectrum at 115 km above New Mexico on 21 February 1955. In this spectrogram, the resonance-lines of (O*I*, $3s^3S^0$–$2p^3P_2$), 1302·2, 1304·9, 1306·0 Å and Lyman $\beta$ of H*I*, 1025·7 Å, are

* Fourth Division, Technical Research Institute, National Defense Agency, Tokyo, Japan.

recorded as a strong emission-line. There is only 0·05 Å difference between $L\beta$ of H*I* and a strong resonance-line of (O*I*, $3d^3D^0$–$2p^3P_2$). This peculiar coincidence should result in resonance. The observed $L\beta$ of H*I* may be the resonance-line of (O*I*, $3d^3D^0$–$2p^3P_2$). Making a correction for collecting field of rocket-borne spectrograph, the ambient intensities of the resonance-lines of O*I* will be greater than the incident intensity of $L\alpha$ of H*I*. The absorption coefficient of H*I* for $L\alpha$ is $10^4$ times as great as that for Lyman limit. It can be conceived that in the solar chromosphere, $L\alpha$-radiation is emitted from the layer where the condition $\tau_\alpha = 1$ is satisfied. This layer is higher and hotter than the emitting layer of the Lyman continuum. Its temperature will be near 12,000°K and it will radiate $L\alpha$ like a black body near 12,000°K. The chromosphere and corona above this layer must be transparent to $L\alpha$. On the other hand, in the solar atmosphere, the resonance-lines of O*I* are emitted from a layer near the emitting layer of the Lyman continuum, its temperature being near 6000°K. It appears that these lines are not "solar", but "ionospheric".

The fact that these resonance-lines of O*I* have been observed in a strong emission at 115 km is significant to the ionization-problem of the ionosphere. From examination of the transfer of radiation of these lines, it must be concluded that the molecular absorption of these lines is very weak in the ionosphere, and that the molecular absorption-coefficients of $O_2$ and $N_2$ measured in the laboratory are too great to be accepted as correct. Considering the fact that the atmosphere is rich in O*I* above 115 km, the resonance-lines of O*I* and $L\beta$ of H*I* observed are not of an incident solar radiation which penetrates directly from the sun down to 115 km, but of a radiation which is scattered through the resonance absorptions of O*I* in the ionosphere and subsequently the spontaneous emissions.

Investigation of the mechanisms of scattering these photons, which penetrate down into the *E*-region and are stored up to form a strong radiation-field, can clear up the mechanisms of ionizing the ionosphere and of dissipating an electron there.

## 2. Processes Dissipating Electrons in the Ionosphere

### 2.1. *New proposal for ionospheric recombination and formation of* $O_2^-$

The writer proposes a new interpretation for the ionospheric recombination. The processes must be those which can explain the facts mentioned in Section 1.3.

As a result of ionization, positive ions of $O^+$ and $N_2^+$ and electrons are yielded directly. $N_2^+$ ions are produced in the upper region only by the incident ionizing radiation coming from the corona, while $O^+$ ions are produced because of the incident radiation as well as the scattered radiation.

In addition, making allowance for some attachment of electrons to O*I* and $O_2$, $O^-$ and $O_2^-$ are produced. The concentration of $O^-$ is too small to have any effect on the dissipating electrons and, as the charged constituents, electrons $e$, $O^-$, $O_2^-$, $O^+$ and $N_2^+$ must be considered by us. Among the chemical reactions between these charged particles, or with participation of the neutral constituents, $N_2$, O*I* and $O_2$, we shall discuss those reactions associated only with dissipating electrons in the ionosphere.

Bates and Massey advocated that the process involving charge transfer of a positive ion and subsequent dissociative recombination might be promising. However, we must meet some difficulties when we apply this process to the ionospheric recombination.

The following reactions will be considered to be the most preferable set of processes:

mutual neutralization
$$\begin{cases} O^+(^4S^0) + O_2^-(^4\Sigma_g^-) \rightarrow O' + O'_2 \\ \qquad\qquad\qquad\qquad \text{or } O' + O'' + O''', \\ N_2^+(X^2\Sigma_g^+) + O_2^-(^4\Sigma_g^-) \rightarrow N'_2 + O'_2 \\ \qquad\qquad\qquad\qquad \text{or } N'_2 + O' + O'', \end{cases}$$

attachment
$$O_2(X^3\Sigma_g^-, v \simeq 1) + e \leftrightarrows O_2^-(^4\Sigma_u^-, v = 0, \text{ or } 1),$$

radiative stabilization
$$O_2^-(^4\Sigma_u^-, v = 0, \text{ or } 1) \rightarrow O_2^-(^4\Sigma_g^-, v = 0) + h\nu,$$

radiative detachment
$$O_2^-(^4\Sigma_g^-) + h\nu \rightarrow O_2^-(^4\Sigma_u^-, v = 0, \text{ or } 1) \rightarrow O'_2(X^3\Sigma_g^-, v \cong 1) + e$$

collisional detachment
$$O_2^-(^4\Sigma_g^-) + N_2(X^4\Sigma_g^+) \rightarrow NO(X^2\Pi) + NO(X^2\Pi) + e$$

The equilibrium concentration of $O_2^-(^4\Sigma_g^-)$ has been derived from these reactions. We have indicated that the effective recombination-coefficient of each layer can be explained in terms of these reactions.

### 2.2. *Ionospheric recombination and resonance-lines of* O*I*

When the mutual neutralization between $O_2^-$ $(^4\Sigma_g^-)$ and $O^+(^4S^0)$ takes place, the resulting O-atoms lie almost entirely in highly excited states, the energy of which is more than 9·11 eV higher than that of the ground state. These excited O-atoms undergo spontaneous transition to the ground state and in so doing emit photons which correspond to their resonance lines. The resonance-lines are (O*I*, $3s^3S^0$–$2p^3P_2$) and (O*I*, $3d^3D^0$–$2p^3P_2$). These lines were observed at 115 km as a strong emission-line by the rocket-borne spectrograph of U.S. Naval Research Laboratory.

## 3. Ionization Mechanism in the Ionosphere

### 3.1. *New proposed basic idea of the scattering theory*

The photons from the resonance lines, which appear in the radiation field as a result of ionospheric recombination, are again absorbed by the surrounding O-atoms: oxygen atoms in the highly excited states are produced which are then either ionized by visible radiation, or return into the ground state, emitting spontaneously resonance lines of O*I*. Thus the photo-ionization and recombination of O*I* may be inferred to be a scattering phenomenon of the ionizing and resonance radiations with the help of the visual radiation.

In a steady state, a disappearance of one photon of the ionizing radiation yields an increase of one photon of the resonance radiation. The converse holds true. Hence, if we consider the ionizing radiation together with the resonance radiation,

the conservation of total photon-flux is substantiated throughout the atmosphere. Therefore, a linear field is realized in the optically deep region.

The photons of the resonance-lines permeate as a scattered radiation down into the $E$-layer, and are then richly stored up in the $E$-region. The ionization in the $E$-layer is that from the highly excited states of O$I$ due to a visual radiation.

3.2. *Radiation fields connected with the ionization of* O$I$

In treating the ionizing radiation fields in the ionosphere, we take into account the fine structure of the energy levels of O$I$. The simplest model of O$I$ is treated, which consists of the ground level, the representative of the excited states, and the ionized level. With regard to the representative of the excited states, we take $3^3S^0$ level.

The writer obtained the cyclic equations concerning the ionization, and also the equations of radiative transfer with respect to the ionizing radiations and resonance radiations.

The solutions of the equations of transfer were calculated. The base of the ionosphere was determined by molecular absorption of the resonance radiations.

By applying the solutions, the writer discussed concretely the identification of each of the observed ionospheric layers.

It was concluded that the incident ionizing radiations come from the chromosphere as well as from the corona.

3.3 *Conclusion*

Such an ionization mechanism as proposed here enables the variations of the $E$-layer during solar eclipses, the solar flare effect of the ionosphere, and the variations of the ionized layers in a solar cycle to be explained.

VOL.
15
1959

Journal of Atmospheric and Terrestial Physics, 1959, Vol. 15, pp. 89 to 94. Pergamon Press Ltd. Printed in Northern Ireland.

# A new theory of formation of the *F2*-layer

TOSHIYUKI YONEZAWA*

**Abstract**—The importance is emphasized of the role played by electron–ion diffusion in the mechanism of formation of the *F2*-layer. Taking into account the electron–ion diffusion in the gravitational field as well as the electron–ion movement in the vertical direction, the velocity of which is assumed to increase exponentially with height, height distributions of electron density for steady-state conditions have been calculated and discussed. The latitudinal distributions of the maximum electron density and the height of its level have also been obtained and compared with observations, resulting in a reasonable agreement at least in their broad features.

## 1. INTRODUCTION

The mechanism of formation of the *F2*-layer does not seem to have been fully understood hitherto. In conventional treatments of this layer the *effective* recombination coefficient has usually been employed, but it has not necessarily been clear to what sorts of atomic processes this effective recombination coefficient corresponds, so that its variation with height, for instance, cannot be argued from the theoretical point of view. The writer wishes to emphasize that, though electron removal is effected by such processes as

$$O^+ + O_2 = O_2^+ + O, \qquad O_2^+ + e = O' + O'' \tag{1}$$

or

$$O^+ + N_2 = NO^+ + N, \qquad N_2^+ + e = N' + N'' \tag{2}$$

as suggested by BATES (1955) and these processes determine the height distribution of electron density at lower levels, the height distribution of electron density *at higher levels* is mainly determined *by electron–ion diffusion* in the gravitational field. Thus, while the temporal rate of electron removal is of the attachment type at lower levels, i.e. the effective recombination coefficient is inversely proportional to the electron density, with the constant of proportionality decreasing exponentially with height, the effective recombination coefficient becomes independent of height at higher levels (see Fig. 1). At intermediate heights, however, such simple variations of the effective recombination coefficient with height cannot be expected.

## 2. BASIC ASSUMPTIONS AND SOLUTION

The differential equation governing the electron density variation when all the above effects as well as the vertical movement of electrons and ions are taken into account is as follows:

$$\frac{\partial N}{\partial t} = Q - L + \frac{\partial}{\partial z}\left\{D_a\left(\frac{\partial N}{\partial z} + \frac{N}{2H}\right)\right\} - \frac{\partial}{\partial z}(Nv) \tag{3}$$

where $N$ is the electron density, $t$ is the time, $z$ is the height, $Q$ is the well-known Chapman function, $L$ is the rate of electron loss due to such processes as given by

* Radio Research Laboratories, Kokubunji, Tokyo, Japan.

(1) or (2), $D_a$ is the ambipolar diffusion coefficient in the vertical direction of electron–ion gas, $H$ is the scale height for atomic oxygen, and $v$ is the vertical velocity of electrons and ions. $Q$, $L$ and $D_a$ are given by the following expressions:

$$Q = Q_0 \exp\left(1 - \frac{z - z_0}{H}\right) - \sec\chi \,.\, \exp\left(-\frac{z - z_0}{H}\right) \tag{4}$$

$$L = B_0 \exp\left(-m\frac{z - z_0}{H}\right) N \tag{5}$$

$$D_a = (b/n_0)\left\{\exp\left(\frac{z - z_0}{H}\right)\right\} \sin^2 I \tag{6}$$

where $\chi$ is the solar zenith angle, $I$ is the magnetic dip, $b$ is a constant of proportionality, $z_0$ is the height of a datum level, $Q_0$ is the rate of electron production

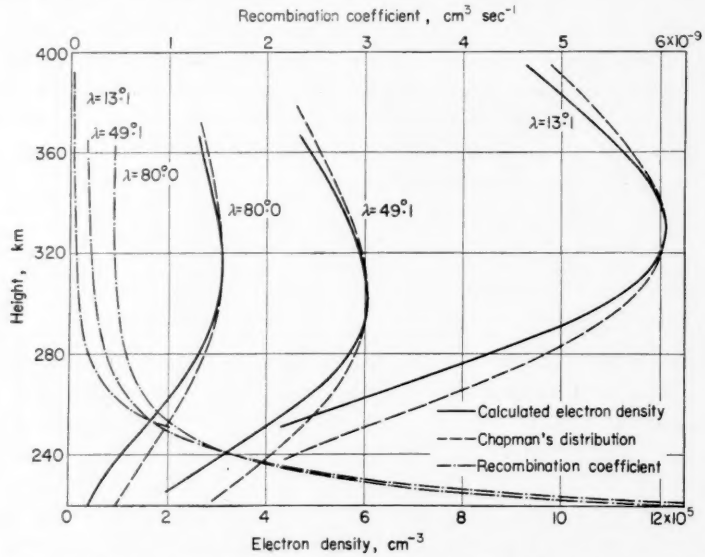


Fig. 1. Calculated electron density distributions in the *F2*-region near noon at the equinoxes. Chapman's distributions and effective recombination coefficients are also shown.

at the datum level for $\chi$ equal to zero, $B_0$ and $n_0$ are the rate coefficients for the electron loss at the datum level and the atmospheric molecular density there, respectively, and $m$ is a constant which will be taken as 2 in the following.

In this report the vertical drift velocity, $v$, of electrons and ions is assumed to increase with height in inverse proportion to the atmospheric molecular density:

$$v = v_0 \exp\left(\frac{z - z_0}{H}\right) \tag{7}$$

The main reason for this assumption is that the mathematical treatment becomes relatively simple in this case, but it does not seem to be quite unreasonable considering that the coefficient of kinematic viscosity seems to decrease rapidly with



VOL. 15 1959

height above the *F2*-region (YERG, 1953) and the analogous is true with the collision frequency of electrons and ions with atmospheric molecules, and consequently with the resistance which they suffer in motion. On this assumption differential equation (3) can be solved for *steady-state conditions*, i.e. if $\partial N/\partial t$ equals zero, and the height distribution of electron density appropriate to the present problem is expressed in the following form:

$$N = \frac{Q_0 e}{B_0 A}\, u^{\frac{1}{2}-\frac{c}{3a^2}} \left\{ I_{-\left(\frac{1}{6}+\frac{c}{3a^2}\right)}(u) \int_u^\infty \exp\left(-A \sec\chi\, x^{2/3}\right) K_{\left(\frac{1}{6}+\frac{c}{3a^2}\right)}(x)\, x^{-\left(\frac{1}{6}+\frac{c}{3a^2}\right)} dx \right.$$
$$\left. + K_{\left(\frac{1}{6}+\frac{c}{3a^2}\right)}(u) \int_0^u \exp\left(-A \sec\chi\, x^{2/3}\right) I_{-\left(\frac{1}{6}+\frac{c}{3a^2}\right)}(x)\, x^{-\left(\frac{1}{6}+\frac{c}{3a^2}\right)} dx \right\} \qquad (8)$$

where $I$ and $K$ are usual Bessel functions with imaginary arguments and

$$a^2 = \frac{b}{n_0 H^2}\sin^2 I, \qquad c = \frac{v_0}{H}, \qquad A = \left(\frac{3}{2}\right)^{2/3} a^{2/3}/B_0^{1/3} \qquad (9\text{a, b, c})$$

and

$$u = \left\{\exp\left(-\frac{3}{2}\frac{z - z_0}{H}\right)\right\} \Big/ A^{3/2} \qquad (10)$$

## 3. Height Distribution of Electron Density

The following values of the parameters have been adopted for the calculations below:

$$z_0 = 200 \text{ km},\ n_0 = 5 \times 10^9 \text{ cm}^{-3},\ Q_0 = 250 \text{ cm}^{-3}\text{ sec}^{-1},$$
$$B_0 = 3 \times 10^{-3} \text{ sec}^{-1},\ H = 60 \text{ km},\ b = 1 \times 10^{19} \text{ cm}^{-1}\text{ sec}^{-1}.$$

Evaluating the left-hand side of equation (8) by numerical methods, with the aid of equations (9) and (10), we have calculated height distributions of electron density for several locations with different latitudes, $v_0$ being assumed to be zero and the earth's rotational axis and magnetic axis to coincide with each other. A few examples of the results are shown in Fig. 1. The effective recombination coefficients required to produce these steady-state distributions of electron density and Chapman's distributions corresponding to these are also depicted. From the figure one will see that the maximum electron density and the height of its level have reasonable values, that the thickness of ionized layers is thinner than that of Chapman's distribution, and that the effective recombination coefficient decreases steeply with height at lower levels but, the decrease becoming slower and slower at higher levels, seems to tend to constant values at very great heights.

## 4. Latitudinal Distribution

In the next place, the latitudinal distributions of the maximum electron density and the height of its level have been calculated using equations (8), (9) and (10), at first neglecting the effect of vertical movement of electrons and ions. The results are shown in Figs. 2 and 3, respectively, by solid lines. Dots in the figures represent observed values at local noon for equinoctial months averaged over observatories

with similar latitudes. One will see that calculated maximum electron densities are higher than observed ones in higher latitudes and lower in lower latitudes. In order to bring about a closer agreement between theory and observation, it becomes necessary to assume a latitudinal distribution of the velocity of vertical movement of electrons and ions such as depicted in the upper-right portion of Fig. 2, which is somewhat similar in shape to the curves of the vertical drift velocity of electrons

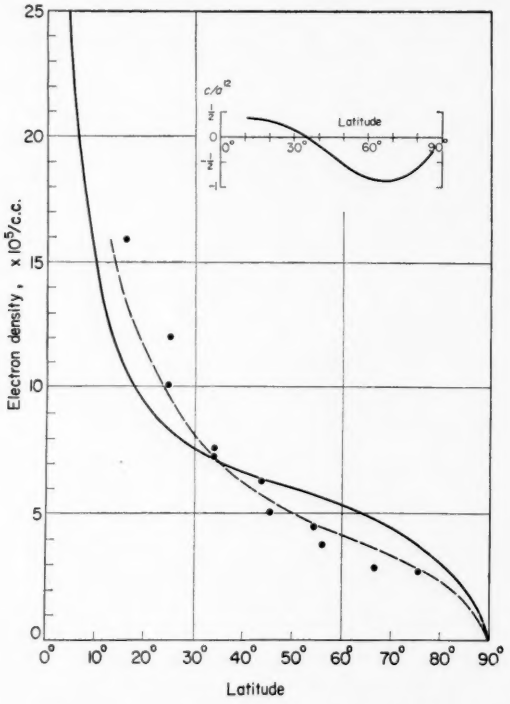


Fig. 2. Variation of the maximum electron density in the *F2*-region with latitude near noon at the equinoxes. For the solid and broken curves, see the text. The dots indicate maximum electron densities at noon observed in March and September 1952 against geomagnetic latitude.

deduced by MARTYN (1947) and by MAEDA (1953). Then, the theoretical curve for the maximum electron density becomes as shown by a broken line in Fig. 2 and agreement between theory and observation is considerably improved, but the magnitude of the vertical velocity needed amounts to as high as 50 km/hr in high latitudes, which seems too large to be readily accepted. As regards the height of the level of maximum ionization, fairly good agreement between theory and observation can be obtained without invoking vertical movement of electrons and ions, except near the equator, and the consideration of this effect does not seem to improve the result to any extent.

Notwithstanding these minor discrepancies, one may conclude that the broad features of the observed latitudinal distributions of the maximum electron density and the height of its level are reproduced by our theory, invoking, if necessary, the

vertical electron–ion movement. In particular, we can understand the reason why the distribution of electron density does not obey the $(\cos \chi)^{1/2}$ law expected from Chapman's theory and is subject to geomagnetic control. (Note that the magnetic dip, $I$, enters explicitly through equation (9a) into expression (8) of electron density distribution even if the vertical drift $v_0$ equals to zero.) We can also

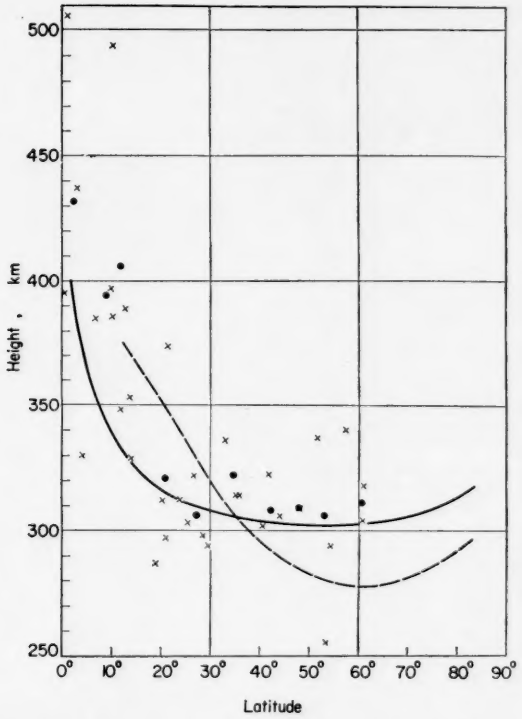


Fig. 3. Variation of the height of the level of maximum electron density in the $F2$-region with latitude near noon at the equinoxes. The meanings of the solid and broken curves are the same as in Fig. 2. The crosses indicate observed heights at respective stations. The dots indicate averages for respective groups of stations with similar geomagnetic latitudes.

understand why the height of ionized layers becomes greater towards the equator without invoking effects of vertical electron–ion movements or of temperature.

## 5. Conclusions

The above considerations have been confined only to steady-state conditions, but, as has been shown by Shimazaki (1959) in some special cases, the time required to attain steady-state conditions above the 300 km level is not long, being of the order of 1 hr or so, so that the steady-state conditions can be taken as representing approximately the actual circumstances.

Our theory cannot be applied on the geomagnetic equator because the horizontal geomagnetic field there prohibits entirely the electron–ion diffusion in the vertical direction and the electron density increases with height unboundedly on the basis

of our theory. As a matter of fact, however, the effect of the radiative recombination between electrons and atomic ions of oxygen, which can be neglected in other cases, manifests itself at very great heights ($\geq$ 500 km) so that we have here also ionized layers. Details are not considered here.

## REFERENCES


| | | |
|---|---|---|
| BATES D. R. | 1955 | *Proc. Phys. Soc.* A **68,** 344. |
| MAEDA K. | 1952 | *J. Geomagn. Geoelect., Kyoto* **4,** 83. |
| MAEDA K. | 1953 | *Rep. Ionos. Res. Japan* **7,** 81. |
| MARTYN D. F. | 1947 | *Proc. Roy. Soc.* A **189,** 241. |
| SHIMAZAKI T. | 1959 | *J. Radio Res. Lab.* **4** |
| YERG D. G. | 1953 | *Basic Ionospheric Research Technical Report* No. 45. Pennsylvania State College. |


VOL.
15
195

Journal of Atmospheric and Terrestrial Physics, 1959, Vol. 15, p. 95. Pergamon Press Ltd. Printed in Northern Ireland

# Excitation of the oxygen red lines in twilight*

(Abstract only)

J. W. CHAMBERLAIN†

**Abstract**—Various mechanisms for exciting the red lines at twilight are investigated. Computations are presented on the twilight enhancement to be expected from resonance scattering of sunlight at $\lambda$6300, which arises from the nebular transition of [O*I*]. The problem differs from that for $\lambda$5893 of Na in two important respects. For [O*I*], secondary scatterings and self-absorption can be neglected and collisional deactivation must be included. The numerical calculations are based on an adopted distribution of O and $O_2$, with the latter constituent assumed to be the source of deactivation. The transmission function for the lower atmosphere is replaced with a simple screening height; this method of comparing theory and observations might be improved if the deactivation coefficient and model atmosphere were precisely known. Observations, when compared with the theory, suggest that very little of the [O*I*] twilight arises from resonance scattering. Similarly, dissociation of $O_2$ in the Schumann–Runge continuum contributes, but does not give by itself the observed absolute intensity or variation in intensity.

While the above-mentioned mechanisms should contribute in the very early twilight, the main effect probably arises from dissociative recombination of $O_2^+$. An elementary theory of the evening twilight variation is presented with this hypothesis and fair agreement with observations is obtained. The same mechanism probably explains the nightglow, with the height of emission in the neighbourhood of 250–300 km. It is speculated that erratic variations and the pre-dawn enhancement observed in winter may arise from diffusion (and other dynamic effects) of ions and $O_2$ in the lower part of the *F*-region.

* The research reported in this paper was supported in part by the Geophysics Research Directorate of the Air Force Cambridge Research Center, Air Research and Development Command, under Contract AF 19(122)-480 with the University of Chicago.

† Yerkes Observatory, University of Chicago. On leave of absence, March–June 1957, at the National Bureau of Standards, Boulder, Colorado.

Journal of Atmospheric and Terrestrial Physics, 1959, Vol. 15, pp. 96 to 98. Pergamon Press Ltd. Printed in Northern Ireland

# Recombination in the *F2*-layer and the oxygen red lines in the airglow*

J. W. CHAMBERLAIN†

THERE has long been doubt that the [O*I*] lines in twilight could be satisfactorily explained by resonance scattering. The observations by CABANNES and GARRIQUE (1936), ELVEY and FARNSWORTH (1942) and DUFAY and TCHENG MAO-LIN (1946) showed a slow decrease with time that implied an enormous scale height if resonance scattering were assumed. It has often been suggested that a consideration of deactivation of the red line might account for this slow decrease; an analysis of the absolute intensity by BATES (1948) suggested that the emission might thus be satisfactorily explained.

Present-day concepts of the upper atmosphere provide considerably less atomic oxygen above 100 km than was adopted in BATES's model. A rediscussion of the problem has recently been carried out (CHAMBERLAIN, 1958) with allowance for deactivation (with various assumed rate coefficients) and for screening of the incident solar flux by the lower atmosphere.

Comparison of the calculations with recent observations by ROBLEY (1956) show that very little of the twilight enhancement can arise from resonance scattering. In the first place, the absolute emission in a vertical square-centimetre column above 135 km cannot be greater than 50 R,‡ whereas the observed value may exceed this value by ten times. Secondly, the observed rate of decrease would require an extremely high deactivation coefficient, which would further reduce the absolute intensity. And finally, the observed decrease, when plotted against shadow height, is quite different for observations in different azimuths from the sun.

Dissociation of $O_2$ in the Schumann–Runge region similarly fails to provide satisfactory agreement. It is interesting to note, however, that in early twilight the excitation by this process provides an intensity comparable to that from resonance scattering, when the $O_2$ abundance at 200 km and above is computed with allowance for diffusion (NICOLET and MANGE, 1954; NICOLET, 1954a; BATES, 1954). The morning enhancement may involve photo-detachment of $O^-$ (BATES, 1948), although the daytime equilibrium of negative ions is too small for the mechanism to explain an appreciable portion of the evening twilight. Laboratory measurements on the electron affinity and attachment rate for atomic oxygen (BRANSCOMB and SMITH, 1955) should make possible an accurate prediction of the dawn enhancement of this process.

* The research reported in this paper was supported in part by the Geophysics Research Directorate of the Air Force Cambridge Research Center, Air Research and Development Command, under Contract AF 19(122)-480.

† Yerkes Observatory, University of Chicago, Williams Bay, Wisconsin.

‡ 1 R (rayleigh) is $10^6$ quanta/cm$^2$ (column)-sec.

CHAMBERLAIN (1958) has also investigated the decay of intensity from dissociative recombination, $O_2^+ + e \rightarrow O^* + O^*$, as ionization disappears after sunset in the *F*-layers. The mechanism appears to be the principal one responsible for recombination in the *F*-layers as BATES and MASSEY (1947) originally suggested. The $O_2^+$ is formed by charge transfer between $O_2$ and $O^+$, with $O^+$ produced by solar radiation. Until recently, there appeared to be severe difficulties with the mechanism: but NICOLET and MANGE's (1954) work on diffusion showed there would be more $O_2$ in the *F*-layer than was previously expected (see NICOLET, 1954b) and BATES (1955) suggested that the rate coefficient for charge transfer might after all be appropriately high, as atom–ion exchange would increase the efficiency of the reaction over what would be obtained with the transfer of only an electron.

BATES (1948) and BARBIER (1957b) suggested that some of the post-twilight enhancement might result from dissociative recombination. The nightglow [O*I*] red lines appear to originate in the *F*-region. Although van Rhijn heights for this emission are not valid, BARBIER has estimated 300 km for the emitting height by relating diurnal changes in the intensity in the eastern and western sky. Also HEPPNER *et al.* (1957) found from rockets that the emission was above 160 km. Moreover, St. AMAND (1955) reported interesting correlations of the red lines with *F*-layer ionization.

Further evidence on the importance of dissociative recombination for the *F*-layers has been presented by the ionospheric analysis of RATCLIFFE *et al.* (1955); also cf. BATES (1954, 1956). In this connexion BARBIER (1957b) has provided further evidence that the *F*-layer is associated with the red lines. He shows that the observed intensity correlates well with a semi-empirical formula involving the critical frequency (which depends on the maximum electron density in the layer) and the virtual height of radio reflection. BARBIER's formula is essentially an expression for the rate of emission at the height of the maximum electron density. His recombination rate coefficient is similar in form to that derived from the radio work by RATCLIFFE *et al.* (1955).

Thus the evidence for dissociative recombination in the nightglow is becoming quite impressive, and in evening twilight it also appears that the mechanism is of dominating importance. CHAMBERLAIN's calculations assumed that $O_2$ remains in diffusive equilibrium throughout twilight. The electron density was assumed not to be affected by diffusion but to be governed entirely by recombination after sunset. With the initial electron density $n_e(O)$ taken as constant with height, for simplicity, the emission rate, integrated over all height, is insensitive to the reaction rates for charge transfer and dissociative recombination. It appears that $n_e(O) \sim 3 \times 10^5$ cm$^{-3}$ gives a good representation of the intensity of [O*I*] throughout twilight. The predicted height of emission is about 220 km at 15 min after sunset in the *F*-layers and rises to 275 km at $2\frac{1}{2}$ hr after sunset. These heights are not inconsistent with the Doppler temperature of $750 \pm 200$°K reported by PHILLIPS (1956) for the [O*I*] twilight.

The lack of correlation between the red and green oxygen lines makes it apparent that very little red-line emission originates around 100 km, where the green-line nightglow is excited. Thus deactivation of the red line at low altitudes

must be significant. A detailed discussion of this problem has been presented by SEATON (1958).

BARBIER (1955; 1957a, c) has observed enhancements in the middle and second half of the night that are not so readily explained. Perhaps a detailed consideration of diffusion of $O_2$ and ions would disclose enhancements later in the night.

## REFERENCES


| | | |
|---|---|---|
| BARBIER D. | 1955 | *The Airglow and Aurorae* (Edited by ARMSTRONG E. B. and DALGARNO A.) p. 38. Pergamon Press, London. |
| BARBIER D. | 1957a | *C. R. Acad. Sci., Paris* **244,** 1809. |
| BARBIER D. | 1957b | *C. R. Acad. Sci., Paris* **244,** 2077. |
| BARBIER D. | 1957c | *C. R. Acad. Sci., Paris* **244,** 1945. |
| BATES D. R. | 1948 | *Emission Spectra of the Night Sky and Aurorae* p. 21. Physical Society, London. |
| BATES D. R. | 1954 | *Rocket Exploration of the Upper Atmosphere* (Edited by BOYD R. L. F. and SEATON M. J.) p. 347. Pergamon Press, London. |
| BATES D. R. | 1955 | *Proc. Phys. Soc.* A **68,** 344. |
| BATES D. R. | 1956 | *Solar Eclipses and the Ionosphere* (Edited by BEYNON W. J. G. and BROWN G. M.) p. 191. Pergamon Press, London. |
| BATES D. R. and MASSEY H. S. W. | 1947 | *Proc. Roy. Soc.* A **190,** 1. |
| BRANSCOMB L. M. and SMITH S. J. | 1955 | *Phys. Rev.* **98,** 1127. |
| CABANNES J. and GARRIQUE H. | 1936 | *C. R. Acad. Sci., Paris* **203,** 484. |
| CHAMBERLAIN J. W. | 1958 | *Astrophys. J.* **128,** 713 |
| DUFAY J. and TCHENG MAO-LIN | 1946 | *Ann. Géophys.* **2,** 189. |
| ELVEY C. T. and FARNSWORTH A. H. | 1942 | *Astrophys. J.* **96,** 451. |
| HEPPNER J. P., STOLARIK J. D. and MEREDITH L. H. | 1957 | *Trans. Amer. Geophys. Un.* **38,** 394. |
| NICOLET M. | 1954a | *The Earth as a Planet* (Edited by KUIPER G. P.) p. 644. University of Chicago Press, Chicago. |
| NICOLET M. | 1954b | *Rocket Exploration of the Upper Atmosphere* (Edited by BOYD R. L. F. and SEATON M. J.) p. 361. Pergamon Press, London. |
| NICOLET M. and MANGE P. | 1954 | *J. Geophys. Res.* **59,** 15. |
| PHILLIPS J. G. | 1956 | *The Airglow and Aurorae* (Edited by ARMSTRONG E. B. and DALGARNO A.) p. 67. Pergamon Press, London. |
| RATCLIFFE J. A., SCHMERLING E. R., SETTY C. S. G. K. and THOMAS J. O. | 1955 | *Phil. Trans.* **248,** 621. |
| ROBLEY R. | 1956 | *C. R. Acad. Sci., Paris* **243,** 2120. |
| SEATON M. J. | 1958 | *Astrophys. J.* In press. |
| ST. AMAND P. | 1955 | *Ann. Géophys.* **11,** 450. |


VOL. 15 1959

Journal of Atmospheric and Terrestrial Physics, 1959, Vol. 15, pp. 99 to 101. Pergamon Press Ltd. Printed in Northern Ireland

# Tides in the *F*-layer

G. J. Gassmann*

In planning further investigations on air-tides under the IGY programme, a comparison of available experimental data with theoretical conceptions was performed for the September 1955 period. The original $h'f$ records of Washington, Puerto Rico, Canal Zone, Talara, Huancayo, and of an air-borne equipment, were analysed in terms of electron density vs. true height. The necessary uniformity of calibration in virtual height and frequency of the records from the different stations was established by the air-borne recorder.

The world-wide three-dimensional plot of the *F*-layer (i.e. electron density vs. true height, vs. latitude and vs. local time) of a single day shows a vertical expansion of the layer beginning at 0800 hours local time at all low and medium latitudes, with a maximum at about 5°N. This maximum of upward expansion near the equator shifts southward within 2 hr into the vicinity of 12°S, the location of the magnetic equator. Simultaneously, at $\pm 20°$ two minima develop, one on either side of the maximum. At 1100 to 1400 hours (see example on Fig. 1) the levels of equal ionization vary more than 150 km along the meridian, which is a 50 per cent increase of height near the magnetic equator. For comparison, the decrease of $f_0F$, connected with the expansion of the layer, is only about 30 per cent. In the late afternoon a downward drift of ionization begins in all low and medium latitudes with a flat maximum near the equator. This movement lasts all night until the early morning hours. The maximum appears near 10°N at 1800 hours and shifts to 5°S at 2400 hours and to 12°S at 0400 hours local time. The speed of these vertical movements which can be estimated from the measurements is of the order of 50 km/hr in the day and 10 km/hr during the night.

The exact locations of the lows and highs, on the world-wide presentation of layer heights, change from day to day by distances up to 1000 km. It is therefore obvious that by using monthly or weekly means of the measured parameters major parts of the phenomenon would be obscured.

The diurnal variations described, although non-symmetrical with respect to the equator and modified by other influences, were compared with the theories of the solar-tide variations (see references). According to these, the electric current system in the *E*-region must be associated with a system of separated positive and negative electrical charges which, in turn, extend their potential lines along the geomagnetic field into the *F*-region, subsequently causing shunt currents and drifts.

The most advanced theoretical derivation of the experimental (Bartels) current system in the *E*-region from the barometric pressure variation has been accomplished by Keneshea and Pfister (1956). Their analysis of the solar tide

* Ionospheric Physics Laboratory, Geophysics Research Directorate, Air Force Cambridge Research Center.

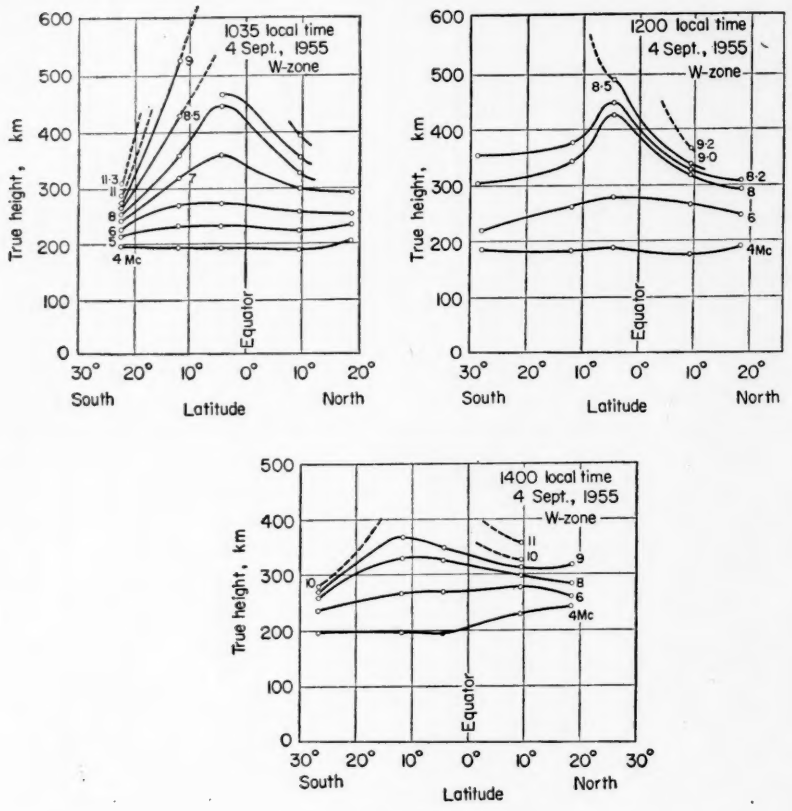


Fig. 1.

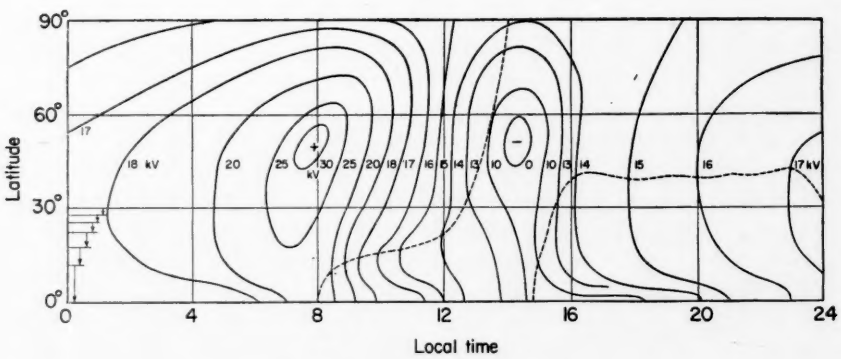


Fig. 2. Charge distribution in *E*-layer (after KENESHEA and PFISTER).



VOL. 15 1959

assumes a tidal wind system in the $E$-region in phase with the one deducible from the barometer on ground, but from 60 to 100 times stronger. In the course of the analysis the system of separated charges in the $E$-region (Fig. 2) is available as a theoretical by-product (not accessible to direct measurement) and the subsequent effects on the $F$-layer can be calculated. The general agreement with the experimental results is good. Even some details can be explained, for example the maxima of $f_0F$ north and south of the equator in the afternoon, the locations of which are not identical with the foci of the current system. This result is obtained by disregarding possible tidal winds in the $F$-layer, the importance of which, therefore, seems to be minor. Thus, the mentioned theoretical principles appear to be a good guide for further experimental work.

## References


| | | |
|---|---|---|
| Baker W. G. and Martyn D. F. | 1953 | *Phil. Trans.* A **246,** 281. |
| Fejer J. A. | 1953 | *J. Atmosph. Terr. Phys.* **4,** 184. |
| Hirono M. | 1952 | *J. Geomagn. Geoelect. Kyoto* **4,** 7. |
| Hirono M. and Kitamura T. | 1956 | *J. Geomagn. Geoelect. Kyoto* **8,** 9. |
| Keneshea T. and Pfister W. | 1956 | URSI Spring Meeting, Washington. |


OL.
15
959

Journal of Atmospheric and Terrestrial Physics 1959, Vol. 15, pp. 102 to 107. Pergamon Press Ltd. Printed in Northern Ireland

# The disturbed *F*-layer over Slough

AUDREY R. ROBBINS* and J. O. THOMAS*

**Abstract**—Electron density profiles for magnetically disturbed days have been compared with those for quiet days. The effect of disturbance on the height of the peak of the *F2*-layer ($h_mF2$), on the maximum electron density ($N_m$) and the total electron content below the *F2*-layer peak ($n_T$), is discussed. It is emphasized that the quantity $h'F2$ frequently used in the past in describing the effect of disturbance is without physical significance, and can be seriously misleading.

Evidence is presented to show that appreciable changes sometimes occur in the ionosphere near the time of a magnetic sudden impulse.

## INTRODUCTION

SEVERAL workers have examined the effects produced in the ionosphere by magnetic storms. All have made use of the published figures describing the layers, of which the most commonly used have been the penetration frequencies (*fF2*, *fF1*, *fE*) and the minimum virtual heights ($h'F2$, $h'F1$, $h'E$) recorded from the different layers. Occasionally the height of the peak of ionization ($h_mF2$, $h_mF1$, $h_mE$) has been used. This has usually been calculated from the $h'(f)$ record on the assumptions that the layer was parabolic, that the earth's field did not influence the radio-wave propagation, and that group retardation in the lower ionosphere was unimportant.

THOMAS *et al.* (1958) have described how they have used $h'(f)$ records made at Slough (latitude 51·5°N, longitude 0·5°W) to deduce the electron density profiles, or $N(h)$ curves, which show how the electron density ($N$) depends on the height ($h$). In their paper they explain how the method (a) allows for the effect of the earth's magnetic field, and (b) gives a monotonically increasing $N(h)$ curve in which the height at which a given electron density is found is the lowest possible height consistent with the observed $h'(f)$ curve, but makes no other *a priori* assumptions about the "shape" of the layer.

Hourly records were analysed for every day at Slough for 6 months, January, September and July 1950 (high sunspot number) and December, September and June 1953 (low sunspot number). A summary of the results for the quiet days was given in the paper referred to above and the detailed results for all days have been published in the form of a book of tables (THOMAS *et al.*, 1957) which is available from the Radio Section, Cavendish Laboratory, Cambridge. The results for the disturbed days have been published separately (THOMAS and ROBBINS, 1958). Here we report some of the main points arising from that study.

It will be shown that the minimum virtual height $h'F2$ frequently used in previous work is completely misleading if it is taken to indicate the height of the *F2*-layer. The new results will be discussed in terms of the parameters $h_mF1$ and $h_mF2$, the true heights of maximum electron density in the *F1*- and *F2*-layers averaged over the disturbed days and compared with the corresponding quantities averaged over the ionospherically quiet days.

* Cavendish Laboratory, Cambridge.

*The heights of the F1- and F2-layers*

In Fig. 1 the lines show the average diurnal variations of $h_mF2$ and $h_mF1$ for the ten international quiet days in each month and the broken curves show the same quantities averaged over the five international disturbed days. It will be noted

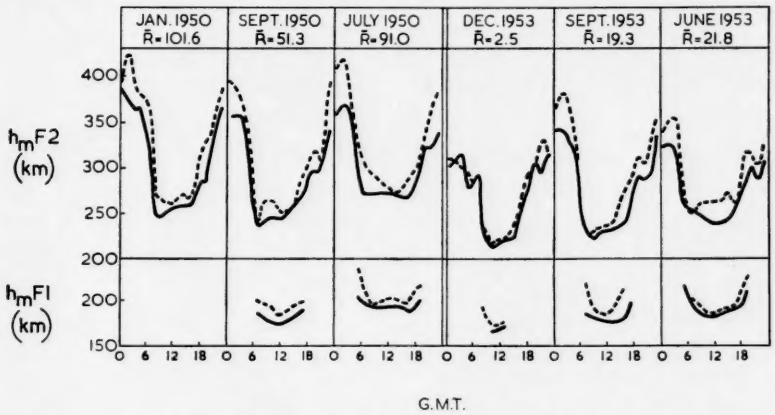


Fig. 1. The average diurnal variation of $h_mF1$ and $h_mF2$ for the ten international quiet days (continuous line) and the five international disturbed days (broken line).

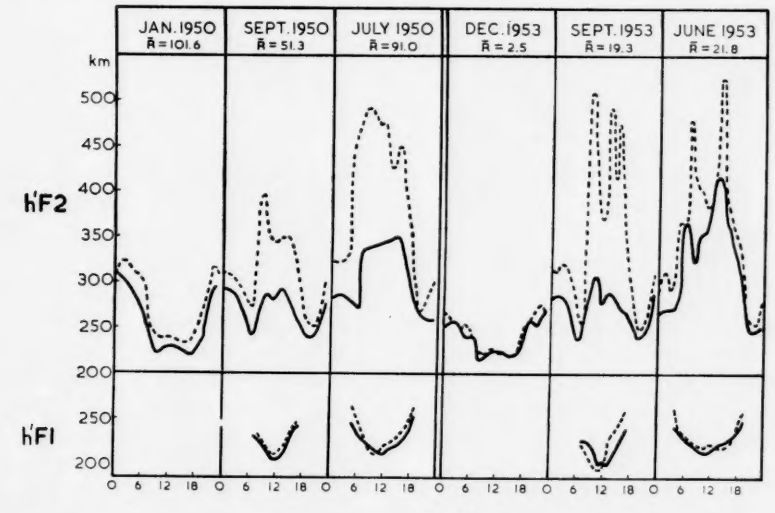


Fig. 2. The average diurnal variation of $h'F2$ and $h'F1$ for the ten international quiet days (continuous line) and the five international disturbed days (broken line).

from Fig. 1 that $h_mF2$ and $h_mF1$ are increased on the disturbed days and that the increase in $h_mF2$ is greatest at night.

The corresponding variations of $h'F1$ and $h'F2$ (quiet and disturbed) are shown in Fig. 2. It is immediately obvious that $h'F2$ depends mainly on the group

retardation in the *F1*-layer and on the closeness of the *F1*- and *F2*-layer critical frequencies, and that movements of the peak of the layer ($h_mF2$) cannot be inferred from a study of $h'F2$.

The lines in Fig. 3 show the variation of a quantity $A(h_mF2)$, which measures the average of $h_mF2$ for each hour on the five international disturbed days minus the average for the same hour for the ten international quiet days. The dashed line shows $A(h'F2)$ and (except possibly when there is no *F1*-layer present) is quite unrelated to $A(h_mF2)$.

*The maximum electron densities and the sub-peak total electron content of the layers*

Fig. 4 shows the variation of the ratio $(\overline{N_mF2})_d/(\overline{N_mF2})_q$, where the bars denote averages over the international disturbed (suffix $d$) and the quiet (suffix $q$) days. Fig. 4 also shows $(\overline{n}_T)_d/(\overline{n}_T)_q$ where $n_T$ is the total electron content from the bottom of the *E*-layer up to $h_mF2$ during the day and from $h_0F2$ up to $h_mF2$ during the night, where $h_0F2$ is the height of the bottom of the *F2*-layer and is assumed to be equal to the minimum virtual height of the *F2*-layer. The form of the variation is similar to that of the $N_m$ ratio.

It is important to note that the behaviour of $N_mF2$ during a storm depends on the local time of commencement of the storm (MARTYN, 1953). If averages are taken for the disturbed days it must be remembered that: (a) the three or four major storms occurring in each of the months have their times of starting differently distributed throughout the day in each month (thus similar individual storms starting at different times in each month can produce average curves which are quite dissimilar); (b) the international disturbed days are disturbed to different degrees. For example an international disturbed day may be quiet for the first 12 hr.

It is thus probably not meaningful to consider averages for the international disturbed days; recourse must be made to a study of individual storms. This is particularly so for studies of the maximum electron densities since it is known that $N_mF2$ sometimes has a positive phase (MARTYN, 1953; APPLETON and PIGGOTT, 1952). The average true heights for the disturbed days are useful because $h_mF2$ at Slough is always increased during a storm. Here again, however, in a detailed analysis attention must be paid to the height changes in individual storms.

It has been found that the average $N_mF1$ for the international disturbed days is less than that for the international quiet days (Fig. 5) (APPLETON and INGRAM, 1935; BERKNER, *et al.*, 1939). There is no indication of a positive phase in the $N_mF1$ variation during a storm.

*Height changes during a magnetic sudden impulse*

On 1 January 1950 nineteen magnetic observatories reporting to the *J. Geophys. Res.* announced a magnetic sudden commencement (*SC*) at 1645 hours GMT. Of fifteen observatories sending in data, none reported a major magnetic storm after this *SC*. At Abinger, the magnetograms showed a sudden impulse (*SI*) at this time. The variation of the horizontal component ($H$) of the earth's magnetic field at Abinger is shown in Fig. 6, curve (a). In curve (b) the quantity plotted is



VOL.
15
195

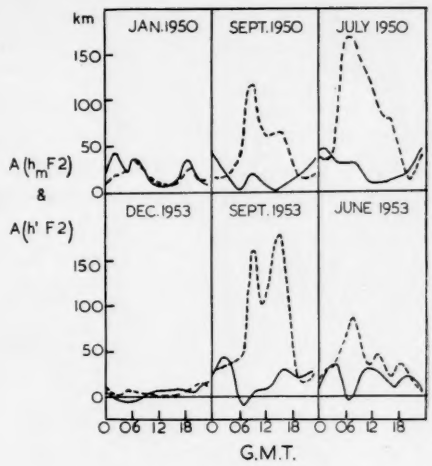


Fig. 3. The variation of $A(h_mF2)$ (continuous line) and $A(h'F2)$ (broken line).

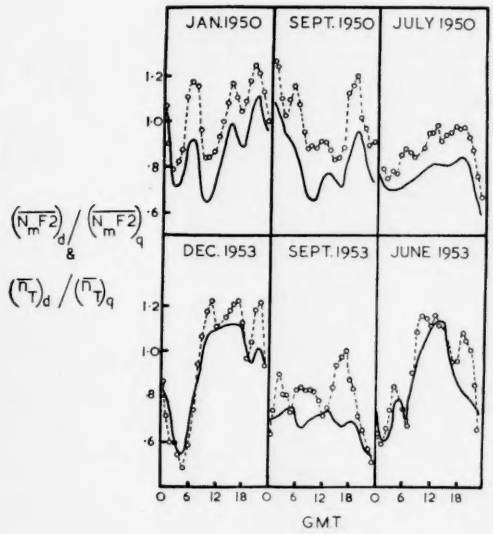


Fig. 4. The diurnal variation of the ratio of the average value of $N_mF2$ for the international disturbed days to that for the international quiet days (continuous line). The circles are the same ratio for the total electron content ($n$ ).

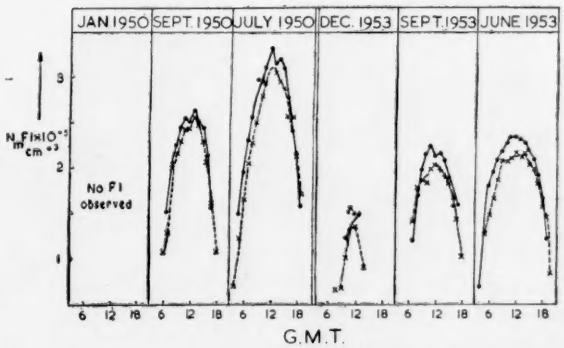


Fig. 5. The average diurnal variation of $N_mF1$ for the ten international quiet days (black circles) and the five international disturbed days (crosses).

$\Delta'H = H_d - Hq$ for each hour. The quite period was taken to be 1100 GMT on second to 1000 GMT on third. The *SI* represents an increase in $H$ of about $15\gamma$.

Between $1\frac{1}{4}$ hr and $2\frac{1}{4}$ hr following the *SI*, $h_mF2$ was observed to increase rapidly to a height of more than 125 km above its normal value—curve (c) ($\Delta h_mF2 = h_mF2 - (h_mF2)_q$ at each hour). The height reached was greater than any observed during the month (465 km instead of the quiet day average of 340 km)

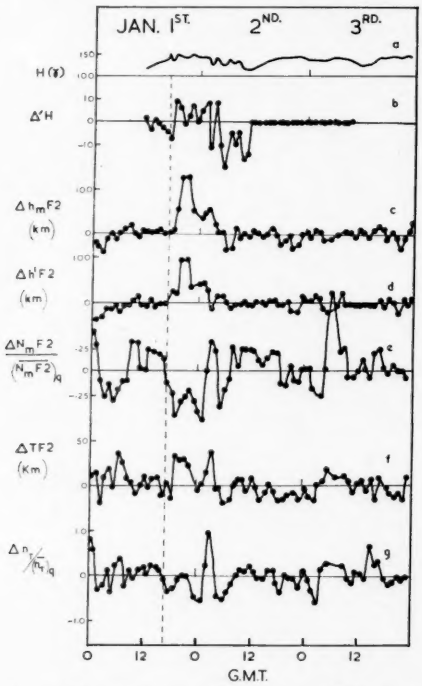


Fig. 6. The magnetic sudden impulse of 1 January 1950 and simultaneous ionospheric observations at Slough. The time of occurrence of the sudden impulse is shown by the broken line.

and was comparable with the heights observed later in the month during large storms.

The value of $h'F2$ also showed a large increase at this time (curve d) which suggests either a real height increase of the whole layer or an increase of ionization low down. The maximum electron density was decreasing before the *SI* and continued to fall sharply. Large fluctuations of $N_mF2$ are, however, common in winter and it is not possible to state that a significant drop in $N_mF2$ occurred, since comparable fluctuations were observed on several quiet days in the month. Fig. 6 curve (e) gives the variation of $\Delta N_mF2/(N_mF2)_q$. The variation of the thickness $TF2$ of the $F2$-layer ($= h_mF2 - h_0F2$ by night and $h_mF2 - h_mE$ by day (no $F1$ present)) is shown in Fig. 6 curve (f) where again the letter $\Delta$ signifies the difference from the mean of the international quiet days. The $\Delta n_T/(n_T)_q$ curve shows no significant change.



VOL. 15 1959

It is clear that the world-wide sudden impulse described above was accompanied by marked height changes in the ionosphere. The association of the two is made clear because the magnetic trace is constant after the *SI*. In the period under review three *SC*s were observed which were also accompained by ionospheric height changes, but since the magnetic trace was disturbed at the time of these height changes they could not be so definitely associated with the *SC*.

Similar ionospheric disturbances have been noted by HARDWICK (1953) which occurred during magnetically quite periods as indicated by the geomagnetic planetary *K*-indices; it may well be that these disturbances were associated with sudden impulses of the same type as that described in this paper.

## REFERENCES


| | | |
|---|---|---|
| APPLETON E. V. and INGRAM L. J. | 1935 | *Nature, Lond.* **136,** 548. |
| APPLETON E. V. and PIGGOTT W. R. | 1952 | *J. Atmosph. Terr. Phys.* **2,** 236. |
| BERKNER L. V., WELLS H. W. and SEATON S. L. | 1939 | *Terr. Magn. Atmos. Elect.* **44,** 283. |
| HARDWICK B. | 1953 | *J. Atmosph. Terr. Phys.* **3,** 347. |
| MARTYN D. F. | 1953 | *Proc. Roy. Soc.* A **218,** 1. |
| THOMAS J. O., HASELGROVE J. and ROBBINS A. R. | 1957 | *Tables of Ionospheric Electron Density, Slough* Series B, No. 1. Cavendish Laboratory, Cambridge. |
| THOMAS J. O., HASELGROVE J. and ROBBINS A. R. | 1958 | *J. Atmosph. Terr. Phys.* **12,** 46. |
| THOMAS J. O. and ROBBINS A. R. | 1958 | *J. Atmosph. Terr. Phys.* **13,** 131. |


OL.
15
959

Journal of Atmospheric and Terrestrial Physics, 1959, Vol. 15, pp. 108 to 115. Pergamon Press Ltd. Printed in Northern Ireland

# Dynamical structure of the ionospheric *F2*-layer as deduced from the world-wide daily variations

TATSUO SHIMAZAKI*

**Abstract**—Recourse was made to numerical calculations to find the effects of various non-uniform vertical motions due to diffusion, thermal and/or tidal variations on daily variations in the *F2*-layer. A method of solving the problem was worked out so that the electron density distribution may return back every 24 hr regardless of non-recurrent motions of each part resulted by several causes. The comparison of calculated and observed variations shows that the Bradbury model is better than the Chapman model in every respect. Special emphasis is placed upon the fact that the effect of non-uniform semi-diurnal vertical drift velocities with height gradient of both amplitude and phase is very important except near the equator.

## 1. INTRODUCTION

IT is well known that the effect of electron movement plays a very important part in the *F2*-regions because the electron disappears very slowly. In practice, in the upper atmosphere there are many kinds of motions, of which thermal and tidal motions have been considered primarily responsible for anomalous behaviours of the ionospheric *F2*-layer. Each individual motion or combination of the two motions may have its own peculiar effect upon the temporal variations of the electron density distribution. Accordingly, we can learn to some extent the dynamical structure of the *F2*-layer by examining the motional effect manifested in the daily variation curves at various locations in different seasons of the year and epochs of the solar cycle.

VOL. 15 1959

## 2. METHOD OF ANALYSIS

When we consider the effect of movement, special attention must be given to the fact that if affected simultaneously by two or more causes, movement of electrons becomes non-recurrent, i.e. any part of the ionosphere does not always return back to the initial level after its long and complicated course of the whole day and night. Nevertheless, the electron density distribution 24 hr later should be the same as the initial one except on days of such a disturbance as ionospheric storm. The writer (SHIMAZAKI, 1956a) worked out a general method of analysis for the purpose of obtaining the distribution of electron density unchanged after 24 hr against the above-mentioned non-recurrent motions. Thus, it is now possible to investigate the joint effect of thermal and tidal motions or the effect of tidal motions with height gradient of both amplitude and phase.

In actual calculations, the path was first traced hour after hour starting from a given initial level, by solving the equation of motion for different assumed motions of the ionosphere. An example of the non-recurrent motions thus traced is shown in Fig. 1, which illustrates the non-uniform semi-diurnal vertical motion. Then, the writer solved the equation of continuity by numerical methods following the path determined above, taking account of electron production, disappearance by attachment-type decay process, and apparent change in electron density due to non-uniform motions, and obtained the electron density at several heights for different hours. As a result, we can depict the electron density profile for each

* Radio Research Laboratories, Kokubunji, Tokyo, Japan.

hour, from which the theoretical daily variations in the maximum electron density and its height were deduced for various assumed motions of the ionosphere.

## 3. Results and Discussion

Result of analysis shows that the Bradbury model of the *F2*-layer is better than the Chapman model in every respect. It is well known that electrons in the *F2* regions will be lost by attachment-type process, the decay coefficient of which decreases with height far more rapidly than the electron production rate (Ratcliffe *et al.*, 1956). In practice the former decreases with molecular oxygen

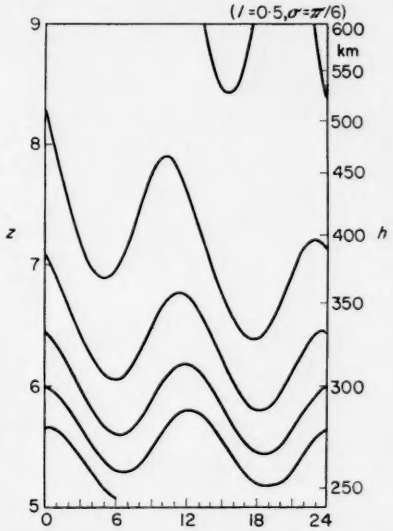


Fig. 1. An example of non-uniform and non-recurrent motions in the ionosphere. The amplitude of semi-diurnal vertical drift velocity is assumed to be inversely proportional to the one-quarter power of molecular density and the phase to advance with height with the rate of gradient of $\sigma = \pi/6$.

density proportionally to $\exp\{-2(1 + \Gamma)z\}$, while the latter varies with atomic oxygen (ionizable constituent) density proportionally to $\exp\{-(1 + \Gamma)z\}$ in regions sufficiently high tone glect the term $\sec \chi . \exp\{-z + z_0{}^m\}$ as compared with $z - z_0{}^m$, where $\Gamma$ is the scale height gradient and $z$ is measured in units of scale height of O atoms.* Now, in these circumstances, enters a difficulty that the electron density will increase upwards without limitation in a steady state, consequently having no maximum. Accordingly, in order to make possible the formation of the *F2*-layer above the *F1*-layer for this model, we must assume that an apparent attachment coefficient decreases with height more slowly in the regions above a certain level—about 300 km. This assumption is practically justified by considering the effect of downward diffusion of electron–ion pairs in the upper atmosphere, which certainly plays an important part in the regions above 300 km. In this connexion Yonezawa (1956) showed that in a steady state the electron density can have its maximum under the influence of downward diffusion of

* The superscript $m$ means the maximum value (for $\chi = 0$).

electron–ion gases in the gravity field. Furthermore, it can be shown by the writer's calculations (SHIMAZAKI, 1957a and 1959) that for any initial distribution electrons produced over 300 km fall down by diffusion rapidly to the lower regions of greater absorption and disappear there, so that the maximum may be produced at about this level (300 km). In the regions above this level the diffusion equilibrium will be established for the electron–ion gases within an hour or so, much shorter than periods of thermal or tidal variations (one day or a half). Thus in these regions of diffusive equilibrium the electron density will distribute proportionally to $\exp\{-(m_1/m + \Gamma)z\}$ and the apparent attachment coefficient varies proportionally to $\exp\{-(1 - m_1/m)z\}$. It is therefore legitimate to assume that an apparent

Table 1. Average heights of the *F2*-layer (in km) at noon and midnight in various seasons and epochs of the solar cycle
(The brackets indicate the day-time in winter, at which the height is extremely low).

| | | March | June | September | December | Mean |
|---|---|---|---|---|---|---|
| *Sunspot maximum* (1947) | | | | | | |
| Northern hemisphere | noon | 386 | 450 | 409 | (361) | 401 |
| | midnight | 387 | 424 | 409 | 392 | 403 |
| Southern hemisphere | noon | 378 | (334) | 364 | 416 | 371 |
| | midnight | 410 | 368 | 392 | 411 | 395 |
| *Sunspot minimum* (1952) | | | | | | |
| Northern hemisphere | noon | 315 | 377 | 331 | (284) | 327 |
| | midnight | 354 | 349 | 353 | 329 | 346 |
| Southern hemisphere | noon | 325 | (275) | 315 | 360 | 319 |
| | midnight | 334 | 333 | 321 | 333 | 330 |

attachment coefficient decreases with height rather slowly proportionally to $\exp\{-0{\cdot}5z\}$ in the regions above 300 km, while it decreases very rapidly proportionally to $\exp\{-2(1 + \Gamma)z\}$ in the regions lower than this level.

By comparing the daily variations calculated theoretically for various assumed motions against the above-mentioned model of the *F2*-layer with the observational results, the following conclusion may be derived (SHIMAZAKI, 1956a, b, 1957a).

(a) An upward scale height gradient has an appropriate effect on the Bradbury *F2*-layer. The calculated daily variations in the maximum electron density become very similar to the observed ones, if we consider the effect of positive scale height gradient with height. Furthermore, it must particularly be noted that this effect enlarges the electron production rate near the level of maximum electron density, which is quite contrary to the result obtained by GLEDHILL and SZENDREI (1950) who carried out the calculations against the Chapman model of the *F2*-layer.

(b) Temperature variations have a striking effect on the height of the layer, but little effect on the shape of daily variations in the maximum electron density. This effect seems to explain well the observed lower height of the layer in sunspot minimum year than in maximum and the fact that the layer reaches the highest and lowest level during the daytime in summer and winter, respectively, as is readily seen in Table 1.



VOL. 15 1959

(c) A non-uniform *semi-diurnal* vertical drift velocity has a serious effect on the daily variations in the *F2*-layer. This effect is very favourable for explaining the observed daily variations in the *F2*-layer at various latitudes and seasons. Remarkable similarities can be clearly seen between the calculated and observed variations at all times and seasons except during the daytime in winter, if we take the non-uniform velocity whose amplitude increases inversely proportionally to a quarter power of the molecular density ($m = 0{\cdot}25$) and whose phase advances ($\sigma > 0$) with height (cf. Fig. 2 and Fig. 3a). During the daytime in winter, however, the situation is quite different and the non-uniform velocity seems to have the opposite characteristics, i.e. the amplitide decreases ($m = -0{\cdot}25$) and the phase lags ($\sigma < 0$) with height (cf. Fig. 2 and Fig. 3b). In both cases, the change with latitudes of daily variations may well be explained by shifting forward gradually the phase, as a whole, with decreasing latitudes, except near the equator. On the other hand, the practical observational results bring about the fact that the *F2*-layer is formed at much lower level during the daytime in winter as is seen in Table 1. Thus, the above-mentioned opposite characteristics of the non-uniform velocities during the daytime in winter may be caused by the difference of the height of the layer at these hours from the heights at other times and seasons. It is therefore concluded that the amplitude increases with height in the *upper F2*-regions and decreases in the *lower F2*-regions. The critical level of these two *upper* and *lower F2*-regions may be situated a little higher than the height of the layer during the daytime in winter—about 350 km in sunspot maximum and 280 km in sunspot minimum. This may correspond to the fact that the kinematic viscosity increases with height in the lower regions, reaching the maximum value somewhere in the *F2*-regions and then decreases with height in the upper regions, as was suggested by YERG (1953). According to his theory, it has the maximum value at about 240–350 km.

(d) A non-uniform *diurnal* vertical drift velocity has not a desirable effect except near the equator. It is generally known that the dynamo field estimated from the daily geomagnetic variations has a large diurnal component and, if this produces the vertical drift motions in the *F2*-regions, the effect of diurnal component of the motion should appear clearly in the observed daily variations in the *F2*-layer. In practice, this is not the case except near the equator, and the effect of the dynamo field will hardly reach the *F2*-regions. This may give evidence that the electric field does not extend so effectively to the *F2*-regions from the lower dynamo regions. This conclusion is supported also by the writer's recent investigation (SHIMAZAKI, 1957b and 1958), which shows that the effect of $S_q$ current system practically disappears in the *F1*-regions although it predominates in the *E*-regions. As a matter of fact, we can see a marked departure from the Chapman theory in the *E*-layer, i.e. the observed $f_0E$ is larger than the theoretical value at lower latitudes and is reversed at higher latitudes. This departure is well explained as the effect of non-uniform vertical drift velocity produced by the $S_q$-field, if the velocity decreases with height (see also APPLETON *et al.*, 1955 and BEYNON and BROWN, 1956). On the other hand, the effect of $S_q$ current system cannot be seen in the *F1*-layer, because this layer shows a very regular variation according to the simple Chapman theory. Thus, it appears true that the diurnal electric field which originated from

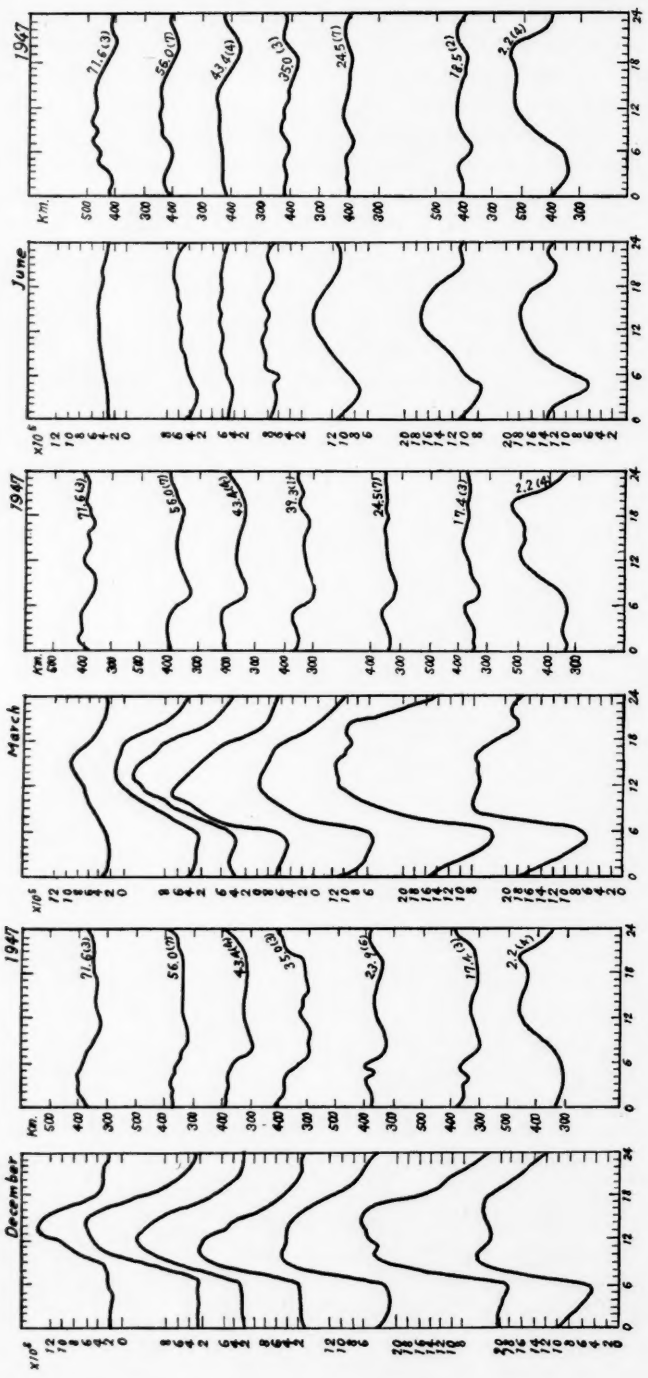
1947
December
March
June
Km.
71.6(3)
56.0(7)
43.4(4)
35.0(3)
23.9(6)
17.4(3)
2.2(4)
24.5(7)
18.5(2)

(a)

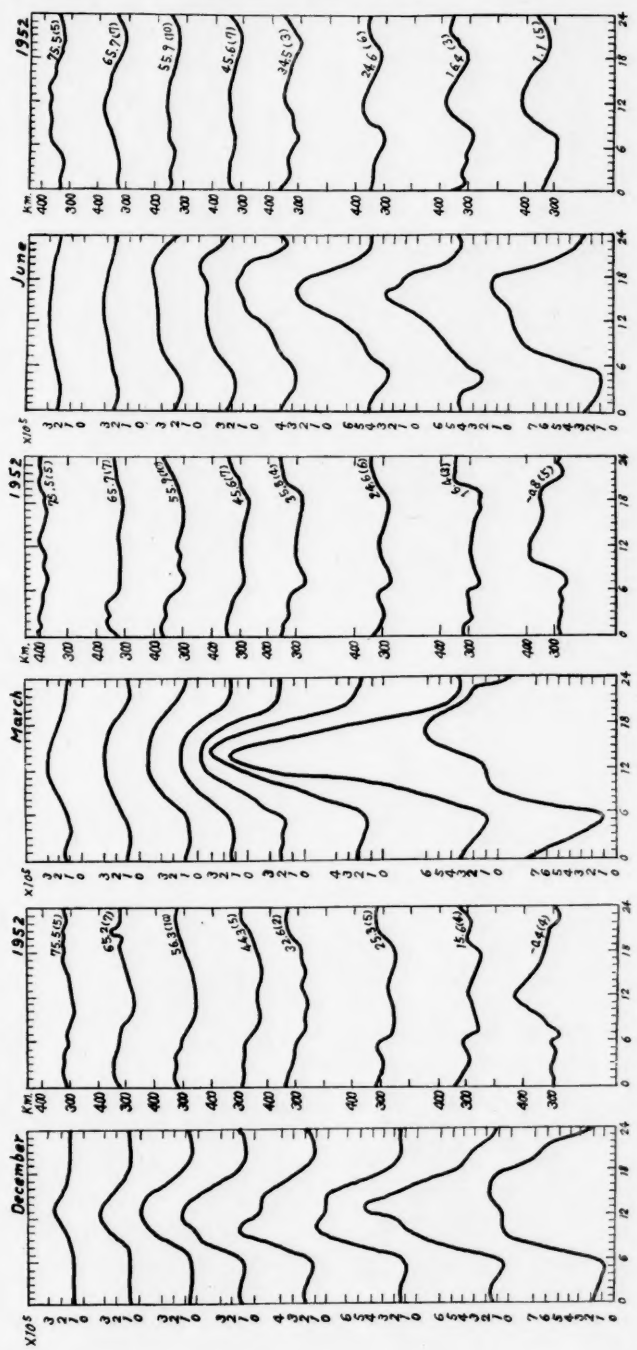


Fig. 2 (a) and (b) Average daily variations in the *F2*-layer observed at different latitudes and seasons in sunspot maximum (1947) and near the minimum (1952) years. The figures on each curve indicate the mean geomagnetic latitude of observatories to obtain the curve, and the figure within brackets is the number of observatories involved in each case. The height of the *F2*-layer was calculated from M(3000)*F2* by the formula (SHIMAZAKI, 1955) $h_pF2 = -176 + 1490/(\mathrm{M3000})F2$.

the lower dynamo regions is not so effective to produce the main features of the observed daily variations in the *F2*-layer. And this may suggest the fact that strong semi-diurnal motions do exist in the *F2*-regions and produce semi-diurnal dynamo fields, which are strong enough to outweigh the diurnal electric field transmitted from the lower dynamo region. As a result, the latter will become

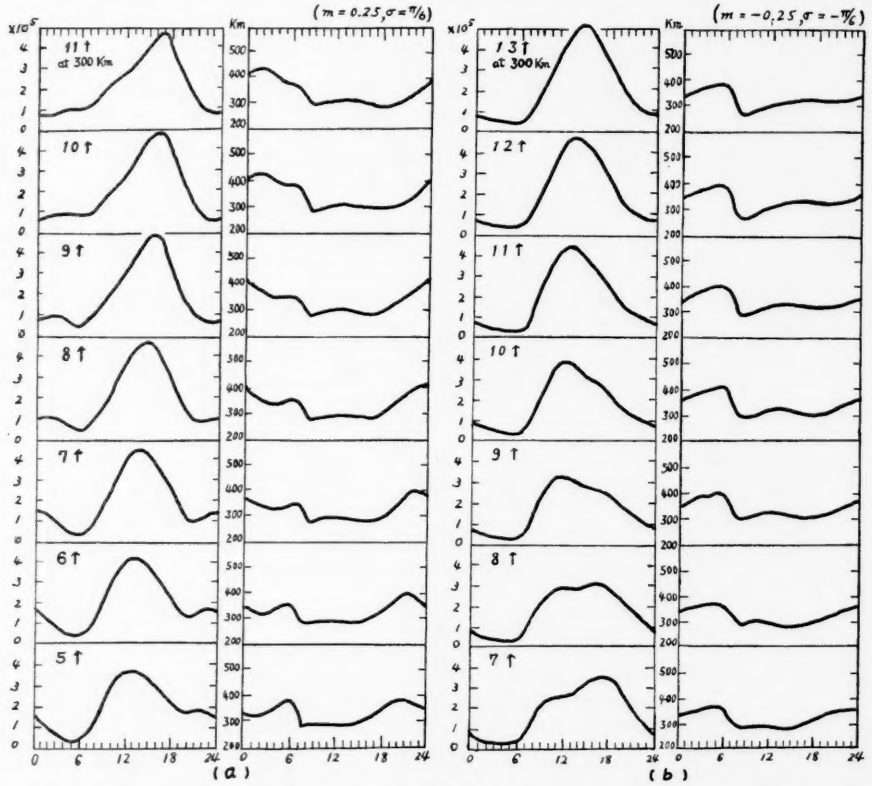


Fig. 3. Illustrating the effect of non-uniform semi-diurnal vertical drift velocities. The left (a) explains well the observed daily variations at various latitudes in all times and seasons except during the daytime in winter, while the right (b) those observed during the daytime in winter.

ineffective except near the geomagnetic equator. In this connexion, it is very interesting to see that the counter electric field due to induction drag much reduces the effect of applied electric field except near the equator (HIRONO, 1953).

## REFERENCES


| | | |
|---|---|---|
| APPLETON E. V., LYON A. J. and TURNBULL, A. G. | 1955 | *Nature, Lond.* **176,** 897. |
| BEYNON W. J. G. and BROWN G. M. | 1956 | *Nature, Lond.* **177,** 583. |
| GLENHILL J. A. and SZENDREI M. | 1950 | *Proc. Phys. Soc.* B **63,** 427. |
| HIRONO M. | 1953 | *J. Geomag. Geoelectr.* **5,** 22. |
| RATCLIFFE J. A., SCHMERLING E. R. and THOMAS, J. O. | 1956 | *Phil. Trans.* A **248,** 621. |




VOL. 15 1959

| | | |
|---|---|---|
| SHIMAZAKI T. | 1955 | *J. Radio Res. Lab.* **2,** 85. |
| SHIMAZAKI T. | 1956a | *Rep. Ionos. Res. Japan* **10,** 124. |
| SHIMAZAKI T. | 1956b | *J. Radio Res. Lab.* **3,** 17. |
| SHIMAZAKI T. | 1957a | *J. Radio Res. Lab.* **4,** 309. |
| SHIMAZAKI T. | 1957b | *J. Radio Res. Lab.* **4,** 37. |
| SHIMAZAKI T. | 1958 | *J. Radio Res. Lab.* **5,** 35. |
| SHIMAZAKI T. | 1959 | *J. Radio Res. Lab.* **6,** 107. |
| YERG D. G. | 1953 | *Scientific Report* No. 45. Ionosphere Lab., State University, Penn., U.S.A. |
| YONEZAWA T. | 1956 | *J. Radio Res. Lab.* **3,** 1. |


OL.
15
959

Journal of Atmospheric and Terrestrial Physics, 1959, Vol. 15, pp. 116 to 120. Pergamon Press Ltd. Printed in Northern Ireland

# Ionospheric *F2*-disturbances associated with geomagnetic storms

TERUO SATO*

**Abstract**—An attempt is made to explain the ionospheric *F2*-disturbances associated with the geomagnetic storms by the electron drift theory. The study is made of the individual states of the disturbances. The results show that the *F2*-disturbances in the equatorial zone and most of disturbances in middle latitudes can be explained as the effects of the vertical drift of electrons.

## 1. INTRODUCTION

IN this paper it is examined whether an individual *F2*-disturbance associated with the geomagnetic storm is explained by the effect of vertical drift of electrons. The drift of electrons is assumed to be caused by the electric field deduced from the geomagnetic disturbance–daily variation. The study is made of the individual state of the disturbance in the equatorial zone and in middle latitudes.

## 2. METHOD OF TREATMENT OF GEOMAGNETIC DATA AND THEORETICAL CONSIDERATIONS

Since it is difficult to derive the disturbance–daily variation of a geomagnetic storm at one station, the following method is taken for the sake of convenience. The values of the horizontal intensity ($H$) and the declination ($D$) of the geomagnetic field for the local time nearest to that of the commencement of the geomagnetic storm are taken, and from these values the mean values of $H$ and $D$ on five international quiet days corresponding to that hour are respectively subtracted. The values thus obtained are the deviative parts at hour zero of the storm time. This process is followed for succeeding 60 hr. They are denoted, respectively, as $\Delta H$ and $\Delta D$. Next the overlapped means of 24 hr of them are calculated for the earlier 48 hr, assuming that the deviative values before the commencement of the geomagnetic storm are zero. Then the variations can be said to correspond to the $D_{st}$ variation of the average state. When these variations are subtracted respectively from $\Delta H$ and $\Delta D$, the parts corresponding to the disturbance–daily variation, $D_s$, of the average state can be derived.

When an anisotropic electrical conductivity of the ionosphere is taken into account, and it is assumed that the winds in the $E$- and $F$-regions have the same directions and magnitudes, and that the earth's magnetic field is produced by a dipole magnet, the vertical velocity of the electrons in the $F$-region is given by (MAEDA, 1955):

$$v = \left(\frac{I_x}{K_{xy}} + \frac{I_y}{K_y}\right) \frac{\sin\theta}{F(1 + 3\cos^2\theta)^{1/2}} \tag{1}$$

where $I_x$ and $I_y$ represent the total electric currents in the $x$ (south) and $y$ (east)

* Geophysical Institute, Kyoto University, Kyoto, Japan.



VOL. 15 1959

directions flowing in the *E*- and *F*-regions, $\theta$ the geomagnetic co-latitude, $F$ the total intensity of the geomagnetic field and

$$K_{xy} = \frac{\Delta}{k_{xy}},\ K_y = \frac{\Delta}{k_x}, \qquad \Delta = k_{xy}^2 + k_x k_y \tag{2}$$

where

$$k_x = \int_E \sigma_{xx}'\, dz + \int_F \sigma_{xx}'\, dz, \quad \text{etc.} \tag{3}$$

and $\sigma_{xx}'$, etc. are the elements of the electrical conductivity tensor $\sigma = \begin{Vmatrix} \sigma_{xx}' & \sigma_{xy}' \\ \sigma_{yx}' & \sigma_{yy}' \end{Vmatrix}$. The integration is carried out for the *E*- and *F*-regions. $I_x$ and $I_y$ are related approximately to the geomagnetic components in $y$- and $x$-directions in such a way that

$$2\pi I_y = -f\Delta X, \qquad 2\pi I_x = +f\Delta Y \tag{4}$$

where $f$ is constant and taken as unity. If the station is situated on the magnetic equator the expression of the vertical velocity is simplified as follows:

$$v = \frac{\Delta X}{2\pi K F} \tag{5}$$

where $K$ is the electrical conductivity on the magnetic equator. The vertical velocity ($v_d$) on the disturbed day is calculated by using $\Delta X$ and $\Delta Y$ derived from the $D_s$-variation.

In the course of the study it is necessary to know the daily variation of the *F2*-region on the quiet day. We assume that the vertical drift of electrons affects the quiet daily variation of the *F2*-region. The vertical velocity ($v_q$) is given by the same expressions as (1) or (5) on substituting the values on the quiet day into the respective terms. The values of $\Delta X$ and $\Delta Y$ are those derived from the mean values of the $S_q$-variations on the five international quiet days in the months when the storms occur.

If the effect of the horizontal velocity and the height gradient of the vertical velocity are not taken into account, the variation of the electron density ($n$) is given by

$$\frac{\partial n}{\partial t} = q(t, z) - \beta n - v\frac{\partial n}{\partial z} \tag{6}$$

where $v$ represents the vertical velocity of the drift, $q$ and $\beta$ the production and the effective attachment rates of the electrons, respectively, $t$ the time and $z$ the height in the unit of the scale height; $q$ is taken as $q_0 \exp(1 - z - e^{-z}\sec\chi)$, where $q_0$ is constant and $\chi$ the solar zenith angle. The height distribution of $\beta$ is shown in Fig. 1. If the velocity $v$ in (6) equals $v_q$ the solution of the equation represents the quiet daily variation and if $v$ equals $(v_q + v_d)$ the solution represents the daily variation on the disturbed day. When the former variation is subtracted from the latter, the residue equals to the deviative part from the normal variation.

### 3. IONOSPHERIC DISTURBANCES IN THE EQUATORIAL ZONE

The *F2*-disturbances in the equatorial zone are studied for the individual state using the data during the years 1938–1939 at Huancayo which is situated on the magnetic equator (SATO, 1956). The electric conductivity is taken as

$$K = 1{\cdot}73 \times 10^{-7} p(t) \quad \text{e.m.u.} \tag{7}$$

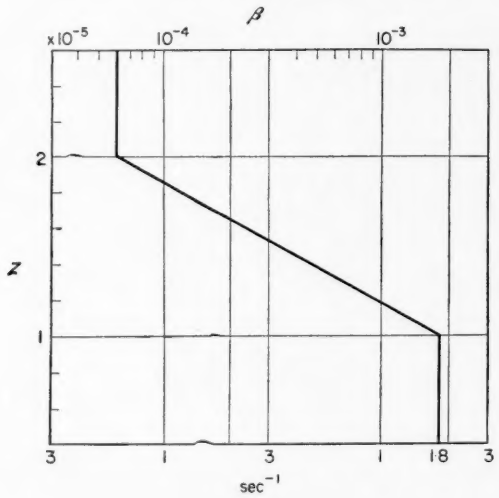


Fig. 1.

both for the quiet and disturbed days. $p(t)$ is the daily variation factor, the seasonal variation of which is neglected. It is shown in Table 1.

Table 1

| Local time (hours) | 0000 | 0200 | 0400 | 0600 | 0800 | 1000 | 1200 | 1400 | 1600 | 1800 | 2000 | 2200 |
|---|---|---|---|---|---|---|---|---|---|---|---|---|
| $p(t)$ | 0·27 | 0·21 | 0·21 | 0·58 | 1·36 | 2·20 | 2·57 | 2·20 | 1·36 | 0·58 | 0·21 | 0·21 |

An example of the observed and calculated variations of the *F2*-disturbances is shown in Fig. 2. The observed values are those for the disturbance at 1600 hours, 2 February 1938 at Huancayo (the time is the nearest local time before the commencement). In Fig. 2 the top part represents the observed deviation of $f_0F2$ ($\Delta f_0F2$, full line, right ordinate) and the observed deviation of $h'F2$ ($\Delta h'F2$, broken line, left ordinate), where $f_0F2$ and $h'F2$ represent, respectively, the critical frequency and the virtual height of the *F2*-region; the centre the corresponding calculated variations (the deviation of the electron density is shown by the full line, right ordinate); and the bottom the disturbance–daily variation of $\Delta H$. It is clear that the agreement between the calculated and the observed deviations is good and that the *F2*-disturbances in the equatorial zone can be explained as the effect of vertical drift of electrons.



VOL. 15 1959

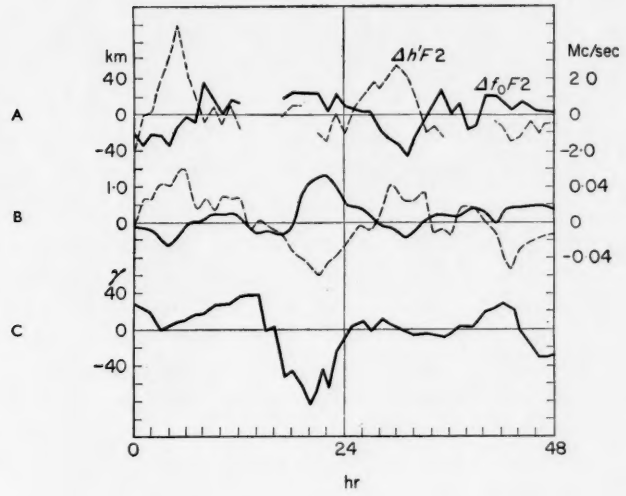
km
40
0
-40
Δh'F2
Δf₀F2
Mc/sec
2·0
0
-2·0
A
1·0
0
0·04
0
-0·04
B
γ
40
0
-40
C
0
24
48
hr

Fig. 2.

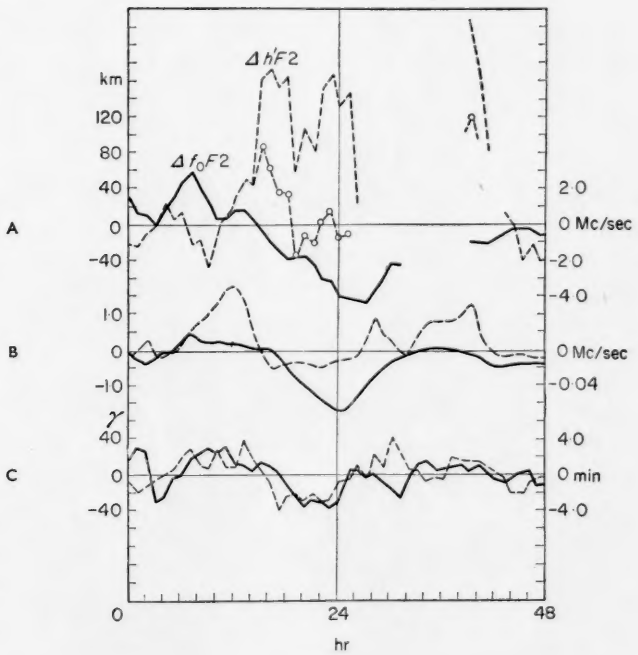
Δh'F2
km
120
80
40
0
-40
Δf₀F2
2·0
0 Mc/sec
-2·0
-4·0
A
1·0
0
-10
0 Mc/sec
-0·04
B
γ
40
0
-40
4·0
0 min
-4·0
C
0
24
48
hr

Fig. 3.

## 4. IONOSPHERIC DISTURBANCES IN MIDDLE LATITUDES

The *F2*-disturbances in middle latitudes are studied using the data at Watheroo during the years 1938–1944 and at Kokubunji (the geomagnetic data are those at Kakioka) during the years 1949–1955. The daily variations of the electrical conductivities, $K_{xy}$ and $K_y$, are taken as

$$K_{xy} = 1{\cdot}6 \times 10^{-8}\, p(t), \quad \text{e.m.u.} \qquad (8)$$
$$K_y = 3{\cdot}0 \times 10^{-8}\, p(t), \quad \text{e.m.u.}$$

for the two stations; $p(t)$ on the disturbed day is different from that on the quiet day and it varies with season, but the details are omitted in the present case.

An example of the calculated and observed deviations of the *F2*-disturbances is shown in Fig. 3. The observed values are those for the disturbance at 1500 hours, 12 November 1940 at Watheroo. In Fig. 3 the top two parts correspond to those in Fig. 2 and the bottom represents the disturbance–daily variations of $\Delta H$ and $\Delta D$ (the former is shown by the full line, left ordinate). Since the observed height deviation includes the effect of the retardation of the radio wave in the day time, the corrected deviation is also shown by the dotted line with the white circle. From Fig. 3 the calculated deviations of the height and electron density seem to be consistent well with the observed values. Since the observed deviation in Fig. 3 is the representative type of the *F2*-disturbances in middle latitudes most of disturbances in those latitudes are considered to be accounted for as the effect of the electron drift. The positive disturbances are also studied and the results show that the height variation, and partially the variation of the electron density, can be explained by the drift theory.

VOL.
15
195

### REFERENCES

MAEDA K. 1955 *Rep. Ionos. Res. Japan.* **9**, 71.
SATO T. 1956 *J. Geomagn. Geoelect, Kyoto* **8**, 129.

Journal of Atmospheric and Terrestrial Physics, 1959, Vol. 15, pp. 121 to 125. Pergamon Press Ltd. Printed in Northern Ireland

# Equatorial spread-*F*

R. W. WRIGHT* and N. J. SKINNER*

**Abstract**—Spread-*F* conditions have been examined for six low-latitude stations—Dakar, Khartoum, Djibouti, Ibadan, Nairobi and Leopoldville.

It is shown that, contrary to the general view, occurrence of disturbed magnetic conditions inhibits the occurrence of spread-*F* layers during the southern solstice at all these stations. The seasonal variation of the occurrence of spread-*F* is considerably changed if, instead of all days, only magnetically quiet days are considered.

In the northern winter there appears to be widespread correlation of occurrence of spread-*F* across Africa. This is shown to be due to the magnetic influence.

## 1. INTRODUCTION

ONE very noticeable phenomenon at most stations of low latitude is the prevalence of spread echoes from the *F*-layer at night. The general properties of this type of behaviour have been observed at Huancayo by WELLS (1954) and at stations further away from the equator by REBER (1954a, b). In a previous paper (WRIGHT *et al.*, 1956) an analysis was made of results observed at Ibadan, Nigeria, where the magnetic latitude is about $2\frac{1}{2}°$S. This analysis is now extended to cover other low latitude stations—Dakar, Khartoum, Djibouti, Nairobi and Leopoldville. The seasonal, diurnal, and magnetic variations of spread-*F* for each station are shown to be similar.

## 2. REDUCTION OF RECORDS FOR SPREAD-*F*

In Table 1 are summarized the geographical locations and magnetic latitudes of the six stations considered. The sources of information and the periods analysed are also indicated. The period 1955–1957 was selected for Leopoldville and Nairobi as that was the only convenient period for which data were available. The period 1952–1953 was selected for the other stations because a maximum of data was available for these years. The magnetic latitude is given in Table 1 and not the geomagnetic latitude. We feel that it is the actual angle of dip in the ionosphere which controls the equatorial anomalies due to the earth's magnetic field. This angle is not likely to be very different from the angle of dip on the ground.

An index of scatter ($S$) is defined as in our previous communication, whereby an integer between 0 and 3 is assigned to each hourly value of $f_0F2$. Thus, when no value of $f_0F2$ can be measured because of the prevalence of spread echoes, the symbol $F$ is normally used in the routine reduction and the corresponding index of scatter is $S = 3$.

Table 2 summarizes the system used to determine the index $S$ from the tables of hourly values of $f_0F2$.

Although Table 2 is based on the internationally agreed method of reduction when spread echoes are present, we realize that individual observers may interpret

* University College, Ibadan, Nigeria.

and reduce their ionograms differently. Consequently, there may be differences in the level of scatter indicated from station to station, and from one observer to another at the same station. One cannot even guarantee that a single observer will be consistent in his reductions over a long period. Furthermore, the value of $S$ is dependent upon the recorder sensitivity. All these factors must therefore be

Table 1

| Station | Latitude | Longitude | Magnetic latitude | Years analysed | Source |
|---|---|---|---|---|---|
| Dakar | 14½°N | 17½°W | 12°N | 1951–1953 | Bulletin O.D. S.P.I.M. |
| Khartoum | 15½°N | 32½°E | 6½°N | 1952–1953 | Bulletin B. Radio Res. Board, Slough. |
| Djibouti | 11½°N | 43°E | 2½°N | 1952–1953 | Bulletin O. Dj. S.P.I.M. |
| Ibadan | 7½°N | 4°E | 2½°S | 1952–1954 | Separate reduction from records. |
| Nairobi | 1°S | 37°E | 10°S | 1955–1957 | Bulletin ETDN. S.A. C.S.I.R. |
| Leopoldville | 4½°S | 15°E | 12°S | 1955–1957 | Bulletin of Bureau de Géophysique, Congo Belge |

VOL.
15
1959

borne in mind when inter-comparison of absolute levels of scatter is made between different stations and for different years. In this paper such comparisons are avoided.

The results have been divided into three seasons, winter (Nov., Dec., Jan., Feb.); summer (May, June, July, Aug.); and equinoxes (March, April, Sept., Oct.).

Table 2

| Index of scatter $S$ | Symbol in $f_0F2$ tables | Explanation |
|---|---|---|
| 3 | $F$ | $f_0F2$ unreadable due to spread echoes |
| 2 | e.g. (6·9)$F$ | $f_0F2$ doubtful due to spread echoes |
| 1 | 6·9$F$ | Some scatter present but $f_0F2$ reliable |
| 0 | 6·9 | No scatter |

These groups have been divided into magnetically quiet nights ($q$) and magnetically disturbed nights ($d$). In the initial treatment accorded to results from Dakar, Djibouti, Khartoum and Ibadan, $d$-nights are those that follow a day when the total of the geomagnetic planetary 3 hr range indices, $K_p$, is greater than 30, while $q$-nights follow days where $K_p$ is less than 16. For the later data for Leopoldville and Nairobi the magnetic conditions were different owing to considerable difference in the sunspot-cycle epoch, and the internationally agreed quiet and disturbed days were used.

Fig. 1 shows the average nocturnal variation of $S$ on $q$- and $d$-nights for the various seasons for all stations. The most important point shown by Fig. 1 is that at all the stations near the southern solstice, spread $F$-layers are more prevalent on magnetically quiet days. Magnetic disturbances *reduce* the likelihood of the occurrence of spread-$F$ layers. As the season changes towards the northern solstice, the effect diminishes effectively to zero. We have already shown (WRIGHT *et al.*, 1956) that in the case of a typical temperate-latitude station, Slough, the spread-$F$ conditions are definitely more prevalent during magnetically disturbed nights for all seasons.

A further result evident from a study of Fig. 1 is that the summer maximum of occurrence of spread-$F$ layers, which has often been remarked, is to some extent dependent upon the inclusion of magnetically disturbed days. If only quiet days are considered then the summer maximum is no longer a dominant feature, at least for the stations studied here. It would be of considerable interest to study the seasonal variations of spread-$F$ on quiet days for other stations, both equatorial and non-equatorial.

Data from two additional low-latitude stations were available at Ibadan: Singapore at 1°N geographic latitude and 10°S magnetic latitude, and Elizabethville at $11\frac{1}{2}$°S geographic latitude and about 20°S magnetic latitude. The Singapore results 1952–1953 were found to show remarkably little spread-$F$ in view of its low latitude, yet OSBORNE (1951) has indicated that a considerable amount does exist, at any rate for 1949–1950. This would suggest that the discrepancy may be due to the manner in which the data were reduced and presented. In any case, spread-$F$ for the period analysed at Singapore shows very little difference between quiet and disturbed nights—though there is a slight suggestion of greater scatter on quiet nights in the northern solstice. At Elizabethville the occurrence of spread-$F$ conditions as recorded in the published bulletin, 1955–1957, is even less. Negligible difference was found between quiet and disturbed nights for any season.

Data for later years at Ibadan have been examined and it is found that the effects shown in Fig. 1 are quite typical of all years.

## 3. Correlation between Stations

Owing to the high correlation shown between the scintillation of radio stars at Accra and the value of $S$ at Ibadan, over a distance of 500 km, we have examined the correlation between values of $S$ obtained at Ibadan, Dakar and Djibouti. A single value of $S$ was assigned to each night and each station. It was found that between Ibadan and Dakar, over a distance of 2300 km, these values had correlation coefficients

$r_{\text{I–Da}}$ (winter) $= 0{\cdot}4$ (no. of nights used $n = 103$) significant at 1 per cent level
$r_{\text{I–Da}}$ (summer) $= -0{\cdot}075$ ($n = 71$)

Between Ibadan and Djibouti, over a distance of 4300 km, the correlation coefficients were:

$r_{\text{I–Dj}}$ (winter) $= 0{\cdot}2$ ($n = 108$) significant at 5 per cent level
$r_{\text{I–Dj}}$ (summer) $= 0{\cdot}02$ ($n = 73$)

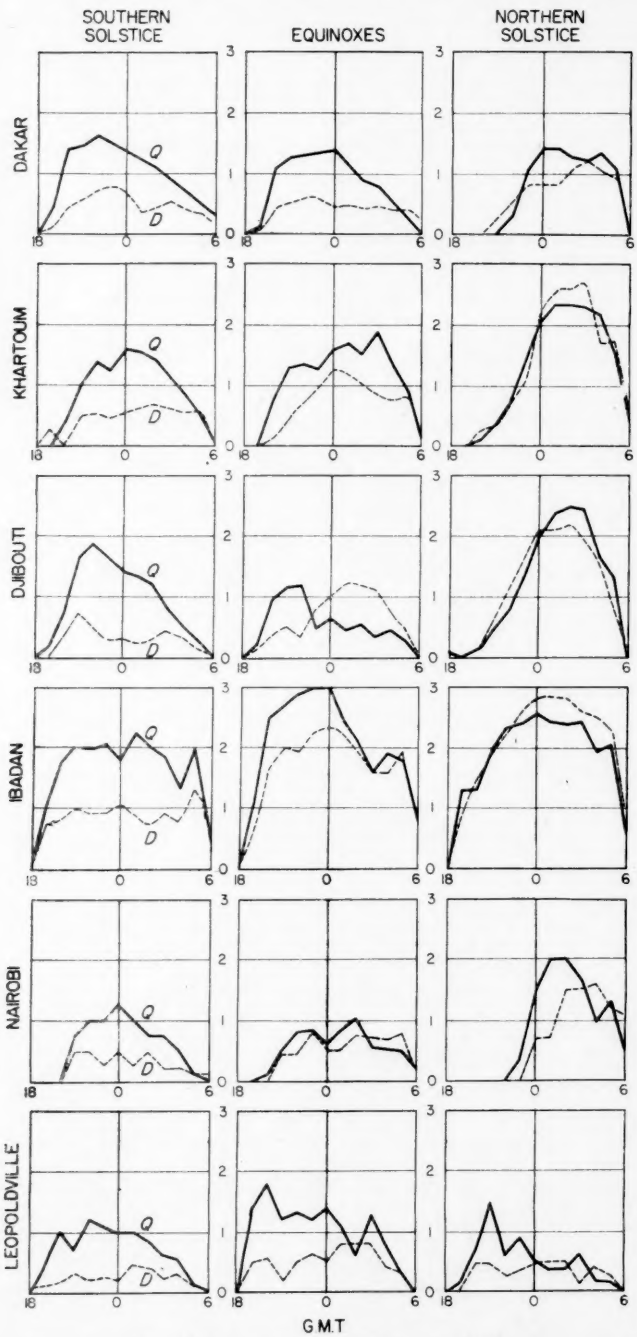


Fig. 1. Showing nocturnal variation of "spread-*F*" for the different seasons for six low-latitude stations. Solid lines for nights following magnetically quiet days. Broken line for nights following magnetically disturbed days.

The correlation in winter is definitely significant and, in view of the large distances involved, might indicate a very widespread occurrence of spread-$F$ layers. However, this large-scale coverage is not due to the inherent nature of spread-$F$ layers as is seen by the negligible correlation during the summer. It is due rather to the pronounced influence on the presence of spread-$F$ in winter of the world-wide magnetic conditions. This is borne out by the fact that the night-time $S$ number and the previous day's $K_p$ number at Ibadan have a correlation coefficient in winter of $-0{\cdot}42$, and at Dakar $-0{\cdot}34$. Furthermore, in winter (on quiet nights only) the correlation coefficient between occurrences of spread-$F$ layer at Ibadan and Dakar is $r_q = 0{\cdot}07$ ($n = 19$), while on disturbed nights only it is $r_d = 0{\cdot}06$ ($n = 26$), neither of which is significant.

## 4. Conclusions

(a) During the southern solstice spread-$F$ conditions are less likely on nights following magnetically disturbed days than those following magnetically quiet days.

(b) The effect is less pronounced during the equinoxes and is negligible in the northern solstice.

(c) The seasonal variation of incidence of spread-$F$ conditions is considerably affected by the inclusion of magnetically disturbed days. If only quiet days are considered, the predominant summer maximum of spread-$F$ occurrence is considerably reduced at the stations considered.

(d) These conclusions are valid for Dakar, Djibouti, Ibadan, Khartoum, Leopoldville and Nairobi. All are low-latitude African stations.

(e) At Elizabethville, further than the other stations from the magnetic equator, the incidence of spread-$F$ conditions recorded in the period studied is insufficient to give conclusive results, but no evidence of the effect was found.

(f) At Singapore also the occurrence of spread-$F$ conditions recorded in the period studied is very low and very little evidence of such an effect is found.

(g) In the northern winter there is a widespread correlation of occurrence of spread-$F$ across Africa. This can be explained in terms of the magnetic influence reported in (a) above.

## References


| | | |
|---|---|---|
| Osborne B. W. | 1951 | *J. Atmosph. Terr. Phys.* **2,** 66. |
| Reber G. | 1954a | *J. Geophys. Res.* **59,** 257. |
| | 1954b | *J. Geophys. Res.* **59,** 445. |
| Wells H. W. | 1954 | *J. Geophys. Res.* **59,** 273. |
| Wright R. W., Koster J. R. and Skinner N. J. | 1956 | *J. Atmosph. Terr. Phys.* **8,** 240. |

Journal of Atmospheric and Terrestrial Physics, 1959, Vol. 15, pp. 126 to 129. Pergamon Press Ltd. Printed in Northern Ireland

# On the occurrence of the $F1\frac{1}{2}$-layer at Tokyo

ISAO KASUYA*

**Abstract**—From a statistical analysis on a basis of routine ionospheric observations at Tokyo (Kokubunji) throughout the last solar cycle, it is found that annual, seasonal and diurnal variations exist in the frequency of occurrence of the intermediate layer, the $F1\frac{1}{2}$-layer at the middle latitude of Tokyo. The $F1\frac{1}{2}$-layer appears mostly in the daytime and is prevalent at both equinoxes, especially remarkable in late spring during years of high solar activity—there has been good correlation between the frequency of occurrence and the number of sunspots.

## 1. INTRODUCTION

IT is well known that we have three most regular and stable ionospheric layers, *F2*-, *F1*- and *E*-layers, of which the electron densities of the *F1*- and *E*- layers are influenced mainly by the solar zenith angle as well as the solar activity. However, the features of the *F2*-layer are not so simple as the variations of *E*- and *F1*-layers. In addition to the layers described above, we have sometimes noticed between *F1* and *F2* the intermediate stratification which seems to appear usually and rather more clearly than the *F1*-layer during years of an active solar cycle. This stratification is called the $F1\frac{1}{2}$-layer (in Japan, this is named *F12* by some workers, NAKATA (1948a, b)).

The layer has not yet been studied thoroughly in terms of its appearance and disappearance, the origin of occurrence, and variations with time, as well as the latitudinal effect of its occurrence, though some work has been done on this subject. Moreover, this has hitherto been considered as an unstable or transient layer which would appear only in the lower latitudinal zone. In this paper, the appearance of the $F1\frac{1}{2}$-layer is examined; whether it has regular variation with time or not, and especially is it influenced or not by solar activity?

## 2. SOURCE OF DATA

This study was conducted on the basis of ionograms obtained by routine observation at Kokubunji (35°42·4′ N, 129°29·3′ E), Tokyo, from January 1947 through June 1956, during nearly one cycle of solar activity. The data before November 1950 were obtained by manual operation of ionospheric sounding equipment, but since December 1950 observation has had recourse to automatic operation. The data obtained by manual operation may not safely be relied on, but they are used for completing the examination of long-period variations.

Now the following points should be noticed to count occurrences of the $F1\frac{1}{2}$-layer from the original ionograms. First, when there appear three clear stratifications in the *F*-region, the intermediate stratification should be counted as the $F1\frac{1}{2}$-layer, excluding the "lunar layer" as it is called. Secondly, when the *F1*-layer is not so clear—as is often the case—and $F1\frac{1}{2}$ cannot be sharply distinguished from *F1*, the frequency of occurrence of $F1\frac{1}{2}$ is counted by scrutinizing the sequential variation of the critical frequency of $F1\frac{1}{2}$.

* Radio Research Laboratories, Tokyo, Japan.



VOL. 15 1959

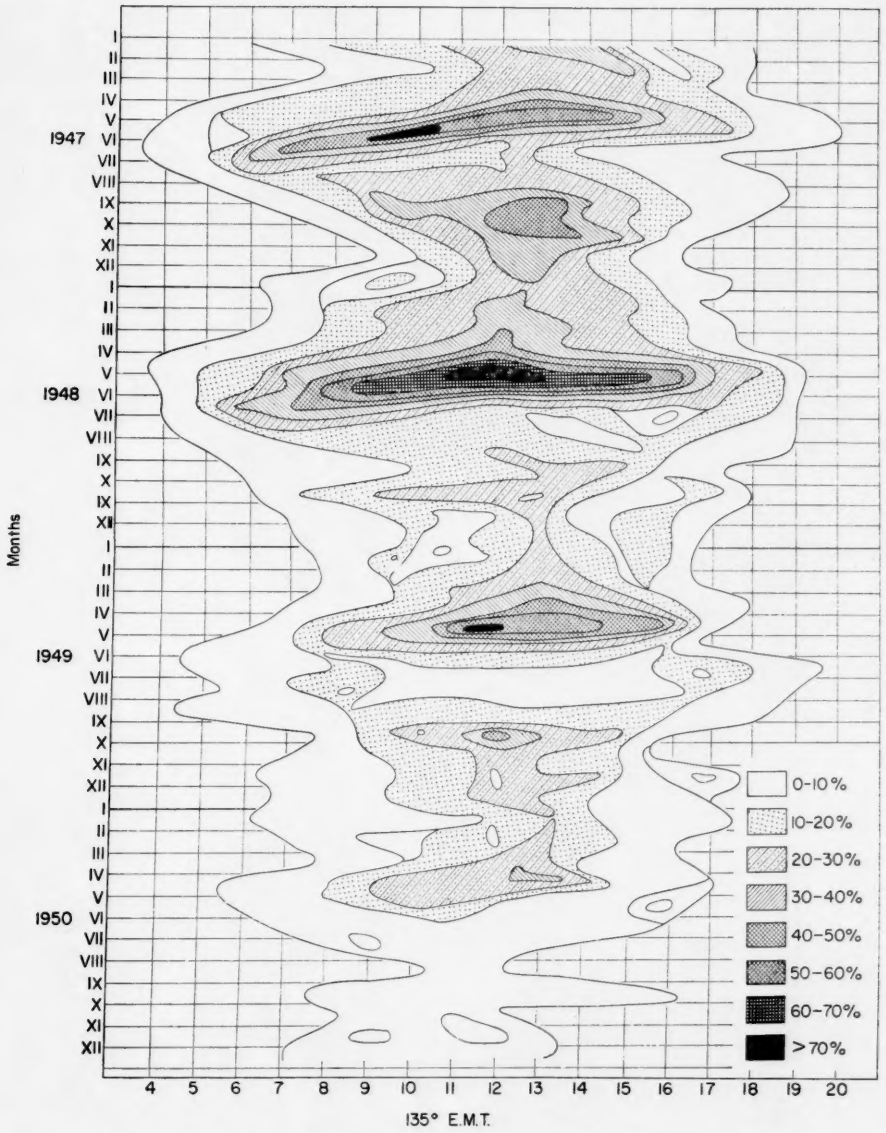


Fig. 1. Monthly variation of hourly percentage frequency of occurrence of the $F1\frac{1}{2}$-layer (frequency of occurrence/observed times 100 for every hour) at Tokyo (Kokubunji).

## 3. STATISTICAL RESULTS

### 3.1. *Diurnal variation*

Consider the monthly percentage of frequency of occurrence of $F1\frac{1}{2}$ with respect to the local time at Kokubunji (Fig. 1). From this diagram, it is obvious that $F1\frac{1}{2}$ has diurnal, seasonal and annual variations. The duration of appearance of $F1\frac{1}{2}$ may be chiefly affected by solar zenith distance, for it is long in summer and short in winter. The maximum frequency of $F1\frac{1}{2}$ is at about noon in winter,

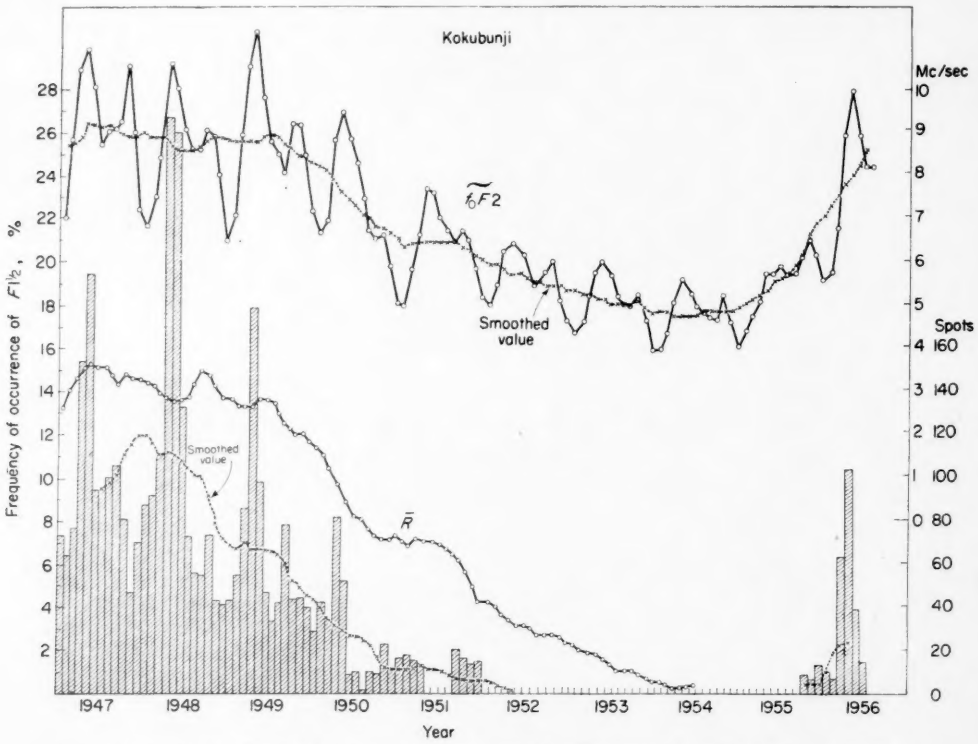


Fig. 2. Annual variation of the percentage frequency of occurrence of the $F1\frac{1}{2}$-layer (frequency of occurrence/total observed hour times 100 for every month) compared with the relative sunspot numbers $\bar{R}$ (smoothed values by 12 months' running average) and $f_0F2$ (mean of the hourly median values for each month).

but it comes earlier than at noon—10–11 a.m. in local time—in spring and summer. The diurnal variation is mostly flat in summer and has a peak in the afternoon in autumn. Sometimes there appear two peaks of occurrence in the morning and in the evening as seen in the summer of 1949.

### 3.2. *Seasonal variation*

The seasonal variation may be seen more clearly in Fig. 2, which shows the monthly percentage of frequency of occurrence regardless of hourly variations. The histogram indicates that there are the maxima of frequency at both equinoxes, the value in spring being higher than in autumn, while on the contrary, the



VOL. 15 1959

minima are at both solstices. The tendency is very similar to the monthly mean variation (denoted by $f_0F2$) of the hourly value of $f_0F2$ as shown in the upper curve in the same figure.

### 3.3. *Annual variation*

Fig. 2 also shows the annual variation of occurrence of $F1\frac{1}{2}$. If we smooth the seasonal variations by taking the running average of monthly histograms, we can pick up the annual variation of occurrence in the broken plots (in the figure it is referred to as the "smoothed value"). In the figure the relative sunspot number $R$ (smoothed value by 12 months' running average) is also illustrated for comparison with the annual variation of $F1\frac{1}{2}$. It can be easily seen that there exists a clearly parallel relationship with each other, and for $R < 40$ (the period from the middle of 1954 to the middle of 1955), $F1\frac{1}{2}$ would disappear. Thus, it is found that the $F1\frac{1}{2}$-layer is affected considerably by solar activity.

## 4. Discussion and Conclusion

As can be shown from the statistics mentioned above, we can ascertain that $F1\frac{1}{2}$ is not only the usual layer but also has diurnal, seasonal and remarkable annual variations in the frequency of occurrence even in the middle latitudinal zone such as Tokyo. Nakata (1948a, b, 1950) has pointed out that this layer must be considered as a not unusual layer. His suggestion agrees in part with the analytical results.

During the years of maximum number of sunspots, we have an almost continuous $h'f$ trace of the $F$-region and the cusp at the critical frequency of $F1$ is not so clear, but the higher stratification than $F1$—this is $F1\frac{1}{2}$—is so distinctive that we are apt to mistake $F1\frac{1}{2}$ for $F1$.

In the same manner as the analysis in case of Tokyo, similar results have been found in the diurnal, seasonal and annual variation of frequency of occurrence of $F1\frac{1}{2}$ at another place, e.g. Yamagawa (31°12·5′N, 130°37·7′E) in Japan situated lower than Tokyo in latitude. The percentage frequency of occurrence at Yamagawa seems to be somewhat more (about 2–3 per cent) than at Tokyo as a whole. The latitudinal effect, however, cannot be hastily deduced only from this result, not until many ionograms are available from the stand-point of the worldwide distribution.

Finally, referring briefly to the critical frequency of $F1\frac{1}{2}$, its value is 6·5 to 7·5 Mc/s or so at Tokyo, and there is no well-defined diurnal variation, but there seem to be some slight peaks in the morning and afternoon. The seasonal variation is also not distinguishable all round the year, having slight maxima at equinoxes.

Further, as to a lunar effect on $F1\frac{1}{2}$, the final conclusion has not yet been reached from the data dealt with above.

## References


| | | |
|---|---|---|
| Nakata Y. | 1948a | *I.A.T.M.E. Oslo.* |
| Nakata Y. | 1948b | *Proc. Inst. for Radio Waves* No. 3 |
| Nakata Y. | 1950 | *Rep. Ionos. Res. Japan*, **4**, No. 1. |

Journal of Atmospheric and Terrestrial Physics, 1959, Vol. 15, pp. 130 to 131. Pergamon Press Ltd. Printed in Northern Ireland

# Latitude dependence of $f_0F2$ over the range of 20°N to 69°S, obtained by ship-borne ionospheric sounder

Masami Ōse*, Kazuo Aida* and Hironobu Okamoto*

On the occasion of the first expedition of Japanese Antarctic Research 1956–1957, routine ionospheric sounding was carried out all the way by the ship-borne sounder on board the *Soya*.

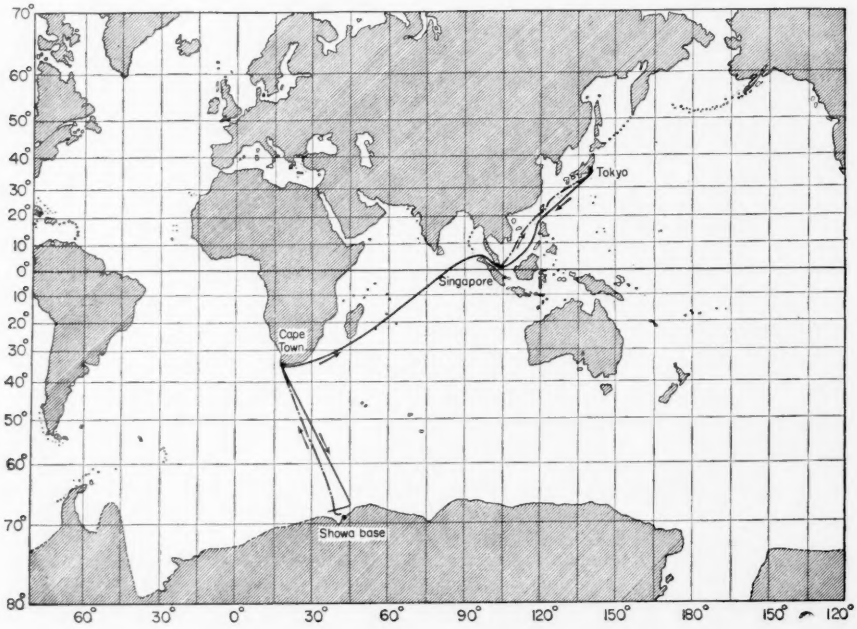


Fig. 1.

The sounding began on 11 November 1956, at the southernmost part of Japan and lasted until the ship came back there on 21 April 1957, keeping in routine observation at every 15 or 30 min. The route of the navigation is shown in Fig. 1. The southernmost latitude reached is 69°15′ in geomagnetic latitude in the Bay of Lützow-Holm.

The results obtained from the above sounding of the magnetic dependence of $f_0F2$ are represented in Figs. 2 and 3, corresponding to their noon and midnight values, respectively, taking the geomagnetic latitude as the abscissa. Here, the full line curve means the outward way and the broken the homeward way. It

* Radio Research Laboratories, Kokubunji, Tokyo.

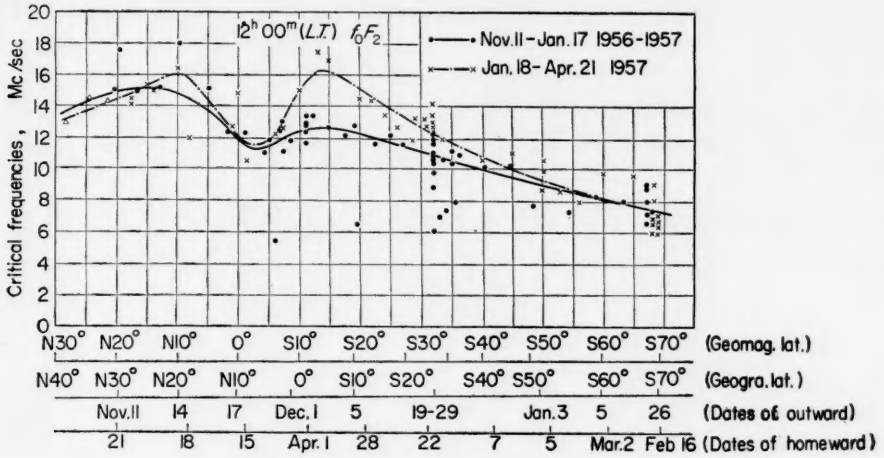
12h 00m (L.T.) foF2
Nov.11-Jan.17 1956-1957
Jan.18-Apr.21 1957
Critical frequencies, Mc/sec
N30° N20° N10° 0° S10° S20° S30° S40° S50° S60° S70° (Geomag. lat.)
N40° N30° N20° N10° 0° S10° S20° S40° S50° S60° S70° (Geogra. lat.)
Nov.11 14 17 Dec.1 5 19-29 Jan.3 5 26 (Dates of outward)
21 18 15 Apr.1 28 22 7 5 Mar.2 Feb.16 (Dates of homeward)

Fig. 2.

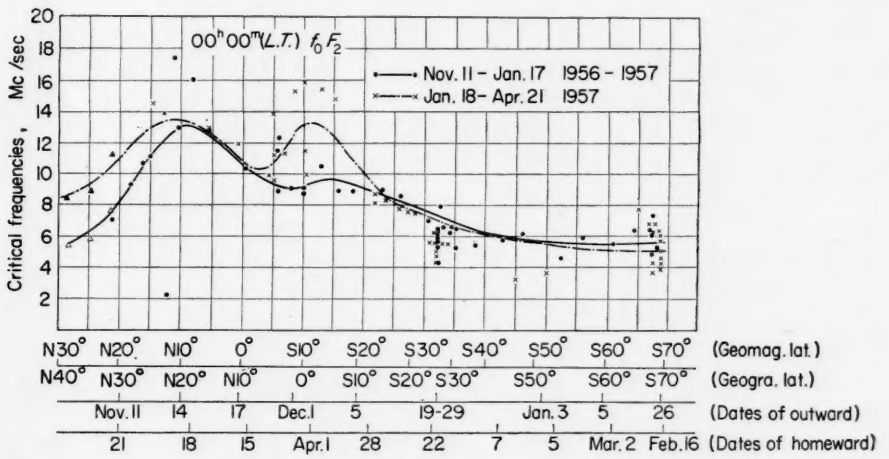
00h 00m (L.T.) foF2
Nov.11 - Jan.17 1956 - 1957
Jan.18 - Apr.21 1957
Critical frequencies, Mc/sec
N30° N20° N10° 0° S10° S20° S30° S40° S50° S60° S70° (Geomag. lat.)
N40° N30° N20° N10° 0° S10° S20° S30° S50° S60° S70° (Geogra. lat.)
Nov.11 14 17 Dec.1 5 19-29 Jan.3 5 26 (Dates of outward)
21 18 15 Apr.1 28 22 7 5 Mar.2 Feb.16 (Dates of homeward)

Fig. 3.

must be noticed that the data were derived from the observations carried out continuously and almost in the same conditions on the whole coverage of latitudes. These curves show the well-known characteristics with dips around the equator and the maxima on both sides of it. But, as they include regular and irregular variations and also longitudinal effects with themselves, it is not yet possible to find precisely the normalized shape of the characteristics free from the above variations and effects, until the necessary hourly values throughout the world are made available.

Journal of Atmospheric and Terrestrial Physics, 1959, Vol. 15, pp. 132 to 136. Pergamon Press Ltd. Printed in Northern Ireland

# Winds in the upper atmosphere

W. G. Elford*

## 1. Introduction

A systematic investigation of winds in the upper atmosphere by the radio observation of drifting meteor trails has been in progress at Adelaide since 1952. These observations have revealed the presence of regular but complex wind systems in that portion of the atmosphere between 75 and 105 km above the ground.

The line-of-sight speeds of drift of meteor trails are recorded automatically by means of a combined continuous wave and pulse system operating on a frequency of 27 Mc/s (Robertson *et al.*, 1953; Elford and Robertson, 1953). To determine the average monthly diurnal wind behaviour, the data for two weeks' continuous observations are first divided into three height groups, each of 10 km interval. All measurements which occur in the same hourly interval of local time are then grouped together and the most probable wind vector for this hour is calculated by a least squares analysis. It is found that the calculated wind vectors are effectively horizontal.

## 2. Results

The results presented here extend over a period of two years' observations from October 1952 to October 1954. The analysis of all the available data has shown that during any one month the diurnal behaviour of the winds in this region can be described in terms of three components: a constant term, a 24 hr periodic component and a 12 hr periodic component. The east–west and north–south components of the winds for each month are given in Table 1.

### 2.1. *Periodic components*

The annual variation of the periodic winds are shown in Figs. 1 and 2 where the 24 hr and 12 hr harmonics of the winds for the months December 1952, March, June, September and December 1953 are plotted in polar form. The diurnal and semi-diurnal oscillations correspond in general to a rotation of the wind vector with time, although during most months the oscillation is markedly elliptical. The sense of rotation of the wind vectors in the height range 75–94 km is anticlockwise, as would be expected for tidal winds in the southern hemisphere.

The amplitude of the 24 hr component is independent of height but varies annually, being a maximum in summer and autumn (30–40 m/sec) and a minimum in winter and spring (10–15 m/sec). The phase is reversed in winter compared with those in the other seasons.

Between 75 km and 94 km height, the amplitude of the 12 hr tidal component is approximately constant, but the phase varies in a complex manner during the year. During summer the phase is approximately constant, but a slow retardation of 6 hr occurs beween March and July and this is followed during October by a rapid return to the summer value.

* Department of Physics, University of Adelaide

Table 1.

| Month | Height (km) | |
|---|---|---|
| October 1952 | 85–94 | $V_{NS} = +\ 0{\cdot}4 + 32{\cdot}3 \cos \pi/12(t - 17{\cdot}5) + 20{\cdot}7 \cos \pi/6(t - 2{\cdot}4)$ |
| | | $V_{EW} = +\ 8{\cdot}6 + 36{\cdot}9 \cos \pi/12(t - 11{\cdot}8) + 7{\cdot}5 \cos \pi/6(t - 2{\cdot}4)$ |
| November 1952 | 85–94 | $V_{NS} = +16{\cdot}6 + 12{\cdot}4 \cos \pi/12(t - 17{\cdot}9) + 19{\cdot}2 \cos \pi/6(t - 10{\cdot}4)$ |
| | | $V_{EW} = +38{\cdot}0 + 28{\cdot}1 \cos \pi/12(t - 9{\cdot}9) + 18{\cdot}8 \cos \pi/6(t - 6{\cdot}5)$ |
| December 1952 | 75–84 | $V_{NS} = +\ 0{\cdot}7 + 15{\cdot}3 \cos \pi/12(t - 0{\cdot}8) + 10{\cdot}1 \cos \pi/6(t - 11{\cdot}4)$ |
| | | $V_{EW} = +28{\cdot}1 + 33{\cdot}4 \cos \pi/12(t - 9{\cdot}6) + 19{\cdot}7 \cos \pi/6(t - 6{\cdot}3)$ |
| | 85–94 | $V_{NS} = +13{\cdot}5 + 25{\cdot}2 \cos \pi/12(t - 19{\cdot}7) + 21{\cdot}5 \cos \pi/6(t - 11{\cdot}6)$ |
| | | $V_{EW} = +47{\cdot}6 + 30{\cdot}8 \cos \pi/12(t - 12{\cdot}0) + 15{\cdot}4 \cos \pi/6(t - 7{\cdot}0)$ |
| | 95–104 | $V_{NS} = +16{\cdot}4 + 18{\cdot}1 \cos \pi/12(t - 22{\cdot}9) + 31{\cdot}1 \cos \pi/6(t - 1{\cdot}3)$ |
| | | $V_{EW} = +56{\cdot}0 + 26{\cdot}6 \cos \pi/12(t - 5{\cdot}6) + 5{\cdot}9 \cos \pi/6(t - 8{\cdot}3)$ |
| March 1953 | 75–84 | $V_{NS} = -\ 7{\cdot}7 + 35{\cdot}7 \cos \pi/12(t - 17{\cdot}4) + 9{\cdot}1 \cos \pi/6(t - 7{\cdot}9)$ |
| | | $V_{EW} = +32{\cdot}3 + 32{\cdot}4 \cos \pi/12(t - 14{\cdot}0) + 14{\cdot}7 \cos \pi/6(t - 7{\cdot}3)$ |
| | 85–94 | $V_{NS} = +\ 5{\cdot}8 + 42{\cdot}1 \cos \pi/12(t - 17{\cdot}3) + 19{\cdot}6 \cos \pi/6(t - 8{\cdot}0)$ |
| | | $V_{EW} = +31{\cdot}1 + 40{\cdot}3 \cos \pi/12(t - 10{\cdot}2) + 10{\cdot}4 \cos \pi/6(t - 4{\cdot}8)$ |
| | 95–104 | $V_{NS} = +\ 5{\cdot}2 + 29{\cdot}7 \cos \pi/12(t - 8{\cdot}7) + 40{\cdot}0 \cos \pi/6(t - 2{\cdot}2)$ |
| | | $V_{EW} = +38{\cdot}4 + 29{\cdot}5 \cos \pi/12(t - 11{\cdot}3) + 6{\cdot}5 \cos \pi/6(t - 4{\cdot}0)$ |
| June 1953 | 75–84 | $V_{NS} = -\ 6{\cdot}9 + 12{\cdot}0 \cos \pi/12(t - 7{\cdot}0) + 4{\cdot}5 \cos \pi/6(t - 11{\cdot}2)$ |
| | | $V_{EW} = +64{\cdot}6 + 32{\cdot}0 \cos \pi/12(t - 22{\cdot}2) + 15{\cdot}9 \cos \pi/6(t - 7{\cdot}8)$ |
| | 85–94 | $V_{NS} = -19{\cdot}8 + 10{\cdot}2 \cos \pi/12(t - 10{\cdot}6) + 4{\cdot}0 \cos \pi/6(t - 5{\cdot}9)$ |
| | | $V_{EW} = +30{\cdot}1 + 12{\cdot}4 \cos \pi/12(t - 23{\cdot}6) + 31{\cdot}0 \cos \pi/6(t - 8{\cdot}5)$ |
| | 95–104 | $V_{NS} = -\ 3{\cdot}6 + 32{\cdot}5 \cos \pi/12(t - 16{\cdot}8) + 2{\cdot}8 \cos \pi/6(t - 3{\cdot}2)$ |
| | | $V_{EW} = +10{\cdot}4 + 14{\cdot}6 \cos \pi/12(t - 15{\cdot}7) + 54{\cdot}2 \cos \pi/6(t - 8{\cdot}0)$ |
| September 1953 | 75–84 | $V_{NS} = -\ 3{\cdot}1 + 16{\cdot}1 \cos \pi/12(t - 18{\cdot}9) + 18{\cdot}4 \cos \pi/6(t - 6{\cdot}3)$ |
| | | $V_{EW} = -\ 5{\cdot}3 + 14{\cdot}0 \cos \pi/12(t - 11{\cdot}9) + 10{\cdot}6 \cos \pi/6(t - 4{\cdot}7)$ |
| | 85–94 | $V_{NS} = +\ 5{\cdot}7 + 7{\cdot}0 \cos \pi/12(t - 17{\cdot}0) + 12{\cdot}0 \cos \pi/6(t - 4{\cdot}7)$ |
| | | $V_{EW} = -14{\cdot}5 + 17{\cdot}5 \cos \pi/12(t - 8{\cdot}0) + 10{\cdot}1 \cos \pi/6(t - 1{\cdot}6)$ |
| | 95–104 | $V_{NS} = +\ 0{\cdot}3 + 26{\cdot}3 \cos \pi/12(t - 18{\cdot}0) + 25{\cdot}1 \cos \pi/6(t - 10{\cdot}9)$ |
| | | $V_{EW} = -14{\cdot}3 + 15{\cdot}9 \cos \pi/12(t - 14{\cdot}8) + 27{\cdot}6 \cos \pi/6(t - 10{\cdot}7)$ |
| December 1953 | 75–84 | $V_{NS} = +\ 1{\cdot}7 + 11{\cdot}3 \cos \pi/12(t - 23{\cdot}6) + 15{\cdot}8 \cos \pi/6(t - 0{\cdot}1)$ |
| | | $V_{EW} = +26{\cdot}7 + 24{\cdot}4 \cos \pi/12(t - 13{\cdot}2) + 24{\cdot}4 \cos \pi/6(t - 7{\cdot}8)$ |
| | 85–94 | $V_{NS} = +\ 5{\cdot}2 + 31{\cdot}5 \cos \pi/12(t - 21{\cdot}0) + 12{\cdot}7 \cos \pi/6(t - 11{\cdot}7)$ |
| | | $V_{EW} = +46{\cdot}5 + 25{\cdot}8 \cos \pi/12(t - 10{\cdot}9) + 12{\cdot}6 \cos \pi/6(t - 5{\cdot}6)$ |
| | 95–104 | $V_{NS} = +\ 2{\cdot}9 + 22{\cdot}1 \cos \pi/12(t - 0{\cdot}9) + 10{\cdot}8 \cos \pi/6(t - 0{\cdot}4)$ |
| | | $V_{EW} = +70{\cdot}4 + 20{\cdot}4 \cos \pi/12(t - 9{\cdot}5) + 20{\cdot}8 \cos \pi/6(t - 7{\cdot}3)$ |
| July 1954 | 75–84 | $V_{NS} = -14{\cdot}6 + 6{\cdot}5 \cos \pi/12(t - 18{\cdot}4) + 10{\cdot}7 \cos \pi/6(t - 6{\cdot}2)$ |
| | | $V_{EW} = +31{\cdot}4 + 21{\cdot}6 \cos \pi/12(t - 13{\cdot}0) + 19{\cdot}5 \cos \pi/6(t - 2{\cdot}1)$ |
| | 85–94 | $V_{NS} = -15{\cdot}8 + 22{\cdot}8 \cos \pi/12(t - 16{\cdot}6) + 31{\cdot}7 \cos \pi/6(t - 4{\cdot}9)$ |
| | | $V_{EW} = +\ 5{\cdot}2 + 13{\cdot}3 \cos \pi/12(t - 18{\cdot}3) + 30{\cdot}2 \cos \pi/6(t - 1{\cdot}7)$ |
| | 95–104 | $V_{NS} = -22{\cdot}8 + 27{\cdot}7 \cos \pi/12(t - 15{\cdot}7) + 28{\cdot}1 \cos \pi/6(t - 3{\cdot}0)$ |
| | | $V_{EW} = +\ 9{\cdot}5 + 15{\cdot}4 \cos \pi/12(t - 19{\cdot}6) + 39{\cdot}6 \cos \pi/6(t - 11{\cdot}4)$ |
| October 1954 | 75–84 | $V_{NS} = +\ 2{\cdot}6 + 19{\cdot}5 \cos \pi/12(t - 17{\cdot}4) + 0{\cdot}5 \cos \pi/6(t - 8{\cdot}8)$ |
| | | $V_{EW} = -19{\cdot}1 + 33{\cdot}9 \cos \pi/12(t - 14{\cdot}9) + 24{\cdot}4 \cos \pi/6(t - 2{\cdot}4)$ |
| 3–16 October 1954 | 85–94 | $V_{NS} = +\ 6{\cdot}5 + 34{\cdot}9 \cos \pi/12(t - 14{\cdot}9) + 9{\cdot}1 \cos \pi/6(t - 1{\cdot}1)$ |
| | | $V_{EW} = -\ 8{\cdot}1 + 28{\cdot}1 \cos \pi/12(t - 10{\cdot}4) + 32{\cdot}1 \cos \pi/6(t - 11{\cdot}2)$ |
| 17 October–3 November 1954 | | $V_{NS} = +\ 9{\cdot}4 + 35{\cdot}5 \cos \pi/12(t - 18{\cdot}5) + 13{\cdot}5 \cos \pi/6(t - 10{\cdot}6)$ |
| | | $V_{EW} = +16{\cdot}6 + 26{\cdot}4 \cos \pi/12(t - 10{\cdot}9) + 4{\cdot}5 \cos \pi/6(t - 6{\cdot}7)$ |
| | 95–104 | $V_{NS} = 0 + 23{\cdot}6 \cos \pi/12(t - 7{\cdot}6) + 35{\cdot}1 \cos \pi/6(t - 11{\cdot}8)$ |
| | | $V_{EW} = +\ 1{\cdot}6 + 30{\cdot}0 \cos \pi/12(t - 14{\cdot}2) + 44{\cdot}1 \cos \pi/6(t - 8{\cdot}5)$ |

OL.
15
959

In the height range 95–104 km, the 12-hr periodic winds show little evidence of the tidal oscillations present in the other height groups. The amplitudes are larger and the oscillations are confined to periodic variations in fixed directions.

During the equinoxial months, March and September, the phase of the 12 hr

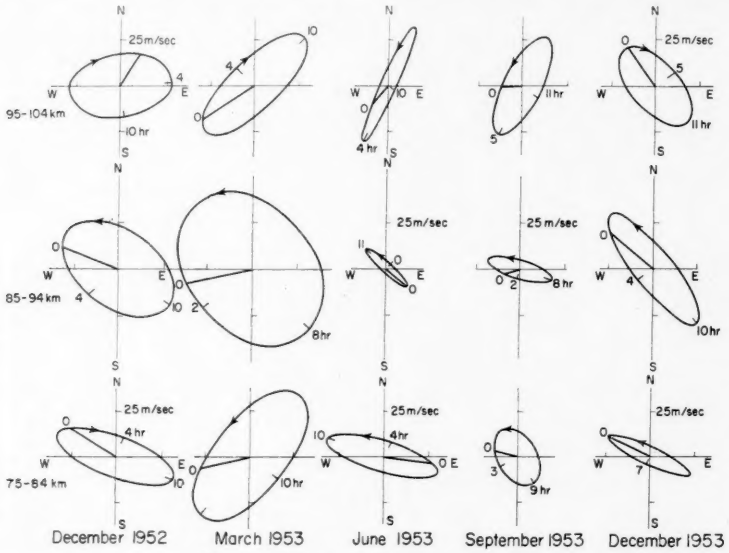


Fig. 1. 24-hr periodic components

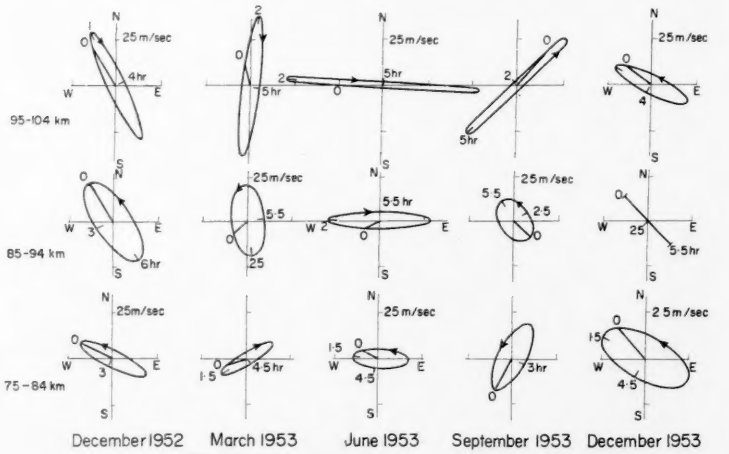


Fig. 2. 12-hr periodic components

tidal component advanced with height at a rate of approximately 5°/km between 75 and 94 km.

2.2. *Prevailing winds*

The average prevailing winds for all months are predominantly in the east–west directions, and during summer and winter exhibit large vertical gradients.



VOL. 15 1959

In Fig. 3 the prevailing components are plotted as a function of height for the months December, March, June and September. The outstanding features of those curves are the large and opposite wind gradients, which exist in the east–west directions during December and June, and the almost complete absence of the gradients during September and March. It can be seen that the prevailing wind

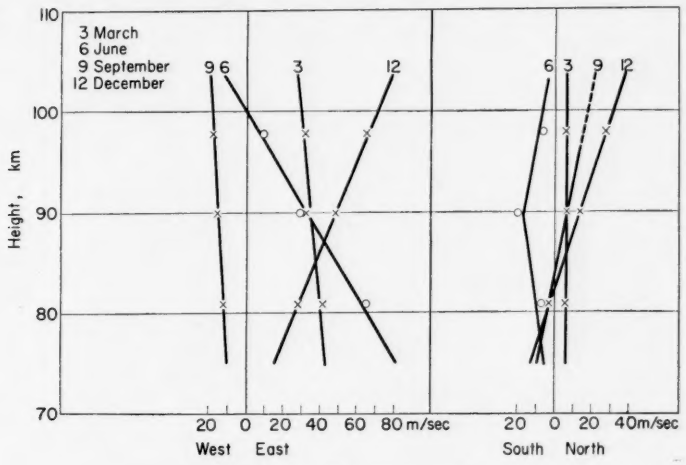


Fig. 3. Prevailing components

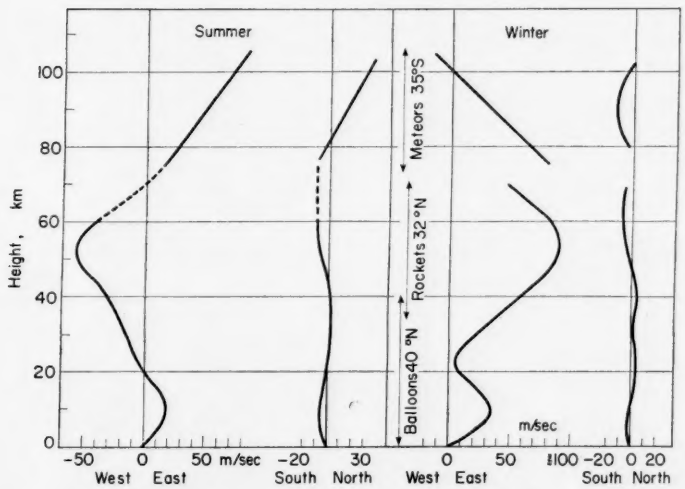


Fig. 4. Prevailing components (vector directions).

would reverse direction from east to west at a height of 100 km in June and at about 70 km in December, while in March it was directed towards the east, and in September towards the west, over the total height range. The average gradient in December was +2·3 m/sec per km and in June −3·3 m/sec per km.

The summer and winter prevailing wind components are complementary to measurements of winds between 0–70 km carried out in similar latitudes in the

northern hemisphere (Brasefield, 1954). These measurements have been obtained from balloon flights and from the explosion of grenades carried on rockets, and the mean winds are reproduced in Fig. 4 together with the meteor results. In summer the agreement is remarkably good and the reversal at approximately 70 km appears conclusive. In winter the winds determined using meteors are considerably stronger than the rocket measured winds, but this is not a serious disagreement since the winds measured between 60 and 70 km refer to only one rocket flight.

During certain months the combination of amplitude gradients of the prevailing winds and phase gradients of the periodic winds give rise to rapid changes of the wind pattern with height. During summer and winter, wind gradients as large as 8 m/sec per km and lasting for several hours are a regular feature of the wind pattern.

### 2.3. *Random winds*

The random component of the observed winds is of the order of 10 m/sec and thus is not an important feature of the wind systems at heights up to 100 km in medium latitudes.

## 3. Conclusions

From the combined results of balloons, rockets and meteors, it is now possible to describe the general circulation in medium latitudes up to a height of about 100 km. In summer and winter, large wind gradients exist in the east–west direction.

Below a height of 90 km the two periodic wind components are of comparable amplitude and are tidal in nature. The phase of the 24 hr component is approximately independent of height and season, whereas the phase of the 12 hr component varies annually and advances with height during the equinoxial months.

VOL. 15 1959

## References


Brasefield C. J. 1954 *J. Geophys. Res.* **59,** 233.

Elford W. G. and Robertson D. S. 1953 *J. Atmosph. Terr. Phys.* **4,** 271.

Robertson D. S., Liddy D. T. and Elford W. G. 1953 *J. Atmosph. Terr. Phys.* **4,** 255.

Journal of Atmospheric and Terrestrial Physics, 1959, Vol. 15, pp. 137 to 140. Pergamon Press Ltd. Printed in Northern Ireland

# Air motions at meteoric heights

L. A. MANNING*

IN previously reported studies, methods have been described for finding ionospheric winds using the Doppler frequency shift imparted to meteoric echoes by drift of the ionization trails. Both average and root mean square values of wind velocities have been measured by these techniques (MANNING, 1950, 1953, 1954). In the original studies the writer and his colleagues found the average horizontal drift velocity of the whole meteoric region to be of the order of 30 m/sec. An average vertical drift velocity of 1·5 m/sec in the downward direction was found with a standard deviation of 2·4 m/sec. The r.m.s. value of the instantaneous values of the horizontal wind components was found to be 50 m/sec, while the r.m.s. value of the vertical wind components was found to be of the order of 12 m/sec, but with an error of observation that would not exclude a value of zero. It was suggested that a horizontally stratified wind structure would serve to explain the results.

Further application of the preceding method was made by ELFORD and ROBERTSON (1953), who found 12 and 24 hr components in mean velocities. GREENHOW has also applied the method and obtained similar results; he has reported in detail on the changes in mean wind properties with time and with height (GREENHOW, 1954).

In the present study the results will be given of a new method of analysing the detailed wind structure at meteoric heights. The results are based on the fading, diversity and aspect properties of meteoric echoes.

It is assumed that when a meteor enters the 80–110 km height region, it produces an initially straight column of ionization perhaps 25 km long (MANNING *et al.*, 1953). This straight trail is acted on by horizontal winds whose direction and magnitude vary with height. As the trail partakes of the motion of the surrounding air, it is distorted into some sinuous shape determined by the vertical wind profile. It is assumed that the deviation from the mean of the north–south and east–west components of the wind profile may be described by Gaussian "noise" functions. There is then some spectrum function describing the relative amplitude of the Fourier components of the wind velocity–height profile. This spectrum function is descriptive of the shears and turbulence.

The strengths of radio signals reflected from the distorted trails may be computed by integral methods involving summation of the elementary scattering contributions from each differential length of trail. The results may be shown to be very nearly the same for practical trail dimensions as from a simple analysis based on "glints". It is assumed that whenever the trail is tangent at a point to an ellipsoid of revolution having the transmitter and receiver as foci, a reflection is obtained. The strength of the reflected power at this "glint" is

* Radio Propagation Laboratory, Stanford University, Stanford, California.

dependent on the radius of curvature of the trail at that point in relation to the curvatures of the ellipsoid. A glint is thus assumed to exist whenever the trail presents a first Fresnel zone to the receiver. A single glint will exist when an echoing trail is first formed. As time advances, the increasing sinuosity of the trail permits additional glints to appear whenever the trail at a given point is turned enough to become tangent to one of the ellipsoids. Parts of the trail remote from the original reflection point on the average develop glints at later times than do near parts; they must be warped more to present a specular reflection condition. Thus as time advances, additional glints appear at a random rate, first near the original reflection point, but gradually extending to include the whole trail. (The rate of addition of glints is of the order of one or two per second.)

Fading of the echo is a result of the addition of signals from two or more glints. At each glint the wind velocity is different, and the signal returned from each glint will possess a distinct Doppler frequency shift. The delay in the start of fading described by GREENHOW (1952) is attributed to the interval when only the first glint is present. The deep regular fading usually seen early in the life of a fading echo results from the beating of signals from a small number of glints.

Statistical properties of the wind must be obtained using many meteors. It is then convenient to think that an aperture distribution of glints is produced by an ensemble of trails. If all the trails of the ensemble were superimposed so that the original reflection points coincide, a Gaussian distribution of power reflection coefficient would exist along the ensemble trail due to the probability density distribution of glints. The Fourier spectrum of this aperture distribution yields the angular autocorrelation function of ensemble average cross-correlation between the fading envelopes measured at separated receivers on the ground. Since the aperture width increases with time, the autocorrelation must be made by summing over the ensemble at a given echo time, measured in fading cycles. Experimental measurements of the fading cross-correlation have been made using a 61 Mc/s video carrier from a television station 1000 km east of Stanford.* The correlation function was found to have the predicted Gaussian shape, when plotted against the product of adjusted fading cycle number and ground spacing. Ground spacings up to 310 m were used both along and across path.

From these correlation measurements a value can be obtained for the ratio of the height gradient of the wind to the mean deviation of velocity from the mean velocity. This ratio in turn is an index of the small-scale cut-off in the size spectrum of shear or turbulence. Let $\Lambda$ be the wavelength of a sinusoidal component of the velocity height profile. Then if the spectral amplitude is assumed to be a Gaussian function of $2\pi/\Lambda$, the amplitude is down to 10 per cent of maximum at $\Lambda = 1{\cdot}1$ km and to 50 per cent at $\Lambda = 1{\cdot}9$ km. If the spectrum is assumed of constant amplitude down to a minimum scale of $\Lambda_0$, but zero for larger $\Lambda$, $\Lambda_0 = 1{\cdot}8$ km. It may also be shown from considerations of convergence that the turbulent spectrum must die off at least as rapidly as $(2\pi/\Lambda)^{3/2}$.

The rate of fading of a meteoric echo is determined by the maximum difference velocity at the effective glints. At first when only two glints are present, the

* The writer is indebted to V. R. ESHLEMAN and O. G. VILLARD for these data.



VOL.
15
1959

fading frequency may be used to deduce the r.m.s. deviation of the pertinent velocity component from the mean. From the 61 Mc/s data referred to above, an r.m.s. N–S component of velocity deviation of 49·7 m/sec was found (all the figures are certainly not significant). Combining this velocity with the diversity effect cross-correlation, an r.m.s. value of the relative maxima of the height gradient of the N–S component of velocity of 99 m/sec per km is found.

Further consideration of the rate of echo fading indicates that the ensemble average fading speed should increase with fading cycle number. The fading frequency is determined by the maximum difference in glint velocity. As time advances, the number of glints increases. Since the velocities of the glints are distributed in a Gaussian manner, the expected maximum difference in glint velocity increases with the number of glints. Thus the model predicts a characteristic increase in fading frequency with time. Near the end of the echo, however, the reduction in trail length rapidly removes glints, and a drop in fading frequency should occur. Both of these effects are found experimentally. The rate of decrease in ensemble average fading frequency drops with fading cycle number, measured from the end of sufficiently long enduring echoes, in conformity with predicted trail length variation (Eshleman, 1957). The rate of rise of fading frequency from the start of the echo has a characteristic shape reproduced experimentally. There is an undetermined constant, however, and its value may be deduced from the measurements. If two glints appear on the trail with a spacing such that the correlation between their velocities is not zero, they are not independent as far as their probability of contributing to a higher fading frequency is concerned. By comparing the actual rate of increase of fading frequency with that predicted on the basis that all the glints had independent velocities, we get the height differential in the atmosphere for which the N–S components of wind deviations are uncorrelated. This height differential is found to be 6·4 km. This is very nearly the atmospheric scale height.

As the trails become increasingly distorted, it is possible to get perpendicular reflection at angles even farther from the original normal. The theoretical prediction of this behaviour has been compared with aspect sensitivity measures by McKinley and Millman (1949). They noted the radar delay in appearance of visual meteors as a function of the deviation of the line of sight from the perpendicular to the trail axis. Delays in appearance of 10 sec or so were found when the trail was seen nearly end on. Application of the present theory to their results predicts the form of the observed aspect dependence, and yields the r.m.s. value of the relative maxima of the height gradient of one component of the wind profile. A value of 96 m/sec per km is found in this way.

A third means of obtaining the height gradient is to compare the theoretical time delay to the start of the fading with Greenhow's (1952) experimental distribution function of the same quantity. Again, a gradient of the order 100 m/sec per km is found.

It may be further remarked that the theory of fading presented here explains quantitatively the "slow fade" described by Greenhow. It is often observed that the envelope amplitude of a fading echo fluctuates at a rate much slower than the fading frequency. For shorter duration echoes, the envelope of the

fading fluctuates more rapidly. This effect is explained by the fact that when a glint is first formed, it is single. But as the trail continues to warp, it splits into two glints quite close together. Thus each glint pair can be thought of as a single glint whose amplitude fluctuates at the slow rate determined by the correlation in the wind profile at small height separations.

From the various measures on meteoric radio echoes, a consistent picture of the wind structure is obtained. The wind is predominantly horizontal, with individual velocities commonly of 50 or 70 m/sec. The region as a whole has a mean drift velocity of the order of 30 m/sec, variable from day to day and containing tidal components. The horizontal velocities of winds separated vertically by a scale height are uncorrelated. The amplitude of the wind components of scale less than 1–2 km is small. The turbulent velocities must die out at least as rapidly as $(2\pi/\Lambda)^{3/2}$. The angular velocities of any small scale turbulent eddies cannot be as large as that due to the large-scale shears. The average vertical velocity of the wind must be no more than a few metres per second, and the r.m.s. vertical velocities cannot be much larger. The mean relative maxima of wind gradients are about 100 m/sec per km. These numerical results are completely consistent with those WHIPPLE (1953) has obtained by photographing drifting meteor trains. The radio observations are based on averages over more meteors, however, and are more definite concerning the low velocities of small-scale irregularities.

## REFERENCES


| | | |
|---|---|---|
| ELFORD W. G. and ROBERTSON D. S. | 1953 | *J. Atmosph. Terr. Phys.* **4,** 271 |
| ESHLEMAN V. R. | 1957 | *J. Atmosph. Terr. Phys.* **10,** 57. |
| GREENHOW J. S. | 1952 | *Proc. Phys. Soc.* **65,** 169. |
| GREENHOW J. S. | 1954 | *Phil. Mag.* **45,** 471. |
| MCKINLEY D. W. R. and MILLMAN P. M. | 1949 | *Proc. Inst. Radio Eng.* **37,** 364. |
| MANNING L. A., VILLARD O. G., JR. and PETERSON A. M. | 1950 | *Proc. Inst. Radio Engrs.* **38,** 877. |
| MANNING L. A. | 1953 | *Bull. Amer. Meteorol. Soc.* **34,** 401. |
| MANNING L. A., VILLARD O. G., JR. and PETERSON A. M. | 1953 | *Trans. Amer. Geophys. Un.* **34,** 16. |
| MANNING L. A., PETERSON A. M. and VILLARD O. G., JR. | 1954 | *J. Geophys. Res.* **59,** 47. |
| WHIPPLE F. L. | 1953 | *J. Met.* **10,** 390. |

Journal of Atmospheric and Terrestrial Physics, 1959, Vol. 15, pp. 141 to 144. Pergamon Press Ltd. Printed in Northern Ireland

# Drift in the *E*-region

K. RAWER*

THE drift observations with KRAUTKRAMER's (1950) fading method are usually interpreted in terms of a random field-strength distribution (BRIGGS and SPENCER, 1954). This means that a rather well-defined physical model of the reflecting layer is supposed, e.g. one which is the result of isotropic turbulence. Both RATCLIFFE (1954) and PUTTER (1955) have stated that the end points of the apparent velocity vectors lie on a circle through the origin (we call it "random circle"). The statistical probability of readings on different parts of this circle has been calculated by BRIGGS and PAGE (1955).

It seemed worthwhile to discuss some other models which could perhaps explain the observations. Since these are observations of shock-waves in the *F*-region it does not appear impossible that, instead of a pattern formed by random interference of many rays, there are fading patterns formed by only a few interfering rays. This must be the case if a well-defined deformation of the reflecting surface is the reason for the observed fadings. Some calculations have been made for different models, each using two rays only.

The first model supposes a small deformation concentrated on a rather small surface. We call it point-deformation. The interference originates between the normally reflected ray and a second one which is reflected from the deformation. In that case the apparent direction is always directed towards the deformation point. Effectively with this model the same circle is found as before for the end-points of the apparent velocity vector. The statistics are somewhat different from the "random case", the distribution being smaller if a finite lifetime of the deformation is supposed.

For the second model we suppose a narrow "line" of deformation, such as would be the case for a wavefront going through the reflecting surface. In that case the apparent velocity must always be equal to the component of the real movement which is perpendicular to the deformation line. Thus in the case of this model, all apparent velocity vectors should here be equal to that velocity which is the only one that could be considered as physically effective. If different directions should appear they should be interpreted, for this model, as indicating different directions of the individual deformation lines.

We know from shock-waves that no completely horizontal movement should be supposed, i.e. there should also be a vertical component. If this is inserted instead of a circle or a point we obtain for both models a spread distribution both in direction and amplitude. Until now nearly all drift-observations have been effectively evaluated for isolated fadings, the corresponding field strength minima or maxima being identified on the three tracks ("method of similar fades"). The automatic recorder of Phillips is also designed to do this. Only very few results have been obtained with the complete statistical correlation method of BRIGGS *et al.* (1950), and rather more with the simplified statistical treatment ("six point correlation") of YERG (1955).

* Ionosphärstation, Freiburg,

If isolated fadings are used, one usually tries to read about ten fadings in a period of about $\frac{1}{4}$ hr. The experimental result is quite clear: the "random-circle" appears only in a few per cent of all cases. The normal result is a good mass plot, with an angular dispersion (upper and lower quartile) of about $\pm 25°$ and an amplitude dispersion of about $\pm 30$ per cent. There can be little doubt that the amplitude is less precisely defined than the direction. This result is difficult to explain not only with the random model but also with any deformation-model using horizontal movement only. We feel thus that vertical components of movements cannot be neglected.

At first one should expect that in this case the complete statistical calculation should yield a different result from that of the random model. This is not certain, since in a statistical treatment many isolated fadings are mixed up so that a random distribution can appear in the statistics even if the isolated fading is well defined. But if we use one or the other method of evaluation we may increase the rate of observations corresponding to the underlying model by selection. If isolated clear fadings are selected, the non-statistical methods will apply to most cases. If on the other hand the behaviour of a period is characterized by equidistant readings of field-strength values, the random evaluation method may be better suited. Fortunately, both methods seem to give fairly concordant results.

At our station at Neuf-Brisach many drift observations have been made from October 1955 until February 1957 (Harnischmacher and Rawer, 1956). These observations are now continued at Breisach (station name: Freiburg). Hourly observations have been made for about 25 per cent of this period. The three tracks (on one film) are evaluated by the methods of similar fades; for every $\frac{1}{4}$ hr interval the median vector is used for the statistics. An example of the results obtained for a winter day is given in Fig. 1; the quartile range is indicated for every period of observation. The data of one month can be presented in a more statistical form by two plots, one for direction and one for amplitude (see, for example, Fig. 2). The direction plot often shows a rather clear daily variation corresponding to one rotation in about 12 hr. This could be caused by a tidal movement. In summer the variation is less regularly seen but it may be that this is due to the appearance of $E_s$; an $E_s$-echo can be reflected at a lower level than the corresponding echo from the normal $E$-layer.

In Fig. 3 the statistical distribution of measured direction values is indicated in detail. For some periods it is not uniform. Apart from one more important concentration there appears a second one which is approximately opposite. This puzzling observation is not merely a statistical result. We had many cases where from the selected "similar fades" of $\frac{1}{4}$ hr, some gave the principal direction and others a nearly opposite one. In such cases we prefer to indicate two different medians instead of mixing all points. Different explanations for this behaviour are under discussion: one is the eventual existence of horizontal wind-eddies; another is the eventual existence of vertical up and down movements causing different vertical velocity components.

It seems to us that the interpretation of drift observations with the fading method should be investigated in more detail. Our present observations correspond nearly all to the median of isolated fadings. This median value certainly has a



VOL.
15
1959

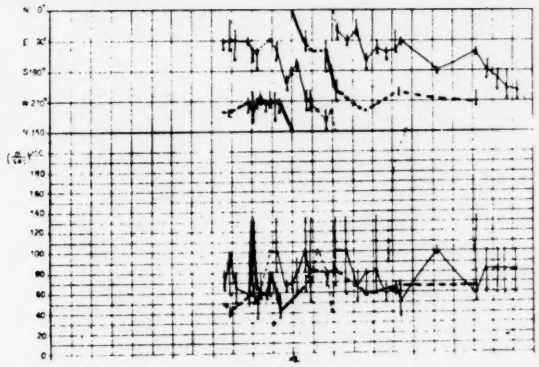

Fig. 1.

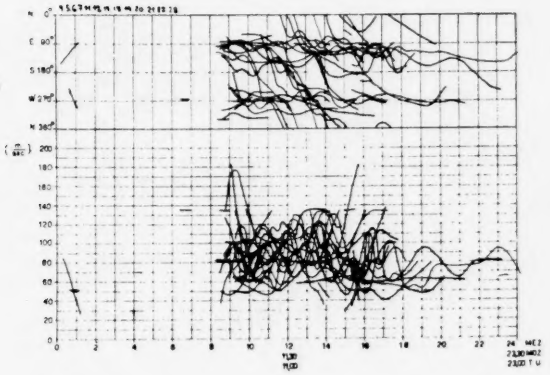

Fig. 2.

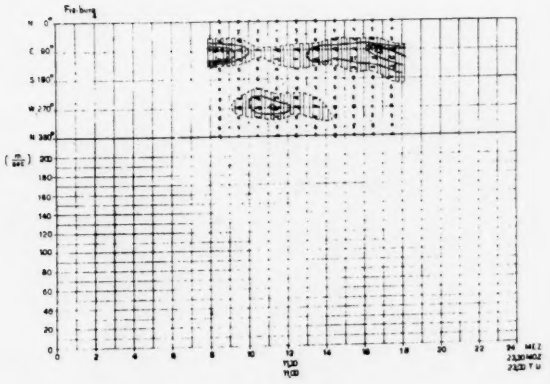

Fig. 3.

physical meaning, but it should be decided what it is and whether it corresponds directly to a horizontal gas- or plasma-velocity. On the other hand the measurements should be intensified in order to obtain a true statistical result for the daily variation. Also the day-to-day changes should be studied.

Finally some of the questions concerning the physical model could be resolved if an arrangement with more than three antennas was used. Only in such circumstances could the form of the pattern be studied and this would be a very important contribution to the problem of correct interpretation of drift measurements.

## REFERENCES


| | | |
|---|---|---|
| BRIGGS B. H., PHILLIPS G. J. and SHINN D. H. | 1950 | *Proc. Phys. Soc.* B **63,** 106. |
| BRIGGS B. H. and SPENCER M. | 1954 | *Rep. Progr. Phys.* **17,** 245. |
| BRIGGS B. H. and PAGE E. S. | 1955 | *Physics of the Ionosphere* pp. 119–122. Physical Society, London |
| HARNISCHMACHER E. and RAWER K. | 1956 | *C.R. Acad. Sci., Paris* **243,** 747, 782. |
| HARMISCHMACHER E. and RAWER K. | 1957 | *Beitr. Phys. Atmosphäre.* |
| KRAUTKRAMER J. | 1945 | *Dtsch. Luftfahrtforsch. FB* Nr. 1761. |
| KRAUTKRAMER J. | 1950 | *Arch. elektr. Übertr.* **4,** 133. |
| RATCLIFFE J. A. | 1954 | *J. Atmosph. Terr. Phys.* **5,** 173. |
| ST. PUTTER P. | 1955 | *Physics of the Ionosphere* pp. 191–201. Physical Society, London. |
| YERG D. G. | 1955 | *J. Geophys. Res.* **60,** 173. |


VOL. 15 1959

Journal of Atmospheric and Terrestrial Physics, 1959, Vol. 15, p. 145. Pergamon Press Ltd. Printed in Northern Ireland

# A propos des grands mouvements verticaux de la région-*F* observés à Casablanca

A. Haubert

**Résumé**—Des mouvements verticaux rapides de la région-*F* sont observés à Casablanca, avec une fréquence d'occurence pouvant atteindre dix jours par mois, vers 21 heures et 5 heures du matin.

Ces mouvements, sans rapports apparents avec les perturbations géophysiques ou solaires, semblent devoir être interprétés comme des phénomènes de marées.

La comparaison systématique des phénomènes solaires et magnétiques avec les anomalies de l'ionosphère ne permet pas seulement de déceler des corrélations, mais aussi de classer certains phénomènes comme totalement indépendants des perturbations classiques.

C'est ainsi que certains grands mouvements verticaux de la région-*F*, observés à Casablanca semblent devoir être plus justement attribués à un processus de marée plus ou moins localisée.

En effet, il a été constaté qu'un abaissement de la region-*F* suivi d'une élévation rapide avec scission en deux couches présentait une tendance marquée à se produire soit vers 21 heures, soit vers 5 heures du matin.

Cette évolution très caractérisée se produit généralement par série pendant quelques jour, cependant pas nécessairement tous les jours au cours d'une série, ni forcément les mêmes jours à 5 heures et 21 heures.

L'évolution est d'autant plus spectaculaire qu'elle est rapide; elle fait penser à l'inversion de champ électrique induit dans un conducteur de rotor de dynamo au passage devant un pôle. Cependant, il est possible que des champs induits horizontaux engendrent des mouvements des électrons à composante verticale, par suite du champ magnétique terrestre permanent.

De semblables mouvements peuvent aussi être observés à d'autres heures de la journée, mais ce sont des cas tout à fait exceptionnels, c'est ainsi qu'en juin 1954 le phénomène s'est produit à Casablanca pendant quelques jours vers 7 à 8 heures du matin, mais ce fut la seule fois en cinq ans. Nous avons appris qu'aux Indes, à Ahmedabad, celà s'est aussi produit à peu près aux mêmes heures locales, mais seulement en décembre 1955. Tandis, qu'en ce qui concerne Casablanca, la fréquence d'occurence à 5 heures et 21 heures peut atteindre 10 jours par mois. Cette fréquence d'occurence paraît plus grande en hiver qu'en été, mais la présence plus fréquence en été de *E*-sporadique peut masquer un certain nombre de cas.

Nous insistons à nouveau sur l'impossibilité de se faire une idée de l'ampleur de tels phénomènes tant que les conditions d'une vue synoptique ne seront pas réalisées par la publication par toutes les stations des anomalies observées et de leurs heures d'occurence.

Journal of Atmospheric and Terrestrial Physics, 1959, Vol. 15, pp. 146 to 150. Pergamon Press Ltd. Printed in Northern Irel and

# Wind systems and drift motions in the ionosphere deduced from the dynamo theory

M. Hirono, H. Maeda and S. Kato*

## 1. Introduction

Since the analyses and theoretical researches of Martyn (1947) and others it is increasingly evident that the ionization drift by electrodynamic force may produce a number of anomalies in the ionosphere.

At first several attempts were made to interpret the semi-diurnal variation in the $F2$-region by the tidal oscillation. However, quantitative theory is not established as yet.

In recent years the equatorial anomaly of the $F2$-region was studied in our university (Maeda, 1953; Hirono and Maeda, 1954) and it was shown that the main part of the anomaly can be interpreted by vertical ionization drift accompanied by solar magnetic variation. From these results it is promising that many other ionospheric anomalies are interpreted by drift due to current system producing daily magnetic variation. At present, therefore, exhaustive researches on this important subject are very necessary.

VOL. 15 1959

The dynamo theory in the ionosphere was already investigated by many workers, but most problems were unsolved as regards daily variation of the anisotropic electrical conductivity. We tried to solve these problems for some different plausible ionospheric parameters.

## 2. Experimental

Hasegawa and Maeda (1951) and Maeda (1952) estimated the daily variation of the electrical conductivity of the $E$-region. According to their results, the ratio of the noon value to the midnight value is about 12 : 1 and this ratio was taken as a most important basis for our analysis. This ratio is, however, different from Chapman's (1919) estimate of 25 : 1.

Electric current $(I_x, I_y)$ integrated with height in the ionosphere is given by

$$\begin{aligned} I_x &= \int \sigma_{xx}\, dh \,.\, E_x + \int \sigma_{xy}\, dh \,.\, E_y \\ I_y &= \int \sigma_{yx}\, dh \,.\, E_x + \int \sigma_{yy}\, dh \,.\, E_y \end{aligned} \qquad (1)$$

where $I_x$ = southward component
$I_y$ = eastward component

## 3. Calculation

(a) First, using global distribution of geomagnetic daily variation $(\Delta H_x, \Delta H_y)$ and the ionospheric conductivity with daily variation, we calculated the distribution of the electric field $(E_x, E_y)$ based on (1) and the relation between $(\Delta H_x, \Delta H_y)$ and $(I_x, I_y)$.

* Kyoto University, Japan.

(b) The electric field $(E_x, E_y)$ consists of two parts: an electrostatic field $(X, Y)$ and a dynamo field $(vH_z, -uH_z)$,

$$\begin{aligned} E_x &= X + vH_z \\ E_y &= Y - uH_z \end{aligned} \tag{2}$$

where $(u, v)$ denotes air velocity and $(X, Y)$ is derived from a potential $S$

$$\begin{aligned} X &= -\partial S/a\partial\theta \\ Y &= -\partial S/a \sin\theta\ \partial\lambda \end{aligned} \tag{3}$$

If we eliminate $(X, Y)$ or $(u, v)$ from (2), we obtain a fundamental equation of the dynamo theory.

(c) To solve the dynamo equation the following three methods were devised.

(i) MAEDA (1955) assumed that the wind velocity is irrotational (scaloidal), i.e.

$$u = -\partial\phi/a\ \partial\theta, \qquad v = -\partial\phi/a \sin\theta\partial\lambda \tag{4}$$

From (2), (3) and (4) we have

$$\cot\theta \frac{\partial^2\phi}{\partial\lambda^2} + \frac{\partial}{\partial\theta}\left(\sin\theta\cos\theta\frac{\partial\phi}{\partial\theta}\right) = \frac{a}{c}\left\{\frac{\partial}{\partial\lambda}E_x - \frac{\partial}{\partial\theta}(E_y\sin\theta)\right\} \tag{5}$$

Expanding $\phi$ in a series of spherical harmonics and under the assumption that the series consists of low-degree terms only: $n \leqq 7$ (for $m = 1$), 8 (for $m = 2$), 9 (for $m = 3$), he obtained a solution of (5), where $m$ and $n$ denote the order and degree of the harmonics, respectively.

(ii) KATO (1956) used the equation of motion

$$\left.\begin{aligned} \frac{\partial u}{\partial t} - 2v\omega\cos\theta &= -\frac{1}{a}\frac{\partial}{\partial\theta}\frac{p'}{\rho_0}, \\ \frac{\partial v}{\partial t} + 2u\omega\cos\theta &= -\frac{1}{a\sin\theta}\frac{\partial}{\partial\lambda}\frac{p'}{\rho_0}. \end{aligned}\right\} \tag{6}$$

From (2) and (3) it follows that

$$\frac{\partial}{\partial\lambda}(vH_z) + \frac{\partial}{\partial\theta}(uH_z\sin\theta) = \frac{\partial}{\partial\lambda}E_x - \frac{\partial}{\partial\theta}(E_y\sin\theta) \tag{7}$$

Eliminating $u$ and $v$ from (6) and (7) and expanding $p'$ in a series of spherical harmonics, and under the assumption that the series consists of low-degree terms only: $n \leqq 8$ (for $m = 1$), 9 (for $m = 2$), he obtained a solution of this differential equation.

(iii) HIRONO and KITAMURA (1956) assumed that the wind velocity is

$$\text{scaloidal:} \quad u = \frac{\partial\psi}{a\ \partial\theta}, \qquad v = \frac{\partial\psi}{a\sin\theta\ \partial\lambda} \tag{8}$$

or

$$\text{toroidal:} \quad u = \frac{\partial\psi}{a\sin\theta\ \partial\lambda}, \quad v = \frac{\partial\psi}{a\ \partial\theta} \tag{9}$$

Then from (2), (3) and (8) it follows that

$$\frac{\partial^2 S}{\partial \theta^2} + \frac{1}{\sin\theta\cos\theta}\frac{\partial S}{\partial \theta} + \frac{1}{\sin^2\theta}\frac{\partial^2 S}{\partial \lambda^2} = -a\left\{\frac{\partial E_x}{\partial \theta} + \frac{E_x}{\sin\theta\cos\theta} + \frac{1}{\sin\theta}\frac{\partial E_y}{\partial \lambda}\right\} \quad (10)$$

or from (2), (3) and (9)

$$\frac{\partial \psi}{\partial \lambda} = \frac{a}{C}\left\{\frac{\partial E_y}{\partial \theta} + E_y \cot\theta - \frac{1}{\sin\theta}\frac{\partial E_x}{\partial \lambda}\right\} \quad (11)$$

They showed that equations (10) or (11) can be solved by numerical integration without any neglect of higher harmonics.

## 4. RESULTS

(a) *Wind velocity*

Let $A_n$ and $T_n$ denote the amplitude of wind velocity in the middle latitudes and the time when the wind is directed northward in the northern hemisphere, respectively, and $n = 1$ and 2 denote the diurnal and semi-diurnal components, respectively.

(i) *Observed results.* BRIGGS and SPENCER (1954) summarize the observed wind by various methods, as follows: the mean velocity is about 80 m/sec and the periodic part is mainly semi-diurnal. In the northern hemisphere $A_2 = 30$ m/sec, $T_2 = 15$ hr.

WEISS (1955) observed wind in the southern hemisphere (Adelaide) using meteor trails and concluded that the main periodic wind is diurnal: $A_1 = 21$ m/sec, $T_1 = 5$ hr.

(ii) *Calculated results.* From our calculations the following results are obtained: $A_1 = 20 \sim 50$ m/sec, $T_1 = 13 \sim 15$ hr, $A_2 = 8 \sim 20$ m/sec, $T_2 = 13 \sim 15$ hr, as shown in Figs. 1, 2, 3 and 4. In any case the amplitudes of diurnal winds are several times as great as those of semi-diurnal winds. This relation agrees with observed results at Adelaide (WEISS, 1955) but differs from BRIGGS and SPENCER's (1954) results. The orders of magnitude agree with those observed but there is some discrepancy as regards phase of the wind.

(b) *Ionization drift*

(i) *Observed results.* According to MARTYN (1947) and others, the vertical drift velocity in the $F2$-region seems to be mainly semi-diurnal at equinox. On the other hand, the horizontal drift velocity in the $F2$-region seems to be mainly diurnal.

BRIGGS and SPENCER (1954) show that the E–W drift velocity in the $F2$-region is of order 100 m/sec and towards the east by day and towards the west by night.

(ii) *Calculated results.* In the $F2$-region the so-called induction drag advocated by COWLING (1945) will be important. The electrostatic field $(X, Y)$ originated in the $E$-region is transmitted to the $F2$-region and produces horizontal ionization drift. This drift will accelerate the air of the $F2$-region up to the velocity $(u, v)$ which is nearly equal to the horizontal ionization drift velocity due to electric field $(X, Y)$, and induces a dynamo field $(vH_z, -uH_z)$ cancelling most part of the original field $(X, Y)$, if the period is much longer than about 40 min. Thus there is

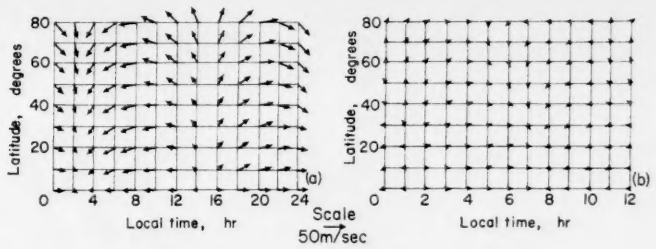


Fig. 1. (by H. MAEDA) Wind system deduced from the dynamo theory. (a) diurnal component; (b) semi-diurnal component.

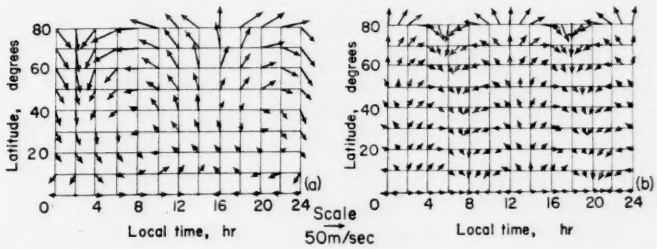


Fig. 2. (by S. KATO) Wind system deduced from the dynamo theory. (a) diurnal component; (b) semi-diurnal component.

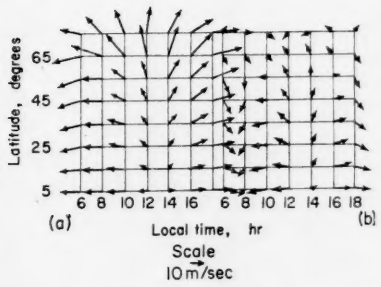


Fig. 3. Scaloidal (by M. HIRONO and T. KITAMURA) (a) diurnal component; (b) semi-diurnal component.

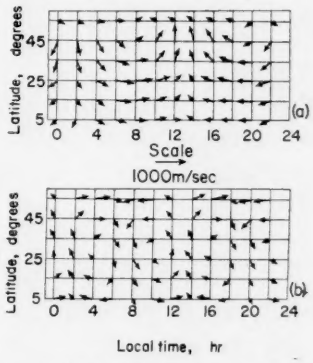


Fig. 4. Toroidal (by HIRONO and KITAMURA) (a) diurnal component; (b) semi-diurnal component.

almost a direct relation between $(X, Y)$ and the horizontal drift, but the vertical drift $\{(Y - uH_z) \cos \phi\}/H$ is not directly related to the electrostatic field, except on the magnetic equator. The calculated horizontal drift velocity of the *F2*-region (HIRONO and KITAMURA, 1956) is mainly diurnal and of order 50 m/sec, and in phase with that observed in high latitudes but opposite to those observed in lower latitudes.

In the lower *F*-region the vertical drift is not seriously affected by induction drag and the order of magnitude is at least sufficient to let some electrons in the *F1*-region descend to the *E*-region at night.

## 5. DISCUSSION

In our calculation of conductivity, it is assumed that the density of negative ions is effectively zero, according to BATES and MASSEY (1951). Recent rocket observation (JOHNSON and HEPPNER, 1956) indicated the existence of considerable negative ions in the $E$-region. If the amount is sufficiently great our calculation should be renewed, and the resulting electrostatic field may have considerably different phase.

Our results are likely to be mainly due to the assumption (HASEGAWA and MAEDA, 1951) that the ratio of noon to night conductivity is about 12 : 1. If the ratio is much greater than this value, we should have different results concerning relative magnitudes of the diurnal and semi-diurnal wind systems. It is clearly desirable to submit it to the direct experimental test. Radio observation of the lower ionosphere seems to support the above mentioned ratio (WATT and BROWN, 1954), but night-time observation of the $E$-region is still too meagre to confirm this situation.

Quite recently GREENHOW and NEUFELD (1956) have made detailed measurements of the wind using meteor radio echoes and have shown that the main periodic wind is semi-diurnal and the phase has a gradient of about 5°/km against altitude. It is very desirable to make these observations in other places of different latitude.

The effect of the general circulation is so far omitted, but in a future study this effect should be considered in addition to the periodic wind system.

## REFERENCES


| | | |
|---|---|---|
| BATES D. R. and MASSEY H. S. W. | 1951 | *J. Atmosph. Terr. Phys.* **2,** 1. |
| BRIGGS B. H. and SPENCER M. | 1954 | *Rep. Progr. Phys.* **17,** 245. |
| CHAPMAN S. | 1919 | *Phil. Trans.* **218,** 1. |
| COWLING T. G. | 1945 | *Proc. Roy. Soc.* A **183,** 453. |
| GREENHOW J. S. and NEUFELD E. L. | 1956 | *Phil. Mag.* **1,** 1157. |
| HASEGAWA M. and MAEDA H. | 1951 | *Rep. Ionos. Res. Japan* **5,** 167. |
| HIRONO M. and MAEDA H. | 1954 | *J. Geomagn. Geoelect., Kyoto* **6,** 127. |
| HIRONO M. and KITAMURA T. | 1956 | *J. Geomagn. Geoelect., Kyoto* **8,** 9. |
| JOHNSON C. Y. and HEPPNER J. P. | 1956 | *J. Geophys. Res.* **61,** 575. |
| KATO S. | 1956 | *J. Geomagn. Geolect., Kyoto* **8,** 24. |
| MAEDA H. | 1952 | *Rep. Ionos. Res. Japan* **6,** 155. |
| MAEDA H. | 1955 | *J. Geomagn. Geoelect., Kyoto* **7,** 121. |
| MAEDA K. | 1953 | *Rep. Ionos. Res. Japan* **7,** 81. |
| MARTYN D. F. | 1947 | *Proc. Roy. Soc.* A **189,** 241. |
| WATT J. W. and BROWN J. N. | 1954 | *J. Geophys. Res.* **59,** 71. |
| WEISS A. A. | 1955 | *Meteors* (Edited by KAISER) p. 195. |

Journal of Atmospheric and Terrestrial Physics, 1959, Vol. 15, pp. 151 to 155. Pergamon Press Ltd. Printed in Northern Ireland

# On the origin of the long-lived solar corpuscular streams which appeared during the last solar cycle 1950-53

KENZI SINNO*

**Abstract**—It is well known that the geomagnetic variation shows a marked 27-day recurrence tendency, especially when the solar activity is on the decrease. In the decreasing epoch of solar activity (1949–1954), the remarkable recurrences of the geomagnetic variation developed without exception. Besides, we verified through investigation by the Bartels' 27-day diagram that the vernal and autumnal maxima belonged to different series of the recurrences which appeared alternately in this period.

For explanation of the above phenomena, the correlations between geomagnetic activities and solar coronal intensities are examined.

It is concluded that the heliographic latitude of coronal intensity and the geomagnetic variation play an important role in these correlations. The corona directed to the earth (e.g. the northern corona in autumn when the earth comes to the north of the heliographic equator and the southern corona in spring when the earth comes to the south of the heliographic equator) shows a remarkable negative correlation with the geomagnetic variation. And the position, from and speed of the corpuscular stream which affects the geomagnetic variation are discussed from the standpoint of inter-correlations with the geomagnetic variation.

## 1. Existence of Semi-annual Period of 27-day Recurrence

THE 27-day recurrence tendency of the international magnetic character figure $C$ has two maxima (BHARGAVA and NAQVI, 1954; SINNO, 1956; TANDON, 1956) around the equinoxes of every year. The amplitudes of these semi-annual waves are somewhat different, but the periods are regular throughout these years. Besides, we can verify that the vernal and autumnal maxima of this curve belong to different sequences of the recurrence which appears alternately in this period, in comparison with the 27-day recurrence diagram of $C$.

In the following investigation, we analyse the data from 1950 to 1953, when the solar activity was decreasing and the 27-day recurrence of geomagnetic activity was very high.

For the practical method of statistical analysis, each row of the Bartels' recurrence diagram, corresponding to one revolution of the sun, takes on the average the same annual phases, respectively, and the diagram for 4 years can be reduced to 1 year. Strictly, the recurrence period is not 27 days, but 27·03 days. This reduced 27·03 day recurrence pattern is shown in Fig. 1. A considerable part of the accidental errors caused by the non-recurrent type disturbances, can be removed and the vernal and autumnal maxima then appear clearly. To help the investigation, the average curves of the rows (the third, fourth and fifth, as the vernal maximum and the tenth, eleventh and twelfth, as the autumnal maximum) and of the columns (the thirteenth, fourteenth and fifteenth as the vernal and the sixth, seventh and eight as the autumnal maximum) which pass through the equinoctial maxima are shown at the bottom and on the right of Fig. 1, respectively. From the average curves of the rows, we can find easily the effect of the $M$-regions which were long-lived in the solar northern and southern hemispheres during these years.

* Hiraiso Radio Wave Observatory, Radio Research Laboratories, Hiraiso, Japan.

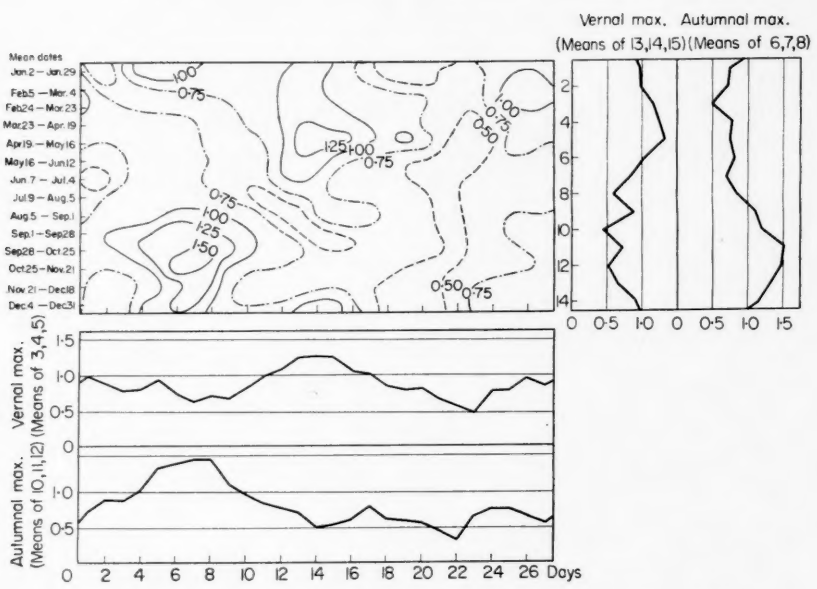


Fig. 1. Diagrams reduced to 1 year from Bartels' diagram are drawn with the lines of the equimagnetic activity (strictly speaking, the reduced diagram is 27·03 days instead of 27 days). On the bottom are the averages of the rows which pass along the vernal (rotations of third, fourth and fifth) and autumnal (rotations of tenth, eleventh and twelfth) maxima. On the right side are the averages of the columns which pass along the vernal (thirteenth, fourteenth and fifteenth days) and autumnal (sixth, seventh and eighth days) maxima.

## 2. Correlations between Geomagnetic Variation and Coronal Intensity

In the following, we examine the state of the corona corresponding to the above described geomagnetic variation. As we have already shown (Sinno, 1956) the disturbances of short-wave propagation and geomagnetic disturbances belonging to the 27-day recurrent type, have fair correspondence with the central meridian passage of sunspots when solar activity is low; solar radio noise intensity and coronal intensity have shown the largest correlation with the 27-day recurrent type of geomagnetic disturbances. The average 27-day (strictly speaking, 27·03 day) variations of coronal intensity during 1950–1953, at every 5° interval, are shown in Fig. 2. For the same reason as the case shown in Fig. 1, accidental and observational errors are removed and we may find where the long-lived $M$-regions lie. In this figure, the days are reduced to the days of central meridian passage across the solar surface and correspond to the day of Fig. 1.

The correlation coefficients between averaged equinoctial geomagnetic variations (averages of the rotation numbers 3, 4, 5 and 10, 11, 12, respectively) and the averaged 27-day variations of coronal intensities which are displaced by a day ahead, are shown in Fig. 3 for each latitude, respectively. The vernal geomagnetic variation has a large negative correlation ($-0{\cdot}7$ to $-0{\cdot}9$) with the coronal intensities



VOL. 15 1959

of the latitudes in the southern hemisphere, while it has a little correlation(0·1–0·2) in the northern hemisphere. Also the autumnal geomagnetic variation appears almost symmetrical with respect to 5–6 degrees south latitude, as shown in Fig. 3 In this discussion, we disregard the difference from the equator. The comparatively higher values of the correlations do not decrease at high latitudes, but it is difficult to consider that the $M$-regions exist at so high latitude. Thus, we come to the conclusion the $M$-regions lie in about $\pm 15°$–$20°$, respectively, and the

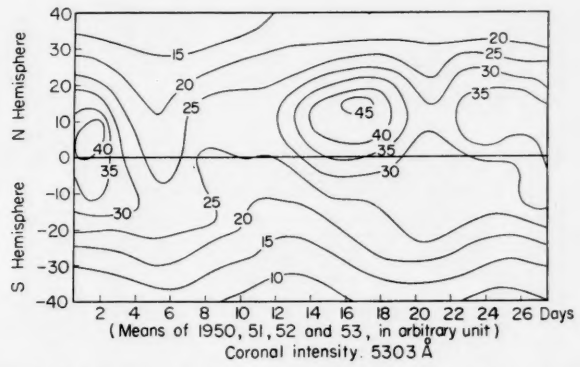


Fig. 2. Averaged 27-day variations of coronal intensity, 1950 to 1953, at every 5 degrees' interval. Scales are in arbitrary unit for the normalization is done every year.

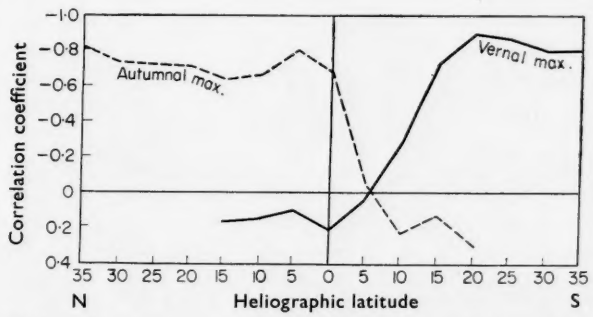


Fig. 3. Correlations between averaged magnetic 27-day variations at equinoxes (the means of rotation of third, fourth, fifth, and tenth, eleventh, twelfth, respectively) and averaged 27-day variations of coronal intensities which are displaced by a day ahead.

northern one controls the geomagnetic variation in autumn and the other does so in spring, according to the motion of the earth in its orbit which is inclined about 7·3° to the heliographic equatorial plane.

Next, in order to find the effect of the coronal intensities $\pm 15°$ on the geomagnetic variation, we calculate the correlation coefficients of the averaged 27-day variation of $C$ with $\pm 15°$ coronal intensities over the year, and the values are smoothed by means of the running average of three rotations. It is remarkable that these two curves closely resemble the curves on the right side of Fig. 1.

Now, using the averaged 27-day variations of $\pm 15°$ coronal intensities and

geomagnetic variations at both equinoxes, we compute the cross-correlation by displacing the days. The vernal geomagnetic variation shows the best correlation with $-15°$ corona with 2 days' lag, and the autumnal one has not any delay in peak value of the correlation with $+15°$ corona. The mean delay of the effect of the corona is about $1\frac{1}{2}$ days, and its dispersion is about 4 days ($53{\cdot}3°$).

From the above discussion, we see that the directivity of corpuscules is about 6° to the latitudinal direction and about 50° to the longitudinal direction of the sun, if the emission is directed radially on the solar surface. Here, the directivity of the stream in space means the probability of the streams which are emitted in its direction.

## 3. Discussion and Conclusion

From the geomagnetic and coronal studies mentioned above, we can definitely say that the corpuscular emission has its origin in the solar northern and southern hemispheres during the decreasing epoch of solar activity and controls the geomagnetic disturbances in autumn and spring, alternately.

In this conclusion, the negative correlations between the geomagnetism and corona are considered to be somewhat curious. The opinion of PECKER and ROBERTS (1955) relating to these negative correlations, is remarkable. According to their opinion, the ion jets leaving the solar surface near the centre of activity are deflected to the quiet region by the active centre field; for instance, the magnetic field. Hence, the ion jets are emitted from the active centre, behaving as jets ejected straight from a region in a low active state.

On the other hand, in recent papers BABCOCK and BABCOCK (1955) have reported that a solar unipolar region at 15°N continued in 1953 corresponds to the recurrent series of geomagnetic disturbances. And they considered that the particles will come out more or less radially from this unipolar region, without dissipating their energy by pronounced collisions; that is different from the particles ejected near a bipolar region.

The above two speculations do not contradict each other and give a fair interpretation of the mechanism concerning ejection of corpuscular stream from the solar surface.

Now there remains to be determined what is the time lag of the maximum correlations with the corona behind the epoch when the earth reaches the highest heliographic latitude, as was pointed out in Figs. 1. The time retards on 6 March and 8 September, when the earth comes to the highest solar latitude ($\pm 7°15'$), are near the times when the angle made by the solar axis with the terrestrial meridian half-plane which passes through the sun's centre reaches a maximum. These times of the maximum angle are on 7 April and 11 October. If we suppose that the electromagnetic collisional cross-section of the earth and the corpuscular beam becomes larger at these times, we can avoid the difficulty. But the theoretical estimation of the collisional cross-section is impossible in the present stage of knowledge.

In this report, we discuss only the long-lived $M$-regions which existed during the decreasing epoch of the last solar activity. We cannot say that the general characteristics of the $M$-regions have been discovered. Further investigations are to be made with observational data covering different periods.



VOL. 15 1959

## References


| | | |
|---|---|---|
| Babcock H. W. and Babcock H. D. | 1955 | *Astrophys. J.* **121,** 349. |
| Bhargava B. N. and Naqvi A. M. | 1954 | *Nature, Lond.* **173,** 498. |
| Pecker J. C. and Roberts W. O. | 1955 | *J. Geophys. Res.* **60,** 33. |
| Sinno K. | 1956 | *J. Radio Res. Lab.* **3,** 155. |
| Tandon J. N. | 1956 | *J. Geophys. Res.* **61,** 211. |


DL.
15
959

Journal of Atmospheric and Terrestrial Physics 1959, Vol. 15, pp. 156 to 160. Pergamon Press Ltd. Printed in Northern Ireland

# Magneto-hydrodynamic waves in the ionosphere

SYUN-ICHI AKASOFU*

**Abstract**—The study is made of the magneto-hydrodynamic waves in the ionosphere and the outer atmosphere. The dispersion relations of Alfvén waves are obtained and it is shown that various types of geomagnetic micropulsations and ionospheric noises appear in the wide range from audio- to very low-frequency. The Alfvén waves with finite amplitude are also studied. It is suggested that the retarded sound-type shock wave may be identified with the descending "cusps" on $h'$-$f$ curve of ionogram.

## 1. INTRODUCTION

RECENT researches on the ionized gas in the interplanetary space and the outer atmosphere have shown that the sun and the earth are not separated *in vacuo*, but in the tenuous ionized gas. This suggests that the solar disturbances propagate through these tenuous media and reach the ionosphere—that is, the ionosphere is situated in the *bottom* of these ionized gas systems.

The above two gas systems may, probably, be treated as *fully* ionized gas systems. However, in the ionosphere, the gas is weakly ionized and it is necessary to study in detail the hydromagnetic effects in the *weakly* ionized gas.

## 2. DISPERSION RELATIONS OF MAGNETO-HYDRODYNAMIC WAVES

The well-known magneto-ionic theory assumes the wave motion of electrons in the immobile background, i.e. neutral particles. When we are concerned with the frequency range corresponding to geomagnetic micropulsations, low-frequency ionospheric noises, and fine structures of the ionosphere—comparable or far below the gyrofrequency of positive ions—the motion of positive ions, and so that of neutral particles, cannot be neglected.

Using SCHLÜTER's (1951) momentum balance equations for these constituents together with Maxwell's equations, we obtain the following dispersion equation for the wave propagation along the magnetic lines of force,

$$\frac{\omega^2}{\kappa^2} = \frac{[BV_A{}^2 + (\omega c^2/4\pi)\{i(W_1 + W_{2zz}) \pm (W_{3z})\}]}{[1 + (\omega/4\pi)\{i(W_1 + W_{2zz}) \pm (W_{3z})\}]} \tag{1}$$

This dispersion equation is applicable to the lower frequency range, in which the motion of positive ions is important, and to the higher one, in which the positive ions are undisturbed, while the electrons play a predominant role.

The effect of a magnetic field on the propagation of magneto-hydrodynamic waves is to split the waves into two waves corresponding to $O$- and $E$-waves of electromagnetic waves in the ionosphere. However, the magneto-hydrodynamic $O$-wave is always damped very strongly in the ionosphere. To illustrate the dispersion relations, the phase velocity is plotted as a function of $\omega$ for the conditions corresponding to $F2$-, $E$- and $D$-regions of the ionosphere in Fig. 1.

* Geophysical Institute, Tôhoku University, Sendai, Japan



VOL.
15
1959

For the waves propagating across the magnetic field, we obtain the following dispersion relations, according to PIDDINGTON (1953):

$$\kappa^4 - \kappa^2 \left\{ \frac{\omega^2}{U^2} - \frac{i\omega(U^2 + V_A{}^2)}{sU^2} \right\} - \frac{i\omega^3}{sU^2} = 0 \tag{2}$$

In the ionospheric conditions, for the frequency range that we are concerned with, we obtain two types of waves. One of them is intrinsically the sound wave (retarded sound wave); the other is the magnetic wave (modified Alfvén wave), whose

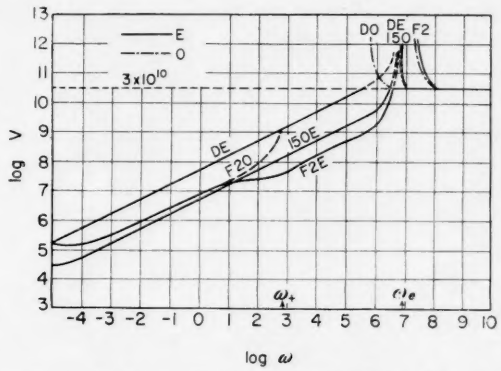


Fig. 1. Dispersion relations for the conditions in the $F2$-, $E$- and $D$-regions of the ionosphere.

velocity is of the order of $H/\sqrt{4\pi\rho_p}$(= velocity of pure Alfvén wave along the magnetic lines of force), where $\rho_p$ is the density of ionized part of gas (cf. AKASOFU, 1956a).

## 3. THEORY OF OUTER ATMOSPHERIC OSCILLATIONS

In this section, we study the global oscillations of the outer atmosphere. We consider an axially symmetrical case through the axis $\theta = 0$ of a system of spherical co-ordinates $(r, \theta, \phi)$. A magnetic dipole is placed at the origin parallel to the axis of symmetry. Then, the equation of small oscillation for the most important mode is (DUNGEY, 1954; KATO and AKASOFU, 1956),

$$\left( 4\pi\rho H_0{}^{-2} \frac{\partial^2}{\partial t^2} - \frac{1}{r^2} \sin\theta \frac{\partial}{\partial\theta} \frac{1}{\sin\theta} \frac{\partial}{\partial\theta} - \frac{\partial^2}{\partial r^2} \right) (r \sin\theta \, E_\phi) = 0 \tag{3}$$

The solution of this equation gives the oscillating electric field in and outside the outer atmosphere, respectively.

$$E_\phi = \sum_n \frac{1}{n\sqrt{x}} [A_n J_{n+1/2}(x) + B_n J_{-n-1/2}(x)] \, P_n{}^1(\mu) \tag{4a}$$

$$E_\phi = \sum_n \frac{1}{n} \left\{ \frac{M_n}{n+1} x^n - \frac{N_n}{\eta} \frac{1}{x^{n+1}} \right\} P_n{}^1(\mu) \tag{4b}$$

Using the boundary conditions, we obtain the equation of period, from which we can estimate the period of oscillations.

$$\phi_n(x) = J_{n+1/2}(x) \cdot J_{-n+1/2}(\beta x) + J_{-n-1/2}(x) \cdot J_{n-1/2}(\beta x) \tag{5}$$

For example, for the atmospheric shell having the thickness of 5 earth's radii, the periods are 378, 182, 118, 87, 69, 57, . . . sec.

## 4. RETARDED SOUND-TYPE SHOCK WAVE

When the electron density variation for the wave-type variation is 10 per cent or so, it is necessary to treat this type of disturbance as a wave of finite amplitude, i.e. shock wave. According to HELFER (1953), there are three types of magneto-hydrodynamic shock waves and in their limiting case of infinitesimal amplitude, they correspond to three waves studied in Section 2. It is very difficult to discuss these shock waves in the weakly ionized gas-mixture. Fortunately, the results obtained in Section 2 form the basis for further treatments.

From the conclusion in Section 2, it becomes apparent that the retarded sound-type shock wave are the most interesting ones, because the velocity is of the order of acoustic waves. On the other hand, the true Alfvén and the modified Alfvén wave have so large a velocity that radio observations cannot detect them, at present.

The fundamental properties of the retarded sound-type wave are that the wave is virtually a sound wave and its motion is not parallel to the direction of magnetic field. We follow the treatment of HELFER. Describing subscripts 1 and 2 as the physical parameters of the medium in front of and behind the advancing shock, respectively, we obtain the velocity of the shock front in terms of the physical condition of the medium, according to Rankine–Hugoniot-like equations

The velocity of shock front in terms of velocity of sound (Mach number) is

$$M = \sqrt{\left(\frac{6}{5}Q\right)} D_1 \cos\theta_1 \tag{6}$$

As the numerical example, we consider the case, in which the shock front propagates at an angle 6° or so to the magnetic lines of force. It seems that in the middle latitude this case appears most frequently. Then, it is seen that the Mach number is of the order of 0·1 in the ionospheric and the outer atmospheric conditions, if the electron density variation is 10 per cent or so. Assuming temperature $T = 1000°$ K, the velocity of sound is of the order of 1000 m/sec. Thus, the velocity of shock front is of the order of 100 m/sec.

According to a recent study by moving pictures of ionograms, rapidly varying disturbances sometimes occur on the $h'$-$f$ curve. Some of them appear at the uppermost *F2*-layer as the "cusps" and come down along the $h'$-$f$ trace to the regions-*F1* and -*E* (see Fig. 2).

BIBL (1951) made the first detailed study of such a phenomenon at Freiburg and Djibouti. According to RAWER (1956), some further information is as follows: The velocity of the apparent movement (virtual height) goes up to some 300 m/sec (vertical movement). The phenomenon is always very rare at night-time.

Moreover, NAKATA (1954) also observed the vertical motion by the sweep frequency $h'$-$t$ and *fct* method. The well-defined form of observed features indicates the horizontal motion from north to south of the order of 7·5 km/min, as well as the vertical motion.

Consequently, it seems that the wavefront has a three-dimensional surface when we assume the shock wave hypothesis. The satisfactory agreement between the

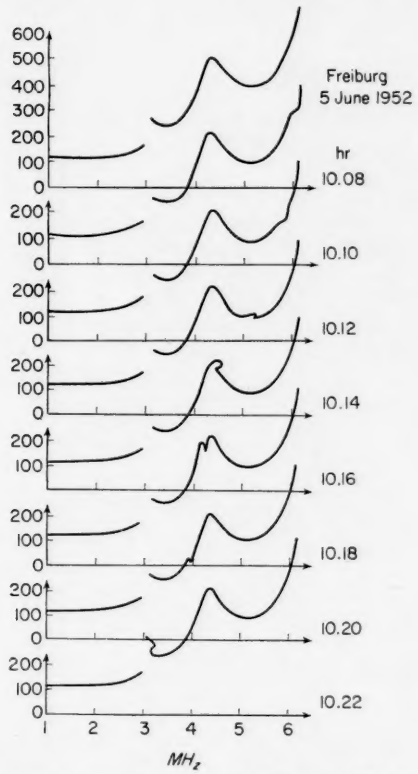


Fig. 2. Transient phenomenon in the $F$-layer (after BIBL, 1953).

observed and the theoretical values provides the possible explanation due to the shock wave. Owing to the non-uniform distribution of temperature, the shock front may not be a flat, but a curved surface, which may give rise to double or triple reflections.

## 5. CONCLUSION

We have seen various types of Alfvén waves in the ionized atmosphere around us. Because of the resemblance between the geomagnetic micropulsation and the shock wave, it is very likely that the solar disturbances may be the ultimate origin of these disturbances.

These disturbances travel through the outer atmosphere, being guided by the earth's magnetic field, and may be observed in the ionosphere by the radio method and by the magnetogram.

Thus, a new tool will have become available for the exploration of the outer atmosphere by the study of the propagation of these shock waves, as well as the "whistler."

*Acknowledgements*—The writer wishes to express his sincere thanks to Prof. Y. KATO of this Institute, Prof. K. MAEDA of Kyoto University, Dr. K. RAWER of Ionosphärenstation, Freiburg and Dr. Y. NAKATA of the Radio Research Laboratories, Tokyo for their kind encouragement and advice.

## REFERENCES


| | | |
|---|---|---|
| AKASOFU S. | 1956a | *Sci. Rep. Tôhoku Univ.* **8,** 24. |
| AKASOFU S. | 1956b | *Rep. Ionos. Res. Japan* **10,** 227. |
| AKASOFU S. | 1957 | *Sci. Rep. Tôhoku Univ.* **8,** 23. |
| BIBL K. | 1951 | *Ann. Géophys.* **7,** 208. |
| BIBL K. | 1953 | *Z. Geophys.* **8,** 138. |
| DUNGEY J. W. | 1954 | *Sci. Rep.* No. 69 Ionosphere Res. Lab. Pennsylvania State University. |
| HELFER H. L. | 1953 | *Astrophys. J.* **117,** 117. |
| KATO Y. and AKASOFU S. | 1956 | *Sci. Rep. Tôhoku Univ.* **7,** 103. |
| NAKATA Y. | 1954 | *J. Radio Res. Lab.* **1,** No. 2. |
| PIDDINGTON J. H. | 1953 | *Mon. Not. R. Astr. Soc.* **113,** 647. |
| RAWER K. | 1956 | Private communication. |
| SCHLÜTER A. | 1951 | *Z. Naturforsch.* **6a,** 73. |


VOL
15
195

Journal of Atmospheric and Terrestrial Physics, 1959, Vol. 15, pp. 161 to 167. Pergamon Press Ltd. Printed in Northern Ireland

# Analysis of pulse-delay data from rockets for the determination of electron density

W. PFISTER* and J. C. ULWICK*

## 1. INTRODUCTION

ROCKET experiments measuring the electron density in the ionosphere, utilizing the pulse-delay method, began in 1946 when the V-2 rockets first became available. The experiment consists in the measurement of the transmission times of pulses at two frequencies, one being delayed by the ionosphere. Comparison transmissions are made both from the ground to the rocket and from the rocket to the ground. Up to the present, useful data for the determination of electron densities have been obtained from two V-2 rockets and nine Aerobee rockets (three standard, four intermediate and two hi). Only part of the records obtained on these rocket flights have been analysed and the results reported are only of preliminary nature.

The first data from a V-2 rocket showed that the measured time-delay fluctuated considerably after the rocket reached a height of 95 km. The conclusion was that the ionosphere is very irregular and patchy in the interval between 95 and 110 km, while the small irregularities at heights above 110 km have negligible effects on the measured time-delays (BETH, 1950). Records from later flights indicated that the fluctuations of the time delay are caused by small clouds of high electron density and the smoothing process had to be done by weighting the smaller time-delays. The results for V-2 No. 24 and Aerobees No. 38 and 39 for rocket ascent showed a bifurcation of the *E*-region (LIEN, LINFORD *et al.*, 1954). In view of the discrepancy of the results with our general concept of the *E*-layer and with the findings of the Naval Research Laboratory from their rocket experiments (SEDDON and JACKSON, 1955; PFISTER *et al.*, 1955), a re-evaluation of the data became desirable.

## 2. RAY PATH AND EQUIVALENT PATH LENGTH

The first consideration in a more careful analysis is to take into account the effects of the earth's magnetic field for tracing the oblique ray paths and for the equivalent path of the wave packet. Vector expressions were derived for a horizontally stratified ionosphere, utilizing an extended analytical treatment of Poeverlein's two-dimensional case based upon crystal optics.

According to HAMILTON (1837), ray directions can be found by drawing normals to the $\mu$-surface, which is in turn obtained by plotting, in space polar co-ordinates, the value of the refractive index as a function of the wave normal.

If we let the $\mu$-surface be represented vectorally by

$$\boldsymbol{\mu} = \mu(\alpha, \chi)$$

* Ionospheric Physics Laboratory, Air Force Cambridge Research Center, Geophysics Research Directorate.

where $\alpha$ is the angle between $\boldsymbol{\mu}$ and $\mathbf{M}$, a unit vector in the direction of the earth's magnetic field, and $\chi$ is the angle between the $\boldsymbol{\mu}\mathbf{M}$-plane and any arbitrary fixed $\mu M$-plane, measured in the direction of $\boldsymbol{\mu} \times \mathbf{M}$, then

$$\frac{\partial \boldsymbol{\mu}}{\partial \alpha} \quad \text{and} \quad \frac{\partial \boldsymbol{\mu}}{\partial \chi}$$

are vectors tangent to the $\alpha$- and $\chi$-curves, respectively, and thus tangent to the $\mu$-surface. Therefore

$$\frac{\partial \boldsymbol{\mu}}{\partial \chi} \times \frac{\partial \boldsymbol{\mu}}{\partial \alpha}$$

is a vector perpendicular to the $\mu$-surface at the point $(\alpha, \chi)$ and pointing outwardly from the $\mu$-surface. The unit vector $\mathbf{S}$ in the direction of this vector is given by

$$\mathbf{S} = \frac{\dfrac{\partial \boldsymbol{\mu}}{\partial \chi} \times \dfrac{\partial \boldsymbol{\mu}}{\partial \alpha}}{\sqrt{\left\{\left(\dfrac{\partial \boldsymbol{\mu}}{\partial \chi} \times \dfrac{\partial \boldsymbol{\mu}}{\partial \alpha}\right) \cdot \left(\dfrac{\partial \mu}{\partial \chi} \times \dfrac{\partial \mu}{\partial \alpha}\right)\right\}}} \tag{1}$$

To calculate $\dfrac{\partial \boldsymbol{\mu}}{\partial \alpha}$ and $\dfrac{\partial \boldsymbol{\mu}}{\partial \chi}$, we chose two unit vectors $\mathbf{e}_1$ and $\mathbf{e}_2$ having the properties that

$$\mathbf{e}_1 \cdot \mathbf{e}_2 = \mathbf{e}_1 \cdot \mathbf{M} = \mathbf{e}_2 \cdot \mathbf{M} = 0$$

Then we may write

$$\boldsymbol{\mu} = \mathbf{e}_1 \mu \sin \alpha \cos \chi + \mathbf{e}_2 \mu \sin \alpha \sin \chi + \mathbf{M} \mu \cos \alpha$$

from which we find

$$\frac{\partial \boldsymbol{\mu}}{\partial \chi} \times \frac{\partial \boldsymbol{\mu}}{\partial \alpha} = \left(\frac{d\mu}{d\alpha} \cos \alpha - \mu \sin \alpha\right)\boldsymbol{\mu} - \mu \frac{du}{d\alpha} \mathbf{M} \tag{2}$$

This vector is in the direction of the unit vector $\mathbf{S}$ normal to the $\mu$-surface at the point $(\alpha, \chi)$. The vector

$$\frac{\boldsymbol{\mu}}{\mu} - \frac{d\mu/d\alpha \cos \alpha \, \mathbf{M}}{d\mu/d\alpha \cos^2 \alpha - \mu \sin \alpha \cos \alpha} \tag{3}$$

evidently has the same direction as (2), and if we define a new parameter

$$\varepsilon = 1 - \frac{d\mu/d\alpha}{d\mu/d\alpha \cos^2 \alpha - \mu \sin \alpha \cos \alpha} \tag{4}$$

which is a measure of the degree of isotropy, we may write

$$\mathbf{S} = \frac{\boldsymbol{\mu}/\mu - (1 - \varepsilon) \cos \alpha \, \mathbf{M}}{\sqrt{(\sin^2 \alpha + \varepsilon^2 \cos^2 \alpha)}} \tag{5}$$

The unit vector $\mathbf{S}$ given by (5) gives the ray direction at the point $(\alpha, \chi)$ of the



VOL.
15
1959

$\mu$-surface. $d\mu/d\alpha$ may be found by differentiating the Appleton–Hartree equation with respect to $\alpha$. Then, from (4)

$$\varepsilon = \frac{(h-1)(1-\mu^2)^2 + a^2}{(h/(1-a)-1)(1-\mu^2)^2 + a^2} \tag{6}$$

where $h = \dfrac{\omega_H{}^2}{\omega^2}$ and $a = \dfrac{\omega_N{}^2}{\omega^2}$

The phase of the wave

$$\exp(i\omega t) \,.\, \exp[-i\omega\phi(x, y, z)/c] \tag{7}$$

may be written in the form

$$\omega cT - \int_0^S \omega(\boldsymbol{\mu} \,.\, \mathbf{S})\, ds \tag{8}$$

where the ray path has been chosen as the path of integration. The Appleton–Hartree equation with $\mu \cos \alpha$ eliminated may be symbolized by

$$\mu(\mu_1, \mu_2, \omega)$$

where $\mu_1$ and $\mu_2$ are constant for a given ray (Snell's law). Solving this equation for $\mu_3$, we have

$$\mu_3 = \mu_3(\mu_1, \mu_2, \omega)$$

Thus $\mu_3$ may be considered a function of the independent variables $\mu_1$, $\mu_2$ and $\omega$. If we call $P(\mu_1\mu_2\omega)$ the phase of the wave (7) we have from (8)

$$P(\mu_1\mu_2\omega) = \omega cT - \int_0^S \omega(\boldsymbol{\mu} \,.\, \mathbf{S})\, ds \tag{9}$$

This is the phase for a wave of angular frequency $\omega$ and incident directions given by $\mu_1$ and $\mu_2$.

For the ray path, according to Kelvin's principle of stationary phase, we must have

$$dP(\mu_1, \mu_2, \omega) = 0$$

Thus since $\mu_1$, $\mu_2$ and $\omega$ are independent

$$\frac{\partial P}{\partial \mu_1} = 0, \quad \frac{\partial P}{\partial \mu_2} = 0, \quad \frac{\partial P}{\partial \omega} = 0 \tag{10}$$

Making use of (9), equations (10) give

$$\int_0^S \left(\frac{\partial \boldsymbol{\mu}}{\partial \mu_1} \,.\, \mathbf{S}\right) ds = 0 \tag{a}$$

$$\int_0^S \left(\frac{\partial \boldsymbol{\mu}}{\partial \mu_2} \,.\, \mathbf{S}\right) ds = 0 \tag{b}$$

$$cT - \int_0^S \frac{\partial}{\partial \omega} \Big\{\omega(\boldsymbol{\mu} \,.\, \mathbf{S})\Big\}_{s=\text{constant}} ds = 0 \tag{c}$$

The first of these equations defines the position of the ray path. The last equation gives the equivalent path length of the ray. These formulae have been used for the analysis of the experimental delay data. The method of analysis is essentially a trial-and-error method using the IBM 704 high-speed computer.

For the evaluation, the ionosphere is assumed to be divided into $\frac{1}{2}$ km layers of constant electron density. The step-wise evaluation begins with the rocket in a position at the top of the first layer. The position of the rocket with respect to the ground transmitter and the delay of the pulse at this position are given by the experimental data. The electron density for the layer and the departure angles for the ray so as to intercept the rocket are estimated. The index of refraction and the direction of the wave-normal are now determined by the simultaneous solution of the Appleton–Hartree equation and Snell's law. The ray path is computed to see if the ray hits the rocket. If not, new departure angles are estimated and the procedure is repeated. Once the correct ray path is determined, the delay is computed and compared with the experimental delay. If the difference between these delays is not within a specified limit, the procedure is repeated from the beginning with a new electron density until this criterion is satisfied. When satisfied, the electron density for the first layer is now known. The procedure is repeated for the next and each succeeding layer until, layer by layer, the electron density profile is determined.

## 3. DELAY-DATA REDUCTION

Fig. 1 shows the delay readings recorded as a function of time of flight and altitude for a frequency of 4·05 Mc/s transmitted from the ground to Aerobee no. 38. Gaps in the data as evidenced here are generally filled in by data obtained from other recording stations. Examination of the data reveals a periodicity of the fluctuations of the readings which agrees with the rocket roll. From these data it is evident that the missile rotates approximately $1\frac{1}{2}$ times/sec with an amplitude range of the fluctuations between $\frac{1}{2}$ and 1 $\mu$sec. The delay data for the 6 Mc/s downward transmission from another flight showed the missile rotated approximately 2 times/sec with an amplitude range of the fluctuations between $1\frac{1}{2}$–2 $\mu$sec (Fig. 1 of PFISTER, 1956). This type of fluctuation can easily be eliminated by integrating over the period of the roll of the rocket.

Fig. 2 shows how this fluctuation is eliminated when the mean values for $\frac{1}{2}$ km intervals are taken. These mean values, however, are still not regular enough to allow an analysis based on the concept of a smooth, stratified ionosphere. Irregularities are still evident at various altitudes, particularly noticeable at 102 and 105 km. These were eliminated by computing running means over 3 km intervals as shown by the solid line. These delays are now used in the analysis.

## 4. RESULTS

As a result of the method of analysis, the electron density distribution obtained is a step curve of $\frac{1}{2}$ km intervals. This is smoothed by a weighted running mean over five such intervals, the weights used being 1, 0·8 and 0·4, respectively. Some of the results of the new careful analysis have been reported at several scientific meetings. These results have so far indicated that the structure of the *E*-layer



VOL. 15 1959

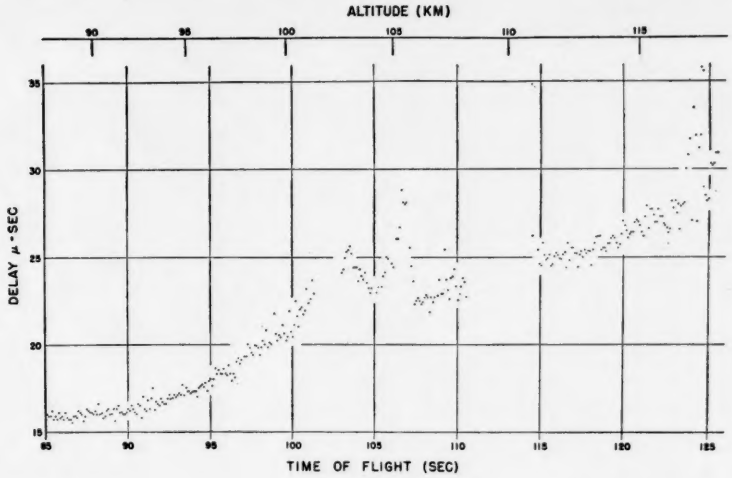


Fig. 1.

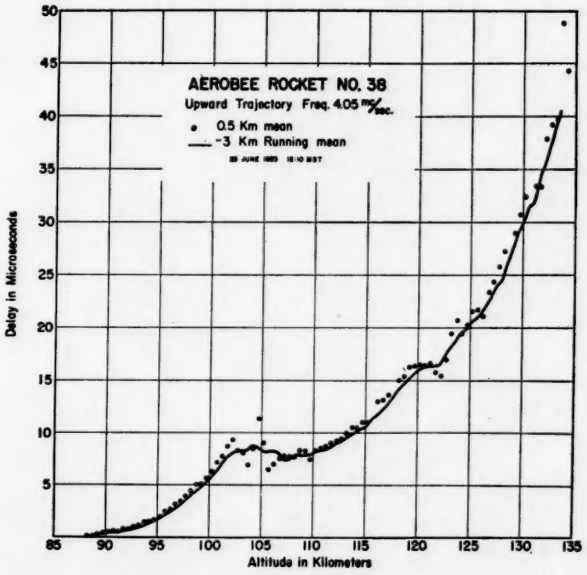


Fig. 2.

appears to be of a laminated nature with about 6 km separation between laminations. The results also show that the conclusion of a bifurcation of the *E*-layer was premature and that a very intense individual blob caused the impression of a bifurcation. As an example of the results, Fig. 3 shows the electron-density profile for rocket descent of Aerobee no. 38 calculated from the data of the two probing frequencies, 4·05 and 4·87 Mc/s. The agreement between the two frequencies is good with respect to the shape of the curves although the values at 107 and 114 km are noticeably different. These we attribute to the different effects the

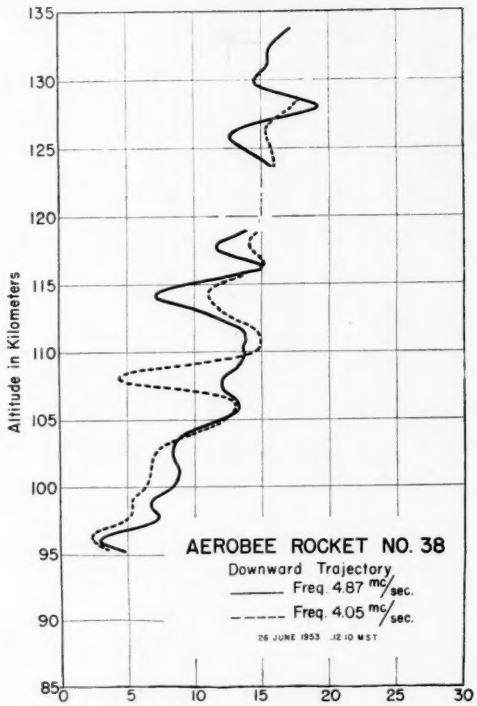


Fig. 3.

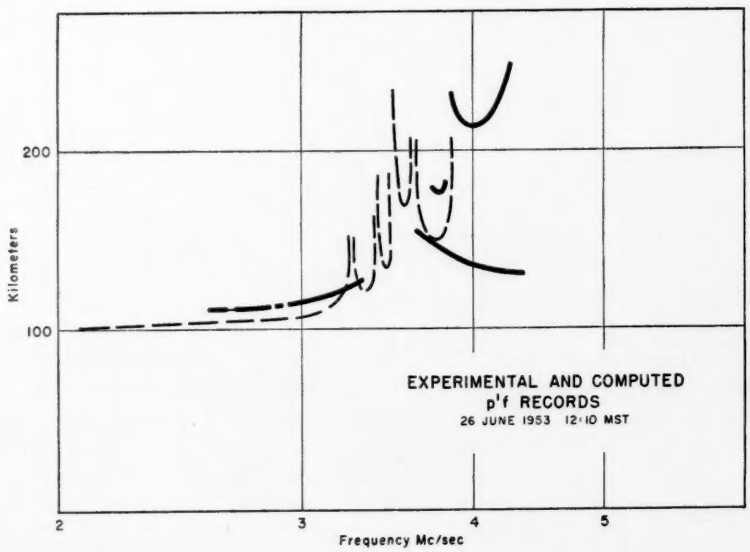


Fig. 4.



VOL.
15
1959

irregularities have on the two frequencies as a result of different ray paths and the smoothing process. Peaks in the curves occur at 106, 111, 117 and 128 km with no data available from 119 to 123 km. From the mean curve of these two frequencies, an $h'f$ curve is constructed and compared with that taken at the White Sands Ionosphere Station about 30 miles away from the Aerobee launching tower as shown in Fig. 4. The conclusion here, as in other flights, is that much finer details can be obtained from the rocket-flight results than the $h'f$ record can provide.

It is apparent from the data and the results that this experiment is feasible for research on the blobby structure of the ionosphere. The combination of the delay data from the four receiving stations which measure at oblique incidence for the downward transmission, and the essentially vertical incidence station for both upward and downward transmissions, gives a fairly good three-dimensional picture of the blob structure. In addition, on the last two rocket flights the signal amplitude fluctuations at three closely spaced receivers were measured to give more details about the fine structure of the ionosphere.

## References


| | | |
|---|---|---|
| Beth E. | 1952 | *Proceedings of Conference on Ionospheric Physics* 1950. Geophysical Research Paper #11, Air Force Cambridge Research Center. |
| Hamilton W. R. | 1837 | *Trans. Roy. Irish Acad.* **17**, 144. |
| Lien J. R., Linford L. B. *et al.* | 1954 | *Rocket Exploration of the Upper Atmosphere.* Interscience, New York. |
| Pfister W. | 1956 | *Scientific Uses of Earth's Satellites.* University of Michigan Press. |
| Pfister W., Ulwick J. C. and Marcou R. J. | 1955 | *Phys. Rev.* **97**, 1183. |
| Seddon J. C. and Jackson J. E. | 1955 | *Phys. Rev.* **97**, 1182. |


OL.
15
959

Journal of Atmospheric and Terrestrial Physics, 1959, Vol. 15, pp. 168 to 174. Pergamon Press Ltd. Printed in Northern Ireland

# Region-*E* and solar activity

W. J. G. Beynon* and G. M. Brown*

Recently there has been renewed interest in the derivation of ionospheric indices of solar activity. Since the various ionospheric layers arise, directly or indirectly, from solar radiation of more than one wavelength, and these radiations may well vary unequally, it is to be anticipated that an index based on one layer only will not adequately represent solar activity changes. In this note we discuss some aspects of region-*E* and solar activity.

## 1. Theoretical Considerations

Under equilibrium conditions the relationship between the peak electron density of the normal *E*-layer (represented by the critical frequency $fE$) and solar zenith angle $\chi$ is approximately given by

$$K(\alpha \,.\, H)(fE)^n \,.\, \sec \chi = S_\infty \tag{1}$$

where $S_\infty$ is the intensity of the ionizing radiation outside the atmosphere, $\alpha$ is the effective recombination coefficient, $H$ is the scale height of the ionized constituent and $K$ is a numerical constant. The index $n$ depends on the effective process of electron dissipation. For large zenith angles, sec $\chi$ must be replaced by the appropriate Chapman function $\mathrm{Ch}(\chi)$.

An expression of the form (1) may be expected to apply to the seasonal variation of noon values of $fE$ and it has been customary to take the "character figure" $(fE)^n \sec \chi$ as proportional to the ionizing radiation $S_\infty$. When the seasonal influence on $fE$ is removed in this way, there remain a number of other minor influences to be considered. These include

(a) the possible influence of seasonal changes in temperature at the layer on the product $(\alpha H)$.

(b) the effect of ellipticity of the earth's orbit. This will give rise at all locations to a 6% increase in intensity of radiation in December–January compared with June–July, causing an annual variation in the values of $fE$ and possibly in the product $(\alpha H)$.

(c) perturbing influences on the parameter $fE$, such as geomagnetic distortion, magnetic disturbance and possible lunar tidal effects. For the data with which we shall be concerned here, these are likely to be quite small.

There is considerable evidence, mainly from solar eclipse data, that the effective radiation $S_\infty$ consists of a number of components, part originating in the active areas in or near sunspot groups, part from the corona, and part from the general undisturbed background of the solar disk. To a first approximation we can allow for the solar cycle effect in $S_\infty$ by writing

$$S_\infty = a + b \,.\, R \tag{2}$$

where $a$ and $b$ are numerical constants and $R$ is the relative sunspot number.

* University College of Swansea

Combining (1) and (2) we have

$$(fE)^n \sec \chi = A + B.R \tag{3}$$

where $A(=a/K\alpha H)$ and $B(=b/K\alpha H)$ may show a seasonal variation.

Equation (3) leads to the following expression for the sensitivity of $fE$ to sunspot number changes

$$\frac{\partial fE}{\partial R} = \frac{B \,.\, \cos^{1/n} \chi}{n(A + BR)^{(n-1)/n}} \tag{4}$$

Thus, for a given station ($n$ = constant), this sensitivity will vary with both $\chi$ and $R$, being largest in local summer for a given $R$, and largest at sunspot

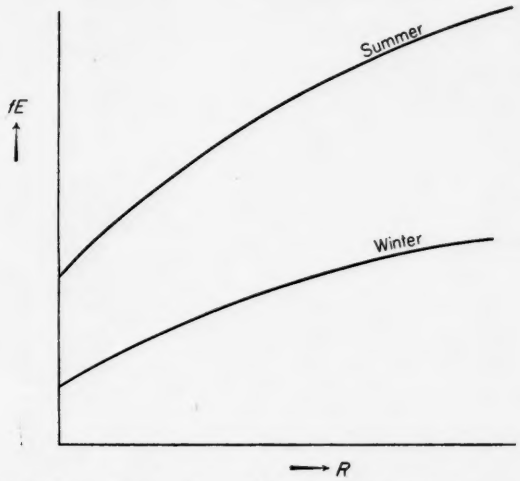


Fig. 1. Theoretical form of the relationship between $fE$ and sunspot number $R$ at one station for two seasons.

minimum for a given value of $\chi$. The forms of the $fE/R$ variations to be expected at any given place are as shown in Fig. 1.

In applying equation (4) to consider the variation of sensitivity ($\partial fE/\partial R$) with latitude, it is to be remembered that the value of the index $n$ itself varies with latitude.

## 2. Long-period (Solar Cycle) Variations

The remarkably close connection between sunspot number and $fE$ is shown from a consideration of the monthly mean values of the two parameters. Taking the monthly mean noon values over an eleven-year period we have determined, for each month, the departures of $fE$ and $R$ from the mean values for the whole period. These departures, $\Delta fE$ and $\Delta R$, are plotted in Fig. 2. It will be noticed that the points cluster closely about a mean curve, 90% lying within 0·1 Mc/s. For small changes the relation between $\Delta fE$ and $\Delta R$ is fairly linear ($\Delta R \leqslant 40$ and $\Delta fE \leqslant 0{\cdot}2$ Mc/s, the departures being measured with respect to the mean values of $R = 73$ and $fE = 3{\cdot}2$ Mc/s for the period under consideration). Within these limits it is found that the average sensitivity of $fE$ at Slough to long-period (solar

cycle) sunspot changes is $\Delta fE/\Delta R = 0{\cdot}0048$ Mc/s per unit $R$. For larger sunspot changes there is clear evidence for departure from linearity.

If years of rising and falling activity are grouped separately there is an interesting division of the points in Fig. 2. This is illustrated in Fig. 3 in which this grouping has been effected. Each point in this diagram represents the mean $\Delta fE$ for successive

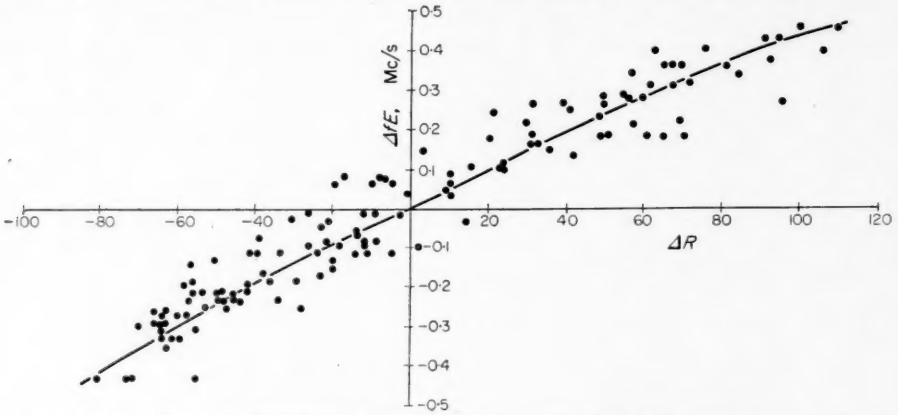


Fig. 2. Monthly mean departures of noon $fE$ at Slough and of sunspot number $R$ for the period 1940–50.

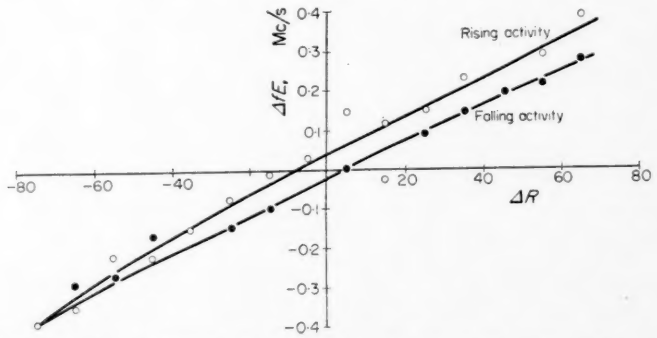


Fig. 3. Mean departures of noon $fE$ at Slough and of sunspot number $R$ over 1940–50 for years of rising and falling solar activity.

intervals of 10 in $\Delta R$, and it is seen that the points for rising and falling sunspot activity lie on separate curves. Bearing in mind that the origin in this diagram refers to the mean $R$ (73) and the mean $fE$ (3·2 Mc/s) for the period, it will be seen that the curves diverge to an increasing extent from zero sunspot number. This difference between rising and falling parts of the solar cycle was first noted by Appleton and Naismith (1940). Fig. 3 indicates that, for a given sunspot number, $fE$ may be up to 0·1 Mc/s larger on the rising than on the falling part of the solar cycle.

In order to determine the relationship between $fE$ and $R$ more precisely we have considered the daily noon values of $fE$ for Slough for the solstice months for the period 1938–52 inclusive. These daily values have been grouped according to the prevailing sunspot number $R$ = 0–20, 20–40, etc. The average values for each

group are plotted in Fig. 4. In this figure the number of values per group is usually about 50, except for the very large sunspot numbers ($R > 150$) for which the number per group falls to 10 or less. In these circumstances we have not felt it justifiable to attempt to subdivide the limited data according to rising and falling parts of the cycle. It will be seen that there is some scatter of the points, but the general shapes of the mean curves are similar to those sketched in Fig. 1. Over limited ranges of $R$ (say $40 < R < 120$) the relationship is approximately linear but there

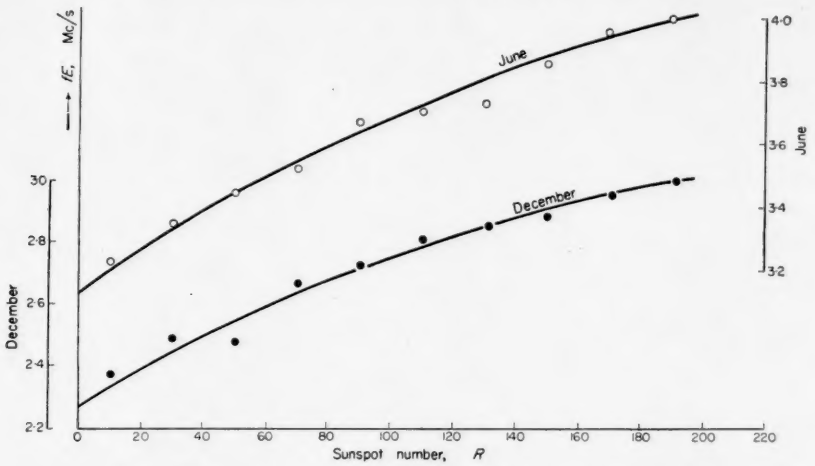


Fig. 4. Relation between $fE$ and $R$ for solstice months at Slough, using daily noon values for 1938–52.

is appreciable divergence from linearity over a large sunspot range.* These considerations are obviously important when any reduction of $fE$ values to a common sunspot number is attempted, and, in particular, extrapolation to *zero* sunspot number on the basis of a linear $fE/R$ relationship may lead to considerable error.

Some representative values of the sensitivity parameter $\Delta fE/\Delta R$ deduced from Fig. 4 are summarized in the table.

Table 1. Values $\Delta fE/\Delta R$ for Slough in Mc/s per unit $R$

| Season | Range in $R$ | |
|---|---|---|
| | 0–60 | 60–200 |
| Summer | 0·0062 | 0·0036 |
| Winter | 0·0052 | 0·0030 |

* It is worth noting that if the alternative method of grouping the data is adopted, i.e. daily values of $R$ grouped for specific values of $fE$, then each curve appears to show a sharp rise to a new level near $R = 100$. We have not yet been able to decide whether this has any significance.

It will be seen that the summer values of $\Delta fE/\Delta R$ are some 20% greater than the winter values. Equation (4) shows that the seasonal change in $\chi$ would, of itself, give rise to a 38% increase from winter to summer at Slough, for which $n = 4$. The difference between this percentage and that observed is to be attributed partly to the seasonal variations in the parameters $A$ and $B$ (i.e. in the product $\alpha H$) and partly to the minor influences indicated above.

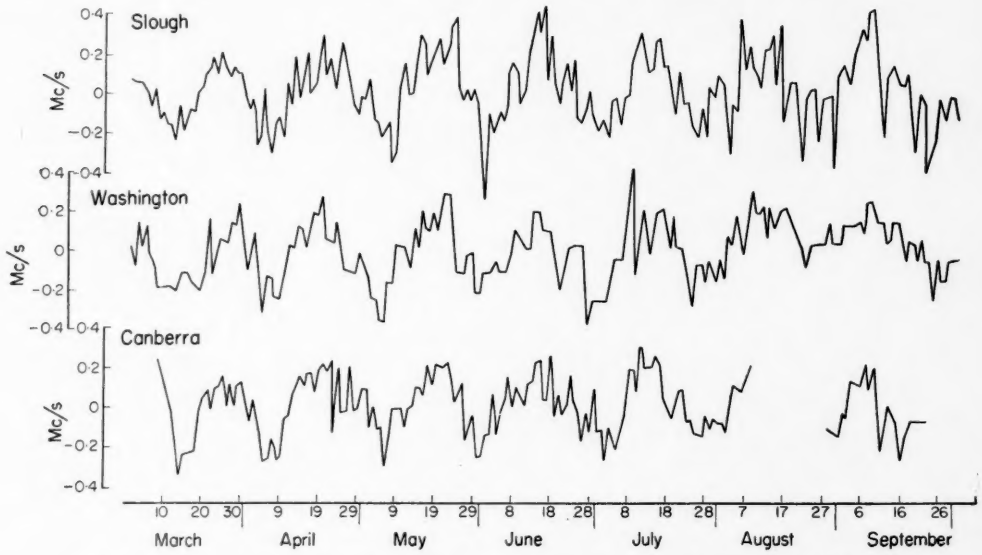


Fig. 5. Daily departures of noon values of $fE$ for the period March–September 1951, for Slough (51·5°N, 0·6°W), Washington (38·7°N, 77·1°W), and Canberra (35·3°S, 149°E).

### 3. Short-period (27 Day) Variations

At certain times there is a striking day-to-day correspondence between $fE$ and $R$. This is especially marked when sunspots are distributed asymmetrically in heliographic longitude, giving rise to recurrence tendencies corresponding to the solar rotation period of 27 days. We have discussed the incidence of this phenomenon in $fE$ data at an earlier meeting of this Commission. Over the months March–September 1951 sunspot numbers showed a very marked series of 27-day oscillations, the largest amplitude of which was associated with the appearance on May 16 of one of the largest spots recorded. From the latter half of July to the end of September the variation was more complex, involving the recurrence of two separate sunspot groups with an appreciable separation in longitude. We have examined ionospheric data over this period for stations distributed over as wide a range of latitude and longitude as possible and Fig. 5 shows for some representative stations, the departures $\Delta fE$ of the noon critical frequency of the $E$ layer from the smooth curve through the monthly mean values. Visual inspection of the graphs clearly reveals a world-wide 27-day recurrence tendency in the ionization density, which is in phase with a similar variation of sunspot number.



VOL. 15 1959

To illustrate the close correspondence between $fE$ and $R$ over short periods we have in Fig. 6 replotted daily values of $\Delta fE$ (noon) and $\Delta R$ over the two months April–May 1951.

Incidentally, it may be added that these marked 27-day "waves" were also evident at this time at all ionospheric levels, being clearly visible in $D$-region data ($-\log \rho$ and $f$-min), $fF1$ and $fF2$. The variations are also discernible for early morning data, showing that the ionization of the $E$-layer follows the solar intensity of radiation almost immediately after sunrise.

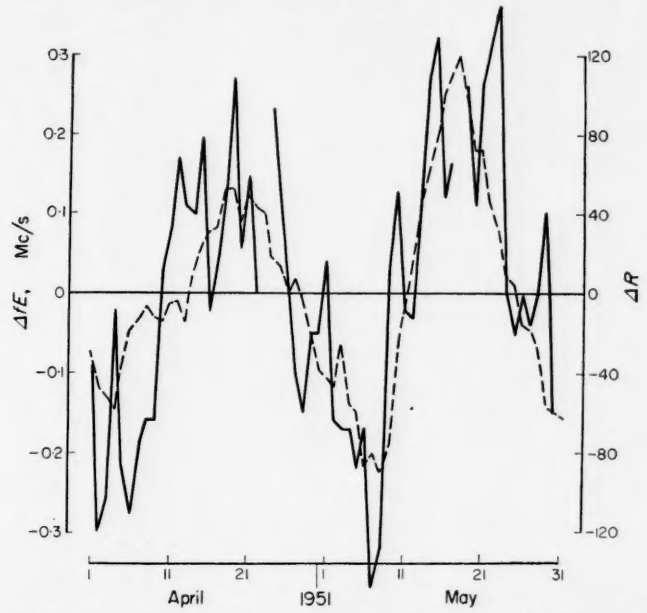


Fig. 6. Simultaneous variations of daily departures of noon values of $fE$ for Slough (———) and of sunspot number $R$ (— — —) for April–May 1951.

In this short period of a few months we have a series of regular sunspot number changes of magnitude normally only found from years of minimum to years of maximum solar activity. Considering the average amplitudes of the five cycles in $R$ and $fE$ over the period up to the middle of July we calculate that the sensitivity of $fE$ at Slough to short-period sunspot changes is about 0·0040 Mc/s per unit $R$. This value, derived for a *summer* period of relatively *low* solar activity, is to be compared with the figure of 0·0024 Mc/s per unit $R$ previously given by us (Beynon and Brown, 1950) from a Fourier analysis of data for the same station covering the *winter* period for the years 1947–50 of *high* solar activity. This difference in sensitivity between two such periods is to be expected from equation (4).

If we compare short- and long-term sensitivities for corresponding seasons and epochs of the solar cycle, we find that the $E$-layer is less sensitive to short-period (27-day) sunspot changes than to long-period (11-year) ones. This difference probably arises from the fact that over short periods the background radiation from the sun remains substantially unchanged and the observed $E$-layer changes

in electron density are to be attributed almost entirely to the temporary increase of radiation associated with centres of activity. In the case of solar cycle changes the effect of sunspots is supplemented by a general increase in the steady background component.

## References


Appleton E. V. and Naismith R. 1940 *Proc. Phys. Soc. Lond.* **152,** 402.

Beynon W. J. G. and Brown G. M 1950 *Proceedings of the 2nd Meeting, Mixed Commission on the Ionosphere*, p. 156. I.C.S.U., Brussels.


VOL.
15
1959

Journal of Atmospheric and Terrestrial Physics, 1959, Vol. 15, p. 175. Pergamon Press Ltd. Printed in Northern Ireland

# Report on spectrographic work at Tromsö and Oslo

L. VEGARD

THIS report deals with some results of spectrographic work carried out at Tromsö and Oslo in order to study the properties of the solar bundles formed by photoelectrons from sunspot regions and neutralized by protons.

(1) In the case of aurorae coming down below, say 110 km, the flux and velocity is much smaller for protons than for electrons.

(2) By the passage through the ionosphere the protons and the electrons are absorbed independently. The protons stop at an altitude ($h_p$) which is considerably greater than that of the electrons ($h_e$).

(3) In the height interval between ($h_p$) and ($h_e$) the H-lines are absent and the excitation of the auroral luminescence is due to electrons only. The spectrum is characterized by the great intensity of molecular bands and few and weak atomic lines. The red $N_2 1P$ bands, which produces the red aurorae of type ($B$) are strong, while the forbidden red OI doublet responsible for red aurorae of the ($A$) type may be absent.

(4) Above ($h_p$) the H-lines appear. The intensity increases upwards to a maximum and gradually decreases. Three spectrograms taken at Oslo in rapid succession were typical for great proton flux. They were practically identical with the exception, that two of them showed H-lines, but the third not. This means that the latter was taken at an altitude too great to show H-line emission. The excitation power of the protons however, was not reduced. All were taken from long auroral rays.

(5) A number of spectrograms of red aurorae of type ($A$) have recently been taken at Oslo and Tromsö. They are characterized by an extremely strong red O*I*-doublet and by the enhancement of other atomic lines, while the bands were unusually weak. In one case the red O*I* doublet was about thirty times as strong as the green auroral line. The typical differences between spectrograms produced by electrons and by protons are shown on many spectrograms from Oslo and Tromsö, and they will be dealt with in a paper to be published in *Fysiske Publikasjoner*, Oslo. These differences and the great variations of the relative proton flux account for many of the observed variations in the spectral composition of the auroral luminescence.

(6) The properties of the solar bundles found by experiment have thus verified their formation through photoelectric effect of solar X-rays from the sunspot regions.

(7) The electron flux being greater than that of the protons, causes an accumulation of negative electricity in the ionosphere, which will set up electric fields, corresponding electric currents, ionospheric winds, and disturb the distribution of electrons and ions responsible for the *F2*-layer, which is normally formed by secondary photoelectrons produced in the ionosphere by the solar X-rays, which we know produce the *E*-layer.

## AUTHOR INDEX

(D denotes participation in Discussions)


AIDA K. 130
AKASOFU S. 156
APPLETON E. V. 9, 19D, 20D, 23D, 24D, 25D, 37D, 57D, 62D, 63D, 64D
BAILEY D. K. 20D
BERKNER L. V. 19D, 24D, 42D, 47D, 62D
BEYNON W. J. G. 13, 20D, 66, 168
BROWN G. M. 168
CHAMBERLAIN J. W. 24D, 52D, 53D, 65D, 95, 96
CHAPMAN S. 18D, 29, 37D, 43, 47D, 52D, 63D
ELFORD W. G. 132
GALLET M. 63D, 65D
GASSMANN G. F. 99
HAUBERT A. 83, 84, 145
HIRONO M. 146
INOUE Y. 85
KASUYA I. 126
KATO S. 146
KIMURA I. 58
LEJAY P. 20D, 27
LEPECHINSKY D. 20D
MAEDA H. 146
MAEDA K. 58
MANNING L. A. 62D, 63D, 137
MARTYN D. F. 19D, 20D, 23D, 25D, 42D
MATSUSHITA S. 20D, 68
MENZEL D. H. 20D, 53D, 65D
MORGAN M. G. 24D, 54, 57D, 62D, 63D
OKAMOTO H. 130
ÔSE M. 130
PAWSEY J. L. 47D, 51
PFISTER W. 161
RATCLIFFE J. A. 19D, 20D, 21, 24D, 25D, 37D, 65D
RAWER K. 20D, 24D, 38, 141
ROBBINS A. R. 21, 102
SATO T. 116
SCOTT J. W. C. 57D
SHIMAZAKI T. 77, 108
SINGER S. F. 47D, 48, 65D
SINNO K. 151
SKINNER N. J. 121
THOMAS J. O. 21, 102
ULWICK J. C. 161
VEGARD L. 175
WATTS J. M. 65D, 73
WRIGHT R. W. 121
YONEZAWA T. 89


VOL. 15 1959

INTERNATIONAL COUNCIL OF SCIENTIFIC UNIONS

JOINT COMMISSION ON RADIO-METEOROLOGY

# PROCEEDINGS OF FOURTH MEETING

NEW YORK UNIVERSITY
14–16 AUGUST 1957

VOL.
15
959

*Editor:*

Sir HAROLD SPENCER-JONES
*ICSU Publications Office, Royal Institution, London W.1*

PERGAMON PRESS, INC.
NEW YORK LONDON PARIS LOS ANGELES

VOL
15
195

## Membership of the Mixed Commission on Radio-Meteorology

*International Scientific Radio Union (U.R.S.I.)*

H. BREMMER, Markt 35, Eindhoven, Netherlands.

C. R. BURROWS, Ford Instrument Company, Long Island City, New York, U.S.A.

W. E. GORDON, School of Electrical Engineering, Cornell University, Ithaca, New York, U.S.A.

J. LUGEON, Station Centrale Suisse de Meteorologie, Krahbuhistrasse 58, Zurich, 7/44, Switzerland.

*International Geodetic and Geophysical Union (U.G.G.I.)*

J. S. MARSHALL, Physics Department, McGill University, Montreal, Quebec, Canada.

A. PERLAT, Meteorologie Nationale, 1 Quai Branly, Paris 7$^0$, France.

P. A. SHEPPARD, Imperial College of Science and Technology, London S.W.7, England.

M. S. P. VENKITESWARAN, Meteorological Institute, Poona, India.

*International Union of Pure and Applied Physics (I.U.P.A.P.)*

E. G. BOWEN, Division of Radiophysics, Scientific and Industrial Research Organization, University Grounds, City Road, Chippendale, N.S.W., Australia.

O. E. H. RYDBECK, Chalmers University of Technology, Gothenburg, Sweden.

VOL. 15 959

The following were present at the New York meeting:

| | |
|---|---|
| Dr. C. R. BURROWS | Dr. M. G. H. LIGDA |
| Dr. W. E. GORDON | Dr. I. van der MARK |
| Dr. J. S. MARSHALL | Dr. M. G. MORGAN |
| Dr. P. MISME (representing A. PERLAT) | Mr. K. A. NORTON |
| Mr. R. BOLGIANO, Jr. | Dr. V. G. PLANK |
| Dr. D. ATLAS | Mr. A. RUVIN |
| Mr. J. H. CHISHOLM | Dr. R. A. SILVERMAN |
| Dr. D. R. FITZGERALD | Dr. L. G. SMITH |
| Dr. W. A. FLOOD | Dr. R. L. SMITH-ROSE |
| Dr. D. R. HAY | Dr. J. P. VOGE |
| Dr. W. F. HITSCHFELD | Dr. A. D. WHEELON |

In each of the five scientific sessions one or more speakers were invited to give introductory papers on the particular subdivision of the field then to be considered. These papers are presented below, together with the discussion which followed. In the latter, where the author is not specifically indicated, the remarks have been prepared by the recording secretary on the basis of his notes taken during the session.

VOL.
15
1959

# CONTENTS


Preface . . . . . 183

*Session* I. *Radio Scattering by Inhomogeneities*

A. D. WHEELON: Radio scattering by tropospheric irregularities . . . . . 185

Discussion . . . . . 204

K. A. NORTON: Recent experimental evidence favouring the $\rho K_1(\rho)$ correlation function for describing the turbulence of refractibility in the troposphere and stratosphere . 206

*Session* II. *Convection and Inhomogeneities*

V. G. PLANK: Convection and refractive index inhomogeneities . . . . . 228

Discussion . . . . . 245

*Session* III. *Lightning*

M. G. H. LIGDA: Radar observation of lighting . . . . . 248

L. G. SMITH: Electric field-change studies of lightning . . . . . 251

Discussion . . . . . 252

D. R. FITZGERALD and H. R. BYERS: Aircraft observations of convective cloud electrification . . . . . 254

Discussion . . . . . 260

*Session* IV. *Radar Studies of "Angels"*

D. ATLAS: Radar studies of meteorological "angel" echoes . . . . . 262

Discussion . . . . . 284

*Session* V. *Radar Weather*

W. F. HITSCHFELD: Convective processes in the atmosphere as revealed by weather radar 288

Discussion . . . . . 292

*Session* VI. *Administration*

Minutes . . . . . 294

Resolutions . . . . . 295


OL.
15
959

VOL.
15
1959

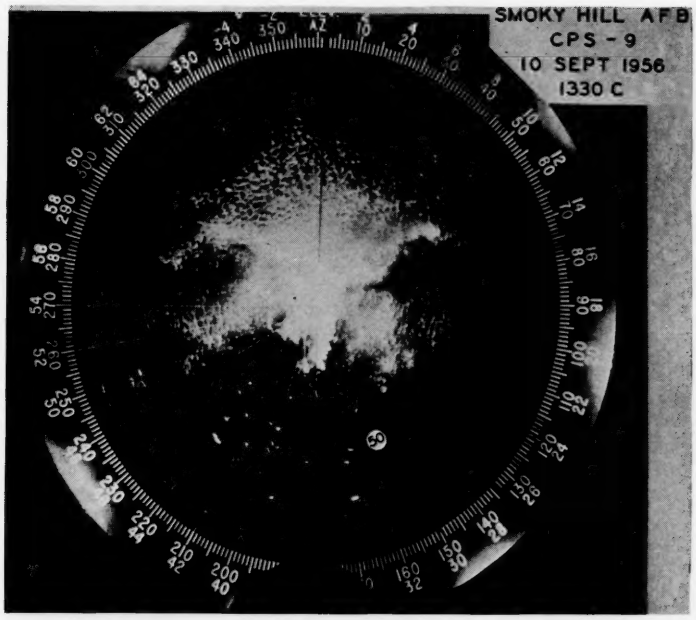


Record of a 3 cm radar PPI presentation on a clear, dry day. Range to 100 miles. The mottled pattern presumably is the result of meteorological effects. (See Atlas, Discussion, Session V, p. 285.)

VOL.
15
1959

Journal of Atmospheric and Terrestrial Physics, 1959, Vol. 15, pp. 183 to 184. Pergamon Press Ltd. Printed in Northern Ireland

# Preface

J. S. MARSHALL

THE technical programme of the 1957 meeting brought together different approaches to common or interrelated phenomena.

Regarding dielectric inhomogeneities, the bubble idea of convection was explored with regard to both cumulus cloud formation and to smaller bubble formations in which condensation was not achieved. The resulting patterns were translated into dielectric terms. Knowledge of radar angels was reviewed and related to the bubble picture. The theory of radio scattering by inhomogeneities was reviewed at the first session, and subsequently scrutinized in relation to convection and to angel observations.

The study by radar of precipitating clouds, and particularly of thunderstorms, was reported. The reportage here emphasized findings from constant-altitude radar displays, new since our last meeting. This provided a satisfactory frame of reference against which to relate lightning observations by radar, with natural emphasis on extensive near-horizontal discharge paths. Electric-field changes at the earth's surface, resulting from lightning discharge in nearby thunderstorms, were reported. The pattern of change at stations a few miles apart, resulting from a single discharge, can be quite different. This is in keeping with the great horizontal extents of discharge observed by radar. A study from aircraft of the horizontal field around cumuli as they approached and achieved precipitation was reported. The formation of graupel in the upper reaches of the cloud, and its fall-out leaving charged cloud behind, appear to be all-important to charge separation and resulting discharge.

The very considerable interrelation of the various topics reviewed and discussed should be apparent to some extent from the foregoing summary. It was powerfully apparent to the participants. Discussion at all sessions involved most of those present, and the discussion among the several specialities represented was notably constructive and mutually helpful.

The original concept of this Joint Commission, as we understand it, was that it should contain radio scientists, meteorologists and others best described by the more general term of physicist. It should be possible to determine a member's classification, presumably, by considering which of the scientific unions held that member's primary allegiance. Reviewing the list of participants at this meeting, it seems to us that, for several of those present, scientific interest fell squarely between URSI and UGGI. Everyone had an interest in Commission II and/or IV of URSI, and at the same time in the IAM within UGGI. Within the IAM, the area of interest could surely be described as physical meteorology; in any case, the appellation either of cloud physics or of atmospheric electricity would be found too narrow.

It seems to us that radiometeorology has become an area of scientific endeavour, rather than merely the name for a common meeting-ground of radio men and

meteorologists. Within this area, to be sure, are many specialities: tropospheric propagation (including its relevance as a means of revealing atmospheric structure), radar observations of precipitation, lightning and dielectric inhomogeneities, the study of lightning by its radiations. The people making these sorts of observations naturally presume to consider the physical processes leading to the phenomena they observe. We could argue from this that the area under discussion should be broadened to include all physical meteorology. Intuitively, to suggest such a broadening would be unwise. The climax of such argument would surely be a common goal of searching after truth, and this would bring under a common head a large number of scientific unions, and organizations even beyond. Our argument, rather, is toward this: that there exists a powerful community of interest among those who study radio waves, either originating in the troposphere, or reflected or scattered, refracted or otherwise modified in the atmosphere. For some of these scientists, the transmission of information is the goal. For some, the driving curiosity is with regard to the physical processes of the troposphere. For both these groups, and for others for whom neither is preponderant, there exists a stimulating excitement in considering radio waves in relation to the medium that either made or moulded them. Our 1957 meeting has demonstrated that all such men can meet and argue constructively together, profitably for all concerned.

This profitable community of interest is covered neither by URSI in itself nor UGGI in itself, although rather well by the two between them. We submit, therefore, that a continuing Joint Commission on Radiometeorology should be retained, with membership from these two Unions, and charged with the responsibility to maintain constructive intercommunications among radiometeorologists, whether their basic interest lies with radio, or meteorology, or purely and simply with the composite appellation.

VOL
15
195

Journal of Atmospheric and Terrestrial Physics, 1959, Vol. 15, pp. 185 to 205. Printed in Northern Ireland

# SESSION I

## Radio Scattering by Inhomogeneities

## Radio scattering by tropospheric irregularities

A. D. Wheelon*

The existence of time-varying irregularities in the tropospheric index of refraction has been firmly established by numerous measurements with microwave refractometers. The physical reality of these apparently random fluctuations poses an important problem for turbulence theory in itself. The effects of such irregularities in scattering radio waves both within and beyond the horizon has raised a much broader and more vital class of questions. The combination of turbulence theory and electromagnetic propagation theory has been used to explain the propagation of microwaves beyond the horizon. The important role of refractive fluctuations is suggested by the fading and band-width limitations of scatter signals. Scintillation of the amplitude and phase of electromagnetic waves propagated through a region of refractive irregularities is discussed with the same techniques.

VOL. 15 959

### 1. Refractive Index Irregularities

#### 1.1. *Characterization of a turbulent medium*

The tropospheric index of refraction varies from point to point in a random manner. To describe this effect, one decomposes the dielectric constant ($\varepsilon = n^2$) into its mean value and a small stochastic component.

$$\varepsilon(\mathbf{r}, t) = \varepsilon_0 + \Delta\varepsilon(\mathbf{r}, t) \tag{1.1}$$

$\varepsilon_0$ is considered to be a function of altitude ($h$) only and its gradient appears in several physical theories of turbulent irregularities. The function $\Delta\varepsilon(\mathbf{r}, t)$ is usually treated as a stationary random process, which is spatially homogeneous and isotropic.

$$\langle \Delta\varepsilon(\mathbf{r}, t)\rangle = 0$$

$$\langle \Delta\varepsilon(\mathbf{r}, t)\Delta\varepsilon(\mathbf{r} + \mathbf{R}, t)\rangle = \langle \Delta\varepsilon^2\rangle C(|\mathbf{R}|) \tag{1.2}$$

Little attention has been paid to higher moments, except to note that they are completely specified in terms of $C(R)$ if the $\Delta\varepsilon$ form a Gaussian random process (Lawson and Uhlenbeck, 1950). The intensity of dielectric fluctuations $\langle \Delta\varepsilon^2\rangle$ is measured experimentally as several parts in $10^{-12}$. The correlation function falls to 0·5 in a distance of several hundred feet, which is called the scale length $l_0$ of the irregularities.

The space correlation function $C(R)$ is the fundamental characterization of the

* The Ramo-Wooldridge Corporation, Los Angeles 45, California.

turbulence. The exponential model $C(R) = \exp -R/l_0$ has been used extensively in the past to analyse scatter propagation. The Gaussian model $C(R) = \exp -R^2/l_0^2$ is frequently used for line-of-sight problems because it can be integrated readily, although it apparently has no foundation in physical theories of turbulence and is inconsistent with scatter-propagation data. The relatively new Bessel model

$$C(R) = \frac{R}{l_0} K_1\left(\frac{R}{l_0}\right)$$

seems to give rather good agreement with both scatter and line-of-sight data, and is equivalent to the turbulent theory of gradient mixing. It should be emphasized that the correlation function represents only a model of the irregularities, and must be discarded if it does not agree with experiment.

It is possible to generalize the above description to include anisotropic and inhomogenous fields. Anisotropic irregularities can be discussed by introducing different scale lengths in orthogonal directions (STARAS, 1955; BOOKER, 1956), for example

$$C(R) = \exp -\left[\frac{x^2}{l_x^2} + \frac{y^2}{l_y^2} + \frac{z^2}{l_z^2}\right]^{1/2} \tag{1.3}$$

and such effects are apparently quite important in the troposphere. Refractometer experiments show that the intensity of dielectric fluctuations decreases with altitude. One can describe an inhomogenous field of this sort with a height dependent $\langle \Delta\varepsilon^2 \rangle$, as long as the intensity does not change significantly in several scale lengths ($l_0$).

A more difficult problem is encountered with the assumption of stationarity. There now seems to be compelling experimental evidence that the dielectric variations either: (a) do *not* form a stationary process, or (b) that there is a great deal of power in the low-frequency part of the spectrum of $\Delta\varepsilon$, which appears as trend when viewed over a short span of time or space. Both explanations are probably correct in part, with a rapidly-fading stationary process superimposed on long-period (diurnal, seasonal) harmonic components. Unfortunately, there is no adequate theory of non-stationary processes now available.

### 1.2. *The spectrum method*

An equivalent characterization of a turbulent medium is the spectrum of irregularities $S(k)$ (WHEELON, 1957; MINTZER, 1953), which is the Fourier decomposition of the space correlation function.

$$\langle \Delta\varepsilon^2 \rangle C(R) = \frac{1}{8\pi^3} \int d^3k \exp(-i\mathbf{k} \cdot \mathbf{R}) S(\mathbf{k}) \tag{1.4}$$

This approach has the advantage of exhibiting an explicit $R$-dependence for the correlation without committing the study to a particular model at the outset. If the medium is isotropic $S(k)$ depends only on $|\mathbf{k}|$, so that the space correlation becomes:

$$\langle \Delta\varepsilon^2 \rangle C(R) = \frac{1}{2\pi^2} \int_0^\infty dk k S(k) \frac{\sin kR}{R} \tag{1.5}$$

The mean square fluctuation at a point,

$$\langle \Delta\varepsilon^2 \rangle = \frac{1}{2\pi^2} \int_0^\infty dk k^2 S(k) \tag{1.6}$$

indicates that the spectrum represents the ability of each blob-size group (i.e. wave-number range) to produce irregularities.

Equation (1.4) may be inverted to compute the spectrum corresponding to a given correlation function. Table 1 indicates the spectra for the Gaussian, exponential, and Bessel models. The small $R$ behaviour of the correlation is determined by the large $k$ range of the spectrum, and vice versa.

Table 1.

| $C(R)$ | $\exp(-R^2/l_0^2)$ | $\exp(-R/l_0)$ | $\frac{R}{l_0} K_1\left(\frac{R}{l_0}\right)$ |
|---|---|---|---|
| $S(k)$ | $\pi^{3/2}\langle\Delta\varepsilon^2\rangle l_0^3 \exp\left(\frac{-k^2 l_0^2}{4}\right)$ | $8\pi \frac{\langle\Delta\varepsilon^2\rangle l_0^3}{[1 + k^2 l_0^2]^2}$ | $6\pi^2 \frac{\langle\Delta\varepsilon^2\rangle l_0^3}{[1 + k^2 l_0^2]^{5/2}}$ |

The spectrum method is particularly well suited to describing the temporal behaviour of dielectric fluctuations. Time variations of $\Delta\varepsilon$ are associated with two types of motion:

1.2.1. *Drifting convection.* The entire (frozen) structure is borne along on prevailing winds, and is equivalent to an additional space-correlation distance $\mathbf{U}\tau$.

1.2.2. *Random motion.* If one rides along with the net flow, there is still motion associated with continuous eddy break-up. The appropriate generalization of equation (1.4) displaced in both space and time becomes (Wheelon, 1957; Silverman, 1957)

$$\langle \Delta\varepsilon(\mathbf{r}, t)\Delta\varepsilon(\mathbf{r} + \mathbf{R}, t + \tau)\rangle = \frac{1}{8\pi^3} \int d^3k S(k) \exp(i\mathbf{k} \cdot (\mathbf{R} + \mathbf{U}\tau) C(k, \tau) \tag{1.7}$$

where $C(k, \tau)$ describes the time-autocorrelation of fluctuations within a fixed wave-number interval $k$. Dimensional arguments show that $C(k, \tau)$ should depend only on $v_0 k_0^{\frac{1}{3}} k^{\frac{2}{3}} \tau$ in the inertial subrange ($\tau$), although no functional dependence has yet been established.

### 1.3. *Physical theories of turbulent irregularities*

The spectrum method makes direct contact with physical theories of turbulent irregularities. Such theories identify three distinct ranges of the spectrum shown in Fig. 1.

(a) $0 < k < k_0$: The input or blob-creating range corresponds to very large scale lengths $l_0 = k_0^{-1}$, which are probably anistropic. Since we do *not* know (in detail) how turbulence is created from a laminar flow, turbulence theories carefully avoid this range. It is important to note that the spectra listed in Table 1 do make definite statements about this range, so the large $R$ behaviour of the corresponding correlation models must be regarded as pure guesswork or extrapolation.

(b) $k_0 < k < k_s$: The inertial subrange is characterized by redistribution of the turbulent "energy" toward higher wave-numbers and represents the progressive subdivision of eddies in the turbulent structure. Dimensional analysis can be used here with considerable confidence. Tropospheric scatter propagation depends principally on this inertial range.

(c) $k_s < k < \infty$: The dissipation range is characterized by a sharp drop in turbulent activity, due to the destructive action of viscosity and diffusion.

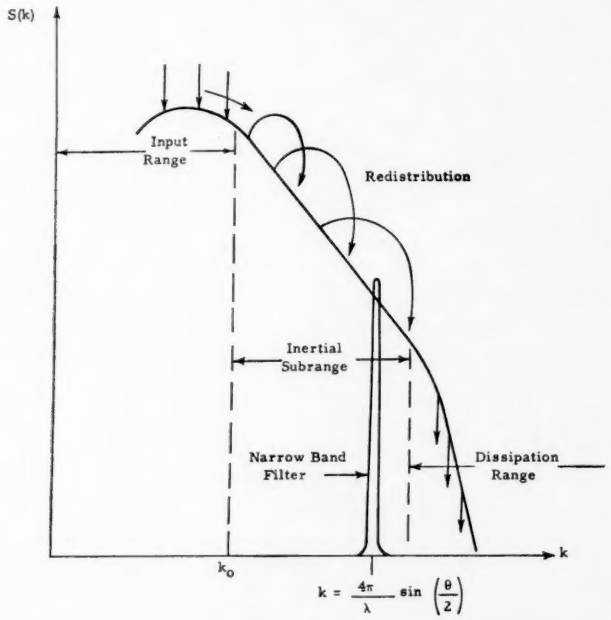


Fig. 1. Typical spectrum of dielectric irregularities showing ranges and narrow-band filter which characterizes trophospheric scattering.

The present survey does not consider the dissipation range, since aperture and recorder smoothing effectively eliminate the contributions of such tiny blobs. In the troposphere $l_s = k_s^{-1}$ is of the order of millimetres and $l_0 = k_0^{-1}$ is 100 m or more (VILLARS and WEISSKOPF, 1954).

Dielectric variations in the lower troposphere are governed principally by water vapour content. One is dealing therefore with the irregularities established in a passive scalar by turbulent movements of the atmosphere's (vector) velocity field. There are three theories which predict $S(k)$:

1.3.1. *Pressure fluctuations.* Fluctuations of the velocity field induce pressure variations according to Bernoulli's law. The variations of pressure, density and water-vapour content are related linearly; the spectrum of dielectric fluctuations is given by (VILLARS and WEISSKOPF, 1954):

$$S(k) = \left(\frac{v_0}{c}\right)^4 \frac{k_0^{\frac{4}{3}}}{k^{\frac{11}{3}}}, \qquad (k > k_0) \tag{1.8}$$

where $v_0$ is the speed of the largest blobs and $c$ the speed of sound. Most authors now agree that this mechanism is unimportant for the troposphere.

1.3.2. *Obukhov's mixing theory.* In this theory, an external source is imagined to feed fluctuations into the spectrum at the largest blob size ($k_0$). Subsequent redistribution down the inertial range is attributed to turbulent convection, for which dimensional arguments give (Obukhov, 1949; Silverman, 1956b; Bolgiano, 1957):

$$S(k) = \langle \Delta\varepsilon^2 \rangle \frac{k_0^{\frac{2}{3}}}{k^{\frac{11}{3}}}, \qquad (k > k_0) \tag{1.9}$$

If the external source is identified only with the mixing of a gradient by the largest blobs,

$$\langle \Delta\varepsilon^2 \rangle \simeq k_0^{-2} \left( \frac{d\varepsilon_0}{dh} \right)^2 \tag{1.9'}$$

1.3.3. *Mixing-in-gradient theory.* In this approach one considers an initial refractive-index gradient and how it is changed by turbulent convection. As the turbulent eddies rotate, they transfer parcels of water vapour from low to high points on the profile, and vice versa. The mechanism for turbulent fluctuations appears explicitly in this theory, and no external source is required. The inertial range is again amenable to dimensional arguments (Villars and Weisskopf, 1955; Wheelon, 1957a)

$$S(k) = \left( \frac{d\varepsilon_0}{dh} \right)^2 \frac{1}{k^5}, \qquad (k > k_0) \tag{1.10}$$

Both of these theories predict that the intensity of turbulent fluctuations is proportional to the gradient of the inhomogeneous mean profile. A good correlation between the strength of scatter signals and the monthly mean refractive gradient has been observed experimentally on many paths (Bean and Meaney, 1955). Since strong scattered signals are associated with large dielectric fluctuations, this must be considered an important success for both mixing theories.

Frequent absence of dielectric irregularities at inversion layers and other stable meteorological interfaces suggests that the mixing-in-gradient models are not applicable to very sharp gradients. It would be valuable to perform controlled experiments to study the correlation between turbulent irregularities and gradients of the mean field.

## 2. Electromagnetic Scattering by Irregularities

The stochastic dielectric constant (1.1) enters into electromagnetic theory through the relation between the electric and displacement vectors,

$$\mathbf{D} = [\varepsilon_0 + \Delta\varepsilon]\, \mathbf{E} \tag{2.1}$$

When the magnetic field is eliminated from Maxwell's equations, the electric vector is found to satisfy (Wheelon, 1955):

$$\nabla^2 \mathbf{E} - \frac{1}{c^2} \frac{\partial^2}{\partial t^2} (\varepsilon \mathbf{E}) = -\nabla \left[ \frac{1}{\varepsilon} \mathbf{E} \,.\, \nabla \varepsilon \right] \tag{2.2}$$

Time derivatives operate principally on $\mathbf{E}$, since the field oscillates much more rapidly than the medium. The vector components of $\mathbf{E}$ are mixed in the right-hand term of (2.2) and give rise to depolarization effects. BALSER (1957) has shown that this term makes no contribution to scattered fields, so that with a harmonic time dependence ($k = \omega/c = 2\pi/\lambda$),

$$[\nabla^2 + k^2(\varepsilon_0 + \Delta\varepsilon)]\,\mathbf{E} = 0 \tag{2.3}$$

Since $\Delta\varepsilon(\mathbf{r}, t)$ is an unknown stochastic function of position, it is impossible to solve (2.3) exactly. The Born approximation is widely used to describe single-scattering by the fluctuations. This is essentially a three-dimensional iteration of the wave equation (2.3), which gives the total field in terms of the unperturbed wave $\mathbf{E}_0(r)$ as

$$\mathbf{E}(R) = \mathbf{E}_0(R) - \frac{k^2}{4\pi}\int_V d^3r\,\frac{\exp\,(-ik\,|\mathbf{R} - \mathbf{r}|\,)}{|R - r|}\,\Delta\varepsilon(r, t)\mathbf{E}_0(r) \tag{2.4}$$

where $V$ is the volume of irregularities illuminated by both the transmitter and receiver. The first term in (2.4) represents the transmitted wave and the integral expression is the scattered wave. To proceed further, one must distinguish between line-of-sight and beyond-the-horizon propagation.

2.1. *Line-of-sight propagation*

Two common line-of-sight propagation paths are shown in Fig. 2. In the relay link problem, both the transmitter and receiver are immersed in a turbulent medium at a distance $L$ from one another. The scattering volume $V$ is thus the entire space containing dielectric irregularities. The total field given by (2.4) induces voltage components in the receiver, as shown in Fig. 2(c). The primary field $E_0$ establishes the phase reference $V_0$ and the scattered term gives rise to both in- and out-of-phase components, corresponding to the real and imaginary parts of the integral term in (2.4), respectively. The total voltage $V_T$ and its phase $\alpha$ are measured by the receiver. It is inherent in the Born approximation that $E_s$ must be small compared with the mean signal $E_0$, so that instantaneous fluctuations of the total amplitude and phase are given by:

$$\frac{\delta V_T}{V_T} \simeq \frac{k^2}{4\pi}\,\mathrm{Re}\int d^3r\,\frac{\exp\,(ik\,|R - r|\,)}{|R - r|}\,\Delta\varepsilon(r)E_0(r) \tag{2.5}$$

$$\alpha \simeq \frac{k^2}{4\pi}\,Im\int d^3r\,\frac{\exp\,(ik|R - r|)}{|R - r|}\,\Delta\varepsilon(r)E_0(r) \tag{2.6}$$

The variances of phase and amplitude fluctuations thus depend upon sixfold integrals of the space correlation function (1.2).

It is common practice to use the geometrical-optics approximation to describe line-of-sight propagation. This is equivalent to a one-dimensional (WKB) solution of the wave equation (2.3) and recognizes only the random speeding-up and slowing-down of the wave as it propagates along the ray path ($z$). The phase of the vector voltage diagram in Fig. 2(c) is given directly by this method.

$$\alpha = \frac{\pi}{\lambda}\int_0^L dz\;\Delta\varepsilon(z, t) \tag{2.7}$$



VOL. 15 1959

This expression is always a good approximation to the volume integral (2.6) and it is generally used to study phase variations because of its simplicity.

Geometrical optics also predict amplitude variations of the received signal. These are due physically to bunching and diverging of the (energy-bearing) rays by random refractive bending.

$$\frac{\delta V}{V} = \frac{\lambda}{2\pi}\int_0^L dz\left[\frac{\partial^2\alpha}{\partial x^2} + \frac{\partial^2\alpha}{\partial y^2}\right] \tag{2.8}$$

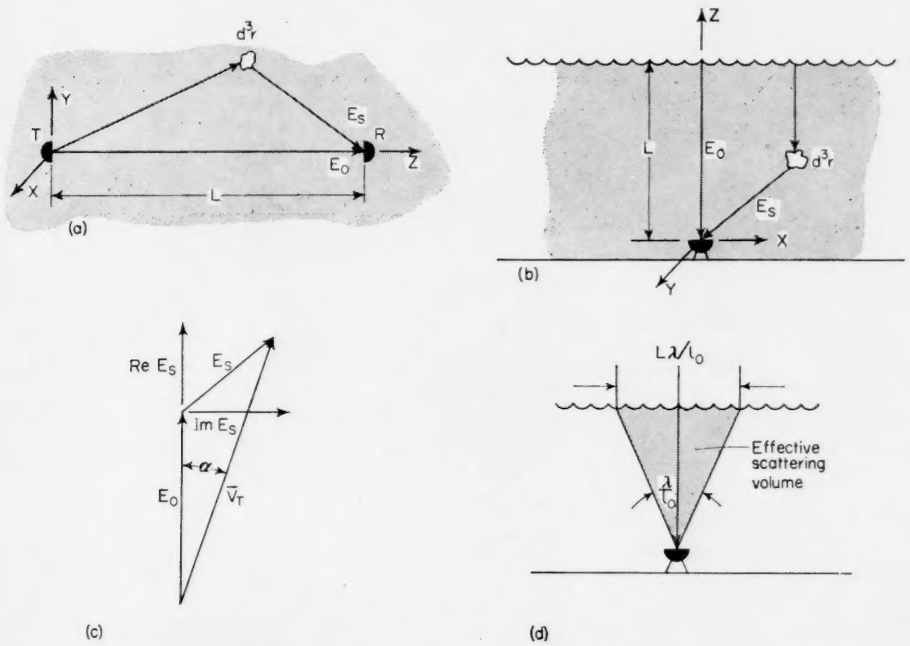


Fig. 2. Geometry for line-of-sight propagation problems and corresponding vector–voltage diagram.
(a): Relay link problem; (b): Radio star problem; (c): Vector–voltage diagram; (d): Effective scattering volume geometry.

This expression is not usually a good approximation to the more precise wave-theory result (2.5).

The geometrical optics approximation is a special case of the single-scattering wave theory of equation (2.4). To understand the correspondence let us note that the scale length of the irregularities $l_0$ is generally much larger than the wave-length of the radiation. The blobs act like very shallow lenses and project almost all of the scattered radiation in a cone of angular opening $\lambda/l_0$ about the line-of-sight. The *effective* scattering volume over a path length $L$ therefore has a maximum width $L\lambda/l_0$ (see Fig. 2(d)). If this width is much less than the average blob size, the scattering volume consists of cylindrical plugs "cored" from successive blobs. The propagation is then substantially one-dimensional and random variations of the phase speed of the wave is the measured effect. This corresponds to Fresnel scattering and is correctly treated by geometrical or ray optics.

The opposite extreme occurs when $L\lambda/l_0 \gg l_0$, so that the receiver sees many whole blobs. The problem is now necessarily three-dimensional and requires the wave solution (2.4). This corresponds to Fraunhofer scattering. The scattering parameter

$$\eta = \frac{L\lambda}{l_0^2} \tag{2.9}$$

is evidently the important variable in these discriminations. If $\eta$ is less than unity, the wave theory expressions (2.5) and (2.6) reduce to the geometrical optical results (2.7) and (2.8). If $\eta$ is greater than or near unity, one must use the full wave theory to compute amplitude scintillations. The ray and wave theory mean-square phase results differ by only a factor of two, so that the distinction between (2.6) and (2.7) is not usually made.

The single-scattering approximation (2.4) breaks down at very large distances and/or high frequencies, since the convergence of the Born series is related to the smallness of the mean-square phase expression,

$$\langle \alpha^2 \rangle = \pi^2 \langle \Delta\varepsilon^2 \rangle \frac{Ll_0}{\lambda^2} \tag{2.10}$$

As the wave progresses deeper into the turbulence, scattering out of the main beam gradually dissipates the primary signal ($V_0$) in Fig. 2(c), so that one is left only with the (correspondingly-increased) random field $E_s$. The method of RYTOV (1937) has been used to describe this "phase-creep" zone, when the amplitude and phase fluctuations are not small.

$$E(R) = E_0(R) \exp - \left[ \frac{k^2}{4\pi E_0(R)} \int d^3r \, \frac{\exp\,(ik|R-r|)}{|R-r|} \, \Delta\varepsilon(r, t) E_0(r) \right] \tag{2.11}$$

This reduces to (2.4) in the limit of small signal variations, but it is *not* clear how this method accounts for multiple scatterings. A number of interesting calculations of phase and amplitude correlations have been made with this technique (OBUKHOV, 1953; CHERNOV, 1954, 1955).

### 2.2. *Scatter propagation*

Typical scatter propagation geometries for narrow- and broad-beam aerials are shown in Figs. 3(a) and 3(b). The radiated (unperturbed) wave $E_0(R)$ in (2.4) must be omitted for propagation beyond the horizon because of earth screening. This means that the reference voltage $V_0$ is absent from the vector-voltage diagram of Fig. 2(c) and the signal is composed only of the complex vector induced by the scattered field $E_s$.

Since the receiver is always many wave-lengths from the scattering blobs, the far-field approximation is used. The ratio of received to transmitted field strengths becomes (VILLARS and WEISSKOPF, 1954)

$$\frac{E_s(R)}{E_0} \simeq \frac{\exp\,(-ikR)}{4\pi R} k^2 \int_V d^3r \exp\,(i\bar{K} \cdot \bar{r}) \, \Delta\varepsilon(r, t) \tag{2.12}$$

where $\bar{K} = \bar{k}_1 - \bar{k}_2$ is the scattering difference vector. The magnitude,

$$|\bar{K}| = \frac{4\pi}{\lambda} \sin \frac{\theta}{2} \tag{2.13}$$

depends jointly on the wavelength of the radiation and the angle $\theta$ through which the scattering proceeds (see Fig. 3).

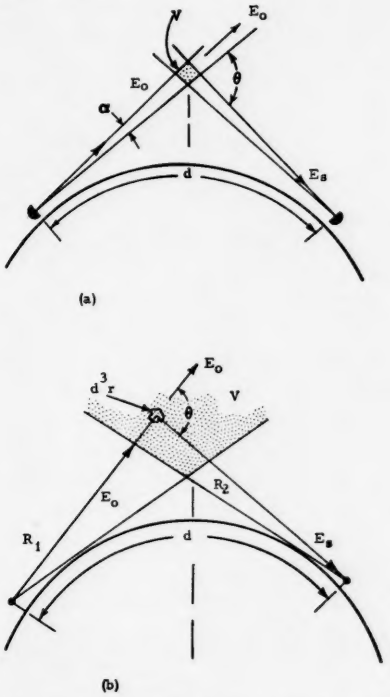


Fig. 3. Geometry for scatter propagation beyond the horizon showing the effective scattering volume $V$ in each case.
(a): Narrow beams; (b): Broad beams.

The scattering cross-section $\sigma(\theta, \lambda)$ per unit volume, per unit solid angle and per unit incident power characterizes the scattering process for each blob.

$$\sigma = \frac{R^2}{V} \left\langle \left| \frac{E_s(R)}{E_0} \right|^2 \right\rangle \tag{2.14}$$

When (2.12) and (2.14) are combined, the cross-section may be expressed either in terms of the space correlation function $C(R)$ or the spectrum $S(k)$.

$$\sigma(\theta, \lambda) = \frac{\pi^2}{\lambda^4} \int_V d^3r \exp (i\bar{K} \cdot \bar{R}) \langle \Delta\varepsilon^2 \rangle C(R) \tag{2.15}$$

or

$$\sigma(\theta, \lambda) = \frac{\pi^2}{\lambda^4} S \left[ \frac{4\pi}{\lambda} \sin \frac{\theta}{2} \right] \tag{2.16}$$

The scattering process acts like a narrow-band filter on the spectrum shown in Fig. 1, emphasizing the wave-number $k = 4\pi/\lambda \sin \theta/2$. Experimental combinations of $\lambda$ and $\theta$ focus attention on the inertial range of $S(k)$.

The angular dependence of $\sigma$ is often interpreted as the scattering polar diagram of an average blob, and reference to Table 1 shows that almost all of the scattered radiation is projected into a cone of angular opening $\lambda/l_0$ about the forward direction.

It has been suggested by Feshbach that multiple-scattering is more efficient than one large-angle scattering. Such effects are certainly more important at higher frequencies, since the convergence of the Born series is related to the smallness of the equivalent line-of-sight mean-square phase shift (2.10) computed along the (kinked) ray path. There is some evidence from round-trip pulse flight-time experiments on scatter circuits which indicate that the energy may well travel along the shorter multiple-scattering path. Further research should be directed to this interesting point.

## 3. LINE-OF-SIGHT PHASE AND AMPLITUDE INSTABILITY

The foregoing discussion has established general expressions for the phase and amplitude scintillations of waves which are propagated through random media. To compare theory and experiment, it is necessary to combine these propagation expressions with the descriptions of the turbulent medium given in Section 1. The results depend both on the propagation geometry and the model chosen to represent the irregularities.

The two most common line-of-sight problems are illustrated by Fig. 2.

(a) Relay link problem: Receiver and transmitter are both immersed in an infinite turbulent region. The transmitter emits spherical waves and the receiver is also assumed to be omni-directional. Reflections from a ground plane are ignored, since they do not contribute scintillations unless moving foliage or water surfaces are present.

(b) Radio star problem: Plane waves are assumed to fall on a semi-infinite turbulent medium, and the receiver is placed a distance $L$ below the interface. The turbulence may be graduated toward its upper boundary by using an inhomogeneous $\langle \Delta\varepsilon^2(r) \rangle$.

The patterns of the transmitter and receiver can be included if more exact comparison is possible. It is significant that the receiver always stands in the (tropospheric) turbulent medium, so that blobs which are just on top of the receiver play an important role. This is to be contrasted with scatter propagation (WHEELON, 1955) for which one can exploit the far-field approximation (2.12).

### 3.1. *Mean-square phase variation*

The calculation of phase variations is usually based on the geometrical optics expression (2.7). Using any of the correlation models in Table 1, the theoretical phase variance becomes (MUCHMORE and WHEELON, 1955)

$$\langle \alpha^2 \rangle = p\pi^2 \langle \Delta\varepsilon^2 \rangle \frac{Ll_0}{\lambda^2} \tag{3.1}$$

where $p$ is a constant of order unity. The wavelength dependence of this result

has been confirmed by simultaneous measurements (HERBSTREIT and THOMPSON, 1955; DEAM and FLANNIN, 1955) of phase shifts on three frequencies: 100, 1000 and 10,000 Mc/s, on line-of-sight paths to mountain tops (see Fig. 4a). The distance $L$ dependence is difficult to check experimentally, since paths of different lengths are apt to go through regions of the troposphere which do not have the same level of turbulent activity. Attempts to correlate phase variations with aircraft refractometer measurements of $\langle \Delta\varepsilon^2 \rangle$ and $l_0$ in the propagation paths have been moderately successful.

To attempt a detailed comparison between theory and experiment, it is necessary to recognize the influence of aperture smoothing and finite data-sample effects on the measured values. These difficult effects can be computed for an arbitrary model of the irregularities, if the spectrum method (see 1.2) is used (WHEELON, 1957b). The mean-square phase is given in terms of the spectrum by:

$$\langle \alpha^2 \rangle = \frac{\pi L}{2\lambda^2} \int_0^\infty dk k S(k) \left[ \frac{2J_1(ka)}{ka} \right]^2 \Lambda(kuT) \tag{3.2}$$

where $a$ is the receiver reflector-dish radius. A uniform convective motion $U$ is assumed to cause time variations of the phase, which are sampled with a data length $T$. The (analytic) function $\Lambda(kuT)$ indicates that the mean-square phase increases with the data-sample length (WHEELON, 1957b) since a finite data-sample effectively removes low frequency components from the record. This effect is observed experimentally although non-stationary effects could give the same result. The aperture smoothing factor effectively eliminates the contributions of very small blobs ($1/k < a$). These factors filter the spectrum $S(k)$ shown in Fig. 1 by providing high and low wave-number cut-offs. A similar small $k$ filter is supplied by finite path length ($L$) corrections (WHEELON, 1957b).

It is significant that the wavelength ($\lambda$) and path length ($L$) variation of the mean in equation (3.2) are established without reference to particular turbulent models (i.e. $S(k)$).

### 3.2. *Space correlation of phase variations*

The correlation between phase variations measured on adjacent propagation paths has been calculated for a variety of turbulence models (MUCHMORE and WHEELON, 1955). It is found that the Bessel model gives good agreement with spaced-receiver experiments (see Figs. 4a and 4b for small baseline distances. At very large separations, however, the experimental correlation falls more slowly than the theory predicts. This is tentatively ascribed to lack of spatial homogeneity or temporal stationarity. Since the correlation at great distances is due to the joint influence of very large blobs on the two propagation paths, the phase correlation should depend on the large $R$ behaviour of $C(R)$, which is *not* tied to physical theories (see Section 1.3).

The space correlation between phase variations measured on rotated propagation paths (see Fig. 4b) can be expressed in terms of the spectrum method (WHEELON, 1957b) by introducing an additional filter factor into (3.2),

$$\langle \alpha_1 \alpha_2 \rangle = \frac{\pi L}{2\lambda^2} \int_0^\infty dk k S(k) \left[ \frac{1}{kD} \int_0^{kD} dx J_0(x) \right] \tag{3.3}$$

For the parallel paths shown in Fig. 4(c),

$$\langle \alpha_1 \alpha_2 \rangle = \frac{\pi L}{2\lambda^2} \int_0^\infty dk k S(k) J_0[kD] \tag{3.4}$$

3.3. *Time correlation of phase variations*

The random variation of phase with time is due to the joint action of drifting convection and turbulent self-motions. The space–time correlation of dielectric

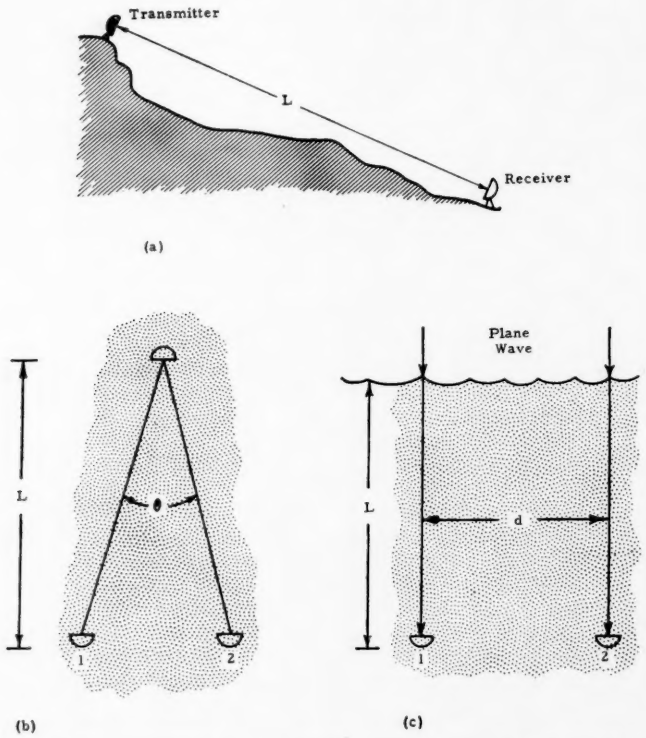


Fig. 4. Line-of-sight propagation experimental path geometry for space correlation calculations.
(a): Profile plan of propagation experiments; (b): Top view of propagation experiments—rotated paths; (c): Top view of propagation experiments—parallel paths

fluctuations (1.7) permits one to calculate the time correlation of phase records for an arbitrary spectrum. If the convective wind blows normal to the propagation path (WHEELON, 1957b):

$$\langle \alpha(t) \alpha(t+\tau) \rangle = \frac{\pi L}{2\lambda^2} \int_0^\infty dk k S(k) J_0[ku\tau]\, C[k, \tau] \tag{3.5}$$

The effect of self-motion is usually discarded since the turbulent speed ($V_0$) is much less than the drift speed ($u$).

The experimental data have generally been expressed in terms of the frequency

spectrum of the phase records.* For drift motion alone (WHEELON, 1957b)

$$W(f) = \frac{\pi L}{2\lambda^2} \int_{2\pi f/u}^{\infty} \frac{dkkS(k)}{[k^2u^2 - (2\pi f)^2]^{\frac{1}{2}}} \tag{3.6}$$

The mixing-in-gradient model (1.10) predicts that the frequency spectrum $W(f)$ should vary as $f^{-4}$ (BEAN, 1956). This behaviour is observed experimentally over several decades of frequency. The variability of such records, however, does not preclude the Obukov model (1.9). The average number of mean (zero) crossings and maxima can be expressed in terms of ratios of moments of the spectrum $S(k)$, and should be compared with accumulating experimental evidence.

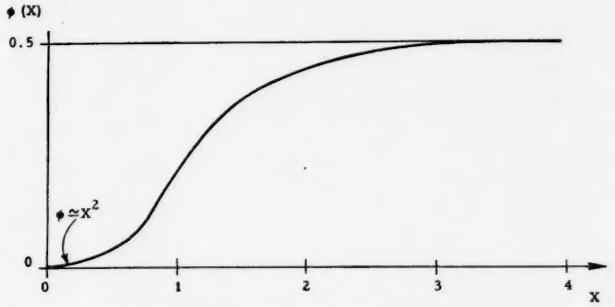


Fig. 5. Scattering function for amplitude fluctuations.

### 3.4. *Amplitude variation*

It was pointed out in Section 2 that the three-dimensional wave theory must be used to describe amplitude variations. Since the variance $\langle |\delta V_T/V_0|^2 \rangle$ involves six-dimensional integrals of the space correlation function (FANNIN, 1956; WHEELON, 1955), the problem has been solved only with the Gaussian model which has important analytical simplifying properties.

The spectrum method may be used to compute the mean-square phase and amplitude fluctuations for an arbitrary correlation model (BOOKER, 1956)

$$\langle \alpha^2 \rangle = \frac{\pi L}{4\lambda^2} \int_0^{\infty} dkkS(k)\,[1 - \Phi(k^2L\lambda)] \tag{3.7}$$

$$\left\langle \left| \frac{\sigma V_T}{V_0} \right|^2 \right\rangle = \frac{\pi L}{4\lambda^2} \int_0^{\infty} dkkS(k)\Phi(k^2L\lambda) \tag{3.8}$$

The function $\Phi$ is plotted in Fig. 5 and depends upon the scattering parameter $\eta_k = k^2L\lambda$ for each blob-size group in the distribution described by $S(k)$. Those blobs in $S(k)$ which stand in the Fraunhofer zone ($\eta_k \gg 1$) produce equal phase and amplitude variations, each one half as great as the ray-theory result (3.2). The Fresnel regime gives the phase result (3.2) directly; while using the small argument behaviour $\Phi(x) \simeq x^2$ the geometrical optics result is realized.

* $W(f) = \int_0^{\infty} d\tau \cos(2\pi f\tau)\,\langle \alpha(t)\alpha(t+\tau) \rangle$

Detailed expressions for the scattering function $\Phi(x)$ can be computed for the radio-star tracking and relay-link problems, as well as the additional spectra factors which describe space and time correlations. Gain variations and phase smoothing produced by coupling between the disturbed phase front and a finite receiving aerial can also be studied in this framework.

Unfortunately, very few experimental data are available for amplitude instability, so that a detailed comparison between the above theory and experiment is not possible at this time.

## 4. Tropospheric Scatter Propagation

Radio communication beyond the optical horizon at microwave frequencies has been observed for many years. The random fading and band-width limitations of the received signals suggest that scattering by turbulent irregularities plays a dominant role in the propagation. Numerous studies of this scattering have been based upon the scattering cross-section expression (2.15) and a phenomenological space-correlation model.

An important recent development has been the use of physical theories for the turbulent spectrum (rather than correlation models) to predict the scattering cross-section with (2.16). This is significant because the turbulence theories do not contain (as many) adjustable parameters. In particular, the mixing-in-gradient theory (1.10) contains *no* turbulence parameters but does depend upon the mean gradient of $\varepsilon_0$ in a way which is consistent with meteorological-scatter power-level correlations (Bean and Meaney, 1955) as noted previously.

The ratio of received-to-transmitted power depends upon the integral of the scattering cross-section over the common volume $V$ defined by the aerial patterns and/or earth screening. If $G_1$ and $G_2$ are antenna gains appropriate to beams which meet at the scattering point $d^3r$,

$$\frac{P_R}{P_T} = \frac{\lambda^2}{16\pi^2}\int_V d^3r \, \frac{2G_1 2G_2 \sigma(\theta, \lambda)}{R_1^2 R_2^2} \tag{4.1}$$

where $R_1$ and $R_2$ are the distances to the scattering point from the transmitter and receiver, respectively. The factors of two are the ideal smooth earth ground reflection factors. Using the result (2.16), this ratio can be expressed in terms of the spectrum of turbulent irregularities.

$$\frac{P_R}{P_T} = \frac{1}{4\lambda^2}\int_V d^3r \, \frac{G_1 G_2}{R_1^2 R_2^2} S\left[\frac{4\pi}{\lambda}\sin\frac{\theta}{2}\right] \tag{4.2}$$

where $\theta$ varies (geometrically) with the integration point ($d^3r$). This ratio is used most often to express the results of narrow-beam scatter experiments.

The majority of broad-beam data are given with respect to the free-space power that would be received over a line-of-sight path of the same length,

$$\frac{P_{\text{f.s.}}}{P_T} = \frac{G_1}{4\pi d^2}\frac{\lambda^2 G_2}{4\pi} \tag{4.3}$$



VOL. 15 1959

This leads to

$$\frac{P_R}{P_{\text{f.s.}}} = \frac{4\pi^2 d^2}{\lambda^4} \int_V d^3r \frac{S\,[(4\pi/\lambda)\sin\theta/2]}{R_1{}^2 R_2{}^2} \tag{4.4}$$

The average patterns of the broad aerials are removed here to cancel the total gains. This integral has occupied the time and efforts of many workers. The problem is mostly one of finding a judicious co-ordinate system in which to do the integrations over the common volume, as limited by earth screening.

In performing the volume integrations, one must eventually recognize a sizable number of refinements to the spherical-earth model. The influence of irregular terrain in modifying the take-off angles led NORTON *et al.* (1955b) to the concept of (effective) angular distance. Refraction of the upgoing and scattered beams by tropospheric refraction has been described so far by variable 4/3 earth modifications of the airless-earth results. BEAN (1956) considered the influence of atmospheric absorption on the same beams and predicted the radio frequency and distance dependence of absorption, as well as the expected correlation with meteorological conditions. The question of scattering by diffracted waves in the shadow region (below the common volume) has been studied by ARONS (1956), who finds that the contributions are very small indeed. The inclusion of ground reflection factors and the inefficiency of ordinary height-gain relations is only partially complete.

### 4.1. *Radio-frequency dependence*

Since only the inertial range ($k_0 < 4\pi/\lambda \sin\theta/2 < k_s$) is involved in most microwave scatter experiments, the turbulent spectra described in Section 2.3 may be used. Because the spectra are simple inverse powers of the wave-number, $k = 4\pi/\lambda \sin\theta/2$, the radio-frequency dependence of the ratios (4.1) and (4.4) can be brought outside the integrations and established quite independent of the volume-integration problems.

The mixing-in-gradient theory of equation (1.10) predicts a linear wave-length dependence for the ratio $P_R/P_{\text{f.s.}}$. This same result has been established experimentally by careful analysis of numerous broad-beam experiments (NORTON *et al.*, 1955b). The same model implies a $\lambda^3$ variation for the ratio $P_R/P_T$ which is also consistent with narrow-beam data. It would appear that the $\lambda^{-\frac{1}{3}}$ dependence predicted by the Obukhov theory (1.9) is not consistent with present radio data.

### 4.2. *Distance dependence*

The distance dependence of (4.2) depends upon careful integration of the spectrum's angular dependence over the common volume which is limited by the transmission distance $d$. The mixing-in-gradient model has no adjustable turbulence constants to influence this distance dependence, but does depend on the mean profile $\theta_0(h)$. Estimations of the integral (4.4) using an exponential variation of $d\varepsilon_0/dh$ up to stratospheric heights predict the observed range dependence of scattered fields quite well out to 700 miles (BOOKER and GORDON, 1956). The narrow-beam data show that the ratio $P_R/P_T$ drops off as a high power ($-9$) of the transmission distance. Further work needs to be done on this subject.

4.3. *Statistical properties of the fading envelope*

The envelope of radio-frequency signals received beyond the horizon is found experimentally to be a random function of time and is Rayleigh-distributed. This is successfully explained by noting that both the real and imaginary parts of the scattered wave in equation (2.12) are Gaussian-distributed, if $\Delta\varepsilon$ is itself a Gaussian normal random-process. The magnitude of the vector sum of two such components with equal variances is known to be Rayleigh-distributed (LAWSON and UHLENBECK, 1950; SILVERMAN and BALSER, 1954). A more general proof which does not rely on the Born approximation applies the central limit theorem to the independent scattering contributions by many blobs in the scattering volume (SILVERMAN, 1955).

Time variations of the signal envelope are physically related to the random addition of Doppler-shifted waves received from different elements of the scattering volume. The drift ($U$) and random ($V_0$) velocities of the eddies impose these frequency shifts on the scattered waves. The basic problem is to predict the radio-frequency and scattering-angle dependence of this fading, and the average rate of fading is taken as a convenient measure of the time-varying envelope. Early studies of this problem (GORDON, 1955; RICE, 1953) considered only the r.m.s sum of these velocities as the effective speed.

$$N \simeq \frac{f}{c}\left\{\left[2U \sin\left(\frac{\bar{\theta}}{2}\right)\right]^2 + \frac{1}{3}\,V_0{}^2\right\}^{\frac{1}{2}} \tag{4.5}$$

where $\bar{\theta}$ is the average scattering angle in the common volume.

A considerable advance in analysing this fading phenomenon was made recently by using the spectral representation of the turbulent dielectric-fluctuations (SILVERMAN, 1956a). The explicit separation of drift- and random-velocity contribution to the space–time correlation of $\Delta\varepsilon$ (1.7) gives the time-displaced generalization of (2.16) as:

$$\frac{P_R}{P_{\text{f.s.}}}\,\rho(\tau) = \frac{4\pi^2 d^2}{\lambda^4}\int d^3rS\left[\frac{4\pi}{\lambda}\sin\frac{\theta}{2}\right]\exp\left(i\bar{K}\,.\,\bar{U}\tau\right)C\left[V_0 R_0{}^{\frac{1}{2}} K^{\frac{2}{3}}\tau\right] \tag{4.6}$$

where $\bar{K}$ is the scattering difference vector defined earlier. Since the major component of the drift speed is usually horizontal—and therefore perpendicular to $\bar{K}$ for midpoint scattering—the significant contribution of drift is made by volume elements which are far from the midpoint. The fading rate, i.e. average rate of mean crossings, is defined in terms of the time correlation $\rho(\tau)$ by the standard expression:

$$N \simeq \frac{1}{\pi}\left[-\left.\frac{d^2\rho}{d\tau^2}\right|_{\tau=0}\right]^{\frac{1}{2}}$$

The fading rate due to self-motion is proportional to $f^{\frac{2}{3}}$, while drift motion gives the usual linear Doppler dependence on frequency. Available data indicate a variable-frequency exponent less than one (NORTON *et al.*, 1955a) so that some mixture of the two effects is indicated. Further experimental results are needed,



VOL. 15 1959

especially with respect to the distance-dependence of $N$. The theory needs to be clarified by evaluating (4.6) for several models.

4.4. *Space correlation of the field*

A combination of two or more spaced receivers is frequently exploited to overcome signal loss during deep fades. This diversity reception depends upon spacing the antennae sufficiently far apart to insure independent fading of the two signals. STARAS (1956) solved the statistical problem of estimating the percentage of time that the *greater* of the two signals is below a specified level as a function of the correlation between the two fields.

The propagation problem is to estimate this space correlation. GORDON (1955) and RICE (1953) presented qualitative analysis which showed that correlation distances normal to the propagation path (horizontal and vertical) ought to be of the order $\lambda a/d$, where $d$ is the transmission distance and $a$ the radius of the earth. The correlation distance $\lambda a^2/d^2$ along the path was also deduced. Precise calculations of all three correlations as functions of the separation were presented by STARAS (1955) using the exponential correlation model. To reach agreement with broad-beam data, he found it helpful to assume anisotropic scattering blobs (cf. equation 1.3) and deduced a vertical-to-horizontal scale length ratio of approximately one-third. Such experiments would appear valuable but more data are needed.

The realization of plane–earth height–gain advantages is limited by space coherence between the actual receiver and its image. The usual height–gain curve is realized if the antenna is less than one-half the vertical correlation distance ($\lambda a/2d$). Only slight improvement is gained above this height by the gradual decrease of the scattering angle. Agreement between theory and experiment on this point is acceptable.

4.5. *Gain-loss and beam swinging*

When very narrow beams are used on scatter circuits, it is found that free-space antenna gains are not realized. This is known as gain loss or antenna-to-medium coupling loss and arises from the fact that signals arrive at the receiver from an extended scattering volume $V$. Narrowing the antenna beam eventually reduces this common volume faster than the aerial gain is increased, so that a relative gain-loss is incurred.

This problem was analysed qualitatively by BOOKER and DE BETTENCOURT (1955) and later generalized by NORTON *et al.* (1955b) and by STARAS (1957) to include non-symmetrical antenna patterns and dissimilar aerial sizes. STARAS evaluated the effect of anisotropic irregularities on the coupling loss. These refined estimates are in good agreement with the experimental data.

BOOKER and DE BETTENCOURT (1955) also considered the effect of swinging the transmitting and receiving aerials simultaneously in azimuth and elevation. In either case, the net effect is to increase the scattering angle and therefore to decrease the received power. They used the exponential correlation model to make estimates of this reduction, which are apparently in good agreement with available data.

4.6. *Band-width limitations*

The signal-frequency band-width which the scatter medium can support without serious distortion is intimately related to the multi-path delays which are experienced. These depend upon the size of the effective scatter volume, which is determined by the antenna beam-widths and/or the scattering pattern of the blobs. When the antenna patterns ($\alpha$) are broad, the multi-path is controlled by the scattering blobs and the approximate result

$$\Delta f = \frac{5ca^2}{d^3} \qquad \alpha \gg \bar{\theta} \tag{4.7}$$

given by GORDON (1955) shows that the band-width decreases rapidly with distance. STARAS (1955) computed the actual frequency-correlation of signals at different frequencies but his results differ by a factor of 8 from (4.7). This problem needs further clarification and resolution with experiment.

A real improvement in band-width capabilities is obtained with very narrow beams. Although some antenna-gain degradation is experienced with narrow beams, the angular distribution of multi-path signals which are admitted to the receiver is reduced and the band-width thereby increased. BOOKER and DE BETTENCOURT (1955) examined this problem for beams narrower than the average scattering angle $\theta = d/a$ and found

$$\Delta f = \frac{4ca}{\alpha d^2} \qquad \alpha \ll \bar{\theta} \tag{4.8}$$

which increases steadily with antenna size and less rapidly with distance. When aircraft fly through the path, the solid bistatic reflections from them supply a multi-path signal of unusual magnitude and the above estimates for broad antenna beams are meaningless.

4.7. *Reflection by elevated layers*

Layers are frequently observed in the troposphere as discontinuities in the vertical profile of refractive-index measurements. It was suggested long ago that partial reflections from these layers might explain scatter propagation (NORTON, 1948). FRIIS *et al.* (1957) have developed this idea in some detail, using uncorrelated reflections from many layer patches in the common volume. These results depend on the size and number of layers, as well as the average refractive discontinuity across the sheets. The ratio $P_R/P_{\text{f.s.}}$ (see Section 4) computed from this theory is proportional to the wave-length, in agreement with experiment. Their predictions of beam-swinging experiments and gain loss are also consistent with experiment. No explanation of fading phenomenon or band-width limitations has been given thus far.

BAUER (1956) has studied the partial reflections from a single spherical layer above the earth. His experimental correlation of scatter-signal strengths with the refractive change across elevated layers in the path is interesting. It is likely that such layers are the seat of intense irregularities, if one believes the mixing models (2.7) or (2.8). The presence of such irregularities at the point of partial reflection

would provide the layer theories with an additional random component to explain fading. The problem may be looked at differently, however, by saying that turbulent blobs are probably created most strongly at layer discontinuities, so that the important scattering volume is near the layer. GORDON (1955) has studied the scattering by elevated turbulent layers briefly. The distinction between such layers and elongated blobs (i.e. anisotropic irregularities) however, is not sufficiently clear.

4.9. *Normal mode theory*

The explanation of radio propagation beyond line-of-sight in terms of coherent partial reflections from a bilinear refractive-index profile has been pursued by CARROLL and RING (1955). Unfortunately, recent expositions of this theory are characterized more by stratagems than comparisons of the theory with experimental data. Two important predictions of normal mode theory emerged from a symposium on this subject at the U.S. Naval Electronics Lab. (1955). The received field strength: (a) varies exponentially with distance and (b) is independent of radio-frequency. The first prediction agrees best with experiments, since it is difficult to distinguish between an exponential variation and a large inverse power of the distance.

The discontinuity in the bilinear profile model of refractive index is of continuing concern to FRIEDMAN and others. Although coherent reflections from stable layers may contribute to the mean signal, normal mode theory offers no explanation of the following important features of scatter propagation: (a) fading envelope, (b) band-width limitations, (c) space correlations, and (d) gain–loss effects.

*Acknowledgements*—This writer benefited from valuable discussions of the subject with R. B. MUCHMORE, K. A. NORTON and H. STARAS. J. B. MCGUIRE kindly helped with the preparation of the paper.

## REFERENCES


| | | |
|---|---|---|
| ARONS L. D. | 1956 | *An Analysis of Radio-Wave Scattering in the Diffraction Region.* Cornell University E.E. Report 312, Ithaca, New York. |
| BALSER M. | 1957 | *Trans. Inst. Radio Engrs., N.Y.* PGAP. |
| BAUER J. R. | 1956 | *The Suggested Role of Stratified Elevated Layers in Transhorizon Shortwave Radio Propagation.* Massachusetts Institute of Technology, Lincoln Laboratory Technical Report No. 124. |
| BEAN B. R. and MEANEY F. M. | 1955 | *Proc. Inst. Radio Engrs., N.Y.* **43,** 1419. |
| BEAN B. R. | 1956 | *Trans. Inst. Radio Engrs., N.Y.* CS **4,** 32. |
| BOLGIANO R. | 1957 | *Turbulent Mixing and Its Role in Radio Scattering.* Cornell University E.E. Report 334, Ithaca, New York. |
| BOOKER H. G. | 1956 | *J. Atmosph. Terr. Phys.* **8,** 204. |
| BOOKER H. G. and DE BETTENCOURT J. T. | 1955 | *Proc. Inst. Radio Engrs., N.Y.* **43,** 281. |

| | | |
|---|---|---|
| BOOKER H. G. and GORDON W. E. | 1956 | *The Role of Stratospheric Scattering in Radio Communication.* Cornell University E.E. Report 308, Ithaca, New York. |
| CARROLL T. J. and RING R. M. | 1955 | *Proc. Inst. Radio Engrs., N.Y.* **43,** 1384. |
| CHERNOV L. A. | 1954 | *Dokl. Akad. Nauk SSSR* **98,** 953. |
| CHERNOV L. A. | 1955 | *Akustich. Zh.* **1,** 89. |
| DEAM A. P. and FANNIN B. M. | 1955 | *Proc. Inst. Radio Engrs., N.Y.* **43,** 1402; *Report* Nos. 6–08, 7–06, Electrical Engineering Research Laboratory, University of Texas. |
| ELLISON T. H. | 1951 | *J. Atmosph. Terr. Phys.* **2,** 14. |
| FANNIN B. M. | 1956 | *Trans. Inst. Radio Engrs., N.Y.* PGAP **AP-4,** 661. |
| FRIIS H. T., CRAWFORD A. B. and HOGG D. C. | 1957 | *Bell Syst. Tech. J.* **36,** 627. |
| GORDON W. E. | 1955 | *Proc. Inst. Radio Engrs., N.Y.* **43,** 23. |
| HEISENBERG W. | 1948 | *Z. Phys.* **124,** 628. |
| HERBSTREIT J. W. and THOMPSON M. C. | 1955 | *Proc. Inst. Radio Engrs., N.Y.* **43,** 1391. |
| LAWSON J. L. and UHLENBECK G. E. | 1950 | *Threshold Signals* Vol. XIII, p. 62. M.I.T. Rad. Lab. Series, McGraw-Hill, New York. |
| MINTZER D. | 1953; 1954 | *J. Acoust. Soc. Amer.* **25,** 922, 1107, **26,** 186. |
| MUCHMORE R. B. and WHEELON A. D. | 1955 | *Proc. Inst. Radio Engrs., N.Y.* **43,** 1437. |
| NORTON K. A. | 1948 | *Advances in Electronics* **1,** 381. |
| NORTON K. A. | 1956 | *Trans. Inst. Radio Engrs. N.Y.* CS **4,** 39. |
| NORTON K. A. | 1959 | Comments at this Symposium. |
| NORTON K. A., RICE P. L., JANES H. B. and BARSIS A. P. | 1955a | *Proc. Inst. Radio Engrs., N.Y.* **43,** 1341. |
| NORTON K. A., RICE P. L. and VOGLER L. E. | 1955b | *Proc. Inst. Radio Engrs., N.Y.* **43,** 1488. |
| OBUKHOV A. M. | 1949 | *Izv. Akad. Nauk SSSR, Ser. Geofiz.* **13,** 58. |
| OBUKHOV A. M. | 1953 | *Izv. Akad. Nauk SSSR, Ser. Geofiz.* No. 2, 155. |
| RICE S. O. | 1953 | *Proc. Inst. Radio Engrs., N.Y.* **41,** 274. |
| RYTOV S. M. | 1937 | *Izv. Akad. Nauk SSSR, Ser. Fiz.* No. 2. |
| SILVERMAN R. A. | 1955 | *Proc. Inst. Radio Engrs., N.Y.* **43,** 1253. |
| SILVERMAN R. A. | 1956a | *J. Appl. Phys.* **27,** 93. |
| SILVERMAN R. A. | 1956b | *J. Appl. Phys.* **27,** 699. |
| SILVERMAN R. H. | 1957 | *J. Appl. Phys.* **28,** 506. |
| SILVERMAN R. A. and BALSER E. M. | 1954 | *Phys. Rev.* **96,** 560. |
| STARAS H. | 1955 | *Proc. Inst. Radio Engrs., N.Y.* **43,** 1374. |
| STARAS H. | 1956 | *J. Appl. Phys.* **27,** 93. |
| STARAS H. | 1957 | *Trans. Inst. Radio Engrs. N.Y.* PGAP **5,** 228. |
| TATARSKII V. I. | 1953 | *Zh. Eksp. Teor. Fiz.* **25,** 74. |
| U.S. NAVY ELECTRONICS LABORATORY | 1955 | *A Summary of the Symposium on Normal Mode Theory.* San Diego, California. |
| VILLARS E. and WEISSKOPF V. F. | 1954 | *Phys. Rev.* **94,** 232. |
| VILLARS F. and WEISSKOPF V. F. | 1955 | *Proc. Inst. Radio Engrs., N.Y.* **43,** 1232. |
| WHEELON A. D. | 1955 | *Proc. Inst. Radio Engrs., N.Y.* **43,** 1459. |
| WHEELON A. D. | 1957a | *Phys. Rev.* **105,** 1706. |
| WHEELON A. D. | 1957b | *J. Appl. Phys.* **28,** 684. |

## Discussion

Dr. V. G. Plank—Dr. Wheelon, you have stated that large $N$-fluctuations are associated with turbulence. How and why is this true for the case of stratified refractive-index transition zones (e.g. subsidence inversions)? Bauer, of Project Lincoln, has flown extensively through such layers and his measurements and analysis indicate that the layers are essentially planar over areas of many square miles.

Dr. Wheelon—As I have pointed out in my paper, both the "mixing" theories indicate that the $N$-fluctuations are proportional to the gradient of mean refractive index. Thus a transition zone such as Dr. Plank describes would be just the place one might expect to find large values of $\Delta N$.

Mr. R. Bolgiano—In partial answer to Dr. Plank's question regarding the existence of blobs in stratified layers I should like to make two points. First, whereas the intensity of turbulence is measured in terms of the r.m.s. value of the turbulent velocities, the intensity of refractive-index fluctuations is controlled primarily by the gradient-of-potential index and the scale of the velocity field in the direction of that gradient. Consequently one might expect that, if there is any correlation between these two intensities it will be negative, since strong turbulence will tend to erase rapidly any deviation of the gradient from its adiabatic value.

Secondly, in recent weeks I have been working on the very problem of the generation of turbulence in the free atmosphere and find that only at such stratified layers, at fronts, is the wind shear likely to be sufficiently intense to overcome the stabilizing influence of the density gradient. Hence, except for thermal convection, it is only in such layers that intense turbulence would be expected.

Dr. D. R. Hay—At the Radio Physics Laboratory (Defence Research Board, Ottawa, Canada), we have been carrying out a study to correlate weather fronts with their effects upon scatter-signal transmissions. Two radio links are operated for this purpose: an 85-mile path at 500 Mc/s and a 185-mile path at 46 Mc/s. For the initial study, position of the weather front through the transmission paths is compared with signal-fading rate and hourly median-signal level. In the absence of weather fronts, the signal-fading rate on both paths has a marked diurnal variation, with minimum around midnight and maximum around early afternoon. The movement of a weather front through the transmission paths generally results in a decrease in hourly median-signal amplitude and an increase in signal-fading rate well above the diurnal maximum. The 46 Mc/s transmissions are affected to the greatest extent by summer fronts (predominantly Polar fronts), but the 500 Mc/s transmissions are affected chiefly by winter fronts (predominantly Arctic fronts). The results of this study will be published shortly in the open literature.

Journal of Atmospheric and Terrestrial Physics, 1959, Vol. 15, pp. 206 to 227. Pergamon Press Ltd. Printed in Northern Ireland

# Recent experimental evidence favouring the $\rho K_1(\rho)$ correlation function for describing the turbulence of refractivity in the troposphere and stratosphere

K. A. NORTON*

## 1. INTRODUCTION

ATMOSPHERIC turbulence influences the propagation of radio waves in many ways. These influences are effectively defined by the detailed description of the variations in time and in space of the scalar refractive index, $n$, of the atmosphere. It is the purpose of this paper to show that in radio propagation studies these variations may be described to a useful degree of accuracy by assuming (a) that the variations in space at a fixed time may be described by the correlation function $\rho K_1(\rho)$, where $K_1$ is the modified Bessel function of the second kind and $\rho = r/l_0$ is a normalized distance between two points in the atmosphere, and (b) that the variations in time at a fixed point may be described by the assumption that this spatial pattern is moved past this point with the mean wind. The above is equivalent to assuming that the random motion of the atmosphere has a negligible effect on the variations with time relative to the time variations resulting from the drift of the frozen-in turbulent structure past the observer. Three independent kinds of experimental evidence are presented:

(a) Direct measurements of the variations of $n$ with time at a fixed location are made with a refractometer. The spectra of these variations are shown to agree with the spectra expected for the above-described $\rho K_1(\rho)$ model. Three constants, the total variance of refractivity, an effective median scale length, and a standard deviation of the characteristic frequencies, are adjusted in fitting the theory to the data so that only the agreement with the shape of the spectrum is significant.

(b) Measurements of the variations with time of the phase of a radio wave received over a line-of-sight path. Again the spectra of these variations are shown to agree with the spectra expected for the $\rho K_1(\rho)$ model. Three constants, the total variance of phase, an effective median scale length, and a standard deviation of the characteristic frequencies are adjusted in fitting the theory to the data so that again only the agreement with the shape of the spectra is of primary significance. However, the three constants required in this case are not inconsistent with those obtained in the refractivity measurements, the latter being made at a time and place different from those used for the observations of phase.

(c) Measurements of the received power of radio waves scattered in the forward direction to a receiving point beyond the radio horizon of the transmitter. In this case, by somewhat arbitrarily identifying one of the parameters of the forward-scatter theory based on the $\rho K_1(\rho)$ model with the variance of the vertical gradient of the refractive index, it is possible, without any other adjustable constants, to

* National Bureau of Standards, Boulder Laboratories, Boulder, Colorado.

calculate the forward-scattered radio power in terms of the variance of this vertical gradient as determined from Rocket Panel data. The agreement with the experimental data is considered satisfactory. The variance of refractive index determined as above from the Rocket Panel data is also in satisfactory agreement with that required to explain the direct measurements on the variance of refractivity and the variance of phase. The present paper contains substantially more information than was presented to the Joint Commission; in particular, data are added on refractivity spectra and on reading-error spectra.

## 2. Forward Scatter of Radio Waves

In recent papers (Norton, 1956; Norton *et al.*, 1955) some evidence was given that the structure of the turbulence of refractivity in the troposphere may be described in the inertial sub-range of blob sizes by the correlation function $\rho K_1(\rho)$ where $K_1$ is the modified Bessel function of the second kind and $\rho = r/l_0$ is a normalized distance between two points in the atmosphere. This particular form of correlation function was suggested to me by Muchmore and independently by Gallet* in order to explain the observed $\lambda$ dependence of the scattering cross-section in the forward scattering of radio waves by the troposphere (Norton *et al.*, 1955). This $\lambda$ dependence is a feature of the Villars and Weisskopf (1955), Gallet (1955), and Wheelon (1957a) models of atmospheric turbulence.

If we assume that the largest blobs in the atmosphere are like pancakes with larger characteristic scales horizontally than vertically, and let $l_h$ denote the effective horizontal scale (an average of the horizontal scales parallel and normal to the mean wind) and $l_v$ the vertical scale, both expressed in metres, then it can be shown (Norton, 1956) on the basis of this $\rho K_1(\rho)$ model that the meteorological parameter, $R$, which directly measures the radio wave power scattered in the forward direction, may be expressed in the following form:

$$R = \langle(\Delta n)^2\rangle l_h/l_v^3 \qquad (1)$$

In the above $\langle(\Delta n)^2\rangle$ is the variance of the refractive index of the atmosphere. Note the relatively greater importance of the vertical scales; in this connexion it should be noted that refractometers flown in aircraft tend to measure only the horizontal scales and thus may systematically give an erroneous picture of the turbulence to the extent that the horizontal and vertical scales have substantially different magnitudes. It should be noted in passing that this influence of anisotropy on the magnitude of $R$ is its principal effect on electromagnetic scattering. In addition, anisotropy will also influence the correlation on spaced antennas and the magnitude of the loss in antenna gain, in the directions stated in two recent papers by Staras (1955, 1957).

* Private communications from R. B. Muchmore, Guided Missile Research Division, Ramo-Wooldridge Corp., Los Angeles, 45, Calif. and from R. Gallet of the National Bureau of Standards, Boulder Laboratories. In fact both Muchmore and Gallet independently obtained expressions for a family of correlation functions of the form $(r/l_0)\mu K\mu(r/l_0)$. It appears now that only the function corresponding to $\mu = 1$ will be required, since this particular function provides predictions most nearly in agreement with the radio data.

Recently, BOOKER and GORDON (1957)*, by somewhat arbitrarily identifying $R$ with an estimate of the variance $V$ of the vertical gradient of refractive index relative to its mean value (see their equation 16), have shown how $R$ may be evaluated for a dry atmosphere (such as is encountered in the stratosphere) and this theory has been further developed by ABBOTT† at the National Bureau of Standards. Thus ABBOTT has determined that the variance of the vertical gradient is about one-third of the mean square refractive-index gradient $\langle(dn/dh)^2\rangle$ for a dry isothermal atmosphere, and may be represented by the following expression which was evaluated by using the Rocket Panel (1952) data on the characteristics of the upper atmosphere:

$$R \simeq V = 0{\cdot}0816\ \langle(dn/dh)^2\rangle = 2{\cdot}37 \times 10^{-16} \exp(-0{\cdot}0002848h) \qquad (2)$$

where $h$ is the height above sea level expressed in thousands of feet. The constant 0·0816 in this equation is equal to $\{(\gamma - 1)/\gamma\}^2$ where $\gamma$ is the ratio of the specific heat at constant pressure to that at constant volume and is approximately 1·4 for air. This expression for a dry isothermal atmosphere should also apply approximately to the actual atmosphere from sea level up to altitudes of more than 200,000 ft; for example, BEAN (1953) has analyzed the gradient of refractive index for several representative climates, and the use of these values in (2) would lead to estimates of $V$ differing from those for the Rocket Panel atmosphere by less than $\pm 3$ dB. At heights above the earth's surface less than, say, 15,000 ft the moisture in the atmosphere begins to play an increasingly more important role and, although this evidently (BEAN, 1953) does not greatly affect the mean gradient, the value of $R$ may be expected to be more variable diurnally and seasonally at these lower heights. Note that correlation functions $(r/l_0)^{\mu}K_{\mu}(r/l_0)$ lead to a meteorological parameter, $R$, with dimensions proportional to $l_0^{-2\mu}$ and this has the same dimensions as the variance of a gradient only for $\mu = 1$.

Using the value of $R$ given by (2) and integrating over the common volume by the methods described by NORTON *et al.* (1955), ABBOTT then calculated the solid curve of $Y(\theta)$ shown on Fig. 1 for the case of a symmetrical path ($\alpha_0 = \beta_0$) with the antennae on the ground ($d_{Lt} = d_{Lr} = 0$). The function $Y(\theta)$ is related to the basic transmission loss expected on a tropospheric forward-scatter path as is indicated by the equation given at the top of Fig. 1. The terms in this equation are defined by NORTON (1956) and NORTON *et al.* (1955); the frequency gain and asymmetry functions given by NORTON (1956) and used in adjusting the data to the values of $Y(\theta)$ shown on Fig. 1 were determined for an assumed inverse height squared variation of $R$ rather than the more appropriate exponential variation represented by (2). Note that the level of this curve is in good agreement with the average of the observations of path losses, and that its variation with distance is in still better agreement. ABBOTT inadvertently omitted a factor 0·1 in calculating the $Y(\theta)$ curve shown on Fig. 1; when the $Y(\theta)$ shown on Fig. 1 is lowered by this factor, i.e. 10 dB, it will evidently be in even better agreement with the data.

* The numerical constant in this paper relating the meteorological parameter, $R$, to the scattered power (equation 14) is smaller by a factor of $1{\cdot}2/\pi$ than the constant obtained by the use of the correlation function $\rho K_1(\rho)$, and ABBOTT has used the latter in his calculations of $Y(\theta)$; the origin of the Booker–Gordon constant is not understood.

† Private communication.



VOL. 15 1959

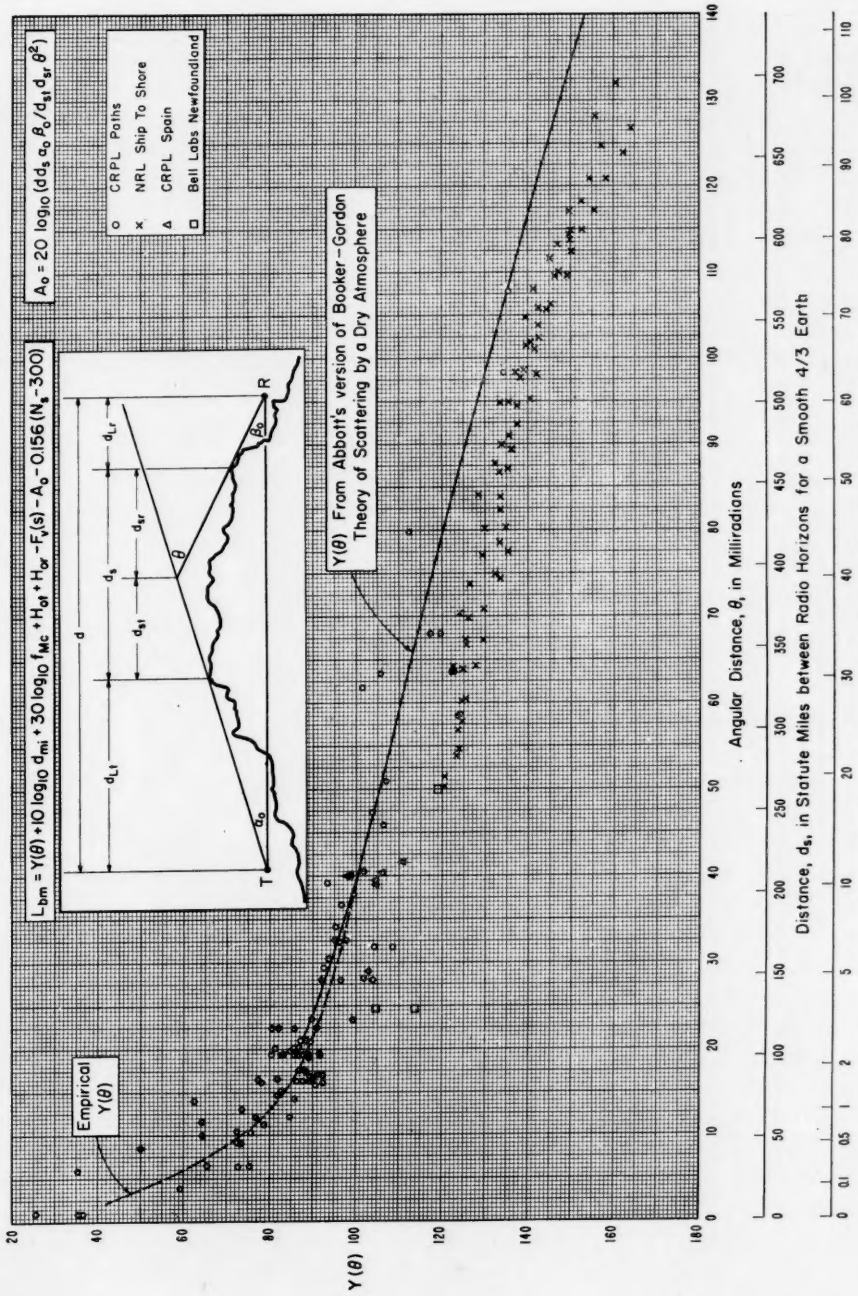
$L_{bm} = Y(\theta) + 10 \log_{10} d_{mi} + 30 \log_{10} f_{Mc} + H_{0f} + H_{0r} - F_y(s) - A_0 - 0.156 (N_s - 300)$
$A_0 = 20 \log_{10} (d d_s a_0 \beta_0 / d_{sf} d_{sr} \theta^2)$
o CRPL Paths
× NRL Ship To Shore
Δ CRPL Spain
□ Bell Labs Newfoundland
Empirical Y(θ)
Y(θ) From Abbott's version of Booker–Gordon Theory of Scattering by a Dry Atmosphere
Y(θ)
Angular Distance, θ, in Milliradians
Distance, $d_s$, in Statute Miles between Radio Horizons for a Smooth 4/3 Earth
Height of Scattering Center in Thousands of Feet above a Smooth Earth
T
R

Fig. 1. Prediction formula for winter afternoon median basic transmission loss, $L_{bm}$.

The NRL data (DINGER *et al.*, 1958) were obtained on a frequency of 412·85 Mc/s in a joint project with the Lincoln Laboratories. Each of the crosses on Fig. 1 represents a value of $Y(\theta)$ corresponding to the median of the observed transmission loss for a 50 min period of time. The data on Fig. 1 were corrected for loss in antenna gain by a method to be described in a forthcoming paper. Since the value (2) of $R$ was determined solely from meteorological data, the agreement of ABBOTT's curve with the data on Fig. 1 provides strong evidence in favour of the correlation function $\rho K_1(\rho)$ as a model for describing the turbulence of refractivity; it appears unlikely to the writer that the use of other functional forms for the correlation function would provide as good a fit. Note in particular that the CRPL and Bell Laboratories data cover a frequency range from 85 to 4090 Mc/s and it is evident on Fig. 1 that the transmission-loss formula fits these radio data quite well over this wide range of frequencies. This theory of forward scattering based on an exponential atmosphere is now being generalized to allow more appropriately for path asymmetry and for frequency gain, and this generalization will shortly be published. (RICE *et al.*, 1959).

### 3. PHASE VARIATIONS ON A LINE-OF-SIGHT PATH

We turn next to more direct evidence relative to the nature of atmospheric turbulence. Thus, Figs. 2 and 3 show measured spectra of the phase variations on a 16 mile line-of-sight path on Maui, Territory of Hawaii. The method of measurement is described in a paper by HERBSTREIT and THOMPSON (1955). Of particular interest is the agreement between these measured spectra and a theory, based on the log-normally modified $\rho' K_1(\rho')$ autocorrelation function, which is described in the Appendix.

The phase variations were simultaneously recorded in two ways. A "low-pass" Esterline–Angus recording was made using a chart speed of 3 in/min and a relatively compressed scale—900 degrees full scale. The frequency response of this circuit was flat from zero to approximately 1 c/s, the response of the recording meter being the limiting factor at the high-frequency end. To remove low-frequency "trends" and thus permit amplification of the higher-frequency variations, the output of the phase meter was also passed through a high-pass filter and recorded on a second Esterline–Angus meter. This is the so-called "band-pass" data, the recording meter again limiting the response at the high-frequency end. The "band-pass" response characteristic is shown at the bottom of Figs. 2 and 3.

The power spectra were obtained by using a 600-point Fourier series coefficient computation programmed for the IBM Type 650 computer. The programme requires as an input 601 values of the variable, evenly spaced in time. Other requirements, common to all methods of spectrum computation using digital input, are: (a) that the observations be spaced closely enough to take into account the highest frequencies present in the data; (b) that the sample of record chosen be long enough to allow for the lowest frequencies present; and (c) that the variable have equal value and equal slope at both ends of the sample. In practice it is difficult to satisfy all of these requirements, but it is felt that they were reasonably well met in the data discussed here. The output of the programme consists of 53 values of $c_i^2 (i = 1, 3, 5, 7, 9, 15, 21, 27, \ldots, 297)$, an estimate of the power



VOL. 15 1959

contained in a band $1/T$ c/s in width with centre frequency $i/T$ c/s, where $T$ is the sample length in seconds. In the spectra discussed here, the ordinate is $Tc_i^2$, which is an estimate of the average power density, $\overline{W(i/T)}$ over this band, expressed in (electrical degrees)$^2$/unit bandwidth, or simply (degrees)$^2$ per c/s. That is,

$$Tc_i^2 \simeq \overline{W\left(\frac{i}{T}\right)} = T\int_{\frac{i}{T}-\frac{1}{2T}}^{\frac{i}{T}+\frac{1}{2T}} W(f)\,df$$

where $W(f)$ is the true power density at frequency $f$.

A semi-automatic chart scaling device was used to obtain the 601 data points required for each spectrum. The device operates in the following way: while the chart moves at a predetermined constant speed across a flat surface, the operator retraces the inked line with a pointer; a timing mechanism geared to the chart drive causes the variable to be sampled at a pre-set rate, and the value of each sample is punched automatically on an IBM card.

Figs. 2 and 3 together with Tables 1 and 2 summarize the results of the spectrum analysis. These particular times were chosen from the large amount of data available because they represent typical night and day conditions, respectively, and also because the low-pass recordings were unusually free from discontinuities. Also, the general character of the variations on the band-pass record remained unchanged throughout each of the periods. This made possible the analysis of a 55-min low-pass sample in the case of Fig. 2 and two 20-min samples in Fig. 3.

The Fourier method of computation using a fixed number of observations suffers from two disadvantages. One is that, while the nature of the low-pass record permitted a relatively large sampling interval so that the 601 points covered a period of up to 55 min, in the case of the band-pass record the rapid variations required a small sampling interval, and 601 points covered only 3·41 min. In other words, the maximum length of record that can be analysed is determined in practice by the highest frequencies present in the record. Another disadvantage is that the individual points on the spectrum are subject to large sampling fluctuations and some means of smoothing or averaging should be employed.

To compensate, at least partially, for these limitations, six 3·41 min samples of band-pass data selected from the period covered by the longer low-pass samples were analysed, and the ordinates of the resulting six spectra averaged to obtain the band-pass spectra shown in Figs. 2 and 3. These spectra have been modified to allow for the recording-circuit frequency response shown at the bottom of each figure, so that they represent as nearly as possible the spectra of the phase variations before filtering.

The errors introduced in the process of scaling the raw data and the rounding of the instantaneous values of the variable before punching them on IBM cards produce errors in the spectra which we may call "reading-error noise". An effort has been made to estimate the spectrum of this noise for each group of data, and these estimated reading error noise spectra are shown on Figs. 2 and 3. They were obtained as follows: a given sample of chart record was scaled several times, keeping all conditions as constant as possible. Then the 601 differences between

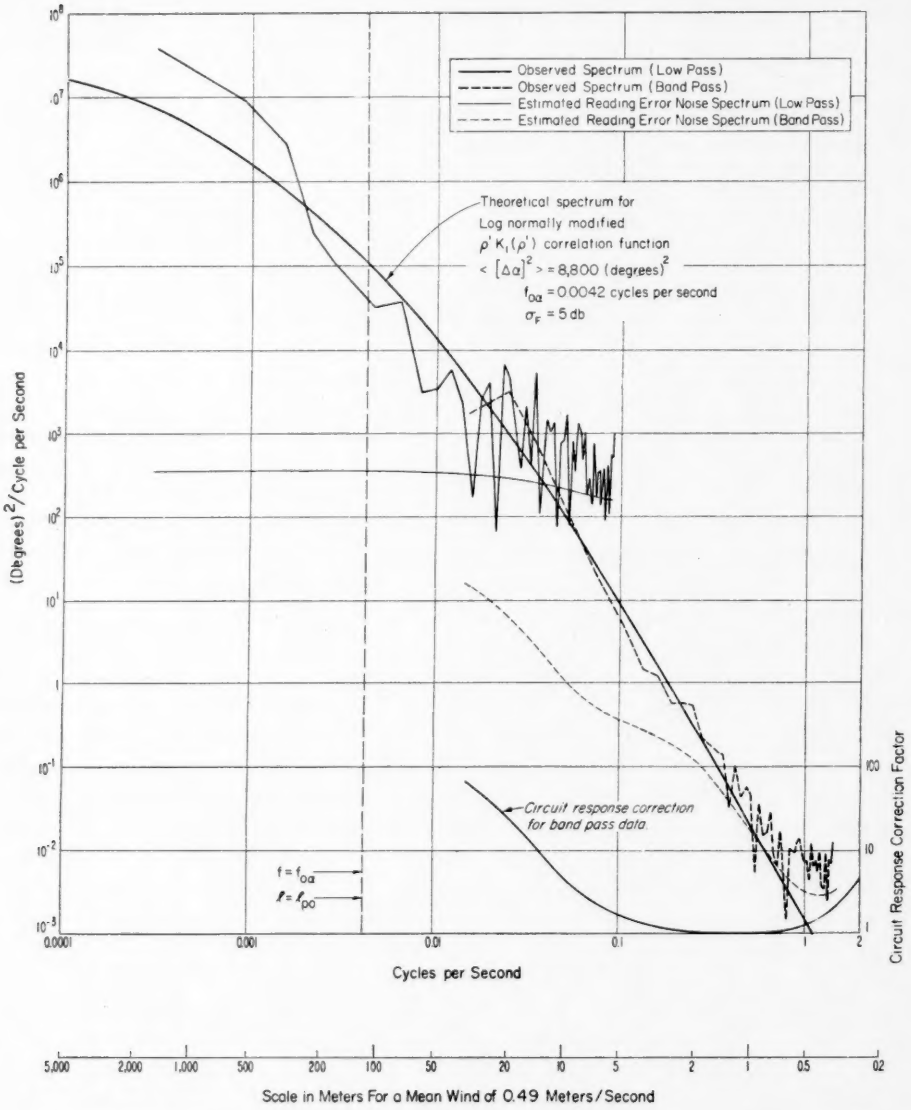


Fig. 2. Power spectrum of 9414 Mc/s single-path phase variations. Haleakala—Puunene path: 0158–0252 hours 7 November 1956.

the first and second trials were obtained and the variance and serial correlation coefficients of these differences computed. The estimated variance of the reading-error noise, $s^2$, is half the variance of these differences. The serial correlation coefficients were compared to two model autocorrelation functions, from either of which the corresponding spectrum can easily be computed. The first model was the autoregressive scheme of first order, called the Markoff scheme, in which the

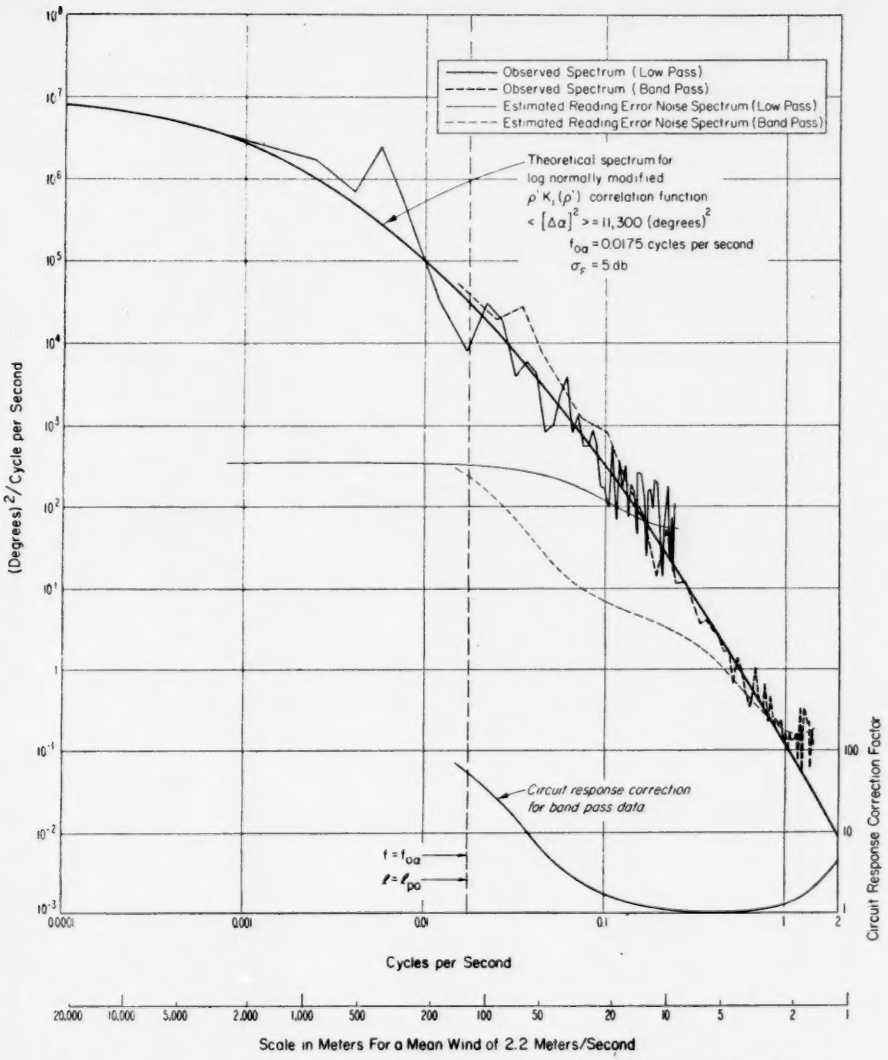
Observed Spectrum (Low Pass)
Observed Spectrum (Band Pass)
Estimated Reading Error Noise Spectrum (Low Pass)
Estimated Reading Error Noise Spectrum (Band Pass)
Theoretical spectrum for log normally modified $\rho' K_1(\rho')$ correlation function
$< [\Delta\alpha]^2 > = 11,300$ (degrees)$^2$
$f_{0\alpha} = 0.0175$ cycles per second
$\sigma_F = 5$ db
Circuit response correction for band pass data
$f = f_{0\alpha}$
$\ell = \ell_{p0}$
(Degrees)$^2$/Cycle per Second
Circuit Response Correction Factor
Cycles per Second
Scale in Meters For a Mean Wind of 2.2 Meters/Second

Fig. 3. Power spectrum of 9414 Mc/s single-path phase variations. Haleakala—Puunene Path: 1300–1400 hours 5 November 1956.

$k$th-order autocorrelation, $\rho_k$, is given by $\rho_k = \rho_1{}^k$, where $\rho_1$ is the first-order autocorrelation and is estimated by $r_1$, the observed serial correlation coefficient of lag 1.

The average power density of the reading noise at frequency $i/T$ under the Markoff scheme is then estimated by

$$Tc_i{}^2 = \frac{4Ts^2}{n}\left[\frac{1 - r_1{}^2}{1 - 2r_1 \cos(2\pi i/n) + r_1{}^2}\right]$$

where $s^2$ is the estimated variance of the reading error in (degrees)$^2$, $T$ is the

Table 1. Phase spectrum information

| Fig. | Data | Approx. time | Length of record (min) | Calibration (degrees full scale) | Sampling interval (sec) | No. of spectra averaged | Variance of data points† (degrees)$^2$ min. | av. | max. |
|---|---|---|---|---|---|---|---|---|---|
| 2 | Single-path phase (low-pass) | 0200–0254 7/X1/56 | 54·54 | 900 | 5·454 | 1 | — | $8{\cdot}82 \times 10^3$ | — |
| 2 | Single-path phase* (band-pass) | 0200–0254 7/X1/56 | 3·41 | 11·25 | 0·341 | 6 | 0·404 | 1·58 | 3·04 |
| 3 | Single-path phase (low-pass) | 1300–1400 5/X1/56 | 20·41 | 900 | 2·041 | 2 | $1{\cdot}03 \times 10^4$ | $1{\cdot}13 \times 10^4$ | $1{\cdot}22 \times 10^4$ |
| 3 | Single-path phase* (band-pass) | 1300–1400 5/X1/56 | 3·41 | 45 | 0·341 | 6 | 23·8 | 38·6 | 46·9 |

* In these spectra, the lowest frequency shown is $3/T$ c/s, since the response correction at $1/T$ c/s was not available.

† These are variances of the output of the recording circuit and do not represent the total variance of the input, except in the case of the low-pass data.

period of record in seconds, and $n$ is the number of data points less 1 (600 in this case). The second model was the autoregressive scheme of second order, known as the Yule scheme. The $k$th-order autocorrelation, $\rho_k$, of the Yule scheme satisfies the equation

$$\rho_k = \alpha\rho_{k-1} - \beta\rho_{k-2}, \qquad k = 1, 2, \ldots$$

with $\rho_0 = 1$, $\rho_{-k} = \rho_k$. The determination of $\alpha$ and $\beta$ depends on the knowledge of the first two autocorrelations. Estimating $\rho_1$ and $\rho_2$ by $r_1$ and $r_2$, the first- and

Table 2. Reading error-noise spectrum information

| Fig. | Data | Autocorrelation model used | No. of independent trials | Variances of reading error (degrees)$^2$ |
|---|---|---|---|---|
| 2 | Single-path phase (low-pass) | Markoff | 2 | 22·46<br>27·84 |
| 2 | Single-path phase (band-pass) | Yule | 4 | 0·0656<br>0·2698<br>0·2727<br>0·1013 |
| 3 | Single-path phase (low-pass) | Markoff | 2 | 33·9<br>132·7 |
| 3 | Single-path phase (band-pass) | Yule | 4 | 1·54<br>12·1<br>1·73<br>3·053 |

second-order serial correlation coefficients, estimates of $\alpha$ and $\beta$ are obtained by $a$ and $b$, respectively, where

$$a = \frac{r_1(1 - r_2)}{1 - r_1^2}, \qquad b = \frac{r_1^2 - r_2}{1 - r_1^2}.$$

Its average power density is then estimated by

$$Tc_i^2 = \frac{4Ts^2}{n(1 - r_1^2)}\left[\frac{1 - r_2^2 - 2r_1^2(1 - r_2)}{1 + a^2 + b^2 - 2a(1 + b)\cos(2\pi i/n) + 2b\cos(4\pi i/n)}\right]$$

Using in each case the model which more closely agreed with the observed serial correlation, the noise spectrum was computed.

It will be seen that the reading-error noise probably contributes much of the power in the phase spectra at the high-frequency end. In fact, the latter should probably be treated with considerable caution wherever the noise-power density at a given frequency becomes greater than about one-tenth of the phase-power density. It is felt that the noise spectra may be somewhat high because of difficulty

Table 3. Refractivity spectrum information

| Spectrum no. | Type of recording | Date | Beginning time | Length of sample | $\delta$ (sec) | Calibration ($N$-units full-scale) | Variance of mean wind speed | | |
|---|---|---|---|---|---|---|---|---|---|
| | | | | | | | Data points ($N$-units)$^2$ | Total (m/sec) | Parallel component* (m/sec) |
| 1 | Low-pass | 24/V/56 | 20:59:00 | 18·8 min | 2·0 | 20·0 | 2·4039 | 3·33 | † |
| 2 | Band-pass | 24/V/56 | 21:20:00 | 2·0 min | 0·2 | 0·667 | 0·0057310 | 3·91 | † |
| 3 | Band-pass | 24/V/56 | 21:21:37 | 10·0 sec | 0·05 | 0·667 | 0·0021643 | 3·13 | † |
| 4 | Band-pass | 24/V/56 | 21:22:55 | 10·0 sec | 0·05 | 0·667 | 0·003017 | 4·36 | † |
| 5 | Band-pass | 24/V/56 | 21:21:54 | 10·0 sec | 0·05 | 0·667 | 0·0013278 | 4·02 | † |
| 6 | Low:pass | 25/V/56 | 09:13:00 | 42·9 min | 4·69 | 20·0 | 7·8520 | 1·94 | 1·42 |
| 7 | Low-pass | 25/V/56 | 09:42:05 | 5·6 min | 0·438 | 20·0 | 0·89907 | 2·68 | 2·56 |
| 8 | Band-pass | 25/V/56 | 09:36:30 | 23·7 sec | 0·04 | 3·33 | 0·16127 | 2·46 | 1·83 |
| 9 | Band-pass | 25/V/56 | 09:34:58 | 26·3 sec | 0·04 | 3·33 | 0·030348 | 0·22 | 0·21 |
| 10 | Band-pass | 25/V/56 | 09:36:02 | 23·4 sec | 0·04 | 3·33 | 0·028429 | 2·01 | 0·45 |

* The refractometer cavity was oriented normal to the Pikes Peak—Garden of the Gods propagation path, i.e., with the openings facing roughly north and south. The "parallel component" of the measured wind velocity approximates the air speed through the cavity.

† Wind direction data not available.

VOL. 15
1959

encountered in taking observations at precisely the same time on the chart in each trial. Any shift in the time scale will tend to increase the apparent reading-noise variance. In an effort to compensate for this error, several determinations of noise variance were made for each group of data, and the trial yielding the smallest variance was used in computing the noise spectrum.

This difficulty came to light when several estimates of reading-noise variance were obtained for each group of data. These showed far greater variability among the estimates than would be expected in view of the large number of degrees of freedom in each estimate. Table 2 contains miscellaneous information about the noise spectra and gives the sample reading-error variances for each group of data.

Table 4. Maximum component of wind speed normal to path during recording periods (m/sec)

| Recording period | Puunene | Haleakala |
|---|---|---|
| hr | m/sec | m/sec |
| 5/X1/56 1300–1400 | 6·49 | 7·45 |
| 7/X1/56 0200–0254 | 3·82 | 0·73 |
| 7/X1/56 1322–1400 | 3·99 | 1·50 |
| 7/X1/56 1418–1439 | 7·67 | 1·21 |

On the assumption that time-scale errors were largely responsible for the wide range of variances obtained, it was decided that the trial yielding the smallest variance had the smallest time-scale error and therefore should be used in computing the reading error-noise spectrum. To test this assumption that the sample variances came from essentially different populations, Cochran's test was applied. Using 144 as a rough estimate of the number of degrees of freedom (to allow for the auto-correlation of the 600 data points), it was found that in almost all cases the variances were significantly different at the 5 per cent significance level. It was also found that in those cases where the variances were not significantly different (i.e. where they appeared to be taken from the same population) the selection of the smallest variance instead of the mean variance could result in an error of no more than 10 per cent in the ordinates of the noise-power spectrum.

It is recognized that in order to extrapolate these data to other situations, a mean drift velocity normal to the path for the period of record is required. Unfortunately, on this particular path the observed wind was blowing in opposite directions at the path terminals during most of the recording periods. To establish an upper bound on these velocities, the Table 4 gives the maximum speed of the component of wind normal to the path for each period.

The theory in the Appendix indicates that the variance of phase $\langle(\Delta\alpha)^2\rangle$ on a line-of-sight path is related to the variance of refractivity $\langle(\Delta n)^2\rangle$ along the path in the following way:

$$\langle(\Delta\alpha)^2\rangle = \pi(360)^2 \langle(\Delta n)^2\rangle l_{po} L/\lambda^2 \quad \text{(degrees)}^2 \qquad (3)$$

where $L$ is the length of the propagation path and $\lambda$ is the free-space wavelength of

the radio waves whose phase variation is being measured. If we use the measured variance $\langle(\Delta\alpha)^2\rangle = 8820$ (degrees)$^2$ for the 7 November record, we find that $\langle(\Delta n)^2\rangle l_{po}$ should be equal to $883{\cdot}2 \times 10^{-12}$ m. The average of $\langle(\Delta n)^2\rangle/l_{po}^2$ as estimated by (2) over the height range involved on the Maui path is equal to $5{\cdot}5 \times 10^{-16}$. Combining these two results we find that $l_{po} = (883{\cdot}2 \times 10^{-12}/5{\cdot}5 \times 10^{-16})^{\frac{1}{3}} = 117$ m on 7 November. In a similar way we find $l_{po} = 127$ m for the 5 November record. These were the median characteristic scales used to determine the ranges of scales shown at the bottom of Figs. 2 and 3. The effective mean wind normal to the path is thus equal to $v_\alpha = l_{po} f_o = 0{\cdot}49$ m/sec on 7 November and equal to 2·2 m/sec on 5 November; these values are not inconsistent with the wind data described above.

The value of $\sigma_F = 5$ dB chosen for fitting the theory of the Appendix to the observed spectra was selected not only because it provided a satisfactory fit, but also because it was in agreement with estimates of this parameter determined from other so-far-unpublished data analyses. Assuming this value, neglecting the variance of $v_\alpha$, and taking $l_{po} = 120$ m we conclude that the atmosphere at various times and locations may be characterized by characteristic scales, $l_p$, ranging, in 90 per cent of the cases, from 18 to 800 m. Considering this great variability, it is not surprising that it has been difficult heretofore to make adequate direct measurements on the atmosphere supporting these forward-scatter theories.

VOL. 15 1959

## 4. Variations of Refractivity Measured with a Stationary Refractometer

Using a refractometer described in a recent report by THOMPSON and VETTER (1957), direct measurements of refractivity were made with this instrument mounted on a pole at a height above the ground of only 22·1 ft. These measurements were made at a site near the Garden of the Gods at Colorado Springs, Colorado, with a ground elevation of 6430 ft above sea level. The refractivity data consist of simultaneous low-pass recordings using an Esterline–Angus meter and band-pass recordings using a high-speed Sanborn meter. Two periods of record were selected for an analysis of the spectrum of refractivity variations. One was from approximately 2059 to 2123 hours on 24 May 1956, and the other from 0913 to 0956 hours on 25 May 1956.

The method of spectrum computation used in these cases was developed by TUKEY (1949), PRESS and TUKEY (1956) and BLACKMAN and TUKEY (1959), and overcomes the principal objections to the Fourier method discussed previously. In particular, there is no restriction on the number of data points to be used, and the random fluctuation in the spectral estimates is greatly reduced. As programmed for the IBM Type 650 computer, the method yields $m + 1 = 31$ estimates of power density at the frequencies $1/8m\delta$ and $q/2m\delta$, where $q = 1, 2, \ldots, 30$, $\delta$ is the sampling interval in seconds, and $m$ is the maximum lag for which the serial correlation was computed.

Fig. 4 summarizes the spectrum analysis of refractivity variations occurring on the evening of 24 May. Shown here are several sample spectra which together cover as much of the frequency range as the record continuity and filter characteristics would permit. One covers the frequency range from 0·00208 to 0·25 c/s and is

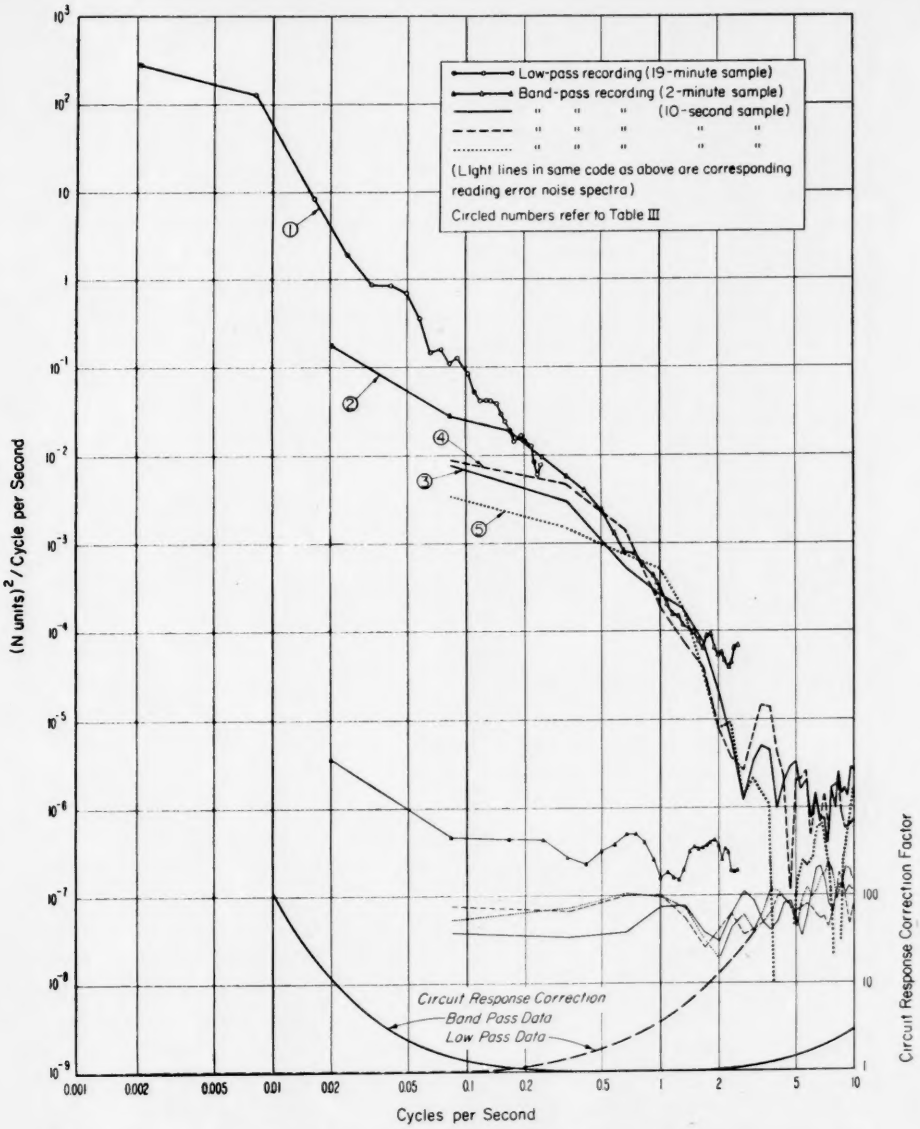


Fig. 4. Power spectrum of refractivity variations. Garden of the Gods site: approximate time, 2059–2123 hours 24 May 1956.

the spectrum of a 19-min sample taken from the Esterline–Angus record. Another covers from 0·0208 to 2·5 c/s and was taken from a 2-min sample of the band-pass Sanborn chart record. In addition, three 10-sec samples from this Sanborn record were analysed to cover the range from 0·0833 to 10 c/s. The spectra of reading and rounding-error noise are shown for the Sanborn data. They were obtained by scaling each record sample twice, and computing by the Tukey method the

spectrum of the differences between corresponding values read in the two trials and allowing for the fact that the expected reading-error variance is just half of the variance of these differences. In these cases the scaling and tabulating was done manually, and shifts in the time scale between the two sets of readings did not constitute a problem. Since the computation involves the serial correlation function for lags from 0 to 30, it differs considerably from the method used in obtaining the reading-error noise spectrum in the phase analysis discussed previously. In the latter case, the serial correlation was computed for lags 1 and 2, and only these values used to determine the form of an autoregressive scheme approximating the actual autocorrelation function. The factors used to correct all of the spectra in this figure and those on Fig. 5 for the recording circuit frequency-response characteristics are plotted at the bottom of the graph.

These sample refractivity spectra are all relatively less reliable at both their low- and high-frequency ends than at intermediate frequencies since we did not sufficiently "pre-whiten" (PRESS and TUKEY, 1956) the records prior to the analysis. The low-frequency end is systematically low since the samples were chosen so that their end points would be about equal, and this tends to lower the low-frequency content; if more "pre-whitening" had been used, this selection would not have been necessary.

Any power in frequency bands higher than the one with its midpoint at $1/2\delta$ c/s, the highest-frequency band taken into account in this process, is added to the computed power in this highest-frequency band and below. This effect will, for these spectra, be most noticeable in the highest-frequency band of each spectrum where, in general, the expected actual power is about half of the observed power. For a more complete discussion of this "aliasing", see PRESS and TUKEY (1956) and BLACKMAN and TUKEY (1959). Also, the reading-error noise is included in the computed spectrum, and since it is relatively constant over the entire spectrum, it is again more noticeable at the high-frequency (low power) end of each spectrum. In fact, it appears to dominate the high-frequency end of the spectra for the 10-sec samples in Fig. 4.

In view of these considerations, it was decided that only the central portion of each should be used in comparing these experimental spectra with the theory. These are shown in Fig. 5, together with the results of a similar analysis performed on data recorded on the morning of 25 May 1956. In both cases the segment comprising the high-frequency end of the composite spectrum is the average of three sample spectra covering that frequency range.

Fig. 5 shows the comparison of these observed spectra with those expected with the log-normally modified $\rho' K_1(\rho')$ correlation function. Note that the effective scales, $l_{po}$, are comparable with those obtained in analysing the Maui phase data; also, the choice $\sigma_F = 5$ dB is evidently satisfactory.

## 5. CONCLUSIONS

Summarizing the above, we have shown that, although atmospheric turbulence is extremely variable, the log-normally modified $\rho' K_1(\rho')$ correlation function may be used to describe the characteristics of refractivity variations as exemplified in three independent kinds of measurement. Furthermore, the existence has been



VOL.
15
1959

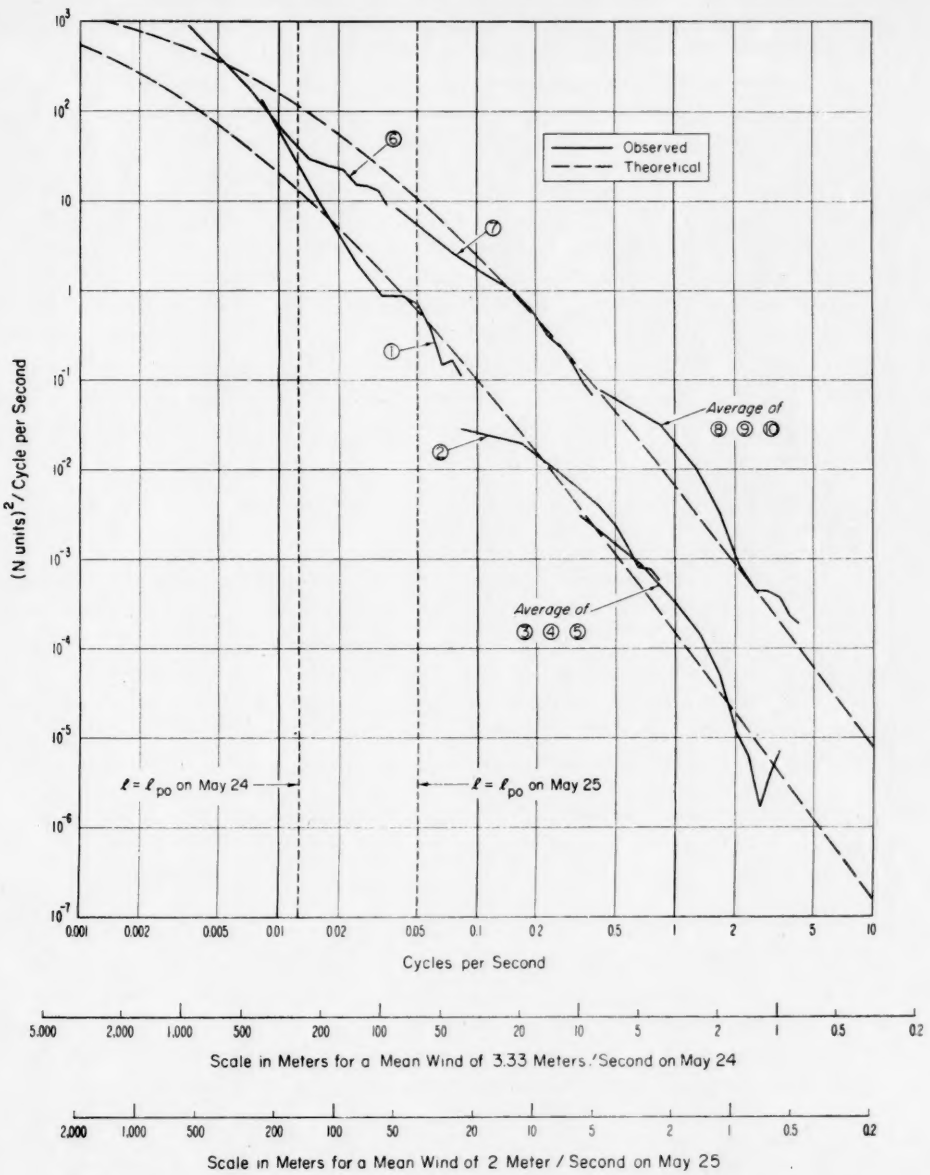
Observed
Theoretical
⑥
⑦
①
②
Average of ⑧ ⑨ ⑩
Average of ③ ④ ⑤
$\ell = \ell_{po}$ on May 24
$\ell = \ell_{po}$ on May 25
(N units)² / Cycle per Second
Cycles per Second
Scale in Meters for a Mean Wind of 3.33 Meters / Second on May 24
Scale in Meters for a Mean Wind of 2 Meter / Second on May 25

Fig. 5. Comparison of observed and theoretical refractivity power spectra. Garden of the Gods site.

established in particular experimental situations of an inertial subrange of blob sizes with a spectrum proportional to the cube of the blob size as predicted in WHEELON's (1957a, b, 1959) analysis. Thus it appears that the "self motion" is the mechanism responsible for the conversion of the pancake-like anisotropic large

blobs into the isotropic smaller blobs which presumably characterize the shorter-wavelength portion of the inertial subrange. In this latter range the time variations in the samples observed are apparently adequately described by the assumption that the "frozen in" turbulent air mass moves relative to the observer with the mean wind, the "self motion" having a negligible influence.

*Acknowledgements*—The research results reported here represent a group effort by a large part of the staff of the Radio Propagation Engineering Division of the National Bureau of Standards, Boulder Laboratories. Some of the key personnel involved in this work were J. W. HERBSTREIT, M. C. THOMPSON, W. E. JOHNSON, C. F. PETERSON, P. L. RICE, K. O. HORNBERG, P. I. WELLS, A. F. BARGHAUSEN, M. J. VETTER, B. R. BEAN, H. B. JANES, R. L. ABBOTT, L. E. VOGLER, ANITA LONGLEY, MARY MATZ, A. W. KIRKPATRICK, F. FREETHEY, W. HARTMANN, R. E. WILKERSON; in addition, E. L. CROW and M. M. SIDDIQUI, Office of the Director of the Boulder Laboratories, assisted with some of the statistical considerations.

*Note added in proof on 8 May 1959*

Recently, experimental data have been reported by THOMPSON and JANES (1959) on the power spectra of the phase variations covering a range of frequencies from 0·0001 to 10 c/s using improved measurement and analysis techniques. For these data the power spectra varied throughout this entire range of frequencies approximately in inverse proportion to the 2·8 power of the frequency. These data are sufficiently improved relative to the data given in the present report so that it appears to be necessary to abandon the assumption (b) in the introduction to this paper, and these new data suggest that the self-motion of the atmosphere exerts a controlling influence on the form of the spectra of the fluctuations of refractivity and of phase with time. A paper is currently being prepared which elaborates on this point of view.

VOL.
15
1959

## APPENDIX

### *A Theory of Atmospheric Turbulence Based on the Log-normally Modified $\rho' K_1(\rho')$ Autocorrelation Function for Describing the Turbulence of Refractivity*

Let $l_p$ denote a characteristic scale of the turbulent refractive-index structure of the atmosphere in the direction that the wind speed, $v_n$, moves the air through an ideal refractometer, i.e. one which does not modify the refractivity characteristics of the atmosphere being measured. We will express $v_n$ in metres per second (m/sec), $l_p$ in metres (m) and their ratio $v_n/l_p \equiv f_c$ in cycles per second (c/s). Assuming the correlation model $\rho' K_1(\rho')$, the autocorrelation function describing the variations of refractivity measured by this ideal refractometer may be obtained simply by setting $\rho' = \tau v_n/l_p \equiv \tau f_c$ with $\tau$ expressed in seconds so that

$$\langle [\Delta n(t, f_c) \cdot \Delta n(t + \tau, f_c)] \rangle = \langle [\Delta n(t, f_c)]^2 \rangle \, \rho' K_1(\rho') \qquad (1)$$

We will further assume that the variation, $\Delta n(t)$, in the refractive index of the atmosphere relative to its mean value, $n_0$, may be expressed as a sum of components, $\Delta n(t, f_c)$, each of which has its own characteristic frequency, $f_c$, and the natural logarithms of these characteristic frequencies are normally distributed about a

mean value $\ln f_{0n}$ with standard deviation, $\sigma_f$. It is convenient to let $F = 10 \log_{10} f_c$, and then $F$ is normally distributed about $F_{0n} = 10 \log_{10} f_{0n}$ with the standard deviation $\sigma_F = (10 \log_{10} e)\sigma_f$ expressed in decibels (dB); a typical value of $\sigma_F = 5$ dB and in this case $\sigma_f = 1{\cdot}1512925$.

This assumption that the characteristic frequencies are log-normally distributed has been made primarily since it makes possible the explanation of experimental data obtained in a wide variety of independent experiments. However this assumption also appears reasonable on physical grounds when $f_c$ is identified as a characteristic frequency at which turbulent energy is introduced into the atmosphere. Thus there must be a continuous input of turbulent energy at each point in the atmosphere. As the wind carries the atmosphere past its environment, the characteristic frequency, $f_c$, of this input energy will change continuously. This will happen by virtue of the fact that the significant environmental factors of the atmosphere, e.g. the surface roughness, the gradient of refractive index, and the instantaneous wind velocity are random functions of location. After the wind has moved a given point in the atmosphere past a representative portion of its environment, this point will have been subject to a wide range of input energies, each resulting in an effective value of $f_c$. Thus, at any specific time, each point in the atmosphere will have associated with it the decaying turbulent energy associated with each of the sources of input energy which have not yet been dissipated by viscosity. In accordance with this picture, each four-dimensional point in the atmosphere will be characterized by the distributions of $f_c$ which have been determined by the environment to which this point was exposed during a preceding time of the order of the dissipation time for a typical source of turbulent energy.

In the frequency band, $df$, the fraction of the total variance, $\langle[\Delta n(t)]^2\rangle$, of refractivity associated with the characteristic frequency, $f_c$, may be considered to be equal to:

$$W_n(f, f_c)\, df = \langle[\Delta n(t)]^2\rangle\, g_n(q')\, dq' \tag{2}$$

where $q' = 2\pi f/f_c$ and $g_n(q')$ is the cosine transform of the autocorrelation function $\rho' K_1(\rho')$:

$$g_n(q') = \frac{2}{\pi}\int_0^\infty \rho' K_1(\rho') \cos(q'\rho')\, d\rho' = [1 + q'^2]^{-3/2} \tag{3}$$

Now the power spectrum of the function $\Delta n(t)$ may be obtained by averaging (3) over all values of $f_c$:

$$W_n(f, \sigma_F)\, df = < [\Delta n(t)]^2 > g_n(q, \sigma_F)\, dq \tag{4}$$

$$g_n(q, \sigma_F)\, dq = \frac{1}{\sqrt{(2\pi)}\sigma_f}\int_0^\infty (1 + q'^2)^{-3/2}\, dq' \exp\left[-\frac{(\ln f_c - \ln f_{0n})}{2\sigma_f{}^2}\right]\frac{df_c}{f_c} \tag{5}$$

where $q = 2\pi f/f_{0n}$. Let $\sqrt{(2)}\sigma_f x = \ln(f_c/f_{0n})$ so that $q' = q \exp(-\sqrt{(2)}\sigma_f x)$ and then (5) becomes:

$$g_n(q, \sigma_F) = \frac{1}{\sqrt{\pi}}\int_{-\infty}^{+\infty} \{1 + q^2 \exp[-2\sqrt{(2)}\sigma_f x]\}^{-3/2} \exp[-\sqrt{(2)}\sigma_f x - x^2]\, dx \tag{6}$$

The function $g_n(q, \sigma_F)$ was evaluated numerically using the I.B.M. 650

computer, and is shown graphically on Fig. 6 as a function of $q$ for several values of $\sigma_F$. Note that for sufficiently large values of $q$:

$$g_n(q, \sigma_F) \simeq q^{-3} \exp(2\sigma_f^2) \tag{7}$$

The above theory applies to an ideal refractometer. Any actual refractometer will tend to filter the received signals, and this filtering action may be allowed for in practice by multiplying the right-hand side of (4) by the filter response function

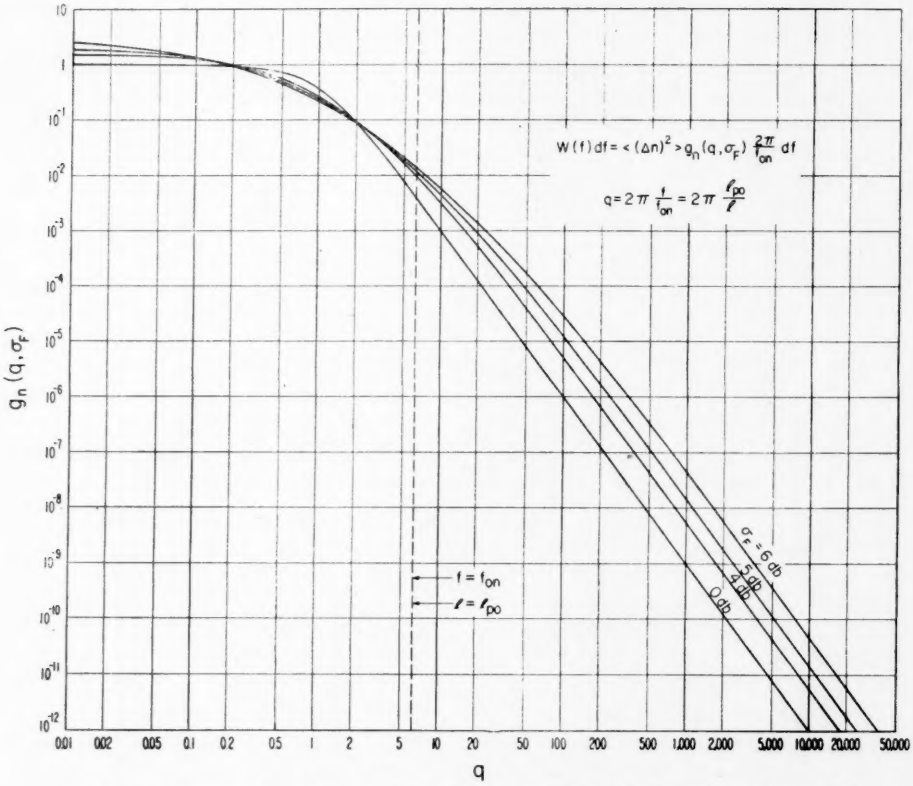


Fig. 6. The spectrum of refractivity for the log-normally modified $\rho' K_1(\rho')$ autocorrelation function.

$R(f)$. The refractometer used in making the measurements described in this paper could be used either as a low-pass or as a band-pass filter; the low-pass filter response, $R(f)$, was down by 3 dB at an upper cut-off frequency $f_u = 0{\cdot}5$ c/s while the band-pass filter response was down by 3 dB at the lower cut-off frequency $f_a = 0{\cdot}4$ c/s, and at the upper cut-off frequency $f_b = 40$ c/s. Thus the measured mean square value of the refractive index was less than its actual value:

$$\langle[\Delta n(t)]^2\rangle_m = \langle[\Delta n(t)]^2\rangle \int_0^\infty g_n(q, \sigma_F) R(f)\, dq \tag{8}$$

For the low-pass filter the integral in (8) is of the order of unity whereas for the band-pass filter this integral is less than 0·01 in many cases.



VOL. 15 1959

We will consider next the variations of the phase of a radiofrequency carrier generated by a source of constant frequency with free-space wavelength, $\lambda$, as received over a line-of-sight path of length $L$. Let $l_e$ denote a characteristic scale of the turbulent refractive-index structure in the direction that the wind speed, $v_\alpha$, moves the air normal to the path at some point along the path. We will assume,

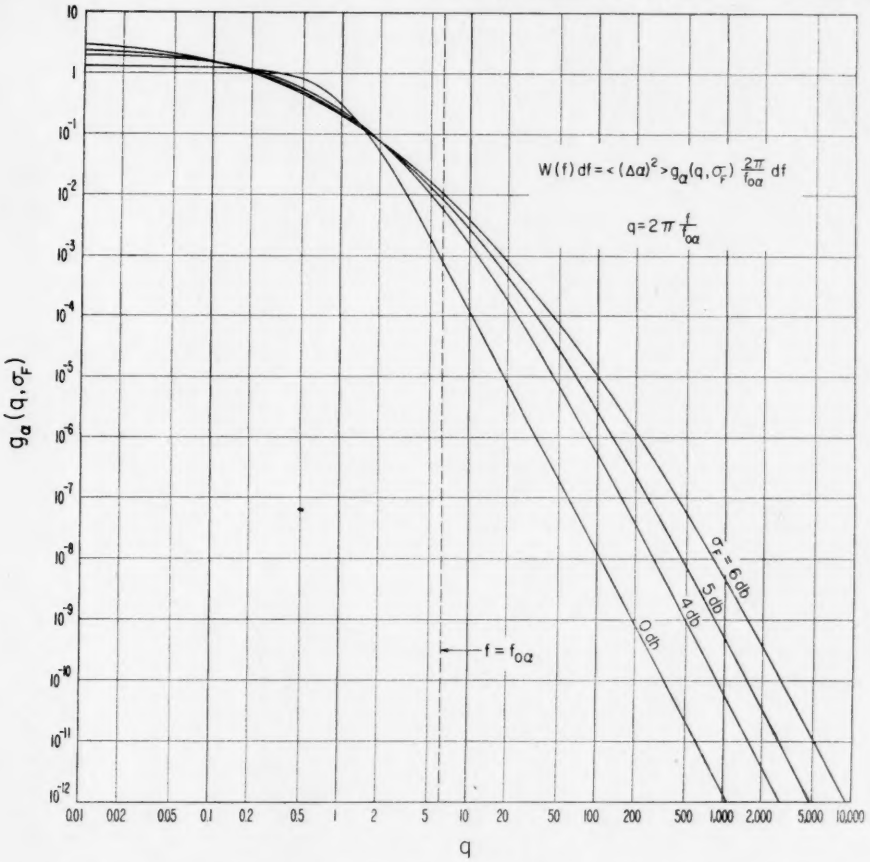


Fig. 7. The spectrum of phase for the log-normally modified $\rho' K_1(\rho')$ autocorrelation function.

as before, that the natural logarithm of the ratio $v_\alpha/l_e = f_c$ is normally distributed about a mean value $\ln f_{0\alpha}$ with standard deviation $\sigma_f$. Assuming, as before, that (1) represents the autocorrelation model for a given value of $f_c$, then it can be shown by methods similar to those used by WHEELON (1957b) and MUCHMORE and WHEELON (1955)* that the autocorrelation function describing the variations of phase with characteristic frequency, $f_c$, may be expressed:

$$\langle[\Delta\alpha(t, f_c) \cdot \Delta\alpha(t + \tau, f_c)]\rangle = \langle[\Delta\alpha(t, f_c)]^2\rangle(1 + \rho') \exp(-\rho') \qquad (9)$$

where $\rho' = \tau v_\alpha/l_e = \tau f_c$ and $\langle[\Delta\alpha(t, f_c)]^2\rangle = 4\pi^3\langle[\Delta n]^2\rangle l_e L/\lambda^2$.

* See also footnote 12 of NORTON (1956).

In the frequency band, $df$, the fraction of the total variance, $\langle[\Delta\alpha(t)]^2\rangle$, of phase associated with the characteristic frequency, $f_c$, may be considered to be equal to:

$$W_\alpha(f, f_c)\, df = \langle[\Delta\alpha(t)]^2\rangle\, g_\alpha(q')\, dq' \tag{10}$$

where $q' = 2\pi f/f_c$ and $g_\alpha(q')$ is the cosine transform:

$$g_\alpha(q') = \frac{2}{\pi}\int_0^\infty (1 + \rho')\exp(-\rho')\cos(q\rho')\, d\rho' = \frac{4}{\pi}[1 + q'^2]^{-2} \tag{11}$$

The power spectrum of the function $\Delta\alpha(t)$ may be obtained by averaging (10) over all values of $f_c$:

$$W_\alpha(f, \sigma_F)\, df = \langle[\Delta\alpha(t)]^2\rangle\, g_\alpha(q, \sigma_F)\, dq \tag{12}$$

$$g_\alpha(q, \sigma_F) = \frac{4}{\pi\sqrt{\pi}}\int_{-\infty}^{+\infty}[1 + q^2\exp(-2\sqrt{2}\,\sigma_f x)]^{-2}\exp(-\sqrt{2}\,\sigma_f x - x^2)\, dx \tag{13}$$

where $q = 2\pi f/f_{0\alpha}$. The function $g_\alpha(q, \sigma_F)$ was evaluated numerically and is shown graphically on Fig. 7. Note that for sufficiently large values of $q$:

$$g_\alpha(q, \sigma_F) \simeq \frac{4}{\pi} q^{-4}\exp(4{\cdot}5\,\sigma_f{}^2) \tag{14}$$

Phase measurements were made with a low-pass filter for which the upper effective cut-off frequency was $f_u = 1{\cdot}4$ c/s, and on a band-pass filter with effective cut-off frequencies of $f_a = 0{\cdot}04$ and $f_b = 1{\cdot}4$ c/s. The measured variance of phase, $\langle[\Delta\alpha(t)]^2\rangle_m$, was less than the actual value by the factor:

$$\frac{\langle[\Delta\alpha(t)]^2\rangle_m}{\langle[\Delta\alpha(t)^2\rangle} = \int_0^\infty g_\alpha(q, \sigma_F)R(f)\, dq \tag{15}$$

For the low-pass filter the integral in (15) is of the order of unity, but for the band-pass filter this integral is less than 0·01 in many cases.

VOL. 15 1959

## REFERENCES


| | | |
|---|---|---|
| BEAN B. R. | 1953 | *Proc. Inst. Radio Engrs. N.Y.* **41,** No. 4, 549. |
| BLACKMAN R. B. and TUKEY J. W. | 1959 | *The Measurement of Power Spectra from the Point of View of Communications Engineering.* Dover Publications, New York. |
| BOOKER H. G. and GORDON W. E. | 1957 | *Proc. Inst. Radio Engrs., N.Y.* **45,** No 9 1223 |
| DINGER H. E., GARNER W. E., HAMILTON D. H., JR. and TEACHMAN A. E. | 1958 | *Proc. Inst. Radio Engrs., N.Y.* **4b** 1401 |
| GALLET R. | 1955 | *Proc. Inst. Radio Engrs., N.Y.* **43,** No. 10, 1240. |
| HERBSTREIT J. W. and THOMPSON M. C. JR. | 1955 | *Proc. Inst. Radio Engrs., N.Y.* **43,** No. 10, 1391. |
| MUCHMORE R. B. and WHEELON A. D. | 1955 | *Proc. Inst. Radio Engrs., N.Y.* **43,** No. 10, 1437. |
| NORTON K. A. | 1956 | *Trans. Inst. Radio Engrs., N.Y.* CS-4, 39; NBS Report 3562. |

| | | |
|---|---|---|
| Norton K. A., Rice P. L. and Vogler L. E. | 1955 | *Proc. Inst. Radio Engrs., N.Y.* **43,** No. 10, 1488. |
| Press H. and Tukey J. W. | 1956 | Bell Telephone System Monograph No. 2606. |
| Rice P. L., Longley A. G. and Norton K. A. | 1959 | *Prediction of the Cumulative Distribution with Time of Ground Wave and Tropospheric Wave Transmission Loss.* NBS Technical Note No. 15, July, Office of Technical Services, U.S. Dept. of Commerce, Washington 25, D.C. |
| The Rocket Panel | 1952 | *Phys. Rev.* **88,** No. 5, 1027. |
| Staras H. | 1955 | *Proc. Inst. Radio Engrs., N.Y.* **43,** No. 10, 1374. |
| Staras H. | 1957 | *Trans. Inst. Radio Engrs., N.Y.* AP-5, No. 2, 228–231. |
| Thompson M. C. and Janes H. B. | 1959 | *J. Res. Nat. Bur. Stand.* 63D, July–August. |
| Thompson M. C., Jr. and Vetter M. J. | 1958 | *Rev. Sci. Instrum.* **29,** No. 12 |
| Tukey J. W. | 1949 | *The Sampling Theory of Power Spectrum Estimates.* Symposium on Applications of Autocorrelation Analysis to Physical Problems, Woods Hole, Massachusetts, 13–14 June 1949. Office of Naval Research, Washington, D.C. |
| Villars F. and Weisskopf V. F. | 1955 | *Proc. Inst. Radio Engrs., N.Y.* **43,** No. 10, 1232. |
| Wheelon A. D. | 1957a | *Phys. Rev.* **105,** No. 6, 1706. |
| Wheelon A. D. | 1957b | *J. Appl. Phys.* **28,** No. 6, 684. |
| Wheelon A. D. | 1959 | *J. Res. Nat. Bur. Stand.* 63D, September–October. |

Journal of Atmospheric and Terrestrial Physics, 1959, Vol. 15, pp. 228 to 247. Pergamon Press Ltd. Printed in Northern Ireland

## SESSION II

CONVECTION AND INHOMOGENEITIES

# Convection and refractive index inhomogeneities

V. G. PLANK*

### 1. INTRODUCTION

THIS paper will review certain observations and theories in the field of cumulus convection and attempt to integrate them into a more or less comprehensive picture. The picture will then be interpreted in terms of refractive index structure.

### 2. CONCEPTS OF CONVECTION

*Parcel method*

The first quantitative model of cumulus cloud growth was the so-called "parcel method" developed by REFSDAL (1930). This method assumed that parcels (or convective cells) would appear in non-saturated air whenever the actual lapse rate of temperature exceeded the dry adiabatic lapse rate (about 10°C/km), or in saturated air whenever the actual lapse rate of temperature exceeded the moist adiabatic lapse rate (approximately 6°C/km). This is the cumulus cloud case.

The parcel, which was completely unspecified as to its physical properties, was assumed not to interact in any way with the surrounding air. Its buoyancy, vertical velocity, total distance of rise, and the excesses of parcel temperature and moisture content over that of the environment were assumed to be completely determinate from a meteorological sounding of the atmosphere and a thermodynamic diagram.

In practical forecasting, this "parcel method" has been extensively used to predict the time of cumulus formation and the degree and rate of growth. The method has been fairly successful, although more and more difficulties have become apparent as our observations of cumulus improved.

*Slice method*

The earliest recognized, and one of the principal defects of the parcel method was the assumption of an undisturbed environment. In an attempt to cure this fault, BJERKNES (1933, 1938), devised the so-called "slice method". This method considered mass continuity, taking into account the fact that masses of air carried upward in the convective cells, i.e. in the cumulus coluds, must be compensated by a counter-balancing descent of air in those clear regions between clouds. The

* Geophysics Research Directorate, Air Force Cambridge Research Center, Air Research and Development Command.



VOL. 15 1959

primary assumptions inherent in the method were that the atmosphere was initially barotropic and that all motions were adiabatic above the surface layers. In practice, the method involved the consideration of a thin slice of the atmosphere, containing convective cells with clear regions between, and an application of the circulation theorem of BJERKNES to determine the rate of change of circulation in the slice. This rate of change measured the layer stability of the atmosphere within the confines of the slice. Other slices were made at altitude levels above and below that of the initial slice and, in this manner, the stability picture of the atmosphere above the local area could be constructed. Stable and unstable layers for rising parcels were redefined, by application of thermodynamic theory, and new criteria for cumulus formation and growth were defined.

As a forecast tool the slice method proved to be much too complicated; and the intended improvement over the "parcel method" was not realized.

*Entrainment*

With the extensive observations and aircraft flight measurements that occurred during and after World War II, it became obvious that both the "parcel" and the "slice" methods were seriously inadequate. For one thing, the majority of cumuli terminated far below the level predicted from parcel considerations. For another, the lapse rate of temperature within clouds was found to be greater than the moist adiabatic lapse rate, which means that the difference in temperature between cloud interior and environment was less than the theoretical. Also, liquid water contents were much smaller than predicted.

DL.
15
959

These observations pointed out one of the chief defects of the two methods. Vertically rising currents, parcels or jets cannot be considered as isolated from their surroundings. A continual mixing between rising air and the environment occurs. In fact, one can demonstrate that lateral mixing, or entrainment, is a required feature of all convective currents of the type observed in the atmosphere. This has been done by STOMMEL (1957), AUSTIN (1951), and others. Without entrainment, atmospheric convective currents would violate the law of mass continuity.

In the first attempts to describe quantitatively the entrainment process, it was assumed that a real atmospheric convective current could be likened to a "jet stream," and that the theories of TOLLMIEN (GOLDSTEIN, 1938) (aerodynamics) and ROSSBY (1936) (oceanography) would apply. The basic idea of the "jet stream" is that whenever a jet, or current of fluid, moves through a large body of fluid at rest there is entrainment of surrounding fluid into the moving fluid so that the total mass subjected to motion increases with distance down stream. Fig. 1 shows the streamlines associated with a "jet stream".

STOMMEL (1947) at Woods Hole Oceanographic Institution, was the first to modify the jet stream theories and apply them to convective currents. HOUGHTON and CRAMER (1951) at Massachusetts Institute of Technology, later worked out the theoretical details of an atmospheric convective jet model and BUNKER (1953) modified the Houghton–Cramer model and used it in a study comparing theory and observation. He demonstrated that the model did explain many of the observations.

AUSTIN (1948) and AUSTIN and FLEISHER (1948) also of MIT, used the entraining jet concept to work out a circulation model for a cumulus cloud. They used observed cloud temperatures and LWC's to compute the amount of entrainment for various assumed updraft velocities and environmental conditions. Essentially, they applied the "jet stream" to the cumulus cloud in the manner shown in Fig. 1.

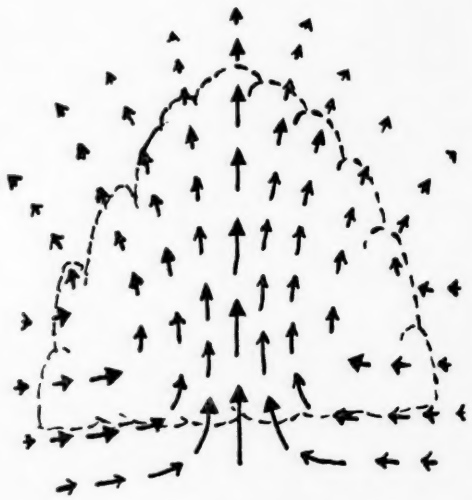

Fig. 1. Sketch of an entraining jet.

The principal findings of this and other work on entrainment have been summarized by Austin (1948) as follows:

1. With entrainment, the theoretical lapse rate of temperature within cumulus clouds is much closer to actual than it is with the moist adiabatic ascent assumption of the parcel method. This is because the mixing of drier air from the surroundings into the moist ascending air of the cumulus reduces the cloud temperature (through evaporation or the reduction of condensation) and thereby reduces the degree of instability.
2. With entrainment, the theoretical LWC's of the air at altitudes above the condensation level are much closer to actual than they are when using the parcel method.
3. With entrainment, the growth of cumulus clouds is governed in an important part by the state of the environmental surroundings, i.e. if during its growth the cloud penetrates a dry environment or a dry layer, then additional growth will be retarded or may be completely stopped.
4. With entrainment, the cloud is in an unstable state and highly turbulent. The average lapse rate of temperature within the cloud is considerably in excess of the moist adiabatic (in fact, it more closely resembles that of the environment), yet each air parcel within the cloud that is actively condensing and rising will cool at a lapse rate intermediate between the average of the cloud and the moist adiabatic. The parcel will rise until its buoyancy is destroyed by mixing, and the rising of innumerable parcels contributes to a highly turbulent state in the cloud interior.

During and subsequent to the major work on entrainment, various observations were made that further verified the general soundness of the concepts just reviewed. For example, various people at the University of Chicago, the Woods Hole Oceanographic Institution, the Radiophysics Laboratory, Commonwealth Scientific and



VOL.
15
1959

Industrial Research Organization, Sydney, Australia and the Air Force Cambridge Research Center flew aircraft through cumulus clouds and obtained data showing that temperatures in clouds generally fluctuated only a few tenths of a degree from ambient, with occasional places in the cloud fluctuating some 1°–4°C. More refined measurements of LWC again verified that they were much less than those computed on the basis of moist adiabatic ascent of a parcel from cloud base. Various synoptic studies of aircraft cloud observations (mainly by the University of Chicago) also revealed that cloud growth and altitude extent are indeed dependent on the state and structure of the environment, primarily on its moisture content.

*Bubble theory of convection*

Until 1953, the emphasis in convection work was slanted toward cloud scale circulations. However, in that year, SCORER and LUDLAM (1953) initiated a new concept of the convection process with the presentation of their "bubble theory of penetrative convection". This theory emphasized and described the smallest element of convection, the photon or bubble. Briefly, the bubble theory is as follows:

It is assumed that the unit of convection is a bubble of buoyant air which sheds its outer skin steadily into a turbulent wake. It is further assumed that the air above the bubble is lifted (and cooled) as the bubble approaches and that it drains down around the outside of the bubble, with the air close to the bubble being mixed into the wake. If the bubble air is unsaturated, the wake air is buoyant, but if it is saturated the wake air may have negative buoyancy (a product of evaporation). A Scorer–Ludlam bubble is shown in Fig. 2.

The bubble also entrains air from the environment. Thus, its life span is in a large measure controlled by the environmental conditions through which it is passing.

SCORER and LUDLAM also hypothesized that bubbles in the real atmosphere just above the ground are very small, that they are formed over local heat or moisture anomalies, and that their breakaway from the surface is aided by a gentle wind drift. As the bubbles rise above the ground, they aggregate into larger ones, the larger ones tending to pull the smaller ones into their wake, presumably through the action of aerodynamic drag forces. They also point out that the warm, moist channels left in the environment by the wakes of previous bubbles are preferred channels for the later passage of other bubbles. These two situations are also indicated in Fig. 2.

As the more favoured bubbles continue to ascend into the atmosphere, they progressively enter regions of fewer and fewer other bubbles and, consequently, above a certain level they no longer collect other bubbles. At this time, they are penetrating previously undisturbed air and they continually waste away as they proceed up. The bubble either wastes away completely, spreads out below a temperature inversion that it cannot penetrate, or passes through the condensation level and acquires a new source of buoyancy through release of the latent heat of condensation.

*Evidence supporting bubble theory*

There is much evidence to support the general framework of the Scorer–Ludlam theory. The precise details of bubble structure and circulation and the mode of bubble interaction with the environment are still unknown, but there is little question that bubbles, in some form, are present in the lower atmosphere and that bubbles are the primary building blocks for cumulus formation and growth. We might review some of this evidence.

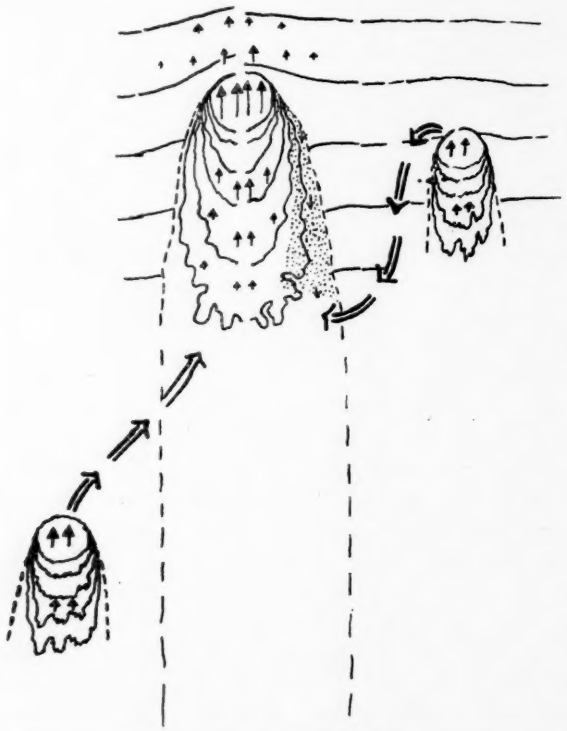

Fig. 2. Velocity field around a rising Scorer–Ludlam bubble and schematic representation of paths of small bubbles relative to that of the larger one. The left half of the large bubble refers to dry ascent; the right half refers to ascent after saturation; and the shaded area represents the region of the wake in which there is sinking motion (after SCORER and LUDLAM 1953).

Observations made by glider pilots provide the best clue as to the nature of convective bubbles below cloud base. They report (YATES, 1953; WELCH, 1953; LUDLAM and SCORER, 1953; Group Discussion on Convection, 1953) that thermals generally exist below most cumulus clouds and there is more or less general agreement that the thermals are of two types: (a) a rather steady updraft into cloud base and (b) updrafts that are intermittent.

The intermittent drafts are definitely bubble-like, and they appear to have horizontal as well as vertical components of motion. Several pilots have managed to stay in such an updraft by clever or fortuitous shifting of their position with



VOL.
15
1959

respect to cloud base, i.e. they stayed in the updraft by correctly forecasting its lateral motion.

Regarding the nature of the thermals encountered by glider pilots, they report the average thermal to be some 1000 ft in diameter at altitudes above 1000 ft and as much as 3000–4000 ft in diameter higher up. Temperatures inside the thermal are 1°–2°F warmer than ambient at the same level. Updraft velocities, as deduced from variometer readings, range up to 15 ft/sec, depending on the day. The updraft is usually steady and major up and down surges within the thermal are not felt. A ring of turbulence and a down-current are clearly evident around the boundary of most thermals and the vertical extent of the thermal is usually several times its diameter. A glider riding such a thermal is buoyed up, strongly at first, then less and less strongly. However, quite frequently before buoyancy is lost completely, a new updraft commences. It is as if successive bubbles are rising up a vertical column.

Sometimes a glider pilot has no difficulty in riding a thermal from below cloud base right up into the cloud. Other times he can get close to the base but not up into the cloud. There apparently is considerable variance in the character of inflow into the cumulus. Certain pilots have reported that the inflow sometimes occurs in one localized area of the cumulus base and that this area is characterized by a hollow in the otherwise flat undersurface. Such hollow may extend as much as 200 ft up into the cumulus.

OL.
15
959

The frequency of occurrence of thermals and their nature have been found to depend primarily on the underlying terrain, on the solar altitude, on the wind velocity and on the wind shear. On an average day over average terrain, the frequency of thermals is about one per 5–15 min per $\frac{1}{2}$ mile$^2$. Terrain with considerable contrast in the way of fields, shrubs and trees produces more thermals than level uniform terrain. Similarly, a hilly region is favourable. The wind has considerable effect. On a calm day, there are few thermals. On a day with light wind, the thermals are rather evenly distributed and have the structure described previously. On a windy day, the thermals tend to be lined up in rows that are oriented up–down wind. Shear of the wind with altitude apparently distorts the bubbles so that their cross-sections are smaller than normal, their lengths are increased, and their long axes lean away from the vertical.

This is the picture above 1000 ft. (However, we must remember that glider pilots are primarily concerned with the larger soarable thermals and that their descriptions may thus be biased.)

Below 100 ft, the picture of thermal structure is even more qualitative. Glider pilots report that soaring thermals are virtually impossible to find, that most updrafts are of small extent and short duration, and that their frequency of occurrence is much higher than at higher altitudes. Evidence revealed by soaring birds and dragonflies (Group Discussion on Convection, 1955; Scorer, 1954) shows: (a) that, in sunshine with no wind, air in the first few metres appears to stream steadily upward from fixed places; (b) that, in sunshine with wind, agglomerations of many small surface thermals periodically rise from the ground, form rather compact masses (bubbles) and continue upward; (c) that convection develops upward (i.e. soaring birds take to the air in the order of their wing

loading, the most heavily loaded ones also being the highest soarers); (d) that thermals are wider and stronger at the higher altitudes and that they react more slowly to surface sun-shadow effects near the ground; and (e) that when convection is intense, the boundaries of the thermals are more sharply edged.

Birds seem to have an uncanny ability to stay within a small thermal and to shift quickly to another one when the original has lost its updraft. Observations of such birds indicate the approximate duration of the thermals to be about 2 min and the lateral extent of the updraft a distance of some tens to a few hundreds of feet.

Other observations also support the general picture of the convective region hypothesized by SCORER and LUDLAM. The most complete are probably those made in England by JAMES (1953, 1954). JAMES made rapid-response aircraft measurements of temperature and humidity as functions of distance below cumulus cloud base and found that the atmosphere could be roughly broken into three main regions:

(a) In the lowest 500–1000 ft above the surface, where the lapse rate of temperature is superadiabatic to some degree, there is a region of intense turbulent mixing, where temperature and humidities fluctuate considerably (some 1°–2°F in temperature). Many parcels (or bubbles) of warm moist air apparently exist in a wide range of sizes.

(b) Between 500–1000 ft and 2500 ft, where the lapse rate of temperature is adiabatic, the temperature–humidity fluctuations are considerably damped over those below 500 ft. For the most part, there is a slow variation of ambient air temperature, broken sporadically by small rapid fluctuations of temperature of the order of 0·1°–0·2°F, lasting over 500–1000 ft distances. Good agreement was noted between the frequency of occurrence of such temperature bursts and the position of cumulus clouds overhead. Other temperature fluctuations lasting over 3000–5000 ft distances were also detected on occasion.

(c) Just below cloud base there is a region called the sub-cloud layer. This is a stable layer that is some 200–400 ft thick. It exists predominantly in the clear regions between clouds after cumulus activity has progressed for some little time. (The existence of this sub-cloud layer was first noted by BUNKER, *et al.* (1949) in observations of trade wind cumulus. Others have also verified its presence.)

Our Unit at the Air Force Cambridge Research Center has also made temperature and refractive index measurements just below cloud base. These data have not yet been analysed, but a casual examination indicates that conditions are sometimes stable. Other times, the presence of bubbles below cumulus is revealed. One pass, made over the British West Indies just beneath cloud base, revealed the presence of seven bubbles below a single cloud. The bubbles ranged in size from 150 to 620 ft; their temperatures were some 1°–2°C warmer than ambient. No bubbles existed in the clear area between clouds.

We see that there is rough qualitative agreement between the observations of of the glider pilots, the aircraft measurements, and the conditions postulated by SCORER and LUDLAM.



VOL. 15 1959

## 3. The Building of Cumulus Clouds

*Initial and subsequent development in an atmosphere without wind shear*

Now let us consider what happens to the bubbles that reach the condensation level and how they act to form cumulus clouds. Fig. 3 shows cumulus clouds at various stages in their development. The sketches and the following discussion combine observation, theory and personal presumption. (A review of convection is necessarily subjective, since present knowledge is sketchy and disconnected.)

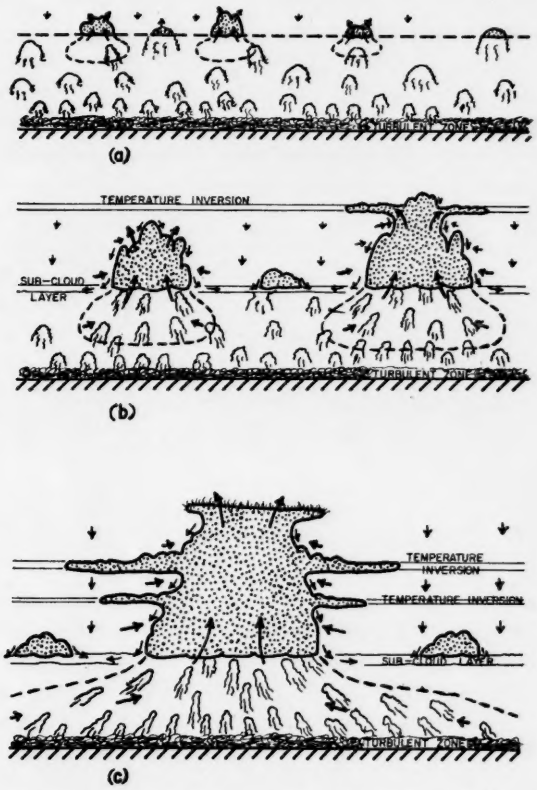


Fig. 3. The several stages of cumulus development in an atmosphere without wind shear. Arrows indicate air motions; dashed lines show the cross-sectional areas of bubble-gathering influence. (a) Early morning; (b) Mid-morning–noon; (c) Noon–afternoon.

In the morning, as the more favoured bubbles first reach the condensation level, they form small puffs of cloud. Some of these puffs subsequently develop, some do not. Apparently, the initial stage of cloud formation under average conditions is pretty much of a statistical process. A volume of air that is moving along at the condensation level and happens to have a bubble move into it and then is further favoured by the reception of other bubbles is likely to develop into a small cumulus cloud. However, another adjacent volume of air that only receives single bubbles at infrequent intervals is not likely to develop.

As a cumulus grows from a small size (perhaps a critical size) it tends to develop more and more of a circulation of its own. Accompanying this strengthened circulation, there is a slight lessening of the atmospheric pressure at levels below the cloud and, as the process proceeds, the cloud becomes more capable of reaching further and further down into the convective region below and diverting or, so to speak, "pulling in" more and more bubbles to feed its subsequent growth. As the cloud grows so does its sphere of bubble gathering influence (as indicated by the areas inside the dashed lines in Fig. 3).

Presumably the gross cloud circulation is similar to the entraining jet model described earlier, with one major exception. That is that evaporation-produced down-drafts exist over most of the cumulus just at the air–cloud boundary (MALKUS, 1955), down-drafts in the sense of a mean motion.

It has been pointed out by SCORER, MALKUS and LUDLAM that the major portion of a visible cumulus is composed primarily of cloudy air from the wakes of bubbles that have risen through the cloud region. They also point out that new bubbles may develop within the cumulus as a result of the spotty release of the latent heat of condensation. Thus, in the mid-morning picture (Fig. 3b) we have bubbles from the convective region entering the sphere of influence of the cumulus and rising into the cloud base. These bubbles may be sufficiently moist and buoyant to proceed all the way up through the cloud or they may enter and be reformed into new ones as latent heat is released.

VOL.
15
1959

This picture of cumulus-cloud mechanics at this stage of development has been deduced primarily from time-lapse pictures of actively growing cumuli and from aircraft measurements made in conjunction with the picture taking. Most of this work has been accomplished at the Woods Hole Oceanographic Institution. A strip of their film that demonstrates the bubble process rather nicely is shown in Fig. 4.

Continuing to develop our picture of convection, we come to a consideration of the sub-cloud layer. The sub-cloud layer is a complicated product of various factors (see BUNKER *et al.*, 1949, 1954; LUDLAM, 1953) but two of the primary ones would appear to be: (a) subsidence of air in those clear regions between clouds as required for the maintenance of mass continuity; and (b) the drainage of cool air down the sides of the cumulus. This cool air presumably moves down to cloud base and spreads out below, serving to intensify the inversion created by subsidence.

The sub-cloud layer should be well formed in those clear areas between clouds after cumulus activity has been going on for some time. Eventually, the layer might become sufficiently thick and stable so that it would prevent new cumulus growth, or seriously impair the continued growth of the smaller existing cumuli because, as the layer intensified, it would slowly choke off the circulation and retard the rate at which these clouds acquire new bubbles.

Also, in the early and mid-afternoon periods, the rising cumulus tends to moisten those temperature-inversion layers that it encounters in the ambient atmosphere as it climbs upward. Each inversion acts as a barrier to the upward growth of a cumulus and, until it "batters its way through", all up-coming bubbles tend to spread out laterally underneath the inversion (see Fig. 3c). The more intense and thick the inversion is, the greater the lateral spreading of moist air.

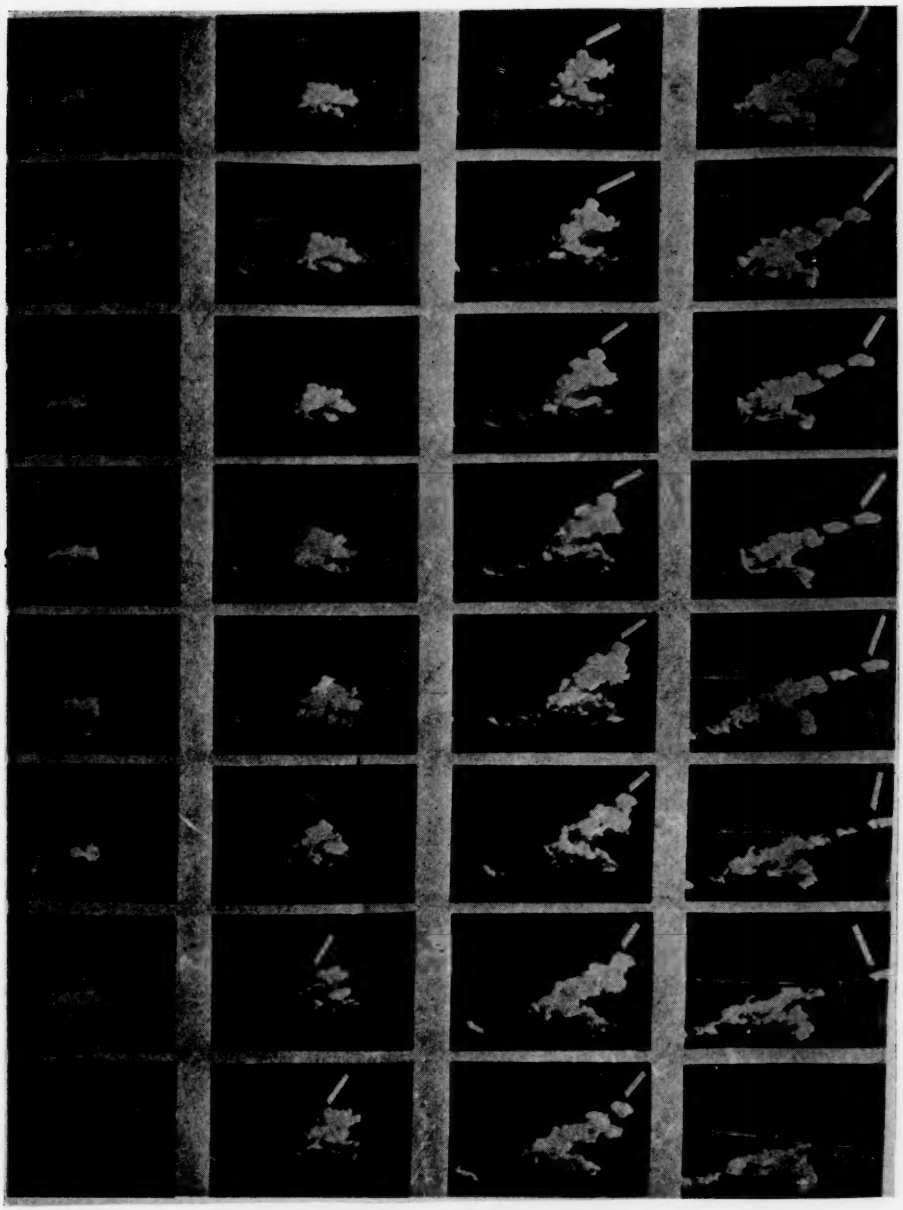

Fig. 4. Series of time-lapse photographs of a cloud over Nantucket Island on 14 August 1950. Successive positions of a particular bubble are indicated by the white arrow. Wind shear on this day was very high, 5m/sec per km (this figure is a reproduction of Fig. 3 in MALKUS and SCORER, 1954).

VOL.
15
1959

*Effects of wind shear*

Thus far we have not considered the effects of wind shear on the cumulus. There are two primary effects, recently described by MALKUS (1949, 1952).

First, in a field of wind shear, the cumulus, in rising from a lower level to a higher one, tends to conserve its original horizontal momentum and carry it into the upper level. If wind speeds increase with altitude, which is the usual case, then that part of the cumulus which is at the higher level becomes a partial barrier for the environmental winds at this level. These winds are forced to go around and over the cumulus top. In fact, some of our aircraft data indicate that on occasion part of the flow may be diverted downward near the up-shear cloud boundary.

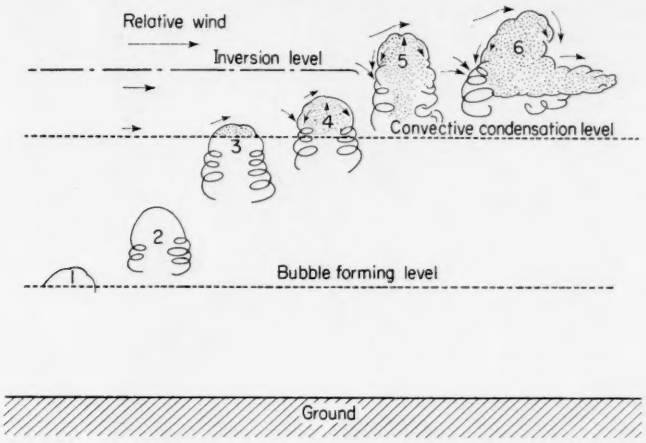


Fig. 5. Stages in the development of a "one bubble" cloud. Above the condensation level, the wake and "skin" of the cloud may fall relative to the ground and to the bubble head because of the cooling effect at the evaporating cloud-clear air boundary. When the cloud rises through a subsidence inversion with wind shear, observations indicate that it acts as a partial block to the upper winds. These winds are forced over and around the cloud, with some of the dry air from above the inversion moving dynamically downward at the up-shear edge.

This occurrence is illustrated in Fig. 5. (On the particular day to which Fig. 5 applies, a subsidence inversion existed at about 10,000 ft altitude. Aircraft passes made just below inversion level revealed the presence of very warm dry air at the up-shear boundary of the cumuli that were penetrating this inversion. Thermodynamic considerations show that this air could only have come from above the inversion; i.e. air from above the inversion was being forced dynamically downward at the up-shear cloud boundary.)

Another effect of wind shear is that the trajectories of bubbles rising through the cloud are slanted from vertical. Clouds building through a field of wind shear build on the up-shear side and decay on the down-shear side. This effect is especially evident in Fig. 4.

The distorting effect of wind shear is also evident in data taken during aircraft traverses made in the up-shear–down-shear direction through cumulus. Such traverses have been made at Woods Hole, at the University of Chicago, and by ourselves. On entering the up-shear side of a cumulus, there is a relatively narrow

transition zone some 100–1000 ft wide (depending on the state and size of the cloud) separating those air properties characteristic of the environment from those characteristic of the cloud. There are also one or two sharp turbulent bumps. The interior region is a relatively homogeneous medium of temperature and vapour content and is moderately turbulent. On exit on the down-shear side, the transition zone is much wider (of the order of 500–3000 ft), and the region of sharp turbulence is likewise wider. ACKERMAN (1957), at the University of Chicago, has shown that this turbulent field extends for a considerable distance outside of the visible cumulus in the down-shear direction.

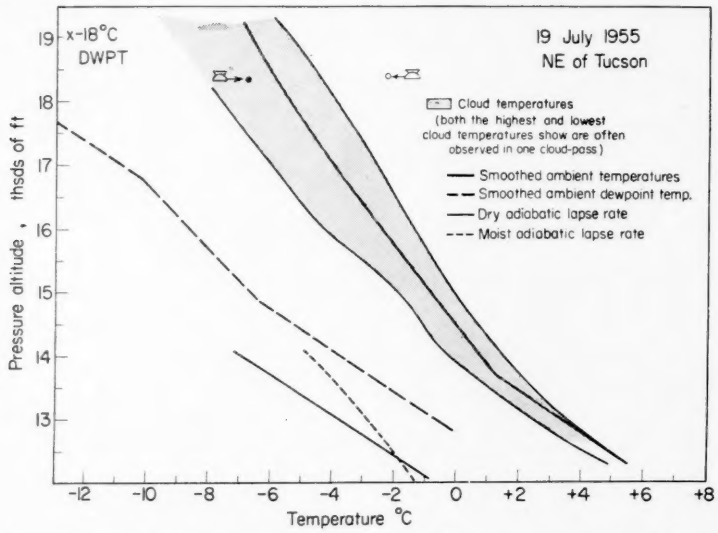


Fig. 6. Envelope of cloud temperatures observed during some thirty cloud passes on 19 July 1955. Solid line within shaded envelope shows the smoothed ambient temperatures.

All of the above effects are, of course, superimposed on the simple convective picture presented in Fig. 3.

One final point should be made before leaving the subject of convection and getting into refractive index inhomogeneities. This is that the clear areas between cumulus are, in general, relatively free of important temperature–humidity fluctuations or turbulence (CUNNINGHAM *et al.*, 1956; BUNKER, 1952).

*Refractive-index structure of convective regions*

Now we may ask, just what does all of the above imply about the refractive-index structure of convective regions? First let us consider the simple cumulus cloud. We have seen that the temperature within such a cloud is generally within 1°–2° of ambient. Data from flights made by our Unit also indicate that certain clouds are predominantly colder than ambient; others are warmer.* But the

* Sharply-defined, solid-appearing, actively-rising clouds are, in general, predominantly warm; whereas clouds with ill-defined, wispy boundaries, that look "washed out," tend to be cold. Individual protuberances (rising bubbles) at the tops of clouds may have a hard, solid appearance, yet be either warm or cold. (We have penetrated a number of cold bubbles at the tops of cumulus with our aircraft. Apparently they are rising due to momentum, having lost their buoyancy at some lower level.) Instrument traces for aircraft penetrations through both warm and cold clouds are shown in Fig. 8 (far left).

average temperature for a number of clouds over an area is very close to the ambient. This is pointed out in Fig. 6.

*Importance of environmental humidity*

Since refractive index is only secondarily dependent on temperature and since temperature is only slightly variable through clouds, this means that the refractive

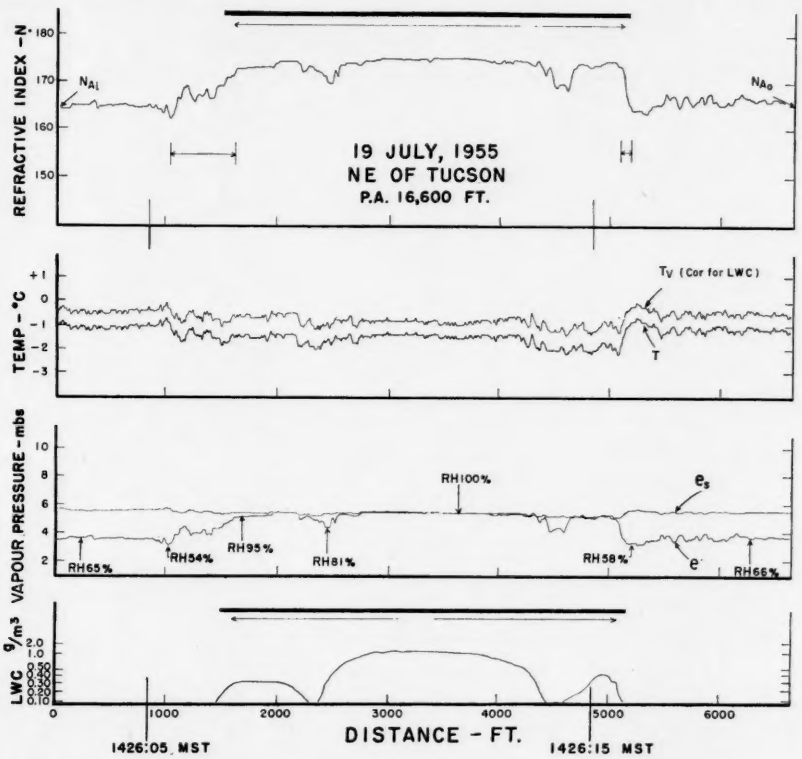


Fig. 7. Measured traces of refractive index, $N$, temperature, $T$, and liquid water content, LWC, and derived traces of vapour pressure, $e$, saturated vapour pressure, $e_s$, and virtual temperature, $T_v$, through a cloud penetrated on 19 July 1955. The solid bars show those periods when the aircraft was inside visual clouds. Note the uniform $N$ values in the interior core of the cloud (between 2500 and 4500 ft distance), the good correlation between the $N$ and $e$ traces, and the smallness of the $N$ variations resulting from $T$ changes.

structure of a cumulus is, to a good first approximation, a function of its water vapour content as opposed to that of the environment. It also means that the interior of a cumulus, where humidity is uniformly 100 per cent, is a relatively homogeneous refractive index medium.

Refractometer and temperature measuring flights through cumulus show the general validity of the above points; Figs. 7, 8 and 9 illustrate.

We can now return to the Fig. 3 pictures of convection and see what the *gross* refractive structure of a convective lower atmosphere will be. Everywhere in these pictures where there are clouds, we can simply assume saturation at the

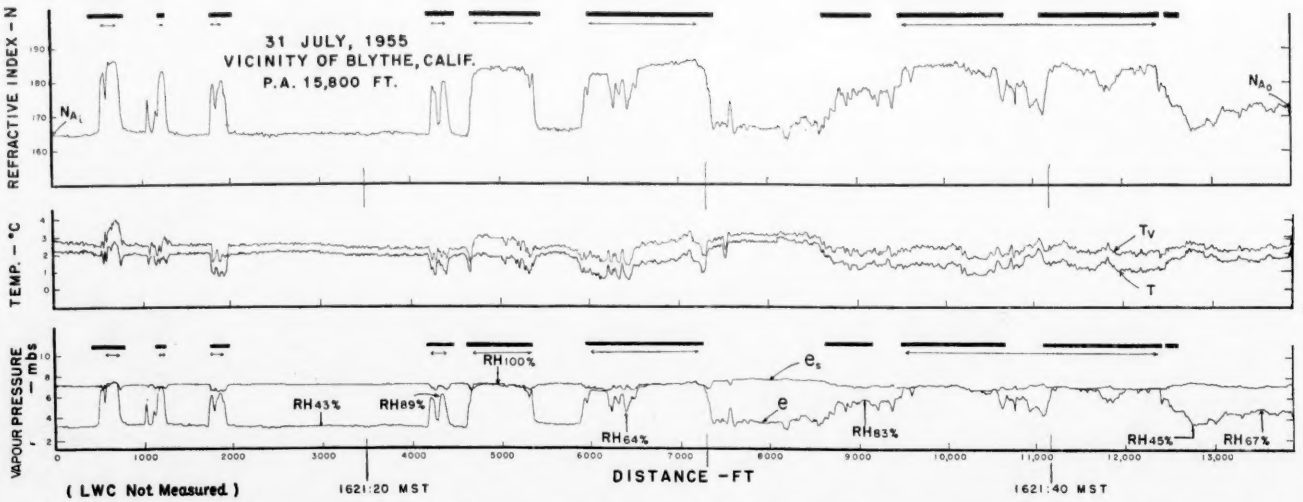


Fig. 8. Traces of measured and derived quantities through an isolated cumulus mass penetrated on 31 July 1955 (see Fig. 7 for trace identification). Note the three clouds on the extreme left; the first is warm (its top was rising at 30 ft/sec), the second neutral, the third cold. Also note the correspondence between the $e$ and $N$ traces and the "square wave" appearance of many of the clouds.

ambient temperature and compute refractive index; or putting it another way, the refractive-index difference between cloud and environment will simply be the humidity difference converted into index.

For most practical purposes, the humidity condition of the environment determines the general "refractivity" of the convective atmosphere. Clouds

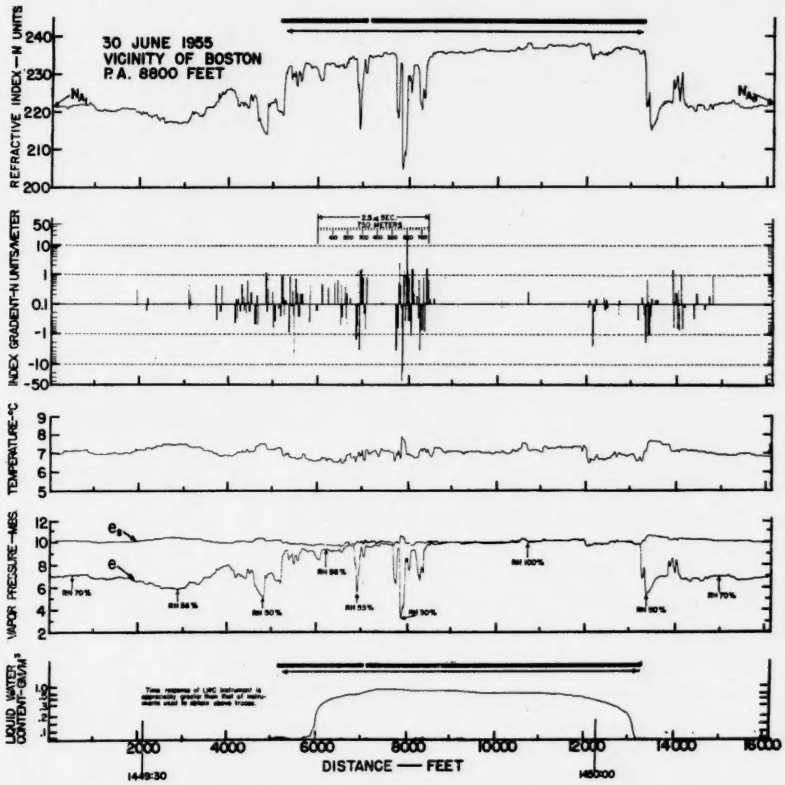


Fig. 9. Traces of measured and derived quantities and plot of the value extent, and position of all gradients exceeding 0·1 N unit/m. The "down shear" side of the cloud is believed to be at left in this figure.

building into a "dry" environment will evidence large index differences across their boundaries; but on the other hand, this same dry atmosphere, or any dry portions or layers in that atmosphere, will also make cumulus activity less extensive and/or less "built up". Clouds building into a "moist" environment will be larger, grow taller and occupy a greater percentage of the total lower atmosphere; but the index difference across their boundaries will be small. Perhaps the most "refractive" situation would be one where the cumuli build through an environment composed of alternate, horizontally-stratified, moist–dry layers.

*Refractive-index gradients in convective regions*

Another important consideration in radio propagation is the structure of the refractive-index gradient regions in a convective atmosphere. Flights through

and around cumulus show that the gradients of consequence are encountered right at the cloud boundary. In fact, with actively growing cumuli, the boundary is a region of extreme index variability. Index values in the region oscillate numerous times between values characteristic of the cloud interior and values approximating those of the ambient atmosphere. Fig. 9 illustrates this point, and Table 1 shows the number of gradients in various value classes for the Fig. 9 aircraft cloud pass (see PLANK *et al.* (1957) for a more comprehensive discussion of this pass.)

The general impression that one obtains when flying through the cloud boundary region and monitoring the instruments is that the saturated central core of the cumulus is covered, on the sides and top, by a layer or layers of bubbles (or eddies) which are themselves bounded by smaller eddies or layers of non-saturated air that has somehow been entrained or otherwise circulated well into the boundary

Table 1. Number and magnitude of $N$ gradients in cloud pass

| | Gradient ($N$ units/m) | | | | | | |
|---|---|---|---|---|---|---|---|
| | 0·1–0·32 | 0·32–1·0 | 1·0–3·2 | 3·2–10 | 10–32 | 32–100 | Total |
| No. of regions | 63 | 55 | 22 | 9 | 2 | 1 | 152 |
| No. of regions in 750 m distance | 9 | 29 | 12 | 4 | 2 | 1 | 57 |

region from outside the cloud. The outer surfaces of the outermost layer of bubbles form the visual cauliflower protuberances of the cumuli.

The spacing between the sharpest and most extensive refractive-index gradients encountered along the flight paths of our various aircraft cloud passes agrees very nicely with the dimensions of the cauliflowers (as triangulated from photographs) at the point of aircraft penetration. The boundaries of the cauliflowers are indicated to be the places of maximum index variation and our penetrations of individual isolated cauliflowers further substantiate this. The boundary of the cauliflower on the side toward the main cumulus mass is indicated to be as sharp (refractive-index-wise) as the outer boundary. It should be reiterated that several layers of cauliflower bubbles, or eddies, seem to be present in the transition zone between the ambient atmosphere and the cloud interior. With wind shear, the up-shear transition zone appears to consist of a single layer of bubbles, whereas the down-shear zone contains several layers.

*The sizes, rate of occurrence and duration of convective elements*

Thus far we have considered the gross effects of cumulus clouds on the refractive index structure of a convective atmosphere and discussed certain features of the index gradients. It would seem appropriate at this time to present some figures on the approximate sizes, rate of occurrence, and duration of the various convective elements. This information is given in Table 2 and Fig. 10.

In conclusion, I would like to say that the subject of convection is still very much an open one. The subject matter presented herein is based on certain broad



VOL. 15 1959

Table 2. Properties of convective elements

| Convective element | Observer | Place of observation | Method used | Range of horizontal dimensions | Frequency of occurrence | Rate of rise | Duration | Temp. diff. from ambient |
|---|---|---|---|---|---|---|---|---|
| *Cumulus clouds* | | | | | | | | |
| Cumulus humilis, congestus | BATTAN *et al.* (1956) | U.S.A. | Aircraft penetration | 500–24,000 ft | — | — | — | — |
| Cumulus humilis, congestus | BATTAN *et al.* (1956) | Caribbean | Aircraft penetration | 1000–20,000 ft | — | — | — | — |
| Cumulus humilis, congestus | PLANK, SPATOLA | Florida | Measmts. on aerial photomaps of cumulus | 500–21,000 ft | — | — | — | — |
| Cumulus congestus | WORKMAN, REYNOLDS (1945) | New Mexico | Triang. of time lapse photos | — | — | — | 10–18 min | — |
| Cumulus humilis | — | — | Estimated | 500–5000 ft | — | — | — | 0·5 to 1°C |
| Cumulus congestus | — | — | Estimated | 5000–30,000 ft | — | — | — | 1 to 3°C |
| Cumulonimbus | — | — | Estimated | 30,000–80,000 ft | — | — | — | — |
| Cauliflower protuberances on cumulus humulis and congestus | MALKUS (1954) | Nantucket Is. | Triang. of time lapse photos | 700–2500 ft | — | 3–30 ft/sec | 60–300 sec | — |
| | PLANK | New England and S.W. U.S. | Triang. of aerial photos | 500–7000 ft | — | 30 ft/sec (1 case) | — | — |
| | PLANK, SPATOLA | Florida | Measmts. on aerial photomaps of cumulus | 500–6000 ft | — | — | — | — |
| | HUNTINGTON (U. of Chi.) | U.S.A. and Caribbean | Time lapse photography | — | One per 5–10 min | — | — | — |
| Thermals above 1000 ft | BUNKER (1953) | New England | Aircraft penetration | 3300–5000 ft | — | 3 ft/sec | — | 0·3 to 0·5°C |
| | JAMES (1953, 1954) | England | Aircraft penetration | 500–5000 ft | — | — | — | 0·05 to 0·1°C |
| | CUNNINGHAM (AFCRC) | Caribbean | Aircraft penetration | 150–620 ft | — | — | — | 1 to 2°C |
| | YATES (1953) WELCH (1953) LUDLAM and SCORER (1953) Group Discussion on Convection (1953) | England | Glider soaring | 1000–4000 ft | One per 5–15 min per $\frac{1}{4}$ sq mile$^2$ (under av. conditions) | up to 15 ft/sec | — | 1 to 2°C |
| Thermals below 1000 ft | BUNKER (1953) | Brookhaven | Measmts. with a maze of temp. elements mounted on tower | 125–800 ft | — | 2·8–4·3 ft/sec | — | 0·5 to 0·6°C |
| | JAMES (1953, 1954) | England | Aircraft penetration | Wide range <450 ft (too small for soaring) | — | — | — | 0·5 to 1°C |
| | YATES 1953) | England | Glider penetration | | Numerous | — | — | — |
| | HANKIN (1913) and GOODHART (Group Discussion on Convection, 1953). | India and England | Observations of soaring birds and dragonflies | 10's to 100's of feet | | | Av. 2 min | — |

areas of well established thought, but the thread that binds the whole is spun from piecemeal information and subjective interpretation.

## References


| | | |
|---|---|---|
| Ackerman B. | 1957 | *J. Meteorol.* In press. |
| Austin J. M. | 1948 | *J. Meteorol.* **5**, 103. |
| Austin J. M. | 1951 | *Compendium of Meteorology* pp. 694–701. American Meteorological Society. |
| Austin J. M. and Fleisher A. | 1948 | *J. Meteorol.* **5**, 240 |
| Battan L. J. and Braham R. R., Jr. | 1956 | *J. Meteorol.* **13**, 587. |
| Bjerknes J. | 1938 | *Quart. J. R. Met. Soc.* **65**, 325. |
| Bjerknes V., Bjerknes J., Solberg H. and Bergeron T. | 1933 | *Physikalische Hydrodynamik.* Springer, Berlin. |
| Bunker A. F. | 1952 | Geophysical Research Paper No. 19, pp. 309–322. Air Force Cambridge Research Center. |
| Bunker A. F. | 1953 | *J. Meteorol.* **10**, 212. |
| Bunker A. F., Haurowitz B., Malkus J. S. and Stommel H. | 1949 | *Pap. Phys. Oceanogr.* **11**, No. 1. |
| Bunker A. F., Ludlam F. H. and Scorer R. S. | 1954 | *Quart. J. R. Met. Soc.* **80**, 102. |
| Cunningham R. M., Plank V. G. and Campen C. F. Jr. | 1956 | Geophysical Research Paper No. 51. Air Force Cambridge Research Center. |
| Goldstein S. (Editor) | 1938 | *Modern Developments in Fluid Dynamics* pp. 592–600. Oxford University Press. |
| Group Discussion on Convection | 1953 | *Quart. J. R. Met. Soc.* **79**, 431. |
| Hankin E. H. | 1913 | *Animal Flight; a Record of Observation.* Iliffe, London. |
| Houghton H. G. and Cramer H. E. | 1951 | *J. Meteorol.* **8**, 95. |
| James D. G. | 1953 | *Quart. J. R. Met. Soc.* **79**, 425. |
| James D. G. | 1954 | Meteor. Res. Paper No. 875. Meteorological Research Committee, London. |
| Ludlam F. H. | 1953 | *Quart. J. R. Met. Soc.* **79**, 430. |
| Ludlam F. H. and Scorer R. S. | 1953 | *Quart. J. R. Met. Soc.* **79**, 317. |
| Malkus J. S. | 1949 | *Trans. Amer. Geophys. Un.* **30**, 19. |
| Malkus J. S. | 1952 | *Quart. J. R. Met. Soc.* **77**, 530. |
| Malkus J. S. | 1955 | *J. Meteorol.* **12**, 350. |
| Malkus J. S. and Scorer R. S. | 1954 | *Pap. Phys. Oceanogr.* No. 54–55; *J. Meteorol.* **12**, 43. |
| Plank V. G., Cunningham R. M. and Campen C. F., Jr. | 1957 | Proceedings of the Sixth Weather Radar Conference, Cambridge, Mass. |
| Refsdal A. | 1930 | *Geofys. Publ.* **5**, No. 12. |
| Rossby C. G. | 1936 | *Pap. Phys. Oceanogr.* **5**, No. 1. |
| Scorer R. S. | 1954 | *Quart. J. R. Met. Soc.* **80**, 68. |
| Scorer R. S. and Ludlam F. H. | 1953 | *Quart. J. R. Met. Soc.* **79**, 94. |
| Stommel H. | 1947 | *J. Meteorol.* **4**, 91. |
| Welch L. | 1953 | *Quart. J. R. Met. Soc.* **79**, 429. |
| Workman E. J. and Reynolds S. E. | 1949 | *Bull. Amer. Meteorol. Soc.* **30**, 359. |
| Yates A. H. | 1953 | *Quart. J. R. Met. Soc.* **79**, 420. |


## Discussion

Dr. R. L. Smith-Rose—I have been interested in listening to Dr. Plank's excellent presentation of the manner in which large "bubbles" evolve from smaller ones, but



VOL. 15 1959

I was at first bothered by the assumption that the distance between the large upward-moving bubbles is large compared with the bubbles themselves. This assumption is necessary if the existence of reasonably stable horizontal layers is to be accepted.

Would it be a fair analogy to picture a medium consisting of layers of two or more liquids of decreasing density but increasing boiling point, e.g. water and a more viscous oil? As the water boils, the bubbles would form, coagulate and then emerge

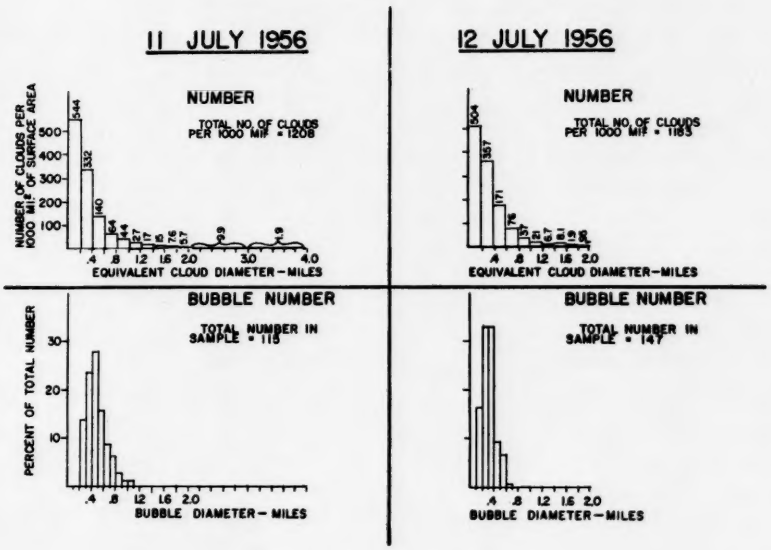
11 JULY 1956
12 JULY 1956
NUMBER
TOTAL NO. OF CLOUDS PER 1000 MI² = 1208
TOTAL NO. OF CLOUDS PER 1000 MI² = 1183
NUMBER OF CLOUDS PER 1000 MI² OF SURFACE AREA
EQUIVALENT CLOUD DIAMETER – MILES
BUBBLE NUMBER
TOTAL NUMBER IN SAMPLE = 115
TOTAL NUMBER IN SAMPLE = 147
PERCENT OF TOTAL NUMBER
BUBBLE DIAMETER – MILES

Fig. 10. Histograms of horizontal cloud and bubble dimensions as obtained from aerial photomaps of cumulus coverage over Florida.

through the oil as large volumes of steam. But this is variable over the interface between the liquids and there remains a stratified surface continuously disturbed by the rising bubbles.

Dr. J. S. Marshall—If with a stable lapse rate a parcel of air is heated beyond its environment and released, it should rise, cooling adiabatically, and come to rest at the level at which it is in hydrostatic equilibrium with the environment. Mixing should modify, but not eliminate, this sort of rise to an equilibrium height.

Suppose that there is a superadiabatic lapse rate within a 100 ft layer next to the ground, a stable lapse rate for the next 1000 ft or so. Suppose that the earth's surface is moist, and so transfers not only heat but also moisture to the adjacent air. Suppose that a shallow cylinder breads away as a bubble. Apart from mixing, the lowest air should rise the highest, the air at 100 ft should rise not at all. The air of the shallow cylinder should end up as a tall thin cylinder in hydrostatic equilibrium with its surroundings. But now we have left a hole where the risen air used to be, because we neglected the contemporary subsidence of the environment. Let us correct for this by allowing the risen bubble and its environment to subside,

the amount of subsidence being proportional to distance down from the top of the bubble. The new lapse rate is the same inside and outside the bubble. The bubble has greater vapour density than its environment at the top of the bubble, but not at the bottom. This concentration of moisture toward the top will be reduced by mixing of a rising bubble. It would be increased, on the other hand, if any considerable part of the heating that produced the superadiabatic layer were by radiation, to which there would be no moisture-transferring concomitant.

It would seem important to recognize that such inhomogeneities in index as were introduced by mixing of moist and drier air as the bubble rose would be relatively slow to fade away once all parts of the bubble had achieved hydrostatic equilibrium.

Regarding the superadiabatic layer at the earth's surface, I have two misgivings that a more careful study of the literature might relieve: First, is its thickness a few metres, or a few tens of metres, or can it be even more? Secondly, since its thickness is more than a few centimetres, what mode of heat transfer produces it? Presumably turbulence would tend to destroy the layer, and so cannot be looked to as its cause. Would the absorption of radiation reflected or emitted from the earth's surface be relevant. Speaking of the literature, it is worthy of mention that SUTTON in his textbook *Micrometeorology* (McGraw-Hill, 1953) discusses bubbles helpfully, and with references, under the heading "Effects of Buoyancy on Heat Transfer".

VOL.
15
1959

When one pictures bubbles that have come to hydrostatic equilibrium with their surroundings, it is important to distinguish between bubbles of clear air in clear air (or bubbles of cloud in cloud) and bubbles of cloud in clear air. At the edges of the latter, there will be continued evaporation and so continued cooling and continued convective circulation. A bubble of clear air in clear air, on the other hand, has no corresponding urge to mix with its environment, and so is liable to retain its identity for a long time.

DR. D. ATLAS—The existence of blobby layers aloft near the base of temperature inversions is a common feature of refractive-index soundings, and must also be inferred from radar back-scattering observations from clear air as well as from forward-scatter propagation measurements. The formation of such blobby layers is most frequently attributed to convection of moist air from the surface into a relatively dry environment, although vertical shear across a horizontal boundary has also been suggested as a possible mechanism. With regard to the former process there appears to be sufficient evidence in the radar back-scatter data of blobby layers aloft at times when significant convection from the surface could not have occurred. (This would appear to be true also of the scatter propagation data with which I am not entirely familiar.) I wonder then if it might not be possible to account for the release of convection aloft (but below the observed blobby layers) as a result of differential radiant heating and emission due to vertical variations in moisture content? For example, an elevated moist layer would cool from the top as a result of radiation upwards, it being transparent to incoming short-wave radiation, and it would heat from below as a result of long-wave radiation from the earth. Subsequent overturning could conceivably convect moist air upwards to form blobby layers during the night and early morning when convection

from the surface layers is restricted. (Note added after the conference: The mechanism proposed above is very strongly supported by observations of nocturnal altocumulus clouds in the absence of any general vertical motion. The formation of such clouds is generally explained as a result of the same process. Indeed, this discussion suggests the correlation of forward and back-scatter measurements with the presence of nocturnal altocumulus.)

OL.
15
959

Journal of Atmospheric and Terrestrial Physics, 1959, Vol. 15, pp. 248 to 250. Pergamon Press Ltd. Printed in Northern Ireland

## SESSION III

LIGHTNING

# Radar observation of lightning*

M. G. H. LIGDA

ECHOES appearing on radar pictures of thunderstorms, and of too short duration to come from precipitation, are safely attributable to lightning. Seldom if ever seen at 3 cm, these lightning echoes appear along with those of precipitation at wavelengths from 10 cm (LIGDA, 1950; MARSHALL, 1953; MILES, 1953; JONES, 1954) to 50 cm and more (Hewitt 1953).

For several years past, many operational radars widely scattered over the United States, at wavelengths 10 and 23 cm, have been routinely photographed and these records studied for weather echoes. In addition to the very extensive precipitation patterns revealed in this way, these PPI photographs contained many instances of lightning echoes.

Because heavy precipitation can produce a strong radar echo even at wavelengths of 23 cm, the detection of echoes from lightning in or near areas of very heavy precipitation is virtually impossible. Accordingly, while undoubtedly many discharges occur in such areas, the discussion which follows is confined to those strokes which occur in areas where precipitation echoes are weak, entirely absent, or at the edges of strong precipitation echoes.

Since cloud-to-ground discharges usually occur in close conjunction with heavy precipitation and may not have appreciable horizontal extent, it may be deduced that they are inconspicuous and difficult echoes to detect on the PPI scope of a radar. In spite of these limitations, however, a fairly large number of echoes that are ascribed to cloud-to-ground discharges have been noted. Fig. 1 shows two fairly typical examples, indicated by the arrows.

It will be noted that most of these occur in a portion of the storm where precipitation was evidently light. Apart from the fact that such conditions are well-nigh essential to the detection of the lightning echoes at all, an additional bit of information is provided by these photographs. Apparently the light precipitation echo is in many cases produced by, or is closely associated with, the anvil top of the cumulonimbus cloud. This conclusion is based upon the manner in which the light precipitation areas were observed to form; that is, after the intense echo had grown to about maximum size, the light precipitation echo grew out of the main echo in a high level, down-wind direction. In those cases where no precipitation echo can be detected there is usually, but not invariably, a strong precipitation

* This summary was prepared by J. S. MARSHALL and W. F. HITSCHFELD.

VOL. 15 1959

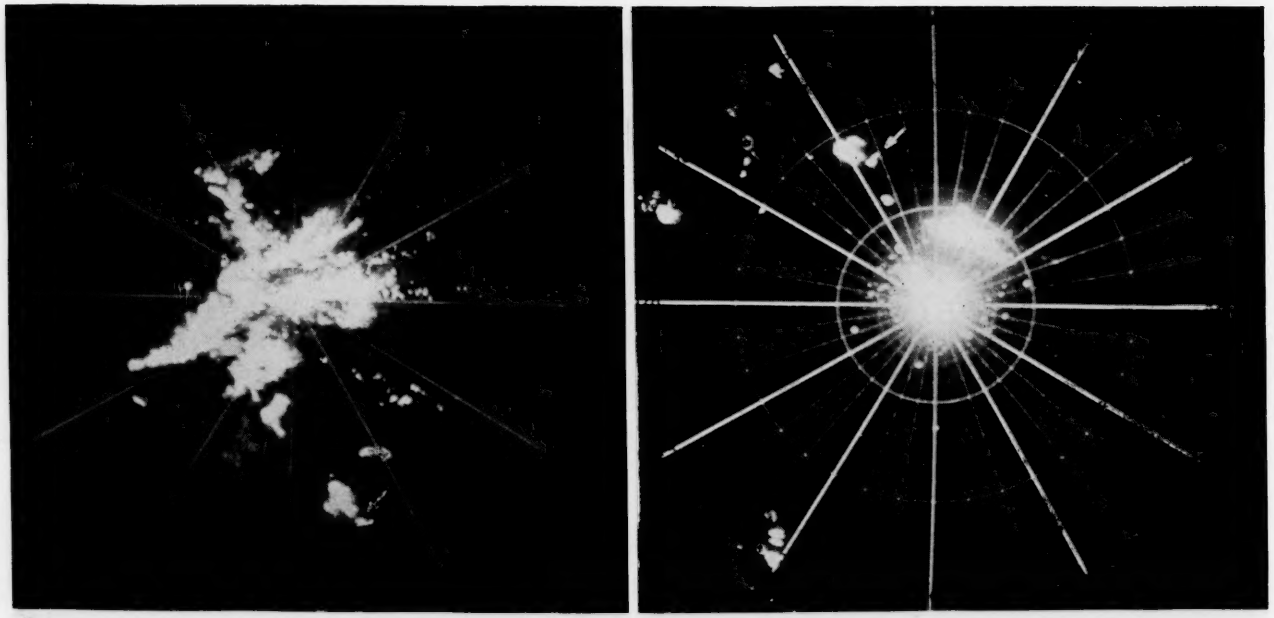

Fig. 1. Lightning echoes associated with isolated storms, believed to be produced by cloud-to-ground strokes (23-cm radar, Amarillo, Texas, 19 June 1955). Length of arrow 10 naut. miles.

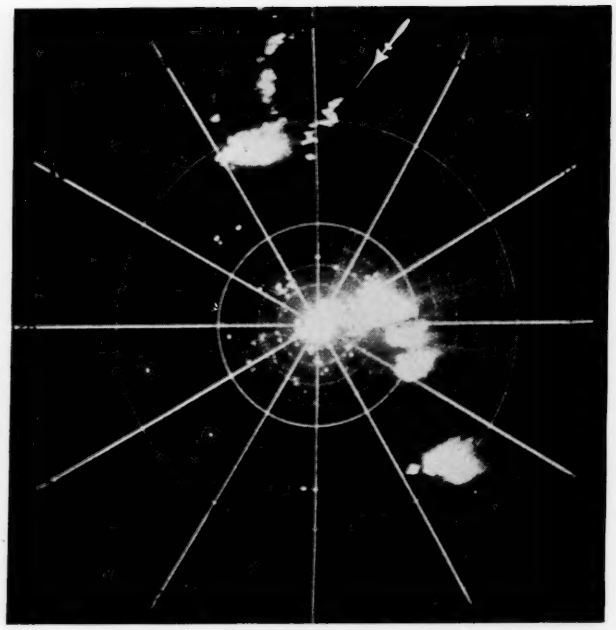

Fig. 2. Arrow points to lightning echo detected in area down-wind of main precipitation area (23-cm radar, Amarillo, Texas, 16 June 1955). All thunderstorms visible on scope in this situation were moving very nearly from west to east. Length of arrow 45 naut. miles.

VOL.
15
1959

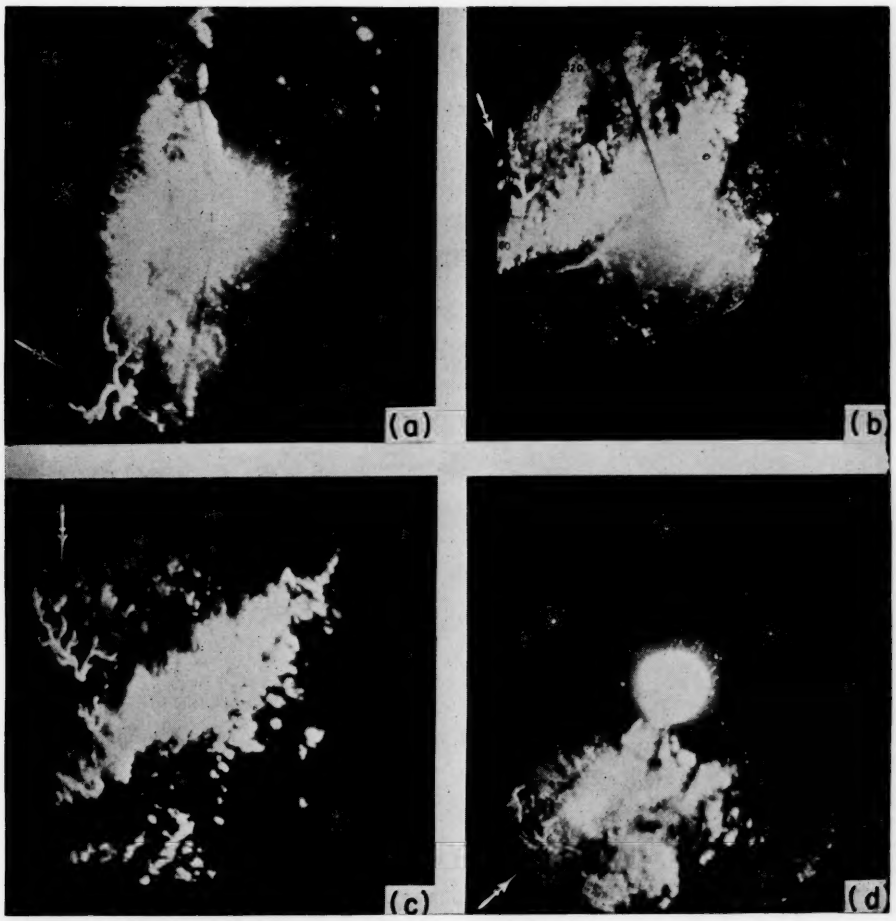


Fig. 3. Extended echoes from instability line-storm in-cloud or cloud-to-cloud discharges. All pictures printed to the same scale with arrow 27 naut. miles in length: (a) 23-cm radar, Belleville, Illinois, 27 May 1955. (b) 23-cm radar, Fordland, Missouri, 19 April 1955 (note the "root-like" structure of the echo at its southern end; this short stubby branching in a direction opposite to branches in other parts of the echo has been observed several times and may indicate regions of high charge concentration). (c) 23-cm radar, Fordland, Missouri, 11 October 1954. This is the longest continuous echo yet found. If the lightning echo south of the long echo is part of the long discharge, this echo is over 100 statute miles in length. Similar gaps have been noticed in other echoes and may be significant. (d) Same storm as (c) but from 10-cm radar, Kirksville, Missouri, 11 October 1954. Note weaker lightning echo relative to precipitation echo.

VOL.
15
1959

echo up-wind from the lightning echo (Fig. 2). Also, in nearly all cases, lightning echoes are detected at moderate-to-long ranges. This suggests that the beam (which in search radars is normally broad in the vertical plane) is at considerable altitude. Cloud-to-ground lightning discharges are not infrequently observed to occur between anvil and ground.

Cloud-to-ground lightning echoes are almost invariably observed when the associated thunderstorm precipitation echoes are large, isolated, and widely scattered. From common observations it is suggested that lightning is but rarely observed unless some portion of the cloud is glaciated.

Far more spectacular, interesting and easy to detect on PPI time-lapse film are the echoes from what are apparently more or less horizontal cloud-to-cloud or in-cloud discharges. These exhibit the same general properties as the cloud-to-ground discharges, i.e. they are visible on just one frame of the sequence (unless the PPI phosphor is sufficiently excited so that persistence is strong enough to allow them to be recorded on the following frame); they can be observed only in areas where the echo from precipitation is weak or absent, and the lightning echoes are very strong. It is deduced that the lightning echoes shown in Fig. 3 are cloud-to-cloud or in-cloud discharges because of their great length.

From the radar observations under discussion, there is compelling evidence that most lightning echoes are obtained from heights of about 20,000 ft. LIGDA (1950), MILES (1953), MARSHALL (1953) and others are all in fair agreement on this point. It is of interest to note that pilots flying for the Thunderstorm Project observed that most strikes on their aircraft occurred near the 15,000 ft level.

Nearly all extended lightning echoes on PPI scopes have been observed at ranges in excess of about 70 miles, and many are detected beyond the 100 mile range. Under normal atmospheric conditions the radar horizon is about 5000 ft above the surface at 100 miles; however, the top of the beam for the radars used to make these observations at that distance exceeds 30,000 ft of altitude (AN/FPS-3). If the echoes originated at low levels, one would expect to see a fair number of them at close ranges, and vice versa if at high levels, because the radar beam increases in height with increased range due to the curvature of the earth and vertical beam-width. This reasoning is strongly supported by the weight of observational evidence, thus substantiating the hypothesis of the high altitude origin of extended lightning echoes. Radar detection of high-level discharges may also be enhanced by the longer persistence of the discharge due to the slower recombination time. However, this may not be a very significant factor.

The detection of lightning echoes on time-lapse PPI-scope film is made more efficient by the following: after the film has been developed, a copy is made of opposite "polarity" to the original (positive if the original is a negative and vice versa). The two film strips may then be matched together, displaced by one frame, placed in the copying machine with a third, unexposed film strip, and a copy made of the matched strips. The resulting film will be a negative showing very little except the lightning echoes, which will be quite dark in contrast with the rest of the scope image. By use of this technique, lightning echoes that might otherwise be overlooked, because of being embedded in regions of relatively intense precipitation echo, may be located with comparative ease. This notion of a

subtractive process has now been extended to developments applicable to operational weather radars. The detection of lightning by radars that also reveal the precipitation pattern is without doubt a procedure of great value.

This account is an extract from a recent paper by Ligda (1956).

## References


| | | |
|---|---|---|
| Hewitt F. J. | 1953 | *Proc. Phys. Soc. Lond.* B **66,** 895. |
| Jones R. F. | 1954 | *Quart. J. R. Met. Soc.* **80,** 579. |
| Ligda M. G. H. | 1950 | *Bull. Amer. Met. Soc.* **31,** 279. |
| Ligda M. G. H. | 1956 | *J. Atmosph. Terr. Phys.* **9,** 329. |
| Marshall J. S. | 1953 | *Canad. J. Phys.* **31,** 194. |
| Miles V. G. | 1953 | *J. Atmosph. Terr. Phys.* **3,** 258. |


VOL.
15
1959

Journal of Atmospheric and Terrestrial Physics, 1959, Vol. 15, pp. 251 to 253. Pergamon Press Ltd. Printed in Northern Ireland

# Electric field-change studies of lightning*

L. G. SMITH†

ELECTRIC field-change studies have extended the investigation of lightning to the interior of the cloud not accessible to photographic techniques and have revealed the importance of relatively slow processes in the discharge.

The photographic studies have shown that each of the several brilliant return strokes from ground to cloud is preceded by a leader, travelling from cloud to ground, which establishes the conducting channel. The first leader of a discharge is slower than subsequent leaders; they have durations of the order of 10 msec and 1 msec, respectively. There is considerable variation between individual discharges and some major types can be distinguished (SCHONLAND, 1956).

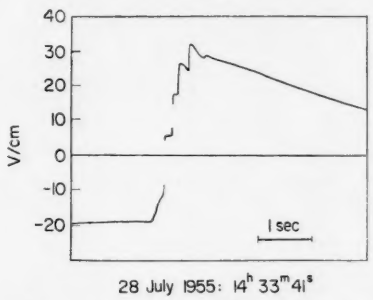


Fig. 1. Electric field-change due to a close lightning discharge having four strokes.

The electric field-change due to a close discharge having four strokes to ground is shown in Fig. 1. The total duration of this field-change is about 1 sec (it is followed by a slow recovery of the field, which is real and not an instrumental effect). The four rapid components are due to the four return strokes and their preceeding leaders. Observations such as this show that the discharge is initiated within the cloud at a time of the order of 100 msec before the first leader is seen to emerge from the cloud. It is found that there may also be a slow change of field between strokes and following the last stroke of the discharge.

Each return stroke neutralizes a region of negative charge in the cloud, about 10 C. By considering the details of the field change MALAN and SCHONLAND (1951) have shown that the return strokes are neutralizing consecutively higher regions of negative charge. The intervals of height are about 0·7 km, the lowest region being at about 3 km for all discharges and the highest at about 9 km for a discharge with many strokes. The slow components of the field-change are interpreted as being due to a junction streamer moving upward within the cloud to tap the successive regions of charge.

* Summary of paper.

† Geophysics Research Directorate, Air Force Cambridge Research Center, Bedford, Massachusetts.

In the case of a discharge having no strokes to ground (i.e. a cloud discharge) the electric field-change is relatively smooth and is most frequently recorded as a gradual change with a duration of the order of 0·3 sec. In a recent study (Smith, 1957) of cloud discharges the field-changes were recorded simultaneously at two stations 13·2 km apart. These observations indicate that cloud discharges most frequently involve the upward movement of negative charge and that the vertical extent of the discharge is of the order of 5 km.

The cloud discharge has much in common with the junction streamer, in vertical extent and in velocity of advance of the streamer ($3 \times 10^6$ cm/sec). Recent measurements of the fine structure of the radiation fields indicate that they have the same mechanism.

## References


| | | |
|---|---|---|
| Schonland B. F. J. | 1956 | *Handbuch der Physik* Bd. 22, p. 576. |
| Malan D. J. and Schonland B. F. J. | 1951 | *Proc. Roy. Soc.* A **209,** 158. |
| Smith L. G. | 1957 | *Quart. J. Roy. Meteorol. Soc.* **83,** 103. |


## Discussion

Dr. W. A. Flood—Examination of records obtained by monitoring a 400-mile distant 915 Mc/s transmitter has disclosed an apparent close correlation between a form of anomalous propagation and the occurrence of thunderstorms near the midpoint of the propagation path. This type of propagation is characterized by short duration "spikes" rising from the median signal level to power levels two to three orders of magnitude (20–30 dB) above the median level. Similar spike-like signals are received during the transmitter bi-hourly silence period, but the amplitude received during these periods is from 30–40 dB less than the amplitudes obtained when the transmitter is on. Correlation between this type of signal and thunderstorm activity is obtained only with thunderstorms near the midpoint of the propagation path. The behaviour of the spike amplitudes and the lack of correlation with local thunderstorms indicate that this phenomenon is distinct from the "sferics" recorded by Hay and Hartz* at 492 Mc/s. It is suggested that our records, when examined in the light of back-scatter data obtained by Marshall,† Ligda‡ and others, offer evidence of forward scattering from ionized regions caused by cloud-to-cloud discharges.

This work was conducted under Contract AF 19(604)-1835, sponsored by Air Force Cambridge Research Center.

The only other comments I have to make are:

(1) Unlike back-scatter (radar) observations, forward-scattered lightning echoes are not obscured by precipitation clutter.

(2) C.W. forward-scatter observations yield the complete amplitude/time history of the ionization produced by the discharge, albeit at the expense of range resolution.

Dr. M. G. Morgan—I want to draw attention to the wide distribution of energy

* Hay D. R. and Hartz T. R. 1955 *Nature, Lond.* **175,** 949.
† Marshall J. S. 1953 *Canad. J. Phys.* **31,** 194.
‡ Ligda M. G. H. 1956 *Atmosph. Terr. Phys.* **9,** 329.



VOL
15
195

associated with whistlers (maximum in the vicinity of 10–20 kc/s), the dispersive character of the propagation mechanism, and the fact that not all lightning discharges produce whistlers.

The discussion then centred on a possible explanation of this latter observation.

Dr. L. G. Smith—Dr. Morgan has noted that whistlers are not observed to follow all discharges. This may be attributed to the relative infrequency of discharges to ground.

Measurements of the electric-field variation indicate that the return strokes of a discharge to ground are the main source of electromagnetic radiation from discharges and can be expected to be the source of whistlers. It is known that cloud discharges are several times more frequent than discharges to ground. Thus, although both cloud discharges and discharges to ground may be observed visually and detected by the radio noise they cause locally, it is only the occasional discharge to ground which is effective as a source of whistlers.

Dr. Smith-Rose—The cloud-to-ground discharges, being more or less vertical, have the wrong polarization for propagation along the earth's magnetic field.

Dr. Ligda—The cloud-to-ground discharges are usually too short in length to be efficient radiators at frequencies of a few kilocycles.

OL.
15
959

Journal of Atmospheric and Terrestrial Physics, 1959, Vol. 15, pp. 254 to 261. Pergamon Press Ltd. Printed in Northern Ireland

# Aircraft observations of convective cloud electrification

D. R. FITZGERALD* and H. R. BYERS*†‡

**Abstract**—A horizontal component of the potential gradient in and around developing trade-wind and extra-tropical cumulus clouds has been measured with field meters mounted in the wingtips of an airplane. Characteristic similarities and differences in the electrostatic behaviour of all-water and of mixed-phase clouds studied in 1953–1955 are discussed. A correlation of these effects with the development of radar echoes in the cloud is given.

## 1. INTRODUCTION

THE Cloud Physics Group at the University of Chicago has been able to conduct a flight research programme on the physical properties of convective clouds through the interest and support of the Air Force Cambridge Research Center. The airplanes used in the programme were equipped with a variety of instruments. The electric-field measurement installation consisted of two field meters operating on the induction principle, mounted facing outward from the airplane wingtips. These were connected by coaxial signal cables to amplifiers and a recorder mounted in the waist of the airplane. The difference of the electric field values recorded for each meter is proportional to the horizontal component of the external electric field transverse to the direction of flight.

The other item of equipment on the airplane of particular value in the study of the cloud electrical properties was an AN/APQ-13 3-cm radar set installed in the nose, with the antenna reflector rotating about the axis of the direction of flight so that a vertical cross-section perpendicular to the flight path was scanned and photographed every 2·6 sec. The receiver sensitivity was adjusted at −76 dB/m to insure that the radar was receiving echoes from precipitation particles.

Flight operations were conducted in the Caribbean area in winter 1953–1954 and autumn 1954, in the midwestern United States in the summer of 1954, and in the southwestern United States in the summer of 1955. Representative examples of the analysis of clouds studied in these regions are given in the next section together with general results of an inspection of all of the flight-programme field-meter data.

## 2. CLOUD AND PRECIPITATION STRUCTURE IN RELATION TO HORIZONTAL ELECTRIC FIELD COMPONENTS

Case studies for a number of interesting trade-wind and extra-tropical cumulus cloud passes have been prepared. Fig. 1 is an example of the kind of structure found in ordinary small trade-wind cumulus. On the left side of the figure, the

* University of Chicago.

† The research reported in this paper has been sponsored in part by the Geophysics Research Directorate of the Air Force Cambridge Research Center, Air Research and Development Command, under Contracts No. AF19(604)-618 and No. AF19(604)-2189.

‡ A longer version of this paper was presented at a Joint Session on Atmospheric Electricity of IAM and IAGA at the Toronto Meeting of IUGG on 6 September 1957.

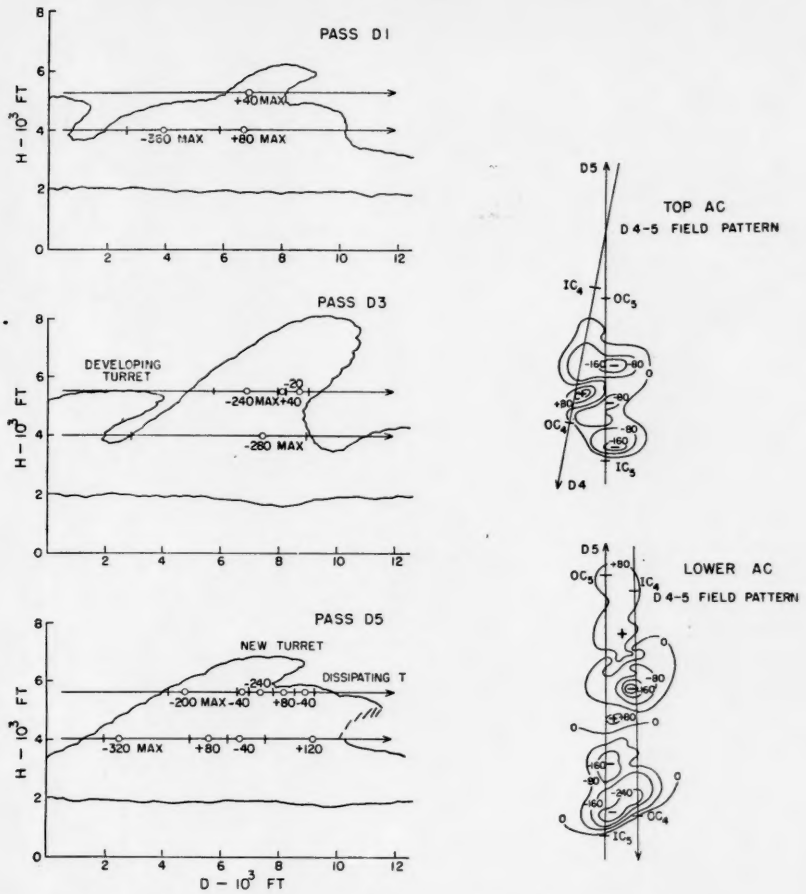


Fig. 1. Flight 189, 15 October 1954. Cloud *D*. Melting level 15,400 ft.

electric field values are plotted in volts per metre (V/m) along the flight paths of two airplanes used to probe this cloud. Sign of the field is indicated on this figure in terms of the unbalanced charge off the right wing. Since the same charge of reversed polarity off the left wing would produce an identical field-meter response, it is necessary to determine the horizontal position of the airplane with respect to the cloud boundaries to infer if the actual charge imbalance in the cloud is positive or negative. With the assumption that most of the charge producing the field is contained within the cloud volume, the field disturbance in small trade-wind cumulus can be interpreted as arising largely from negative excess charge accumulations in the principal draft columns.

An example of the kind of field patterns that may be constructed from sets of successive probes of the same cloud is given on the right side of Fig. 1. One sees clearly-defined patterns at the two flight levels which appear to be associated with the cloud draft structure.

In this particular cloud, maximum fields and liquid-water contents were observed at the lower flight level. Other cases indicate larger maximum fields and liquid-water content at the higher airplane flight level.

A total of 691 probes of trade-wind cumulus have been examined for strong horizontal field effects. All but one of the clouds produced weak fields of order of from 1 to 10 V/cm. The exception had convective turrets extending to sub-zero temperatures. This cloud is shown in Fig. 2. At the bottom of the figure a PPI-type radar echo contour is shown with the electric field values in volts per centimetre (V/cm) plotted along the flight path. One notes a development in the field

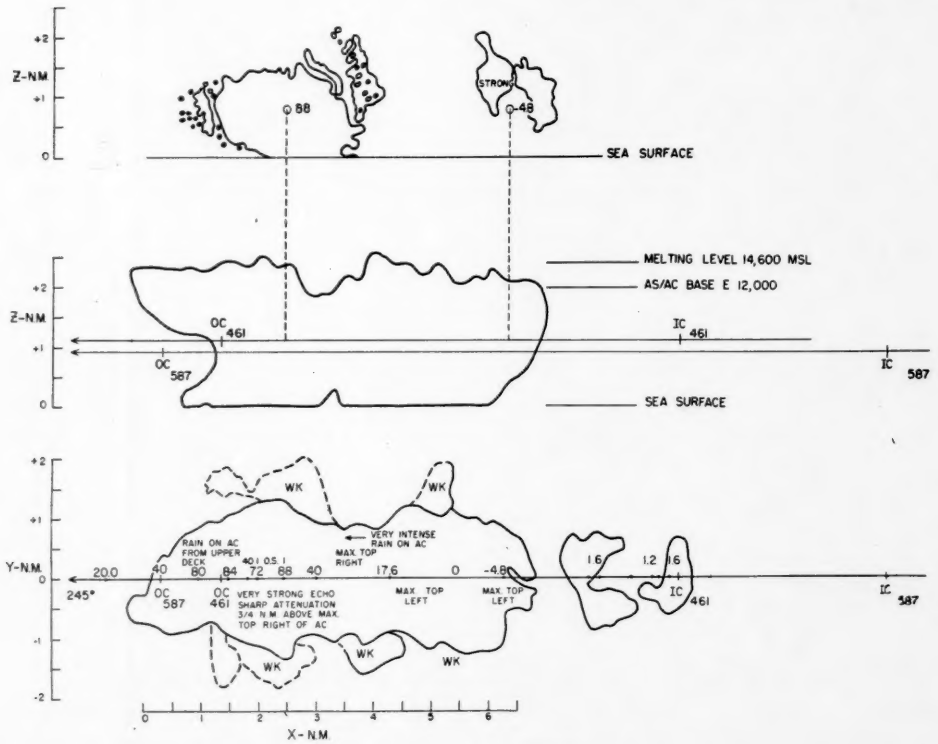


Fig. 2. Flight 188, 14 October 1954.

to an off-scale value greater than 88 V/cm in the region of heavy rain. The unbalanced charge in this case may be interpreted as a positive charge excess off the side of the airplane where the tallest convective towers are indicated by the radar set.

The central portion of the figure is an RHI-type presentation along the flight path showing the height variations of the radar cloud and the airplane tracks. The upper portion shows two single-frame radar cross-sections perpendicular to the flight direction and field values synchronous with the cross-sections. The RHI and PPI presentations were derived from sets of these single-frame photographs of the radarscope.

This cloud is the only tropical cloud flown through that exhibited fields of the order of magnitude of those found frequently in extra-tropical cumulus known to contain ice.

A typical example of the effects observed during flight in and around the upper portions of moderate sized cumulus congestus clouds over the continental United States is shown in Figs. 3 and 4.

Fig. 3 indicates the airplane flight track, PPI echo areas, and electric field values in volts per centimetre (V/cm). The points of entry and exit from visible

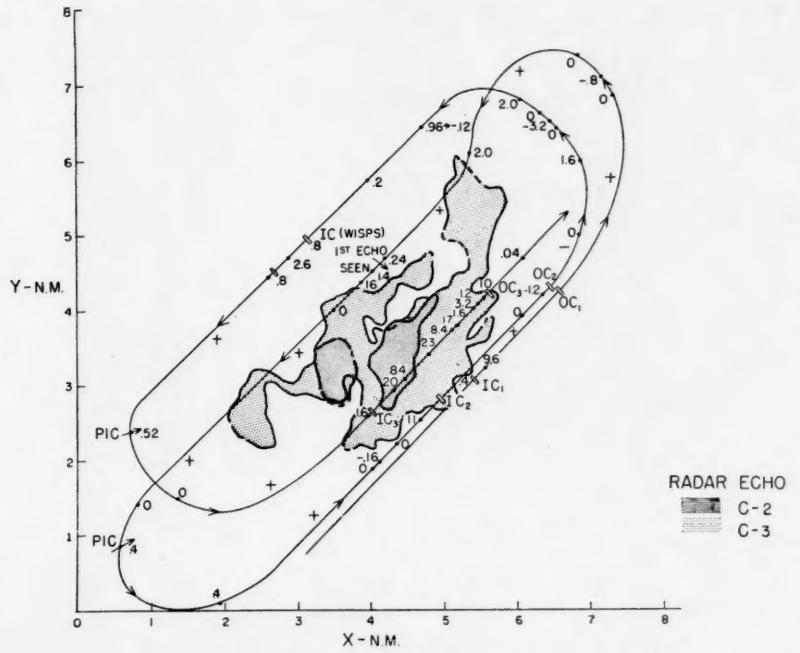


Fig. 3. Flight 259, 27 August 1955. Cloud *C*.

cloud are given by the IC and OC indicators. This cloud had a top estimated at 23,000 ft and base estimated at from 12,000 to 15,000 ft on the first pass and no precipitation echo. The first echo developed during the downwind leg following pass 1. The pattern of this echo development is shown in three dimensions on Fig. 4 by use of the analysis described in connexion with Fig. 2. One sees that a rather large field of 9·6 V/cm was observed on the first pass with no visible or radar precipitation evident in the cloud. On the second pass, 7 min after the first, the field was approximately the same with no visible precipitation at flight level. The radar echo at this time was growing off to the left side of the airplane track and virga was visible from the base before entry. On the third pass, 13 min after the first, the airplane penetrated a rather large radar cloud, visible precipitation in the form of steady soft snow pellets or grain was falling past the airplane, and the electric field reached a maximum of 23 V/cm.

If the imbalance of the charge distribution about the airplane can be associated with the maximum radar-echo regions, it is clear from this and other cases that the solid precipitation carried an excess positive charge.

The electric field records for 389 cloud passes in midwestern United States convective clouds have been examined. Altitudes of these passes ranged from 10,000 to 20,000 ft. Distinct field effects were observed on seventy-nine of the passes. A similar examination was made of cloud penetrations in Arizona. These flights were all at from 17,000 to 20,000 ft. Thirty-eight cloud passes were examined

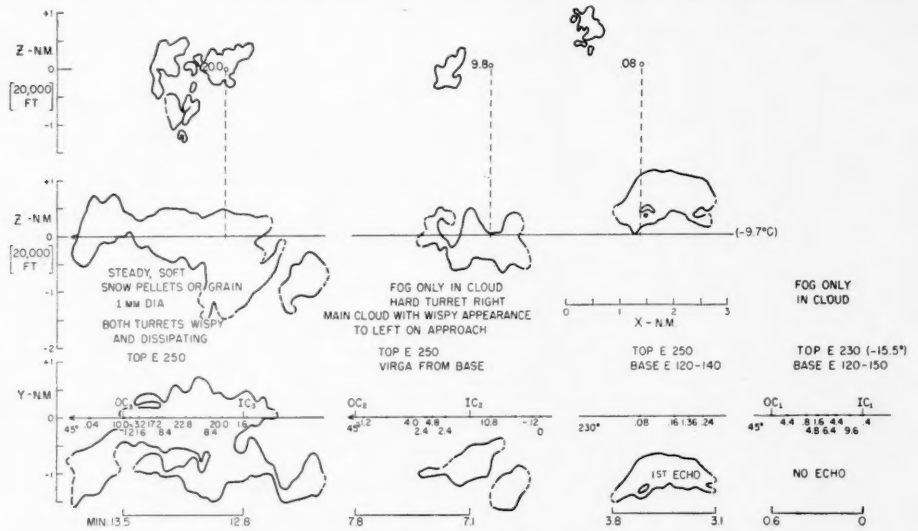


Fig. 4. Flight 259, 27 August 1955. Cloud *C*.

and distinct electrical effects were observed on twenty-five of these. These data are in agreement with well-known evidence that maximum electrical effects on aircraft occur in the vicinity of the melting level when heavy convective precipitation is present.

## 3. SUMMARY

The observations described in this paper provide information on three questions of current importance in precipitation-electricity research. They are:

(1) To what extent do all-water clouds produce appreciable electric fields, and what are the conditions for a static discharge from such a cloud?

(2) Do appreciable electric fields precede or follow the detection of radar precipitation echoes from clouds?

(3) What is the polarity of charged liquid and solid precipitation particles at the altitudes of precipitation initiation in convective clouds, and what is the time scale for the development of pronounced electrical effects?

With respect to the first question, the horizontal electrostatic field has been observed on 691 passes through trade-wind cumulus clouds. The clouds studied had bases from 1500 to 2500 ft above sea level, and tops from a few hundred feet above base to above 15,000 ft. Most of the clouds studied had tops ranging from 7000 to



VOL. 15 1959

9000 ft above sea level. A pronounced external field effect, such as is commonly seen in clouds known to contain ice, was observed on only one tropical cloud pass. This cloud had convective tops extending through an altocumulus–altostratus cloud deck to altitudes colder than 0°C. Very heavy rain was observed at the flight levels of 6500 and 5500 ft of the two airplanes penetrating this cloud.

These observations are in agreement with the paucity of reports of strong electrical activity from warm clouds and, when examined on a case-study basis, suggest a possible mechanism for the occasional build-up of charge in such a cloud to the point where a static discharge may occur. The case studies show that negative-charge centres in warm clouds may be found in the principal draft columns, and that the field magnitudes are larger at the altitudes of higher measured liquid-water concentrations. It may be suggested that entrainment of atmospheric ions into the draft, and selective capture of the negative ions on the larger water droplets in accordance with the predictions of the Wilson ion-capture theory, will account for the effects observed in the cases studied, and it may be that very high entrainment rates, or rapid growth of precipitation on some occasion could lead to sufficient charge separation in this manner for a few static discharges to occur.

The question of the relation of strong electrical effects to the development of radar precipitation in the cloud is illuminated by the observations that many trade-wind cumulus clouds developed strong radar echoes and rain without pronounced electric-field effects. On the other hand, it was common to note the presence of weak, and on occasion, pronounced external field effects before the radar echo appeared in the mixed-phase clouds studied in the midwestern and southwestern United States.

The question of the polarity of liquid and solid precipitation charge in the regions of formation of the precipitation may be examined if one considers that the wingtip field meters' response to external horizontal fields is proportional to the imbalance of the charge distribution about the airplane. Although there is an initial ambiguity in the sign of the unbalanced charge, it seems likely that most of the charge in question will be found in the cloud volume giving the largest radar echo return.

If this criterion is employed, the weak-field tropical clouds are found to exhibit negative charge in statistical excess in the regions of greatest liquid-water content in the cloud. This relation did not continue to hold in any obvious fashion for the one strong-field cloud studied in the Caribbean region.

Regions of high liquid-water content in the mixed-phase clouds, as delineated by rates of rime ice formation or observations that the precipitation was predominantly rain, also appeared to be regions of excess negative-charge accumulation. Magnitudes of the fields associated with these regions were generally less than was observed in positive-charge regions in the same cloud. These smaller fields may be accounted for on the assumption that the negative charge on solid-precipitation streamers was distributed in a rather inhomogeneous manner within the cloud volume. Laboratory support for the view that negative charge exhibits a remarkably greater affinity for association with water vapour and droplets than does positive charge may be found in the early researches carried out by TOWNSEND (1897) and by ZELENY (1900).

A number of clouds examined at altitudes of from 11,000 to 20,000 ft above sea level exhibited strong field build-ups coincident with or somewhat before the observation of solid precipitation in the form of snow pellets or graupel, snow grain, or heavy snow, at flight level. With the assumption that the electric-field anomaly is associated with the maximum radar cloud volume, the sign of the charge on recently formed solid precipitation was found to be predominantly positive over the flight altitudes used. Magnitudes of the fields encountered in clouds known to contain solid precipitation were from ten to a hundred times the usual fields encountered in all-water water clouds. It was common to find that the increase of field in these clouds took place rather suddenly with most of the growth occurring over a period of 5 or 10 min.

The cold cloud observations can be most simply accounted for by the hypothesis that a rapid change from the liquid to solid phase of cloud drops approaching precipitation size is accompanied by an electrical effect which places positive charge on the solid particles with the liberated negative charge left to combine with the ambient water vapour and cloud droplets. If this is so, it follows that one should be able to study the respective roles of precipitation growth by coalescence and by sublimation processes through examination of the precipitation charges at various altitudes in the cloud and, incidentally, to determine from a field measurement outside the cloud whether or not ice is present in it—a question of interest in cloud seeding experiments.

VOL.
15
1959

## References

Townsend J. S. 1897 *Proc. Camb. Phil. Soc.* **9,** 244.
Zeleny J. 1900 *Phil. Trans.* A **195,** 193.

## Discussion

Dr. Smith—What is the relation of these clouds to thunder showers? It seems that the values of field strength given are low for thunder showers and I wonder by what means airborne equipment was calibrated.

Dr. Fitzgerald—The coefficient of proportionality or "form factor" for this installation was determined by banking the airplane at a low altitude during fair-weather conditions and measuring the component along the wing of the vertical fair-weather field at the same time that the field value at the ground was measured. It was then assumed that the air conductivity increased uniformly with altitude and that a constant fair-weather conduction current existed so that the field at flight level could be simply related to the field at the ground through the application of Ohm's law.

Calculations based on this simple model of the lower atmosphere and the observed fields lead to an intensification factor of 220 for the wingtip installation. All field data plotted in the figures shown at this meeting were measured as indicated fields 220 times as large as the plotted values.

Theoretical estimates of the effects of the wing geometry on intensification of the field suggest a factor of perhaps $\frac{1}{10}$ that calculated above, so no great reliance can be placed on the absolute values of field indicated. However, the development in field from one cloud pass to another is independent of the airplane form-factor

and it is this development in relation to the other meteorological events observed that is of the greatest importance.

Subsequent discussions of the problem of obtaining accurate form-factor calibrations for airplanes used in atmospheric electricity research have been held with Dr. J. F. CLARK of the United States Naval Research Laboratory. Dr. CLARK has been able to make detailed theoretical calculations of form factors and to make rather accurate flight observations of the form factor for wingtip mounted field meters. He obtained a result of 53 for a P4Y type airplane which has roughly the same dimensions as the B-17 used in our experiment.

This accurate result has lead to a re-examination of the possible effects of the exchange layer on the day of the B-17 experiment. A small temperature and moisture inversion was present at 0900 hours CST about 500 ft above the altitude at which the experiment was performed at 1300 hours CST. The 1500 hours CST sounding indicated a nearby adiabatic lapse rate. It now appears likely that a space charge sufficient to increase the field at flight level by a factor of about 4 was still present above the airplane during the experiment. This completely invalidates the assumption made about the relation of the field at the ground to that at flight level. In the absence of a direct measurement of the field at flight altitude during the experiment, and for convenience in changing already computed fleld values to reflect the more accurate form-factor determination, a new form factor of 55 or one-quarter that previously calculated has been adopted. The field magnitudes given on the accompanying figures have been changed to accord with this new value assigned the form factor.

OL.
15
959

Journal of Atmospheric and Terrestrial Physics, 1959, Vol. 15, pp. 262 to 287. Pergamon Press Ltd. Printed in Northern Ireland

## SESSION IV

RADAR STUDIES OF "ANGELS"

# Radar studies of meteorological "angel" echoes

D. ATLAS*

Air Force Cambridge Research Center, Air Research and Development Command,
L. G. Hanscom Field, Bedford, Massachusetts

**Abstract**—A review, supplemented by new data, is presented of "angel" echoes from meteorological sources. The major angel types are: (a) non-stratified discrete-coherent echoes which occur randomly in the convective mixing zone, and groups of incoherent echoes associated with pre- and sub-cumulus thermals; (b) mantle echoes associated with, and in the form of, cumulus cloud boundaries; and (c) stratified echoes, generally incoherent when viewed obliquely (at large ranges), coherent at vertical incidence and associated with layers of sharp moisture lapse or minima. Such layers may also act as plane reflectors giving coherent echoes. Special angel types, such as those associated with the sea breeze front add to the impressive evidence of the association of angels with meteorologically induced gradients in refractive index. In every case, however, the gradients required by theory exceed "reasonable" or measured values by at least one or two orders of magnitude, apparently due in large part to the lack of high resolution refractometer measurements. The observations indicate frequent conditions suitable for enhanced forward scatter beyond the horizon and also testify to the feasibility of FRIEND's 1939 proposal to use radio reflections for sounding air-mass boundaries.

VOL.
15
1959

## INTRODUCTION

"ANGEL" echoes from the troposphere have been observed ever since WATSON-WATT *et al.* (1936) first pointed their short-pulse (20 $\mu$sec) 50-m wavelength radio antenna toward the ionosphere over Orford Ness, England, in May 1935. However, it was PIDDINGTON (1939) who first suggested that these echoes were probably due to sharp variations in the atmospheric dielectric constant, and FRIEND (1939) who simultaneously demonstrated the validity of PIDDINGTON's thesis experimentally. Indeed, FRIEND was so convinced of the relationship by 1939 that he proposed the continuous sounding of air-mass boundaries by radio reflections. So it may seem a bit odd that we should still be debating the reality of atmospheric "angels" 18 years later.

Yet this is what we shall be doing in part in this paper, for, despite the accumulation of a vast store of evidence relating "angel" echoes to atmospheric inhomogeneities, we have not been able to reconcile the magnitude of the observed reflection coefficients to the sharpness of the gradients required theoretically. Doubt in the reality of meteorological angels is further compounded by the fact that many so-called angels may adequately be accounted for by birds and insects.

In this paper, I hope to prove the existence of atmospheric angels once and for all, while not denying the co-existence of insect and bird angels. Furthermore, we shall discuss the characteristics of various types of angels and the associated weather, and estimate the discrepancy between theory and observation in the reflection coefficients.

* Geophysics Research Directorate, Weather Radar Unit, Blue Hill Meteorological Observatory, Milton, Mass.

This report will not be a comprehensive historical review of the subject. Such a history has already been provided in an excellent work by PLANK (1956). Instead, we shall restrict the discussion to the most recent observations of various types of angel activity and draw upon historical records for support and refutation.

## DISCRETE–COHERENT ANGELS

Because of their resemblance to bird and insect activity, the discrete–coherent angel echoes are probably the most controversial type. On the PPI and RHI scopes they appear as point or dot echoes, similar to those from small aircraft, and sometimes occur in tremendous numbers, as in Fig. 1. Some reports show correlation of echo velocities with the wind; others do not. Still others indicate direction of motion with the wind but at differing speeds, sometimes as great as 700 miles/hr (PLANK, 1956).

On the RHI or on the A-scope of a fixed vertically-pointing beam this type of echo is usually transitory, lasting no more than a few seconds, although rare angels have been tracked for as long as 20 min on the PPI (PLANK, 1956). Assuming the angels to be wind-borne, PLANK (1956) computed their sizes from their durations and concluded that, although many angels behave like point sources, their probable size is a few tens of feet. BALDWIN (1943, 1948) thought them to be some tens of yards (see also ANON., 1947).

While this type of angel is entirely coherent or non-fluctuating, in contrast to a noise-like precipitation echo, this does not necessarily indicate that the target itself is a single coherent mass, but only that the contributing reflecting surfaces are maintaining nearly constant phase positions with respect to the transmitted waves. In the atmosphere, however, it seems unlikely that a complex array of parcels could furnish a non-fluctuating echo persisting for 1 sec or more. Therefore the most likely target would appear to be a discrete parcel, perhaps with a rough boundary, or at most three or four parcels maintaining fixed relative positions with respect to each other.* We shall deal with fluctuating or incoherent angels later.

Discrete-coherent angels occur under two predominant meteorological conditions: (a) at all levels in the convective mixing layer, usually on hot moist days; and (b) at inversions associated with sharp moisture gradients. Under the latter conditions, the echoes frequently appear in the form of layers and the reflection mechanism may differ somewhat from that associated with the non-stratified type. We shall restrict the discussion to individual non-stratified angels for the moment.

By far the most comprehensive study of the meteorological behaviour of angels is that by PLANK (1956). His results, some of which are seen in Fig. 2, may be summarized as follows:

(1) The seasonal variation of activity in New England shows a broad maximum in the summer months with heaviest activity in July, and trailing off slowly to December. Although PLANK reported no angels in January and February, we have since observed them in February (CHMELA and ARMSTRONG, 1955).

(2) Activity increases with surface temperature. Both the number and height to which the angels extend have a fairly pronounced diurnal variability with

* AUSTIN (1952) has shown that the fluctuation spectrum for five randomly-positioned particles closely approximates that for a large number of particles.

maxima in the early afternoon, but slightly earlier than the maximum temperature. Also, activity drops off more rapidly than temperature beyond the maximum. Although this is not particularly striking in Fig. 2, it is believed to be significant.

(3) The maximum height of angel activity corresponds well to the height of the convective mixing zone or to the maximum range of detection if the mixing layer is deep.

(4) Angels tend to bunch in layers in the vicinity of sharp moisture gradients located within the convective mixing zone.

(5) The greatest activity occurs on days with relatively low wind speed.

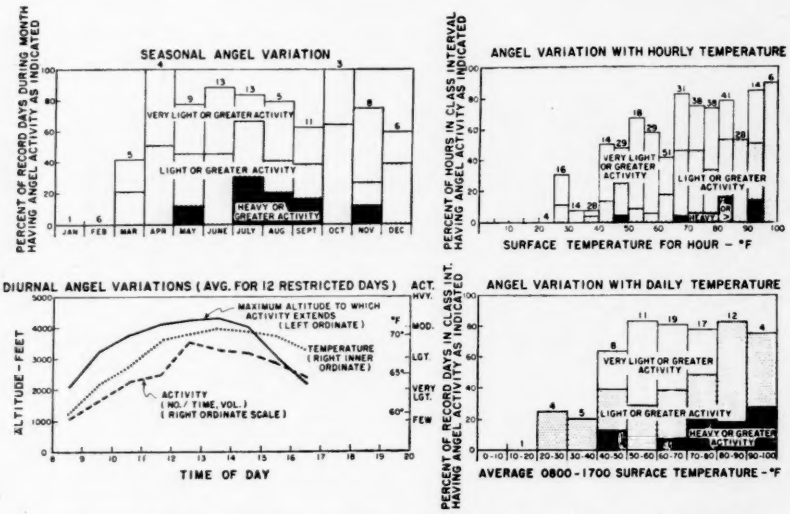
SEASONAL ANGEL VARIATION
PERCENT OF RECORD DAYS DURING MONTH HAVING ANGEL ACTIVITY AS INDICATED
VERY LIGHT OR GREATER ACTIVITY
LIGHT OR GREATER ACTIVITY
HEAVY OR GREATER ACTIVITY
JAN FEB MAR APR MAY JUNE JULY AUG SEPT OCT NOV DEC
ANGEL VARIATION WITH HOURLY TEMPERATURE
PERCENT OF HOURS IN CLASS INTERVAL HAVING ANGEL ACTIVITY AS INDICATED
SURFACE TEMPERATURE FOR HOUR - °F
DIURNAL ANGEL VARIATIONS (AVG. FOR 12 RESTRICTED DAYS)
ALTITUDE - FEET
MAXIMUM ALTITUDE TO WHICH ACTIVITY EXTENDS (LEFT ORDINATE)
TEMPERATURE (RIGHT INNER ORDINATE)
ACTIVITY (NO./TIME, VOL.) (RIGHT ORDINATE SCALE)
ACT.
HVY.
MOD.
LGT.
VERY LGT.
FEW
TIME OF DAY
ANGEL VARIATION WITH DAILY TEMPERATURE
PERCENT OF RECORD DAYS IN CLASS INT. HAVING ANGEL ACTIVITY AS INDICATED
AVERAGE 0800-1700 SURFACE TEMPERATURE - °F

Fig. 2. The seasonal, diurnal, and temperature dependence of discrete–coherent angels in the New England area. The bar graph (*upper left*) shows the percentage of record days in individual months having angel activity exceeding the degree indicated. The diagram (*lower left*) shows semidiurnal variations of (1) maximum altitude reached by angels, (2) frequency of occurrence (activity), and surface temperature. The graphs at right show the percentage occurrence of angel activity in various temperature classes, the upper being based on hourly observations, the lower on daily averages. Data based on observations made with vertically-pointing 1·25 cm-radar (after PLANK, 1956).

Except for the association of strong activity with low wind speeds, all of the above point to a relation between angels and the convective mechanism; convective thermals or bubbles seem to be likely angel sources. The lack of angels in January and February may be related to both the low moisture content in the air and the frozen ground. In this regard, PLANK (1956) has noted a qualitative relation between high angel activity and ground moisture.

As for the bunching of angels at the level of a sharp moisture gradient in the mixing zone, it is apparent that this is the level at which we may expect a maximum difference in vapour density and refractive index between a buoyant parcel originating at the surface and the environment. Since such a parcel retains much of the vapour content with which it was released at the ground, its refractive index differs more and more from that of the environment as the environmental vapour content decreases, the greatest differences occurring in the zone of sharp moisture lapse.



VOL. 15 1959

OL.
15
959

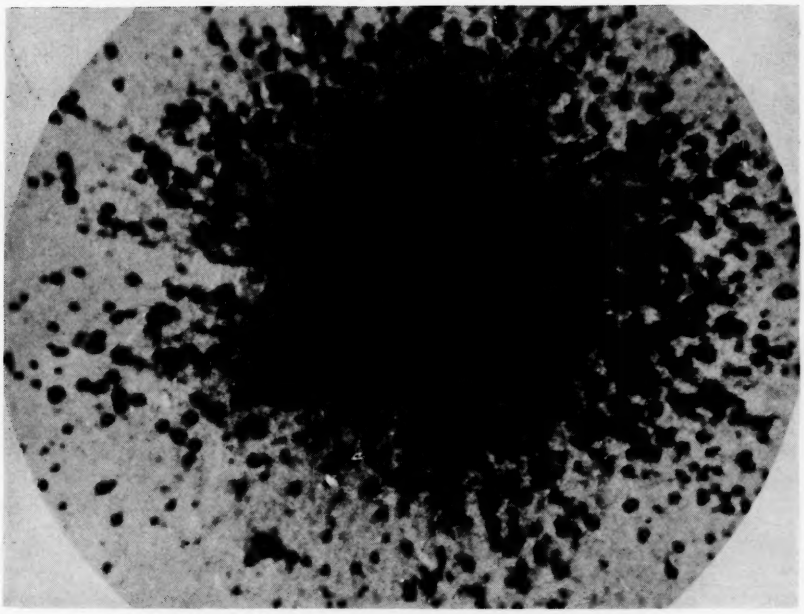

Fig. 1. A large swarm of angels seen on the 10-cm AN/CPS-1 radar at 2100 EST 26 September 1952 on Long Island, N.Y. Range: 15 miles; low beam MTI. Weather: high scattered clouds; wind east at 10 knots. This picture may be due either to meteorological angels or birds. (*Courtesy of Airborne Instrument Laboratories.*)

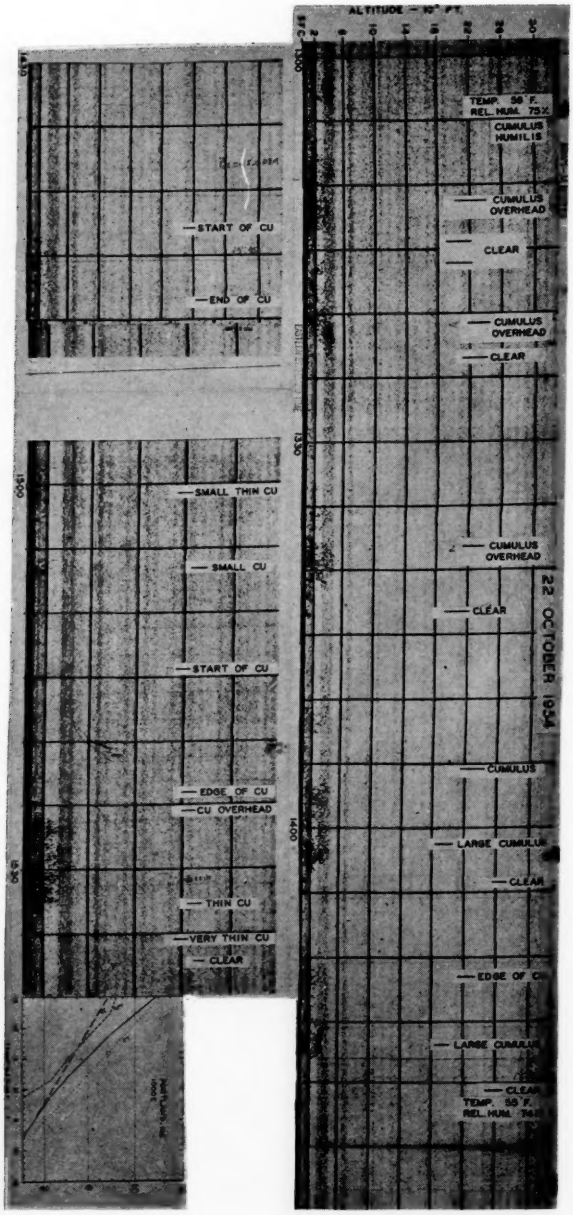


Fig. 3. A 1·25-cm radar time–height record (vertically pointing beam) taken at Lexington, Mass. on 22 October 1954. Note groups of angel echoes up to heights of 5000 ft such as those at 1308–1313, 1338–1342, 1357–1403 and 1526–1533. Each angel group is associated with the passage overhead of a cumulus cloud as noted by comments on record. Horizontal dark bands of noise are imperfections in recording. Sounding at lower right taken at Portland, Me. at 1000 EST: temperature (solid); moist adiabat (dotted); dry adiabat (large dash); dew point (small dash). (After CHMELA and ARMSTRONG, 1955).

VOL. 15 1959

As convection proceeds, however, any such moisture gradient which may have existed initially would itself be destroyed by the convection process. Thus angel activity would tend to decrease in the mid-afternoon, as is actually observed. Stratified angel activity could persist only where the moisture gradient occurs at and above an inversion which caps the convective mixing layer. At such a height, moist parcels rising from the surface would be carried by inertia slightly beyond the inversion where they would display a sharp contrast in refractive index with the dry air, and then settle down below the inversion level to diffuse into a moist environment.

PLANK also noted that the index contrast between rising parcel and environment would be reduced by turbulent mixing. He proposed this as a possible source for the reduction in angel activity with high winds, since the mixing process increases with wind speed.

While all this indicates a fairly definite correlation between the characteristics of angel activity and the behaviour of convective bubbles, it is still somewhat circumstantial evidence. If the bubble or thermal is indeed the echo source, surely we should detect angels under cumulus clouds. Furthermore, the visual boundaries of cumulus clouds should also furnish strong angel reflections. This type of direct evidence is now accumulating in sufficient abundance to leave no doubt of the angel–thermal relationship.

For example, CHMELA and ARMSTRONG (1955) made the observations shown in Fig. 3 with a 1·25-cm vertically-pointing radar. Each dark mass of echoes shown on the facsimile record from the surface to a height of 5000 ft, (e.g. 1357–1403), is a large group of closely spaced, but discrete and coherent angels. Every one of these angel groups is associated with the passage overhead of a cumulus cloud, as can be seen by the notations on the record; several times the beginning and end of an angel group correspond exactly to the edges of the cumulus cloud. Only the cumulus observed at 1515 ft fails to show a well-defined group of angels, although they may be obscured in the noisy record below 2000 ft. Background angel activity between cloud passages was roughly 24/min and occurred below 2000 ft; this increased to about 150/min during cloud passage and extended to a fairly sharp cut-off level at about 4500 or 5000 ft. The cloud bases were at 5800 ft. Assuming that the angel sources or bubbles were carried through the 0·35° beam with the wind (which averaged 13 miles/hr in the lowest 5000 ft), this corresponds to a bubble concentration of $2/10^6$ ft$^3$, or a bubble spacing of roughly 80 ft. Therefore, on a poorer resolution radar or at greater range, it seems likely that these masses of coherent angels would have appeared incoherent, provided that they moved with respect to each other. Indeed, we shall see that the radar resolution frequently determines whether an angel echo will be steady or fluctuate.

The association of the angels in Fig. 3 with the cumulus seems more than coincidental. Each cumulus cloud carries its own band of angels along with it. Glider pilots and seagulls have long been familiar with the thermals under convective clouds, and the refractive-index fluctuations associated with such thermals have been measured in aircraft traversals by GERHARDT *et al.* (1956). Thus the correspondence of the angel masses to thermals is implicit. The only evidence lacking to make the identification positive in the cited case are refractive-index

measurements through the thermals simultaneous with the radar observations. While we have made no concerted effort to repeat these observations, HARPER *et al.* (1957) have recently also reported a clear association between angels and cumulus clouds. They too have associated the angels with refractive effects at the edges or caps of rising clear-air thermals.

## INCOHERENT ANGELS

The short-range observations of CHMELA and ARMSTRONG suggest that the thermals of their clouds were comprised of a large number of discrete bubbles or blobs, which should therefore present an incoherent echo when viewed with a wider beam or at a greater range. This is illustrated in Fig. 4, which shows a series of RHI cuts made through a line of cumulus with the 10-cm high-power FPS-6 radar. While mantle echoes are observed from the mountain-like boundaries of the cumulus clouds at all azimuths (we shall discuss mantle echoes later), a column of echo is seen to extend from the ground to the peak of the cloud at 249°. This might be thought to be strong ground echo such as that at 23–26 naut. miles; however, it is seen to disappear 20 min later at 249° and reappear in the 261° picture, having moved northward with the wind. The column is believed to be a major thermal under the cumulus cloud. While the writer did not have an A-scope available, the thermal echo appeared almost certainly to be incoherent, as we should expect from the observations of CHMELA and ARMSTRONG. On the other hand, HARPER *et al.* (1957) have reported discrete-coherent angel echoes rising toward rapidly-building congestus clouds and have photographed one such angel rising into the centre of a mantle echo (Fig. 5). Since their pulse volume was much too large to resolve the closely-packed coherent angels of CHMELA and ARMSTRONG, their angels must have been either individual bubbles or a few such bubbles moving in concert. However, some of their coherent angels did twinkle a bit as they moved so that their reflective properties were not thought to be constant.

In other recent observations with the FPS-6 at South Truro, the writer has seen what appeared to be diffuse trails of echoes, extending from the ground up to the base of the clouds, tilted in the direction of the wind shear, just as we would expect thermals to be oriented. Some of these can be seen weakly in Figs. 6(a) and 6(b). In these photographs, the stronger echoes at 7000 to 9000 ft (7–16 naut. miles) are associated with the cumulus clouds, although a point-to-point echo to cloud correlation was not made. The weak tilted column, extending from the ground to the cloud level at about 15–17 naut. miles, is believed to be the thermal. The so-called thermal echoes could barely be discerned on individual frames (the film was under-exposed) although they were fairly clear on the scope itself. In order to bring them out, repeated exposures of ten consecutive frames were made on one print. Thus all photos in Fig. 6 represent integrations of ten vertical scans of the antenna over a period of 30 sec. No single echo in the thermal could be followed from one frame to another; rather, the echoes twinkled rapidly, indicating incoherence.

In order to understand better the probable origin of the thermal echoes, it may be noted that the radar was directed at an azimuth of 144° and the wind



VOL. 15 1959

METEOROL.
QC915
.A59

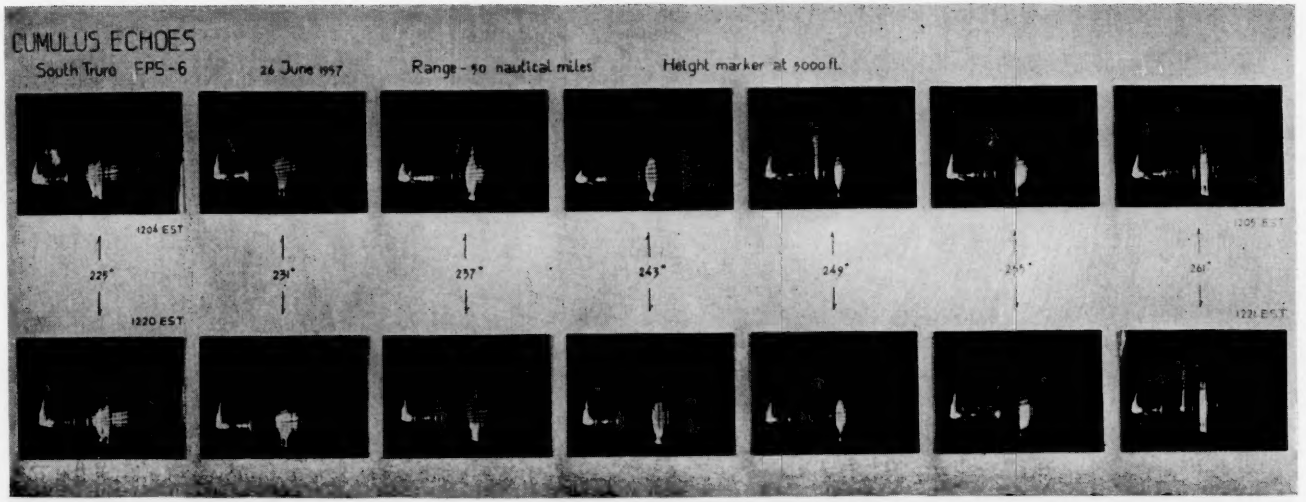


Fig. 4. Cumulus mantle and thermal echoes seen on RHI scope of 10-cm AN/FPS-6 radar at South Truro, Mass. on 26 June 1957. Horizontal range 50 naut. miles; markers 10 naut. miles; top of photo is at height of 15,000 ft. Upper series taken at 6° azimuth steps starting at 225° at 1204–1205 EST; lower at 1220–1221 EST. Thermal column first appears at 249° (*top*), and later at 261° (*bottom*) at range 16–17 naut. miles. Strong echoes extending from below horizon to considerable heights are ground clutter.

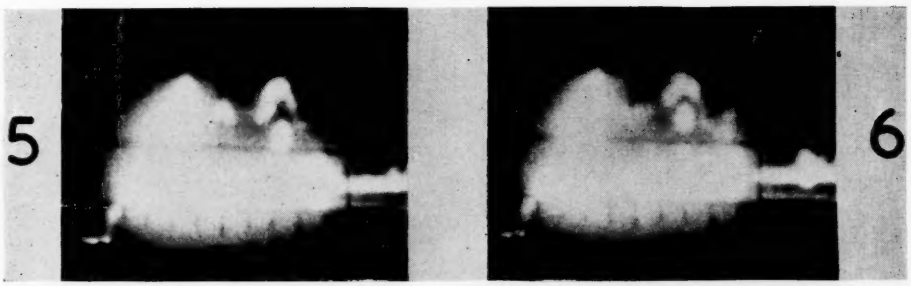


Fig. 5. In the centre of the pictures is a cumulus mantle echo with top at 5000 ft. An isolated (apparently) coherent angel echo beneath it ascends about 500 ft during the 2 min between the pictures taken at 1608, 1610 GMT, 26 July 1956, at Dunstable, England (10-cm radar). (After HARPER *et al.*, 1957).

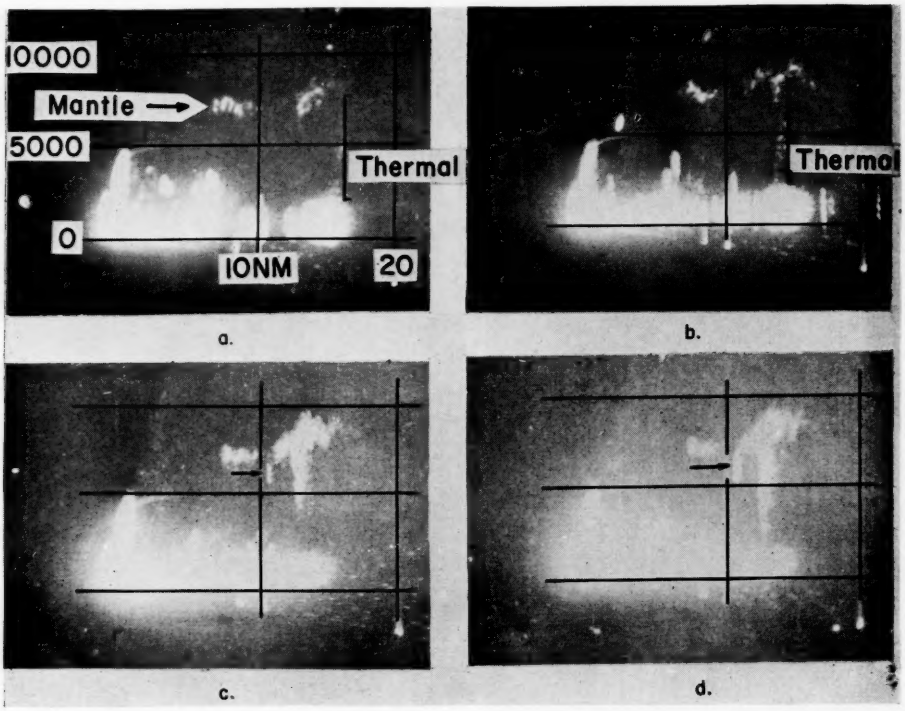


Fig. 6. Cumulus mantles and thermals on the 10-cm FPS-6, South Truro, Mass., 11 July 1957, all at 144° azimuth. Scales and times as indicated. Each photo is an integration of ten consecutive exposures of individual frames taken originally at one frame per scan (3 sec each). Note the weak incoherent thermal column marked in *A* and *B*. Also note the (apparently) coherent echo (arrow) in *C* and *D* which persisted for at least 1 min and the rapid downward projection of the angel column in the 30 sec between *C* and *D*. No droplets were observed.

VOL.
15
1959

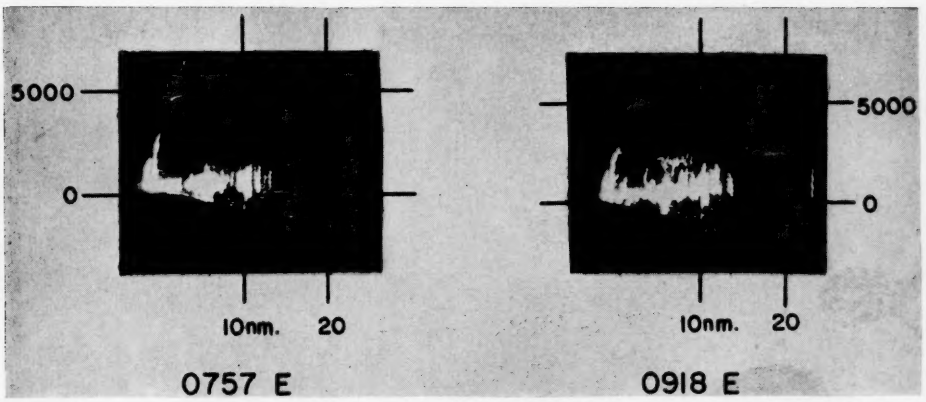


Fig. 7. Pre-cumulus angels seen on FPS-6, South Truro, Mass., 17 July 1957. Azimuth 160°; scales indicated. (*Left*): normal clutter at 0757 EST. (*Right*): low level angels develop at 6–9 naut. miles at 0918, about 20 min prior to first observation of tiny cumulus cloud in same position.

OL.
15
959

VOL.
15
1959

was blowing lightly from between W and WNW at all levels up to about 9000 ft. The radar station at South Truro is located on the north–south peninsula of the Cape, so that views toward the west are over Cape Cod Bay and views to the east are over the ocean, except for nearby ground. It is of interest to point out that the position of the thermal echoes in Fig. 6 lies approximately 5 miles to the east (leeward) of the east–west arm of Cape Cod.* Thus, westerly winds leaving this arm of the peninsula must have had essentially a land history. This air would then display a significant moisture and refractive-index contrast with both the air to the north and south which passed over Cape Cod Bay and Nantucket Sound, respectively. Since this stream of dry air must also have been considerably warmer than that to the north and south, the horizontal N-gradients would be further enhanced. The observation of thermal echo down to the ground level supports this explanation, since adequate refractive contrast in the horizontal could not occur there as a result of vertical lifting. Furthermore, the echo column occurred only in the region directly east of the east–west arm of the Cape, while cumulus clouds and their associated mantle echoes occurred roughly in a north–south line lying parallel to and leeward of the peninsula. Thus convection induced by the peninsula was widespread. Finally, it will be noted that the cumulus-mantle echoes are higher over the thermal echo column than elsewhere, indicating that convection is intensified there in accordance with the proposed hypothesis.

While organized sub-cloud thermal echoes such as those in Figs. 3 to 6 have been observed on occasion, the observation is comparatively rare. At least, there was no evidence of well-defined angel groups in most of the 1·25-cm (low power) vertically-pointing records studied by PLANK (1956). However, the thermals seem more readily detectable with the high power 10-cm FPS-6 equipment. Of course, we should not expect to detect the thermals once the clouds have become well developed, since the sub-cloud layer would be well mixed by then and rising parcels would display little moisture contrast with the environment. On the other hand, evaporative cooling on the boundaries of well-developed cumulus can lead to downdrafts of relatively dry air from aloft into the moist sub-cloud layer where the difference in vapour content may be detectable. The downward development of an echo column, which may be associated with such a mechanism, is shown in Figs. 6(c) and 6(d) at a range of from 12 to 14 naut. miles. Incidentally, the echo at about 11 naut. miles and from 5000 to 7000 ft in these photos was one of the few that appeared coherent on this day.

Fig. 7 illustrates thermals detected prior to the actual formation of cumulus clouds. The photo on the left shows the normal ground clutter; 1 hr 21 min later, we observed the picture on the right in perfectly clear air. We maintained a continuous radar and cloud watch at this direction with both radar and cloud cameras; about 20 min later a small cumulus developed, while the rest of the sky remained clear. The cloud decayed and a new one formed in the same place, evidently triggered by convection over a small peninsula. In this case, the pre-cumulus angels appeared incoherent, although a few unidentified echoes at closer range (possibly from sea gulls) were discrete and coherent in character.

* The presence of ground echoes directly under the thermal echo is believed to be a false indication resulting from the detection of land to the south on a side-lobe of the radiation pattern.

Summarizing to this point, we see that both the discrete coherent and the incoherent non-stratified angels are closely associated with the convection mechanism. The former occur primarily in an apparently random fashion in the convective mixing zone (PLANK, 1956) and only occasionally are associated with particular cumulus clouds. The latter appear most frequently to be associated with pre- and sub-cumulus thermals. While they appear incoherent with poor resolving power, the little available evidence indicates that they are comprised of an array of individual coherent targets when seen with better resolution (CHMELA and ARMSTRONG, 1955). Thus both types of angels seem to behave like convective bubbles or eddies.

## BUBBLE CONVECTION

The idea that atmospheric thermals are comprised of bubbles, and not of a uniform jet is due largely to SCORER and LUDLAM (1953). The bubbles which appear at the cauliflower tops of cumulus clouds strongly support their theory. However, even if SCORER and LUDLAM had not proposed this idea, the writer believes that the radar observations probably would have forced us to conclude that thermals were composed of some sort of blobs.

In their paper, SCORER and LUDLAM visualize a bubble, such as that shown in Fig. 8, with a fairly sharply defined spherical top and a diffuse wake. The left side represents conditions for a dry bubble; the right side represents a cloudy bubble. Note that the air motion is downwards on the edges of a cloudy bubble, where evaporation of the cloud cools the air and causes it to sink. While the sharpest vapour-gradients undoubtedly occur along the top of the bubble, the eddies along the boundary of the wake may overbalance the smaller vapour-discontinuities there to provide an increased reflectivity. On the other hand, the spherical shape of the top boundary may contribute a focusing effect which would enhance the reflectivity of the sharp boundary there for vertically-directed beams.

Large bubbles, perhaps 300 m in diameter, are said to form from an aggregation of the warm moist wakes of many small ones released in the superadiabatic layer at the ground. If there is no wind, the large bubble must draw a supply of fresh smaller ones from the same piece of ground, thereby exhausting its heat and inhibiting further growth. A general wind drift is said, therefore, to assist the growth of the larger bubbles.

Once a group of bubbles has organized into a thermal, the associated small hydrostatic reduction in pressure below would tend to maintain the thermal column as the path of least resistance for further convection. In addition, the release of latent heat during formation and development of a cumulus cloud would tend to reinforce this effect, so that as the cloud moves it sweeps up new bubbles like a vacuum cleaner. This is evidently the means by which a cloud carries its angels or thermals with it and, of course, it is the only process by which a travelling cumulus can build to cumulonimbus proportions.

In our later attempts to deduce the bubble reflectivity, it will be necessary to make some reasonable estimate of the bubbles' vapour-content relative to the environment. In this regard, it is usually assumed that a bubble rises from the surface retaining essentially all of the vapour content without mixing with the



VOL.
15
1959

environment. PLANK (1956) attempted to compute the correct vapour content by assuming it to mix with the environment to various degrees. However, in their experimental cloud-index studies, CUNNINGHAM *et al.* (1956) note that the core "bubbles or more continuous type thermals in larger clouds (appear to) rise without mixing appreciably with the air around them", since the theoretical convection condensation-level frequently checked with the actual cloud base. SCORER and LUDLAM (1953) have also pointed out that the moist wake of one bubble will protect subsequent bubbles from excessive mixing with the dry

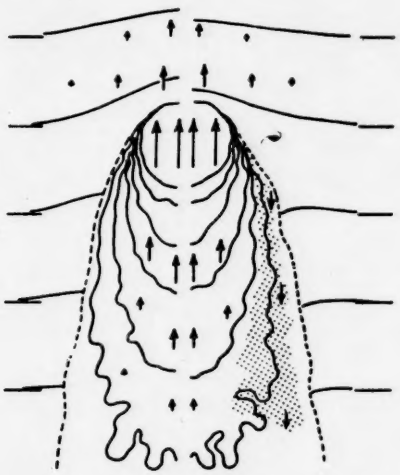

Fig. 8. Model of a rising bubble. The left half of the diagram refers to dry ascent; at the right, condensation has occurred in the bubble and the shaded area represents the region of the wake in which there is sinking motion. Arrows indicate the velocity field; smooth continuous lines show displacement of environment air particles from their original level. (After SCORER and LUDLAM, 1953.)

environment, and CHMELA and ARMSTRONG's angel observations indicate that the bubbles may sometimes be so closely packed in a broad thermal that only those on the boundaries will be subjected to appreciable mixing with the environment.

## BUBBLE SIZES

As for bubble sizes, there is evidently a difference according to angel type. The values quoted earlier for the observations of PLANK (1956) and BALDWIN (1943, 1948) range from a few tens of feet to a few tens of yards for the lone angels. A few index measurements in flight below cumulus indicate sizes ranging from 150 to 650 ft and a small tendency for the larger ones to display higher index contrast with the environment.* The sizes of the cauliflower bubbles on cumulus tops, as reported by SCORER and LUDLAM (1953) and by MALKUS and SCORER (1955), range from 660 to 3000 ft. More extensive observations by PLANK and SPATOLA (1957) show sizes from 525 to 5800 ft. However, these sizes cannot be used as a reliable

* Private communication from CUNNINGHAM, PLANK and SPATOLA, Geophysics Research Directorate, Air Force Cambridge Research Center.

estimate of the sub-cloud sizes because: (a) the large cauliflower bubbles which stand out to the eye are almost certainly composites of smaller bubbles which may be seen as bumpy nodules on the larger ones; (b) on the other hand, the visual bumps begin to erode on emergence from the cloud top; and (c) LUDLAM has shown that the bubbles expand linearly with height.* Considering all these factors and the finding by CHMELA and ARMSTRONG (1955) of a bubble spacing of about 80 ft, the sub-cloud bubbles are placed in the size range from about 30 to 700 ft. Presumably, the closely packed bubbles are near the lower end and the agglomeration of small ones makes the bigger ones, in accordance with the SCORER–LUDLAM theory. It is interesting that BIRNBAUM and BUSSEY (1955) reported blob scale sizes† from about 40 to 400 ft from index measurements on a tower at a height of 375 ft.

## REFLECTIVITIES

The primary reason to doubt the reality of meteorological angels in the past has been the difficulty of accounting for their observed cross-sections theoretically. Therefore, let us review the theory.

ADEN (1951) has shown that the cross-section, $\sigma$, of a dielectric sphere large with respect to the wavelength is given by the product of the plane reflection coefficient, $\rho^2$, and the geometric area of the sphere of diameter, $D$, or

$$\sigma = \rho^2(\pi D^2/4) \tag{1}$$

For an infinitely sharp discontinuity from air to dielectric of index $n$,

$$\rho_s{}^2 = (n - 1)^2/(n + 1)^2 \tag{2}$$

or

$$\rho_s{}^2 = (\Delta N)^2 \times 10^{-12}/4 \tag{2a}$$

in modified $N$ units‡ and for $n \simeq 1$. The subscript $s$ denotes "sharp." Substituting in (1),

$$\sigma_s = [(\Delta N)^2 \times 10^{-12}/4][\pi D^2/4] \tag{3}$$

It is of interest to compare this cross-section with that which we may deduce from the Booker–Gordon scattering theory (BOOKER and GORDON, 1956). In that theory, BOOKER and GORDON consider the spatial variation of refractive index by assuming it to have an exponential correlation function such that the correlation coefficient drops to $1/e$ at a distance $l$, which is called the "scale" of turbulence. This is approximately the blob diameter, $D$. In terms comparable to (3), the reflectivity $\eta$, or total back-scatter cross-section for a unit volume containing many blobs is

$$\eta = \Sigma\sigma = \overline{(\Delta N)^2} \times 10^{-12}/2D \tag{4}$$

where $\overline{(\Delta N)^2}$ is the mean square departure of the index from the average. If we now assume that the entire scattering volume is filled by closely spaced bubbles of

* Private communication to be reported shortly.

† The Birnbaum–Bussey scale size refers to a mean size which is more or less conventional in present scattering theory.

‡ A modified $N$ unit is defined as $N = (n - 1)10^6$.



VOL. 15 1959

equal size such that the number per unit volume is $1/D^3$, we find that the equivalent mean cross-section of a hypothetical unit Booker–Gordon blob is

$$\bar{\sigma} = [\overline{(\Delta N)^2} \times 10^{-12}/4]2D^2 \tag{5}$$

In other words, the cross-section of such a hypothetical unit blob is just $8/\pi$ times that of the simple sharp-edged dielectric sphere of ADEN. The difference is probably due to the manner of integration and the difference between the turbulence "scale" and bubble diameter.

The difficulty in applying equation (3) is that there can be no true discontinuity in refractive index in the atmosphere. In order to approach reality, we may apply SWINGLE's (1950) result for the power reflection coefficient of a plane layer in which there is a linear $N$ gradient $\Delta N/\Delta Z$:

$$\rho_g{}^2 = [(\Delta N)^2 \times 10^{-12}/4][(\lambda/4\pi\Delta Z)^2] \tag{6}$$

This holds for $(\lambda/\Delta Z) \leq 4\pi$, and the subscript $g$ refers to "gradient". By analogy with (1), it seems reasonable to assume that the cross-section of an electrically large dielectric sphere having a shell in which there occurs a linear gradient of $N$ would be approximately

$$\sigma_g = \rho_g{}^2\pi D^2/4 \tag{7}$$

Using (3), (6) and (7) we see that the ratio of the cross-section of a bubble with linear gradient shell to that of a sharp-edged bubble is

$$F = \sigma_g/\sigma_s = (\lambda/4\pi\Delta Z)^2 \tag{8}$$

In other words, the gradient shell bubble may be considered to be sharp-edged when $\Delta Z = \lambda/4\pi$.

It has been suggested that even SWINGLE's equation (6) overestimates the power reflection coefficient because of the discontinuities in gradient at the boundaries of the transition zone. While this is true mathematically, it is felt that the reality of discontinuities in $N$ gradient has been adequately demonstrated (e.g. by CUNNINGHAM *et al.*, 1956). The reader who wishes to consider reflections from regions having smooth transitions in index at their boundaries is referred to the work of FRIEND (1949). In this regard, it may be noted that FRIEND's smooth transition layer is practically equivalent to a sharp-edged layer when $\Delta Z = \lambda/4\pi$, the same criterion as found by SWINGLE.

The radar cross-sections of sharp-edged spherical bubbles calculated according to (3) are plotted as a function of index and diameter in Fig. 9. Also shown there are the approximate cross-sections deduced by various observers on the basis of observed ranges or signal intensities and the nominal radar characteristics.

It is evident that cross-sections up to a maximum of about 10 cm$^2$ may be accounted for by bubbles of not unreasonable index and diameter, provided that they are sharp-edged. However, it is difficult to conceive of 100–1000 m-diameter bubbles having transition shells of only 0·1–1 cm thickness, in accordance with the requirement of equation (6) at wavelengths of from 1 to 10 cm. Transition zones of at least 10–100 cm would seem to come closer to reality, in which case the

theoretical cross-sections of Fig. 9 would be reduced by at least $10^{-2}$–$10^{-6}$. In that event, we could just barely account for the smallest observed cross-sections of $10^{-2}$ cm$^2$. Of course, there are eddies in which the refractive index rises gradually to a peak in distances corresponding to many wavelengths. Obviously, these would have extremely small cross-sections and it seems unlikely that they could be responsible for any reported angels.

Thus, despite an overwhelming amount of empirical evidence indicating an association between angels and convective bubbles or eddies, we cannot yet account

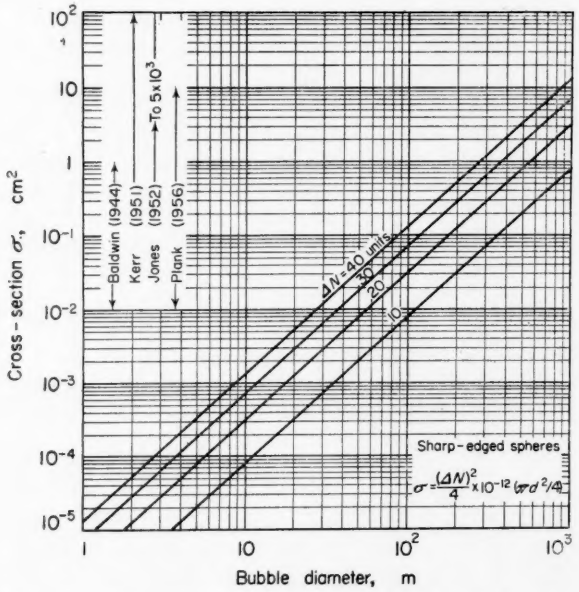


Fig. 9. Radar cross-sections of sharp edged spherical bubbles (cm$^2$) vs. their diameter (m) for various values of $\Delta N$, bubble to environment contrast in units of modified index of refraction.

for the observed cross-sections theoretically, assuming a reasonable bubble model. While the theory needs to be examined more carefully, it can hardly be questioned in the limiting case of sharp discontinuities. Is it possible then that angels are due to the rare bubbles with sharp boundaries which do not constitute our picture of what is reasonable? Alternatively, could there be another reasonable model of an eddy or bubble with enhanced cross-section corresponding to, or even exceeding, that of the sharp-edged spherical model? In this regard, it has been suggested by GORDON* that a bubble or eddy might have a rough surface. Indeed, it seems possible that the concept of a simple spherical bubble may be entirely wrong. Instead, convection may take place in the form of irregular whirling eddies in which sheaths of moist and dry air envelope each other in complex patterns similar to those we see frequently in cigarette smoke. The difficulty here lies largely in the

* Verbally at the initial presentation of this paper at the meeting of the Joint Commission on Radio Meteorology, New York City, 14 August 1957.



VOL. 15 1959

problem of obtaining coherent echoes from such complex transitory targets. In any case these possibilities cannot yet be ignored.

Of course, equations (3) and (6) suggest a means of determining whether or not the targets are sharp-edged. If simultaneous measurements at several wavelengths show no wavelength sensitivity of the measured cross-section, the target must be assumed sharp. Unfortunately, existing data on discrete angels are inconclusive in this regard.

Incidentally, the above discussion casts a shadow of doubt over the validity of the BOOKER–GORDON (BOOKER and GORDON, 1950) cross-sections for back- (and forward-) scatter since they appear to correspond to the limiting values for sharp-edged discontinuities.

## CUMULUS MANTLE ECHOES

Until 1957 no one, to our knowledge, had reported angel echoes from the boundaries of cumulus clouds, where some of the sharpest index gradients have been observed (CUNNINGHAM *et al.*, 1956). Early in 1957 HARPER *et al.* reported such echoes for the first time.* Two of their photos were shown in Fig. 6. These echoes, in the form of an inverted U or V on a 10-cm height finder, are persistent, though weak and diffuse, with a fluctuating character like that of precipitation echoes. The correspondence between the echo and cumulus boundaries was checked on a number of occasions by theodolite. Some of the associated clouds were so small as to exclude the possibility of drizzle droplets as the echo source. Furthermore, the mantles were never seen on a 3-cm radar of comparable sensitivity for precipitation. Consequently, HARPER *et al.* have attributed the echoes to abrupt refractive gradients at the cloud edges.

In June and July 1957, the writer verified the above report, using the high power 10-cm FPS-6 radar at South Truro, Cape Cod. Some of these observations are shown in Figs. 4, 10 and 11. Fig. 10 shows several examples. At the upper and lower right are shown two clear-cut inverted V's associated with the visual cloud peaks. The other photos also show the cloud-boundary echoes and some diffuse echoes below. In Fig. 4 the radar scans through a line of cumulus in various directions, the two sequences being taken 16 min apart. Although the cloud boundaries are strongest, some of the pictures show complete echo mounds (e.g. 225° at 1204). Note also that the cloud towers have moved north with the southerly winds in the 16 min between sequences, so that the structures at 237°, 243° and 249° in the 1204 series are found in roughly the same shape at 249°, 255° and 261° in the 1220 series.

Fig. 11 shows a time-lapse series at approximately ½ min intervals from 1208 to 1218. Note that the cloud mantle is almost completely echo-filled at first with the thermal column extending from ground to cloud peak. After 1214, however, the pattern is more in the form of an umbrella with the thermal representing the handle. When shown as a film, the audience is usually in agreement that the outer

* SIR ROBERT WATSON-WATT (1946) has written: "There is some doubt about the date of the first observed radar echoes from clouds. An experimental 30-cm installation at Bawdsey (England) in 1938 appeared to give echoes from cumulus, but was so unstable that though echoes were correlated with cloud, and absence of echoes with absence of cloud, the observers hesitated to make a firm statement". In the light of present knowledge, the long wavelength and low power of the radar in association with the reported "cumulus" clouds would seem to place this early report in the category of mantle echoes.

boundaries are moving down the slope; but echo motion below the base of the cumulus appears first to be downwards and then upwards. However, it is virtually impossible to track an individual echo from one frame to the next, i.e. the echoes are incoherent.

The reflectivities computed for the mantle echoes, according to the theoretical radar equations and measured echo powers, range from about $10^{-16}$ to $2 \times 10^{-14}$ $cm^{-1}$. The droplets in cumulus cloud have reflectivities ranging from about $10^{-18}$ to $10^{-15}$ $cm^{-1}$ at 10-cm wavelength. Thus, it appears that a few well-developed cumulus clouds may be detectable at short ranges with the powerful FPS-6, solely by virtue of droplet scattering. However, we have never been able to detect even bulging cumulus on the powerful 3·2 cm CPS-9 which has a range of from 5 to 10 miles on a target of $10^{-13}$ $cm^{-1}$ (the maximum expected value for a cumulus at 3·2 cm).* Of course, the strongest echoes from the droplets would be in the core of the cloud, while the mantles are associated with the boundaries. On both counts then, the implication is that the mantle echoes are due to the sharp index gradients at the cloud boundaries.

In addition to the detection of cumulus in all stages of development, the FPS-6 has displayed echoes at close ranges from most other forms of water clouds when experience has indicated that equally sensitive 1- and 3-cm radars would not have detected their particle content. It therefore seems fairly conclusive that: (a) mantle and mound echoes are due to the refractive-index gradients at the cloud boundaries, and (b) this type of angel has greater cross-section at the longer wavelengths. Such a wavelength sensitivity is in accord with theoretical expectation (i.e. equation 6).

The observations of CUNNINGHAM *et al.* (1956) as represented in Fig. 12 provide an excellent picture of the refractive-index structure of cumulus clouds and show us why we should obtain mantle echoes. Index cross-sections at various levels through an average active cloud on one particular day are shown on the right, while the cloud structure and circulation are depicted on the left. We see that the cloud boundaries have extremely sharp index gradients as well as a number of rapid fluctuations. The index minima found just inside the cloud boundaries (side and top) are attributed to the entrainment of dry environmental air, as indicated by the circulation currents. There are few such fluctuations in the core of the cloud itself, thus suggesting that the core region should not reflect any significant amount of radiation. These observations fit the picture of the classical mantle echo nicely. Those cases in which the mantle is echo-filled may readily be attributed to the simultaneous detection of the tangential cloud boundaries by a beam wider than the cloud.

Although the observations of CUNNINGHAM *et al.* give us a fine qualitative understanding of mantle echoes, calculations made by PLANK *et al.* (1957) on the basis of those observations fail to provide reflectivities of sufficient magnitude to explain the observations. Using the refractometer data, they computed the power reflection coefficient on the basis of SWINGLE's gradient equation for a plane layer

* A verbal report has been received from the MIT Weather Radar Project that simultaneous quantitative measurements have been made on mantle echoes with 3 and 10 cm-radars. These observations definitely show that the 10-cm reflectivity exceeds that at 3 cm.



VOL.
15
195

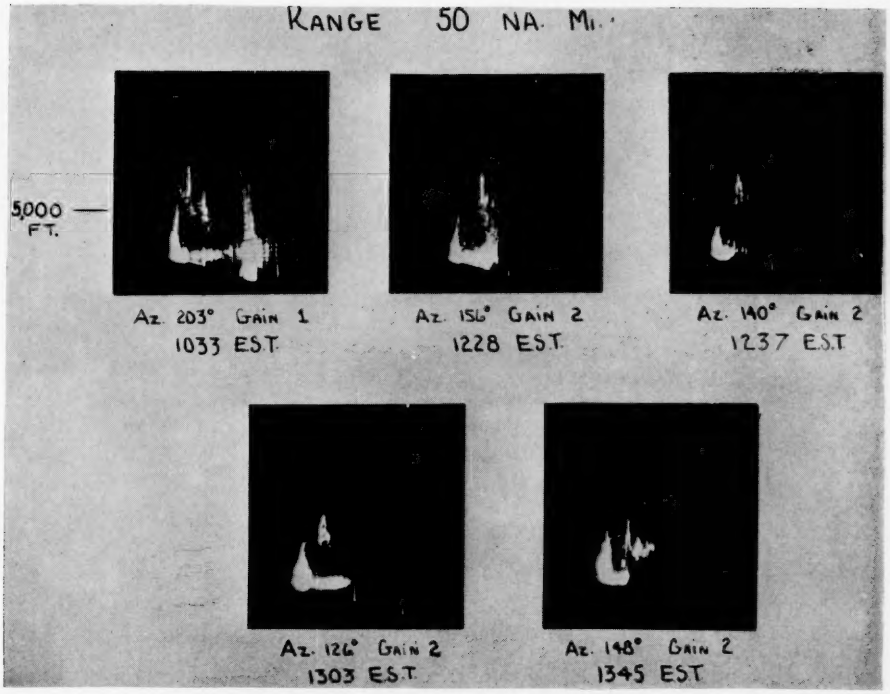


Fig. 10. Cumulus mantle echoes seen on FPS-6 at South Truro, Mass., 26 June 1957. Scales, azimuths, times and gains as indicated. Gain 2 is 5 dB down from maximum receiver sensitivity of −105 dB/m which is gain 1.

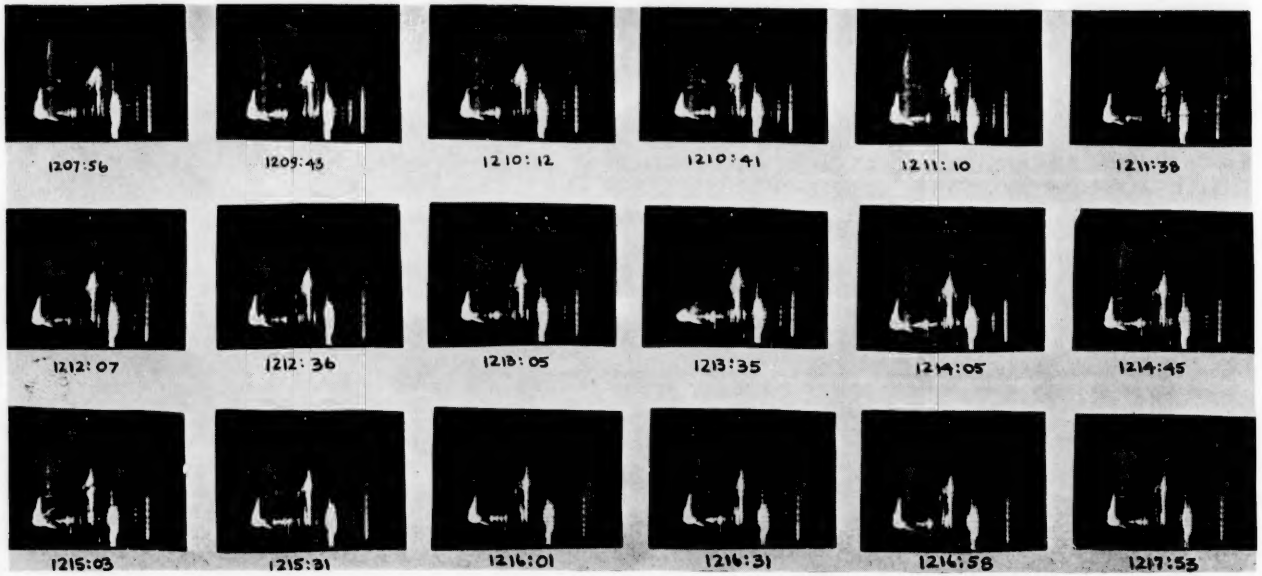


Fig. 11. Time-lapse series of cumulus mantle and associated thermal echoes; FPS-6, South Truro, Mass., 26 June 1957. Azimuth 240°; range, 50 naut. miles, cloud echo top at from 9000 to 10,000 ft. Pictures at from 29 to 30 sec intervals except first and last.

VOL. 15
1958

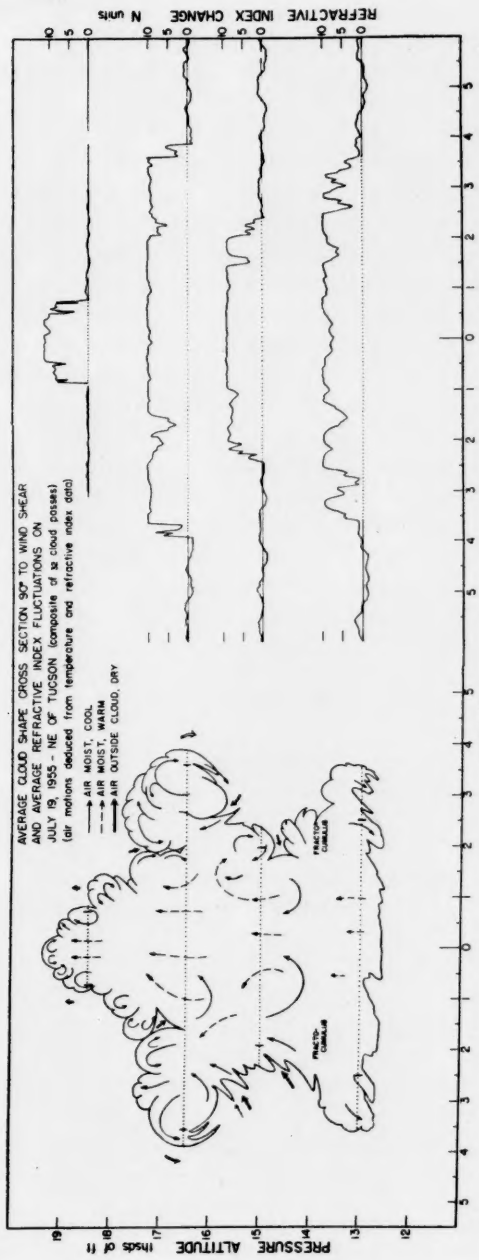
AVERAGE CLOUD SHAPE CROSS SECTION 90° TO WIND SHEAR
AND AVERAGE REFRACTIVE INDEX FLUCTUATIONS ON
JULY 19, 1955 - NE OF TUCSON (composite of 32 cloud passes)
(air motions deduced from temperature and refractive index data)
AIR MOIST, COOL
AIR MOIST, WARM
AIR OUTSIDE CLOUD, DRY
FRACTO-CUMULUS
FRACTO-CUMULUS
PRESSURE ALTITUDE hnds of ft
DISTANCE hnds of ft
REFRACTIVE INDEX CHANGE N units

Fig. 12. Average cloud model and refractive index cross-sections through it for 19 July 1955 in the area north-east of Tucson, Arizona. This is a composite of thirty-two cloud passes. (After CUNNINGHAM *et al.*, 1956.)

(essentially equation 6). At $\lambda = 300$ cm, they found $\rho^2 = 4{\cdot}85 \times 10^{-11}$. At 10 cm, this would be $5{\cdot}4 \times 10^{-13}$. If we now use equation (1) and assume that all the blobs are of uniform diameter $D$ and closely packed with concentration $1/D^3$, the cross-section per unit volume may be written

$$\eta = \bar{\sigma}/D^3 = \rho^2\pi/4D \tag{9}$$

With $\rho^2 = 5{\cdot}4 \times 10^{-13}$, $\eta = 4{\cdot}2 \times 10^{-14}/D$. Thus, closely packed blobs of 100-m diameter would have a reflectivity of $4 \times 10^{-18}$ cm$^{-1}$. Our measurements with the 10 cm FPS-6 at South Truro place $\eta$ for mantle echoes fairly reliably in the range between $2 \times 10^{-16}$ and $2 \times 10^{-14}$ cm$^{-1}$, or roughly from 2 to 4 orders of magnitude greater. To bring the calculations from the aircraft index data into line with the observations would require either blobs smaller than 1 m in diameter, which is not likely, or bubble gradients from ten to a hundred times as sharp as those measured with the air-borne refractometer.* Of course, it is possible that the cloud chosen by PLANK *et al.* is not representative of those clouds from which mantle echoes are received. Obviously, there is a need for simultaneous radar and refractometer reconnaissance of the same clouds.

Again, we must either assume the existence of gradients sharper than those measured by CUNNINGHAM *et al.* (1956) or postulate cloudy bubbles with rough edges of a scale not now measurable. While the minimum distance resolvable by the aircraft refractometer is about 1 m, and changes as great as 29 $N$ units have been reported in this distance or less, a large majority of the observed gradients are more gradual. Thus, even if we question the resolving power of the refractometer, sufficiently sharp-edged clouds are comparatively rare while mantle echoes appear to be quite common.

## STRATIFIED ANGELS

Stratified angel activity is treated most comprehensively by FRIEND (1949) and in the excellent review by PLANK (1956). Coherent layer-type echoes have been observed at vertical incidence at all wavelengths from 1 cm to 300 m since 1935 and have been well correlated with layers of sharp moisture-gradients. While these layer echoes have generally appeared steady for long durations at the very long wavelengths, practically all the observations at microwaves have shown them to be of comparatively short duration, though still coherent. Also, though the layers may appear for many hours at microwaves, the duration of any one echo is generally well under 30 sec (GOULD, 1952).

Until 1957, very few observations had been made at other than vertical incidence. In 1952, JONES reported discrete dot angels on a 10-cm RHI in narrow layers with dimensions no greater than the beam width. These echoes were insensitive to viewing angles up to about 19 degrees. On the PPI the echoes sometimes appeared almost continuously out to 20 miles, usually moving in the approximate direction of the wind but in excess of the wind speed. Radar cross-sections were said to be of

* Careful experiments have been made of the echoes from rainfall in which the measured echo power ranges from 4 to 7 dB below the theoretical values computed for the observed drop-size distributions. The situation is reversed for mantle angels by some 20 to 40 dB, i.e. they reflect much better than expected. This could hardly be due to an actual radar sensitivity greater than that calculated, especially since the system was checked regularly and found to be operating close to its rated values.



VOL.
15
1959

the order of 0·5 m² and a tendency was noted for increased activity after sunset if they were observed in the afternoon. GOLDSTEIN *et al.* (1951) also note a preference for calm summer nights. While the characteristics of JONES' angel echoes strongly suggest a meteorological phenomenon, the reported cross-section of 0·5 m² is suspiciously high even for sharp-edged discontinuities (Fig. 9).

Clear air layer echoes were also a very frequent occurrence on the RHI scope of the 10-cm FBS-6 during my observations on Cape Cod. Two outstanding cases are illustrated in Figs. 13 and 14. In Fig. 13, we see an upper cirrus cloud deck,

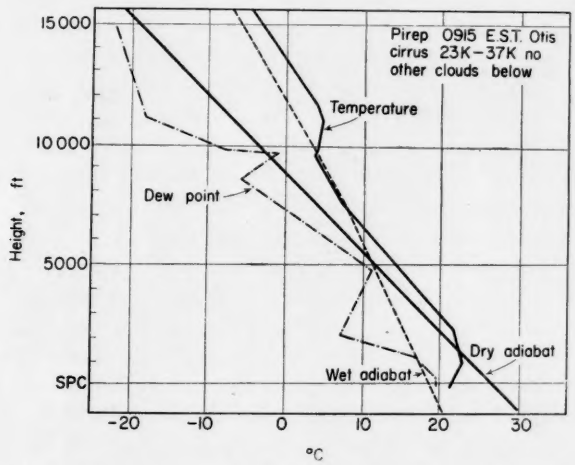


Fig. 13. Scope photos show cirrus echoes above 27,000 ft and blobby clear-air echo layers at 11,000, 8000 and 9000 ft (*top*); at 8000, 6000 and 2000 ft (*centre*); from 7000 to 9000 (*bottom*) on FPS-6 at South Truro, Mass., 15 July 1957. Range: approx. 25 naut. miles. Azimuth and time indicated. Radio-sounding at right taken at Nantucket, Mass. at 0700 EST. Note insert pilot report at upper right.

based at 24,000 to 30,000 ft, and three or four other echo layers below, depending on the direction of the RHI cut. At 220°, layers are seen at about 4000, 8000 and 11,000 ft. At 50°, they appear at about 2000, 6000 and 8000 ft and 20 min later at only 8000 ft at 40°. The Nantucket sounding about 2 hr prior to the observations shows a subsidence inversion at 10,000 to 11,000 ft accompanied by an extremely sharp lapse in dew point corresponding to the strong 11,000 ft echo layer. Other dew point minima are shown at 2000 and 8000 ft, corresponding to two of the other three echo layers. At 0915 the writer requested a jet pilot to make a cloud sounding in the vicinity of Otis Field to the southwest. He found only the cirrus deck and no other clouds below. Note that the echoes are quite blobby, apparently incoherent in structure (although it was not possible to view them on an A-scope). Layer reflectivities varied from $\eta = 3{\cdot}7 \times 10^{-16}$ to $2{\cdot}3 \times 10^{-15}$ cm$^{-1}$.

A most interesting set of observations was taken on 10 July 1957. The FPS-6 showed a weak layer at about 8800 to 10,200 ft; it appeared strongest at 238° in the southwest quadrant. A 2-min exposure of the scope is shown at the right in Fig. 14. A simultaneous reconnaissance flight was made by the Lincoln Laboratory Convair with a refractometer. Since the layer appeared centred at 9500 ft, the

writer vectored the plane out at 238° from South Truro at this level. However, a 400-ft altimeter correction later put them at 9900 ft MSL. The horizontal run is seen at the top of Fig. 14; it shows fluctuations of only about 1 $N$ unit maximum. Obviously, this run was above any appreciably turbulent layer. At 20 naut. miles and 238° from South Truro, a spiral descent was made at 500 ft/min. This shows a strong inversion and sharp moisture lapse based at 8900 ft. In the 25 ft above the 8950 ft level, $N$ drops off by 10 units, and another 8 units in the next 175 ft. In the 100-ft layer below 8950 ft, we observe fluctuations of from 5 to 10 units per 25 ft of height, or per 750 ft of horizontal flight in the spiral descent. Thus, this 100-ft layer at the very base of the inversion appears blobby in nature. Such blobbiness below the inversion is typical, especially when the lapse rate below the inversion is adiabatic, as it is in this case. However, both the blobs and the strong $N$ gradient are so close to each other that it is impossible to say that the echo layer is due to one or the other. However, the incoherent nature of the echoes and the low angles of incidence strongly suggest that the blobs are responsible in this case, although the echo layer appears to lie mostly above 9000 ft.*

Blobby layers would appear to explain all of the FPS-6 clear air layers of incoherent echoes as well as JONES (1952) stratified coherent angel echoes. Since all of these echoes appeared at low angles of incidence and seem isotropic in reflectivity over some 10° to 15° of elevation, it does not seem at all likely that a plane layer could be responsible. Such blobby layers could also explain many of the coherent angels seen at vertical incidence, since the smaller pulse volumes attainable at closer ranges would contain many fewer blobs. For example, the FPS-6 pulse volume is $75 \times 10^6$ m$^3$ in size at 10 naut. miles and only $3 \times 10^6$ m$^3$ at 2 naut. miles. Thus it could encompass some seventy-five bubbles of 100-m diameter when looking at a 2-mile-high layer at low angles of incidence compared with only three such bubbles at vertical incidence. Many of the microwave vertical observations have been made with even smaller pulse volumes (GOULD, 1952; PLANK, 1956).

This does not mean that plane layers of strong $N$ gradient do not reflect detectable amounts of energy at near vertical incidence. On the contrary, at the long wavelengths approaching 100 cm and longer, it is not difficult to detect sufficiently sharp, though still reasonable, $N$ gradients in homogeneous layers. Furthermore, at these wavelengths, small deviations from horizontal uniformity do not upset the requirement that the layers must be plane to within a fraction of the wavelength. Thus at the longer wavelengths, continuous coherent echo may be received from conceivable atmospheric layers. At the short microwaves, however, both the sharpness and planeness criteria of a layer are more difficult to meet in the real atmosphere. Nevertheless, there are far too many observations which can be explained only on the basis of extremely sharp plane layers. The noted preference of stratified layers for calm summer nights describes conditions under which we should expect little or no blobbiness below the inversion; rather, there should be a strong lapse in vapour pressure at a very stable inversion. The fact that the associated echoes are evidently of shorter duration at the short microwaves, though still coherent, while the longer wavelength layers appear more or less continuous,

* Perhaps due to residual height errors in both the aircraft and radar observations.



VOL. 15 1959

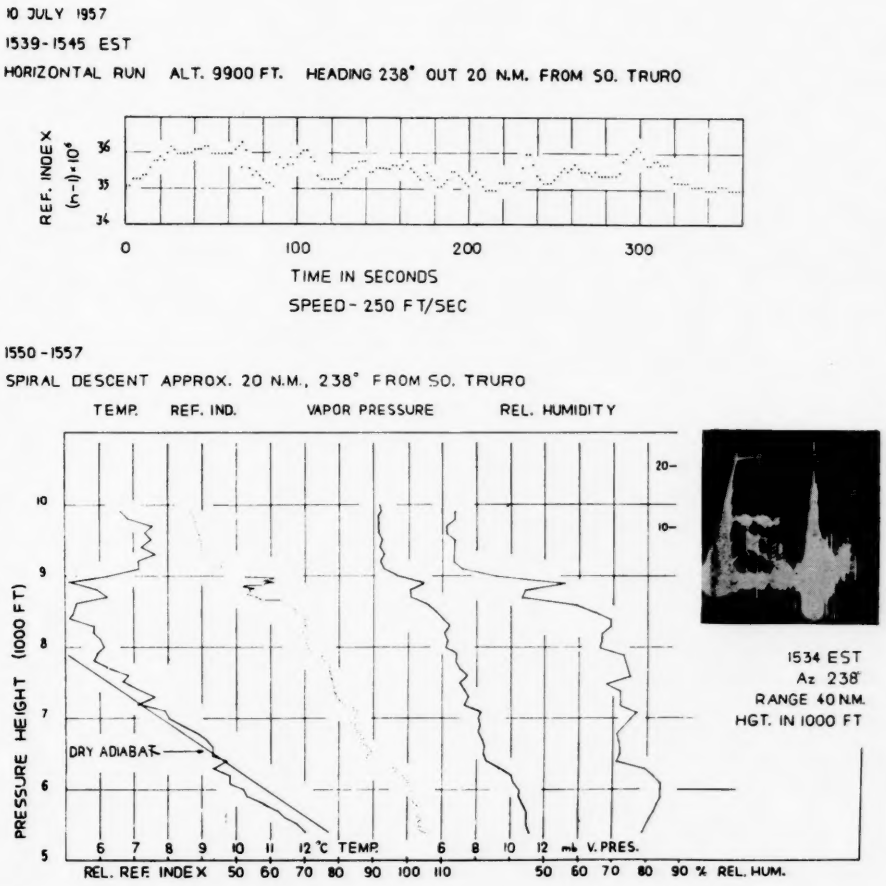


Fig. 14. Scope photo (*insert right*) shows 2 min exposure of FPS-6 scope with echo layer at from 9000 to 10,000 ft (scattered altocumulus in area at approximately same altitude). Aircraft soundings of temperature, refractive index, vapour pressure and relative humidity, left to right. Horizontal refractometer record at 9900 ft level is shown at top. (Aircraft data furnished by J. MEYER, MIT Lincoln Laboratory.)

VOL.
15
1959

suggests that the sharpness and planeness of the layers fluctuate about their critical values at short wavelengths, but can be maintained within the much less critical values at the longer ones. This, too, is as we should expect.

The maximum clear-air layer reflectivities which the writer measured with the 10-cm FPS-6 were about $10^{-15}$ cm$^{-1}$, which corresponds to a power reflection coefficient of $10^{-14}$. This is the same value as reported by FRIEND (1949) for some of his strongest layers. Such coefficients can be obtained either with bubbles or with plane layers, provided that the $N$ gradients at the boundaries are fairly sharp in either case. For example, we would obtain such a 10-cm reflection coefficient from a plane layer with gradient of $10N$ units per 40 cm. Other observations at 1·25 cm (ATLAS *et al.* 1953*) would require gradients of $15N$ units per cm. While such sharp gradients are difficult to imagine, they approach conceivability if we recall the boundaries which are frequently observed when flying at the top of haze layers. For example, it is not uncommon that a pilot can fly with his head in the clear and his body in the haze.

To summarize the situation for stratified echoes then, we see that:

(1) There is a considerable store of evidence associating clear-air echo layers with both sharp moisture-gradients and minima in the atmosphere. Furthermore, the behaviour of the angels is consistent with rational meteorological phenomena; the association is not merely a statistical one.

(2) Many of the microwave observations have the characteristics of blobby layers at the base of an inversion or in zones of moisture minima.

(3) At wavelengths longer than 10 cm, persistent coherent stratified echoes can be explained as the result of sharp, though not unreasonable, vertical gradients in plane layers. Although the gradient and uniformity requirements of the plane layer theory are quite severe at the shorter wavelengths, the theory is hardly questionable. Therefore, the evidence indicates that the requirements can be fulfilled for brief, closely-spaced, intervals (up to 30 sec each) so that an almost continuous echo layer is observed for many hours.

(4) In short, stratified angels are probably due both to blobby layers as well as to sharp transition plane layers. In either case, however, the index gradients have to be sharper than now generally felt reasonable, though what we feel reasonable now may be altered with new high-resolution meteorological equipment.

Since the forward-scatter from a blobby layer should exceed the back-scatter by several orders of magnitude, depending upon the angle of incidence (BOOKER and GORDON, 1950), the radar data provide important direct evidence of the existence of conditions adequate to account for scatter propagation beyond the horizon. In addition, the recent observations with high sensitivity systems testify to the feasibility of FRIEND's (1939) remarkable proposal to sound air mass boundaries by radio.

Although there are many other interesting cases of atmospheric angels, we shall review only a few of the more striking ones.

## SEA BREEZE ANGELS

A preliminary report on radar detection of the sea breeze was presented in 1953

* As corrected by PLANK (1956, p. 79). See also the section on sea breeze angels.

(ATLAS *et al.*). Since then the data have been reviewed more carefully and new features have come to light. The observations shown in Fig. 15 were made at the MIT Round Hill Field Station at South Dartmouth on Buzzards Bay, with both a horizontally-oriented beam directed SSE out over the water and a vertically-pointing beam. While looking out over the water to the south with the horizontal beam (elevated at 1°), a front of fluctuating echoes started to move in from a distance of 10,000 ft range. Nothing could be seen visually. However, when the echoes reached the shoreline, the temperature dropped sharply and the turbulent fluctuations ceased; the wind direction shifted from north to south; the refractive index rose rapidly. Obviously, this is the sea breeze. At 1234, when the sea breeze progressed $\frac{1}{2}$ mile inland and passed over the radar, we switched to the vertical beam and observed coherent echoes from the sea-breeze inversion at about 1000 ft.

The explanation is as follows: The cold sea-breeze air moving in over the warm shallow water near the shore gave rise to a strong superadiabatic surface layer which permitted bubbles of moist air to boil upwards into drier air at the 170 ft level of the beam. These provided the incoherent echoes on the horizontal beam. The bubbles then continued upward to the sea-breeze inversion where the moisture apparently diffused and provided a sharp moisture-contrast with the dry air aloft. The horizontal change in index across the front was about $30N$ units which, if applied to the vertical contrast across the inversion, would have to occur in a 2-cm layer in order to explain the observed echo intensity and coherent nature of the inversion layer on the vertical beam. We see that this gradient cannot be maintained for long, however, and the inversion echo disappears about 10 min after its initial detection (1245), evidently as a result of mixing. This radar observation, along with its meteorological documentation, constitutes the most powerful evidence yet of the reality of atmospheric angels.

Note, by the way, that there were few small-scale fluctuations in the refractometer record taken at a height of 28 ft during the passage of the sea breeze inland. At such a low level, the refractometer lies in the more or less homogeneous moist air which does not show contrast with the dry air until it rises to the higher levels of the radar beam. This is in contrast to the record of Fig. 16, where the sea breeze has been in progress for more than 1 hr. Here, the dry land air has evidently broken through the inversion in great eddies and settled to the lowermost levels where it is swept shoreward with the force of the sea-breeze air and is seen in the violent $N$ fluctuations of the refractometer. This mixing across the inversion has also prevented the formation of a coherent-echo layer at the inversion level. Such a breakdown of the inversion at some distance behind the sea-breeze front may also be seen in the vertical cross-sections of the temperature and moisture field drawn by CRAIG *et al.* (1945) on the basis of wire-sonde measurements.

## SQUALL PRECURSOR LINE

With the more widespread use of long-range long-wavelength radars for meteorological studies in recent years have come frequent reports of a thin band of diffuse echo which lies some 5 to 20 miles in advance of a squall line and moves with it. This line of echo has been dubbed the precursor line. Present evidence indicates that there is no precipitation associated with it, but it is frequently

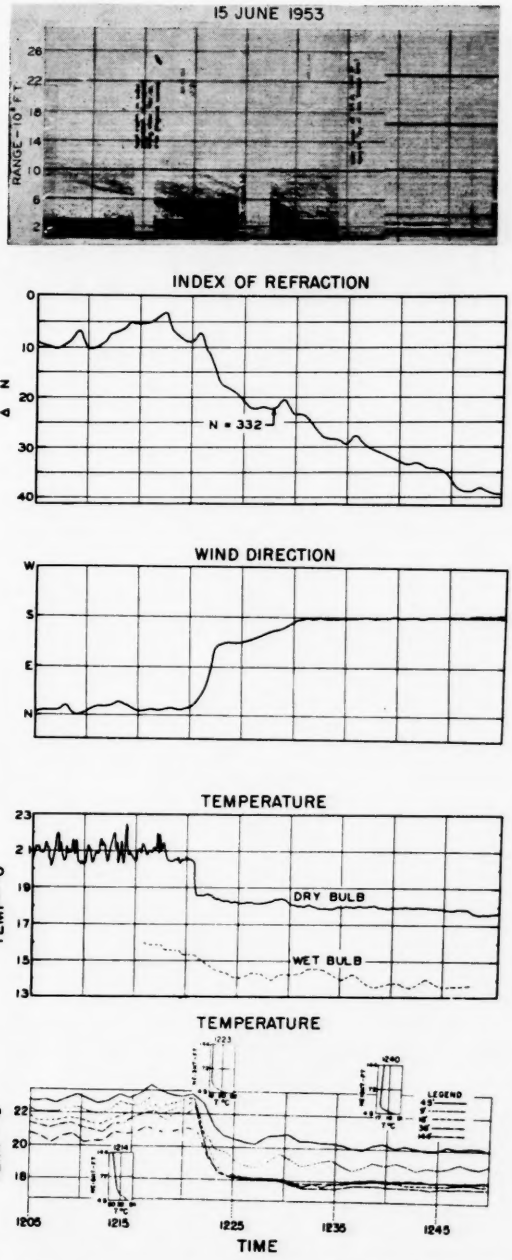


Fig. 15. (*Top*): Range vs. time record of 1·25-cm echoes during onset of sea breeze at South Dartmouth, Mass., 15 June 1953. When solid echo appears out to 3000-ft range, beam is directed horizontally toward SSE; elsewhere it is vertical. Echoes in layer at from 900 to 1000 ft altitude (1235–1245 EST) are from sea breeze inversion. Meteorological records below were made on shore just under the radar beam.

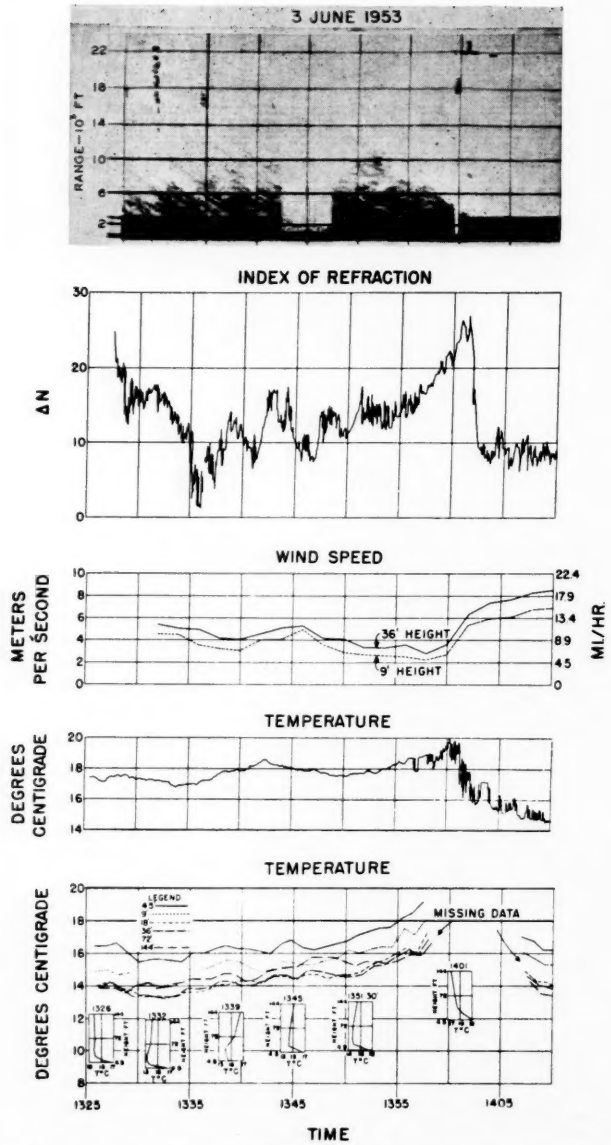


Fig. 16. Similar to Fig. 15 but for 3 June 1953. Sea breeze has been in progress approximately 1½ hr. Note sharp fluctuations in refractive index (scale reversed from that in Fig. 15).

VOL.
15
1959

accompanied by pressure jumps, wind shifts and slight temperature changes at the surface. The precursor line is detected best by 23-cm radars such as the FPS-3 on which it first appears at a range of about 50 to 60 naut. miles. At Blue Hill, we have detected only one such band with the 3-cm CPS-9. On other occasions, the 23-cm radar at South Truro detected the precursor, while the 3-cm CPS-9 did not. The one line detected at 3 cm extended from the ground to about 20,000 ft and was bowed outward at the middle levels in the direction of motion. However, no clouds or noticeable meteorological events occurred as it passed the station.

A study of midwest U.S. precursor bands by LEACH (1957) has attributed them to sharp refractive index gradients.

### ANOMALOUS ECHOES OVER CAPE COD BAY

On a number of occasions, the 3-cm CPS-9 on Blue Hill has detected wiggly bands of echo over Cape Cod Bay, such as those shown in Fig. 17. The echoes are diffuse and incoherent; they are low level, rarely extending above 1000 ft, and almost always associated with anomalous propagation. Occasional checks have shown that the water was calm; thus, sea clutter is fairly well eliminated. The motion of the band is slow and erratic, not in agreement with the winds. It sometimes lasts for several hours.

The most persistent wiggle in the band frequently seems to parallel the outline of the Provincetown peninsula. This, and the lack of regular motion, suggested the possibility that an eddy of cold water from the north, injected into the warmer water on both shores of the bay, might cause differential cooling and moistening of the surface air, thus providing the index boundaries necessary for reflection. A water-temperature chart of the bay furnished by Woods Hole Oceanographic Institution (Fig. 18) does show such sharp temperature differences. This map was prepared over a 3-day period and undoubtedly does not show the eddies as they might appear at any instant. Sharper temperature gradients would be expected in a chart prepared synoptically. Since the air in contact with the water may be expected to be close to saturation at the water temperature, contrasts up to about 5 mbar in vapour pressure and 20 $N$ units could readily occur. While the differential cooling idea is tentative, we have not been able to arrive at a more logical explanation.

### CONCENTRIC RING ANGELS

Probably the most tantalizing angels yet observed are those in the form of concentric rings, which expand like ripples in a pond when a pebble is thrown into it. The observations were made by ELDER (1957) on a 23-cm FPS-3 radar at Ypsilanti, Michigan, and are illustrated in Fig. 19.

Although all of the rings reported by ELDER were observed in JANUARY 1956, he has advised the writer that they have been observed in all seasons of the year at Ypsilanti. However, to my knowledge, they have never been seen on the 23-cm radar at South Truro, Cape Cod (though attempts have been made to find them). There is an apparent maximum occurrence in the late afternoon, after the daily maximum in temperature, but there was no other apparent correlation with weather observed at the surface. Low-level inversions were not observed in the Selfridge

Field radiosonde records on all days of ring angels, but might have developed at the time and place of observation.

The rings expanded at an average speed of about 42 knots, though a few had speeds as great as 100 knots. Average spacing between adjacent rings on one day was 3 naut. miles. The centres of most rings were fixed, but once the centre moved in agreement with the observed wind direction. The strong preference for certain fixed areas of occurrence suggests a phenomenon associated with the ground. However, the most frequent rings to the south-east occurred over nearly level farm land. A few rings occurred over two state institutions, but none were observed over more industrialized areas within the range in which smoke-stack sources were most powerful.

ELDER has suggested that the echoes are due to refraction of the transmitted energy by a gravity wave triggered at a point source and propagating on an atmospheric inversion. The transmitted energy is believed to be refracted to ground targets, which scatter directly back to the radar. Therefore it is said that the rings can move with twice the speed of the reflecting medium. While this seems to be the most logical explanation, no mechanism could be proposed for a point-source disturbance. For example, aircraft echoes were not evident in the vicinity on most occasions, though a few rings seem to emanate from a point echo.

## SUMMARY AND CONCLUSIONS

In the foregoing we have attempted to present a review and reinterpretation of some of the most significant observations and studies of angel echoes from meteorological sources. This has been done in the light of extensive new data presented here for the first time. Three primary angel types have been distinguished:

(1) Non-stratified angels of both the discrete–coherent and incoherent types are closely associated with convective bubbles or eddies. The former occur primarily in an apparently random fashion in the convective-mixing zone and show no particular correlation with specific cumulus clouds. The latter are almost always associated with organized pre- and sub-cumulus thermals; when viewed with high resolution, the thermals may appear as groups of closely packed discrete angels.

(2) Mantle echoes in the form of inverted U's in vertical cross-sections on 10-cm radars are found to correspond to the boundaries of cumulus clouds. This and the failure to observe similar echoes on equally sensitive 3-cm radars indicate beyond reasonable doubt that the echoes are angel reflections from the sharp index gradients at the cloud boundaries.

(3) Stratified angel echoes generally appear incoherent when viewed obliquely with a vertically-scanning beam, and coherent when viewed from below with a fixed-vertical beam. The echo layers are strongly correlated with strata of sharp moisture lapse or moisture minima. These zones are those in which moist air parcels rising from lower levels display maximum index contrast with the environment, providing either incoherent or coherent echoes, depending upon radar resolution. At vertical incidence, steady coherent echoes at long wavelengths, and less steady but still coherent ones at the shorter wavelengths, indicate that the layers of sharp moisture lapse may also act as plane partial reflectors, especially on calm nights when convection is suppressed.

VOL. 15 1959

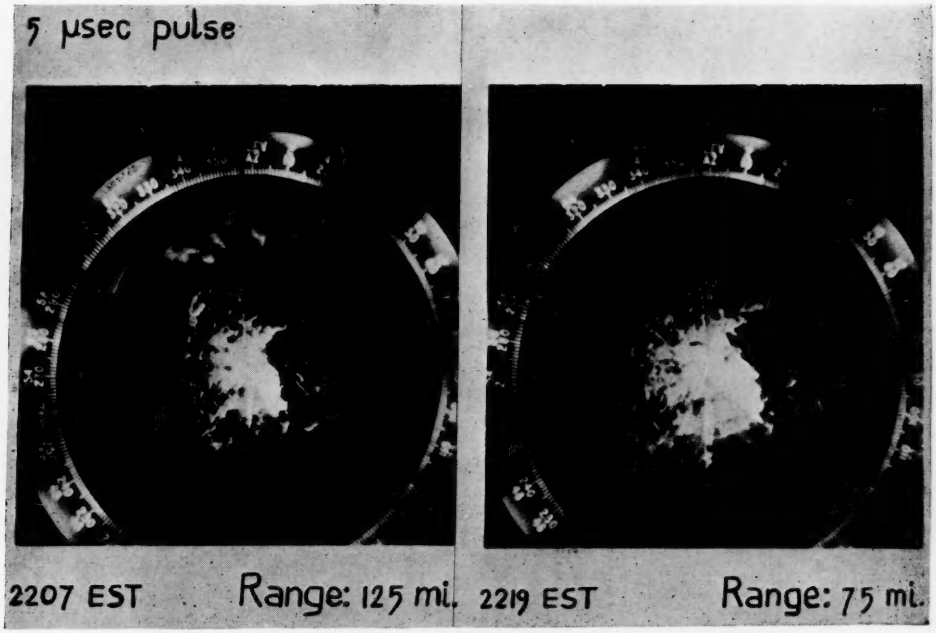


Fig. 17. Anomalous echoes over Cape Cod Bay seen on 3-cm AN/CPS-9 on Great Blue Hill, Milton, Mass., on 29 April 1957. Wiggly echo pattern appears north-west of Cape Cod peninsula which shows only during anomalous propagation. Range and time as indicated.

Fig. 18. Surface water temperature map (°F) of Boston harbour and Cape Cod Bay made over three day period in August 1951. (*Courtesy of Woods Hole Oceanographic Institution.*)

VOL.
15
1959

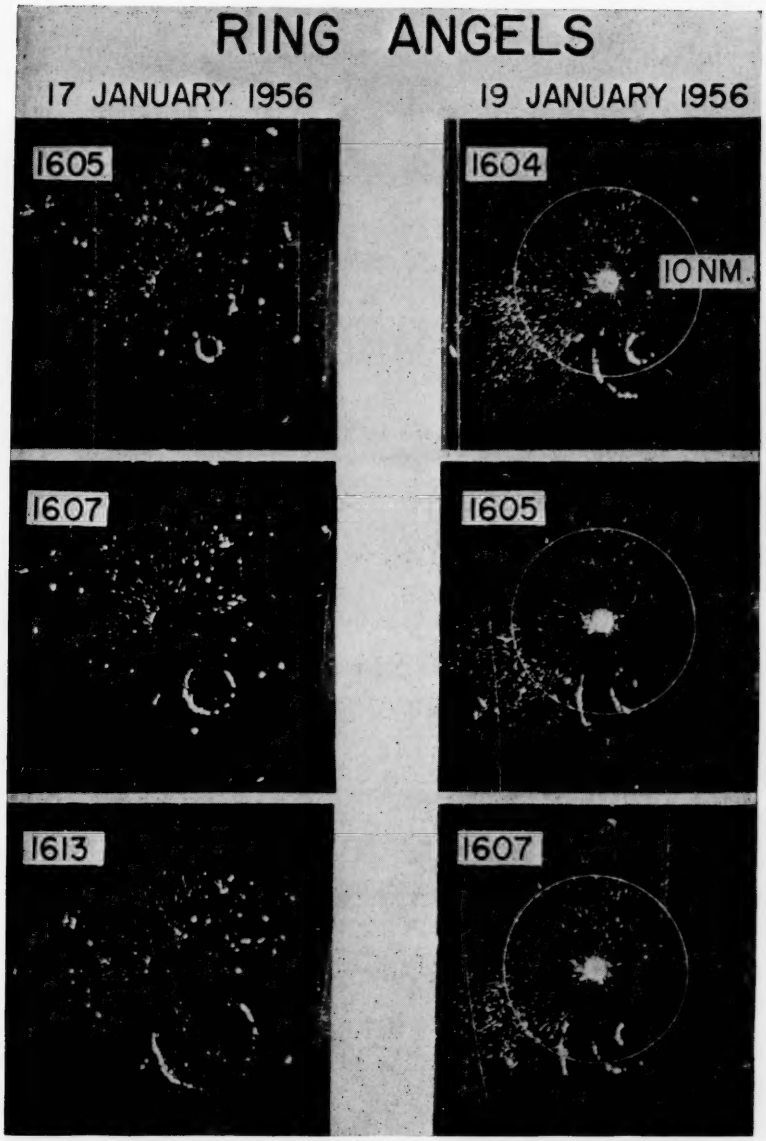


Fig. 19. Expanding ring angels seen on the 23-cm AN/FPS-3 radar at Ypsilanti, Michigan. Dates, times and range as indicated. Moving target indication in use. (After ELDER, 1957.)

VOL.
15
1959

Other special angels such as those associated with the sea-breeze front add incontrovertible support to the overwhelming empirical evidence of the association between angel echoes and meteorologically induced gradients in refractive index. The detection of birds and insects, although occasionally confusing, can hardly be used to explain more than a small fraction of the observations (of type (1) above).

The problem is to account for the observed radar cross-sections and plane reflection coefficients theoretically. In every case, the refractive-index gradients required by theory exceed "reasonable" or measured gradients by at least one or two orders of magnitude. While our concept of a "reasonable" gradient is strongly biased by measurements with low-resolution meteorological instruments and refractometers, index measurements through cumulus clouds show only relatively rarely gradients at the limit of resolving power. Until more extensive measurements are available with high resolution instruments, we are obliged to assume either that the angels are due to those relatively rare sharp-edged bubbles or eddies, or that the spherical model of a bubble is incorrect. Of course, the scattering theory itself is not without question. In the case of coherent echoes from stable plane layers where both theory and model seem reasonable, the radar measurements themselves appear to be the best available evidence of extremely sharp gradients of refractive index.

All the radar angel observations, and especially those due to elevated blobby layers, indicate the frequent existence of conditions adequate for the enhanced forward-scatter of electromagnetic waves beyond the horizon. The data also testify to the feasibility and foresightedness of FRIEND's 1939 proposal to use radio reflections for the continuous sounding of air-mass boundaries. Mantle echoes from cloud boundaries and other angels suggest further research and operational applications.

*Acknowledgements*—The writer wishes to express his appreciation to the staff of the South Truro Field Station of MIT Lincoln Laboratory, and especially to A. WING, R. FARRELL and E. LANE for their wholehearted efforts in operating and calibrating the FPS-6 radar; to J. MEYER and J. BAUER, of Lincoln Laboratory, for obtaining the aircraft refractometer data of 10 July 1957; to DR. R. CUNNINGHAM and V. PLANK, of the Geophysics Research Directorate, for Figs. 12 and 2, respectively; and to MR. J. GRAY, of Airborne Instrument Laboratories, for Fig. 1. A. CHMELA, of my laboratory, assisted invaluably in the field work and analysis, and R. LOESER in the analysis and preparation of illustrations.

## REFERENCES


| | | |
|---|---|---|
| ADEN A. L. | 1951 | *J. Appl. Phys.* **22**, 601. |
| ANON. | 1947 | *Bell Lab. Record* **25**, 75. |
| ATLAS D., PAULSEN W. H., DONALDSON R. J., CHMELA A. C. and PLANK V. G. | 1953 | *Proceedings of Conference on Radio Meteorology*, Paper XI 6, University of Texas. |
| AUSTIN P. M. | 1952 | Weather Radar Research Technical Report No. 17. Massachusetts Institute of Technology. |
| BALDWIN M. W. | 1943 | Bell Telephone Lab. Memoranda Nos. MM 44-150-2, 3 and 4. |

| | | |
|---|---|---|
| BALDWIN M. W. | 1948 | *Proc. Inst. Radio Engrs., N.Y.* **36**, 363. |
| BIRNBAUM G. and BUSSEY H. E. | 1955 | *Proc. Inst. Radio Engrs., N.Y.* **43**, 1412. |
| BOOKER H. G. and GORDON W. E. | 1950 | *Proc. Inst. Radio Engrs., N.Y.* **38**, 401. |
| CHMELA A. C. and ARMSTRONG G. M. | 1955 | *Proceedings Fifth Weather Radar Conference, Asbury Park*, pp. 63–66. |
| CRAIG R. A., KATZ I. and HARNEY P. J. | 1945 | *Bull. Amer. Meteorol. Soc.* **26**, 405. |
| CUNNINGHAM R. M., PLANK V. G. and CAMPEN C. M. | 1956 | Geophysical Research Paper No. 51. Air Force Cambridge Research Center; |
| ELDER F. C. | 1957 | *Proceedings Sixth Weather Radar Conference*, pp. 281–290. American Meteorological Society, Boston. |
| FRIEND A. W. | 1939 | *Bull. Amer. Met. Soc.* **20**, 202. |
| FRIEND A. W. | 1949 | *Proc. Inst. Radio Engrs., N.Y.* **37**, 116. |
| GERHARDT J. R., CRAIN C. M. and CHAPMAN H. | 1956 | *Bull. Amer. Met. Soc.* **37**, 251. |
| GOLDSTEIN H., KERR D. E. and BENT A. E. | 1951 | *Propagation of Short Radio Waves* Ch. 7. Radiation Laboratory Series, Vol. 13. McGraw-Hill, New York. |
| GOULD W. B. | 1952 | *Proceedings Third Weather Radar Conference*, McGill University pp. F 25–28, F 38. |
| HARPER W. G., LUDLAM F. H. and SAUNDERS P. M. | 1957 | *Proceedings Sixth Weather Radar Conference* pp. 267–272. American Meteorological Society, Boston. |
| JONES R. F. | 1952 | *Proceedings Third Weather Radar Conference*, McGill University pp. F 39–40. |
| LEACH W. | 1957 | Scientific Report No. 2, Contract AF19 (604)-1564. Department of Oceanography and Meteorology, Texas A and M College. |
| MALKUS J. S. and SCORER R. S. | 1955 | *J. Meteorol.* **12**, 43. |
| PIDDINGTON J. H. | 1939 | *Proc. Phys. Soc. Lond.* **51**, 129 and 547. |
| PLANK V. G. | 1956 | Geophysics Research Paper No. 52. Air Force Cambridge Research Centre. |
| PLANK V. G., CUNNINGHAM R. M. and CAMPEN C. F. | 1957 | *Proceedings Sixth Weather Radar Conference*, pp. 273–280. American Meteorological Society, Boston. |
| PLANK V. G. and SPATOLA A. A. | 1957 | *Some Characteristics of Cumulus Clouds over Florida.* 151st National Meeting of American Meteorological Society, Chicago, Illinois. |
| SCORER R. S. and LUDLAM F. H. | 1953 | *Quart. J. R. Met. Soc.* **79**, 94. |
| SWINGLE D. M. | 1950 | TR No. 112. Cruft Laboratory, Harvard University. |
| WATSON-WATT R. | 1946 | *J. Instn. Elect. Engrs.* **93**, 374. |
| WATSON-WATT R., WILKINS A. F. and BOWEN E. G. | 1936 | *Proc. Roy. Soc.* **161**, 81. |


## DISCUSSION

DR. V. G. PLANK—DR. ATLAS, you have expressed the belief that sharper and sharper gradients of refractive index will be found in the atmosphere as we improve the space resolution of our instrumentation and that these gradients might explain observed angel activity. In certain cases, such as the vertical gradients associated with stratified layers or the caps of rising bubbles this may be true; however, I am

dubious about finding gradients of sufficient sharpness and extent to explain (using current theory) the angel reflections that one receives looking quasi-horizontally at convective elements.

To review for a moment what we require, refractive-index-gradient wise, to account for an angel signal: if we use SWINGLE's (SCEL) equation, we need a very sharp gradient and it doesn't matter what the total $N$ difference is across the gradient region: if we use BAUER's (Project Lincoln) equations, then we need a sharp gradient and a large total $N$ change across the gradient region. I personally am partial to BAUER's equation, because it reduces to the situation of Fresnel reflection in the case of an infinitely thin gradient region and because BAUER used continuous functions in the mathematics, whereas SWINGLE did not.

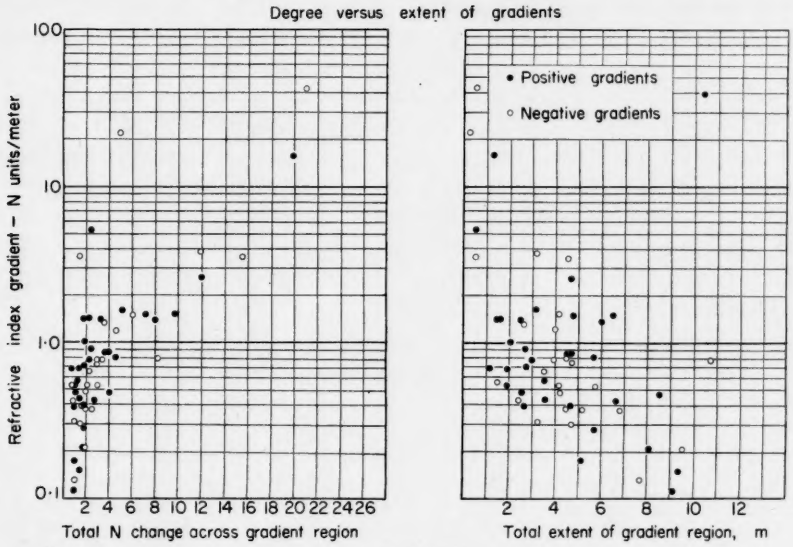
Degree versus extent of gradients
Refractive index gradient – N units/meter
100
10
1·0
0·1
2 4 6 8 10 12 14 16 18 20 22 24 26
Total N change across gradient region
• Positive gradients
○ Negative gradients
2 4 6 8 10 12
Total extent of gradient region, m

Fig. D-1.

Therefore I am presupposing that, to explain an angel echo, we require a gradient region that is both sharp and extensive. Now, my point is that our flights through cumulus clouds, using instrumentation with a resolution capability of some 3–5 ft, indicate that we are already resolving the thickness of those gradient regions having large total $N$ change. My analysis of the Fig. 9 cloud pass in the paper I presented at this meeting shows that the sharpest gradient regions are the most extensive ones (extensive meaning total $N$ change across the gradient region), and vice versa. This is clearly shown in Fig. D-1 which pertains to that aircraft pass. The same gradient structure is also shown in other passes.

As I pointed out in my paper, the sharp, extensive gradient regions have a spacing which agrees with the dimensions of the cauliflower protuberances on cumulus, and there are many reasons for believing that the air–cloud boundaries of these cauliflowers are the places where the sharpest, most extensive, gradients actually occur. The cauliflowers are indicated as being the primary eddies that drive the other and smaller eddies of the turbulent decay process.

Expanding this, large eddies are indicated to be associated with large $N$ differences across thin transition zones at the eddy boundaries (this means large $N$ gradients at the boundary). Now as we consider smaller and smaller size eddies, we observe that the $N$ differences (from inside the eddy to outside) become progressively smaller, and that the transition zone at the eddy boundary becomes progressively larger. (Meaning a progressive decrease in values of the $N$ gradient at the eddy boundaries with decreasing eddy size.) My point is that in the light of this trend, it is unreasonable to expect that very small eddies, of scale of the order of centimetres or fractions thereof, will have large $N$ differences and sharp gradients.

As mentioned, we presently appear to be resolving the sharpest and most extensive gradient regions in our aircraft passes. If we improved our space resolution, I personally do not feel that we would find a whole new spectrum of sharper and more extensive $N$ gradients.

Mr. R. Bolgiano—Dr. Atlas's presentation on radar observations of refractive index inhomogeneities has been most interesting and enlightening. However, I must join with Dr. Plank in wondering if the sharp boundaries which are required on a coherent-scattering basis can possibly be maintained or even exist in the first place in the free atmosphere. On the other hand, I must object when Dr. Plank suggests that, as the boundary of a cell is broken up by turbulence, all gradients are diminished and that the sharp gradients required cannot be associated with the small blobs.

Consider for the moment the fluctuations of, say, moisture vapour, represented by $w$. $\overline{W}$ is the mean distribution of moisture and $W$ the total. Then, from the conservation of matter (neglecting evaporation and condensation for the moment),

$$\frac{\partial W}{\partial t} = -U_i \frac{\partial W}{\partial x_i} + D \frac{\partial^2 W}{\partial x_r \partial x_r}$$

where $U_i$ ( $= \bar{U}_i + u_i$) is the vector velocity and $D$ the molecular diffusivity of water vapour. Taking the average of this equation, subtracting that average from the total expression and assuming local homogeneity of the fluctuating components, we obtain the familiar conservation equation for the fluctuating term

$$\frac{\partial w}{\partial t} = -u_i \frac{\partial \overline{W}}{\partial x_i} - U_i \frac{\partial w}{\partial x_i} + D \frac{\partial^2 w}{\partial x_r \partial x_r}$$

Multiplying both sides by $2w$, averaging and invoking the local homogeneity assumption in the time domain as well yields

$$2\overline{u_i w} \frac{\partial \overline{W}}{\partial x_i} = -2D \overline{\left(\frac{\partial w}{\partial x_i}\right)^2}$$

or

$$K(\text{grad } \overline{W})^2 = D\overline{(\text{grad } w)^2}$$

where $K$ is the eddy diffusivity. Since it is well known that in atmospheric turbulence the eddy diffusivity is several orders of magnitude greater than the molecular diffusivity, it is apparent that the "local" gradient of moisture vapour often far exceeds the mean gradient.

DR. W. E. GORDON—A single but very remarkable observation has been reported to me. I will describe the observation, suggest an explanation, and call your attention to the fact that the explanation provides an alternative to DR. ATLAS's factor which he dislikes but associates with the thickness of the reflecting layer.

Two observers, one at the scope of an X-band radar, the other at the bore-sight telescope attached to the radar antenna, were attempting to receive echoes from wispy cumulus clouds. The telescope observer directed the pointing of the antenna to several such clouds but no radar echoes were observable. The 'scope observer, however, indicated that a strong echo was available and directed the antenna to it. The echo was easily tracked automatically, so that both observers could look through the telescope. They agreed nothing was visible. The 'scope observer returned and verified that the echo was still present. At about this time a wispy cumulus formed in the centre of the field of the telescope and the radar echo disappeared.

The suggested explanation is that the radar echo was due to scattering in the thin turbulent shell of a bubble, which in this case became an element of a cumulus cloud. The turbulence was maintained by the shear across the surface of the bubble due to its vertical velocity. The turbulence rapidly decayed and the radar echo disappeared when the bubble reached the condensation level where a stable layer suppressed the vertical motion.

The model proposed by DR. ATLAS imagines that scattering takes place throughout the volume of the bubble and gives him theoretical echoes that are too strong. The turbulent shell substantially reduces the scattering volume and will, I believe, give echo strengths that are of the same order of magnitude as those observed.

DR. LIGDA suggested that the loss of echo might be due to a change of state of the water content from vapour to liquid. Refractometer observations through bubbles and through clouds indicate large sudden changes in index at the boundaries in both cases. I therefore conclude that the change of state cannot substantially alter the difference in refractive index between the bubble or cloud and its surroundings and the loss of echo must be associated with a decrease of turbulence.

OL.
15
959

Journal of Atmospheric and Terrestrial Physics, 1959, Vol. 15, pp. 288 to 293. Pergamon Press Ltd. Printed in Northern Ireland

## SESSION V

RADAR WEATHER

# Convective processes in the atmosphere as revealed by weather radar

W. F. HITSCHFELD*

THIS contribution is a brief summary of some of recent work by the Stormy Weather Group at McGill University. It is but a sample of the extensive research now carried on in some two dozen laboratories, a "status report" on which may be found in the Proceedings of the Sixth Weather Radar Conference (1957). A critical review of the whole field including associated propagation problems has been given by MARSHALL and GORDON (1957).

Weather radar has been developed principally as a tool for tracing and studying the development of precipitation in the atmosphere. In the great majority of cases, the atmospheric particles responsible for meteorological echoes are raindrops and snowflakes with diameters of a few-tenths of a millimetre or more.

The two broad classes into which precipitation patterns fall are closely related to the two commonly recognized mechanisms of precipitation: the continuous type, which is the result of laminar upglide of air on a frontal surface—most of our snow and much of our rain are formed this way—and the showery type of precipitation, exemplified by thunderstorms, which is the result of convective upbubbling of air over the heated ground.

Convective processes of sorts play important parts in the larger framework of the continuous upglide as well. In our experience, continuous precipitation originates in most cases in discrete cells embedded in a *stable* atmosphere. These cells move more or less with the ambient wind and are of the order of one mile in diameter. Fig. 1 shows the levels of occurrence of these cells in the scheme of the frontal stratification of the atmosphere; while cells can occur in any air mass, just above the maritime front would seem to be their most favoured breeding ground. The heights of formation vary from 8000 to 20,000 ft with a corresponding temperature range from $-5°$ to $-35°$C. Convective lifting to a height of from 1000 to 2000 ft observed in these cells, in stable air, can be explained if one assumes that the air taken in at the base contains vapour at water equilibrium, while that released at the top contains only vapour at ice equilibrium, and at the colder temperature prevailing at that greater height. The source of the water substance could be the droplets of stratus cloud or the water-saturated vapour in the vicinity of such cloud. Of these two possibilities, the latter is much the more potent (because the latent heat released in this case is so much greater), and presumably

* McGill University, Montreal.



VOL. 15 1959

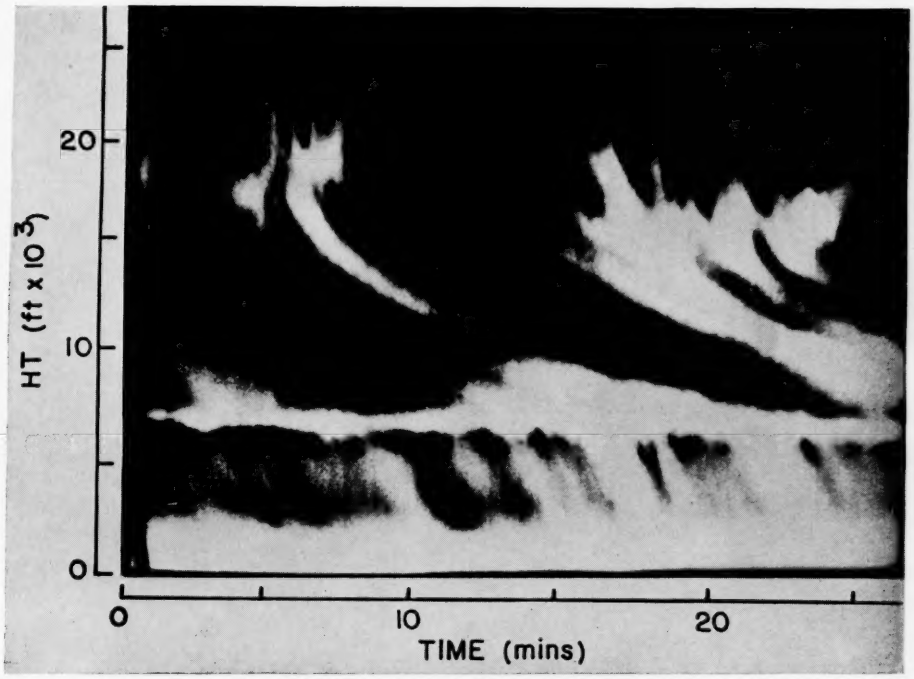


Fig. 2. Generating cells and snow trails as seen by zenith-pointing radar. Horizontal "bright band" at 7000 ft altitude is the melting region. Streaks below are rain streamers. (From GUNN and MARSHALL, 1955.)

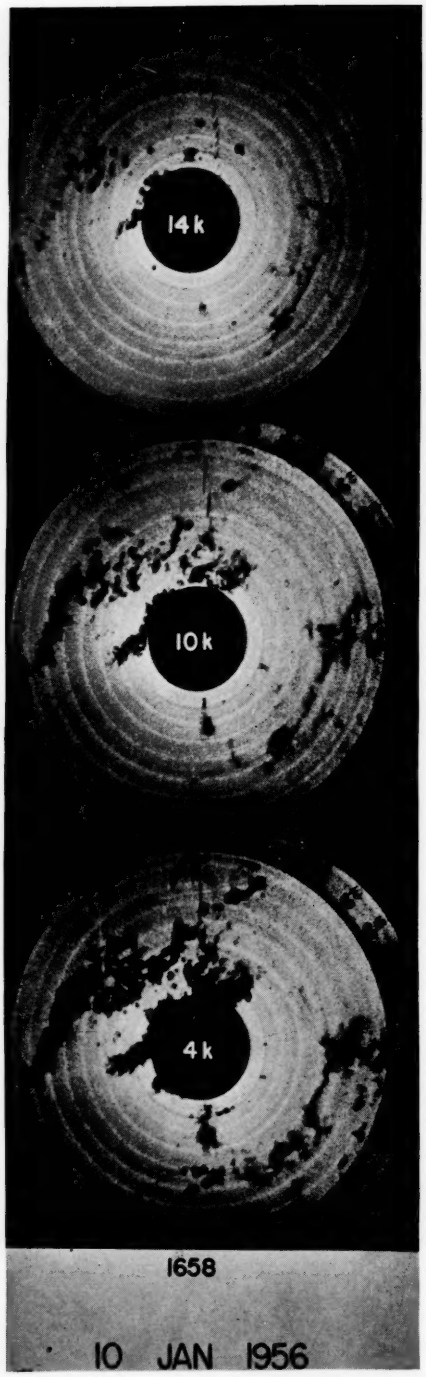


Fig. 3. CAPI (= constant altitude plan indicator) records of snow-generating cells at 14,000 ft (*top*), and the trails falling from them as they appear at 10,000 and 4000 ft (*middle and bottom*). The radar is at the centre of each picture, radius is 75 miles in each case. (From LANGLEBEN, 1957.)

VOL.
15
1959

the more likely process. The turbulence which accompanies the convection is probably required for the aggregation of the snow crystals to full-size flakes. (There is radar evidence that such aggregation takes place in the cells (LANGLEBEN, 1954).

The flakes, in falling out of their turbulent generating cells, penetrate into layers of different, generally lower, wind speeds; hence they tend to lag behind, and long drawn-out snow trails results, such as can be seen rather well by zenith-pointing radar (Fig. 2). Near the OC-isotherm (at about 7000 ft), the particles melt to rain and fall more quickly, hence showing the rather steeper trajectories of the lower part of the figure. The melting region itself shows up as a horizontal region of enhanced echo, called the "bright band".

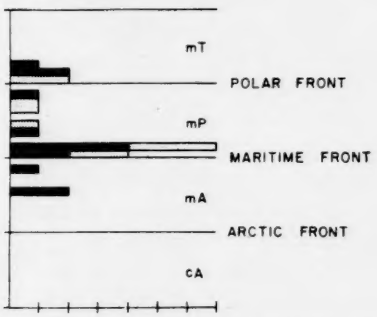


Fig. 1. Position of generating cells within the air masses, and their proximity to the frontal surfaces separating them. (Stippled data obtained in 1952, black from 1954.) (Diagram from DOUGLAS *et al.*, 1957.)

The distribution of generating cells in the horizontal is best revealed by a recently perfected technique of utilizing PPI radar pictures to produce maps of the precipitation echo at any constant height above ground. Fig. 3 is an example of three such "CAPI-maps" of snow, showing generating cells forming an array at 14,000 ft, and horizontal sections through the diffuse trail pattern at 10,000 and 4000 ft. The broadening and intensification of the pattern at the lower levels suggests that there is further growth of the precipitation below the generating cells.

Another instance of convection associated with continuous precipitation are the downdrafts that may be engendered by the rapid evaporation of particles at the lower edge of a precipitation trail above a layer of dry air. The resulting pattern, as shown by zenith-pointing radar, is illustrated in Fig. 4; the downward extensions of the echo layer have been named "stalactites" and are due to the sublimational cooling of the air.

Fig. 5 shows an example of *instability* snow showers, as revealed by the CAPI technique. Here, small-scale convection in unstable air gives rise to many small and low showers at time 2140, while subsequent pictures (at 2309 and 0147) indicate an intensification and a coarsening of the pattern. The temperatures at the three heights (4000, 6000 and 8000 ft) are indicated on the right edge of the figure. They are so low (from $-10°$ to $-16°$ C) as to suggest that the echoing material was ice at all stages.

Convection is the main mechanism in summer showers. We illustrate three different patterns, as revealed by the CAPI radar technique. Fig. 6 shows the development of two line arrays of storms with the second one reaching rather impressive levels of intensity, accompanied by sporadic and light hail fall. In the first column of pictures (1529 local standard time) several well-defined convection cells may be distinguished in a larger diffuse echo mass. The odd cell reaches the considerable height of 40,000 ft. In the course of the next $1\frac{1}{2}$ hr, this line moves (at a rate of about 30 miles/hr) to the east. A number of firm cells clustered around the one reaching 40,000 ft are in the lead, while the extensive diffuse echo behind them grows appreciably. To the west, an as-yet short line is making its appearance, which grows rapidly, till at 1811 it is fully developed and about 80 miles long. Diffuse echo masses appear in connexion with this line only at the higher levels while, oddly enough, the humidity at the low levels was rising, that at high levels falling, as indicated by radiosondes.

On 23 July (Fig. 7) the atmosphere aloft was dry; many small scattered thundershowers occurred, all of which developed in a similar manner. Echoes first appeared at around 10,000 ft, developing within 20 min to a maximum height of 30,000 ft (at a rate of about 1000 ft/min), while the horizontal extent became a maximum (about 10 miles in diameter). Echo tops stayed at their maximum height for a period varying from a few minutes to over an hour, and after this declined in height at a rate of some 250 ft/min. The lifetime of a typical shower was about 1 hr, although one or two showers of apparently no greater development or intensity than the others lasted for well over 2 hr.

In a few instances hail was associated with these isolated showers. (Information about such hail was supplied by observers on the ground.) When hail was observed, it lasted for 2-3 min, reaching the ground within 20 min of the first appearance of an echo.

From sets of pictures, such as Fig. 7, one every few minutes or so, it is easy to plot echo trajectories. Nearly all echoes appeared to move in straight lines, and the motion at all heights of any given echo was nearly identical, even in the face of considerable wind shear. The echo velocity seemed most closely related to that of the wind at low levels (from 5000 to 10,000 ft), but the two were nowhere identical. The magnitude of the vector deviation from the nearest wind was up to 15 miles/hr. On one day (not illustrated here) two initially adjoining echoes diverged at an angle of about 68°, deviating from the wind between ground and 25,000 ft by 30° and 38°, respectively.

Fig. 8 shows a striking phenomenon observed on several occasions of great windshear and high humidities aloft. In the figure, echoes of large isolated showers are seen to develop very long diffuse extensions which we have called plumes. The first column of pictures shows a plume (at 15,000, 25,000 and 35,000 ft) at the stage of its greatest development, when it reached a length of some 60 miles. At the western edge of these 75-mile maps, an as-yet small storm makes its appearance, which in the second column, 45 min later, is the most prominent feature. Here, the second storm has reached great intensity, and at 35,000 ft is just sprouting a plume, which in fact required another 45 min to reach the stage of our first plume in the earlier pictures. This first plume is still in evidence at time 1600, but

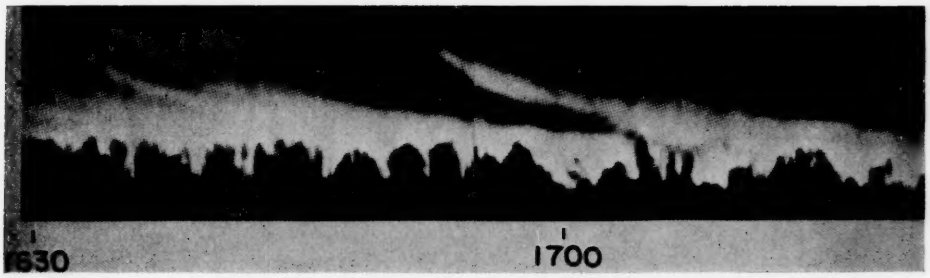


Fig. 4. Zenith-pointing radar record of "stalactite" formations resulting when snow particles from trails fall into, and evaporate rapidly in, dry air.

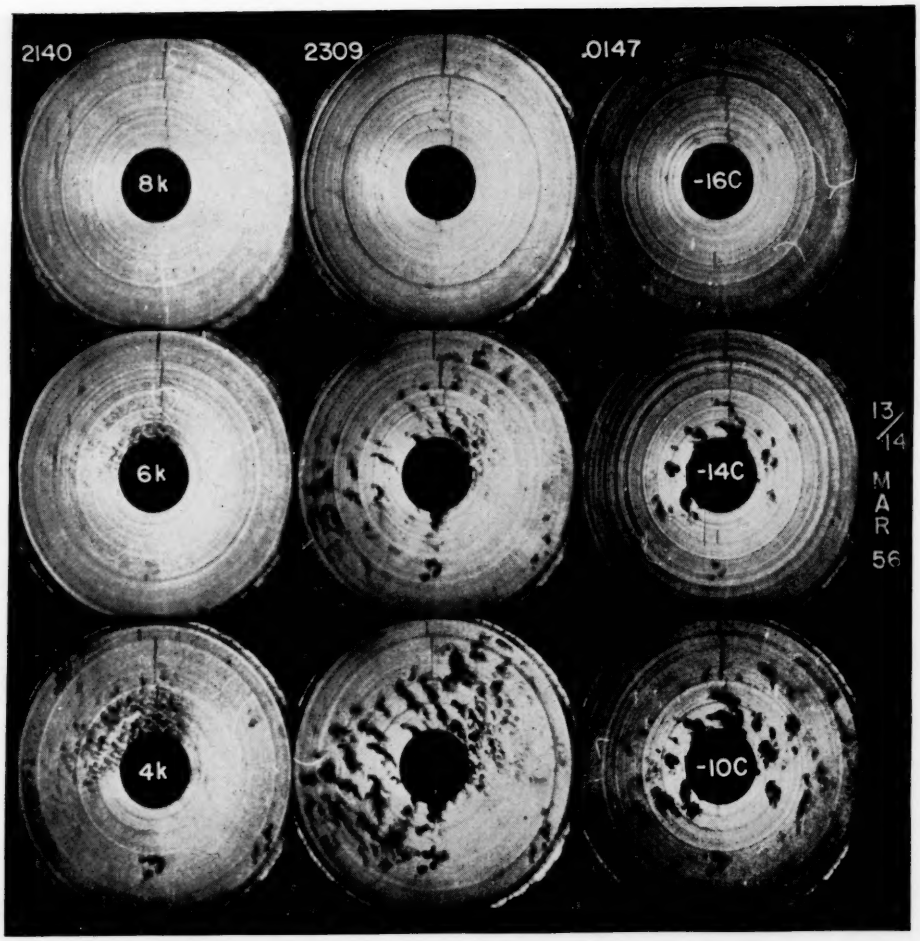


Fig. 5. CAPI records of snow showers. Top row of pictures are8 000 ft mapsat 2140, 2390 and 0147 on 13-14 March 1956, respectively. Middle and bottom row at the same times are for heights of 6000 and 4000 ft. Showers are low convective developments in an unstable environment yielding ice-only precipitation. Turbulence scale changes remarkably from left to middle column.

VOL.
15
1959

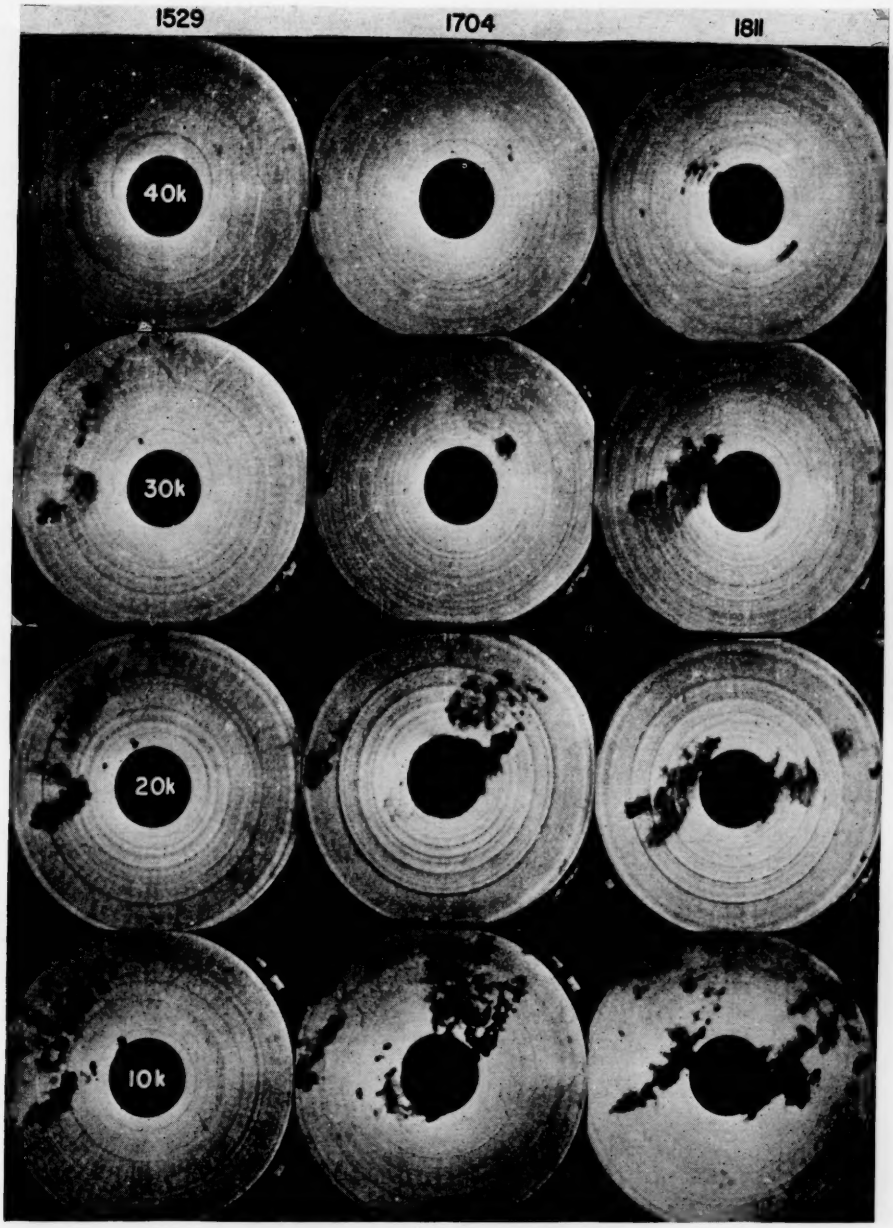


Fig. 6. CAPI records of intense summer thunderstorms arrayed in line developments and accompanied by large and diffuse echo masses. As for all CAPI pictures, the radius of each picture is 75 miles; heights of successive rows are 10,000, 20,100, 30,000 and 40,000 ft.

Fig. 7. CAPI records, again 75 miles in radius, of small scattered showers. Heights are 5000, 15,000 and 25,000 ft, respectively.

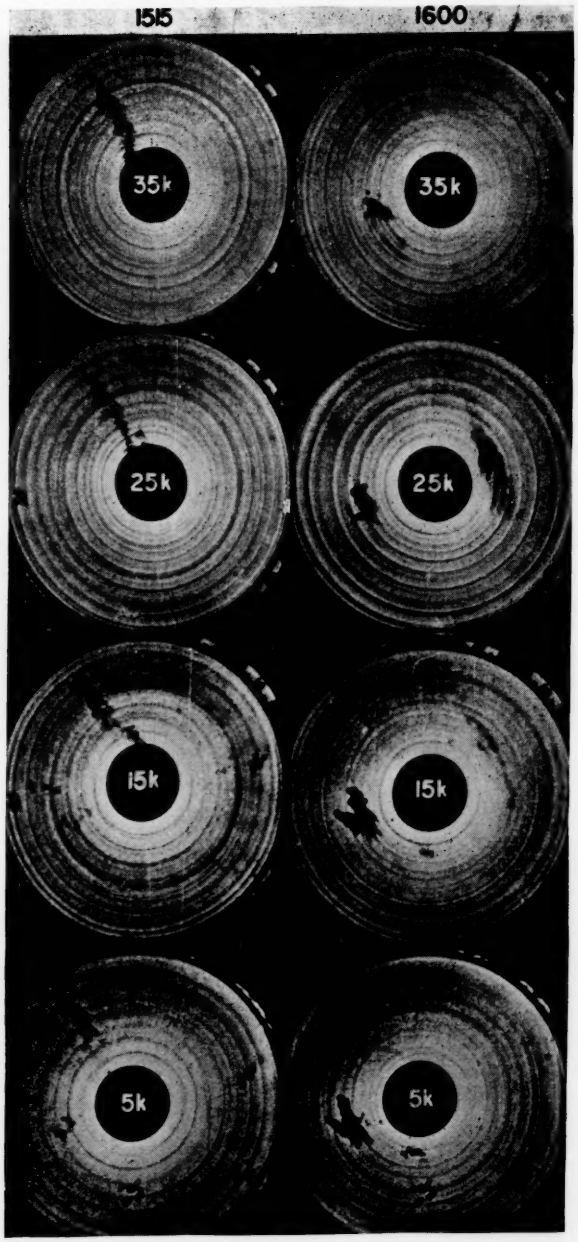


Fig. 8. Large isolated showers with high-level "plumes". Intense black echoes are convective elements; fuzzy elongated echoes are the plumes. In the bottom row, at 5000 ft, black spots to south and south-east of each picture are echoes from hills. (The same echo can also be seen in the 4000 ft pictures of Fig. 3 and 5, and the 5000 ft picture of Fig. 7).

VOL.
15
1959

only at 15,000 and 25,000 ft. The convective chimney which gave rise to it in the first place has subsided, and only a small remnant of it, detached from the plume, shows at 5000 and 15,000 ft.

There were several large isolated storms on this day, and each of them shot forth a plume oriented at about 340°. The motion of the showers at 45 miles/hr was almost exactly west–east, which was also the direction of the wind at low levels. At high levels, the wind was much stronger (130 miles/hr) and had a strong component from the north (about 320°). It thus appears that the velocity of the wind at, say, 35,000 ft, relative to the storm was 110 miles/hr and from bearing

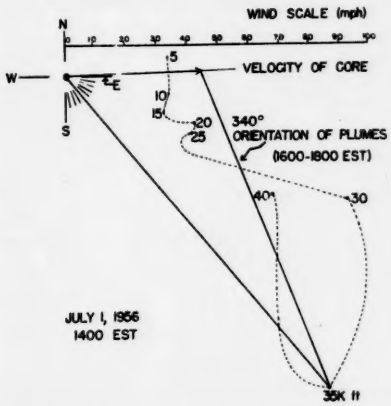


Fig. 9. Dashed line is the hodograph of the winds prevailing at the time of Fig. 8. The echo core at all heights moved W→E at 45 miles/hr. Plumes are oriented at 340° which is the direction of the 35,000 ft wind relative to the echo cores.

340° (see Fig. 9). This is precisely the alignment of the plume, hence suggesting the conclusion that the plume consists of (snow) particles thrown clear of the convective chimneys at a height of about 35,000 ft. While the convective cells of the storm at all *heights* move at the same velocity, the snow in the plume travels with the high-level wind. Experience of some pilots seems to indicate that these plumes may be seats of important electrical activity. But this matter remains to be investigated in detail.

## References


| | | |
|---|---|---|
| American Meteorological Society | 1957 | *Proc. Sixth Weather Radar Conf.* |
| Douglas R. H., Gunn K. L. S. and Marshall J. S. | 1957 | *J. Meteorol.* **14,** 95. |
| Langleben M. P. | 1954 | *Quart. J. Roy. Meteorol. Soc.* **80,** 174. |
| Langleben M. P. | 1957 | *Proc. Sixth Weather Radar Conf.* pp. 89-98. American Meteorological Society. |
| Marshall J. S. and Gordon W. E. | 1957 | *Radiometeorology.* Meteorological Monographs, American Meteorological Society, Boston. |


## Discussion

Dr. J. S. Marshall—Bubbling, apparently, is the process by which a superadiabatic layer next to the earth's surface overturns with the air above; on a

summer morning that air above may be stable, so that the bubbles rise to hydrostatic equilibrium. In winter, when snow falls into dry air, we assume that a superadiabatic layer is formed aloft, at the upper limit of the dry air, as snow evaporates. The "stalactites" of Dr. HITSCHFELD's Fig. 4 are the result of overturning between this thin superadiabatic layer aloft and the stable air below. I suggest, then, that Fig. 4 might usefully be studied, inverted, as a first approximation to the summer-morning pattern, with moist, but clear, bubbles risen into a stable environment.

DR. J. S. MARSHALL summarized the Report on Canadian Simultaneous Forward-Scatter Weather-Radar Observations, prepared by S. A. STONE of the National Research Council:—

In 1956 the National Research Council established a microwave link from Ottawa to Dorval Airport, near Montreal. The Dorval receiver was placed in a hut adjacent to the room containing the control console for a 3-cm weather radar operated by the McGill University Stormy Weather Group. It was then possible to observe when the precipitation fell on the path. By taking high-speed recordings of received field strength before, during, and after rain fell on the path, it was hoped to discover the effects of this rain on beyond-the-horizon propagation.

Transmission was one-way, Ottawa to Dorval, a distance of 90 miles, at a frequency of 2720 Mc/s, and with peak pulse power of 100 kW. Antennae were 6 ft paraboloid reflectors. The receiving antenna was inclined some 40 min, which placed the lower beam intersection 32 miles from Dorval and 2000 ft up. The important scattering volume was taken to be: height 2000 ft; width 5000 ft; length 9600 ft, as suggested by GORDON. The common volume for the 4° beamwidths is some sixty times greater. From theoretical considerations, the ratio of rain to tropospheric scattering cross-sections was $R^{1.6} \times 10^{-5}$, where $R$ is rainfall rate (mm/hr). Assuming rain fills the common volume, a precipitation rate of 100 mm/hr is required to double the scattered power. This requirement therefore rules out precipitation scatter having any marked effect on the signal.

The high-speed recordings of field strength during frontal passages show an increase in the fading rate (positive-slope crossings of the median level) during and after a frontal passage. On several occasions the signal level rose 10 or 20 dB. This rise in signal level was accompanied by a compression of the fading range of the signal, which indicates that some propagation mechanism other than tropospheric scattering was occurring, such as trapping in a wet duct.

Correlation of signal level with frontal passages shows more cases of amplitude decreasing than otherwise, the trend being more marked for cold fronts than for warm fronts.

Another feature was the rise of signal level most nights. This is probably due to anomalous propagation occasioned by radiation cooling.

DR. D. ATLAS—In the afternoon of 10 September 1956, the scope of the 3-cm CPS-9 radar at Smoky Hill AFB, Salina, Kansas displayed a vast area of diffuse echoes, out to a range of 100 miles in places. No precipitation and only a few scattered high clouds were reported. The internal pattern of the echo area consisted largely of polygonal cells and some striated bands very similar in appearance to forms of altocumulus clouds. Only vaguely could one discern what may have



VOL. 15 1959

been ground features in this mysterious echo pattern, although in the clear areas to the SW, fixed, discrete echoes associated with towns were observed at ranges beyond the normal horizon (out to 80 miles).

However, super-refraction in the normal sense was highly unlikely because the observations were made during the heat of the day when extensive convection precluded the required stratification. It was thought at first that the echoes were due to reflections from the boundaries of Benard cells, established by convection between the surface and a subsidence inversion at about 9500 ft. The light winds in this layer and small shear would favour the formation of such a regular convection pattern. Also, the horizontal cell dimensions agreed in magnitude with that to be expected from theory and observation. The necessary refractive-index gradients at the cell boundaries could be attributed to eddies of dry air brought down from aloft (below the inversion) enveloped in or enveloping relatively moist surface air and carried upwards in the vertical circulation arms of the Benard cells. However, the vertical radar cross-sections showed the echoes to extend only to a height of about 1000 ft, which would have precluded their detection out to 100 miles, except by a secondary scattering mechanism (i.e. forward-scatter by nearby blobs to others beyond the horizon and back). This placed a doubly severe requirement on the sharpness of the $N$-gradients which already had to be stretched to account for direct back-scattering.

Although it is still questionable, the most reasonable explanation appears to be forward-scatter from the eddies to the ground and back again, the forward-scatter signal from the blobs being much greater than the back-scatter. In this manner, relatively featureless terrain would present a pattern of the elevated "mirror" through which it is viewed by the radar. In other words, the pattern of the Benard convection cells is seen in the terrain return. Of course, hills aligned perpendicular to the radar would be seen best; this is evidently the reason for a tendency toward circumferential alignment of the cell boundaries. Also the presence of the vague ground features among the generally diffuse echoes fits in with this hypothesis. The presence of only prominent ground targets to the south-west appears to be due to a weakening of atmospheric scattering in that direction.

Journal of Atmospheric and Terrestrial Physics, 1959, Vol. 15, pp. 294 to 296. Pergamon Press Ltd. Printed in Northern Ireland

# SESSION VI

## ADMINISTRATION

### Minutes

THE meeting was convened at 2.15 p.m. Those in attendance were: J. S. MARSHALL, W. E. GORDON, P. M. MISME, Col. E. HERBAYS, R. L. SMITH-ROSE, J. H. CHISHOLM, J. P. VOGE, J. VAN DER MARK and R. BOLGIANO, Jr.

Dr. GORDON initiated the discussion by reading from the proposed rules of ICSU for Mixed Commissions, particularly that part relating to areas of interest and programme. He noted that these rules clearly state that a mixed commission must define its area of concern by choosing one or, at most, several specific topics for future consideration.

Dr. MARSHALL then said that for him a prime objective in attending the meetings was to decide as to the existence of an area of common interest between the radio-propagation people on the one hand and the meteorologists on the other. He read a summary (see Preface) of the meetings, which he had prepared, including his conclusions on this matter.

Dr. SMITH-ROSE suggested that it might be of some appreciable value to discuss and determine a programme for the future before attempting to decide the fate of the commission.

There followed an extended discussion of which the major objective was the definition of the area of interest for JCRM. Dr. SMITH-ROSE questioned the inclusion of thunderstorms and lightning flashes as being relevant to tropospheric propagation. Mr. CHISHOLM pointed out that with today's high-gain systems atmospheric noise is of interest to u.h.f. and s.h.f. communications engineers, but that Commission IV of URSI has not been considering this frequency range. Dr. MARSHALL contended that since thunderstorm activity appears to be a direct outgrowth of convective turbulence, which topic is certainly of interest from the meteorologist's point of view, it cannot be separated. The culmination of this discussion was:

(A) A statement of the general area of interest of JCRM, namely "studies of physical meteorology made by or immediately relevant to radio".

(B) The choice of two topics to constitute the programme for the next period:

(1) The study of vertical and horizontal air-movements and refractive-index structure, including the formation of clouds and precipitation, and the application of results to radio-wave propagation and to meteorology.

(2) The study of electric fields in the atmosphere, with special reference to thunderstorms.



VOL. 15 1959

There was also some appreciable discussion regarding the nature of the meetings. M. MISME suggested that:

(a) The programme should be established by URSI and UGGI 3 years in advance of the next meeting, the president of the commission choosing one or two select topics if the programme was too broad.

(b) The meetings should *not* be a general symposium.

(c) The French language should be understood.

(d) Papers should be restricted to unpublished material.

(e) The commission officers should choose, for presentation and publication, the most significant of the papers submitted. Also, papers should be submitted 3 months in advance.

Dr. MARSHALL expressed enthusiasm for the relatively informal character of the meetings as conducted during these sessions. He felt, and there was general agreement on this point, that more information was exchanged and more valuable personal contact made under such circumstances.

Dr. GORDON requested suggestions for the interval until the next meetings. After brief discussion it was agreed that the next sessions should be held in 3 years, regardless of the timing and location of UGGI or URSI international meetings.

Next Dr. GORDON inquired regarding the lack of representation of IUPAP. It was agreed that that organization should be asked if it wishes to participate in the 1960 meetings in view of the topics constituting the programme; and that, if the answer were affirmative, IUPAP be requested to appoint some active representatives. Following this, there was some consideration of representatives in general. M. VOGE made the suggestion that, if possible, some thought should be given to discussion leaders for the next sessions, in view of the programme topics selected, when appointments are made.

It was agreed that, considering his long association with the Commission and intimate interest therein, Dr. GORDON should serve as President during the next 3 years and that he should select a secretary after representation on the Commission has been reviewed by the member Unions.

## Resolutions

It was agreed:

That the 1957 meetings had provided a successful forum in which specialists in radio science, meteorology and physics had a unique opportunity to describe their experiences and to exchange knowledge about phenomena in the lower atmosphere in which they had a mutual scientific interest.

The following resolutions were adopted unanimously:

(1) That the Joint Commission should continue as a forum with a reasonable balance of radio-scientists, meteorologists and, as may be necessary, other physicists, in which the meteorologists can exchange knowledge and experience.

(2) That the programme for the immediate future should be: (a) study of vertical and horizontal air-movements and refractive-index structure including formation of clouds and precipitation and application of the results to radio-wave

propagation and meteorology; (b) study of electrical fields in the atmosphere with special reference to thunderstorms.

(3) That the constituent Unions be invited to review their representation on the Commission and make fresh appointments where necessary.

(4) That the next meeting of the Commission be held in 1960.

(5) That the papers for presentation at the next meeting be submitted to the President of the Commission for approval 3 months before the meeting.

(6) That the Commission conveys its warmest gratitude to the President of New York University and his staff, particularly Prof. M. KLINE, for the facilities, assistance and hospitality provided in connexion with the Commission's meeting.

## AUTHOR INDEX

(D denotes participation in Discussion)

ATLAS D. 262, 245D, 292D
BOLGIANO R. 203D, 286D
BYERS H. R. 254
FITZGERALD D. R. 254, 260D
GORDON W. E. 286D
HAY D. R. 204D
HITSCHFELD W. F. 288
LIGDA M. G. H. 248, 287D
MARSHALL J. S. 183, 244D, 291D
NORTON K. A. 206
PLANK V. G. 203D, 228, 284D
SMITH L. G. 251, 260D
SMITH-ROSE R. L. 244D
WHEELON A. D. 185, 203D

VOL.
15
195

OL.
15
959